



**STUDIES IN ORGANO-  
TRANSITION METAL CHEMISTRY**

by

Michael John Liddell  
B.Sc.(Hons) (Otago),  
M.Sc. (Monash)

A Thesis presented for the  
Degree of Doctor of Philosophy

Department of Physical and Inorganic Chemistry  
University of Adelaide

June 1989

# TABLE OF CONTENTS

	Page
<i>LIST OF FIGURES</i>	vii
<i>LIST OF TABLES</i>	x
<i>LIST OF SCHEMES</i>	xii
<i>ABBREVIATIONS</i>	xiii
<i>NUMBERING OF COMPLEXES</i>	xvii
<i>STATEMENT</i>	xviii
<i>ACKNOWLEDGEMENTS</i>	xix
<b>SUMMARY</b>	1
<b>CHAPTER ONE</b>	5
<b>Cycloaddition reactions of 1,1-dicyano-2,2-bis(trifluoromethyl)ethene with transition-metal acetylides</b>	
<b>1.1. Introduction</b>	6
<b>1.2. Results and Discussion</b>	12
1.2.1. Cyclobutenyl complexes	12
1.2.2. Butadienyl complexes	23
1.2.3. Allyl complexes	28
1.2.4. Hydrolysis of (13)	32
1.2.5. Nitrile-substituted cyclobutenyl complexes	36
1.2.6. Electrochemistry	50
<b>1.3. Conclusions</b>	53
<b>1.4. Experimental</b>	54
<i>Syntheses:</i>	
1.4.1. $W\{\overline{C=CPhC(CF_3)_2C(CN)_2}\}(CO)_3(\eta-C_5H_5)$ (13)	57

	Page
1.4.2. $\text{Mn}\{\overline{\text{C}=\text{CPhC}(\text{CF}_3)_2\text{C}(\text{CN})_2}\}(\text{CO})_3(\text{dppe})$ (14)	58
1.4.3. $\text{Fe}\{\overline{\text{C}=\text{CPhC}(\text{CF}_3)_2\text{C}(\text{CN})_2}\}(\text{CO})_2(\eta\text{-C}_5\text{H}_5)$ (15)	58
1.4.4. $\text{Ru}\{\overline{\text{C}=\text{CPhC}(\text{CF}_3)_2\text{C}(\text{CN})_2}\}(\text{dppe})(\eta\text{-C}_5\text{H}_5)$ (16)	59
1.4.5. $\text{Ru}\{\overline{\text{C}=\text{CPhC}(\text{CF}_3)_2\text{C}(\text{CN})_2}\}(\text{PPh}_3)_2(\eta\text{-C}_5\text{H}_5)$ (17)	60
1.4.6. $\text{Ru}\{\overline{\text{C}=\text{CMeC}(\text{CF}_3)_2\text{C}(\text{CN})_2}\}(\text{PPh}_3)_2(\eta\text{-C}_5\text{H}_5)$ (18)	60
1.4.7. $\text{Ru}\{\overline{\text{C}=\text{CPhC}(\text{CF}_3)_2\text{C}(\text{CN})_2}\}(\text{CO})(\text{PPh}_3)(\eta\text{-C}_5\text{H}_5)$ (19)	61
1.4.8. $\text{W}\{\text{C}=\text{C}(\text{CN})_2\}\text{CPh}=\text{C}(\text{CF}_3)_2\}(\text{CO})_3(\eta\text{-C}_5\text{H}_5)$ (20) and $\text{W}\{\eta^3\text{-C}(\text{CF}_3)_2\text{CPhC}=\text{C}(\text{CN})_2\}(\text{CO})_2(\eta\text{-C}_5\text{H}_5)$ (24)	62
1.4.9. $\text{Ni}\{\text{C}=\text{C}(\text{CN})_2\}\text{CPh}=\text{C}(\text{CF}_3)_2\}(\text{PPh}_3)(\eta\text{-C}_5\text{H}_5)$ (21)	63
1.4.10. $\text{Ru}\{\text{C}=\text{C}(\text{CN})_2\}\text{CPh}=\text{C}(\text{CF}_3)_2\}(\text{CO})(\text{PPh}_3)(\eta\text{-C}_5\text{H}_5)$ (22)	64
1.4.11. $\text{Ru}\{\text{C}=\text{C}(\text{CN})_2\}\text{CPh}=\text{C}(\text{CF}_3)_2\}(\text{dppe})(\eta\text{-C}_5\text{H}_5)$ (23)	64
1.4.12. $\text{Ru}\{\eta^3\text{-C}(\text{CF}_3)_2\text{CPhC}=\text{C}(\text{CN})_2\}(\text{PPh}_3)(\eta\text{-C}_5\text{H}_5)$ (25)	65
1.4.13. $\text{Ru}\{\eta^3\text{-C}(\text{CF}_3)_2\text{CMeC}=\text{C}(\text{CN})_2\}(\text{PPh}_3)(\eta\text{-C}_5\text{H}_5)$ (26)	66
1.4.14. $\text{W}\{\overline{\text{NH}=\text{C}(\text{OH})\text{C}(\text{CN})=\text{C}}\}\text{CPh}=\text{C}(\text{CF}_3)_2\}(\text{CO})_2(\eta\text{-C}_5\text{H}_5)$ (27)	67
1.4.15. $\text{Ru}\{\overline{\text{C}=\text{CPhC}(\text{CF}_3)_2\text{C}(\text{CN})_2}\}(\text{NCMe})(\text{PPh}_3)(\eta\text{-C}_5\text{H}_5)$ (29)	68
1.4.16. $\text{Ru}\{\overline{\text{C}=\text{CPhC}(\text{CF}_3)_2\text{C}(\text{CN})_2}\}(\text{NCCH}=\text{CH}_2)(\text{PPh}_3)(\eta\text{-C}_5\text{H}_5)$ (31)	68
1.4.17. $\text{Ru}\{\overline{\text{C}=\text{CPhC}(\text{CF}_3)_2\text{C}(\text{CN})_2}\}\{(\text{NC})\text{C}_6\text{H}_2(\text{CN})_3\}(\text{PPh}_3)(\eta\text{-C}_5\text{H}_5)$ (32)	69
1.4.18. $\text{Ru}\{\overline{\text{C}=\text{CPhC}(\text{CF}_3)_2\text{C}(\text{CN})_2}\}\{(\text{NC})\text{C}_6\text{H}_4(\text{CN})\text{-}o\}(\text{PPh}_3)\text{-}$ $(\eta\text{-C}_5\text{H}_5)$ (33)	70
1.4.19. $\text{Ru}\{\overline{\text{C}=\text{CPhC}(\text{CF}_3)_2\text{C}(\text{CN})_2}\}\{(\text{NC})\text{C}_6\text{F}_4(\text{CN})\text{-}o\}(\text{PPh}_3)(\eta\text{-C}_5\text{H}_5)$ (34) and $\{\text{Ru}\{\overline{\text{C}=\text{CPhC}(\text{CF}_3)_2\text{C}(\text{CN})_2}\}(\text{PPh}_3)\}(\eta\text{-C}_5\text{H}_5)_2\text{-}$ $\{\mu\text{-}(\text{NC})_2\text{C}_6\text{F}_4\text{-}o\}$ (37)	70
1.4.20. $\text{Ru}\{\overline{\text{C}=\text{CPhC}(\text{CF}_3)_2\text{C}(\text{CN})_2}\}\{(\text{NC})\text{C}_6\text{F}_4(\text{CN})\text{-}p\}(\text{PPh}_3)\text{-}$ $(\eta\text{-C}_5\text{H}_5)$ (35)	70
1.4.21. $\text{Ru}\{\overline{\text{C}=\text{CPhC}(\text{CF}_3)_2\text{C}(\text{CN})_2}\}\{\textit{trans}\text{-}(\text{NC})\text{CH}=\text{CH}(\text{CN})\}(\text{PPh}_3)\text{-}$ $(\eta\text{-C}_5\text{H}_5)$ (36) and two isomers of $\{\text{Ru}\{\overline{\text{C}=\text{CPhC}(\text{CF}_3)_2\text{C}(\text{CN})_2}\}\text{-}$ $(\text{PPh}_3)(\eta\text{-C}_5\text{H}_5)\}_2\{\mu\text{-}\textit{trans}\text{-}(\text{NC})\text{HC}=\text{CH}(\text{NC})\}$ (38a) and (38b)	71

	Page
1.4.22. Three isomers of $\{\text{Ru}[\overline{\text{C}=\text{CPhC}(\text{CF}_3)_2\text{C}(\text{CN})_2}](\text{PPh}_3)(\eta\text{-C}_5\text{H}_5)\}_2\text{-}\{\mu\text{-(NC)}_2\text{C}=\text{C}(\text{CN})_2\}$ (39a), (39b) and (39c)	72
1.4.23. Two isomers of $\{\text{Ru}[\overline{\text{C}=\text{CPhC}(\text{CF}_3)_2\text{C}(\text{CN})_2}](\text{PPh}_3)(\eta\text{-C}_5\text{H}_5)\}_2\text{-}\{\mu\text{-(NC)}_2\text{C}=\text{C}(\text{CF}_3)_2\}$ (40a), (40b) and two isomers of $\{\text{Ru}[\overline{\text{C}=\text{CPhC}(\text{CF}_3)_2\text{C}(\text{CN})_2}](\text{PPh}_3)(\eta\text{-C}_5\text{H}_5)\}_2\{\mu\text{-(NC)}_2\overline{\text{C}=\text{C}(\text{CF}_3)_2\text{O}}\}$ (42a) and (42b)	72
1.4.24. Reaction of complexes (40) with O <sub>2</sub>	74
1.5. References	88
 <b>CHAPTER TWO</b>	 91
<b>Cycloaddition reactions of <i>trans</i>-1,2-bis(carbomethoxy)-1-cyano-ethene and related chemistry</b>	
2.1. Introduction	92
2.2. Results and Discussion	97
2.2.1. Three isomers of $\text{Ru}[\overline{\text{C}=\text{CPhCH}(\text{CO}_2\text{Me})\text{C}(\text{CO}_2\text{Me})(\text{CN})}](\text{CO})(\text{PPh}_3)(\eta\text{-C}_5\text{H}_5)$	97
2.2.2. Conrotatory ring-opening	105
2.2.3. Allyl complex $\text{Ru}\{\eta^3\text{-CH}(\text{CO}_2\text{Me})\text{CPhC}=\text{C}(\text{CO}_2\text{Me})(\text{CN})\}\text{-}(\text{CO})(\eta\text{-C}_5\text{H}_5)$	109
2.2.4. Cycloaddition of tetracyanoethene to manganese and iron $\sigma$ -acetylide complexes	113
2.2.5. Reactions of $\text{Fe}(\overline{\text{C}=\text{CFCF}_2\text{CF}_2})(\text{CO})_2(\eta\text{-C}_5\text{H}_5)$	121
2.3. Conclusions	126
2.4. Experimental	130
<i>Syntheses:</i>	

	Page
2.4.1. Two isomers of $\text{Ru}\{\overline{\text{C}=\text{CPhCH}(\text{CO}_2\text{Me})\text{C}(\text{CO}_2\text{Me})-\text{(CN)}}\}\text{(CO)}(\text{PPh}_3)(\eta\text{-C}_5\text{H}_5)$ ( <b>5a</b> ), ( <b>5b</b> )	130
2.4.2. Solid state conversion of ( <b>5a</b> ) and ( <b>5b</b> ) to a third isomer of $\text{Ru}\{\overline{\text{C}=\text{CPhCH}(\text{CO}_2\text{Me})\text{C}(\text{CO}_2\text{Me})\text{(CN)}}\}\text{(CO)}(\text{PPh}_3)(\eta\text{-C}_5\text{H}_5)$ ( <b>5c</b> )	132
2.4.3. $\text{Ru}\{\text{C}[\text{=C}(\text{CO}_2\text{Me})\text{(CN)}]\text{CPh}=\text{CH}(\text{CO}_2\text{Me})\}\text{(CO)}(\text{PPh}_3)(\eta\text{-C}_5\text{H}_5)$ ( <b>6</b> )	133
2.4.4. $\text{Ru}\{\eta^3\text{-CH}(\text{CO}_2\text{Me})\text{CPhC}=\text{C}(\text{CO}_2\text{Me})\text{(CN)}\}\text{(CO)}(\eta\text{-C}_5\text{H}_5)$ ( <b>7</b> )	135
2.4.5. $\text{Mn}\{\overline{\text{C}=\text{CPhC}(\text{CN})_2\text{C}(\text{CN})_2}\}\text{(CO)}_3(\text{dppe})$ ( <b>9</b> )	136
2.4.6. $\text{Fe}\{\overline{\text{C}=\text{CPhC}(\text{CN})_2\text{C}(\text{CN})_2}\}\text{(CO)}_2(\eta\text{-C}_5\text{H}_5)$ ( <b>10</b> )	136
2.4.7. $\text{Mn}\{\text{C}[\text{=C}(\text{CN})_2]\text{CPh}=\text{C}(\text{CN})_2\}\text{(CO)}_3(\text{dppe})$ ( <b>11</b> )	137
2.4.8. $\text{Fe}\{\text{C}[\text{=C}(\text{CN})_2]\text{CPh}=\text{C}(\text{CN})_2\}\text{(CO)}_2(\eta\text{-C}_5\text{H}_5)$ ( <b>12</b> )	137
2.4.9. $\text{W}\{\overline{\text{NH}=\text{C}(\text{OH})\text{C}(\text{CN})=\text{CPh}=\text{C}(\text{CN})_2}\}\text{(CO)}_2(\eta\text{-C}_5\text{H}_5)$ ( <b>13</b> )	138
2.4.10. $\text{Fe}\{\overline{\text{C}=\text{CFCF}_2\text{CF}_2}\}\text{(CO)}_2(\eta\text{-C}_5\text{H}_5)$ ( <b>14</b> )	139
2.4.11. Attempted ring-opening reactions of ( <b>14</b> )	139
2.4.12. $\text{Fe}\{\overline{\text{C}=\text{CFCF}_2\text{CF}_2}\}\text{(CO)}(\text{NCMe})(\eta\text{-C}_5\text{H}_5)$ ( <b>15</b> )	140
2.4.13. $\text{Fe}\{\overline{\text{C}=\text{CFCF}_2\text{CF}_2}\}\text{(CO)}(\text{PPh}_3)(\eta\text{-C}_5\text{H}_5)$ ( <b>16</b> )	141
2.4.14. Reaction of ( <b>14</b> ) with CO	142
2.5. References	143

## CHAPTER THREE 145

### New reactions of $\text{Ru}_5(\mu_5\text{-}\eta^2, P\text{-C}_2\text{PPh}_2)(\mu\text{-PPh}_2)(\text{CO})_{13}$

3.1. Introduction	146
3.2. Results and Discussion	161
3.2.1. Further observations on the synthesis of $\text{Ru}_5(\mu_5\text{-}\eta^2, P\text{-C}_2\text{PPh}_2)(\mu\text{-PPh}_2)(\text{CO})_{13}$ ( <b>1</b> )	161
3.2.2. Pyrolysis reactions of ( <b>1</b> )	167
3.2.3. CO substitution by $\text{P}(\text{OEt})_3$ in ( <b>1</b> )	180
3.2.4. CO substitution by $\text{PMe}_2\text{Ph}$ in ( <b>1</b> )	191
3.2.5. CO substitution by $\text{PPh}_3$ in ( <b>1</b> )	192

	Page
3.2.6. Synthesis of and ligand substitution in $\text{Au}_2\text{Ru}_5(\mu_5\text{-}\eta^2, P\text{-C}_2\text{PPh}_2)(\mu\text{-PPh}_2)(\text{CO})_{12}(\text{PPh}_3)_2$ (35)	198
3.2.7. Oxidative addition of haloacids and $\text{AuCl}(\text{PPh}_3)$ to (1)	206
3.2.8. Addition of allyl halides to (1)	212
3.2.9. Reaction of (1) with mercuric chloride	218
3.2.10. Reaction of (1) with ethene and 1-butene	219
3.2.11. $^{31}\text{P}$ NMR studies on some $\text{Ru}_4$ , $\text{Ru}_5$ and $\text{Au}_2\text{Ru}_5$ clusters	233
3.3. Conclusions	238
3.4. Experimental	241
<i>Syntheses:</i>	
3.4.1. $\text{Ru}_5(\mu_5\text{-}\eta^2, P\text{-C}_2\text{PPh}_2)(\mu\text{-PPh}_2)(\text{CO})_{13}$ (1)	242
3.4.2. Pyrolyses of $\{\text{Ru}_3(\text{CO})_{11}\}_2(\mu\text{-dppa})$ under different conditions	243
3.4.3. $\text{Ru}_4(\mu_4\text{-}\eta^2\text{-C}_2)(\mu\text{-PPh}_2)_2(\text{CO})_{12}$ (7)	245
3.4.4. $\text{Ru}_5(\mu_4\text{-PPh})\{\mu_3\text{-}\eta^2, P\text{-CCPh}(\text{PPh}_2)\}(\text{CO})_{12}$ (26)	246
3.4.5. $\text{Ru}_5(\mu\text{-H})(\mu_4\text{-PPh})\{\mu_4\text{-}\eta^4\text{-CCPh}(\text{C}_6\text{H}_4)\}(\mu_3\text{-PPh})(\text{CO})_{10}$ (27)	246
3.4.6. $\text{Ru}_5(\mu_4\text{-PPh})\{\mu_4\text{-}\eta^4\text{-CCPh}(\text{C}_6\text{H}_4)\}(\mu\text{-PPh}(\text{OMe}))(\text{CO})_{11}$ (28)	248
3.4.7. Three isomers of $\text{Ru}_5(\mu_5\text{-}\eta^2, P\text{-C}_2\text{PPh}_2)(\mu\text{-PPh}_2)(\text{CO})_{12}\{\text{P}(\text{OEt})_3\}$ (29a), (29b), (29c) and $\text{Ru}_5(\mu_5\text{-}\eta^2, P\text{-C}_2\text{PPh}_2)(\mu\text{-PPh}_2)\text{-}$ $(\text{CO})_{11}\{\text{P}(\text{OEt})_3\}_2$ (30)	251
3.4.8. $\text{Ru}_5(\mu_5\text{-}\eta^2, P\text{-C}_2\text{PPh}_2)(\mu\text{-PPh}_2)(\text{CO})_{11}(\text{PMe}_2\text{Ph})_2$ (31)	253
3.4.9. $\text{Ru}_5(\mu_5\text{-}\eta^2, P\text{-C}_2\text{PPh}_2)(\mu\text{-PPh}_2)(\text{CO})_{12}(\text{PPh}_3)$ (32) and $\text{Ru}_5(\mu_4\text{-PPh})(\mu_3\text{-}\eta^2\text{-PhC}_2\text{Ph})(\mu\text{-PPh}_2)_2(\text{CO})_{10}$ (33)	254
3.4.10. $\text{Ru}_5(\mu_4\text{-PPh})\{\mu_3\text{-}\eta^2\text{-PhC}_2(p\text{-tolyl})\}(\mu\text{-PPh}_2)\text{-}$ $\{\mu\text{-P}(p\text{-tolyl})_2\}(\text{CO})_{10}$ (34)	255
3.4.11. $\text{Au}_2\text{Ru}_5(\mu_5\text{-}\eta^2, P\text{-C}_2\text{PPh}_2)(\mu\text{-PPh}_2)(\text{CO})_{12}(\text{PPh}_3)_2$ (35)	256
3.4.12. $\text{Au}_2\text{Ru}_5(\mu_5\text{-}\eta^2, P\text{-C}_2\text{PPh}_2)(\mu\text{-PPh}_2)(\text{CO})_{12}(\text{PPh}_3)\{\text{P}(\text{OEt})_3\}$ (39), $\text{Au}_2\text{Ru}_5(\mu_5\text{-}\eta^2, P\text{-C}_2\text{PPh}_2)(\mu\text{-PPh}_2)(\text{CO})_{11}(\text{PPh}_3)\text{-}$	

	Page
$\{P(OEt)_3\}_2$ (40) and $Au_2Ru_5(\mu_5-\eta^2, P-C_2PPh_2)-$ $(\mu-PPh_2)(CO)_{11}(PPh_3)_2 \{P(OEt)_3\}$ (41)	258
3.4.13. $Ru_5(\mu-H)(\mu_5-\eta^2, P-C_2PPh_2)(\mu-PPh_2)(\mu-Cl)(CO)_{13}$ (42)	259
3.4.14. $Ru_5(\mu-H)(\mu_5-\eta^2, P-C_2PPh_2)(\mu-PPh_2)(\mu-Br)(CO)_{13}$ (43)	260
3.4.15. $Ru_5(\mu-H)(\mu_5-\eta^2, P-C_2PPh_2)(\mu_3-I)(\mu-PPh_2)(CO)_{12}$ (44)	261
3.4.16. $AuRu_5(\mu_5-\eta^2, P-C_2PPh_2)(\mu-PPh_2)(\mu-Cl)(CO)_{13}(PPh_3)$ (45)	262
3.4.17. $Ru_5\{\mu_4-\eta^4, O-C_2C(O)C_3H_5\}(\mu-PPh_2)_2(\mu-Cl)(CO)_{11}$ (46o) and isomer $Ru_5Cl(CO)_{12}(C_3H_5)(dppa^*)$ (46b)	263
3.4.18. $Ru_5\{\mu_4-\eta^4, O-C_2C(O)C_3H_5\}(\mu-PPh_2)_2(\mu-Br)(CO)_{11}$ (47o) and isomer $Ru_5Br(CO)_{12}(C_3H_5)(dppa^*)$ (47b)	264
3.4.19. Two isomers of $Ru_6(CO)_{11}(dppa^*)$ (48o), (48y)	264
3.4.20. $Ru_4\{\mu_4-\eta^2, P,O-C_5H_4O(PPh_2)\}(\mu-PPh_2)(CO)_{11}$ (49) and two isomers of $Ru_5(\mu_4-PPh)\{\mu_3-\eta^3-CC(C_2H_2)(C_2H_3)\}(\mu-PPh_2)-$ $(CO)_{12}$ (50b), (50o)	264
3.4.21. Two isomers of $Ru_5(\mu_4-PPh)\{\mu_3-\eta^3-CC(C_4H_6)(C_4H_7)\}(\mu-PPh_2)-$ $(CO)_{12}$ (51b), (51o)	267
3.4.22. $Ru_5(\mu_4-PPh)(\mu-PPh_2)(\mu-CO)(CO)_{10}\{\eta^5-C_5H_3(C_2H_3)Me\}$ (52)	268
<b>3.5. References</b>	270
 <b>APPENDIX 1</b>	 275
Supplementary data for $Ru_5(\mu_4-PPh)\{\mu_4-\eta^4-CCPh(C_6H_4)\}\{\mu-PPh(OMe)\}(CO)_{11}$ (28)	
 <b>APPENDIX 2</b>	 290
Publications by the author arising from this work	

## LIST OF FIGURES

	Page
<b>CHAPTER ONE</b>	
1. PLUTO plot of $W\{\overline{C=CPhC(CF_3)_2C(CN)_2}\}(CO)_3(\eta-C_5H_5)$ (13)	16
2. PLUTO plot of $Mn\{\overline{C=CPhC(CF_3)_2C(CN)_2}\}(CO)_3(dppe)$ (14)	17
3. PLUTO plot of $Fe\{\overline{C=CPhC(CF_3)_2C(CN)_2}\}(CO)_2(\eta-C_5H_5)$ (15)	18
4. PLUTO plot of $Ru\{\overline{C=CPhC(CF_3)_2C(CN)_2}\}(CO)(PPh_3)(\eta-C_5H_5)$ (19)	19
5. PLUTO plot of $Ru\{C=C(CN)_2\}CPh=C(CF_3)_2\}(CO)(PPh_3)(\eta-C_5H_5)$ (22)	26
6. PLUTO plot of $Ru\{\eta^3-C(CF_3)_2CPhC=C(CN)_2\}(PPh_3)(\eta-C_5H_5)$ (25)	30
7. PLUTO plot of $W\{\overline{NH=C(OH)C(CN)=CCPh=C(CF_3)_2}\}(CO)_2(\eta-C_5H_5)$ (27)	33
8. PLUTO plot of $Ru\{\overline{C=CPhC(CF_3)_2C(CN)_2}\}(NCMe)(PPh_3)(\eta-C_5H_5)$ (29)	39
9. PLUTO plot of $\{Ru[\overline{C=CPhC(CF_3)_2C(CN)_2}](PPh_3)(\eta-C_5H_5)\}_2-$ $\{\mu-(NC)_2C=C(CF_3)_2\}$ (40a)	41
10. Alternative isomeric possibilities for complexes (39a), (39b) and (39c)	43
11. Cyclic voltammogram of complex (40a) ( $200\text{ mV s}^{-1}$ ) in $CH_2Cl_2$	51
<b>CHAPTER TWO</b>	
1. Conrotatory and disrotatory opening of cyclobutene	92
2. Correlation of orbitals	93
3. State correlation diagrams	93
4. 'Outward' and 'inward' transition structures for conrotatory ring-opening of <i>trans</i> -3,4-dihydroxycyclobutene	95
5. PLUTO plot of $Ru\{\overline{C=CPhCH(CO_2Me)C(CO_2Me)(CN)}\}(CO)(PPh_3)-$ $(\eta-C_5H_5)$ (5a)	100
6. PLUTO plot of $Ru\{\overline{C=CPhCH(CO_2Me)C(CO_2Me)(CN)}\}(CO)(PPh_3)-$ $(\eta-C_5H_5)$ (5b)	101

## LIST OF FIGURES (cont.)

	Page
7. PLUTO plot of Ru{C[=C(CO <sub>2</sub> Me)(CN)]CPh=CH(CO <sub>2</sub> Me)}(CO)(PPh <sub>3</sub> )- (η-C <sub>5</sub> H <sub>5</sub> ) (6)	107
8. PLUTO plot of Ru{η <sup>3</sup> -CH(CO <sub>2</sub> Me)CPhC=C(CO <sub>2</sub> Me)(CN)}(CO)(η-C <sub>5</sub> H <sub>5</sub> ) (7)	111
9. PLUTO plot of Fe{C[=C(CN <sub>2</sub> )]CPh=C(CN <sub>2</sub> )}(CO) <sub>2</sub> (η-C <sub>5</sub> H <sub>5</sub> ) (12)	116
10. <sup>13</sup> C NMR spectrum of (14), cyclobutenyl ring carbon resonances, showing various <i>J</i> <sub>F-C</sub> couplings (Hz)	122
11. PLUTO plot of Fe( $\overline{\text{C}=\text{CFCF}_2\text{CF}_2}$ )(CO) <sub>2</sub> (η-C <sub>5</sub> H <sub>5</sub> ) (14)	124
12. PLUTO plots of the two independent molecules of Fe( $\overline{\text{C}=\text{CFCF}_2\text{CF}_2}$ )- (CO)(PPh <sub>3</sub> )(η-C <sub>5</sub> H <sub>5</sub> ) (16)	125

## CHAPTER THREE

1. Molecular structure of (1)	162
2. Cyclic voltammogram of (1) (200 mV s <sup>-1</sup> ) in CH <sub>2</sub> Cl <sub>2</sub>	163
3. PLUTO plot of Ru <sub>4</sub> (μ <sub>4</sub> -PPh){μ <sub>4</sub> -η <sup>2</sup> , <i>P</i> -PhC <sub>2</sub> PPh <sub>2</sub> }(μ-CO) <sub>2</sub> (CO) <sub>8</sub> .MeOH (5)	165
4. PLUTO plot of Ru <sub>5</sub> (μ <sub>4</sub> -PPh){μ <sub>3</sub> -η <sup>2</sup> , <i>P</i> -CCPh(PPh <sub>2</sub> )}(CO) <sub>12</sub> (26)	168
5. PLUTO plot of Ru <sub>5</sub> (μ-H)(μ <sub>4</sub> -PPh){μ <sub>4</sub> -η <sup>4</sup> -CCPh(C <sub>6</sub> H <sub>4</sub> )}(μ <sub>3</sub> -PPh)(CO) <sub>10</sub> (27)	170
6. JACKAL space filling plot of (27)	177
7. PLUTO plot of Ru <sub>5</sub> (μ <sub>4</sub> -PPh){μ <sub>4</sub> -η <sup>4</sup> -CCPh(C <sub>6</sub> H <sub>4</sub> )}(μ-PPh(OMe))(CO) <sub>11</sub> . 2MeOH.H <sub>2</sub> O (28)	178
8. PLUTO plot of Ru <sub>5</sub> (μ <sub>5</sub> -η <sup>2</sup> , <i>P</i> -C <sub>2</sub> PPh <sub>2</sub> )(μ-PPh <sub>2</sub> )(CO) <sub>12</sub> {P(OEt) <sub>3</sub> } (29a)	183
9. PLUTO plot of Ru <sub>5</sub> (μ <sub>5</sub> -η <sup>2</sup> , <i>P</i> -C <sub>2</sub> PPh <sub>2</sub> )(μ-PPh <sub>2</sub> )(CO) <sub>12</sub> {P(OEt) <sub>3</sub> } (29c)	184
10. PLUTO plot of Ru <sub>5</sub> (μ <sub>5</sub> -η <sup>2</sup> , <i>P</i> -C <sub>2</sub> PPh <sub>2</sub> )(μ-PPh <sub>2</sub> )(CO) <sub>11</sub> {P(OEt) <sub>3</sub> } <sub>2</sub> (30)	185
11. PLUTO plot of Ru <sub>5</sub> (μ <sub>4</sub> -PPh)(μ <sub>3</sub> -η <sup>2</sup> -PhC <sub>2</sub> Ph)(μ-PPh <sub>2</sub> ) <sub>2</sub> (CO) <sub>10</sub> .CH <sub>2</sub> Cl <sub>2</sub> (33)	194
12. Possible structures for complexes (39) and (40)	201

## LIST OF FIGURES (cont.)

	Page
13. PLUTO plot of $\text{Au}_2\text{Ru}_5(\mu_5\text{-}\eta^2, P\text{-C}_2\text{PPh}_2)(\mu\text{-PPh}_2)(\text{CO})_{11}(\text{PPh}_3)_2\text{-}$ $\{\text{P}(\text{OEt})_3\}$ (41)	202
14. PLUTO plot of $\text{Ru}_5(\mu\text{-H})(\mu_5\text{-}\eta^2, P\text{-C}_2\text{PPh}_2)(\mu\text{-PPh}_2)(\mu\text{-Br})(\text{CO})_{13}$ (43)	207
15. PLUTO plot of $\text{Ru}_5(\mu\text{-H})(\mu_5\text{-}\eta^2, P\text{-C}_2\text{PPh}_2)(\mu_3\text{-I})(\mu\text{-PPh}_2)(\text{CO})_{12}$ (44)	208
16. PLUTO plot of $\text{Ru}_5\{\mu_4\text{-}\eta^4, O\text{-C}_2\text{C}(\text{O})\text{C}_3\text{H}_5\}(\mu\text{-PPh}_2)_2(\mu\text{-Br})(\text{CO})_{11}$ (47o)	216
17. PLUTO plot of $\text{Ru}_4\{\mu_4\text{-}\eta^2, P, O\text{-C}_5\text{H}_4\text{O}(\text{PPh}_2)\}(\mu\text{-PPh}_2)(\text{CO})_{11}$ (49)	222
18. PLUTO plot of $\text{Ru}_5(\mu_4\text{-PPh})\{\mu_3\text{-}\eta^3\text{-CC}(\text{C}_2\text{H}_2)(\text{C}_2\text{H}_3)\}(\mu\text{-PPh}_2)(\text{CO})_{12}\cdot$ $\text{CH}_2\text{Cl}_2\cdot\text{MeOH}$ (50b)	224
19. PLUTO plot of $\text{Ru}_5(\mu_4\text{-PPh})(\mu\text{-PPh}_2)(\mu\text{-CO})(\text{CO})_{10}\{\eta^5\text{-C}_5\text{H}_3(\text{C}_2\text{H}_3)\text{Me}\}\cdot$ $\text{C}_6\text{H}_{14}$ (52)	226

## LIST OF TABLES

	Page
<b>CHAPTER ONE</b>	
1. Cyclobutenyl, butadienyl and allyl complexes derived from dcfe	13
2. Selected bond distances (Å) and angles (°) for the cyclobutenyl complexes (13), (14), (15), (19), (29)	20
3. Selected bond distances (Å) and angles (°) for complexes (12) and (22)	27
4. Selected bond distances (Å) and angles (°) for complex (25)	31
5. Selected bond distances (Å) and angles (°) for complex (27)	34
6. Nitrile-substituted cyclobutenyl complexes	36
7. Selected bond distances (Å) and angles (°) for complex (40a)	42
8. Analytical data for the nitrile complexes	75
9. FAB MS data for the nitrile complexes	76
10. Infrared data for the nitrile complexes	79
11. <sup>1</sup> H and <sup>19</sup> F NMR data for the nitrile complexes	82
12. UV/Visible data for the nitrile complexes	84
13. Electrochemical data for the nitrile complexes	85
14. Electrochemical and UV/Visible data for the nitrile ligands	87
<b>CHAPTER TWO</b>	
1. Selected bond distances (Å) and angles (°) for complexes (5a), (5b), (6) and (7)	102
2. Structural parameters for tetracyanobutadienyl ligands in four metal complexes	117
3. Selected bond distances (Å) and angles (°) for complexes (14) and (16)	126

## LIST OF TABLES (cont.)

	Page
<b>CHAPTER THREE</b>	
1. Crystallographically characterized pentaruthenium clusters	147
2. Selected bond distances (Å) and angles (°) for (26)	169
3. Selected bond distances (Å) and angles (°) for (27)	171
4. Selected bond distances (Å) and angles (°) for (28)	179
5. Selected bond distances (Å) and angles (°) for complexes (29a), (29c), and (30)	186
6. Selected bond distances (Å) and angles (°) for complex (33)	195
7. Selected bond distances (Å) and angles (°) for complex (41)	203
8. Selected bond distances (Å) and angles (°) for complexes (43) and (44)	209
9. Selected bond distances (Å) and angles (°) for complex (47o)	217
10. Selected bond distances (Å) and angles (°) for complex (49)	223
11. Selected bond distances (Å) and angles (°) for complex (50b)	225
12. Selected bond distances (Å) and angles (°) for complex (52)	227
13. $^{31}\text{P}\{^1\text{H}\}$ NMR data for some $\text{Ru}_4$ , $\text{Ru}_5$ and $\text{Au}_2\text{Ru}_5$ clusters	236

## LIST OF SCHEMES

	Page
<b>CHAPTER ONE</b>	
1. Reactions of <i>tcne</i> with transition-metal acetylides	7
2. Reactions of <i>dcfe</i> with transition-metal $\sigma$ -acetylides	22
3. Formation of (27) from (13)	35
<b>CHAPTER TWO</b>	
1. Interconversion of isomers (5a), (5b) and (5c)	103
2. Ring-opening transformations involving (5a) and (5b)	108
3. Conversion of (6) to (7)	112
4. Summary of cycloaddition reactions involving <i>tcne</i>	113
<b>CHAPTER THREE</b>	
1. Core transformations for pentaruthenium clusters	146
2. Reactivity patterns for (1)	152
3. Reactivity patterns for (2)	154
4. Syntheses of (1) and (5) from (4)	166
5. Formation of (26) and (27) from (1)	173
6. Reaction of (27) with MeOH to form (28)	177
7. Reaction of (1) with P(OEt) <sub>3</sub>	188
8. Reactions of (1) with PPh <sub>3</sub> and P( <i>p</i> -tolyl) <sub>3</sub>	197
9. Reactions of (1) with allyl halides	215
10. Reaction of (1) with ethene	232
11. Reactivity pathways established for (1)	240

## ABBREVIATIONS

*In General*

Anal.	Analysis
AR	Analytical Reagent
Calcd	Calculated
cod	1,5-cyclooctadiene
cp	cyclopentadienyl
Cy	Cyclohexyl
dcfe	1,1-dicyano-2,2-bis(trifluoromethyl)ethene
dme	1,2-dimethoxyethane
dpam	bis(diphenylarsino)arsine methane
dpp	2,3-bis(2-pyridyl)pyrazine
dppa	1,2-bis(diphenylphosphino)ethyne
dppb	1,4-bis(diphenylphosphino)butane
(dppa*)	ligand combination derived from dppa
dppe	1,2-bis(diphenylphosphino)ethane
dpph	$\alpha,\alpha'$ -diphenyl- $\beta$ -picrylhydrazyl
dppm	bis(diphenylphosphino)methane
ESR	Electron Spin Resonance
ETC	Electron Transfer Catalysis
$\Delta H_{pp}$	linewidth (peak to peak)
HP	High Pressure
HV	High Vacuum
LP	Low Pressure
LR	Laboratory Reagent
M	Molar

## ABBREVIATIONS (cont.)

m.p.	melting point
MP	Medium Pressure
$M_r$	relative molecular weight
Na/BPK	sodium benzophenone ketyl solution
phen	1,10-phenanthroline
ppn	bis(triphenylphosphine)iminium
resp.	respectively
$R_f$	Retardation factor (TLC)
rjo	<i>trans</i> -CH(CO <sub>2</sub> Me)=C(CN)(CO <sub>2</sub> Me)
r.t.	room temperature
SEP	Skeletal Electron Pair
tcnq	tetracyanoquinodimethane
tcne	tetracyanoethene
thf	tetrahydrofuran
TLC	Thin Layer Chromatography

*For Infrared Spectroscopy (IR)*

br	broad
m	medium
s	strong
(sh)	shoulder
vs	very strong
vw	very weak
w	weak

*For X-Ray Crystallography*

$D_c$	Density calculated
-------	--------------------

## ABBREVIATIONS (cont.)

$D_m$	Density measured
esd	estimated standard deviation
$F$	structure factor(s)
$F_o$	observed structure factor(s)
$F_c$	calculated structure factor(s)
$R_{\text{amal}}$	agreement index for amalgamation of observed reflections

*For Mass Spectrometry (MS)*

EI MS	Electron Impact Mass Spectra
FAB MS	Fast Atom Bombardment Mass Spectra
$[M]^+$	molecular ion
R.I.	Relative Intensity

*For Nuclear Magnetic Resonance Spectroscopy (NMR)*

$\delta$	chemical shift (ppm)
d	doublet
dd	doublet of doublets
dm	doublet of multiplets
dt	doublet of triplets
m	multiplet
s	singlet
t	triplet
p	pentuplet
q	quadruplet

## ABBREVIATIONS (cont.)

### *For Electronic Absorption Spectroscopy (UV/Visible)*

$\lambda$	wavelength (nm)
$\epsilon$	extinction coefficient ( $M^{-1} \text{ cm}^{-1}$ )

### *For Electrochemistry*

const.	constant
CV	Cyclic Voltammetry
decr.	decrease
$\Delta E_v$	peak separation at scan rate $v$
$n_{\text{meas}}$	number of electrons - measured against $\text{Fe}(\text{cp})_2$
$i_p$	peak current ( $\mu\text{A}$ )
$i_{pa}$	anodic peak current ( $\mu\text{A}$ )
$i_{pc}$	cathodic peak current ( $\mu\text{A}$ )
$n_{\text{rel}}$	relative number of electrons transferred
Irrev.	Irreversible process
mV	millivolt(s)
N-Rev.	Near Reversible process
ox	oxidation process
Q-Rev.	Quasi-Reversible process
red	reduction process
Rev.	Reversible process
SCE	Saturated Calomel Electrode
SW	Square Wave
$v$	scan rate ( $\text{mV s}^{-1}$ )

## NUMBERING OF COMPLEXES

The numbering of complexes applies only to the chapter being discussed in the text as each chapter is self-contained.

**STATEMENT**

This thesis contains no material which has been accepted for the award of any other degree or diploma in any University and, to the best of my knowledge and belief, contains no material previously published or written by another person except where due reference is made in the text. The author consents to the thesis being made available for photocopying and loan if accepted for the award of the degree.

**M.J. LIDDELL**

15/6/89

## ACKNOWLEDGEMENTS

I would like to thank my supervisor, Professor M.I. Bruce, for providing enthusiasm and guidance in this research project. Special thanks go to Dr. E.R.T. Tiekink for his expertise with the X-ray crystal studies and for plotting all the structural diagrams. I am also indebted to Drs. D.N. Duffy, B.K. Nicholson, B.W. Skelton and Professor A.H. White for their contributions to the X-ray crystallographic work. My appreciation is extended to the various people who assisted me during my experimental work, in particular George and Paul. For helping me to use the ZAB-2HF and CXP-300 spectrometers effectively I would like to thank Mr. T. Blumenthal and Mrs. A.M. Hounslow, respectively.

## SUMMARY

During the past decade a great deal of research has been directed towards understanding the reactivity of alkynes when coordinated to transition metals. This interest is due, in part, to the use of transition metal catalysts in industrial processes and also to the variety of reaction mechanisms which may occur on metal substrates. Organic chemistry now makes use of a wide variety of transition metal reagents and catalysts to alter product distributions and/or change reaction pathways. Elucidation of the chemistry operating in these systems, or models of them, is therefore of much importance. This thesis deals with various aspects of the acetylene chemistry of mono- or multi-nuclear complexes.

The first chapter discusses the cycloaddition reactions of 1,1-dicyano-2,2-bis(trifluoromethyl)ethene with transition metal  $\sigma$ -acetylides. Initially, cyclobutenyl complexes are formed. Thermolysis of these compounds results in ring cleavage to form the isomeric butadienyl derivatives which may react further (thermally or photochemically) to form allyl complexes, if the metal possesses a labile ligand. Structural studies have been carried out on a number of cyclobutenyl adducts  $[M]\{\overline{C=CPhC(CF_3)_2C(CN)_2}\}$  where  $[M] = Fe(CO)_2(\eta-C_5H_5)$ ,  $W(CO)_3(\eta-C_5H_5)$ ,  $Mn(CO)_3(dppe)$ , and the first complete series of cyclobutenyl, butadienyl and allyl complexes derived from  $Ru(C_2Ph)(CO)(PPh_3)(\eta-C_5H_5)$  has been crystallographically characterized. In conjunction with these structural studies, spectroscopic comparisons have been made that now allow the assignment of structural types from FAB mass spectrometry,  $^{19}F$  NMR and infrared data. Reaction of the tungsten cyclobutenyl complex with  $Me_3NO$  gave a five-membered metallacycle  $\overline{W\{NH=C(OH)C(CN)=CCPh=C(CF_3)_2\}}(CO)_2(\eta-C_5H_5)$  instead of the expected allyl complex. The cycloaddition reaction of  $Ru(C_2Ph)(PPh_3)_2(\eta-C_5H_5)$  with  $(CN)_2C=C(CF_3)_2$  in acetonitrile proceeded to give  $Ru\{\overline{C=CPhC(CF_3)_2C(CN)_2}\}-(NCCH_3)(PPh_3)(\eta-C_5H_5)$ . This compound reacted with the fluoro-olefin to give the diamagnetic deep blue complex  $\{Ru[\overline{C=CPhC(CF_3)_2C(CN)_2}](PPh_3)(\eta-C_5H_5)\}_2\{\mu-(NC)_2C=C(CF_3)_2\}$ . Extending this synthetic strategy has allowed the isolation of a number of nitrile-substituted mononuclear and dinitrile-bridged binuclear complexes. Electrochemical and  $^{19}F$  NMR studies have been used to characterize these rather unstable

compounds, which exist in a number of isomeric forms. The intense colour of several of these complexes, initially attributed to the presence of bridging groups, has been shown to be due to charge transfer absorptions associated with the electron-deficient, unsaturated dinitrile ligands, whether or not they are bridging.

Chapter Two investigates the direction of the ring-opening process in the cyclobutenyl complexes, using the olefin *trans*-1,2-bis(carbomethoxy)-1-cyano-ethene. Addition of this olefin to  $\text{Ru}(\text{C}_2\text{Ph})(\text{CO})(\text{PPh}_3)(\eta\text{-C}_5\text{H}_5)$  gave two isomeric cyclobutenyl derivatives. Thermal ring-opening of each of these isomers gave the same butadienyl product, which was formed by a conrotatory ring-opening, as predicted by the Woodward-Hoffmann rules. Under these conditions an allyl complex was also formed by loss of the triphenylphosphine ligand rather than CO. A solid-state (supported on silica) transformation of the cyclobutenyl isomers to a third cyclobutenyl complex was studied by NMR. Further investigation of the reaction of tetracyanoethene with  $\text{Fe}(\text{C}_2\text{Ph})(\text{CO})_2(\eta\text{-C}_5\text{H}_5)$  has shown that this reaction also proceeds through a cyclobutenyl complex to the structurally-characterized butadienyl complex. Attempts to isomerize the complex  $\text{Fe}(\overline{\text{C}=\text{CFCF}_2}\text{CF}_2)(\text{CO})_2(\eta\text{-C}_5\text{H}_5)$  were unsuccessful, only CO-substitution products being characterized.

Recent developments in the chemistry of pentaruthenium clusters are summarized at the beginning of the third chapter, as an introduction to the chemistry of  $\text{Ru}_5(\mu_5\text{-}\eta^2, P\text{-C}_2\text{PPh}_2)(\mu\text{-PPh}_2)(\text{CO})_{13}$  [Complex (A)]. The synthesis of this complex has been investigated in detail. At temperatures slightly higher than those used in the original synthesis, P-C and C-H bond cleavage reactions gave initially  $\text{Ru}_5(\mu_4\text{-PPh})\{\mu_3\text{-}\eta^2, P\text{-CCPh}(\text{PPh}_2)\}(\text{CO})_{12}^*$  and then  $\text{Ru}_5(\mu\text{-H})(\mu_4\text{-PPh})\{\mu_4\text{-}\eta^4\text{-CCPh}(\text{C}_6\text{H}_4)\}(\mu_3\text{-PPh})(\text{CO})_{10}^*$ . The latter reacted at room temperature with methanol to form  $\text{Ru}_5(\mu_4\text{-PPh})\{\mu_4\text{-}\eta^4\text{-CCPh}(\text{C}_6\text{H}_4)\}\{\mu\text{-PPh}(\text{OMe})\}(\text{CO})_{11}$ , this reaction proceeding through several intermediates. Ligand substitution of complex (A) favoured a hinge site under thermal conditions, whereas wing-tip sites were favoured under

---

\* molecular structure determined by other workers

Me<sub>3</sub>NO promotion. Cleavage of P-C bonds and phenyl migration occurred during mild pyrolysis of Ru<sub>5</sub>(μ<sub>5</sub>-C<sub>2</sub>PPh<sub>2</sub>)(μ-PPh<sub>2</sub>)(CO)<sub>12</sub>(PPh<sub>3</sub>) to give Ru<sub>5</sub>(μ<sub>4</sub>-PPh)(μ<sub>3</sub>-η<sup>2</sup>-PhC<sub>2</sub>Ph)(μ-PPh<sub>2</sub>)<sub>2</sub>(CO)<sub>10</sub>\*.

The cluster core geometry of complex (A) remained basically the same upon reduction. This was inferred from the formation of Au<sub>2</sub>Ru<sub>5</sub>(μ<sub>5</sub>-P-C<sub>2</sub>PPh<sub>2</sub>)(μ-PPh<sub>2</sub>)(CO)<sub>12</sub>(PPh<sub>3</sub>)<sub>2</sub> when a reduced solution of (A) was treated with AuCl(PPh<sub>3</sub>). This Au<sub>2</sub>Ru<sub>5</sub> cluster was also formed in high yield by reacting the parent cluster with [(AuPPh<sub>3</sub>)<sub>3</sub>O]BF<sub>4</sub>/[ppn][Co(CO)<sub>4</sub>]. Ligand substitution with P(OEt)<sub>3</sub> gave Au<sub>2</sub>Ru<sub>5</sub>(μ<sub>5</sub>-P-C<sub>2</sub>PPh<sub>2</sub>)(μ-PPh<sub>2</sub>)(CO)<sub>12</sub>(PPh<sub>3</sub>){P(OEt)<sub>3</sub>}, Au<sub>2</sub>Ru<sub>5</sub>(μ<sub>5</sub>-η<sup>2</sup>, P-C<sub>2</sub>PPh<sub>2</sub>)(μ-PPh<sub>2</sub>)(CO)<sub>11</sub>(PPh<sub>3</sub>)<sub>2</sub>{P(OEt)<sub>3</sub>}\* and Au<sub>2</sub>Ru<sub>5</sub>(μ<sub>5</sub>-P-C<sub>2</sub>PPh<sub>2</sub>)(μ-PPh<sub>2</sub>)(CO)<sub>11</sub>(PPh<sub>3</sub>){P(OEt)<sub>3</sub>}<sub>2</sub>, illustrating the lability of the gold-bound phosphines as well as substitution on the Ru<sub>5</sub> cluster.

Oxidative addition of halo-acids to complex (A) gave clusters with a 'scorpion' geometry. Examples are Ru<sub>5</sub>(μ-H)(μ<sub>5</sub>-η<sup>2</sup>, P-C<sub>2</sub>PPh<sub>2</sub>)(μ-PPh<sub>2</sub>)(μ-Br)(CO)<sub>13</sub>\* (from HBr) and Ru<sub>5</sub>(μ-H)(μ<sub>5</sub>-η<sup>2</sup>, P-C<sub>2</sub>PPh<sub>2</sub>)(μ<sub>3</sub>-I)(μ-PPh<sub>2</sub>)(CO)<sub>12</sub>\* (from HI). The reaction with allyl bromide gave a cluster with a 'spiked square' geometry Ru<sub>5</sub>(μ<sub>4</sub>-η<sup>4</sup>, O-C<sub>2</sub>C(O)C<sub>3</sub>H<sub>5</sub>)(μ-PPh<sub>2</sub>)<sub>2</sub>(μ-Br)(CO)<sub>11</sub>\*. Reaction with HgCl<sub>2</sub> gave two isomers of Ru<sub>6</sub>(C<sub>2</sub>PPh<sub>2</sub>)(μ-PPh<sub>2</sub>)(CO)<sub>11</sub>.

The thermal reaction of ethene or 1-butene with complex (A) gave as primary products two isomers of Ru<sub>5</sub>(μ<sub>4</sub>-PPh){μ<sub>3</sub>-η<sup>3</sup>-CC(C<sub>n</sub>H<sub>2n-2</sub>)(C<sub>n</sub>H<sub>2n-1</sub>)}(μ-PPh<sub>2</sub>)(CO)<sub>12</sub>\* [n = 2 (ethene); n = 4 (1-butene)] under 5-20 atmospheres of the olefin. These isomers interconverted under nitrogen, ethene or butene (no exchange of olefins was observed). From the ethene reaction Ru<sub>4</sub>{μ<sub>4</sub>-η<sup>2</sup>, P,O-C<sub>5</sub>H<sub>4</sub>O(PPh<sub>2</sub>)}(μ-PPh<sub>2</sub>)(CO)<sub>11</sub>\* was also formed. Ambient pressure reaction of ethene with (A) gave a much greater number of products, from which Ru<sub>5</sub>(μ<sub>4</sub>-PPh)(μ-PPh<sub>2</sub>)(μ-CO)(CO)<sub>10</sub>{η<sup>5</sup>-C<sub>5</sub>H<sub>3</sub>(C<sub>2</sub>H<sub>3</sub>)Me}\* was isolated. This product was also formed in the reaction of Ru<sub>5</sub>(μ<sub>4</sub>-PPh){μ<sub>3</sub>-η<sup>3</sup>-CC(C<sub>2</sub>H<sub>2</sub>)(C<sub>2</sub>H<sub>3</sub>)}(μ-PPh<sub>2</sub>)(CO)<sub>12</sub> with ethene at atmospheric pressure.

X-ray crystallography has been essential to this investigation. The molecular structures of all cluster complexes marked with an asterisk have been determined by others and that of

$\text{Ru}_5(\mu_4\text{-PPh})\{\mu_4\text{-}\eta^4\text{-CCPh(C}_6\text{H}_4)\}\{\mu\text{-PPh(OMe)}\}(\text{CO})_{11}$  by the author. Finally, the many structural types of phosphorus ligands found in this and previous work have been correlated with  $^{31}\text{P}$  NMR data, allowing more or less ready identification of some of the non-crystallographically characterized products.



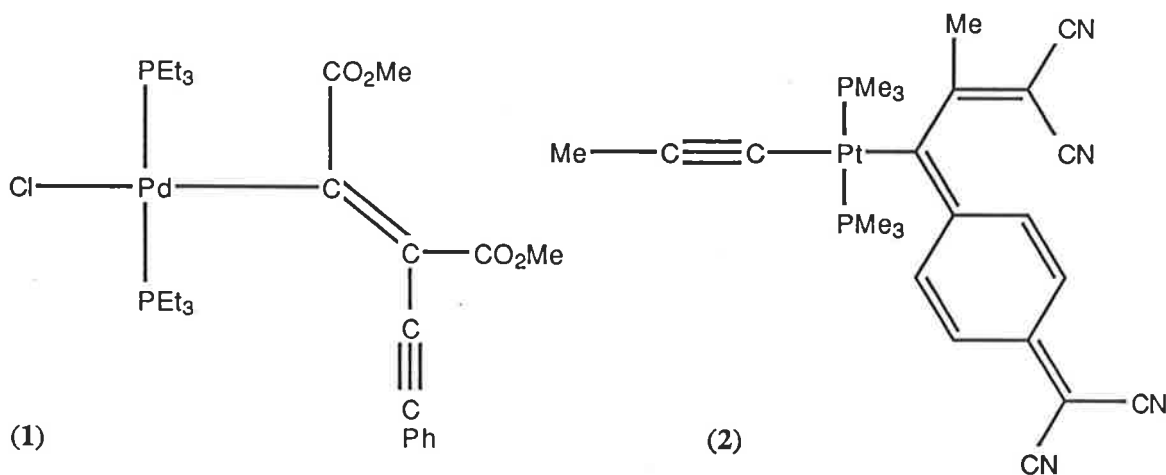
## CHAPTER ONE

### Cycloaddition reactions of 1,1-dicyano-2,2-bis(trifluoromethyl)-ethene with transition-metal acetylides

	Page
1.1. Introduction	6
1.2. Results and Discussion	12
1.3. Conclusions	53
1.4. Experimental	54
1.5. References	88

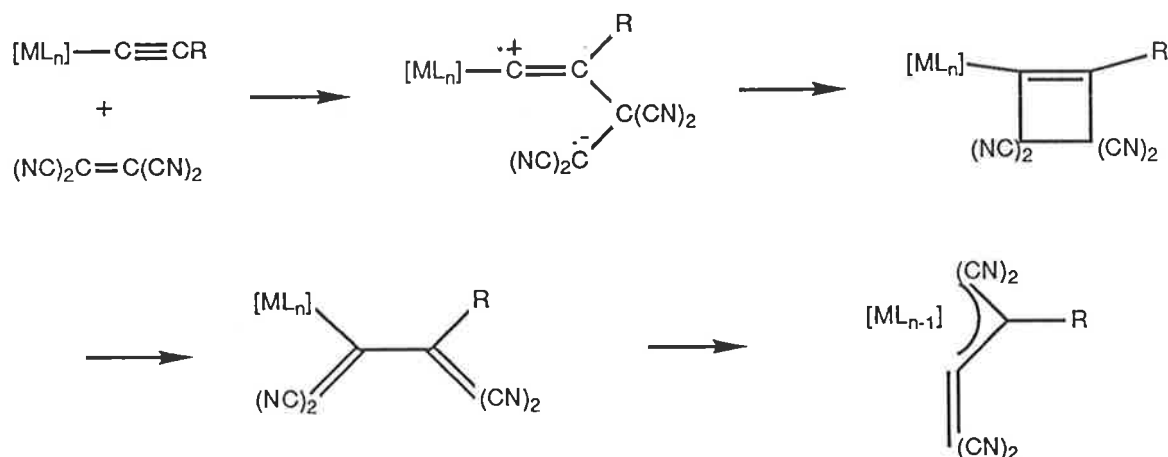
## 1.1. Introduction

Molecular orbital studies of transition-metal  $\sigma$ -acetylide complexes have indicated that the HOMO is localized (10 - 30%) on the  $\beta$ -carbon atom.<sup>1</sup> As expected, the addition of electrophilic reagents such as  $H^+$ ,  $Cl^+$  and  $N_2Ar^+$  to this carbon results in the formation of vinylidene complexes.<sup>2</sup> The addition of other electrophilic reagents, such as electron-deficient olefins and alkynes, has been shown to give cycloaddition and insertion complexes, both of which have been isolated from platinum and palladium acetylide systems.<sup>3</sup> For example, the reactions between tetracyanoethene (tcne) and *trans*-Pt(C<sub>2</sub>H)<sub>2</sub>(PMe<sub>2</sub>Ph)<sub>2</sub> or *trans*-Pt(C<sub>2</sub>Me)<sub>2</sub>(AsMe<sub>3</sub>)<sub>2</sub> afforded the complexes *trans*-Pt{C(CN)<sub>2</sub>C(CN)<sub>2</sub>C<sub>2</sub>H}(C<sub>2</sub>H)(PMe<sub>2</sub>Ph)<sub>2</sub> and *trans*-Pt{C(CN)<sub>2</sub>C(CN)<sub>2</sub>C<sub>2</sub>Me}(C<sub>2</sub>Me)(AsMe<sub>3</sub>)<sub>2</sub>, respectively. Similarly, the addition of dimethyl acetylenedicarboxylate to *trans*-PdCl(C<sub>2</sub>Ph)(PEt<sub>3</sub>)<sub>2</sub> gave an insertion product *trans*-PdCl{C(CO<sub>2</sub>Me)=C(CO<sub>2</sub>Me)C<sub>2</sub>Ph}(PEt<sub>3</sub>)<sub>2</sub> (1).<sup>4</sup> The reaction of *trans*-Pt(C<sub>2</sub>Me)<sub>2</sub>(PMe<sub>3</sub>)<sub>2</sub> with tetracyanoquinodimethane has also been described, and the butadienyl product (2) subsequently identified by X-ray structural analysis.<sup>5</sup>



The addition of tetracyanoethene to various transition-metal  $\sigma$ -acetylide substrates has been thoroughly investigated.<sup>6-10</sup> Tetracyanoethene is a well known (2 + 2) cycloaddition reagent in organic reactions with olefins,<sup>11</sup> but not with alkynes. Therefore, the transition-metal-assisted reactions are of considerable interest. The established reactivity patterns of tcne with  $\sigma$ -acetylide complexes are shown in Scheme 1.

**Scheme 1.** Reactions of tcne with transition-metal acetylides



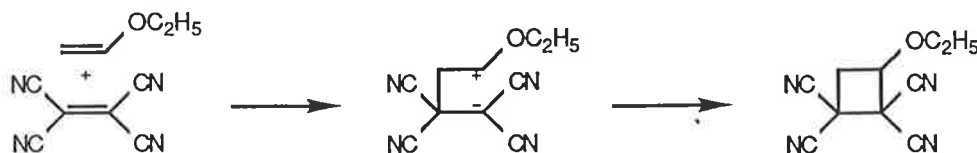
$[ML_n] = Ru(PPh_3)_2(\eta-C_5H_5)$ ;  $Ru(CO)(PPh_3)(\eta-C_5H_5)$ ,  $Ru(PPh_3)[P(OMe)_3](\eta-C_5H_5)$ ,

$Ru[P(OMe)_3]_2(\eta-C_5H_5)$ ,  $Ru(dppe)(\eta-C_5H_5)$ ,  $Ru(CNBU^t)(PPh_3)(\eta-C_5H_5)$ ,  $Ru(CNBU^t)_2(\eta-C_5H_5)$ ,

$W(CO)_3(\eta-C_5H_5)$ ,  $Fe(CO)_2(\eta-C_5H_5)$ ,  $Ni(PPh_3)(\eta-C_5H_5)$ ;  $[ML_{n-1}] = Ru(PPh_3)(\eta-C_5H_5)$ ,  $W(CO)_2(\eta-C_5H_5)$ ;

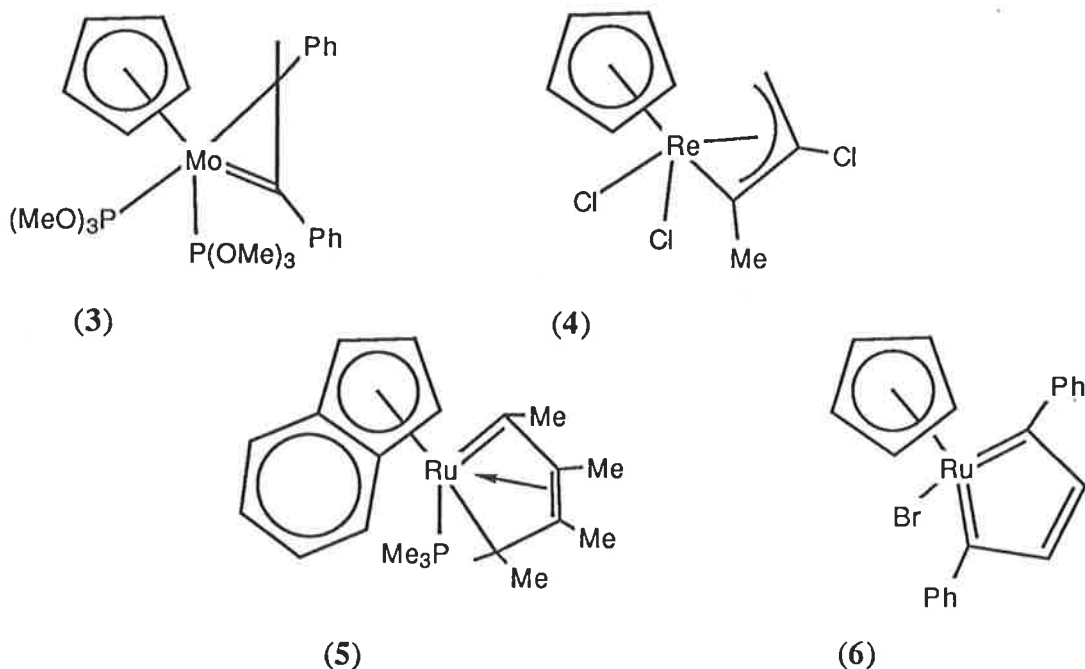
$R = Ph, Me$  (Not all combinations).

The tcne cycloaddition reactions were found to proceed through highly-coloured ESR-active intermediates to give, initially,  $\sigma$ -cyclobutenyl complexes, which isomerized in solution to form the related  $\sigma$ -buta-1,3-dien-2-yl derivatives. Where the metal centre possessed a labile ligand, the butadienyl derivatives transformed readily into  $\eta^3$ -allylic complexes; treatment of these allylic compounds with other ligands (e.g. CO, CNBu<sup>t</sup>) resulted in the reformation of the butadienyl ligand. The nature of the first-formed radical species has not been fully established, but it appears to be the dipolar biradical species shown in Scheme 1. The cycloaddition reactions of polar electron-deficient olefins with electron-rich olefins, which have been shown to proceed through tetramethylene zwitterionic intermediates,<sup>12</sup> support this view. An example is the reaction between tcne with ethoxyethene:



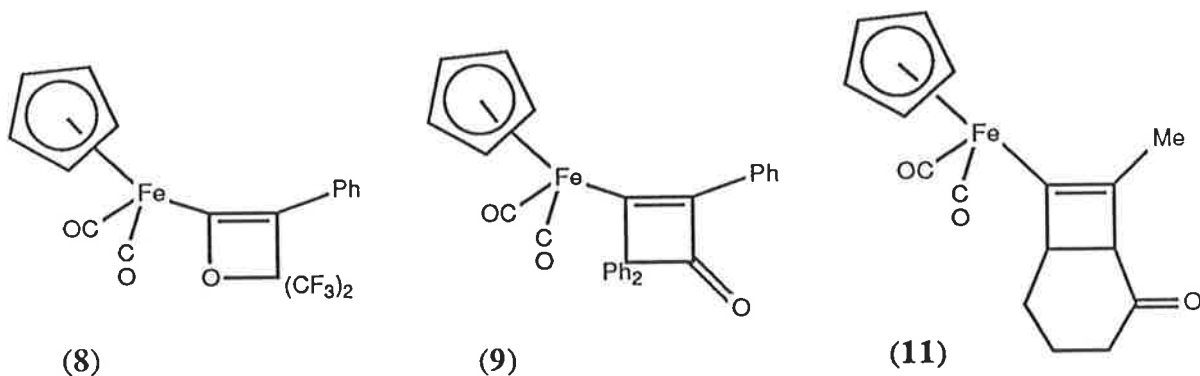
With radical-stabilizing substituents on the olefins, biradical tetramethylenes have been proposed as intermediates in these organic reactions.<sup>13</sup> The related reactions of tcne with metal propargyl (2-alkynyl) complexes proceeded via the initial formation of a non-radical dipolar intermediate to give formal (3 + 2) cycloaddition products.<sup>14</sup>

Examples of each of the three  $\sigma$ -acetylide/tcne derivatives (cyclobutenyl, butadienyl, allyl) have been crystallographically characterized.<sup>6,7,15</sup> The structural results, in conjunction with <sup>13</sup>C NMR studies, have shown that the  $\alpha$ -carbon of the butadienyl and allyl derivatives is highly electron-deficient, and indicate a significant M=C contribution in the bonding of these systems. Recently, many examples of M=C(*sp*<sup>2</sup>) multiple bonds between second and third row transition-metals have been reported and examples containing  $\eta^2(3e)$ -vinyl,<sup>16-18</sup>  $\eta^3(4e)$ -allylidene,<sup>19</sup>  $\eta^4(5e)$ -butadienyl,<sup>20</sup> and butenediyl ligands<sup>21,22</sup> are known. Some examples are complexes (3),<sup>16</sup> (4),<sup>19</sup> (5)<sup>20</sup> and (6).<sup>21</sup> The butenediyl complexes may be regarded as metallacyclopentatriene systems, the degree of planarity of which depends critically on the *d* electron count.<sup>22,23</sup> A related nitrogen-containing metallacycle has also been described.<sup>24</sup>



The reaction of  $\text{CuC}_2\text{Ph}$  with tcne gave an organic product, phenylethynyltricyanoethene, implying that a cycloaddition reaction had not occurred.<sup>25</sup> Oxidative adducts  $\text{Rh}(\text{C}_2\text{R})\text{-}[\eta^2\text{-C}_2(\text{CN})_4]\text{L}(\text{PPh}_3)_2$  ( $\text{L} = \text{MeCN}, \text{CO}$ ;  $\text{R} = \text{Me}, \text{Et}, \text{Ph}$ ) were formed from the reactions of

$\text{Rh}(\text{C}_2\text{R})\text{L}(\text{PPh}_3)_2$  with tcne:<sup>26,27</sup> this seems to indicate that attack by tcne at the vacant metal coordination site is preferred over cycloaddition. Davison and Solar<sup>28</sup> suggested that the reactions of tcne and the acetylide complex  $\text{Fe}(\text{C}_2\text{Ph})(\text{CO})_2(\eta\text{-C}_5\text{H}_5)$  (7) led to the formation of the zwitterionic intermediate  $\text{Fe}[\text{C}^+=\text{CPhC}(\text{CN})_2\text{C}^-(\text{CN})_2](\text{CO})_2(\eta\text{-C}_5\text{H}_5)$  and the cycloadduct  $\text{Fe}\{\overline{\text{C}=\text{CPh}(\text{CN})_2\text{C}(\text{CN})_2}\}(\text{CO})_2(\eta\text{-C}_5\text{H}_5)$  (N.B: this reaction has been re-investigated in Section 2.2.4). The same workers also reported a (2 + 2) cycloaddition product  $\text{Fe}\{\overline{\text{C}=\text{CPhC}(\text{CF}_3)_2\text{O}}\}(\text{CO})_2(\eta\text{-C}_5\text{H}_5)$  (8) from the reaction of (7) with hexafluoroacetone.<sup>28</sup> Reaction of diphenylketene with (7) gave a cyclobut-1-en-3-onyl derivative  $\text{Fe}\{\overline{\text{C}=\text{CPhC}(\text{O})\text{CPh}_2}\}(\text{CO})_2(\eta\text{-C}_5\text{H}_5)$  (9).<sup>28</sup>



A related (2 + 2) cycloadduct was obtained using  $\text{Ni}(\text{C}_2\text{H})(\text{PPh}_3)(\eta\text{-C}_5\text{H}_5)$  (10).<sup>29</sup> In contrast, the reaction of (10) with aryl isocyanates gave linear adducts  $\text{Ni}(\text{C}_2\text{CCONHR})(\text{PPh}_3)(\eta\text{-C}_5\text{H}_5)$  (R = Ph, *p*-tolyl), formed by the insertion of isocyanates into the acetylenic CH bond.<sup>30</sup> These reactions may be compared with those observed for the propargyl-metal complexes  $[\text{ML}_n]\text{CH}_2\text{C}_2\text{R}$  ( $[\text{ML}_n] = \text{Fe}(\text{CO})_2(\eta\text{-C}_5\text{H}_5), \text{Mo}(\text{CO})_3(\eta\text{-C}_5\text{H}_5), \text{W}(\text{CO})_3(\eta\text{-C}_5\text{H}_5), \text{Mn}(\text{CO})_5; \text{R} = \text{H}, \text{CH}_3, \text{Ph})$ ), where cycloaddition reactions with *p*- $\text{CH}_3\text{C}_6\text{H}_4\text{S}(\text{O})_2\text{NCO}$  gave a series of (3 + 2) cycloadducts.<sup>31</sup> In the presence of  $\text{AlBr}_3$ , totally regioselective cycloaddition took place between  $\text{Fe}(\text{C}_2\text{Me})(\text{CO})_2(\eta\text{-C}_5\text{H}_5)$  and cyclohexanone to give (11), a reaction that has much potential for useful development.<sup>32</sup>

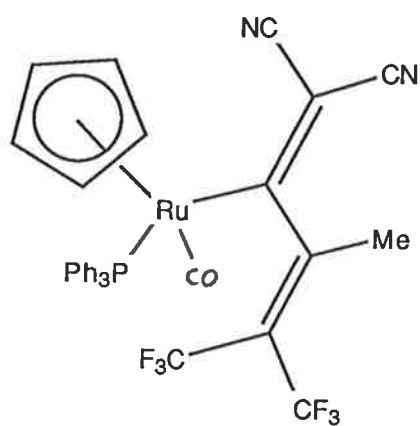
Cycloaddition reactions have also been found to occur with vinylidene complexes. In contrast to the acetylide reactions, these proceed by addition to the  $\alpha$ -carbon. For instance,

(7) reacted with  $[\text{Fe}(\text{C}=\text{CHPh})(\text{CO})_2(\eta\text{-C}_5\text{H}_5)]^+$  to give  $[\text{Fe}\{\overline{\text{C}=\text{CPhC}[\text{Fe}(\text{CO})_2(\eta\text{-C}_5\text{H}_5)]\text{CHPh}}\}(\text{CO})_2(\eta\text{-C}_5\text{H}_5)]^+$ .<sup>33</sup> The rhodium complex  $[\text{Rh}(\text{C}=\text{CHPh})(\text{PPr}^i_3)(\eta\text{-C}_5\text{H}_5)]$  reacted readily with the arylazide  $\text{N}_3\text{C}_6\text{H}_4\text{-}o\text{-NO}_2$  to form the aziridinyl-metal derivative  $\text{Rh}\{\overline{\text{C}[\text{C}=\text{CHPh}]\text{N}(\text{C}_6\text{H}_4\text{-}o\text{-NO}_2)}\}(\text{PPr}^i_3)(\eta\text{-C}_5\text{H}_5)$ ,<sup>34</sup> and with benzoyl azide to form  $(\eta\text{-C}_5\text{H}_5)\text{Rh}\{\overline{\text{C}[\text{C}=\text{CHPh}]\text{N}=\text{C}(\text{Ph})\text{O}}\}(\text{PPr}^i_3)$ , the latter containing a five-membered ring.<sup>35</sup> Addition of oxygen to the olefinic bond of  $[\text{Ru}(\text{C}=\text{CHPh})(\text{PPh}_3)_2(\eta\text{-C}_5\text{H}_5)]^+$  is thought to proceed via a (2 + 2) cycloaddition, followed by ring cleavage, to give  $[\text{Ru}(\text{CO})(\text{PPh}_3)_2(\eta\text{-C}_5\text{H}_5)]^+$  and benzaldehyde.<sup>36</sup>

The (2 + 2) cycloaddition reactions of olefins with  $\sigma$ -acetylide complexes are limited, at present, to those involving the more electrophilic olefins. For example, the reactions of  $\text{Ru}(\text{C}_2\text{Ph})(\text{PPh}_3)_2(\eta\text{-C}_5\text{H}_5)$  with 4-XC<sub>6</sub>H<sub>4</sub>CH=C(CN)<sub>2</sub> gave the respective Ru( $\eta^3$ -allyl)-(PPh<sub>3</sub>)( $\eta\text{-C}_5\text{H}_5$ ) complexes in yields of 78% (X = Ph) and 14% (X = H), but when X = NMe<sub>2</sub>, no reaction was observed.<sup>37</sup> A recent review by Schore,<sup>38</sup> describing the transition-metal-mediated cycloaddition reactions of alkynes in organic synthesis, illustrates the importance of obtaining further information on the nature of the  $\sigma$ -acetylide-based cycloaddition reactions.

This chapter deals with an extension of transition metal  $\sigma$ -acetylide (2 + 2) cycloaddition chemistry using the olefin 1,1-dicyano-2,2-bis(trifluoromethyl)ethene [ $\text{C}(\text{CN})_2=\text{C}(\text{CF}_3)_2$ , dcf<sub>e</sub>]. The first cycloaddition work with this olefin by Green *et al.*<sup>39</sup> demonstrated that 1,3-addition of the olefin to ( $\eta^4$ -triene)irontricarbonyl complexes gave only one isomeric product type, with the CF<sub>3</sub>-substituted carbon being added to C<sup>1</sup> of the triene. The olefin dcf<sub>e</sub> has also been found to be an exceedingly active reagent for 1,4-insertion reactions with various silane, germane and borane reagents.<sup>40</sup> Swincer *et al.*<sup>41</sup> have crystallographically characterized a butadienyl complex  $\text{Ru}\{\text{C}[\text{C}=\text{C}(\text{CN})_2]\text{CMe}=\text{C}(\text{CF}_3)_2\}(\text{CO})(\text{PPh}_3)(\eta\text{-C}_5\text{H}_5)$  (**12**), which was obtained by carbonylating the product formed by reacting dcf<sub>e</sub> with  $\text{Ru}(\text{C}_2\text{Me})(\text{PPh}_3)_2(\eta\text{-C}_5\text{H}_5)$ . The complex  $\{\text{Ru}[\overline{\text{C}=\text{CPhC}(\text{CF}_3)_2\text{C}(\text{CN})_2}]\text{PPh}_3(\eta\text{-C}_5\text{H}_5)\}_2\{\mu\text{-}(\text{NC})_2\text{C}=\text{C}(\text{CF}_3)_2\}$  was obtained by Swincer from the reaction of  $\text{Ru}(\text{C}_2\text{Ph})(\text{PPh}_3)_2(\eta\text{-C}_5\text{H}_5)$  with dcf<sub>e</sub>.<sup>42</sup> This complex had a significant unpaired electron density (0.04 electrons per molecule) which did not

accord with the structure determined by X-ray analysis. We have therefore reinvestigated the synthesis and properties of the binuclear compound in more detail.



(12)

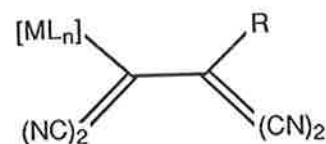
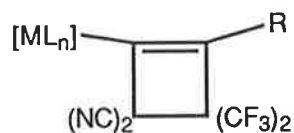
## 1.2. Results and Discussion

### 1.2.1. Cyclobutenyl complexes

The reactions between dcf<sub>e</sub> and various  $\sigma$ -acetylide complexes have given a series of cyclobutenyl complexes [(13) - (19)] (Table 1). Generally, the reaction conditions were chosen to give the cyclobutenyl complexes rather than the butadienyl or allyl derivatives. The cyclobutenyl compounds were formed in good yield by performing the reactions at ambient temperature. Choice of solvent was also important; for complexes (14), (17) and (18), the products precipitated directly from solution [benzene (14); acetonitrile (17), (18)]. Short reaction times were used in the syntheses of (13) (CH<sub>2</sub>Cl<sub>2</sub>) and (15) (diethyl ether), to avoid side reactions. The products obtained were crystalline solids, the stability of individual complexes being dependent on the oxidative stability of the metal centre rather than that of the ring. Ligand substitution was observed in the reaction of Ru(C<sub>2</sub>Ph)(PPh<sub>3</sub>)<sub>2</sub>( $\eta$ -C<sub>5</sub>H<sub>5</sub>) with dcf<sub>e</sub> under a CO atmosphere, where the monocarbonyl (19) was formed as the major product. A range of nitrile-substituted cyclobutenyl derivatives is discussed in Sections 1.2.5 and 1.2.6.

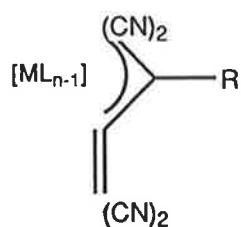
The IR spectra of the cyclobutenyl complexes characteristically show very weak  $\nu$ (CN) bands between 2230 and 2250 cm<sup>-1</sup> and very weak to weak  $\nu$ (C=C) bands between 1550 and 1620 cm<sup>-1</sup>. Strong  $\nu$ (CF) bands were generally found between 1300 and 1100 cm<sup>-1</sup>. A tricarbonyl group was confirmed for (13) by the three-band  $\nu$ (CO) pattern, while for (14), the pattern observed was characteristic of a *fac*-M(CO)<sub>3</sub> group and was similar to that of the phenylethynyl precursor. In the case of (15), a two-band  $\nu$ (CO) pattern confirmed the dicarbonyl formulation, while the single  $\nu$ (CO) band observed for (19) indicated a monocarbonyl complex.

The <sup>1</sup>H NMR spectra of the cycloadducts contained resonances for the cyclopentadienyl ligands [ $\delta$  5.72 (13), 4.95 (15), 4.71 (16), 4.64 (18), 5.02 (19)] and the phenyl [ $\delta$  7.5 - 7.3 (13), 7.32 (15)] or methyl substituents [ $\delta$  0.53 (18)] on the ring, as well as the usual resonances for the phosphine ligands [complexes (14), (16), (18) and (19)].

**Table 1.** Cyclobutenyl, butadienyl and allyl complexes derived from dcfe

Cmpd	[ML <sub>n</sub> ]	R
(13)	W(CO) <sub>3</sub> (η-C <sub>5</sub> H <sub>5</sub> )	Ph
(14)	Mn(CO) <sub>3</sub> (dppe)	Ph
(15)	Fe(CO) <sub>2</sub> (η-C <sub>5</sub> H <sub>5</sub> )	Ph
(16)	Ru(dppe)(η-C <sub>5</sub> H <sub>5</sub> )	Ph
(17)	Ru(PPh <sub>3</sub> ) <sub>2</sub> (η-C <sub>5</sub> H <sub>5</sub> )	Ph
(18)	Ru(PPh <sub>3</sub> ) <sub>2</sub> (η-C <sub>5</sub> H <sub>5</sub> )	Me
(19)	Ru(CO)(PPh <sub>3</sub> )(η-C <sub>5</sub> H <sub>5</sub> )	Ph
(20)	Ru(NCMe)(PPh <sub>3</sub> )(η-C <sub>5</sub> H <sub>5</sub> )	Ph

Cmpd	[ML <sub>n</sub> ]	R
(12)	Ru(CO)(PPh <sub>3</sub> )(η-C <sub>5</sub> H <sub>5</sub> )	Me <sup>†</sup>
(20)	W(CO) <sub>3</sub> (η-C <sub>5</sub> H <sub>5</sub> )	Ph
(21)	Ni(PPh <sub>3</sub> )(η-C <sub>5</sub> H <sub>5</sub> )	Ph
(22)	Ru(CO)(PPh <sub>3</sub> )(η-C <sub>5</sub> H <sub>5</sub> )	Ph
(23)	Ru(dppe)(η-C <sub>5</sub> H <sub>5</sub> )	Ph



Cmpd	[ML <sub>n</sub> ]	R
(24)	W(CO) <sub>2</sub> (η-C <sub>5</sub> H <sub>5</sub> )	Ph
(25)	Ru(PPh <sub>3</sub> )(η-C <sub>5</sub> H <sub>5</sub> )	Ph
(26)	Ru(PPh <sub>3</sub> )(η-C <sub>5</sub> H <sub>5</sub> )	Me

†Reference 41

In the cases of (14) and (16), one of the phenyl groups appeared at considerably higher field than is usually observed (*viz.*  $\delta$  7.5 - 6.7), as two triplets and one doublet [ $\delta$  7.00, 6.61, 5.22 (14); 6.95, 6.72, 5.27 (16);  $J_{av} = 7$  Hz]. The butadienyl derivative  $\text{Ru}\{\text{C}[\text{C}(\text{CN})_2]\text{-CPh}=\text{C}(\text{CF}_3)_2\}(\text{dppe})(\eta\text{-C}_5\text{H}_5)$  (see Section 1.2.2), does not show this pattern of resonances, and this suggests that the dppe ligand is restricting the orientation of the phenyl substituent on the cyclobutenyl ring. This restricting effect of the dppe ligand is also seen in the crystal structure of (14). The phenyl substituent on the ring is presumably deshielded by ring current interactions with the phenyl groups of the phosphine ligand. Molecular modelling of both compounds has shown that the phenyl group on the ring is constrained in a gap between the  $\text{CH}_2$  and  $\text{PPh}_2$  groups, and that it is possible for phenyl groups on the dppe ligand and the ring to become approximately coplanar.

Characteristic  $^{19}\text{F}$  NMR resonances were observed for the cyclobutenyl products between  $\delta$  -65.5 and  $\delta$  -66.5, which is about 4 ppm upfield from that of the free olefin ( $\delta$  -61.8). For most of the complexes examined, a single resonance (singlet) was observed [ $\delta$  -66.3 (13); -65.2 (16); -66.3 (18)] indicating that the  $\text{CF}_3$  groups are equivalent. For complex (19), two quartets were found at  $\delta$  -66.0 and -66.4, showing that the  $\text{CF}_3$  groups are inequivalent. The inequivalence of the  $\text{CF}_3$  groups is due to the chirality at the metal centre and is also observed in the nitrile-substituted cyclobutenyl compounds (see Section 1.2.5).  $^{13}\text{C}$  NMR studies were performed on (16) and (19) only. Resonances were observed for  $\text{C}_\alpha$  [ $\delta$  178.6 (multiplet), 172.7 (doublet), resp.], phenyl groups [ $\delta$  147.2 - 128.4, 136.2 - 126.7, resp.], CN [ $\delta$  115.6, 114.8 (doublet), 113.4 (doublet), resp.] and cyclopentadienyl groups [ $\delta$  85.4, 87.3, resp.]. A carbonyl resonance was observed at  $\delta$  219.6 for (19) and the  $\text{CH}_2$  resonance for (16) was a triplet ( $J_{\text{P-C}} = 22$  Hz) at  $\delta$  29.2.

Fast atom bombardment (FAB) mass spectrometry has proven valuable in the characterization of thermally-sensitive, involatile or ionic organometallic complexes.<sup>43</sup> The fragmentation processes observed are generally the same as those obtained by electron impact ionization. For the cycloadducts, the softer ionization of FAB does permit the observation of processes which are not apparent in their EI mass spectra. Thus, in the case of the

cyclobutenyl complexes, the loss of dcfe from the parent ion (or a carbonyl-free ion) is a characteristic fragmentation, which is essentially the reverse of the synthetic procedure. This route is not found in the isomeric butadienyl complexes, since the C=C double bond originally present in the olefin has been cleaved in these derivatives. As the conversion from the cyclobutenyl to butadienyl isomers occurs upon thermal activation, the EI method of ionization is clearly not suitable for distinguishing between the two structural types.

The mass spectra of (13) - (19) show that these complexes lose  $\text{CF}_3$ , F (from  $\text{CF}_3$ ) and CN groups. In the case of (14), transfer of F and CN to the metal centre occurred. Major ions for the carbonyl complexes were  $[\text{M} - n\text{CO}]^+$  ( $n = 1-3$ ). For the phosphine-containing complexes, loss of phenyl groups and phenyl transfer to the metal was observed in all cases. Throughout this work, complexes containing  $\text{Ru}(\text{PPh}_3)(\eta\text{-C}_5\text{H}_5)$  have shown the ion  $[\text{Ru}(\text{PPh}_3)(\text{C}_5\text{H}_5)]^+$  as the base peak in their spectra. For the bis-triphenylphosphine complexes (17) and (18),  $[\text{M} - \text{PPh}_3]^+$  was a major ion. This parallels the solution chemistry of bis-triphenylphosphine complexes, where loss of triphenylphosphine is a facile process. A marked effect was observed when the substituent on the ring was changed from phenyl to methyl. The latter appears to give the ring greater stability against fragmentation and, as a result, loss of dcfe was not observed for (18), fragmentation and loss of the phosphine ligands being the only processes noted.

Single-crystal X-ray diffraction studies of (13), (14), (15) and (19) have been carried out to determine whether cyclobutenyl or butadienyl ligands were present. Plots of the four molecules are shown in Figures 1 - 4 and Table 2 collects and compares significant structural data using a common numbering scheme (which differs from the X-ray numbering schemes).

The  $\text{W}(\text{CO})_3(\eta\text{-C}_5\text{H}_5)$ ,  $\text{Mn}(\text{CO})_3(\text{dppe})$ ,  $\text{Fe}(\text{CO})_2(\eta\text{-C}_5\text{H}_5)$  and  $\text{Ru}(\text{CO})(\text{PPh}_3)(\eta\text{-C}_5\text{H}_5)$  groups are similar to those found in related complexes, such as  $\text{W}\{\overline{\text{C}=\text{CPhC}(\text{CN})_2\text{C}(\text{CN})_2}\}(\text{CO})_3(\eta\text{-C}_5\text{H}_5)$ ,<sup>15</sup>  $\text{Mn}(\text{C}_2\text{Bu}^t)(\text{CO})_3(\text{dppe})$ ,<sup>44</sup>  $\text{Fe}\{\overline{\text{C}=\text{CPhC}(\text{CN})\{\text{Fe}(\text{CO})_2(\eta\text{-C}_5\text{H}_5)\}\text{CHPh}}\}(\text{CO})_2(\eta\text{-C}_5\text{H}_5)$ ,<sup>33</sup> and  $\text{Ru}\{\text{C}(\text{OPri})=\text{CHPh}\}(\text{CO})(\text{PPh}_3)(\eta\text{-C}_5\text{H}_5)$ .<sup>45</sup>

**Figure 1.** PLUTO plot of  $W\{\overline{C=CPhC(CF_3)_2C(CN)_2}\}(CO)_3(\eta-C_5H_5)$  (13)  
(by M.R. Snow and E.R.T. Tiekink )

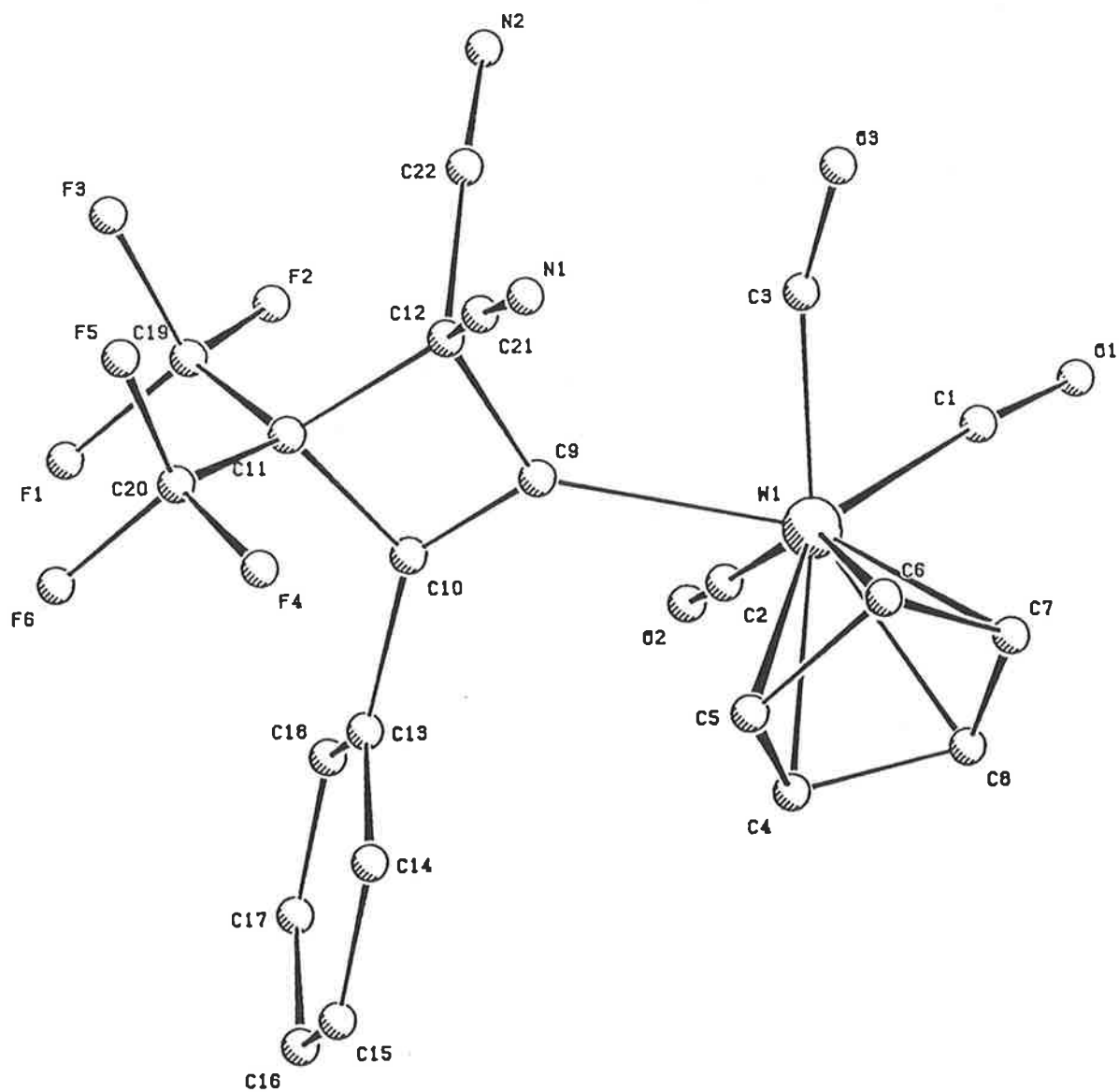


**Figure 2.** PLUTO plot of  $\text{Mn}\{\text{C}=\text{CPhC}(\text{CF}_3)_2\text{C}(\text{CN})_2\}(\text{CO})_3(\text{dppf})$  (**14**)  
 (by M.R. Snow and E.R.T. Tiekink )

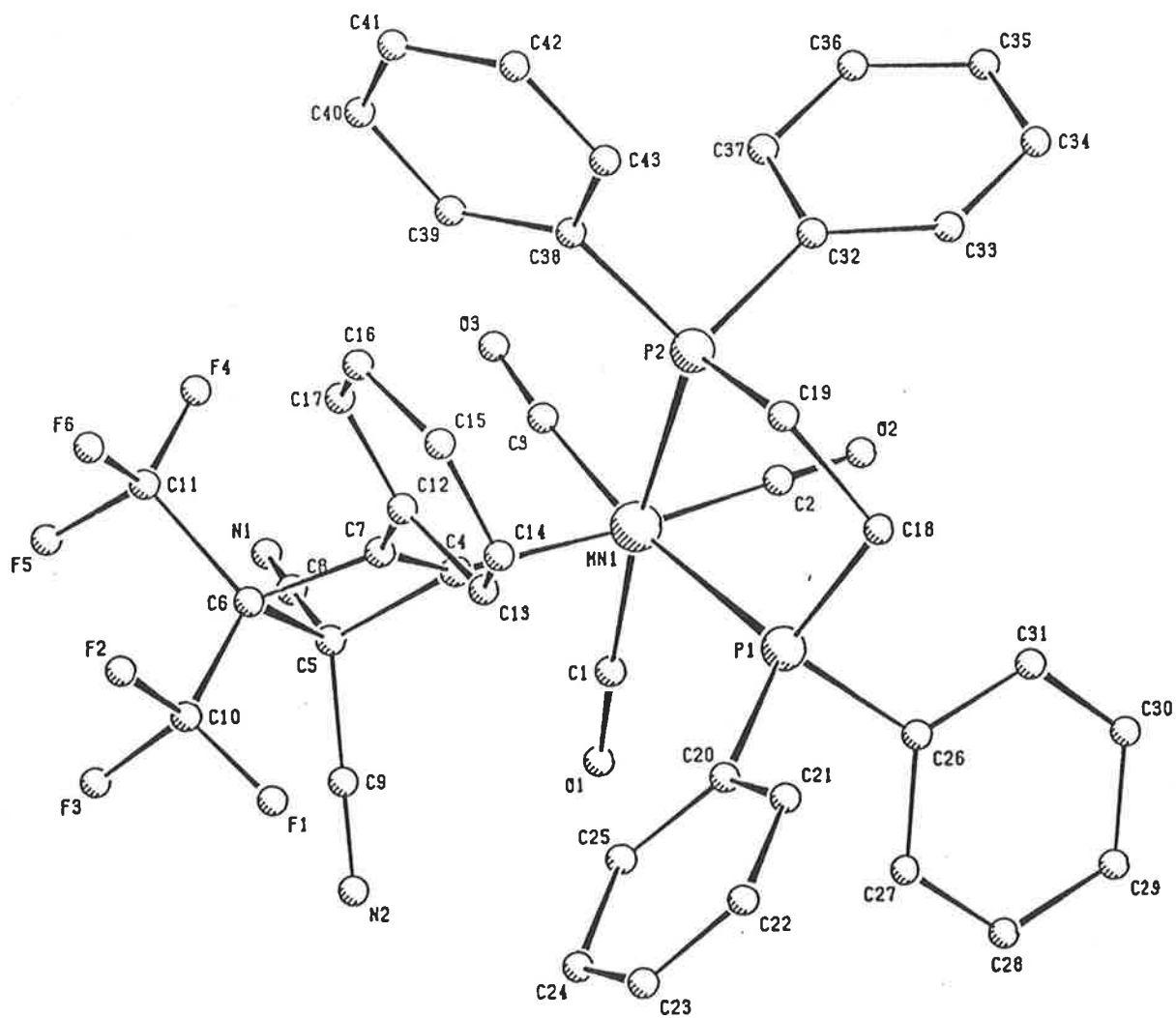


**Figure 3.** PLUTO plot of  $\text{Fe}\{\text{C}=\text{CPhC}(\text{CF}_3)_2\text{C}(\text{CN})_2\}(\text{CO})_2(\eta\text{-C}_5\text{H}_5)$  (15)  
(by M.R. Snow and E.R.T. Tiekink)

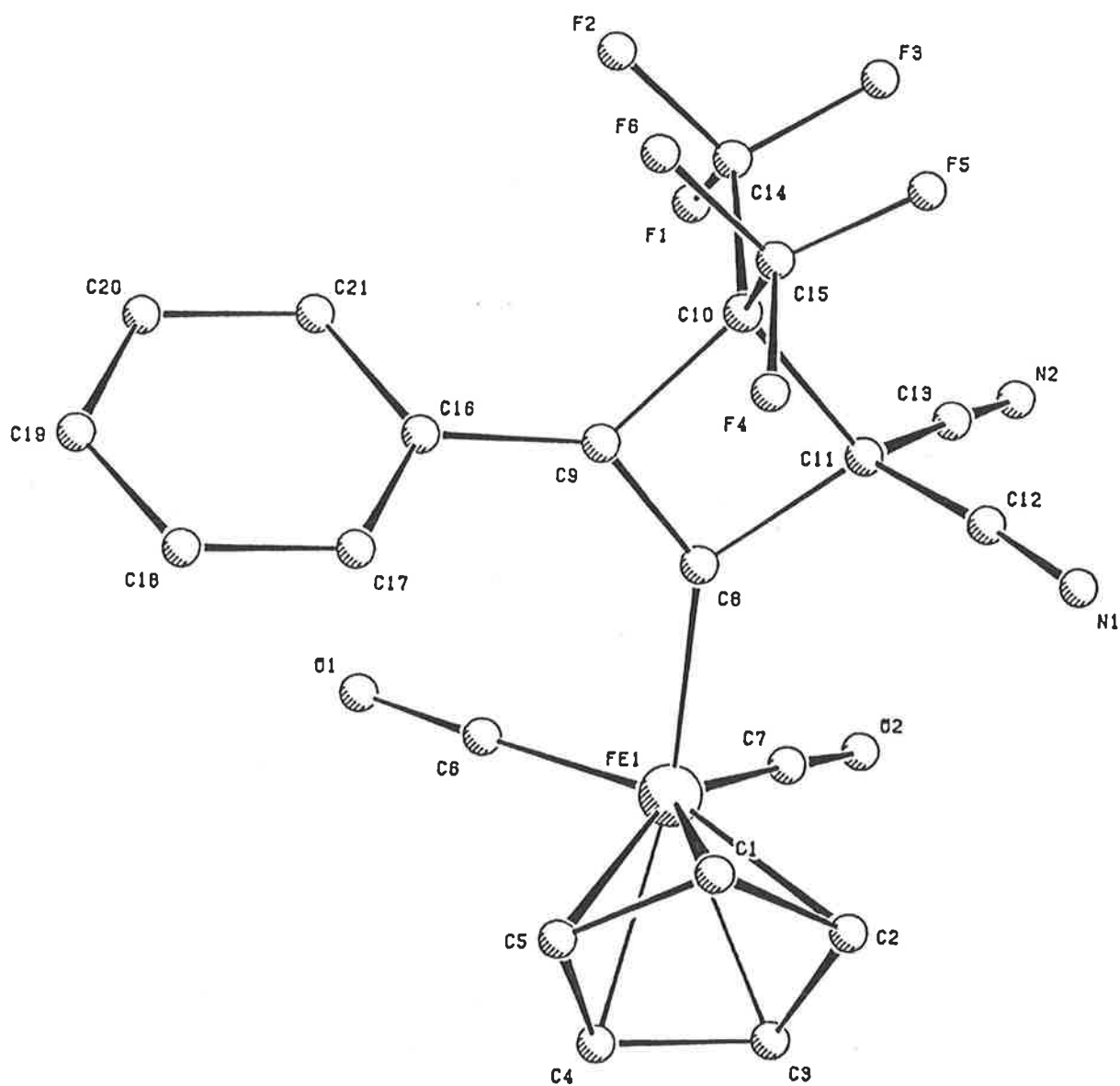


**Figure 4.** PLUTO plot of  $\text{Ru}\{\overline{\text{C}=\text{CPhC}(\text{CF}_3)_2\text{C}(\text{CN})_2}\}(\text{CO})(\text{PPh}_3)(\eta\text{-C}_5\text{H}_5)$  (19)  
(by M.R. Snow and E.R.T. Tiekink )

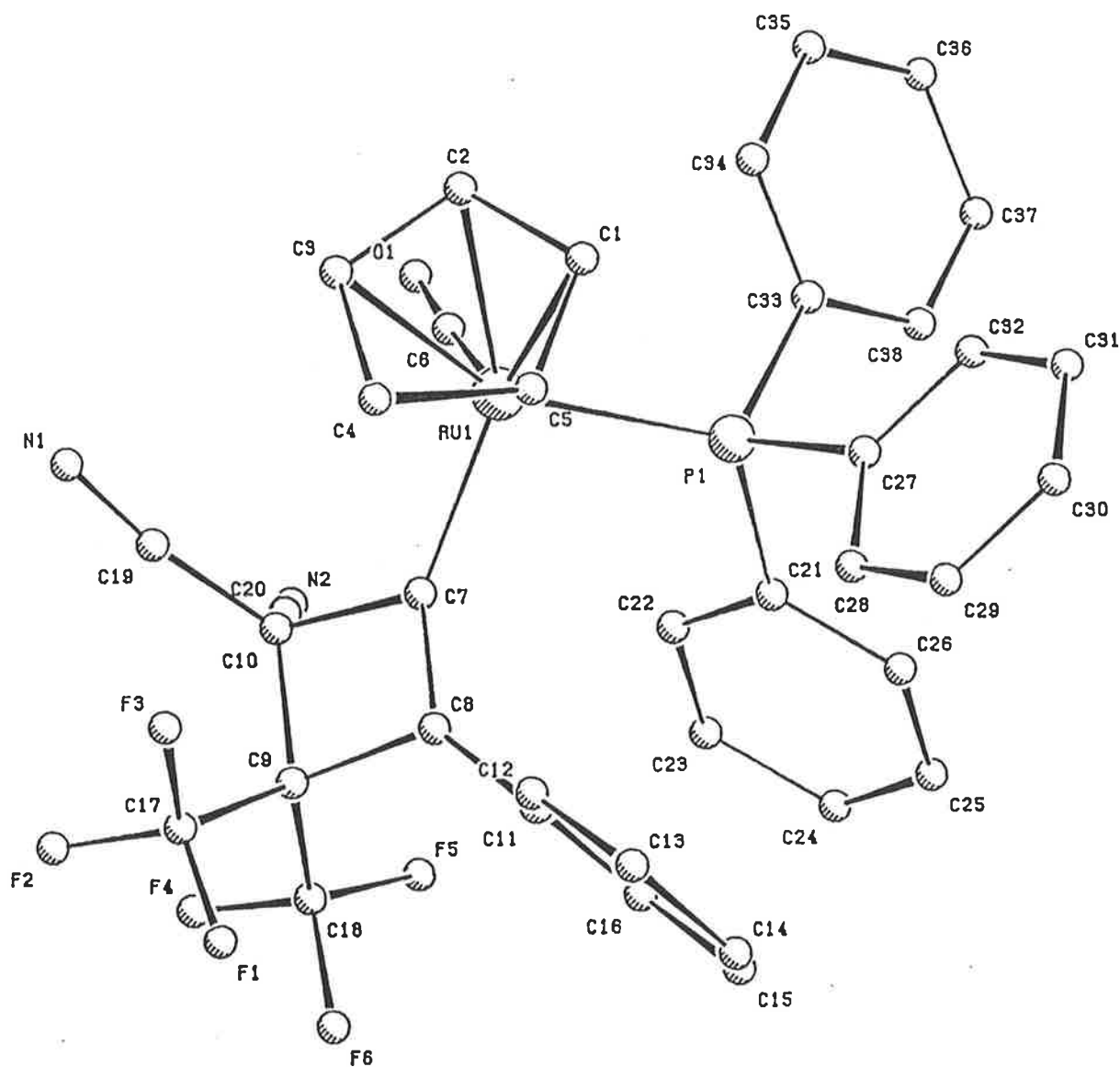
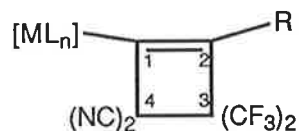


**Table 2.** Selected bond distances (Å) and angles (°) for the cyclobutenyl complexes (13), (14), (15), (19) and (29)

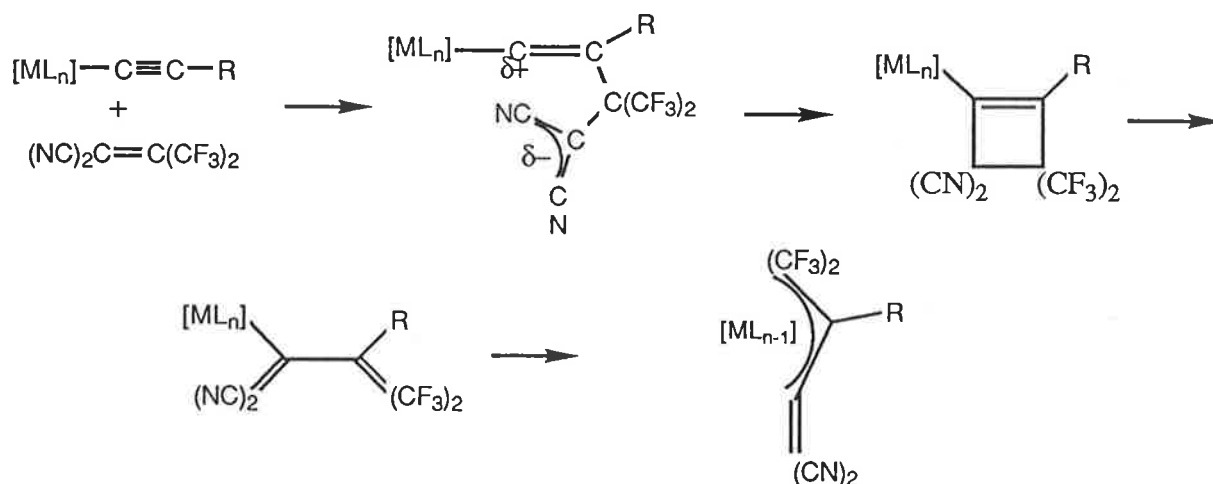


Parameter	Compound				
	(13)	(14)	(15)	(19)	(29)
M-C(1)	2.24(2)	2.099(7)	1.949(4)	2.054(8)	2.034(7)
C(1)-C(2)	1.30(3)	1.337(9)	1.342(5)	1.35(1)	1.359(9)
C(2)-C(3)	1.56(3)	1.52(1)	1.534(5)	1.53(1)	1.53(1)
C(3)-C(4)	1.55(3)	1.58(1)	1.596(6)	1.57(1)	1.58(1)
C(1)-C(4)	1.52(3)	1.610(9)	1.577(5)	1.57(1)	1.58(1)
M-C(1)-C(2)	134(2)	147.2(5)	137.6(3)	140.9(6)	139.7(5)
M-C(1)-C(4)	132(2)	122.4(4)	129.6(3)	126.1(6)	126.7(5)
C(2)-C(1)-C(4)	94(2)	89.6(5)	92.8(3)	91.0(6)	90.8(6)
C(1)-C(2)-C(3)	95(2)	99.0(5)	96.6(3)	97.3(6)	97.5(5)
C(2)-C(3)-C(4)	84(2)	84.7(5)	85.2(3)	84.8(6)	84.7(5)
C(1)-C(4)-C(3)	87(2)	86.3(5)	85.4(3)	86.8(6)	86.9(5)

For (13), the tungsten is in a seven-coordinate environment, the C<sub>5</sub>H<sub>5</sub> group occupies three sites [W-C(cp) 2.29 Å av.] and the remaining four sites are occupied by three carbonyls [W-CO 2.03(3), 1.98(2), 1.96(4) Å] and the cyclobutenyl ligand. The manganese atom in (14) is six-coordinate, being bonded to three carbonyl ligands [Mn-CO 1.820, 1.811, 1.812(8) Å], a dppe ligand [Mn-P 2.334(2), 2.338(2) Å] and the cyclobutenyl ligand. Coordination about iron in (15) and ruthenium in (19) is distorted octahedral. The cyclopentadienyl ligand occupies three sites [Fe-C(cp) 2.103 Å av. (15); Ru-C(cp) 2.258 Å av. (19)], and the remaining sites are occupied by carbonyl [Fe-CO 1.780(5), 1.771(5) Å (15); Ru-CO 1.843(9) Å (19)], phosphine [Ru-P 2.309(2) Å (19)] and cyclobutenyl ligands.

The M-C(sp<sup>2</sup>) distances [W, 2.24(2) Å (13); Fe, 1.949(4) Å (15); Ru, 2.054(8) Å (19)] compare well with those found in the related complexes mentioned above [W, 2.202(9) Å; Fe, 2.09 Å av.; Ru, 2.103(6) Å]. The crystal structure for (14) includes the first determination of a Mn-C(sp<sup>2</sup>) distance. The value of 2.099(7) Å is consistent with the value calculated (2.07 Å) on the basis of the observed Mn-C(sp) separation in Mn(C<sub>2</sub>Bu<sup>t</sup>)(CO)<sub>3</sub>(dppe) [1.996(6) Å] and the difference between C(sp) and C(sp<sup>2</sup>) radii (0.07 Å). The molecule of (19) is chiral at Ru, and as the unit cell contains only one enantiomer, the compound has spontaneously resolved during the crystallization process.

Within the cyclobutenyl rings, the double bonds C(1)=C(2) are normal [1.30(3) - 1.35(1) Å] as is C(2)-C(3) [1.52(1) - 1.53(1) Å]. The tungsten complex has considerably higher esd's than the other structures and tends to show anomalous results: in this case C(2)-C(3) is longer [1.56(3) Å]. The two C-C bonds, opposite the double bond C(3)-C(4) [1.57(1) - 1.596(6) Å], and from the metal-bonded carbon C(1)-C(4) [1.577(5) - 1.610(9) Å], show a degree of lengthening that is also seen in the related tene cyclobutenyl complex  $\overline{\text{W}\{\text{C}=\text{CPhC}(\text{CN})_2\text{C}(\text{CN})_2\}(\text{CO})_3(\eta\text{-C}_5\text{H}_5)}$  [C(3)-C(4) 1.60(1); C(1)-C(4) 1.55(1) Å]. Lengthening of C(3)-C(4) is consistent with the isomerization process giving the butadienyls, but the long C-C bond adjacent to the metal may reflect some separation of charge, not fully shared on ring closure of the proposed zwitterionic intermediate (see Scheme 2). The apparent electron deficiency (as revealed by bond lengthening) in the C(1)-C(4) bond would preclude

Scheme 2. Reactions of dcfe with transition-metal  $\sigma$ -acetylides

the electron transfer which occurs during the ring-opening process. This helps to explain why it is easier to isomerize the tcne complexes than the dcfe-derived cyclobutenyls.

The four-membered rings are all essentially planar, with deviations from the least-squares plane through C(1)C(2)C(3)C(4) being  $< 0.04 \text{ \AA}$ . Angles within the  $C_4$  rings are in the ranges  $89.6(5) - 99.0(5)^\circ$  [at  $C(sp^2)$ ] and  $84.8(6) - 86.8(6)^\circ$  [at  $C(sp^3)$ ].

As revealed by the structural studies, dcfe reacts with the phenylethynyl complexes in a preferred direction so that the  $C(CN)_2$  group becomes attached to the  $\alpha$ -carbon of the acetylide. No evidence for the formation of the isomer that would be produced by addition in the reverse direction has been obtained. While these findings may be the result of the bulk of the  $CF_3$  groups directing the addition in this way, it seems more likely that an intermediate may be stabilized by delocalization of charge on the dicyanomethylene group, rather than on the  $C(CF_3)_2$  group. Such a proposal is consistent with the known stability of cyanocarbon anions and was first suggested in regard to the tcne/ $Fe(C_2Ph)(CO)_2(\eta-C_5H_5)$  reaction by Davison and Solar.<sup>28</sup>

Unlike tetracyanoethene cycloaddition reactions, there are no long-lasting deep-coloured intermediates involved in the cycloaddition; only a very slight blue colouration was observed on larger scale reactions and this very quickly dispersed. According to  $^1H$  NMR studies, the

reaction of  $\text{Ru}(\text{C}_2\text{Ph})(\text{CO})(\text{PPh}_3)(\eta\text{-C}_5\text{H}_5)$  with dcfe in  $d^6$ -benzene was complete within three minutes, which illustrates the rapid transformation from the presumed dipolar intermediate to the cyclobutenyl complex. This is consistent with the organic chemistry of dcfe, where the olefin was found to be a more active enophile than tcne in cycloaddition reactions with styrenes.<sup>46</sup> The olefin dcfe is more polarizable than tcne and can form polar (charge-separated) intermediates or transition states more readily than can tcne.

### 1.2.2. Butadienyl complexes

A feature of the chemistry of the  $\sigma$ -cyclobutenyl complexes derived from tcne is their isomerization to the corresponding butadienyl complexes (Scheme 1), which is often so rapid as to preclude isolation of the cyclobutenyl derivatives. The analogous butadienyl complexes derived from dcfe [(20) - (23), see Table 1] isomerize much less readily. In this study, considerable thermal activation (reflux in benzene, toluene or xylene) was required to bring about the ring-opening. Under these forcing conditions, the ligands on the metal centres are also prone to dissociate, which allows the formation of the related allyl complexes. Thus, mixtures of the related butadienyl and allyl complexes were obtained upon ring-opening of (13) or (18). Swincer obtained complex (12) as a minor product from the carbonylation of complex (18), which he had obtained by a different route.<sup>41</sup>

The IR bands of the butadienyl complexes [(20) - (23)] that are characteristically different from those of the cyclobutenyl complexes are the  $\nu(\text{CN})$  bands ( $2190 - 2220 \text{ cm}^{-1}$ ), which are of weak to medium intensity [relative to the strong bands observed ( $1140 - 1340 \text{ cm}^{-1}$ ) for the  $\text{CF}_3$  groups]. Generally, the  $\nu(\text{C}=\text{C})$  bands ( $1570 - 1630 \text{ cm}^{-1}$ ) are slightly stronger than those of the cyclobutenyls, but they are still of weak to medium intensity. Characteristic  $\nu(\text{CO})$  absorptions for monocarbonyl and tricarbonyl complexes were observed for compounds (22) and (20), respectively.

Proton NMR spectra for the complexes (20) - (23) showed the presence of phenyl groups ( $\delta$  7.6 - 6.8) and cyclopentadienyl ligands ( $\delta$  5.80, 5.30, 4.61 and 4.30, respectively). In the case of (23), a minor isomer (20%) with a  $\text{C}_5\text{H}_5$  resonance at  $\delta$  4.67 was detected. This

product could not be separated by chromatography or crystallization. A similar isomerization has been noted for the complex  $\text{Ru}\{\text{C}=\text{C}(\text{CN})_2\}\text{CPh}=\text{C}(\text{CN})_2\}\text{(dppe)}(\eta\text{-C}_5\text{H}_5)$ .<sup>7</sup> In that case, the difference between the two isomers was attributed to different rotational conformations in solution. A molecular model of (23) showed that the  $\text{-CPh}=\text{C}(\text{CF}_3)_2$  arm of the butadienyl was prone to interactions ( $\text{Ph}:\text{Ph}$ ;  $\text{CF}_3:\text{Ph}$ ) with the phenyl groups on the dppe ligand. The isomerization appears to arise from the phenyl group of the butadienyl being locked on different sides of the  $\text{PPh}_3$  group. A reinvestigation of the structure of (12) using molecular modelling suggests that even in this case, where only triphenylphosphine is present, it is possible to have the butadienyl ligand in different configurations. The major (non-crystallographically characterized) isomer in this system may be related to the minor isomer (12) by rotation of the butadienyl ligand so that the trifluoromethyl groups are in a sterically less demanding position. Such a rotation would be restricted by the triphenylphosphine ligand.

Fluorine NMR results have been obtained for (21), (22) and (23). They show  $\text{CF}_3$  signals (between  $\delta$  -53 and  $\delta$  -57) in a region different <sup>from</sup> to those of the cyclobutenyl ligands. In all cases, the two  $\text{CF}_3$  groups are inequivalent. This is to be expected from the X-ray structural results for (22) and (12), which indicate that the  $\text{CF}_3$  groups should be in different environments. For (22), the higher field multiplet ( $\delta$  -56.6) is considerably broader than the quartet observed at  $\delta$  -53.2 for the other  $\text{CF}_3$  group. Examination of the structure using molecular modelling suggests that the  $\text{CF}_3$  group closest to the phosphine may interact with the phenyl protons on the phosphine. This could give rise to small through-space couplings, which would appear as a broadening of the signal (selective decoupling was not available when these spectra were recorded). The spectrum of (23) shows that the two isomers present have similar CF environments [ $\delta$  -53.1, -55.9 (isomer i); -53.2, -55.7 (isomer ii)], suggesting that the  $\text{CPh}=\text{C}(\text{CF}_3)_2$  groups are in closely related positions in each of the isomers.

Mass spectral results for the butadienyl derivatives were similar to those for the cyclobutenyls, except that the loss of dcfе was not apparent in any of the spectra obtained. The FAB MS result for the Ni complex (21), where loss of dcfе was not observed, was in

accordance with the IR and  $^{19}\text{F}$  NMR results and has allowed a butadienyl structure to be ascribed to this complex. The intermediate cyclobutenyl isomer was not detected in the synthesis of (21) (refluxing benzene) and no reaction was found to occur between the acetylide and dcfe at room temperature. Similarly, an intermediate which was isolated during the synthesis of the allyl complex  $\text{Ru}\{\eta^3\text{-C}(\text{CF}_3)_2\text{CMeC}=\text{C}(\text{CN})_2\}(\text{PPh}_3)(\eta\text{-C}_5\text{H}_5)$  (see Section 1.2.3), is presumed to be the butadienyl  $\text{Ru}\{\text{C}[\text{C}(\text{CN})_2]\text{CMe}=\text{C}(\text{CF}_3)_2\}(\text{NCMe})(\text{PPh}_3)(\eta\text{-C}_5\text{H}_5)$ , on the basis of spectroscopic data. This compound is presumably formed via an acetonitrile-cyclobutenyl complex, which would be related to the structurally-characterized complex  $\text{Ru}\{\overline{\text{C}=\text{CPhC}(\text{CF}_3)_2\text{C}(\text{CN})_2}\}(\text{NCMe})(\text{PPh}_3)(\eta\text{-C}_5\text{H}_5)$  (see Section 1.2.5).

A plot of a molecule of (22) is shown in Figure 5, and relevant interatomic parameters are listed in Table 3. As with (19), the molecule is chiral at the ruthenium, but in this case both enantiomers are present in equal amounts in the unit cell. The coordination about the ruthenium is again distorted octahedral, the  $\eta\text{-C}_5\text{H}_5$  group being somewhat asymmetrically attached to the metal [Ru-C(cp) 2.235-2.283(6), av. 2.256 Å]. The other three positions are occupied by CO [Ru-C(6) 1.852(16) Å],  $\text{PPh}_3$  [Ru-P(1) 2.332(1) Å] and the substituted buta-1,3-dien-2-yl group [Ru-C(7) 2.100(5) Å]. The slight asymmetry found in the Ru-C(cp) bond distances can be ascribed to the steric interaction between the  $=\text{C}(\text{CN})_2$  group of the organic ligand and the cyclopentadienyl ring. In order to minimize this interaction, the cyclopentadienyl ring is shifted slightly from the ideal octahedral face. This effect is also found in the related complex (12). The butadienyl ligand is non-planar [torsion angle C(10)C(7)C(8)C(9) 73.1°] and as a result, the C-C single and C=C double bonds are localized [C(7)-C(8) 1.480(7) Å; C(7)-C(10) 1.367(7) Å; C(8)-C(9) 1.356(7) Å]. This structural feature has been noted previously,<sup>7</sup> and arises because the bulk of the substituents on C(9) and C(10) precludes the adoption of a planar  $\text{C}_4$  skeleton. There are no major differences between the ligand in (22) and that of the Me derivative (12).

Figure 5. PLUTO plot of  $\text{Ru}\{\text{C}=\text{C}(\text{CN})_2\}\text{CPh}=\text{C}(\text{CF}_3)_2\}(\text{CO})(\text{PPh}_3)(\eta\text{-C}_5\text{H}_5)$  (22)

(by M.R. Snow and E.R.T. Tiekink )

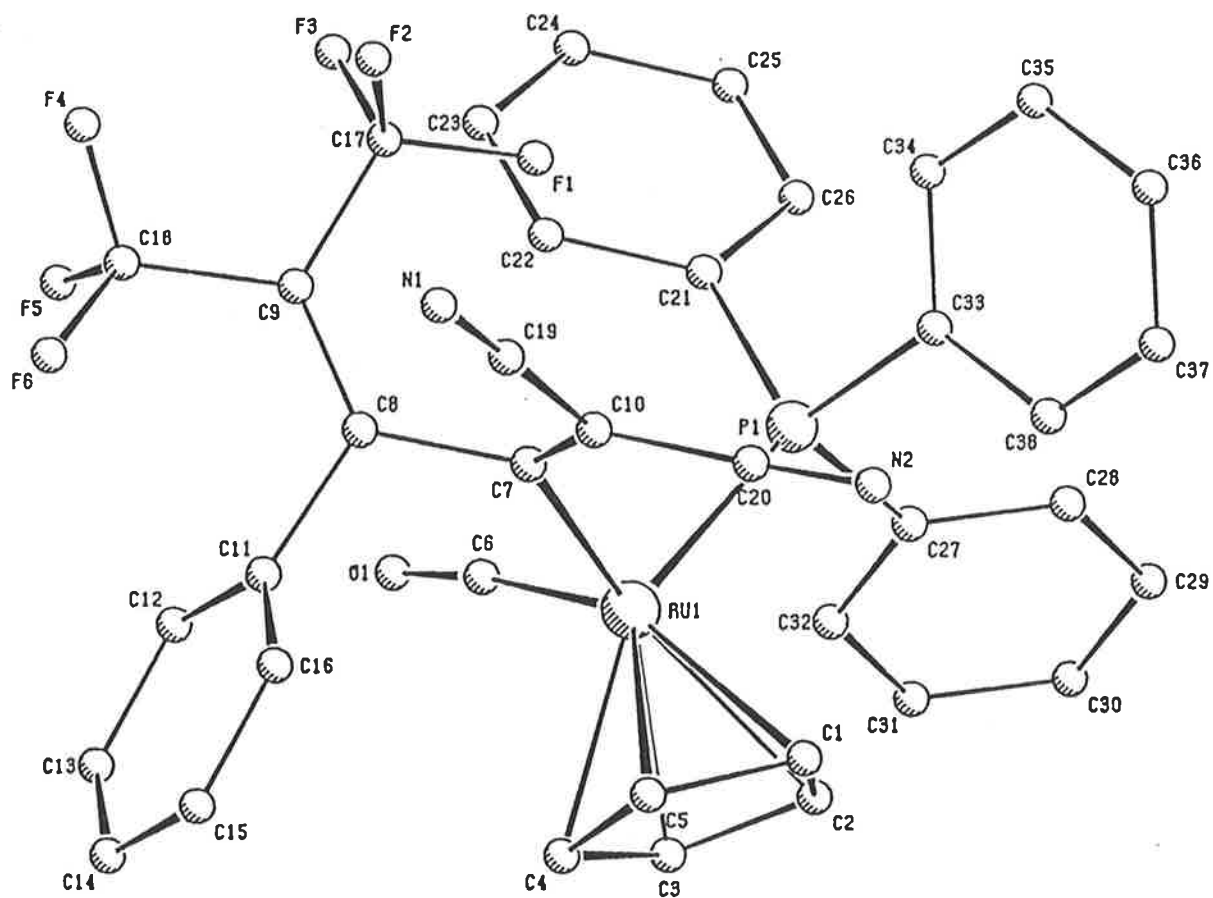


Table 3. Selected bond distances (Å) and angles (°) for complexes (12)<sup>†</sup> and (22)

Parameter	Compound	
	(12)	(22)
Ru-P(1)	2.347(1)	2.332(1)
Ru-C(7)	2.106(5)	2.100(5)
C(7)-C(8)	1.493(8)	1.480(7)
C(7)-C(10)	1.362(8)	1.367(7)
C(8)-C(9)	1.328(8)	1.356(7)
Ru-C(7)-C(8)	116.7(4)	120.0(3)
Ru-C(7)-C(10)	128.3(4)	123.9(3)
C(8)-C(7)-C(10)	113.2(5)	113.5(4)
C(7)-C(8)-C(9)	126.5(5)	125.1(4)
Ru-C(7)-C(8)-C(11)	70.5	58.3
Ru-C(7)-C(8)-C(9)	113.2	124.4
C(10)-C(7)-C(8)-C(9)	80.8	73.1
C(10)-C(7)-C(8)-C(11)	95.5	104.3

<sup>†</sup>Reference 41; complex (12) renumbered according to complex (22).

### 1.2.3. Allyl complexes

The formation of  $\eta^3$ -allyl complexes from the corresponding butadienyl complexes comes about as a result of the loss of a two-electron donor ligand from the metal core. This process has been shown to be reversible for the tene derivative  $\text{Ru}\{\eta^3\text{-C}(\text{CN})_2\text{CPhC}=\text{C}(\text{CN})_2\}\text{-}(\text{PPh}_3)(\eta\text{-C}_5\text{H}_5)$ , where substitution of CO or CNBu<sup>t</sup> gave the related butadienyl derivatives.<sup>7</sup> In the present study, three allyl complexes [(24) - (26), see Table 1] have been isolated by different routes. Synthesis of (24) was achieved by heating the cyclobutenyl precursor (13) in refluxing xylene for 2 hours 45 minutes; this gave the butadienyl product (20) and a 26% yield of orange crystalline (24). The formation of the allyl complex (25) by the irradiation of (22) has completed the first series of transformations:  $\sigma$ -cyclobutenyl  $\rightarrow$   $\sigma$ -butadienyl  $\rightarrow$   $\eta^3$ -allyl derived from the same metal-ligand combinations. Attempted conversion of (18) to the corresponding butadienyl by heating in acetonitrile for several hours gave instead yellow crystalline  $\text{Ru}\{\eta^3\text{-C}(\text{CN})_2\text{CMeC}=\text{C}(\text{CN})_2\}\text{(PPh}_3)(\eta\text{-C}_5\text{H}_5)$  (26) in 66% yield. Confirmation of the allyl structures for these complexes was obtained by an X-ray structural determination for (25).

Infrared spectra of the allyl complexes contain medium - strong intensity bands for the  $\nu(\text{CN})$  absorptions at around  $2220\text{ cm}^{-1}$  and for  $\nu(\text{C}=\text{C})$  at  $1560 - 1590\text{ cm}^{-1}$ . Strong  $\nu(\text{CF})$  bands were observed between  $1080$  and  $1310\text{ cm}^{-1}$ , and for (24) there were two  $\nu(\text{CO})$  absorptions which confirmed the dicarbonyl configuration.

In the  $^1\text{H}$  NMR spectra of the three complexes, cyclopentadienyl resonances were found at  $\delta$  5.79 (24), 4.72 (25) and 4.49 (26). Phenyl resonances were also observed in all cases and, for (26), the methyl resonance was found at  $\delta$  2.06. The  $^{19}\text{F}$  NMR spectra for all three compounds showed two quartets [at  $\delta$  -51.9, -52.5 (24); -48.6, -56.0 (25); -53.0, -56.4 (26)], indicating, as did the molecular structure of (25), that the  $\text{CF}_3$  groups are inequivalent. The chemical shift range is wider than that of the other cycloadducts and reflects the greater effect on the CF environment of the metal-ligand combination. This is not surprising, as the  $\text{C}(\text{CF}_3)_2$  group in these allyl complexes is now also bonded to a metal.

The FAB mass spectra for all three compounds show molecular ions, but less information was obtained from their fragmentation patterns than from those of the cyclobutenyl or butadienyl derivatives. For the ruthenium complexes, transfer of CN was again seen to form the ion  $[\text{Ru}(\text{CN})(\text{PPh}_3)(\text{C}_5\text{H}_5)]^+$ . Weak aggregate ions (< 5% R.I.), of nominal formulation  $[\text{M}_2]^+$  and  $[\text{M}_2 - \text{PPh}_3]^+$ , were found in the spectrum of (26).

Figure 6 is a plot of a molecule of (25); selected parameters are given in Table 4. In (25), the metal is coordinated to the  $\eta\text{-C}_5\text{H}_5$  group [Ru-C(cp) 2.218 - 2.273(8), av. 2.236 Å], a  $\text{PPh}_3$  ligand [Ru-P(1) 2.411(2) Å] and the allylic ligand [Ru-C(6) 1.977(7), Ru-C(10) 2.138(7), Ru-C(11) 2.202(7) Å] formed by chelation of the butadienyl via the C(8)=C(9) double bond [cf. (22)] with loss of CO.

The mode of attachment of the  $\text{C}_3$  ligand, one terminal carbon of which is involved in an *exo*-allylic double bond, is interesting. In addition to complexes such as  $[\text{Fe}(\text{CO})_3\{\eta^3\text{-C}(\text{CO}_2\text{Me})_2\text{CHC}=\text{O}\}]^-$ , whose structure was inferred from spectroscopic data,<sup>47</sup> several other examples have been characterized by X-ray analyses, including  $\text{Mo}\{\text{OC}(\text{O})\text{C}_3\text{F}_7\}(\text{bpy})\{\eta^3\text{-CH}_2\text{C}(\text{CONHMe})\text{C}=\text{CH}_2\}$ <sup>48</sup> and  $\text{ML}_n\{\eta^3\text{-C}(\text{CN})_2\text{CPhC}=\text{C}(\text{CN})_2\}$  [ $\text{ML}_n = \text{W}(\text{CO})_2(\eta\text{-C}_5\text{H}_5)$ ,<sup>6</sup>  $\text{Ru}(\text{PPh}_3)(\eta\text{-C}_5\text{H}_5)$ ].<sup>8</sup> These ligands are distinguished from classical  $\eta^3$ -allylic ligands by the pattern of their M-C and C-C bond lengths. They have two longer M-C bonds, consistent with an  $\text{M}-\eta^2\text{-C}=\text{C}$  interaction, and a short M-C bond involving C(6). This short separation indicates a degree of multiple-bond character between the ruthenium and C(6). In addition, the two C-C bonds in the  $\text{C}_3$  unit are similar. While that for C(10)-C(11) [1.46(1) Å] is also consistent with a strong olefin-metal interaction, C(6)-C(10) [1.42(1) Å] is considerably shorter than expected for a C-C single bond.

**Figure 6.** PLUTO plot of  $\text{Ru}\{\eta^3\text{-C}(\text{CF}_3)_2\text{CPhC}=\text{C}(\text{CN})_2\}(\text{PPh}_3)(\eta\text{-C}_5\text{H}_5)$ .  
 $0.5\text{CH}_2\text{Cl}_2\cdot\text{H}_2\text{O}$  (25) (by M.R. Snow and E.R.T. Tiekink )

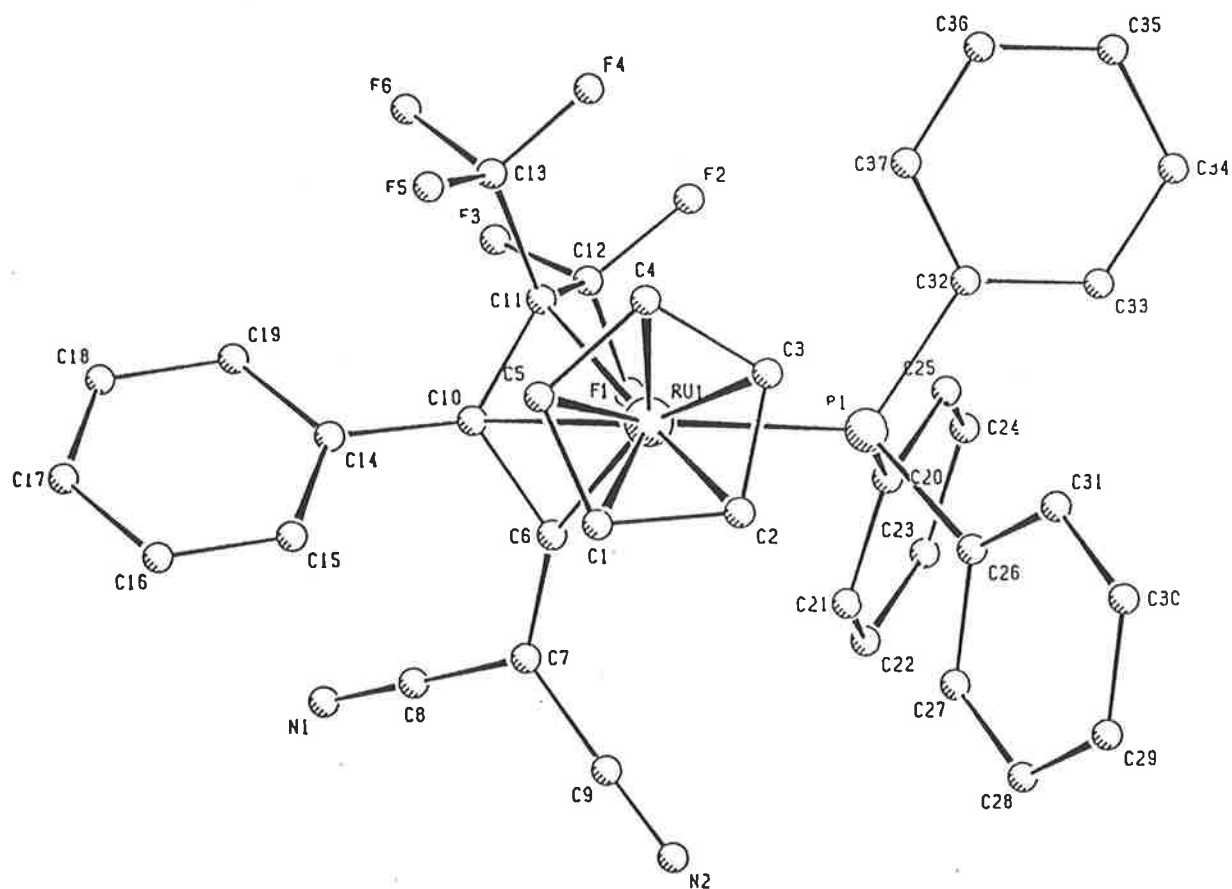


**Table 4.** Selected bond distances (Å) and angles (°) for complex (25)

Ru-P(1)	2.411(2)	Ru-C(1)	2.218(8)
Ru-C(2)	2.229(8)	Ru-C(3)	2.237(8)
Ru-C(4)	2.273(8)	Ru-C(5)	2.226(8)
Ru-C(6)	1.977(7)	Ru-C(10)	2.138(7)
Ru-C(11)	2.202(7)	C(6)-C(7)	1.37(1)
C(6)-C(10)	1.42(1)	C(10)-C(11)	1.46(1)
Ru-C(6)-C(7)	149.9(6)	Ru-C(6)-C(10)	76.0(5)
Ru-C(10)-C(6)	63.8(4)	Ru-C(10)-C(11)	68.0(4)
Ru-C(11)-C(10)	68.0(4)	Ru-C(10)-C(14)	119.3(6)
C(6)-C(10)-C(11)	113.5(6)	C(7)-C(6)-C(10)	131.4(7)

#### 1.2.4. Hydrolysis of (13)

In an attempt to convert (13) to an allylic derivative, the complex was treated with trimethylamine oxide ( $\text{Me}_3\text{NO} \cdot 2\text{H}_2\text{O}$ ) in acetone to give an orange crystalline product  $\text{W}\{\text{NH}=\text{C}(\text{OH})\text{C}(\text{CN})=\text{CCPh}=\text{C}(\text{CF}_3)_2\}(\text{CO})_2(\eta\text{-C}_5\text{H}_5)$  (27) in 24% yield. The IR spectrum contains two  $\nu(\text{CO})$  bands and a strong  $\nu(\text{CN})$  absorption. A group of bands between 3380 and 2730  $\text{cm}^{-1}$  were assigned to  $\nu(\text{OH})$ ,  $\nu(\text{NH})$  and  $\nu(\text{CH})$  absorptions. No resonances attributable to the OH or NH groups were found in the  $^1\text{H}$  NMR spectra, probably because of the broad signals found for this type of group and the relative instability of this complex in solution. The FAB mass spectrum had a molecular ion at  $m/z$  638, which suggested that (27) was related to (13) by loss of a CO ligand and addition of  $\text{H}_2\text{O}$ .

The molecular structure of (27) was determined by X-ray methods and is illustrated in Figure 7. Table 5 lists the bond distances and angles. The tungsten atom is coordinated to two CO groups [ $\text{W-CO}$  2.00(2), 1.98(2) Å] and a  $\text{C}_5\text{H}_5$  ligand [ $\text{W-C}(\text{cp})$  2.27(1) - 2.39(2), av. 2.34 Å], together with carbon and nitrogen atoms of a chelating 1-hydroxy-1-imido-2-cyano-4-phenyl-5,5-bis(trifluoromethyl)penta-2,4-dien-3-yl ligand [ $\text{W-N}(1)$  2.145(8);  $\text{W-C}(8)$  2.15(1) Å]. The  $\text{W-C}(8)$  bond is 0.1 Å shorter than that found in the precursor (13). The ligand is related to the cyclobutenyl ligand originally present in (13) by ring-opening [cleavage of  $\text{C}(11)\text{-C}(12)$  cf. (13)] and the addition of a molecule of water across one of the CN groups. The resulting imido-function displaces a CO group to give a five-membered  $\overline{\text{W-N=C-C=C}}$  chelate ring. This transformation is represented in Scheme 3. Although we cannot establish at which stage the cyclobutenyl ring is cleaved to form the butadienyl group, it would appear, from the observed failure of (20) to form (27) when treated with  $\text{Me}_3\text{NO} \cdot 2\text{H}_2\text{O}$ , that it is after the removal of the CO group.

Figure 7. PLUTO plot of  $\overline{W\{NH=C(OH)C(CN)=CCPh=C(CF_3)_2\}(CO)_2(\eta-C_5H_5)}$  (27)  
(by M.R. Snow and E.R.T. Tiekink )

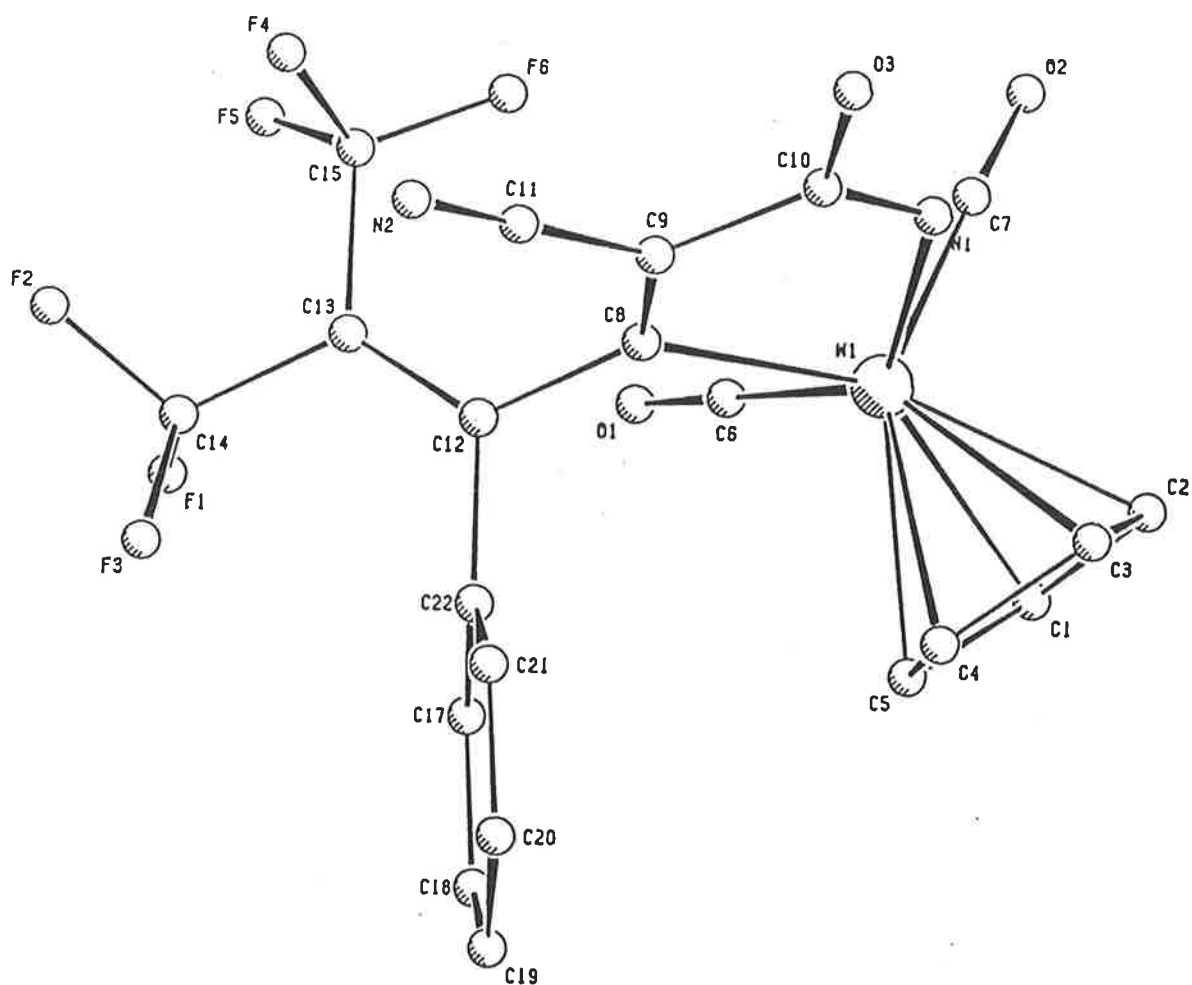
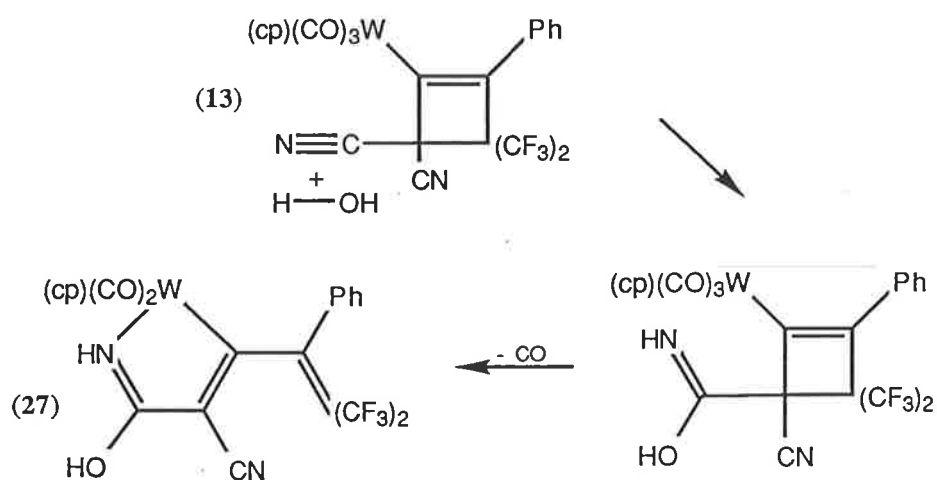


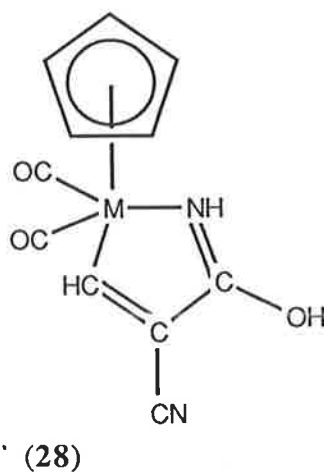
**Table 5.** Selected bond distances (Å) and angles (°) for complex (27)

W-C(1)	2.27(1)	W-C(2)	2.32(1)
W-C(3)	2.39(2)	W-C(4)	2.37(1)
W-C(5)	2.33(1)	W-C(6)	2.00(2)
W-C(7)	1.98(2)	W-C(8)	2.15(1)
W-N(1)	2.145(8)	C(8)-C(9)	1.38(2)
C(9)-C(10)	1.44(2)	C(10)-N(1)	1.26(1)
C(10)-O(3)	1.35(2)	C(9)-C(11)	1.44(2)
C(11)-N(2)	1.13(1)	C(8)-C(12)	1.47(2)
C(12)-C(13)	1.34(2)		
W-C(8)-C(9)	114.4(8)	W-N(1)-C(10)	119.4(7)
W-C(8)-C(12)	126.5(8)	N(1)-W-C(8)	73.9(4)
C(8)-C(9)-C(10)	115.5(9)	N(1)-C(10)-C(9)	116(1)
C(8)-C(12)-C(13)	125(1)	C(14)-C(13)-C(15)	116(1)
N(1)-C(10)-O(3)	122(1)	C(9)-C(10)-O(3)	123.0(9)
C(10)-C(9)-C(11)	118.7(9)	C(8)-C(9)-C(11)	126(1)
C(9)-C(8)-C(12)	118.4(9)	C(8)-C(12)-C(22)	111.6(9)
C(13)-C(12)-C(22)	124(1)		

Scheme 3. Formation of (27) from (13)



The reaction is not consistent with the usual behaviour of polycyano-olefins towards water. The olefin dcf<sub>e</sub>, for example, reacts with water to give hydroxybis(trifluoromethyl)methylmalononitrile (at low pH) or bis(trifluoromethyl)methylenemalonamide (at high pH).<sup>46</sup> However, our reaction has precedent in the observations of King and Saran,<sup>49</sup> who described the formation of  $\overline{M\{NH=C(OH)C(CN)=CH\}(CO)_2(\eta-C_5H_5)}$  ( $M = Mo$  or  $W$ ) (28) when the 1-chloro-2,2-dicyanovinyl complexes  $M\{CCl=C(CN)_2\}(CO)_3(\eta-C_5H_5)$  were treated with alumina containing adsorbed water. Carty<sup>50</sup> has synthesized the compound  $Ru_4(\mu_4-\eta^2-CCHPr^i)(\mu_3-OH)(\mu-PPh_2)(CO)_{10}$ , in which the vinylidene hydrogen atom and the hydroxy-ligand were assumed to come from a water molecule of  $Me_3NO \cdot 2H_2O$  employed in the synthesis.



### 1.2.5. Nitrile-substituted cyclobutenyl complexes

An acetonitrile-substituted cyclobutenyl complex  $\text{Ru}\{\overline{\text{C}=\text{CPhC}(\text{CF}_3)_2\text{C}(\text{CN})_2}\}(\text{NCMe})\text{-}(\text{PPh}_3)(\eta\text{-C}_5\text{H}_5)$  (**29**) was prepared by treating  $\text{Ru}(\text{C}_2\text{Ph})(\text{PPh}_3)_2(\eta\text{-C}_5\text{H}_5)$  (**30**) with dcfe in acetonitrile at room temperature. The lability of the acetonitrile ligand in (**29**) permitted the synthesis of a number of other mononuclear [(**31**) - (**36**)] and binuclear [(**37**) - (**40**)] nitrile complexes (see Table 6). One of the binuclear complexes, (**40a**), had previously been isolated by Swincer<sup>42</sup> from the reaction of dcfe and (**30**) in benzene, and was characterized by means of an X-ray study (see below). The magnetic properties of the complex gave rise to a broad ESR signal corresponding to 0.04 unpaired electrons per molecule and could not be resolved in terms of the molecular structure. We have therefore re-examined the synthesis and properties of (**40a**). In the early stages of this work, it was supposed that the polynitrile ligands were behaving as bridging groups in all cases. This was later shown to be incorrect, as both mononuclear and binuclear complexes were formed in several of these reactions.

As noted above, the synthesis of (**29**) involved treating (**30**) with dcfe in acetonitrile. Initially, complex (**17**) (see Section 1.2.1) formed as a precipitate; this was then collected and suspended in acetonitrile for 1.5 days, forming a pale yellow solution from which yellow crystalline (**29**) was isolated in 43% yield. Complex (**29**) was characterized by analysis and spectroscopic data. In the FAB mass spectrum a molecular ion was found at  $m/z$  785, which fragmented by loss of MeCN, CN,  $\text{CF}_3$  and phenyl groups. A weak ion was found at  $m/z$  530 corresponding to  $[\text{M} - \text{MeCN} - \text{dcfe}]^+$ , allowing the identification of (**29**) as a cyclobutenyl complex. The IR spectrum of (**29**) shows  $\nu(\text{CN})$  bands at 2267 and 2235  $\text{cm}^{-1}$  of medium and weak intensities respectively, and  $\nu(\text{C}=\text{C})$  bands at 1613, 1590 and 1576  $\text{cm}^{-1}$ . Other bands attributable to  $\nu(\text{CF})$  absorptions were found between 1099 and 1310  $\text{cm}^{-1}$ . In the  $^1\text{H}$  NMR spectrum a doublet signal at  $\delta$  1.95 ( $J_{\text{P-H}} = 1.2$  Hz) was found for the  $\text{CH}_3$  group, and at  $\delta$  4.41 for the  $\eta\text{-C}_5\text{H}_5$  group, while a series of resonances between  $\delta$  7.4 - 6.5 were attributable to the phenyl groups. The  $^{19}\text{F}$  resonances at  $\delta$  -66.2 and -66.4 showed that the two  $\text{CF}_3$  groups were inequivalent in solution. An X-ray structure determination of (**29**) has been performed which confirms the mononuclear structure expected from spectroscopic data.

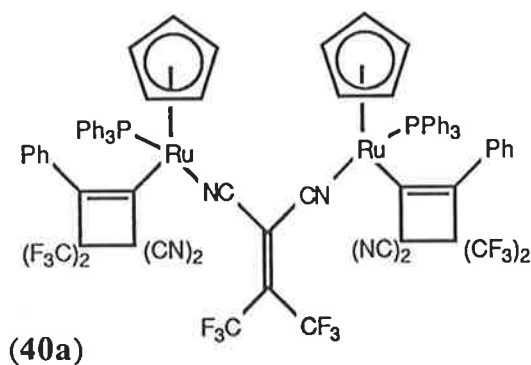
Table 6. Nitrile-substituted cyclobutenyl complexes

Mononuclear complexes  $[\text{Ru}]^{\dagger}\text{L}$ 

Cmpd	L
(29)	NCMe
(31)	NCCH=CH <sub>2</sub>
(32)	(NC)C <sub>6</sub> H <sub>2</sub> (CN) <sub>4</sub> -1,2,4,5
(33)	(NC)C <sub>6</sub> H <sub>4</sub> (CN)- <i>o</i>
(34)	(NC)C <sub>6</sub> F <sub>4</sub> (CN)- <i>o</i>
(35)	(NC)C <sub>6</sub> F <sub>4</sub> (CN)- <i>p</i>
(36)	<i>trans</i> -(NC)CH=CH(CN)

Binuclear complexes  $[\text{Ru}]_2\text{L}$ 

Cmpd	L
(37)	(NC)C <sub>6</sub> F <sub>4</sub> (CN)- <i>o</i>
(38)	<i>trans</i> -(NC)CH=CH(CN)
(39)	(NC) <sub>2</sub> C=C(CN) <sub>2</sub>
(40)	(NC) <sub>2</sub> C=C(CF <sub>3</sub> ) <sub>2</sub>



$\dagger[\text{Ru}] = \text{Ru}\{\text{C}=\text{CPhC}(\text{CF}_3)_2\text{C}(\text{CN})_2\}(\text{PPh}_3)(\eta\text{-C}_5\text{H}_5)$

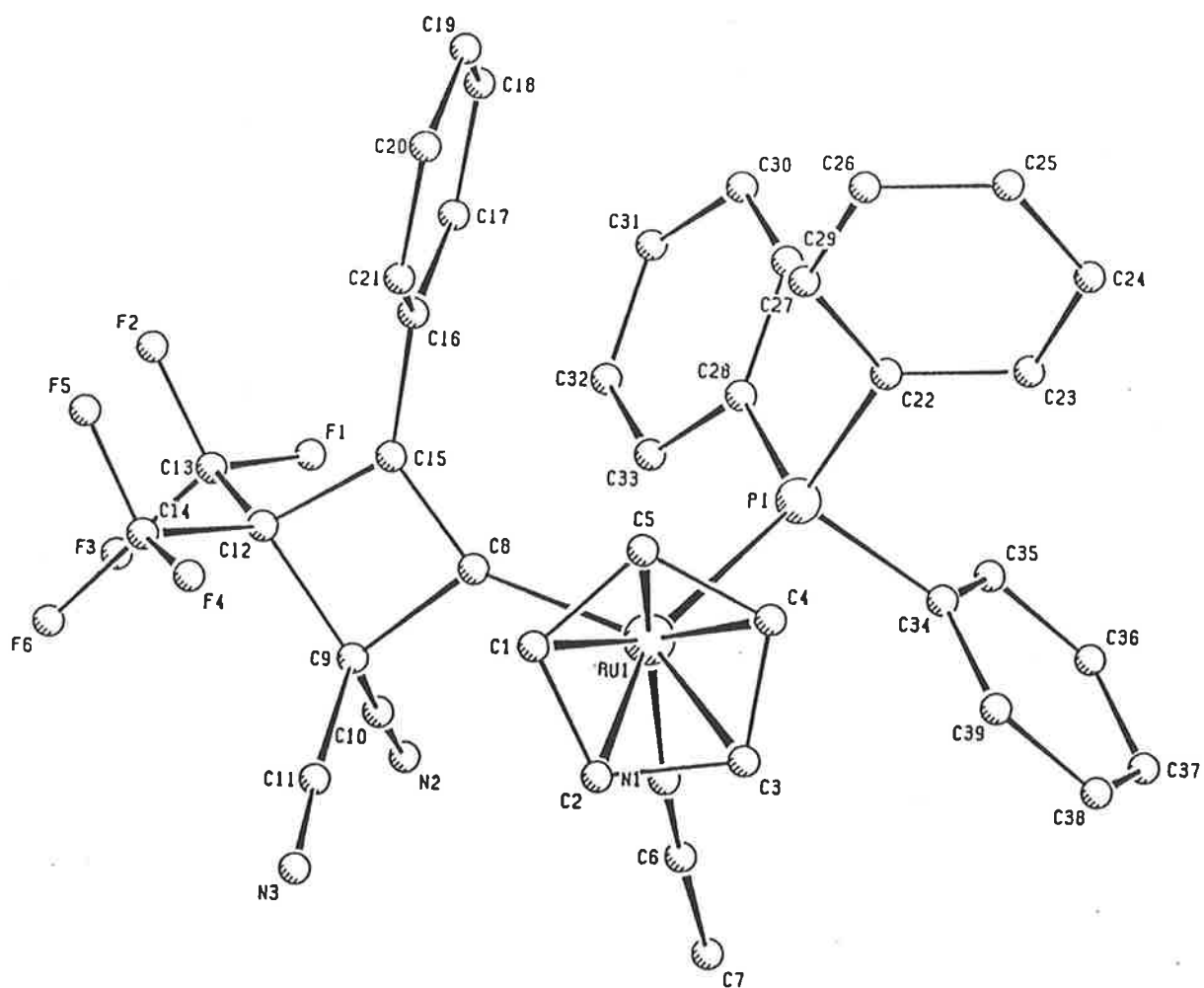
Figure 8 shows a plot of the molecular structure of (29), and significant bond distances were listed in Table 2 (Section 1.2.1). Complex (29) is chiral at the ruthenium, with both enantiomers being found in the unit cell, as for (22). The ruthenium atom is coordinated to MeCN [Ru-N(1), 2.033(6) Å], PPh<sub>3</sub> [Ru-P 2.297(2) Å] and C<sub>5</sub>H<sub>5</sub> ligands [Ru-C(cp) 2.191(7) - 2.243(8), av. 2.224 Å], all distances being within the ranges normally found for complexes containing these ligands.<sup>27,51</sup> The observed C(sp<sup>2</sup>)-Ru distance [2.034(7) Å] is similar to the examples noted in Section 1.2.1, as are the differences in the ring C-C bond lengths (see Table 2).

The room temperature reaction of a benzene solution of (29) with dcfe gave us a new route to the synthesis of pure, diamagnetic {Ru[ $\overline{\text{C}=\text{CPhC}(\text{CF}_3)_2\text{C}(\text{CN})_2}$ ](PPh<sub>3</sub>)( $\eta$ -C<sub>5</sub>H<sub>5</sub>)}<sub>2</sub>-{ $\mu$ -(NC)<sub>2</sub>C=C(CF<sub>3</sub>)<sub>2</sub>} (40a). Unit cell parameters for (40a) were in good agreement with the crystallographically-characterized complex.<sup>42</sup> Another isomer, (40b), was isolated using chromatographic procedures different from Swincer's.<sup>42</sup> Isomers (40a) and (40b) do not appear to interconvert in solution, since no extra peaks were observed in the <sup>1</sup>H NMR spectra of (40a) after seven days in a *d*<sup>6</sup>-benzene solution.

The dcfe derivatives are soluble in hydrocarbon solvents, their IR spectra showing only two bands in the  $\nu(\text{CN})$  region, while in Nujol mullscoplex four-band  $\nu(\text{CN})$  patterns were found. The presence of four bands instead of two is probably due to solid-state and/or solution effects.<sup>52</sup>

In the <sup>1</sup>H NMR spectrum of (40a), one  $\eta$ -C<sub>5</sub>H<sub>5</sub> resonance was found at  $\delta$  5.03, demonstrating the equivalence of the two cyclopentadienyl ligands in solution. This is confirmed by the solid-state structure of (40a), which shows the cyclopentadienyl groups in similar environments. Only two CF<sub>3</sub> signals ( $\delta$  -66.0, -66.4) attributable to the cyclobutenyl rings were found in the <sup>19</sup>F NMR spectrum of (40a). This is consistent with the chiral nature of the complex showing that the two cyclobutenyl rings are equivalent in solution and the two CF<sub>3</sub> groups within each cyclobutenyl ring are inequivalent.

Figure 8. PLUTO plot of  $\text{Ru}\{\text{C}=\text{CPhC}(\text{CF}_3)_2\text{C}(\text{CN})_2\}(\text{NCMe})(\text{PPh}_3)(\eta\text{-C}_5\text{H}_5)$  (**29**)  
(by M.R. Snow and E.R.T. Tiekink)



The CF<sub>3</sub> groups on the bridging nitrile had a signal at  $\delta$  -61.5. Similarly, two CF<sub>3</sub> signals were found for the cyclobutenyl CF<sub>3</sub> groups in (40b) at  $\delta$  -65.8 and -66.3, and the bridging ligand at  $\delta$  -59.8. Molecular ions were found in the FAB mass spectra at  $m/z$  1703 for both (40a) and (40b). Oxidation processes were observed for the compounds (40a) and (40b), where [M + O]<sup>+</sup> ions were formed at  $m/z$  1720. The relative abundance of these ions is initially comparable to that of [M]<sup>+</sup>, but increases with time.

The X-ray structure of (40a) is shown in Figure 9 and bond distances are shown in Table 7. The ruthenium atoms again have pseudo-octahedral geometry and the cyclopentadienyl and triphenylphosphine ligands are within normal bonding distances [(Ru(1)-P(1) 2.314(6), Ru(2)-P(2) 2.316(6) Å; Ru-C(cp) 2.20(1) - 2.27(2), av. 2.23 Å]. The observed Ru-C(*sp*<sup>2</sup>) distances [Ru(1)-C(24) 2.07(2); Ru(2)-C(61) 2.01(2) Å] are similar to those for the examples noted in Section 1.2.1. Each ruthenium centre is chiral; both enantiomers of the molecule shown are present in the unit cell. Within the cyclobutenyl groups, the same trends as found in Section 1.2.1 are apparent. The differences in CC distances between the cyclobutenyl rings are within 3 $\sigma$ , the esd's being rather high. The most notable feature of the structure is the presence of the bridging dcfе group. The Ru-N distances [Ru(1)-N(5) 1.98(1); Ru(2)-N(6) 1.98(2) Å] are slightly shorter than that observed for (29) [Ru-N(1) 2.033(6) Å]. This suggests stronger bonding, but because of the large esd's, the differences are not significant.

The reaction of the nitriles acrylonitrile, 1,2,4,5-C<sub>6</sub>H<sub>2</sub>(CN)<sub>4</sub>, C<sub>6</sub>H<sub>4</sub>(CN)<sub>2-*o*</sub> and C<sub>6</sub>F<sub>4</sub>(CN)<sub>2-*p*</sub> with (29) in benzene at room temperature gave the mononuclear complexes (31), (32), (33) and (35), respectively. Partially characterized binuclear complexes were also obtained from the tetrafluoroterephthalonitrile and tetracyanobenzene reactions, spectroscopic data for these being reported in Sections 1.4.17 and 1.4.20. Both mononuclear and binuclear complexes were isolated from the reactions of (29) with the dinitriles *trans*-CH(CN)=CH(CN) and *p*-C<sub>6</sub>F<sub>4</sub>(CN)<sub>2</sub> in benzene. Two isomeric binuclear products, (38a) and (38b), and a mononuclear product, (36), were obtained from the fumaronitrile system. The tetrafluorophthalonitrile reaction gave a mononuclear complex (34) and a binuclear complex (37).

**Figure 9.** PLUTO plot of  $\{\text{Ru}[\text{C}=\text{CPhC}(\text{CF}_3)_2\text{C}(\text{CN})_2](\text{PPh}_3)(\eta\text{-C}_5\text{H}_5)\}_2\text{-}\{\mu\text{-}(\text{NC})_2\text{C}=\text{C}(\text{CF}_3)_2\}$  (40a) (by T.W. Hambley, J.R. Rodgers, and M.R. Snow)

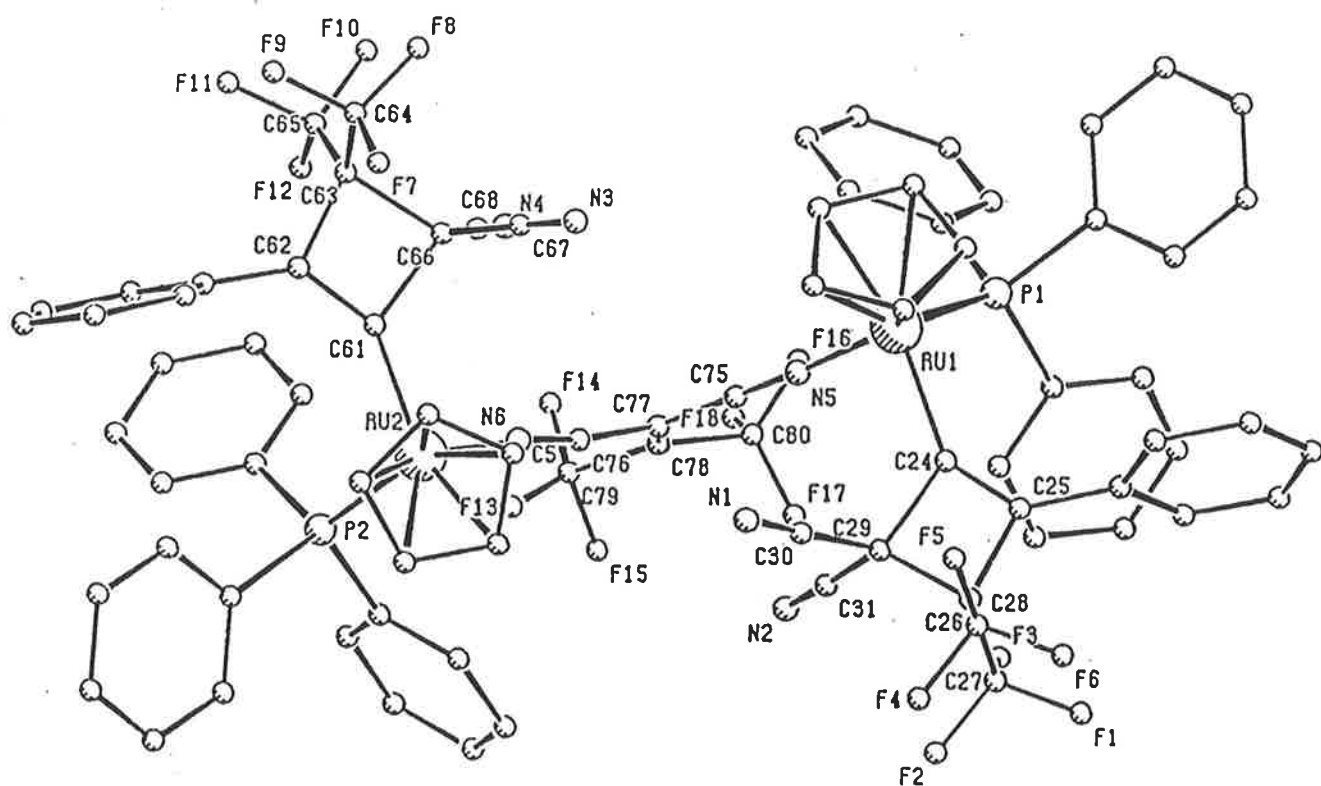
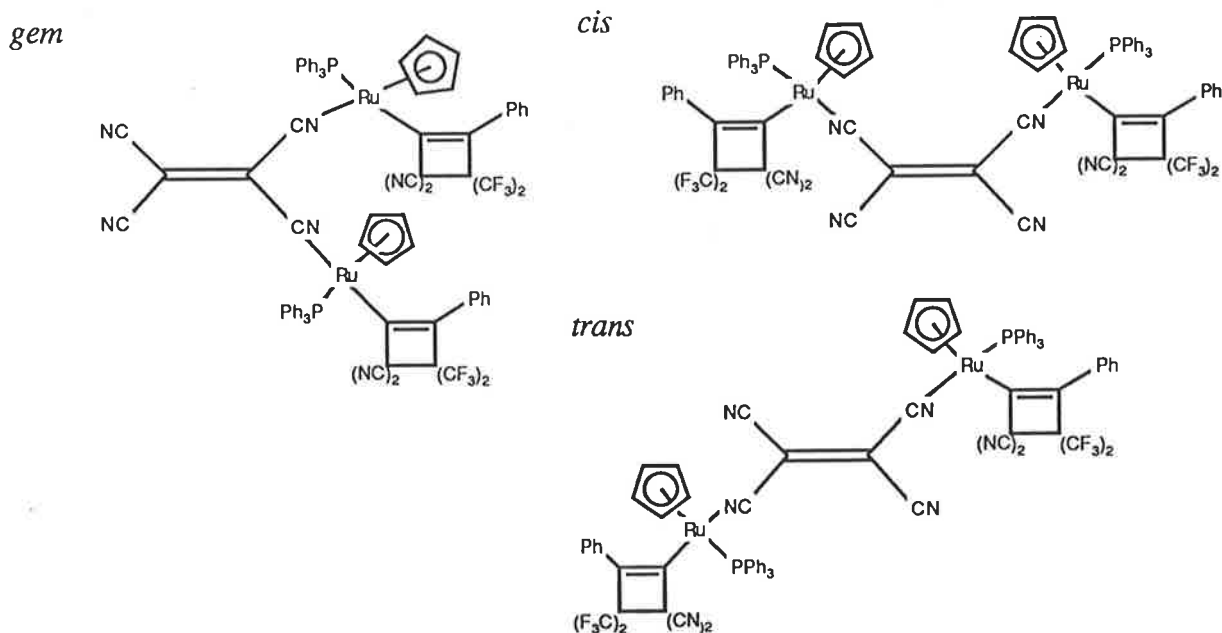


**Table 7.** Selected bond distances (Å) and angles (°) for complex **(40a)**

Ru(1)-P(1)	2.314(6)	Ru(2)-P(2)	2.316(6)
Ru(1)-C(24)	2.07(2)	Ru(2)-C(61)	2.01(2)
C(24)-C(25)	1.30(3)	C(61)-C(62)	1.39(3)
C(25)-C(26)	1.53(3)	C(62)-C(63)	1.55(4)
C(26)-C(29)	1.53(3)	C(63)-C(66)	1.67(4)
C(29)-C(24)	1.60(3)	C(66)-C(61)	1.67(3)
Ru(1)-N(5)	1.98(1)	Ru(2)-N(6)	1.98(2)
N(5)-C(75)	1.17(2)	N(6)-C(76)	1.15(3)
C(75)-C(77)	1.42(3)	C(76)-C(77)	1.41(3)
C(77)-C(78)	1.37(3)	C(78)-C(79)	1.61(4)
C(78)-C(80)	1.57(4)		
C(25)-C(24)-C(29)	91(2)	C(62)-C(61)-C(66)	91(2)
C(24)-C(25)-C(26)	97(2)	C(61)-C(62)-C(63)	99(2)
C(25)-C(26)-C(29)	86(1)	C(62)-C(63)-C(66)	85(2)
C(24)-C(29)-C(26)	86(1)	C(61)-C(66)-C(63)	99(2)
Ru(1)-C(24)-C(25)	143(1)	Ru(2)-C(61)-C(62)	141(2)
Ru(1)-N(5)-C(75)	176(2)	Ru(2)-N(6)-C(76)	172(2)
C(75)-C(77)-C(76)	110(2)	C(79)-C(78)-C(80)	115(2)
N(5)-C(75)-C(77)	177(2)	N(6)-C(76)-C(77)	171(3)
C(75)-C(77)-C(78)	127(2)	C(76)-C(77)-C(78)	123(2)

Only binuclear complexes were isolated from the reaction of tcne with (29), three isomers [(39a), (39b), (39c)] being obtained. The mononuclear and binuclear complexes from these reactions were characterized by microanalysis, FAB mass spectrometry, electrochemistry (see Section 1.2.6) and, where appropriate, by  $^1\text{H}$  and  $^{19}\text{F}$  NMR. The spectral properties of complexes (31) - (36) (see Tables 9 - 12, Section 1.4) are similar to those of (29), and suggest that related structures are likely for these complexes, with a  $\eta^1$ , *N*-bound nitrile ligand attached to the  $\text{Ru}\{\text{C}=\text{CPhC}(\text{CF}_3)_2\text{C}(\text{CN})_2\}(\text{PPh}_3)(\eta\text{-C}_5\text{H}_5)$  core. Similarly, the spectral data for the binuclear complexes (37) - (39) (see Tables 9 - 12, Section 1.4) show that they have structures related to (40a). The alternative isomeric possibilities for the tcne structures are illustrated in Figure 10.

**Figure 10.** Alternative isomeric possibilities for complexes (39a), (39b) and (39c)



In the case of the fumaronitrile and dcfe ligands it is probably not the olefin itself which is responsible for the isomerism, but alternative orientations of the ruthenium centres arising from interactions between the phosphine and cyclobutenyl ligands. For tcne the possibility of *cis*, *trans* and *gem* isomers also exists, as well as for orientational isomerism.

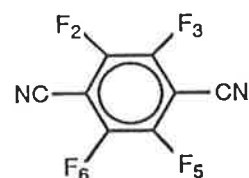
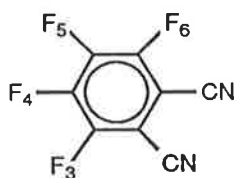
The IR data for the mononuclear complexes (31) - (36) was similar to that of (29). Very weak  $\nu(\text{CN})$  bands were observed between 2220 and 2250  $\text{cm}^{-1}$  for the ring CN groups and medium to strong intensity bands for the nitrile ligands (2170 - 2270  $\text{cm}^{-1}$ ), the more electron-deficient ligands having the lower  $\nu(\text{CN})$  stretching frequencies. The  $\nu(\text{C}=\text{C})$  bands varied in intensity from very weak to strong, with contributions from the double bonds of the nitrile ligands evident in several of the spectra [e.g. 1574s (31), 1590m (36)  $\text{cm}^{-1}$ ]. Strong  $\nu(\text{CF})$  bands were found for all complexes in the range 1088 - 1310  $\text{cm}^{-1}$ . The IR spectra of the binuclear complexes have slightly less intense  $\nu(\text{C}=\text{C})$  bands than their mononuclear counterparts, but are otherwise very similar. The  $\nu(\text{CN})$  bands were shifted to higher frequency (by 2 to 40  $\text{cm}^{-1}$ ) and were fewer in number and/or had smaller line widths (indicative of fewer overlapping bands) than the mononuclear derivatives.

An examination of the stronger  $\nu(\text{CN})$  bands (2200 - 2010  $\text{cm}^{-1}$ ) for the binuclear complexes has suggested a correlation between the number of bands observed and the symmetry of the products. For the isomers of (38), the one-band pattern suggests a highly symmetrical orientation of the two  $\text{Ru}\{\text{C}=\text{CPhC}(\text{CF}_3)_2\text{C}(\text{CN})_2\}(\text{PPh}_3)(\eta\text{-C}_5\text{H}_5)$  groups. In the case of the tcne derivatives, two of the isomers [(39a) and (39b)] have a two-band pattern, while the third isomer (39c) has a one-band pattern. It seems likely that the third isomer has a *trans* symmetry similar to the isomers of (38).

Cyclopentadienyl resonances were observed in the  $^1\text{H}$  NMR spectra of complexes (31) - (36) (see Table 11, Section 1.4). As expected, the effect of increasing the electron deficiency of the nitrile ligands was to shift the cyclopentadienyl resonance downfield [e.g.  $\delta$  4.82  $(\text{NC})\text{C}_6\text{H}_2(\text{CN})_3$  and  $\delta$  4.82  $(\text{NC})\text{C}_6\text{F}_4(\text{CN})\text{-}o$ , versus  $\delta$  4.41  $\text{NCMe}$ ]. Also observed for all the complexes were phenyl resonances in the range  $\delta$  7.6 - 6.4. A mononuclear formulation was assigned to (36) on the basis of the  $^1\text{H}$  NMR spectrum: signals were found for the two CH groups in the fumaronitrile ligand and for the cyclopentadienyl group at  $\delta$  6.03, 5.49 and 4.56, respectively (relative intensities 1:1:5). This formulation was supported by microanalytical results. Complex (31) had  $^1\text{H}$  NMR signals assigned to the  $\text{CH}(\text{CN})$  ( $\delta$  5.74) and  $\text{CH}_2=$  ( $\delta$  5.55) protons of the acrylonitrile ligand, and the  $\eta\text{-C}_5\text{H}_5$  group ( $\delta$  4.50); these

signals had intensities in the ratio 1:1:5. The  $^1\text{H}$  NMR spectra of the binuclear compounds were similar to that of (40a), and show that the two cyclopentadienyl ligands in each complex are equivalent in solution. Integration of the  $\text{CH}:\text{C}_5\text{H}_5$  signals (2:10) for each of the isomers of (38) confirmed their binuclear formulations.

The fluorine NMR spectra showed that the  $\text{CF}_3$  groups in all the complexes are inequivalent, with two quartets for each complex found between  $\delta$  -65.7 and -66.5. As noted above, this is indicative of a chiral metal centre which creates different CF environments on either side of the cyclobutenyl ring. Complex (35) was shown to have a mononuclear formulation by comparison of the two  $\text{CF}_3$  quartets ( $\delta$  -66.1 and -66.4), with the signals observed at higher field for the  $\text{C}_6\text{F}_4(\text{CN})_2$  ligand (intensities 3:3:4). Comparison of the signals for the fluorines in the coordinated nitrile and in the free ligand ( $\delta$  -130.6),<sup>53</sup> showed that  $\text{F}_2$  and  $\text{F}_6$  are inequivalent ( $\delta$  -130.5, -131.4) and are shifted upfield slightly, while  $\text{F}_3$  and  $\text{F}_6$  are deshielded ( $\delta$  -128.7). The spectrum of (34) showed signals for the  $\text{CF}_3$  groups in the normal region ( $\delta$  -66.1, -66.4) while the nitrile ligand displayed signals for  $\text{F}_3$  and  $\text{F}_6$  ( $\delta$  -127.3, -128.3) and for  $\text{F}_4$  and  $\text{F}_5$  ( $\delta$  -142.0, -144.5). The signals observed for the fluoronitrile ligands in (34) and (35) result from fluorine-fluorine (including cross-ring) coupling and from coupling to phosphorus: the expected  $\text{AA}'\text{XX}'\text{Y}$  systems<sup>54</sup> were not fully resolved. The  $^{19}\text{F}$  spectra of complexes (37) - (39) were similar to those of (40) (see Table 11, Section 1.4). The tetrafluorophthalonitrile derivative (37) was given a binuclear formulation by comparison of the  $\text{CF}_3$  and  $\text{C}_6\text{F}_4$  integrals (6:6:4). Two doublets were observed for the  $\text{C}_6\text{F}_4(\text{CN})_2$  group at  $\delta$  -128.7 and -145.5 ( $J_{\text{av}} = 13$  Hz). These have been assigned to  $\text{F}_3, \text{F}_6$  and  $\text{F}_4, \text{F}_5$  respectively. The binuclear complex formed from the reaction of tetrafluoroterephthalonitrile with (29) showed the integrals 6:6:4 for the  $\text{CF}_3$  to  $\text{C}_6\text{F}_4$  groups. The signal for the  $\text{C}_6\text{F}_4$  group was a doublet at  $\delta$  -132.7 ( $J = 14$  Hz), which is again upfield from the free ligand ( $\delta$  130.6) and demonstrates that all fluorines are equivalent. A small difference in chemical shifts between the mononuclear and binuclear complexes of a given series was noted, the shifts for the mononuclear fluoronitrile ligands being at a lower field (1 - 2 ppm) than those of the binuclear complexes.



The fast atom bombardment spectra for the mononitrile complexes are somewhat confusing, as ion/molecule aggregates are formed at higher mass. The principal aggregate  $[M_2 - \text{nitrile}]^+$  appears to be formed by intermolecular association. This illustrates the problems that are faced in assigning molecular ions in complexes containing relatively labile ligands. The FAB mass spectra of the binuclear complexes showed weak molecular ions and fragmentation patterns similar to the mononuclear derivatives. An ion  $[M - \text{C}=\text{CPhC}(\text{CF}_3)_2\text{C}(\text{CN})_2]^+$  was found only in the binuclear complexes. The ion  $[M - \text{nitrile} - \text{dcfe}]^+$  ( $m/z$  530), characteristic of the presence of a dcfe-cyclobutenyl ring (see Section 1.2.1), was found in the spectra of all the mononuclear and binuclear complexes.

In all spectra, ions were also found at  $m/z$  1488 and  $m/z$  744. The high mass ion was assigned to  $[\{\text{Ru}[\text{C}=\text{CPhC}(\text{CF}_3)_2\text{C}(\text{CN})_2](\text{PPh}_3)(\text{C}_5\text{H}_5)\}_2]^+$ , which shows a significant fragmentation, with loss of  $\text{PPh}_3$  and  $\overline{\text{C}=\text{CPhC}(\text{CF}_3)_2\text{C}(\text{CN})_2}$ . The ion at  $m/z$  744 was assigned to  $[\text{Ru}\{\overline{\text{C}=\text{CPhC}(\text{CF}_3)_2\text{C}(\text{CN})_2}\}(\text{PPh}_3)(\text{C}_5\text{H}_5)]^+$ , which has the same formulation as the molecular ion of the allyl complex (25). Fragments from the  $m/z$  744 peak result from the loss of  $\text{CN}$  and  $\text{CF}_3$ . The remaining peaks in the spectra result from the usual fragmentation of  $\text{Ru}(\text{PPh}_3)(\eta\text{-C}_5\text{H}_5)$ ,<sup>55</sup> with breakdown and loss of the phosphine groups and the cyclopentadienyl ligand.

In solution, the nitrile compounds show intense colours which range from red (35) through yellow (29) to dark blue (32). The electronic absorption spectra for (29) - (40) and complexes (30) and  $\text{RuCl}(\text{PPh}_3)_2(\eta\text{-C}_5\text{H}_5)$  (41) have common features. Strong peaks are present at around 234 nm (with shoulders at 286 and 336 nm, not resolved in all cases), which have been ascribed to intraligand transitions associated with the  $\text{Ru}(\text{PPh}_3)(\eta\text{-C}_5\text{H}_5)$  core and, where appropriate, with the nitrile groups. For complexes with electron-deficient nitrile ligands containing unsaturated substituents, two charge-transfer absorptions were observed in the range 400 - 1000 nm. These are presumably MLCT transitions,  $\text{Ru}(\text{II}) \rightarrow \text{nitrile} (d_\pi \rightarrow p_\pi^*)$ .<sup>56</sup> The two CT bands observed for each binuclear complex were found at lower energy (30 - 80 nm) than those of the related mononuclear complexes. This is in accordance with results obtained by Peterson *et al.* for the luminescent complexes  $\{[\text{RuL}_2]_m(\text{dpp})\}$

[L = phen, bpy; m = 1 - 2; dpp = 2,3-bis(2-pyridyl)pyrazine].<sup>56</sup> They found the Ru(II)  $\rightarrow$  dpp transition was shifted to lower energy (71 nm) when the ligand was bridging, as a result of stabilization of the  $\pi^*$ -acceptor orbital on dpp.

Lower energy shifts in the CT bands were found for the most electron-deficient nitriles [546, 644 (32); 470, 510 (34); 484, 534 nm (35)]. The position of the CT bands for the binuclear compounds also reflected the nature of the ligand [tcne 646, (> 900) nm (39a) > dcfe 560, 770 nm (40a) > tetrafluoroterephthalonitrile 562, 586 nm (see Section 1.4.20) > tetrafluorophthalonitrile 506, 552 nm (37)  $\approx$  fumaronitrile 492, 548 nm (38b)]. This pattern could not be related directly to donor strengths but the observed lowering in the energy of the nitrile  $\pi^*$ -acceptor orbitals (hence lower energy absorption) with the more electron-withdrawing groups is as expected. The maxima of the first CT absorption for the isomers of (39) was found between 634 and 646 nm, while the second absorption had maxima greater than 900 nm.

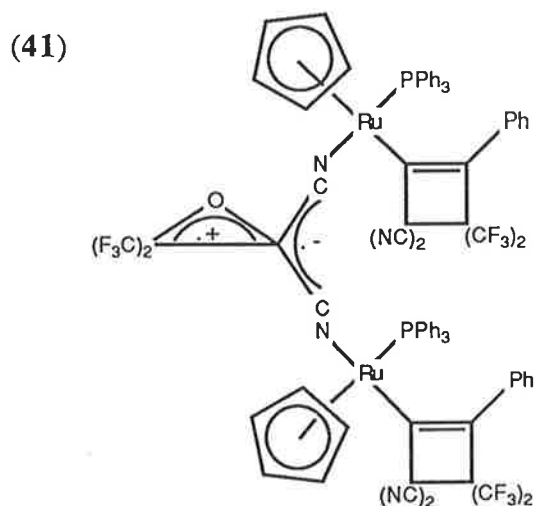
All the reactions of the nitriles with (29) were performed with  $\approx$  1:1 stoichiometry. In cases where binuclear complexes were formed, the same products were obtained when an excess of reactant (29) was used, but the reactions did not go to completion. The nitriles used were chosen to evaluate the effects of (a) increasing the number of the nitrile sites available, (b) changing the steric requirements at the sites and (c) varying the electronic properties of the nitrile. Examples of structurally characterized RuX(PPh<sub>3</sub>)<sub>2</sub>( $\eta$ -C<sub>5</sub>H<sub>5</sub>) complexes [X = C(CN)<sub>3</sub>, C(CN)<sub>2</sub>C(CN)C(CN)<sub>3</sub>], containing *N*-bound tricyanomethanide and pentacyanopropenide anions have been described.<sup>57,58</sup> Related manganese complexes {Mn(CO)<sub>2</sub>( $\eta$ -C<sub>5</sub>H<sub>4</sub>Me)}<sub>n</sub>X (X = tcne, terephthalonitrile, tetrafluoroterephthalonitrile, n = 1 - 4) which contain bridging or terminal nitrile ligands have been synthesized by Kaim and Gross.<sup>59</sup> A binuclear complex was formed from tetrafluoroterephthalonitrile, whereas the product obtained using terephthalonitrile was a mononuclear derivative. The difference in reactivity was related to tetrafluoroterephthalonitrile being a stronger  $\pi$ -acceptor ligand. Previous work by Wallis *et al.*<sup>53</sup> had led to the synthesis of several cationic mononuclear derivatives of [Ru(PPh<sub>3</sub>)<sub>2</sub>( $\eta$ -C<sub>5</sub>H<sub>5</sub>)L]<sup>+</sup> [L = MeCN, CH<sub>2</sub>=CHCN, C<sub>6</sub>H<sub>4</sub>(CN)<sub>2-*o*</sub>, C<sub>6</sub>F<sub>4</sub>(CN)<sub>2-*o*</sub>] as well as to the bridged binuclear

compounds  $[\{\text{Ru}(\text{PPh}_3)_2(\eta\text{-C}_5\text{H}_5)\}_2\text{L}]^{2+}$  [ $\text{L} = \text{C}_6\text{F}_4(\text{CN})_{2-p}, \text{C}_6\text{H}_4(\text{CN})_{2-m}, \text{NC}(\text{CH}_2)\text{CN}$ ]. The formation of the binuclear complexes was favoured when the nitrile groups were in a near-linear arrangement, which minimized interactions between the bulky  $\text{PPh}_3$  groups on the two metal centres.

The synthesis of (29) works successfully because the small acetonitrile ligand readily replaces one of the bulky triphenylphosphine ligands. Molecular modelling of complex (17) has shown that there are mutual interactions between the two triphenylphosphine ligands, as well as with the cyclobutenyl phenyl substituent and the  $\text{CF}_3$  groups. Loss of phosphorus ligands is not a feature of the chemistry of the related complexes  $\text{RuX}(\text{PR}_3)_2(\eta\text{-C}_5\text{H}_5)$  [ $\text{R} = \text{Me}, \text{OMe}; \text{X} = \text{Cl}, \text{C}_2\text{Ph}, \overline{\text{C}=\text{CPh}(\text{CN})_2\text{C}(\text{CN})_2}$ ].<sup>60,61</sup> This is to be expected, as the cone angles of these *P*-donor ligands [ $\text{PMe}_3$  118°,  $\text{P}(\text{OMe})_3$  107°] are considerably smaller than that of  $\text{PPh}_3$  (145°).

Two green complexes were also discovered in the reactions of (29) [or (30)] with dcf; these were found to be isomers of the oxygen adduct  $\{\text{Ru}[\overline{\text{C}=\text{CPhC}(\text{CF}_3)_2\text{C}(\text{CN})_2}](\text{PPh}_3)(\eta\text{-C}_5\text{H}_5)\}_2\{\mu\text{-}(\overline{\text{NC})_2\text{CC}(\text{CF}_3)_2\text{O}}\}$  (42a) and (42b), formed by oxidation of (40a) and (40b) respectively. The analytical and FAB mass spectrometric results confirm the dimeric structure of (42b); (42a) has properties similar to (42b), but reliable analyses were not obtained. In the IR spectra of (42a) and (42b), the  $\nu(\text{CN})$  region contained a two-band pattern. The upper band is at higher frequency than the corresponding bands in either (40a) or (40b). As these strong  $\nu(\text{CN})$  bands are assigned to the *N*-bound nitrile it is clear that the oxidation has taken place at the bridging group. No absorptions assignable to  $\nu(\text{OH})$  were found in the IR spectra of the two isomers of (42). These compounds had fingerprint regions similar to (40a) and (40b), but the  $\nu(\text{C}=\text{C})$  bands were less intense. Molecular ions were found in the FAB mass spectra at  $m/z$  1720 for (42a) and (42b), the fragmentation patterns being similar to the other binuclear complexes mentioned previously. The proton NMR spectra of (42a) and (42b) were nearly featureless, with only very weak, broad resonances being found in the phenyl region. The reduction process observed for the dcf ligand (see Section 1.2.6) in complexes (40a) and (40b) was completely absent from (42b). It seems likely that this reduction

process is associated with the LUMO localized on the ligand, which in turn suggests that the LUMO on the bridging group has either been raised in energy or changed in character altogether in the transformation from (40) to (42). From these results it appears that addition of 'O' to the bridging group in (40) has removed the  $\pi$ -system and a radical cation has been formed, this having an oxidation potential outside the solvent window. A structure involving an epoxide diradical group is consistent with these observations. Ready oxidation of free cyanolefins e.g. tcne, by  $\text{H}_2\text{O}_2$  has been described and proceeds to give epoxides.<sup>62</sup>



The ESR spectra of (40a), (40b) and both isomers of (42) all show the same broad signal (31G peak to peak linewidth) at  $g$  2.038. This was investigated further and found to be the result of small amounts of the isomers of (42) being present in solutions of (40a) or (40b), even after chromatography. Partial conversion of (40a) to (42a) and of (40b) to (42b) took place over four days in benzene solutions under  $\text{O}_2$ . The conversion of (40a) to (42a) (major amount) and (42b) (minor amount) was also facilitated by supporting the complex on silica. A possibility that a catalytic route may be involved in the syntheses of (42a) and (42b) is supported by the increased conversion of (40a) to (42a) and (42b) on silica. These results suggest that the paramagnetic species are the two isomers of (42). Small amounts of these isomers are always present in solutions of (40a), explaining the anomalously low value of unpaired electrons observed by Swincer for (40a).<sup>42</sup>

### 1.2.6. Electrochemistry

It was decided to undertake an electrochemical study of the nitrile complexes to see if the number of couples observed and their  $E_{1/2}$  values could be used to determine whether the complexes formed were mononuclear or binuclear. Recent investigations<sup>63-65</sup> have shown that the redox chemistry of  $\text{Ru}(\text{R})(\text{L})_2(\eta\text{-C}_5\text{R}'_5)$  compounds (where  $\text{R} = \text{C}_2\text{Ph}, \text{C}_2\text{Bu}^t, \text{Me}, \text{CH}_2\text{Ph}, \text{Cl}$ ;  $\text{L} = \text{CO}, \text{PPh}_3$ ;  $\text{L}_2 = \text{dppe}$ ;  $\text{R}' = \text{H}, \text{Me}$ ) is characterized by the one-electron oxidation process  $\text{Ru}(\text{II}) \rightarrow \text{Ru}(\text{III})$ . For the  $\text{C}_5\text{H}_5$  complexes, this process is quasi-reversible and occurs at around 0.5 V. Our results for  $\text{Ru}(\text{C}_2\text{Ph})(\text{PPh}_3)_2(\eta\text{-C}_5\text{H}_5)$  (**30**) agree well with those reported by Bitcon and Whiteley,<sup>63</sup> which are for a quasi-reversible process occurring at  $E_{1/2} = 0.60$  V (0.56V corrected for  $\text{FeCp}_2/\text{FeCp}_2^+$  couple), (Lit.<sup>63</sup> 0.56 V). We also looked at the oxidation process observed for  $\text{RuCl}(\text{PPh}_3)_2(\eta\text{-C}_5\text{H}_5)$  (**41**) which had an  $E_{1/2} = 0.74$ V, and found that this was near-reversible but was not diffusion-controlled.

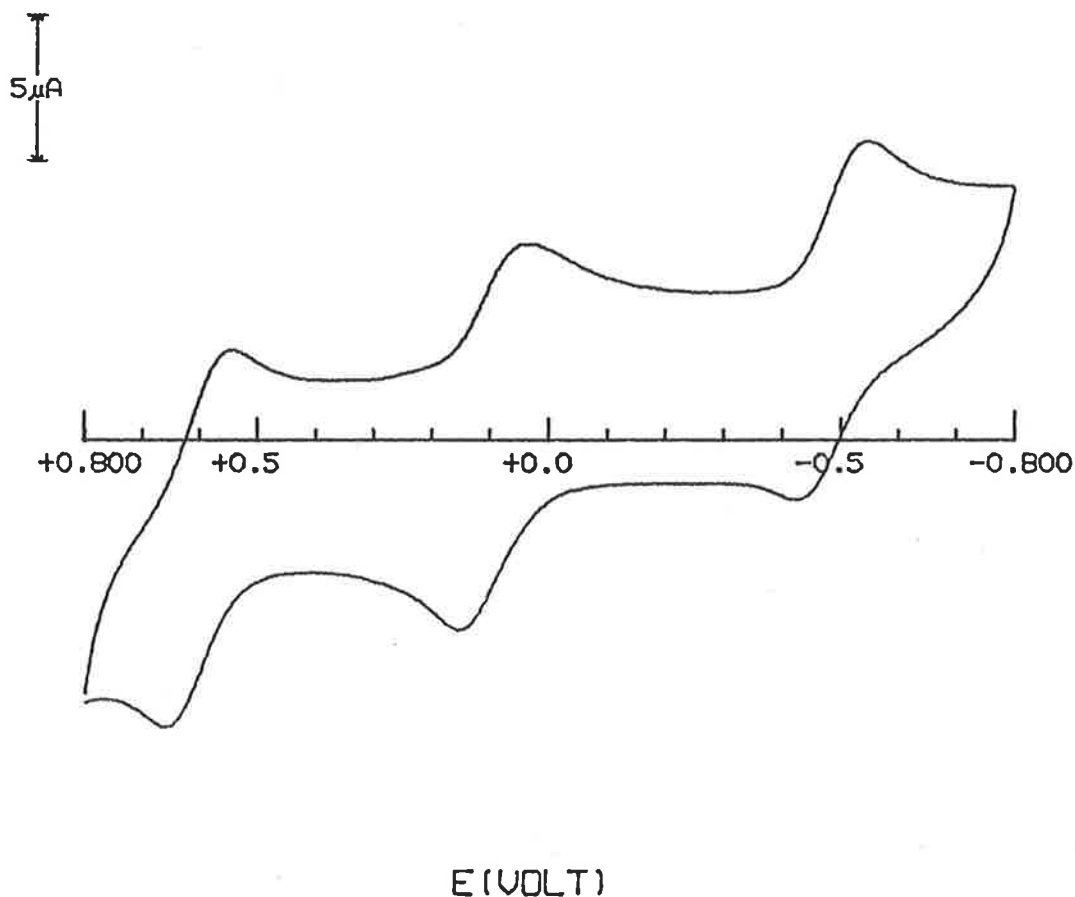
The cyclobutenyl and nitrile ligands shift the  $\text{Ru}(\text{II}) \rightarrow \text{Ru}(\text{III})$  couple to 0.89 V for (**29**) and 0.87 V for (**31**). Higher oxidation potentials were observed when the more deficient nitrile ligands were present:  $E_{1/2}$  1.07 (**32**), 0.95 (**33**), 1.07 (**34**), 1.05 (**35**) and 0.97 V (**36**) (see Table 13, Section 1.4). The chemical reversibility of the processes in (**29**) and (**34**) suggests that it might be possible to modify the environment of the ruthenium with substituents other than  $\text{C}_5\text{Me}_5$ ,<sup>63</sup> to obtain relatively stable 17-electron  $\text{Ru}(\text{III})$  radical cations. Related 17-electron  $\text{Fe}(\text{III})$  cations have been characterized for several  $\text{FeRL}_2(\eta\text{-C}_5\text{H}_5)$  complexes ( $\text{L} = \text{CO}, \text{PPh}_3$ ;  $\text{L}_2 = \text{dppe}$ ;  $\text{R} = \text{Cl}, \text{Br}, \text{H}, \text{Me}$ ),<sup>66,67</sup> but not for the ruthenium analogues investigated.<sup>64</sup> The oxidation processes observed for the other mononuclear compounds were either quasi- or near-reversible and, in some instances, were diffusion-controlled [(**32**), (**33**) and (**34**)].\*

\* The criterion for diffusion control was  $\frac{i^p}{\sqrt{v}} = \text{constant}$ , with variation of  $v$  between 50 and 500  $\text{mV s}^{-1}$ .

Criteria for reversibility in CV (given for an oxidation process):  $\frac{i^{\text{pa}}}{i^{\text{pc}}} = 1.0$  reversible;  $\frac{i^{\text{pa}}}{i^{\text{pc}}} < 1.2$  near-

reversible;  $i^{\text{pa}} > i^{\text{pc}}$  quasi-reversible; no apparent cathodic peak irreversible.

Figure 11. Cyclic voltammogram of complex (40a) ( $200 \text{ mV s}^{-1}$ ) in  $\text{CH}_2\text{Cl}_2$ .



The electrochemistry of complexes (37) - (42b) is summarized in Table 13 (Section 1.4). Using square wave voltammetry, two oxidation processes were measured in each complex, confirming that they are all binuclear. As an example, the CV spectrum of complex (40a) is shown in Figure 11. The cyclic voltammetry results for (37) did not resolve the two processes, which appeared as one two-electron process. Most of these processes were quasi-reversible, although those of (40a), (40b) and (42b) were fully reversible. The oxidation potentials for (42b) [ $E_{1/2}$  0.10, 0.66 V] were in good agreement with those found for the isomers of (40) [ $E_{1/2}$  0.13, 0.67 V (40a); 0.10, 0.67 V (40b)], confirming a related binuclear structure for (42b).

Reduction processes associated with the nitrile ligand were found for (32) - (36). In general, the reduction of the coordinated ligand took place at more negative potential than that observed for the free ligand (see Tables 13 and 14, Section 1.4). For (32) and (35), the reduction processes were chemically reversible. In contrast, those of the free ligands were quasi-reversible. It appears that the metal stabilizes the radical anion associated with the nitrile ligand by charge delocalization. The other mononuclear complexes show irreversible behaviour for the reduction process. A comparison of CV and SW voltammetric currents for the first reduction of (32) with those of the oxidation of ferrocene under stirred conditions<sup>64,65</sup> suggested that this was a one-electron process. The diffusion coefficient for (32) appears to be only slightly smaller than that of ferrocene ( $i_p \propto D^{1/2}$ ), which is somewhat unexpected. Comparison of the Ru(II)  $\rightarrow$  Ru(III) oxidation<sup>65</sup> with the first reduction process helps to confirm that the reduction involves a one-electron transfer.

For the binuclear compounds other than (37), the ratio of the number of electrons involved in the reduction to those involved in the two oxidation processes was 1:1:1. For (37), the ratio was 1:2. The reduction processes observed for (37) - (40) were either quasi-reversible or irreversible and took place at the same or at slightly more negative potentials than those of the free ligands. Little difference was found between the oxidation and reduction potentials of related mononuclear and binuclear complexes, the variations being within the scale of experimental error.

### 1.3. Conclusions

The (2 + 2) cycloaddition reactions between dcfe and transition-metal  $\sigma$ -acetylides gave cyclobutenyl, butadienyl and allylic complexes. In all cases, the dicyanomethylene group became attached to the  $\alpha$ -carbon of the acetylide. This direction of addition appears to be favoured because of charge delocalization on the dicyano groups stabilizing the proposed dipolar intermediate. Addition of dcfe in the opposite direction would result in significant  $\text{CF}_3/\text{PPh}_3$  interactions. Hydrolysis of the cyclobutenyl derivative (13) in the presence of  $\text{Me}_3\text{NO}\cdot 2\text{H}_2\text{O}$  was found to give (27), which contains the unusual  $\text{W}-\text{N}(\text{H})=\text{C}(\text{OH})-\text{C}=\text{C}$  chelate ring.

An acetonitrile-cyclobutenyl complex (29) was formed by treating the bis-triphenylphosphine complex (17) with acetonitrile. This reaction was probably driven by the replacement of the bulky  $\text{PPh}_3$  with the smaller MeCN ligand. Displacement of the acetonitrile ligand in (29) by other nitriles has allowed a number of mononuclear and binuclear nitrile-substituted cyclobutenyl complexes to be synthesized. The reaction of (29) with dcfe gave the binuclear complex (40a), which had been synthesized earlier by Swincer.<sup>42</sup> Complex (40a) was then thought to be paramagnetic, even though an X-ray structure determination suggested otherwise. We have found that small amounts of the proposed epoxy radical species (42a) and (42b), formed by the oxidation of (40a), were invariably present in solutions of (40a).

Electrochemical studies were carried out on each of the nitrile complexes to determine whether they were mononuclear or binuclear. The presence of two metal-centred oxidation processes confirmed the formulation as a binuclear complex, while the presence of only one indicated that it was mononuclear. For the complexes containing the nitriles MeCN, dcfe and *ortho*- $\text{C}_6\text{F}_4(\text{CN})_2$ , the oxidation processes were reversible, which implies that it should be possible to isolate stable 17-electron species by modifying the ligands attached to the ruthenium.

## 1.4. Experimental

**General conditions.** All reactions were performed under nitrogen using dried, degassed solvents; no special precautions were taken to exclude air during workup since most complexes proved to be stable in air as solids and for short times in solution. The nitrogen used was high purity grade (Commonwealth Industrial Gases). Solvents used for chromatography were LR grade; spectroscopic grade solvents were used for spectroscopy; all other solvents used were AR grade and/or were dried and distilled under a nitrogen atmosphere.<sup>68</sup> The petroleum spirit used was a fraction of b.p. 62-66 °C. In the text, 'removal of solvent under reduced pressure' or 'evaporated to dryness' refer to the use of a Buchi rotary evaporator and 'removal of solvent under vacuum' refers to the use of a rotary pump and a trap cooled to -196 °C.

*Melting points :* Melting points were measured in sealed capillaries using a Gallenkamp melting point apparatus and are uncorrected.

*Chromatography:* Flash chromatography was performed under N<sub>2</sub>, using a water-jacketed 15 x 350 mm column with silica (200-325 Mesh, AJAX) or florisil (60-100 Mesh, BDH) as adsorbents. Thin layer chromatography (TLC) was performed on 20 x 20 cm glass plates using a 0.5 mm thick silica adsorbent (60 GF<sub>254</sub>, Merck).

*Photochemistry:* Photochemical reactions were carried out using the following UV sources: Applied Photophysics 16W LP, 400W MP or Phillips 100W HP Hg lamps in quartz immersion wells.

*Pressurized Reactions:* A large autoclave (1L, Baskerville & Lindsay) was used for reactions up to 250 atm. For reactions at less than 80 atm, a small autoclave (Roth, 100 mL) equipped with Teflon gaskets and a glass liner was used. Low-pressure syntheses were performed in thick-walled Carius tubes fitted with Rotaflow high-vacuum taps. The Carius tubes were heated in a Gallenkamp tube oven.

*Analyses:* Microanalyses were performed by the Canadian Microanalytical Service, New Westminster, British Columbia, Canada. Electron microprobe analyses were by the Electron Optical Service, University of Adelaide.

*Molecular modelling:* Molecular modelling was performed using the CHEM-3D program for Apple Macintosh computers, Cambridge Scientific Computing (1987). The covalent radii, bond distances and angles were those found in the CHEM-3D parameters set. They were modified where necessary to values obtained from crystallographic data.

### **Instrumentation.**

*IR:* Perkin-Elmer 683 double-beam and Perkin-Elmer 1720X FT spectrometers, NaCl optics, calibrated using polystyrene absorption at  $1601.4\text{ cm}^{-1}$ .

*NMR:* Bruker CXP 300 ( $^1\text{H}$  NMR at 300.13 MHz,  $^{19}\text{F}$  NMR at 282.35 MHz,  $^{31}\text{P}$  NMR at 121.49 MHz,  $^{13}\text{C}$  NMR at 75.47 MHz) and Bruker WP 80 ( $^1\text{H}$  NMR at 80 MHz,  $^{13}\text{C}$  NMR at 20.1 MHz) spectrometers. Chemical shifts (300 K) to low field are denoted positive; the internal references were  $\text{SiMe}_4$  ( $^{13}\text{C}$  and  $^1\text{H}$  NMR) and  $\text{CFCl}_3$  ( $^{19}\text{F}$ ); the external reference for  $^{31}\text{P}$  NMR was 0.1M HCl/0.01M  $\text{H}_3\text{PO}_4$  in  $\text{D}_2\text{O}$  ( $\delta +0.8$  ppm). The shifts quoted for the  $^{31}\text{P}$  NMR spectra are relative to 85%  $\text{H}_3\text{PO}_4$ . With spectra recorded in non-deuterated solvents  $\text{D}_2\text{O}$  in a concentric tube was used for the field lock.

*ESR:* Varian E.P.R. E-9 spectrometer operating in the X-band;  $\text{dpph}$  was used as a 'g-marker'.

*Electronic spectra:* Electronic spectra were recorded on a Hewlett-Packard 8452A diode array spectrometer, using a 1cm quartz cell.

*Mass spectra:* FAB mass spectra were obtained on a VG ZAB 2HF instrument equipped with a FAB source. Argon or xenon were used as FAB gases, with source pressures typically  $10^{-6}$  bar; the FAB gun voltage was 7.5 kV, current 1 mA. The ion-accelerating potential was 7 kV. The complexes were made up as  $\approx 0.5$  M solutions in  $\text{CH}_2\text{Cl}_2$ ; a drop was added to a

drop of matrix (3-nitrobenzyl alcohol), and the mixture was applied to the FAB probe tip. Spectra are reported below in the form:  $m/z$ , assignment, relative intensity; multi-isotopic species are normalized on the most abundant metal isotope ( $^{56}\text{Fe}$ ,  $^{58}\text{Ni}$ ,  $^{102}\text{Ru}$ ,  $^{184}\text{W}$ ). All metal-containing ions with relative intensities greater than 10% of the base peak are listed as well as assigned minor ions. Peaks marked with an asterisk are the strongest of multiplets related to the assigned formulation by addition or loss of one or two H atoms. Most of the spectra were recorded within two minutes of sample introduction to avoid decomposition and/or side reactions. EI MS were obtained on a GEC-Kratos MS3074 mass spectrometer (70 eV ionizing energy, 4 kV accelerating potential).

*Electrochemistry:* Electrochemical analyses were performed using a BAS-100 electrochemical analyser with a cell containing Pt-disc (Bioanalytical Systems) working, Pt-wire counter and SCE reference electrodes. The reference electrode was separated from the cell by a bridge containing electrolyte, which was fitted with a fine glass frit. A 0.1M solution of  $[\text{NBu}_4][\text{BF}_4]$  in  $\text{CH}_2\text{Cl}_2$  was used as the supporting electrolyte and the concentration of compounds was approximately  $2 \times 10^{-4}$  M. Spectra were recorded at 25 °C and all potentials are in V relative to SCE, at which  $E_{\text{p}}^{\text{ox}}$  for  $\text{Fe}(\text{cp})_2$  was at 0.60 V (differential pulse).

The CV peaks listed were recorded at a scan rate of 200  $\text{mV s}^{-1}$ . The criterion for diffusion control was  $\frac{i_{\text{p}}}{\sqrt{v}} = \text{constant}$ , with variation of  $v$  between 50 and 500  $\text{mV s}^{-1}$ . Criteria for reversibility (given for an oxidation process):  $\frac{i_{\text{pa}}}{i_{\text{pc}}} = 1.0$  reversible;  $\frac{i_{\text{pa}}}{i_{\text{pc}}} < 1.2$  near reversible;  $i_{\text{pa}} > i_{\text{pc}}$  quasi-reversible; no apparent cathodic peak irreversible. For a multi-process CV scan, the ratio of the peak current for the process being measured to that of the process with the smallest peak current, was expressed as an integer value,  $n_{\text{rel}}$ . The number of electrons,  $n_{\text{meas}}$ , involved in a SW process was determined by comparison with  $\text{Fe}(\text{cp})_2/\text{Fe}(\text{cp})_2^+$  under stirred voltammetry conditions. Square wave parameters: sweep width amplitude 25 mV, frequency 15 Hz, step E 4 mV; sweeps were performed in a negative direction  $+1.50 \rightarrow -1.50$  V. Differential pulse parameters: pulse amplitude 50 mV, pulse width 60 ms, pulse period 1000 ms; sweeps were performed in a negative direction at 4  $\text{mV s}^{-1}$ .

**Starting Materials.** Literature methods were used to prepare  $W(C_2Ph)(CO)_3(\eta-C_5H_5)$ ,<sup>69</sup>  $Fe(C_2Ph)(CO)_2(\eta-C_5H_5)$ ,<sup>69</sup>  $Ni(C_2Ph)(PPh_3)(\eta-C_5H_5)$ ,<sup>69</sup>  $Mn(C_2Ph)(CO)_3(dppe)$ ,<sup>70</sup>  $Ru(C_2Ph)(CO)(PPh_3)(\eta-C_5H_5)$ ,<sup>71</sup>  $Ru(C_2Ph)(dppe)(\eta-C_5H_5)$ ,<sup>71</sup>  $Ru(C_2Ph)(PPh_3)_2(\eta-C_5H_5)$ ,<sup>71</sup>  $Ru(C_2Me)(PPh_3)_2(\eta-C_5H_5)$ <sup>71</sup> and  $C(CN)_2=C(CF_3)_2$  (dcfe)<sup>46</sup>. The other nitriles and  $Me_3NO \cdot 2H_2O$  (Aldrich) were commercial samples and were used as received.

## Syntheses

### Syntheses of cyclobutenyl complexes

#### 1.4.1. $W\{\overline{C=CPhC(CF_3)_2C(CN)_2}\}(CO)_3(\eta-C_5H_5)$ (13)

A solution of  $W(C_2Ph)(CO)_3(\eta-C_5H_5)$  (250 mg, 0.57 mmol) and dcfe (160 mg, 0.75 mmol) in  $CH_2Cl_2$  (30 mL) was stirred in the dark for 45 min. The volume was then reduced (to 5 mL, HV) and a mixture of EtOH (2 mL) and petroleum spirit (5 mL) added. Further reduction in volume and cooling resulted in the formation of a yellow precipitate. The solution was syringed off and the precipitate washed with petroleum spirit and dried under vacuum. Chromatography of the product (TLC: petroleum spirit/acetone 5:2) separated a major yellow band ( $R_f$  0.55) from four yellow-orange bands. Crystallization of the major product ( $CH_2Cl_2$ /petroleum spirit) yielded yellow crystals of  $W\{\overline{C=CPhC(CF_3)_2C(CN)_2}\}(CO)_3(\eta-C_5H_5)$  (13) (330 mg, 0.49 mmol, 86%), m.p. 157-158 °C. Anal. Calcd for  $C_{22}H_{10}F_6N_2O_3W$ : C, 40.77; H, 1.56; N, 4.32;  $M_r$  648. Found: C, 40.67; H, 1.59; N, 4.33;  $M_r$  648 (mass spectrometry). IR ( $CH_2Cl_2$ ):  $\nu(CN)$  2244vw;  $\nu(CO)$  2039s, 1960s, 1946s  $cm^{-1}$ . IR (Nujol):  $\nu(CC)$  1612w, 1579w;  $\nu(CF)$  1294(sh), 1277s, 1252(sh), 1232(sh), 1222(sh), 1205s; other bands at 1490w, 1430w, 1152w, 1111m, 1098w, 1077w, 1062w, 1015w, 950m, 940(sh), 844m, 819w, 770w, 723m, 710w, 700w, 630w  $cm^{-1}$ .  $^1H$  NMR ( $CDCl_3$ ):  $\delta$  7.5-7.3 (m, 5H, Ph); 5.72 (s, 5H,  $C_5H_5$ ).  $^{19}F$  NMR ( $CDCl_3$ ):  $\delta$  -66.3 (s,  $CF_3$ ). FAB MS: 648,  $[M]^+$ , 74; 620\*,  $[M - CO]^+$ , 8; 592,  $[M - 2CO]^+$ , 100; 579\*,  $[M - CF_3]^+$ , 9; 564,  $[M - 3CO]^+$ , 68; 495,  $[M - 3CO - CF_3]^+$ , 31; 406,  $[WC_2PhCC(CN)(CF_3)]^+$ , 14; 368\*,  $[W_2?]^+$ , 22; 350,  $[M - 3CO - dcfe]^+$ , 29; 305,  $[W(CO)_2(C_5H_5)]^+$ , 40; 287\*,  $[WC_2Ph]^+$ , 67.

Aggregate ions above  $m/z$  648 were observed at  $m/z$  (%) 688 (6), 702 (14), 717 (18), 732 (8), 1128 (8), 1142 (2) and 1156 (2).

#### 1.4.2. $\text{Mn}\{\overline{\text{C}=\text{CPhC}(\text{CF}_3)_2\text{C}(\text{CN})_2}\}(\text{CO})_3(\text{dppe})$ (14)

The olefin (80 mg, 0.37 mmol) was added to a solution of  $\text{Mn}(\text{C}_2\text{Ph})(\text{CO})_3(\text{dppe})$  (200 mg, 0.31 mmol) in benzene (20 mL). After the solution was stirred for 18 h, the white precipitate was filtered off and washed with benzene and petroleum spirit. Crystallization ( $\text{CH}_2\text{Cl}_2/\text{EtOH}$ ) gave white crystals of  $\text{Mn}\{\overline{\text{C}=\text{CPhC}(\text{CF}_3)_2\text{C}(\text{CN})_2}\}(\text{CO})_3(\text{dppe})$  (14) (200 mg, 0.23 mmol, 75%), m.p. 193-195 °C. Anal. Calcd for  $\text{C}_{43}\text{H}_{29}\text{F}_6\text{MnN}_2\text{O}_3\text{P}_2$ : C, 60.57; H, 3.43; N, 3.28;  $M_r$  852. Found: C, 60.39; H, 3.45; N, 3.30;  $M_r$  852 (mass spectrometry). IR ( $\text{CH}_2\text{Cl}_2$ ):  $\nu(\text{CN})$  2241vw;  $\nu(\text{CO})$  2109s, 1943s  $\text{cm}^{-1}$ . IR (Nujol):  $\nu(\text{CC})$  1610vw, 1590vw, 1578vw, 1555vw;  $\nu(\text{CF})$  1290(sh), 1272s, 1250w, 1218w, 1197s, 1181(sh); other bands at 1482w, 1440m, 1308w, 1109m, 941w, 740w, 722w, 707m, 688m, 676w, 662w, 630w  $\text{cm}^{-1}$ .  $^1\text{H NMR}$  ( $\text{CDCl}_3$ ):  $\delta$  8.0 - 7.3 (m, 20H, PhP); 7.00 (t,  $J_{\text{H-H}} = 7$  Hz, 1H, Ph); 6.61 (t,  $J_{\text{H-H}} = 7$  Hz, 2H, Ph); 5.22 (d,  $J_{\text{H-H}} = 8$  Hz, 2H, Ph); 2.8 - 1.6 (m, 4H,  $\text{CH}_2$ ). FAB MS: 853,  $[\text{M} + \text{H}]^+$ , 4; 852,  $[\text{M}]^+$ , 4; 797\*,  $[\text{M} - 2\text{CO}]^+$ , 2; 768,  $[\text{M} - 3\text{CO}]^+$ , 50; 742,  $[\text{M} - 3\text{CO} - \text{CN}]^+$ , 4; 691,  $[\text{M} - 3\text{CO} - \text{Ph}]^+$ , 5; 554,  $[\text{M} - 3\text{CO} - \text{dcfe}]^+$ , 8; 537,  $[\text{Mn}(\text{CO})_3(\text{dppe})]^+$ , 5; 479,  $[\text{Mn}(\text{CN})(\text{dppe})]^+$ , 8; 472,  $[\text{MnF}(\text{dppe})]^+$ , 100; 453,  $[\text{Mn}(\text{dppe})]^+$ , 15; 259,  $[\text{MnF}(\text{PPh}_2)]^+$ , 16.

#### 1.4.3. $\text{Fe}\{\overline{\text{C}=\text{CPhC}(\text{CF}_3)_2\text{C}(\text{CN})_2}\}(\text{CO})_2(\eta\text{-C}_5\text{H}_5)$ (15)

Addition of dcfe (260 mg, 1.20 mmol) to a solution of  $\text{Fe}(\text{C}_2\text{Ph})(\text{CO})(\eta\text{-C}_5\text{H}_5)$  (200 mg, 0.72 mmol) in diethyl ether (30 mL) followed by stirring in the dark for 40 min resulted in a yellow solution. Reduction of the volume (to 5 mL) followed by filtration removed a small amount of an unidentified precipitate which was washed with petroleum spirit (10 mL). The volume of the combined filtrates was then reduced until a yellow precipitate formed. After cooling (-20 °C), the pale solution was syringed off and the precipitate washed with petroleum spirit. Crystallization ( $\text{CH}_2\text{Cl}_2/\text{petroleum spirit}$ ) gave pale yellow crystals of  $\text{Fe}\{\overline{\text{C}=\text{CPhC}(\text{CF}_3)_2\text{C}(\text{CN})_2}\}(\text{CO})_2(\eta\text{-C}_5\text{H}_5)$  (15) (350 mg, 0.71 mmol, 98%), m.p. 96-97 °C. Anal.

Calcd for  $C_{21}H_{10}F_6FeN_2O_2$ : C, 51.25; H, 2.05; N, 5.69;  $M_r$  492. Found: C, 50.47; H, 2.08; N, 5.97;  $M_r$  492 (mass spectrometry). Rapid decomposition of the solid sample precluded more accurate analytical figures being obtained. IR ( $CH_2Cl_2$ ):  $\nu(CN)$  2243vw;  $\nu(CO)$  2044s, 1995s  $cm^{-1}$ . IR (Nujol):  $\nu(CC)$  1615w, 1590w, 1580w;  $\nu(CF)$  1275s, 1222(sh), 1212(sh), 1200s, 1190(sh), 1155m, 1110s; other bands at 1440m, 1425m, 1370w, 1320w, 1300w, 1160w, 1079m, 1060m, 1035m, 1020m, 1010m, 970(sh), 950s, 934s, 885w, 858s, 843m, 840m, 817s, 800(sh), 772s, 710m, 696s, 675w, 658(sh), 640m, 620w  $cm^{-1}$ .  $^1H$  NMR ( $CDCl_3$ ):  $\delta$  7.32 (m, 5H, Ph); 4.95 (s, 5H,  $C_5H_5$ ). FAB MS: 493,  $[M + H]^+$ , 18; 492,  $[M]^+$ , 11; 466,  $[M - CN]^+$ , 7; 436,  $[M - 2 CO]^+$ , 100; 417,  $[M - 2 CO - F]^+$ , 21; 410,  $[M - 2 CO - CN]^+$ , 23; 398,  $[M - 2 CO - 2F]^+$ , 7; 367,  $[M - 2 CO - CF_3]^+$ , 8; 277\*,  $[M - dcfe]^+$ , 37; 222,  $[M - 2 CO - dcfe]^+$ , 6; 186,  $[Fe(C_5H_5)_2]^+$ , 27; 177,  $[Fe(CO)_2(C_5H_5)]^+$ , 17. The spectrum also contained many ions between  $m/z$  500 and  $m/z$  1420 with relative intensities < 2%, as well as those at  $m/z$  557, 613, 872 and 918, which had relative intensities 10-15%.

#### 1.4.4. $Ru\{\overline{C=CPhC(CF_3)_2C(CN)_2}\}(dppe)(\eta-C_5H_5)$ (16)

A mixture of  $Ru(C_2Ph)(dppe)(\eta-C_5H_5)$  (100 mg, 0.15 mmol) and dcfe (60 mg, 0.28 mmol) in benzene (10 mL) was stirred for 24 h. To the filtered solution was added octane (5 mL) and the volume then reduced to 5 mL. The resulting pale yellow precipitate was washed with petroleum spirit and dried under vacuum. Crystallization (benzene/petroleum spirit) gave yellow microcrystalline  $Ru\{\overline{C=CPhC(CF_3)_2C(CN)_2}\}(dppe)(\eta-C_5H_5)$  (16) (105 mg, 0.12 mmol, 80%), m.p. 230-231 °C. Anal. Calcd for  $C_{45}H_{34}F_6N_2P_2Ru$ : C, 61.43; H, 3.89; N, 3.18;  $M_r$  880. Found: C, 61.63; H, 4.00; N, 3.14;  $M_r$  880 (mass spectrometry). IR (Nujol):  $\nu(CN)$  2233vw;  $\nu(CC)$  1606w, 1586w, 1573w;  $\nu(CF)$  1292(sh), 1274s, 1250(sh), 1230s, 1220(sh), 1208s, 1199s, 1165s, 1110s; other bands at 1546w, 1310(sh), 1105(sh), 1077w, 1068w, 1030w, 1002w, 969m, 942m, 910w, 855w, 817m, 788w, 770w, 751m, 739m, 722s, 708(sh), 700s, 675s, 630w  $cm^{-1}$ .  $^1H$  NMR ( $CDCl_3$ ):  $\delta$  8.0 - 6.6 (m, 20H, PPh); 6.95 (t, overlaps with other phenyl resonances); 6.72 (t,  $J_{H-H} = 7Hz$ , 3H, Ph); 5.27 (d,  $J_{H-H} = 8Hz$ , 2H, Ph); 4.71(s, 5H,  $C_5H_5$ ); 2.52 (m, 4H,  $CH_2$ ).  $^{13}C\{^1H\}$  NMR ( $CDCl_3$ ):  $\delta$  178.6 (m,  $C_\alpha$ ); 147.2 - 128.4 (m, Ph); 115.6 (m, CN); 85.4 (s,  $C_5H_5$ ); 29.2

(t,  $J_{P-C} = 22$  Hz, CH<sub>2</sub>); other minor peaks at  $\delta$  71.6(s), 70.0(s), 58.7(s), 8.4(s). <sup>19</sup>F NMR (CDCl<sub>3</sub>):  $\delta$  -65.2 (s, CF<sub>3</sub>). FAB MS: 880, [M]<sup>+</sup>, 61; 803, [M - Ph]<sup>+</sup>, 14; 734, [M - Ph - CF<sub>3</sub>]<sup>+</sup>, 5; 666, [M - dcfe]<sup>+</sup>, 91; 601\*, [M - dcfe - (C<sub>5</sub>H<sub>5</sub>)]<sup>+</sup>, 7; 589\*, [M - dcfe - Ph]<sup>+</sup>, 7; 581\*, [565 + O]<sup>+</sup>, 5; 565, [Ru(dppe)(C<sub>5</sub>H<sub>5</sub>)]<sup>+</sup>, 100; 499\*, [Ru(dppe)]<sup>+</sup>, 12; 459\*, [Ru(P<sub>2</sub>Ph<sub>3</sub>)(C<sub>5</sub>H<sub>5</sub>)]<sup>+</sup>, 13; 393\*, [RuP<sub>2</sub>Ph<sub>3</sub>]<sup>+</sup>, 13; 378\*, [Ru(PPh<sub>2</sub>C<sub>2</sub>)(C<sub>5</sub>H<sub>5</sub>)]<sup>+</sup>, 26; 363\*, [Ru(PPh<sub>3</sub>)]<sup>+</sup>, 12; 351\*, [Ru(PPh<sub>2</sub>)(C<sub>5</sub>H<sub>5</sub>)]<sup>+</sup>, 47; 317\*, [RuP<sub>2</sub>Ph<sub>2</sub>]<sup>+</sup>, 17; 299\*, [RuC<sub>2</sub>(PPh)(C<sub>5</sub>H<sub>5</sub>)]<sup>+</sup>, 14; 244\*, [RuPh(C<sub>5</sub>H<sub>5</sub>)]<sup>+</sup>, 14; 167, [Ru(C<sub>5</sub>H<sub>5</sub>)]<sup>+</sup>, 13.

#### 1.4.5. Ru{ $\overline{C=CPhC(CF_3)_2C(CN)_2}$ }(PPh<sub>3</sub>)<sub>2</sub>( $\eta$ -C<sub>5</sub>H<sub>5</sub>) (17)

The olefin (76 mg, 0.36 mmol) was added to a suspension of Ru(C<sub>2</sub>Ph)(PPh<sub>3</sub>)<sub>2</sub>( $\eta$ -C<sub>5</sub>H<sub>5</sub>) (200 mg, 0.25 mmol) in MeCN (50 mL). After 1 min all the solid had dissolved and the reaction mixture was cooled to 0 °C. The resulting precipitate was collected after 5 min and washed with MeCN, petroleum spirit and dried under vacuum to give a yellow powder Ru{ $\overline{C=CPhC(CF_3)_2C(CN)_2}$ }(PPh<sub>3</sub>)<sub>2</sub>( $\eta$ -C<sub>5</sub>H<sub>5</sub>) (17) (192 mg, 0.19 mmol, 76%), m.p. 145-146 °C (dec.). Anal. Calcd for C<sub>55</sub>H<sub>40</sub>F<sub>6</sub>N<sub>2</sub>P<sub>2</sub>Ru: C, 65.67; H, 4.01; N, 2.78;  $M_r$  1006. Found: C, 65.36; H, 4.02; N, 3.05;  $M_r$  1006 (mass spectrometry). IR (Nujol):  $\nu$ (CN) 2239vw;  $\nu$ (CC) 1587w, 1572vw;  $\nu$ (CF) 1287(sh), 1269vs, 1219m, 1199vs; other peaks at 1520w, 1435s, 1244w, 1238w, 1160w, 1138w, 1115(sh), 1106m, 1088m, 1077(sh), 1063w, 1027w, 1002w, 947m, 848w, 831m, 817m, 754m, 745m, 740m, 720m, 704s, 698s, 681w cm<sup>-1</sup>. FAB MS: 1006, [M]<sup>+</sup>, 14; 929, [M - Ph]<sup>+</sup>, 1; 792, [M - dcfe]<sup>+</sup>, 11; 744, [M - PPh<sub>3</sub>]<sup>+</sup>, 34; 691, [Ru(PPh<sub>3</sub>)<sub>2</sub>(C<sub>5</sub>H<sub>5</sub>)]<sup>+</sup>, 38; 530, [M - dcfe - PPh<sub>3</sub>]<sup>+</sup>, 7; 453\*, [M - dcfe - Ph - PPh<sub>3</sub>]<sup>+</sup>, 10; 444\*, [429 + O]<sup>+</sup>, 9; 429, [Ru(PPh<sub>3</sub>)(C<sub>5</sub>H<sub>5</sub>)]<sup>+</sup>, 100; 350\*, [Ru(PPh<sub>2</sub>)(C<sub>5</sub>H<sub>5</sub>)]<sup>+</sup>, 21; 244, [RuPh(C<sub>5</sub>H<sub>5</sub>)]<sup>+</sup> 19. As this complex is unstable in solution no NMR data could be obtained.

#### 1.4.6. Ru{ $\overline{C=CMeC(CF_3)_2C(CN)_2}$ }(PPh<sub>3</sub>)<sub>2</sub>( $\eta$ -C<sub>5</sub>H<sub>5</sub>) (18)

To a suspension of Ru(C<sub>2</sub>Me)(PPh<sub>3</sub>)<sub>2</sub>( $\eta$ -C<sub>5</sub>H<sub>5</sub>) (200 mg, 0.27 mmol) in MeCN (35 mL) was added dcfe (74 mg, 0.35 mmol). The solid quickly went into solution and after stirring for 24 h the resulting yellow precipitate was filtered off, washed with MeCN, petroleum spirit

and dried under vacuum. Low temperature crystallization ( $\text{CH}_2\text{Cl}_2$ /petroleum spirit) gave yellow microcrystalline  $\text{Ru}\{\overline{\text{C}=\text{CMeC}(\text{CF}_3)_2\text{C}(\text{CN})_2}\}(\text{PPh}_3)_2(\eta\text{-C}_5\text{H}_5)\cdot 0.25\text{CH}_2\text{Cl}_2$  (**18**) (210 mg, 0.22 mmol, 81%), m.p. 179-180 °C (dec.). Anal. Calcd for  $\text{C}_{50}\text{H}_{38}\text{F}_6\text{N}_2\text{P}_2\text{Ru}\cdot 0.25\text{CH}_2\text{Cl}_2$ : C, 62.84; H, 4.00; N, 2.90;  $M_r$  944 (unsolvated). Found: C, 62.84; H, 4.02; N, 2.93;  $M_r$  944 (mass spectrometry). IR (Nujol):  $\nu(\text{CN})$  2238vw;  $\nu(\text{CC})$  1572m;  $\nu(\text{CF})$  1282(sh), 1270vs, 1255(sh), 1236(sh), 1220s, 1197vs, 1185(sh); other peaks at 1488s, 1311w, 1158w, 1140m, 1112w, 1087s, 1078(sh), 1036w, 1014w, 1000m, 933m, 873m, 838m, 825(sh), 810m, 752s, 750(sh), 747(sh), 739m, 713(sh), 700vs, 680(sh)  $\text{cm}^{-1}$ .  $^1\text{H}$  NMR ( $\text{CDCl}_3$ ):  $\delta$  7.2 - 6.9 (m, 30H, Ph); 5.30 (s, 0.5H,  $\text{CH}_2\text{Cl}_2$ ); 4.64 (s, 5H,  $\text{C}_5\text{H}_5$ ); 0.53 (s, 3H, Me).  $^{19}\text{F}$  NMR ( $\text{CDCl}_3$ ):  $\delta$  -66.3 (s,  $\text{CF}_3$ ). FAB MS: 944,  $[\text{M}]^+$ , 25; 867,  $[\text{M} - \text{Ph}]^+$ , 3; 691\*,  $[\text{Ru}(\text{PPh}_3)_2(\text{C}_5\text{H}_5)]^+$ , 7; 682\*,  $[\text{M} - \text{PPh}_3]^+$ , 55; 625\*,  $[\text{Ru}(\text{PPh}_3)_2]^+$ , 6; 613\*,  $[\text{M} - \text{Ph}]^+$ , 6; 427\*,  $[\text{Ru}(\text{PPh}_3)(\text{C}_5\text{H}_5)]^+$ , 100; 363\*,  $[\text{Ru}(\text{PPh}_3)]^+$ , 13; 350\*,  $[\text{Ru}(\text{PPh}_2)(\text{C}_5\text{H}_5)]^+$ , 20; 244\*,  $[\text{RuPh}(\text{C}_5\text{H}_5)]^+$ , 19.

#### 1.4.7. $\text{Ru}\{\overline{\text{C}=\text{CPhC}(\text{CF}_3)_2\text{C}(\text{CN})_2}\}(\text{CO})(\text{PPh}_3)(\eta\text{-C}_5\text{H}_5)$ (**19**)

(a) A mixture of dcfе (80 mg, 0.37 mmol) and  $\text{Ru}(\text{C}_2\text{Ph})(\text{CO})(\text{PPh}_3)(\eta\text{-C}_5\text{H}_5)$  (100 mg, 0.18 mmol) in benzene (10 mL) was stirred for 20 h. The volume was reduced to 5 mL and *n*-octane (5 mL) was added. Further volume reduction resulted in a white precipitate. This was collected, washed with petroleum spirit, dried under vacuum and crystallized ( $\text{CH}_2\text{Cl}_2$ /petroleum spirit) yielding colourless crystals of  $\text{Ru}\{\overline{\text{C}=\text{CPhC}(\text{CF}_3)_2\text{C}(\text{CN})_2}\}(\text{CO})(\text{PPh}_3)(\eta\text{-C}_5\text{H}_5)$  (**19**) (117 mg, 0.15 mmol, 84%), m.p. 206-207 °C. Anal. Calcd for  $\text{C}_{38}\text{H}_{25}\text{F}_6\text{ON}_2\text{P-Ru}$ : C, 59.15; H, 3.27; N, 3.63;  $M_r$  772. Found: C, 59.13; H, 3.27; N, 3.65;  $M_r$  772 (mass spectrometry). IR ( $\text{CH}_2\text{Cl}_2$ ):  $\nu(\text{CN})$  2240vw;  $\nu(\text{CO})$  1960s  $\text{cm}^{-1}$ . IR (Nujol):  $\nu(\text{CC})$  1611w, 1572w;  $\nu(\text{CF})$  1295(sh), 1278s, 1250(sh), 1222m, 1210s; other peaks at 1487m, 1150w, 1114w, 1100m, 1095m, 1077w, 1065w, 1030w, 1002w, 948m, 900w, 840m, 821s, 760m, 748w, 722m, 708m, 697s, 680w, 638w  $\text{cm}^{-1}$ .  $^1\text{H}$  NMR ( $\text{CDCl}_3$ ):  $\delta$  7.4 - 7.2 (m, 15H, PPh); 7.0 - 6.8 (m, 5H, Ph); 5.02 (s, 5H,  $\text{C}_5\text{H}_5$ ).  $^{13}\text{C}\{^1\text{H}\}$  NMR ( $\text{CDCl}_3$ ):  $\delta$  219.6 [s(br), CO]; 172.7 (d,  $J_{\text{P-C}} = 35\text{Hz}$ ,  $\text{C}_\alpha$ ); 136.2 - 126.7 (m, Ph); 114.8(d,  $J = 11\text{Hz}$ , CN); 113.4 (d,  $J = 8\text{Hz}$ , CN); 87.3 (s,  $\text{C}_5\text{H}_5$ ); other minor peaks at  $\delta$  154.0 (s), 42.5 (s), 35.3 (s).  $^{19}\text{F}$  NMR

(CDCl<sub>3</sub>):  $\delta$  -66.0 (q,  $J_{F-F} = 10$  Hz, CF<sub>3</sub>); -66.4 (q,  $J_{F-F} = 10$  Hz, CF<sub>3</sub>). FAB MS: 772, [M]<sup>+</sup>, 84; 744\*, [M - CO]<sup>+</sup>, 15; 667, [M - CO - Ph]<sup>+</sup>, 15; 558, [M - dcfe]<sup>+</sup>, 11; 529\*, [M - dcfe - CO]<sup>+</sup>, 7; 482, [M - PPh<sub>3</sub> - CO]<sup>+</sup>, 12; 456\*, [M - PPh<sub>3</sub> - CO - CN]<sup>+</sup>, 20; 453\*, [M - dcfe - Ph - CO]<sup>+</sup>, 28; 429\*, [Ru(PPh<sub>3</sub>)(C<sub>5</sub>H<sub>5</sub>)]<sup>+</sup>, 100; 363\*, [Ru(PPh<sub>3</sub>)]<sup>+</sup>, 22; 350\*, [Ru(PPh<sub>2</sub>)(C<sub>5</sub>H<sub>5</sub>)]<sup>+</sup>, 32; 285\*, [Ru(PPh<sub>2</sub>)]<sup>+</sup>, 18; 244, [RuPh(C<sub>5</sub>H<sub>5</sub>)]<sup>+</sup>, 23; 167\*, [Ru(C<sub>5</sub>H<sub>5</sub>)]<sup>+</sup>, 24.

(b) <sup>1</sup>H NMR study of the formation of (19): Ru(C<sub>2</sub>Ph)(CO)(PPh<sub>3</sub>)( $\eta$ -C<sub>5</sub>H<sub>5</sub>) (15 mg, 0.027 mmol) dissolved in C<sub>6</sub>D<sub>6</sub> (0.5 mL) was added to dcfe (6 mg, 0.03 mmol) and then placed in an NMR tube. After three min the formation of (19) was complete.

(c) A solution of Ru(C<sub>2</sub>Ph)(PPh<sub>3</sub>)<sub>2</sub>( $\eta$ -C<sub>5</sub>H<sub>5</sub>) (290 mg, 0.37 mmol) in benzene (50 mL) was saturated with CO and dcfe (167 mg, 0.78 mmol) was added. The reaction was left under positive CO pressure for 5 d. After this time, the volume was reduced (to 10 mL) and n-octane (10 mL) was added. Further evaporation resulted in precipitation of an off-white solid. This was purified by TLC (petroleum spirit/acetone 2:1) to give a white band (R<sub>f</sub> 0.60) of (19) (180 mg, 0.23 mmol, 63%), identified by FAB MS, <sup>1</sup>H NMR and IR.

### Syntheses of butadienyl and allyl complexes

#### 1.4.8. Synthesis of W{C[=C(CN)<sub>2</sub>]CPh=C(CF<sub>3</sub>)<sub>2</sub>}(CO)<sub>3</sub>( $\eta$ -C<sub>5</sub>H<sub>5</sub>) (20) and W{ $\eta^3$ -C(CF<sub>3</sub>)<sub>2</sub>CPhC=C(CN)<sub>2</sub>}(CO)<sub>2</sub>( $\eta$ -C<sub>5</sub>H<sub>5</sub>) (24)

A solution of (13) (130 mg, 0.20 mmol) in xylene (50 mL) was refluxed for 2 h 45 min. After cooling, the solvent was removed under vacuum and the residue purified by TLC (petroleum spirit/acetone 2:1) which eluted two major yellow bands and three minor bands (the latter uncharacterized). The first yellow band (R<sub>f</sub> 0.60) was crystallized (CH<sub>2</sub>Cl<sub>2</sub>/petroleum spirit) to give yellow crystalline W{C[=C(CN)<sub>2</sub>]CPh=C(CF<sub>3</sub>)<sub>2</sub>}(CO)<sub>3</sub>( $\eta$ -C<sub>5</sub>H<sub>5</sub>) (20) (11 mg, 0.017 mmol, 8%), m.p. 184-185 °C. Anal. Calcd for C<sub>22</sub>H<sub>10</sub>F<sub>6</sub>N<sub>2</sub>O<sub>3</sub>W: C, 40.77; H, 1.56; N, 4.32; M<sub>r</sub> 648. Found: C, 40.56; H, 1.53; N, 4.29; M<sub>r</sub> 648 (mass spectrometry). IR (CH<sub>2</sub>Cl<sub>2</sub>):  $\nu$ (CN) 2219w;  $\nu$ (CO) 2044s, 1972s, 1950s cm<sup>-1</sup>. IR (Nujol):  $\nu$ (CC) 1626w, 1622w, 1616w;  $\nu$ (CF) 1254s, 1255m, 1210m, 1161s; other bands at 1448w, 1336m, 1138w,

1121w, 1080w, 1063m, 1015w, 1002w, 966m, 883w, 868w, 860(sh), 846m, 824w, 773w, 756w, 730w, 721(sh), 710w, 700m  $\text{cm}^{-1}$ .  $^1\text{H}$  NMR ( $\text{CDCl}_3$ ):  $\delta$  7.44 (m, 5H, Ph); 5.80 (s, 5H,  $\text{C}_5\text{H}_5$ ). FAB MS: 648,  $[\text{M}]^+$ , 58; 620,  $[\text{M} - \text{CO}]^+$ , 75; 593\*,  $[\text{M} - 2 \text{CO}]^+$ , 33; 564,  $[\text{M} - 3 \text{CO}]^+$ , 100; 545\*,  $[\text{M} - 3 \text{CO} - \text{F}]^+$ , 38; 517\*,  $[\text{W}_2\text{F}(\text{C}_5\text{H}_5)_2]^+$ , 17; 497\*,  $[\text{M} - 3\text{CO} - \text{CF}_3]^+$ , 9; 452\*,  $[\text{W}_2\text{F}(\text{C}_5\text{H}_5)]^+$ , 8; 314,  $[\text{W}(\text{C}_5\text{H}_5)_2]^+$ , 24.

The second yellow band ( $R_f$  0.50) was crystallized ( $\text{CH}_2\text{Cl}_2/\text{MeOH}$ ) to give orange crystalline  $\text{W}\{\eta^3\text{-C}(\text{CF}_3)_2\text{CPhC}=\text{C}(\text{CN})_2\}(\text{CO})_2(\eta\text{-C}_5\text{H}_5)$  (**24**) (32 mg, 0.05 mmol, 26%), m.p. 230-234 °C. Anal. Calcd for  $\text{C}_{21}\text{H}_{10}\text{F}_6\text{N}_2\text{O}_2\text{W}$ : C, 40.67; H, 1.63; N, 4.52;  $M_r$  620. Found: C, 40.57; H, 1.63; N, 4.50;  $M_r$  620 (mass spectrometry). IR ( $\text{CH}_2\text{Cl}_2$ ):  $\nu(\text{CN})$  2219m;  $\nu(\text{CO})$  2052s, 2004s  $\text{cm}^{-1}$ . IR (Nujol):  $\nu(\text{CC})$  1579w, 1575m, 1567w;  $\nu(\text{CF})$  1295m, 1266w, 1234m, 1210w, 1195s, 1186m, 1140s; other bands at 1439(sh), 1190w, 1145(sh), 1110w, 1094m, 1060m, 1022w, 1003w, 967m, 920w, 862w, 840m, 830w, 816m, 803m, 780w, 749m, 727w, 717w, 702s, 648w  $\text{cm}^{-1}$ .  $^1\text{H}$  NMR ( $\text{CDCl}_3$ ):  $\delta$  7.33 (m, 5H, Ph); 5.79 (s, 5H,  $\text{C}_5\text{H}_5$ ).  $^{19}\text{F}$  NMR ( $\text{CDCl}_3$ ):  $\delta$  -51.9 (q,  $J_{\text{F-F}} = 10$  Hz,  $\text{CF}_3$ ); -52.5 (q,  $J_{\text{F-F}} = 10$  Hz,  $\text{CF}_3$ ). FAB MS: 620\*,  $[\text{M}]^+$ , 100; 564\*,  $[\text{M} - 2 \text{CO}]^+$ , 71; 545\*,  $[\text{M} - 2\text{CO} - \text{F}]^+$ , 57.

#### 1.4.9. $\text{Ni}\{\text{C}[\text{C}(\text{CN})_2]\text{CPh}=\text{C}(\text{CF}_3)_2\}(\text{PPh}_3)(\eta\text{-C}_5\text{H}_5)$ (**21**)

A mixture of  $\text{Ni}(\text{C}_2\text{Ph})(\text{PPh}_3)(\eta\text{-C}_5\text{H}_5)$  (200 mg, 0.41 mmol) and dcfe (140 mg, 0.65 mmol) was refluxed in benzene (50 mL) for 24 h. The solution was cooled, filtered and evaporated to dryness. Two crystallizations ( $\text{CH}_2\text{Cl}_2/\text{EtOH}$ ) followed by slow recrystallization ( $\text{CH}_2\text{Cl}_2/\text{petroleum spirit}$ ) gave yellow-green crystalline  $\text{Ni}\{\text{C}[\text{C}(\text{CN})_2]\text{CPh}=\text{C}(\text{CF}_3)_2\}(\text{PPh}_3)(\eta\text{-C}_5\text{H}_5)\cdot 0.25\text{CH}_2\text{Cl}_2$  (**21**) (80 mg, 0.1 mmol, 28%), m.p. 156-157 °C. Anal. Calcd for  $\text{C}_{37}\text{H}_{25}\text{F}_6\text{N}_2\text{NiP}\cdot 0.25 \text{CH}_2\text{Cl}_2$ : C, 61.92; H, 3.63; N, 3.88;  $M_r$  (unsolvated) 700. Found: C, 61.66; H, 3.52; N, 3.85;  $M_r$  700 (mass spectrometry). IR (Nujol):  $\nu(\text{CN})$  2220m;  $\nu(\text{CC})$  1620m, 1600w;  $\nu(\text{CF})$  1332s, 1252s, 1215s, 1167m, 1157s; other bands at 1439(sh), 1190w, 1145(sh), 1110w, 1094m, 1060m, 1022w, 1003w, 967m, 920w, 862w, 840m, 830w, 816m, 803m, 780m, 749m, 727w, 717w, 702s, 648w  $\text{cm}^{-1}$ .  $^1\text{H}$  NMR ( $\text{CDCl}_3$ ):  $\delta$  7.6 - 6.8 (m, 20H, Ph); 5.30 (s, 5.5H,  $\text{C}_5\text{H}_5 + 0.5 \text{CH}_2\text{Cl}_2$ ).  $^{19}\text{F}$  NMR ( $\text{CDCl}_3$ ):  $\delta$  -54.1

(q,  $J_{F-F} = 8$  Hz,  $CF_3$ ); -56.4 (q,  $J_{F-F} = 9$  Hz,  $CF_3$ ). FAB MS: 700,  $[M]^+$ , 31; 635,  $[M - (C_5H_5)]^+$ , 5; 582\*,  $[M - C_2F_5]^+$ , 17; 385,  $[Ni(PPh_3)(C_5H_5)]^+$ , 100; 320,  $[Ni(PPh_3)]^+$ , 77; 241\*,  $[Ni(PPh_2)]^+$ , 67.

#### 1.4.10. $Ru\{C[=C(CN)_2]CPh=C(CF_3)_2\}(CO)(PPh_3)(\eta-C_5H_5)$ (22)

A solution of (19) (100 mg, 0.13 mmol) in xylene (30 mL) was refluxed vigorously for 2 d. After cooling the solvent was removed under reduced pressure and the residue purified by TLC (petroleum spirit/acetone/ $CH_2Cl_2$  4:1:1). The major yellow band ( $R_f$  0.46) was crystallized ( $CH_2Cl_2$ /petroleum spirit) to give yellow crystals of  $Ru\{C[=C(CN)_2]CPh=C(CF_3)_2\}(CO)(PPh_3)(\eta-C_5H_5)$  (22) (20 mg, 0.026 mmol, 20%), m.p. 250-251 °C (dec.). Anal. Calcd for  $C_{38}H_{25}F_6N_2OPRu$ : C, 59.15; H, 3.27; N, 3.63;  $M_r$  772. Found: C, 59.06; H, 3.29; N, 3.65;  $M_r$  772 (mass spectrometry). IR ( $CH_2Cl_2$ ):  $\nu(CN)$  2210m, 2205m;  $\nu(CO)$  1974s, 1957(sh)  $cm^{-1}$ . IR (Nujol):  $\nu(CC)$  1609m, 1597w, 1577w;  $\nu(CF)$  1245s, 1217m, 1206s, 1152vs; other peaks at 1482m, 1436m, 1329m, 1318m, 1130m, 1110(sh), 1098(sh), 1090m, 1072(sh), 1061(sh), 1057m, 1019w, 1000m, 961s, 864m, 802w, 840s, 829(sh), 820s, 777m, 754s, 750(sh), 738s, 729w, 712(sh), 702s, 691s, 682(sh), 647m, 636m  $cm^{-1}$ .  $^1H$  NMR ( $CDCl_3$ ):  $\delta$  7.4 - 7.2 (m, 20H, Ph); 4.61 (s, 5H,  $C_5H_5$ ).  $^{19}F$  NMR ( $CDCl_3$ ):  $\delta$  -53.2 (q,  $J_{F-F} = 9$  Hz,  $CF_3$ ); -56.6 [m(br),  $CF_3$ ]. FAB MS: 772,  $[M]^+$ , 14; 744,  $[M - CO]^+$ , 11; 667,  $[M - CO - Ph]^+$ , 4; 482,  $[M - PPh_3 - CO]^+$ , 10; 456\*,  $[M - PPh_3 - CO - CN]^+$ , 37; 453\*,  $[RuC_2(PPh_3)(\eta-C_5H_5)]^+$ , 28; 429,  $[Ru(PPh_3)(C_5H_5)]^+$ , 100; 363\*,  $[Ru(PPh_3)]^+$ , 11; 350\*,  $[Ru(PPh_2)(C_5H_5)]^+$ , 16; 244,  $[RuPh(C_5H_5)]^+$ , 10; 167,  $[Ru(C_5H_5)]^+$ , 12. Other minor/trace bands (8) were observed but not characterized.

#### 1.4.11. $Ru\{C[=C(CN)_2]CPh=C(CF_3)_2\}(dppe)(\eta-C_5H_5)$ (23)

A solution of (16) (50 mg, 0.057 mmol) in xylene (20 mL) was refluxed for 5 h, cooled, and the solvent removed under reduced pressure. The residue was purified by TLC (petroleum spirit/EtOH/Et<sub>2</sub>O 4:1:1) to give a major yellow band ( $R_f$  0.18) which was collected and crystallized ( $CH_2Cl_2$ /petroleum spirit) giving yellow crystalline  $Ru\{C[=C(CN)_2]CPh=C(CF_3)_2\}(dppe)(\eta-C_5H_5).0.25CH_2Cl_2$  (23) (15mg, 0.017 mmol, 30%), m.p. 223-224 °C.

Anal. Calcd for  $C_{45}H_{34}F_6N_2P_2Ru \cdot 0.25CH_2Cl_2$ : C, 60.32; H, 3.86; N, 3.11;  $M_r$  880 (unsolvated). Found: C, 60.54; H, 3.90; N, 3.12;  $M_r$  880 (mass spectrometry). IR (Nujol):  $\nu(CN)$  2205m, 2190m;  $\nu(CC)$  1590m, 1570m;  $\nu(CF)$  1243s, 1218s, 1199s, 1140s; other peaks at 1489w, 1438s, 1427s, 1329s, 1319s, 1092w, 1046m, 1029w, 1000w, 952m, 872w, 850m, 840m, 819m, 772w, 750m, 723m, 697s, 627m, 645w  $cm^{-1}$ .  $^1H$  NMR ( $CDCl_3$ ):  $\delta$  7.4 - 7.2 (m, 25H, Ph); 5.30 (s, 0.5H,  $CH_2Cl_2$ ); 4.67 (s, 1H,  $C_5H_5$ ); 4.30 (s, 4H,  $C_5H_5$ ); 3.5 - 2.5 (m, 4H,  $CH_2$ ).  $^{19}F$  NMR ( $CDCl_3$ ):  $\delta$  -53.1\* (q,  $J_{F-F} = 10$  Hz,  $CF_3$ ); -53.2 (q,  $J_{F-F} = 10$  Hz,  $CF_3$ ); -55.9\* (q,  $J_{F-F} = 10$  Hz,  $CF_3$ ); -55.7 (q,  $J_{F-F} = 10$  Hz,  $CF_3$ ) - mixture of isomers, peaks marked with \* have approx. four times the intensity of the other isomer. FAB MS: 880,  $[M]^+$ , 38; 803,  $[M - Ph]^+$ , 8; 565,  $[Ru(dppe)(C_5H_5)]^+$ , 100; 499\*,  $[Ru(dppe)]^+$ , 6; 378\*,  $[RuC_2(PPh_2)(C_5H_5)]^+$ , 13; 349\*,  $[Ru(PPh_2)(C_5H_5)]^+$ , 21; 317\*,  $[RuP_2Ph_2]^+$ , 8; 299\*,  $[RuC_2(PPh)(C_5H_5)]^+$ , 8; 244\*,  $[RuPh(C_5H_5)]^+$ , 9; 167,  $[Ru(C_5H_5)]^+$ , 5.

#### 1.4.12. Photochemical synthesis of the allyl complex

##### $Ru\{\eta^3-C(CF_3)_2CPhC=C(CN)_2\}(PPh_3)(\eta-C_5H_5)$ (25)

A solution of (22) (30 mg, 0.039 mmol) in dme (15 mL) was irradiated for 24 h at 24 °C. The solvent was then removed and the residue purified by TLC (petroleum spirit/acetone/ $CH_2Cl_2$  3:1:1). Of the eight bands observed only an orange band ( $R_f$  0.67) was isolated. This crystallized ( $CH_2Cl_2$ /petroleum spirit) as orange crystalline  $Ru\{\eta^3-C(CF_3)_2CPhC=C(CN)_2\}(PPh_3)(\eta-C_5H_5) \cdot 0.5CH_2Cl_2 \cdot H_2O$  (25) (7 mg, 0.009 mmol, 23%), m.p. 211-212 °C. Anal. Calcd for  $C_{37}H_{25}F_6N_2PRu \cdot 0.5CH_2Cl_2 \cdot H_2O$ : C, 56.01; H, 3.25; N, 3.48;  $M_r$  744 (unsolvated). Found: C, 55.92; H, 3.28; N, 3.52;  $M_r$  744 (mass spectrometry). IR (Nujol):  $\nu(CN)$  2220s, 2217(sh);  $\nu(CC)$  1567vs;  $\nu(CF)$  1291s, 1279m, 1243s, 1195vs, 1182(sh), 1161m, 1130vs, 1092s; other peaks at 2060w, 1499(sh), 1492(sh), 1484m, 1450m, 1442s, 1417m, 1347s, 1320w, 1308m, 1221w, 1087(sh), 1075(sh), 1033m, 1000w, 954s, 886m, 857m, 842s, 820m, 805s, 777m, 764(sh), 752s, 740s, 727w, 711(sh), 702s, 690m, 669(sh), 640w, 629w  $cm^{-1}$ .  $^1H$  NMR ( $CDCl_3$ ):  $\delta$  8.0 - 7.3 (m, 20H, Ph); 5.29 (s, 1H,  $CH_2Cl_2$ ); 4.72 (s, 5H,  $C_5H_5$ ).  $^{19}F$  NMR ( $CDCl_3$ ):  $\delta$  -48.6 (q,  $J_{F-F} = 9$  Hz,  $CF_3$ ); -56.0 (q,  $J_{F-F} = 7$  Hz,  $CF_3$ ). FAB MS: 744,  $[M]^+$ , 40; 456\*,  $[Ru(CN)(PPh_3)(C_5H_5)]^+$ , 21, 429\*,

$[\text{Ru}(\text{PPh}_3)(\text{C}_5\text{H}_5)]^+$ , 100; 350\*,  $[\text{Ru}(\text{PPh}_2)(\text{C}_5\text{H}_5)]^+$ , 13.

#### 1.4.13. Thermal synthesis of the allyl complex



A suspension of (18) (200 mg, 0.21 mmol) in MeCN (30 mL) was refluxed for 4 h and then cooled to r.t. Unreacted starting material was then filtered off and the solvent removed under reduced pressure. The residue was chromatographed (column: florisil), eluting with petroleum spirit to remove  $\text{PPh}_3$ . A yellow band removed with  $\text{CH}_2\text{Cl}_2$  was crystallized ( $\text{CH}_2\text{Cl}_2$ / petroleum spirit) to give yellow crystalline  $\text{Ru}\{\eta^3\text{-C}(\text{CF}_3)_2\text{CMeC}=\text{C}(\text{CN})_2\}\text{-}(\text{PPh}_3)(\eta\text{-C}_5\text{H}_5)\cdot 0.5\text{CH}_2\text{Cl}_2$  (26) (100 mg, 0.14 mmol, 66%), m.p. 192-194 °C. Anal. Calcd for  $\text{C}_{32}\text{H}_{23}\text{F}_6\text{N}_2\text{PRu}\cdot 0.5\text{CH}_2\text{Cl}_2$ : C, 53.84; H, 3.33; N, 3.86;  $M_r$  682(unsolvated). Found: C, 53.64; H, 3.33; N, 3.83;  $M_r$  682 (mass spectrometry). IR (Nujol):  $\nu(\text{CN})$  2222s;  $\nu(\text{CC})$  1587s;  $\nu(\text{CF})$  1303s, 1276m, 1240s, 1230s, 1207(sh), 1201s, 1188m, 1167m, 1144s, 1122s, 1095s, 1086s; other peaks at 1482m, 1442s, 1417m, 1368s, 1358s, 1314m, 1060m, 1029s, 1022s, 1002w, 992w, 967s, 933s, 850m, 843s, 824m, 801s, 760m, 752m, 739s, 723m, 712s, 706s, 693s, 681w, 662w  $\text{cm}^{-1}$ .  $^1\text{H}$  NMR ( $\text{CDCl}_3$ ):  $\delta$  7.9 - 7.4 (m, 15H, Ph); 5.29 (s, 1H,  $\text{CH}_2\text{Cl}_2$ ); 4.49 (s, 5H,  $\text{C}_5\text{H}_5$ ); 2.06 (s, 3H, Me).  $^{19}\text{F}$  NMR ( $\text{CDCl}_3$ ):  $\delta$  -53.0 (q,  $J_{\text{F-F}} = 10$  Hz,  $\text{CF}_3$ ); -56.4 (q,  $J_{\text{F-F}} = 11$  Hz,  $\text{CF}_3$ ). FAB MS: 682,  $[\text{M}]^+$ , 51; 605\*,  $[\text{M} - \text{Ph}]^+$ , 3; 593\*,  $[\text{M} - \text{CPh}]^+$ , 5; 456\*,  $[\text{Ru}(\text{CN})(\text{PPh}_3)(\text{C}_5\text{H}_5)]^+$ , 15; 429\*,  $[\text{Ru}(\text{PPh}_3)(\text{C}_5\text{H}_5)]^+$ , 100; 350\*,  $[\text{Ru}(\text{PPh}_2)(\text{C}_5\text{H}_5)]^+$ , 14; weak ions (<5%) observed at  $m/z$  1100 and 1363.

Shortening the duration of the reaction of  $\text{Ru}\{\overline{\text{C}=\text{CMeC}(\text{CF}_3)_2\text{C}(\text{CN})_2}\}(\text{PPh}_3)_2(\eta\text{-C}_5\text{H}_5)$  in MeCN to 10 min (until all the starting material had dissolved) allowed the isolation of  $\text{Ru}\{\text{C}[\text{C}(\text{CN})_2]\text{CMe}=\text{C}(\text{CF}_3)_2\}(\text{NCMe})(\text{PPh}_3)(\eta\text{-C}_5\text{H}_5)$  which was purified by TLC ( $R_f$  0.38; petroleum spirit/acetone/MeCN 12:4:1) and precipitated from cyclohexane. This complex could not be effectively prepared as a crystalline or free-flowing solid for analysis, but the spectroscopic properties are as follows: IR (Nujol):  $\nu(\text{CN})$  2268w, 2238w;  $\nu(\text{CC})$  1690w(br), 1659w(br), 1592w;  $\nu(\text{CF})$  1288(sh), 1221vs, 1251(sh), 1216m, 1196s, 1182(sh); other peaks at 1483m, 1439(sh), 1435m, 1377m, 1160w, 1145w, 1137w, 1095m,

1029w, 998m, 936m, 874w, 847w, 832w, 801w, 747m, 719m, 711(sh), 700(sh), 693m, 688(sh)  $\text{cm}^{-1}$ .  $^1\text{H NMR}$  ( $\text{CDCl}_3$ ):  $\delta$  7.4 - 7.3 (m, 30 H, Ph); 4.54 (s, 5H,  $\text{C}_5\text{H}_5$ ); 1.81 (s, 3H, MeCN); 1.11 (s, 3H, Me). FAB MS: 723,  $[\text{M}]^+$ , 5; 682,  $[\text{M} - \text{MeCN}]^+$ , 23; 612\*,  $[\text{682} - \text{CF}_3]^+$ , 4; 605,  $[\text{682} - \text{Ph}]^+$ , 5; 429\*,  $[\text{Ru}(\text{PPh}_3)(\text{C}_5\text{H}_5)]^+$ , 100; 363\*,  $[\text{Ru}(\text{PPh}_3)]^+$ , 11; 350\*,  $[\text{Ru}(\text{PPh}_2)(\text{C}_5\text{H}_5)]^+$ , 21; 285\*,  $[\text{Ru}(\text{PPh}_2)]^+$ , 10; 244,  $[\text{RuPh}(\text{C}_5\text{H}_5)]^+$ , 18; 167,  $[\text{Ru}(\text{C}_5\text{H}_5)]^+$ , 14.

**1.4.14. Synthesis of  $\overline{\text{W}\{\text{NH}=\text{C}(\text{OH})\text{C}(\text{CN})=\text{CPh}=\text{C}(\text{CF}_3)_2\}}(\text{CO})_2(\eta\text{-C}_5\text{H}_5)$  (27)**

To a solution of (13) (150 mg, 0.23 mmol) in acetone (20 mL) was added  $\text{Me}_3\text{NO}\cdot 2\text{H}_2\text{O}$  (8.5 mg, 0.84 mmol). After 1.5 h of stirring in the dark, the solvent was removed under vacuum. The orange residue was purified by TLC (petroleum spirit/acetone/ $\text{CH}_2\text{Cl}_2$  2:1:1) when the product separated as a major orange band ( $R_f$  0.50) from six trace bands. Crystallization of the orange band ( $\text{CH}_2\text{Cl}_2$ /petroleum spirit) gave orange crystalline  $\overline{\text{W}\{\text{NH}=\text{C}(\text{OH})\text{C}(\text{CN})=\text{CPh}=\text{C}(\text{CF}_3)_2\}}(\text{CO})_2(\eta\text{-C}_5\text{H}_5)\cdot 0.25\text{CH}_2\text{Cl}_2$  (27) (35 mg, 0.055 mmol, 24%), m.p. 222 °C (dec.). Anal. Calcd for  $\text{C}_{21}\text{H}_{12}\text{F}_6\text{N}_2\text{O}_3\text{W}\cdot 0.25\text{CH}_2\text{Cl}_2$ : C, 38.71; H, 1.91; N, 4.25;  $M_r$  638 (unsolvated). Found: C, 38.34; H, 1.91; N, 4.31;  $M_r$  638 (mass spectrometry). IR (Fluorolube A):  $\nu(\text{OH}, \text{NH}, \text{CH})$  3379s, 3335s, 3240s, 3199(sh), 2962m, 2938m, 2880m, 2730w  $\text{cm}^{-1}$ . IR ( $\text{CH}_2\text{Cl}_2$ ):  $\nu(\text{CN})$  2199w, 1622s;  $\nu(\text{CO})$  1971s, 1895s  $\text{cm}^{-1}$ . IR (Nujol):  $\nu(\text{CC}, \text{CN})$  1546s, 1619w, 1614w;  $\nu(\text{CF})$  1334s, 1250s, 1231(sh), 1215m, 1158s, 1150s; other bands at 1133w, 1064m, 982s, 867w, 842m, 831m, 739w, 714w, 703s  $\text{cm}^{-1}$ .  $^1\text{H NMR}$  ( $\text{CDCl}_3$ ):  $\delta$  7.39 (m, 5H, Ph); 5.30 (s, 0.5H,  $\text{CH}_2\text{Cl}_2$ ); 4.91 (s, 5H,  $\text{C}_5\text{H}_5$ ). FAB MS: 638,  $[\text{M}]^+$ , 100; 613\*,  $[\text{M} - \text{CO}]^+$ , 7; 598\*,  $[\text{M} - 2\text{F}]^+$ , 14; 583\*,  $[\text{M} - 2\text{CO}]^+$ , 37; 562\*,  $[\text{M} - \text{Ph}]^+$ , 93; 517,  $[\text{M} - 2\text{CO} - (\text{C}_5\text{H}_5)]^+$ , 83; 284\*,  $[\text{W}(\text{C}_2\text{Ph})]^+$ , 49. Peaks at higher mass were found at  $m/z$  (%) 661 (14), 719 (10), 724 (5), and 748 (4).

### Syntheses of nitrile-substituted cyclobutenyl complexes

(see Tables 8-13 after Section 1.4.24 for analytical and spectroscopic data for these complexes)

#### 1.4.15. $\text{Ru}\{\overline{\text{C}=\text{CPhC}(\text{CF}_3)_2\text{C}(\text{CN})_2}\}(\text{NCMe})(\text{PPh}_3)(\eta\text{-C}_5\text{H}_5)$ (29)

(a) To a suspension of  $\text{Ru}(\text{C}_2\text{Ph})(\text{PPh}_3)_2(\eta\text{-C}_5\text{H}_5)$  (400 mg, 0.51 mmol) in MeCN (50 mL) was added dcfe (140 mg, 0.65 mmol). With vigorous stirring the suspension quickly dissolved and, after cooling (to 0 °C), a yellow precipitate of  $\text{Ru}\{\overline{\text{C}=\text{CPhC}(\text{CF}_3)_2\text{C}(\text{CN})_2}\}(\text{PPh}_3)_2(\eta\text{-C}_5\text{H}_5)$  (17) formed. This was collected and washed with MeCN (3 x 5 mL). The precipitate was suspended in MeCN (80 mL) and stirred at r.t. for 1.5 d giving a clear pale yellow solution. The solution was filtered and the volume reduced (HV) until a yellow microcrystalline product formed. This was washed with EtOH and petroleum spirit, and dried under vacuum, giving  $\text{Ru}\{\overline{\text{C}=\text{CPhC}(\text{CF}_3)_2\text{C}(\text{CN})_2}\}(\text{NCMe})(\text{PPh}_3)(\eta\text{-C}_5\text{H}_5)$  (29) (170 mg, 0.22 mmol, 43%). [The analytical sample was prepared by crystallization ( $\text{CH}_2\text{Cl}_2$ /petroleum spirit) at -15 °C.] Addition of EtOH to the combined filtrates followed by volume reduction gave a further yellow precipitate of (29) (162 mg, 0.21 mmol, 41%) which, after washing with EtOH, petroleum spirit and drying, was suitable for further preparative chemistry but was not analytically pure.

(b) A solution of  $\{\text{Ru}[\overline{\text{C}=\text{CPhC}(\text{CF}_3)_2\text{C}(\text{CN})_2}]\text{PPh}_3(\eta\text{-C}_5\text{H}_5)\}_2\{\mu\text{-(NC)}_2\text{C}=\text{C}(\text{CF}_3)_2\}$  (40a) (96 mg, 0.056 mmol) in MeCN (50 mL) was refluxed for 4 h by which time the solution had changed from blue to yellow. The solvent was removed from the filtered solution under vacuum and the product crystallized twice ( $\text{CH}_2\text{Cl}_2$ /petroleum spirit) to give large dark yellow crystals of  $\text{Ru}\{\overline{\text{C}=\text{CPhC}(\text{CF}_3)_2\text{C}(\text{CN})_2}\}(\text{NCMe})(\text{PPh}_3)(\eta\text{-C}_5\text{H}_5)$  (29) (35 mg, 0.044 mmol, 40%).

#### 1.4.16. $\text{Ru}\{\overline{\text{C}=\text{CPhC}(\text{CF}_3)_2\text{C}(\text{CN})_2}\}(\text{NCCH}=\text{CH}_2)(\text{PPh}_3)(\eta\text{-C}_5\text{H}_5)$ (31)

Acrylonitrile (24 mg, 0.46 mmol) was added to a solution of (29) (100 mg, 0.13 mmol) in benzene (20 mL). After stirring for 15 h the solvent was removed from the yellow solution

under reduced pressure. The residue was chromatographed (TLC: CH<sub>2</sub>Cl<sub>2</sub>/petroleum spirit 1:1), and a major yellow band (R<sub>f</sub> 0.53) was collected and crystallized (CH<sub>2</sub>Cl<sub>2</sub>/MeOH) to give yellow crystalline Ru{ $\overline{\text{C}=\text{CPhC}(\text{CF}_3)_2\text{C}(\text{CN})_2}$ }(NCCH=CH<sub>2</sub>)(PPh<sub>3</sub>)( $\eta$ -C<sub>5</sub>H<sub>5</sub>) (31) (68 mg, 0.087 mmol, 68%). The other three minor/trace bands were not characterized.

**1.4.17. Ru{ $\overline{\text{C}=\text{CPhC}(\text{CF}_3)_2\text{C}(\text{CN})_2}$ }{(NC)C<sub>6</sub>H<sub>2</sub>(CN)<sub>3</sub>}(PPh<sub>3</sub>)( $\eta$ -C<sub>5</sub>H<sub>5</sub>) (32)**

1,2,4,5-Tetracyanobenzene (19 mg, 0.11 mmol) was added to (29) (100 mg, 0.13 mmol) in benzene (20 mL). Stirring for 15 h resulted in a dark blue solution. The solvent was removed under reduced pressure and the residue separated by TLC (petroleum spirit/CH<sub>2</sub>Cl<sub>2</sub>/acetone 6:2:1). A major blue band (R<sub>f</sub> 0.57) was collected, and this product crystallized (CH<sub>2</sub>Cl<sub>2</sub>/hexane) as dark blue plates of Ru{ $\overline{\text{C}=\text{CPhC}(\text{CF}_3)_2\text{C}(\text{CN})_2}$ }{(NC)C<sub>6</sub>H<sub>2</sub>(CN)<sub>3</sub>}(PPh<sub>3</sub>)( $\eta$ -C<sub>5</sub>H<sub>5</sub>) (32) (31 mg, 0.034 mmol, 26%). A further major green band (R<sub>f</sub> 0.7) was collected and tentatively characterized as {Ru{ $\overline{\text{C}=\text{CPhC}(\text{CF}_3)_2\text{C}(\text{CN})_2}$ }(PPh<sub>3</sub>)( $\eta$ -C<sub>5</sub>H<sub>5</sub>)<sub>3</sub>{ $\mu$ -(NC)<sub>2</sub>C<sub>6</sub>H<sub>2</sub>(CN)<sub>2</sub>} (37 mg, 0.22 mmol, 35%). However, another compound (probably an isomer) ran with precisely the same R<sub>f</sub> and could not be separated from the green compound, the proportions of the two compounds varying with the duration of the reaction. Spectroscopic data for the impure green complex is as follows: IR (Nujol):  $\nu(\text{CN})$  2238vw, 2171s;  $\nu(\text{CC})$  1610w, 1573w;  $\nu(\text{CF})$  1290(sh), 1270s, 1220(sh), 1201s; other peaks at 1480m, 1436m 1109m, 1094m, 1071w, 1027w, 942w, 832w, 814(sh), 807w, 769w, 747m, 719m, 704(sh), 694m, 630w cm<sup>-1</sup>. <sup>1</sup>H NMR (C<sub>6</sub>D<sub>6</sub>):  $\delta$  7.2 - 6.6 [m, Ph + C<sub>6</sub>H<sub>2</sub>(CN)<sub>4</sub>]; 5.01 (d, *J* = 3.0 Hz, 4H, C<sub>5</sub>H<sub>5</sub>); 4.51 (s, 1H, C<sub>5</sub>H<sub>5</sub>, impurity). FAB MS (selected ions): 2410\*, [M]<sup>+</sup>, 1; 2096\*, [M - C=CPhC(CF<sub>3</sub>)<sub>2</sub>C(CN)<sub>2</sub>]<sup>+</sup>, 0.1; 1666, [1488 + C<sub>6</sub>H<sub>2</sub>(CN)<sub>4</sub>]<sup>+</sup>, 0.5; 1488\*, [{Ru{ $\overline{\text{C}=\text{CPhC}(\text{CF}_3)_2\text{C}(\text{CN})_2}$ }(PPh<sub>3</sub>)( $\eta$ -C<sub>5</sub>H<sub>5</sub>)<sub>2</sub>}]<sup>+</sup>, 0.7; 1350, [1488 -  $\overline{\text{C}=\text{CPhC}(\text{CF}_3)_2\text{C}(\text{CN})_2}$ ]<sup>+</sup>, 0.5; 1226\*, [1488 - PPh<sub>3</sub>]<sup>+</sup>, 0.3; 1173\*, [1488 -  $\overline{\text{C}=\text{CPhC}(\text{CF}_3)_2\text{C}(\text{CN})_2}$ ]<sup>+</sup>, 0.5; 911\*, [1173 - PPh<sub>3</sub>]<sup>+</sup>, 0.8; 744, [Ru{ $\overline{\text{C}=\text{CPhC}(\text{CF}_3)_2\text{C}(\text{CN})_2}$ }(PPh<sub>3</sub>)( $\eta$ -C<sub>5</sub>H<sub>5</sub>)<sub>2</sub>}]<sup>+</sup>, 16; 429\*, [Ru(PPh<sub>3</sub>)( $\eta$ -C<sub>5</sub>H<sub>5</sub>)<sub>2</sub>]<sup>+</sup>, 100. The green fraction and (32) appeared to interconvert in solution (after further TLC). Three minor blue-purple bands were also collected. These were examined by FAB MS; two appeared to be isomers of {Ru{ $\overline{\text{C}=\text{CPhC}(\text{CF}_3)_2\text{C}(\text{CN})_2}$ }(PPh<sub>3</sub>)( $\eta$ -C<sub>5</sub>H<sub>5</sub>)<sub>2</sub>}{ $\mu$ -(NC)<sub>2</sub>C<sub>6</sub>H<sub>2</sub>(CN)<sub>2</sub>} ([M]<sup>+</sup> 1666, ratio of ions [M]<sup>+</sup>/[RuPPh<sub>3</sub>(C<sub>5</sub>H<sub>5</sub>)<sub>2</sub>]<sup>+</sup> >1%) and the third

a hydration product  $\text{Ru}\{\text{C}_2\text{PhC}(\text{CN})_2\text{C}(\text{CF}_3)_2\}\{\text{C}_6\text{H}_2(\text{CN})_4\cdot\text{H}_2\text{O}\}(\text{PPh}_3)(\eta\text{-C}_5\text{H}_5)$  ( $[\text{M}]^+$  940).

**1.4.18.  $\text{Ru}\{\overline{\text{C}=\text{CPhC}(\text{CF}_3)_2\text{C}(\text{CN})_2}\}\{(\text{NC})\text{C}_6\text{H}_4(\text{CN})\text{-}o\}(\text{PPh}_3)(\eta\text{-C}_5\text{H}_5)$  (33)**

Phthalonitrile (22 mg, 0.17 mmol) was added to a solution of (29) (100 mg, 0.13 mmol) in benzene (10 mL). The solution became orange over 16 h, after which time the solvent was removed under reduced pressure and the residue chromatographed (TLC: petroleum spirit/acetone 2:1). A major orange band ( $R_f$  0.73) was quickly removed and precipitated ( $\text{CH}_2\text{Cl}_2$ /pentane) as an orange powder of  $\text{Ru}\{\overline{\text{C}=\text{CPhC}(\text{CF}_3)_2\text{C}(\text{CN})_2}\}\{(\text{NC})\text{C}_6\text{H}_4(\text{CN})\text{-}o\}(\text{PPh}_3)(\eta\text{-C}_5\text{H}_5)$  (33) (35 mg, 0.04 mmol, 32%). This complex was somewhat unstable in solution and slow crystallization was unsuccessful.

**1.4.19.  $\text{Ru}\{\overline{\text{C}=\text{CPhC}(\text{CF}_3)_2\text{C}(\text{CN})_2}\}\{(\text{NC})\text{C}_6\text{F}_4(\text{CN})\text{-}o\}(\text{PPh}_3)(\eta\text{-C}_5\text{H}_5)$  (34)  
and  $\{\text{Ru}[\overline{\text{C}=\text{CPhC}(\text{CF}_3)_2\text{C}(\text{CN})_2}](\text{PPh}_3)(\eta\text{-C}_5\text{H}_5)\}_2\{\mu\text{-}(\text{NC})_2\text{C}_6\text{F}_4\text{-}o\}$   
(37)**

Tetrafluorophthalonitrile (33 mg, 0.17 mmol) was added to a solution of (29) (100 mg, 0.13 mmol) in benzene (10 mL). The resulting deep red solution was evaporated to dryness after 48 h and the products separated by TLC (petroleum spirit/ $\text{CH}_2\text{Cl}_2$  1:1). A magenta band ( $R_f$  0.68) was collected and crystallized ( $\text{CH}_2\text{Cl}_2$ /hexane) to give dark purple crystals of  $\{\text{Ru}[\overline{\text{C}=\text{CPhC}(\text{CF}_3)_2\text{C}(\text{CN})_2}](\text{PPh}_3)(\eta\text{-C}_5\text{H}_5)\}_2\{\mu\text{-}(\text{NC})_2\text{C}_6\text{F}_4\text{-}o\}$  (37) (18 mg, 0.011 mmol, 17%). The next major red band ( $R_f$  0.35) was removed quickly and precipitated ( $\text{CH}_2\text{Cl}_2$ /pentane) as a dark red powder of  $\text{Ru}\{\overline{\text{C}=\text{CPhC}(\text{CF}_3)_2\text{C}(\text{CN})_2}\}\{(\text{NC})\text{C}_6\text{F}_4(\text{CN})\text{-}o\}(\text{PPh}_3)(\eta\text{-C}_5\text{H}_5)$  (34) (73 mg, 0.077 mmol, 61%). Two other trace green bands were not collected. The two compounds (34) and (37) appeared to interconvert in solution; in the case of (34) this precluded slow crystallization.

**1.4.20.  $\text{Ru}\{\overline{\text{C}=\text{CPhC}(\text{CF}_3)_2\text{C}(\text{CN})_2}\}\{(\text{NC})\text{C}_6\text{F}_4(\text{CN})\text{-}p\}(\text{PPh}_3)(\eta\text{-C}_5\text{H}_5)$  (35)**

A mixture of tetrafluoroterephthalonitrile (40 mg, 0.20 mmol) and (29) (100 mg, 0.13 mmol) in benzene (20 mL) was stirred for 16 h resulting in a deep red solution. The

solvent was removed and the residue purified by TLC (cyclohexane/Et<sub>2</sub>O/CH<sub>2</sub>Cl<sub>2</sub> 6:2:1). A major burgundy-coloured band (R<sub>f</sub> 0.5) was quickly removed and precipitated (CH<sub>2</sub>Cl<sub>2</sub>/petroleum spirit) as a dark red powder of Ru{ $\overline{\text{C}=\text{CPhC}(\text{CF}_3)_2\text{C}(\text{CN})_2}$ }-{(NC)C<sub>6</sub>F<sub>4</sub>(CN)-*p*}(PPh<sub>3</sub>)(η-C<sub>5</sub>H<sub>5</sub>) (35) (68 mg, 0.072 mmol, 57%). This product was separated from a minor purple band (R<sub>f</sub> 0.6) which had a tendency to crystallize on TLC plates. Apparent interconversion in solution was observed between (35) and this purple complex. The purple compound, which appears to be {Ru[ $\overline{\text{C}=\text{CPhC}(\text{CF}_3)_2\text{C}(\text{CN})_2}$ ](PPh<sub>3</sub>)(η-C<sub>5</sub>H<sub>5</sub>)<sub>2</sub>{μ-(NC)<sub>2</sub>C<sub>6</sub>F<sub>4</sub>-*p*}}, could not be purified effectively for analysis. Spectroscopic data for this complex is as follows: IR (Nujol): ν(CN) 2242vw, 2192s; ν(CC) 1692w(br), 1650w(br), 1611w, 1572w; ν(CF) 1288(sh), 1273s, 1201s; other peaks at 1497m, 1439m, 1400w, 1322w, 1219w, 1165w, 1109(sh), 1098m, 987w, 943w, 869w, 836w, 807w, 748w, 719w, 705(sh), 697m, 641w cm<sup>-1</sup>. <sup>1</sup>H NMR (CDCl<sub>3</sub>): δ 7.3 - 6.4 (m, 40H, Ph); 4.66 (d, J<sub>P-H</sub> = 3.1 Hz, C<sub>5</sub>H<sub>5</sub>, 10H). <sup>19</sup>F NMR (CDCl<sub>3</sub>): δ -66.1 (q, J<sub>F-F</sub> = 9 Hz, 6F, CF<sub>3</sub>); -66.4 (q, J<sub>F-F</sub> = 9 Hz, 6F, CF<sub>3</sub>); -132.7 (d, J<sub>F-F</sub> = 14 Hz, 4F, F<sub>o</sub>). FAB MS (selected ions): 1688, [M]<sup>+</sup>, 1; 1488, [{Ru[ $\overline{\text{C}=\text{CPhC}(\text{CF}_3)_2\text{C}(\text{CN})_2}$ ](PPh<sub>3</sub>)(η-C<sub>5</sub>H<sub>5</sub>)<sub>2</sub>]<sup>+</sup>, 0.8; 1173, [1488 -  $\overline{\text{C}=\text{CPhC}(\text{CF}_3)_2\text{C}(\text{CN})_2}$ ]<sup>+</sup>, 0.9; 911, [1173 - PPh<sub>3</sub>]<sup>+</sup>, 2; 744, [Ru{ $\overline{\text{C}=\text{CPhC}(\text{CF}_3)_2\text{C}(\text{CN})_2}$ }- (PPh<sub>3</sub>)(η-C<sub>5</sub>H<sub>5</sub>)]<sup>+</sup>, 31; 667\*, [744 - Ph]<sup>+</sup>, 6; 429\*, [Ru(PPh<sub>3</sub>)(η-C<sub>5</sub>H<sub>5</sub>)]<sup>+</sup>, 100; 362\*, [Ru(PPh<sub>3</sub>)]<sup>+</sup>, 15; 352\*, [Ru(PPh<sub>2</sub>)(η-C<sub>5</sub>H<sub>5</sub>)]<sup>+</sup>, 25; 244\*, [RuPh(η-C<sub>5</sub>H<sub>5</sub>)]<sup>+</sup>, 17. UV/Visible (CH<sub>2</sub>Cl<sub>2</sub>): 586 (2.2\*); 562 (2.1\*); 256 (4.8\*); 232 (7.6\*) nm; \* ε are relative values.

**1.4.21. Ru{ $\overline{\text{C}=\text{CPhC}(\text{CF}_3)_2\text{C}(\text{CN})_2}$ }{*trans*-(NC)CH=CH(CN)}(PPh<sub>3</sub>)-(η-C<sub>5</sub>H<sub>5</sub>) (36) and two isomers of {Ru[ $\overline{\text{C}=\text{CPhC}(\text{CF}_3)_2\text{C}(\text{CN})_2}$ ]- (PPh<sub>3</sub>)(η-C<sub>5</sub>H<sub>5</sub>)<sub>2</sub>{μ-*trans*-(NC)HC=CH(NC)} (38a) and (38b)**

Fumaronitrile (11 mg, 0.14 mmol) was added to a solution of (29) (100 mg, 0.13 mmol) in benzene (15 mL). A ruby-red solution developed over 16 h, after which time the solvent was removed and the residue separated by TLC (petroleum spirit/CH<sub>2</sub>Cl<sub>2</sub> 1:1). Three major bands were collected and crystallized (CH<sub>2</sub>Cl<sub>2</sub>/petroleum spirit): the first purple band (R<sub>f</sub> 0.78) was identified as {Ru[ $\overline{\text{C}=\text{CPhC}(\text{CF}_3)_2\text{C}(\text{CN})_2}$ ](PPh<sub>3</sub>)(η-C<sub>5</sub>H<sub>5</sub>)<sub>2</sub>{μ-*trans*-(NC)HC=CH-(NC)} (38a) (20 mg, 0.013 mmol, 20%), the next purple band (R<sub>f</sub> 0.72) as {Ru[ $\overline{\text{C}=\text{CPhC}(\text{CF}_3)_2\text{C}(\text{CN})_2}$ ]-

$\overline{\text{C}(\text{CF}_3)_2\text{C}(\text{CN})_2}(\text{PPh}_3)(\eta\text{-C}_5\text{H}_5)_2\{\mu\text{-trans}(\text{NC})\text{HC}=\text{CH}(\text{NC})\}$  (38b) (25 mg, 0.016 mmol, 25%) and the third orange band ( $R_f$  0.34) as  $\text{Ru}\{\overline{\text{C}=\text{CPhC}(\text{CF}_3)_2\text{C}(\text{CN})_2}\}\{\text{trans}(\text{NC})\text{CH}=\text{CH}(\text{CN})\}(\text{PPh}_3)(\eta\text{-C}_5\text{H}_5)$  (36) (41 mg, 0.050 mmol, 39%).

**1.4.22. Three isomers of  $\{\text{Ru}[\overline{\text{C}=\text{CPhC}(\text{CF}_3)_2\text{C}(\text{CN})_2}](\text{PPh}_3)(\eta\text{-C}_5\text{H}_5)_2\text{-}\{\mu\text{-(NC)}_2\text{C}=\text{C}(\text{CN})_2\}$  (39a), (39b) and (39c)**

A solution of (29) (100 mg, 0.13 mmol) and tcne (7 mg, 0.055 mmol) in benzene (15 mL) was stirred for 16 h. Removal of the solvent from the blue solution followed by TLC (petroleum spirit/acetone/ $\text{CH}_2\text{Cl}_2$  6:2:1) of the residue separated two blue bands and a green band from a complex mixture of products which remained near the base line. The first blue band ( $R_f$  0.70) crystallized ( $\text{CH}_2\text{Cl}_2$ /cyclohexane) as light blue needles of  $\{\text{Ru}[\overline{\text{C}=\text{CPhC}(\text{CF}_3)_2\text{C}(\text{CN})_2}](\text{PPh}_3)(\eta\text{-C}_5\text{H}_5)_2\}\{\mu\text{-(NC)}_2\text{C}=\text{C}(\text{CN})_2\}$  (39a) (10 mg, 0.0062 mmol, 10%), the next band ( $R_f$  0.67) crystallized ( $\text{CH}_2\text{Cl}_2$ /pentane) as light blue plates of  $\{\text{Ru}[\overline{\text{C}=\text{CPhC}(\text{CF}_3)_2\text{C}(\text{CN})_2}](\text{PPh}_3)(\eta\text{-C}_5\text{H}_5)_2\}\{\mu\text{-(NC)}_2\text{C}=\text{C}(\text{CN})_2\}$  (39b) (13 mg, 0.0080 mmol, 13%) and the green band ( $R_f$  0.63) crystallized ( $\text{CH}_2\text{Cl}_2$ /pentane) as green plates of  $\{\text{Ru}[\overline{\text{C}=\text{CPhC}(\text{CF}_3)_2\text{C}(\text{CN})_2}](\text{PPh}_3)(\eta\text{-C}_5\text{H}_5)_2\}\{\mu\text{-(NC)}_2\text{C}=\text{C}(\text{CN})_2\}$  (39c) (25 mg, 0.015 mmol, 24%). To avoid interconversion recrystallizations of all three compounds were performed quickly.

**1.4.23. Two isomers of  $\{\text{Ru}[\overline{\text{C}=\text{CPhC}(\text{CF}_3)_2\text{C}(\text{CN})_2}](\text{PPh}_3)(\eta\text{-C}_5\text{H}_5)_2\text{-}\{\mu\text{-(NC)}_2\text{C}=\text{C}(\text{CF}_3)_2\}$  (40a), (40b) and two isomers of  $\{\text{Ru}[\overline{\text{C}=\text{CPhC}(\text{CF}_3)_2\text{C}(\text{CN})_2}](\text{PPh}_3)(\eta\text{-C}_5\text{H}_5)_2\text{-}\{\mu\text{-(NC)}_2\text{C}=\text{C}(\text{CF}_3)_2\text{O}\}$  (42a) and (42b)**

(a) The olefin dcfе (75 mg, 0.35 mmol) was added to a benzene (10 mL) solution of  $\text{Ru}(\text{C}_2\text{Ph})(\text{PPh}_3)_2(\eta\text{-C}_5\text{H}_5)$  (225 mg, 0.28 mmol). The colour changed from yellow to blue over a period of 4 h; after 15 h more  $\text{Ru}(\text{C}_2\text{Ph})(\text{PPh}_3)_2(\eta\text{-C}_5\text{H}_5)$  (20 mg, 0.025 mmol) was added and the solution stirred for 1 h before removal of the solvent (HV). The residue was separated by TLC ( $\text{CH}_2\text{Cl}_2$ /petroleum spirit 2:3). The first white band ( $R_f$  0.85) was identified as  $\text{PPh}_3$  (FAB MS, spot TLC). A second, purple, band ( $R_f$  0.70) was crystallized

(CH<sub>2</sub>Cl<sub>2</sub>/petroleum spirit - analysis; benzene/octane - unit cell) as dark purple crystalline {Ru[ $\overline{\text{C}=\text{CPhC}(\text{CF}_3)_2\text{C}(\text{CN})_2}$ ](PPh<sub>3</sub>)( $\eta$ -C<sub>5</sub>H<sub>5</sub>)}<sub>2</sub>{ $\mu$ -(NC)<sub>2</sub>C=C(CF<sub>3</sub>)<sub>2</sub>} (40a) (45 mg, 0.026 mmol, 19%); the unit cell dimensions compared well with those reported previously.<sup>42,72</sup> The next blue band (R<sub>f</sub> 0.65) crystallized (CH<sub>2</sub>Cl<sub>2</sub>/petroleum spirit) as blue microcrystalline {Ru[ $\overline{\text{C}=\text{CPhC}(\text{CF}_3)_2\text{C}(\text{CN})_2}$ ](PPh<sub>3</sub>)( $\eta$ -C<sub>5</sub>H<sub>5</sub>)}<sub>2</sub>{ $\mu$ -(NC)<sub>2</sub>C=C(CF<sub>3</sub>)<sub>2</sub>} (40b) (24 mg, 0.014 mmol, 10%) and a minor green band (R<sub>f</sub> 0.35) crystallized (CH<sub>2</sub>Cl<sub>2</sub>/octane) as dark green crystals of {Ru[ $\overline{\text{C}=\text{CPhC}(\text{CF}_3)_2\text{C}(\text{CN})_2}$ ](PPh<sub>3</sub>)( $\eta$ -C<sub>5</sub>H<sub>5</sub>)}<sub>2</sub>{ $\mu$ -(NC)<sub>2</sub> $\overline{\text{C}=\text{C}(\text{CF}_3)_2\text{O}}$ } (42b) (13 mg, 0.0075 mmol, 5%). Another minor green band (R<sub>f</sub> 0.27) was also collected (42a) and identified spectroscopically as an isomer of (42b): IR (Nujol):  $\nu$ (CN) 2165s, 2047vs;  $\nu$ (CC) 1613w, 1577m;  $\nu$ (CF) 1291(sh), 1276vs, 1237(sh), 1216(sh), 1198s; other peaks at 1482w, 1437m, 1358m, 1320m, 1158w, 1128w, 1113m, 1097m, 1072w, 1054w, 1037w, 1000w, 987w, 946m, 926m, 878w, 831m, 818w, 745m, 719m, 702(sh), 693m, 633m cm<sup>-1</sup>; <sup>1</sup>H NMR (CDCl<sub>3</sub>): No signals detected; FAB MS (selected ions): 1720, [M]<sup>+</sup>, 9; 1404\*, [M -  $\overline{\text{C}=\text{CPhC}(\text{CF}_3)_2\text{C}(\text{CN})_2}$ ]<sup>+</sup>, 1; 812, [1405 - PPh<sub>3</sub> - CF<sub>3</sub>]<sup>+</sup>, 3; 744\*, [Ru{ $\overline{\text{C}=\text{CPhC}(\text{CF}_3)_2\text{C}(\text{CN})_2}$ }(PPh<sub>3</sub>)( $\eta$ -C<sub>5</sub>H<sub>5</sub>)]<sup>+</sup>, 17; 429\*, [Ru(PPh<sub>3</sub>)( $\eta$ -C<sub>5</sub>H<sub>5</sub>)]<sup>+</sup>, 100; 352\*, [Ru(PPh<sub>2</sub>)( $\eta$ -C<sub>5</sub>H<sub>5</sub>)]<sup>+</sup>, 16; 244\*, [RuPh( $\eta$ -C<sub>5</sub>H<sub>5</sub>)]<sup>+</sup>, 13.

As noted below, complex (40a) converts into (42a), and (40b) into (42b), when placed in solution. Pure solutions of (40a) or (40b), when subjected to TLC, invariably show minor amounts of the corresponding isomers of (42). The ESR spectra of all four complexes show a common broad absorption ( $g = 2.038$ ,  $\Delta H_{pp} 31\text{G}$ ). None of the other 7 bands present in the initial TLC separation was identified. A reaction carried out in CH<sub>2</sub>Cl<sub>2</sub> gave none of the complexes (40) or (42), and of the 16 products only PPh<sub>3</sub> was characterized (IR, <sup>1</sup>H NMR).

(b) Complexes (40a), (40b) and (42b) were isolated from the reaction of (29) (130 gm, 0.16 mmol) with dcfe (35 mg, 0.16 mmol) in benzene (20 mL). After 7 h the solvent was removed from the blue solution and the residue purified by preparative TLC (petroleum spirit/CH<sub>2</sub>Cl<sub>2</sub> 3:2). Three bands were collected and identified (IR, <sup>1</sup>H NMR, and FAB MS) as: (40a) (R<sub>f</sub> 0.8, purple), (40b) (R<sub>f</sub> 0.7, blue) and (42b) (R<sub>f</sub> 0.3, green).

#### 1.4.24. Reaction of complexes (40) with O<sub>2</sub>

(a) A solution of (40a) (2 mg, 0.001 mmol) in benzene (5 mL) was degassed with O<sub>2</sub> and left under normal lighting conditions for 4 days. At this stage spot TLC indicated a significant proportion of (42a) present in solution. ESR confirmed the presence of a paramagnetic complex with a broad signal at g 2.038.

(b) Similarly a solution of (40b) (4 mg, 0.002 mmol) was left for 4 days under O<sub>2</sub>. Spot TLC analysis of the solution indicated a significant amount of (42b) (an ESR signal was observed at g 2.038) and a trace amount of (40a).

(c) A solution of (40a) (1 mg, 0.0005 mmol) in CH<sub>2</sub>Cl<sub>2</sub> was supported on silica (287 mg, 200 mesh) and left in the dark for 4 d. At this stage the silica had a green colouration and the adsorbed complex was removed (CH<sub>2</sub>Cl<sub>2</sub>/MeOH) and evaporated to dryness under reduced pressure. The residue was separated by TLC (petroleum spirit/CH<sub>2</sub>Cl<sub>2</sub>/acetone 4:2:1) to give a green band (R<sub>f</sub> 0.7) identified (spot TLC, FAB MS) as (42b) and a blue-green band (R<sub>f</sub> 0.65) identified (spot TLC, FAB MS) as (42a).

Table 8. Analytical data for the nitrile complexes

Cmpd	m.p. (°C)	Formula (Empirical)	Calculated (%)			Found (%)		
			C	H	N	C	H	N
(29)	154-155	C <sub>39</sub> H <sub>28</sub> F <sub>6</sub> N <sub>3</sub> PRu.0.75CH <sub>2</sub> Cl <sub>2</sub>	56.27	3.50	4.95	56.33	3.84	4.88
(31)	169-172	C <sub>40</sub> H <sub>28</sub> F <sub>6</sub> N <sub>3</sub> PRu	60.30	3.54	5.28	59.73	3.52	5.23
(32)	265(dec.)	C <sub>47</sub> H <sub>27</sub> F <sub>6</sub> N <sub>6</sub> PRu.0.5CH <sub>2</sub> Cl <sub>2</sub>	59.17	2.93	8.72	59.76	3.33	8.52
(33)	156-157	C <sub>45</sub> H <sub>29</sub> F <sub>6</sub> N <sub>4</sub> PRu	62.00	3.35	6.43	62.38	3.47	6.31
(34)	146-148	C <sub>45</sub> H <sub>25</sub> F <sub>10</sub> N <sub>4</sub> PRu	57.27	2.67	5.94	56.93	2.66	6.29
(35)	185-187	C <sub>45</sub> H <sub>25</sub> F <sub>10</sub> N <sub>4</sub> PRu	57.27	2.67	5.94	56.67	2.67	6.12
(36)	174-176	C <sub>41</sub> H <sub>27</sub> F <sub>6</sub> N <sub>4</sub> PRu	59.93	3.31	6.82	59.64	3.38	6.70
(37)	154-155	C <sub>82</sub> H <sub>50</sub> F <sub>16</sub> N <sub>6</sub> P <sub>2</sub> Ru <sub>2</sub>	57.84	3.44	4.67	56.95	3.30	4.60
(38 a)	178-179	C <sub>78</sub> H <sub>52</sub> F <sub>12</sub> N <sub>6</sub> P <sub>2</sub> Ru <sub>2</sub> .CH <sub>2</sub> Cl <sub>2</sub>	57.62	3.39	5.08	57.50	3.30	5.09
(38 b)	187-189	C <sub>78</sub> H <sub>52</sub> F <sub>12</sub> N <sub>6</sub> P <sub>2</sub> Ru <sub>2</sub> .1.5CH <sub>2</sub> Cl <sub>2</sub>	56.40	3.33	4.96	56.62	3.39	4.95
(39 a)	300(dec.)	C <sub>80</sub> H <sub>50</sub> F <sub>12</sub> N <sub>8</sub> P <sub>2</sub> Ru <sub>2</sub>	59.48	3.12	6.94	60.09	3.45	6.72
(39 b)	260(dec.)	C <sub>80</sub> H <sub>50</sub> F <sub>12</sub> N <sub>8</sub> P <sub>2</sub> Ru <sub>2</sub> .0.5CH <sub>2</sub> Cl <sub>2</sub>	58.32	3.10	6.76	58.61	3.26	6.69
(39 c)	265(dec.)	C <sub>80</sub> H <sub>50</sub> F <sub>12</sub> N <sub>8</sub> P <sub>2</sub> Ru <sub>2</sub>	59.48	3.12	6.94	59.60	3.22	6.83
(40 a)	179-182	C <sub>80</sub> H <sub>50</sub> F <sub>18</sub> N <sub>6</sub> P <sub>2</sub> Ru <sub>2</sub>	56.48	2.96	4.94	55.24	3.09	4.72
(40 b)	110-112	C <sub>80</sub> H <sub>50</sub> F <sub>18</sub> N <sub>6</sub> P <sub>2</sub> Ru <sub>2</sub>	56.48	2.96	4.94	56.98	3.55	4.69
(42 b)	150(dec.)	C <sub>80</sub> H <sub>50</sub> F <sub>18</sub> N <sub>6</sub> O <sub>2</sub> P <sub>2</sub> Ru <sub>2</sub>	55.95	2.93	4.89	56.78	3.41	4.74

Table 9. FAB MS data for the nitrile complexes

		Compounds							
		(29)	(31)	(32)	(33)	(34)	(35)	(36)	(37)
Molecular Ion:									
[M] <sup>+</sup>	m/z	785	797	922	872	944	944	822	1688
	(%)	(8)	(6)	(2)	(5)	(5)	(2)	(2)	(2)
Common Fragment <sup>†</sup> or Aggregate Ions									
[M <sub>2</sub> -L] <sup>+</sup>	m/z	1529	1541	1666	1616	1688	1688	1566	-
	(%)	(0.9)	(2)	(0.6)	(0.4)	(0.4)	(0.6)	(0.7)	-
[M-ring] <sup>+</sup>	m/z	-	-	-	-	-	-	-	1373
	(%)	-	-	-	-	-	-	-	(2)
[M-dcfe] <sup>+</sup>	m/z	-	-	-	-	-	-	-	-
	(%)	-	-	-	-	-	-	-	-
[MO] <sup>+</sup>	m/z	-	-	-	-	-	-	-	-
	(%)	-	-	-	-	-	-	-	-
[M-ring] <sup>+</sup>	m/z	-	-	-	-	-	-	-	-
	(%)	-	-	-	-	-	-	-	-
m/z									
1488	%	1	1	0.1	0.5	0.7	0.5	0.4	1
1226	"	0.3	0.6	0.2	0.5	0.4	0.2	0.3	0.4
1173	"	2	1	0.4	0.6	0.4	1	0.5	0.8
911	"	1	1	1	1	0.7	0.7	0.6	1
744	"	36	29	18	17	49	25	24	40
718	"	3	2	2	1	-	3	2	3
675	"	3	2	3	2	3	3	2	3
667	"	6	5	5	6	6	6	4	6
596	"	3	3	3	3	2	2	1	3
530	"	3	3	3	7	3	2	2	3
482	"	6	6	7	6	6	6	5	6
453	"	9	10	9	7	8	9	6	8
445	"	6	6	8	6	7	8	5	8
429	"	100	100	100	100	100	100	100	100
362	"	10	9	10	12	10	11	8	9
351	"	17	16	18	50	15	17	12	13
285	"	7	7	8	17	7	7	6	7
244	"	13	12	14	20	1	13	9	12
167	"	167	11	11	22	10	-	8	10

Table 9. FAB MS data for the nitrile complexes (continued)

		Compounds							
		(38a)	(38b)	(39a)	(39b)	(39c)	(40a)	(40b)	(42b)
Molecular Ion:									
[M] <sup>+</sup>	m/z	1566	1566	1616	1616	1616	1703	1703	1720
	(%)	(2)	(1)	(6)	(3)	(1)	(1)	(2)	(10)
Common Fragment <sup>†</sup> or Aggregate Ions									
[M <sub>2</sub> -L] <sup>+</sup>	m/z	-	-	-	-	-	-	-	-
	(%)	-	-	-	-	-	-	-	-
[M-ring] <sup>+</sup>	m/z	-	-	-	-	-	-	-	-
	(%)	-	-	-	-	-	-	-	-
[M-dcfe] <sup>+</sup>	m/z	-	-	-	-	-	1488	1488	-
	(%)	-	-	-	-	-	(0.4)	(0.6)	-
[MO] <sup>+</sup>	m/z	-	-	-	-	-	1720	1720	-
	(%)	-	-	-	-	-	(1)	(3)	-
[M-ring] <sup>+</sup>	m/z	1251	1251	1301	1301	1301	1387	1387	1403
	(%)	(0.6)	(0.6)	(1)	(0.6)	(0.4)	(0.4)	(0.5)	(0.9)
<u>m/z</u>									
1488	%	1	1	0.2	0.2	0.1	0.4	0.6	-
1226	"	0.3	0.5	0.3	0.2	-	-	-	-
1173	"	0.8	1	0.4	0.3	0.2	0.6	0.5	0.2
911	"	0.9	2	1	1	0.5	-	0.6	0.8
744	"	25	31	20	13	8	20	23	14
718	"	3	4	3	2	1	-	-	-
675	"	3	5	5	3	2	-	-	2
667	"	5	7	6	4	2	4	4	2
596	"	-	4	4	3	2	-	-	2
530	"	3	5	5	3	3	3	3	3
482	"	7	9	11	8	6	7	10	7
453	"	9	15	13	7	7	9	15	9
445	"	12	11	10	8	6	13	8	-
429	"	100	100	100	100	100	100	100	100
362	"	15	19	10	12	10	13	-	8
351	"	26	36	22	28	22	18	16	15
285	"	14	17	9	12	13	9	-	5
244	"	18	25	14	18	17	18	-	13
167	"	21	22	12	18	16	14	-	10

† Assignments for the listed ions in the FAB Mass Spectra:

1488\*, [ $\{\text{Ru}(\overline{\text{C}=\text{CPhC}(\text{CF}_3)_2\text{C}(\text{CN})_2})(\text{PPh}_3)(\eta\text{-C}_5\text{H}_5)\}_2\}^+$ ]; 1226\*, [1488 - PPh<sub>3</sub>]<sup>+</sup>; 1173\*, [1488 -  $\overline{\text{C}=\text{CPhC}(\text{CF}_3)_2\text{C}(\text{CN})_2}$ ]<sup>+</sup>; 911\*, [1173 - PPh<sub>3</sub>]<sup>+</sup>; 744, [ $\text{Ru}\{\overline{\text{C}=\text{CPhC}(\text{CF}_3)_2\text{C}(\text{CN})_2}\}(\text{PPh}_3)(\eta\text{-C}_5\text{H}_5)\}^+$ ]; 718\*, [744 - CN]<sup>+</sup>; 675\*, [744 - CF<sub>3</sub>]<sup>+</sup>; 667\*, [744 - Ph]<sup>+</sup>; 596\*, [ $\{\text{Ru}(\eta\text{-C}_5\text{H}_5)\}_2(\text{PPh}_3)\}^+$ ]; 530\*, [ $\text{Ru}(\text{C}_2\text{Ph})(\text{PPh}_3)(\eta\text{-C}_5\text{H}_5)\}^+$ ]; 482\*, [ $\text{Ru}\{\overline{\text{C}=\text{CPhC}(\text{CF}_3)_2\text{C}(\text{CN})_2}\}^+$ ]; 453\*, [ $\text{RuC}_2(\text{PPh}_3)(\eta\text{-C}_5\text{H}_5)\}^+$ ]; 445\*, [ $\text{Ru}(\text{PPh}_3)(\eta\text{-C}_5\text{H}_5)\text{O}\}^+$ ]; 429\*, [ $\text{Ru}(\text{PPh}_3)(\eta\text{-C}_5\text{H}_5)\}^+$ ]; 362\*, [ $\text{Ru}(\text{PPh}_3)\}^+$ ]; 352\*, [ $\text{Ru}(\text{PPh}_2)(\eta\text{-C}_5\text{H}_5)\}^+$ ]; 283\*, [ $\text{Ru}(\text{PPh}_2)\}^+$ ]; 244, [ $\text{RuPh}(\eta\text{-C}_5\text{H}_5)\}^+$ ]; 167, [ $\text{Ru}(\eta\text{-C}_5\text{H}_5)\}^+$ ].

[M-ring]<sup>+</sup> = [ $\text{M} - \overline{\text{C}=\text{CPhC}(\text{CF}_3)_2\text{C}(\text{CN})_2}$ ]<sup>+</sup>;

[M<sub>2</sub>-L]<sup>+</sup> = [2 x [M] - nitrile ligand]<sup>+</sup>.

Table 10. Infrared data<sup>†</sup> for the nitrile complexes

Cmpd	IR (cm <sup>-1</sup> , nujol)			
	v(CN)	v(CC)	v(CF)	Other bands
(29)	2267m, 2235w.	1613m, 1590w. 1576m.	1310(sh), 1293(sh), 1281s(br), 1246(sh), 1222s, 1200s, 1190(sh), 1099s.	1968w, 1900w, 1825w, 1670w, 1491m, 1482s, 1445(sh), 1439s, 1436s, 1161m, 1148m, 1090s, 1072m, 1060m, 1050w, 1030w, 1028w, 1016w, 1000w, 989m, 942s, 921w, 855m, 1110s, 840m, 817m, 808m, 771m, 750s, 740(sh), 701s, 698s, 633s, 600m.
(31)	2240(sh), 2223s.	1614m, 1601(sh), 1587w, 1574s.	1269s, 1200s, 1183(sh), 1107s, 1096s, 1089(sh).	1964w, 1908w, 1825w, 1772w, 1672w, 1488(sh), 1479s, 1442(sh), 1435s, 1408w, 1377m, 1366w, 1361w, 1341w, 1159m, 1142m, 1071m, 1058m, 1048m, 1024m, 1012m, 997m, 985m, 951s, 938s, 920(sh), 898w, 895s, 850(sh), 837s, 814(sh), 804s, 770m, 752(sh), 747s.
(32)	2242w, 2180s.	1611w, 1696(sh), 1587m, 1572(sh).	1290(sh), 1266s, 1237m, 1193s, 1097(sh), 1088(sh).	1527m, 1481m, 1435m, 1158w, 1139w, 1107m, 1071w, 1057w, 1025w, 1008(sh), 998w, 990(sh), 941m, 918m, 876w, 832m, 810(sh), 808m, 768w, 749m, 737(sh), 719m, 703(sh), 694s, 631w.
(33)	2244(sh), 2240m, 2211s.	1612w, 1593m, 1571m.	1310(sh), 1295(sh), 1272s, 1223s, 1197s, 1208(sh).	1471m, 1448m, 1146w, 1110m, 1099m, 1073w, 1060w, 1031w, 1011w, 990w, 988(sh), 943s, 885(sh), 870s, 849m, 835s, 818s, 810s, 769s, 757(sh), 748s, 722s, 700vs, 649(sh), 634s.
(34)	2239vw, 2193s.	1612w, 1577w.	1290(sh), 1272s, 1250(sh), 1241(sh), 1202s.	1513s, 1490m, 1483(sh), 1438m, 1154w, 1110m, 1099m, 1092(sh), 1076w, 1062w, 1030w, 976w, 944m, 838w, 811m, 772w, 749m, 721m, 705(sh), 698s, 633w.

<sup>†</sup> All spectra were recorded as Nujol mulls.

Table 10. Infrared data (continued)

Cmpd	IR (cm <sup>-1</sup> , nujol)			
	v(CN)	v(CC)	v(CF)	Other bands
(35)	2249w, 2199(sh), 2179s.	1644m, 1610w, 1569w.	1290(sh), 1269s, 1219s, 1200s, 1182(sh).	1497s, 1480w, 1437m, 1324m, 1161w, 1145w, 1108m, 1098(sh), 1090(sh), 1075w, 1058w, 1028w, 990m, 941m, 868w, 834w, 809w, 750m, 720m, 705(sh), 695m, 629w.
(36)	2236vw, 2226vw, 2186s, 2179s.	1611w, 1597(sh), 1590m, 1570w.	1270s, 1219m, 1198s.	1481w, 1436m, 1139w, 1108m, 1097w, 1088m, 1071w, 1059w, 1027w, 999w, 989w, 949w, 937m, 865m, 854m, 814w, 800m, 769w, 747m, 719m, 695s, 630w.
(37)	2242vw, 2204(sh), 2195s.	1612vw, 1577vw.	1293(sh), 1273s, 1204s.	1515m, 1481m, 1439m, 1221w, 1188w, 1111m, 1100(sh), 1092w, 979w, 945w, 838w, 819w, 773w, 750m, 721m, 708s, 699s.
(38 a)	2240w, 2200s.	1610w, 1580w, 1564w.	1268s, 1220m 1198s, 1184(sh).	1489(sh), 1480m, 1436m, 1156w, 1142w, 1095m, 1107m, 1080(sh), 1072w, 1059w, 1028w, 997w, 987w, 941m, 909w, 866w, 835m, 812m, 770m, 749s, 719m, 696s, 684(sh), 648w.
(38 b)	2239w, 2202s.	1610w, 1575w.	1291(sh), 1268s, 1219m, 1198s, 1181(sh).	1489(sh), 1482m, 1436m, 1158w, 1107m, 1095m, 1070w, 1058w, 1026w, 1008w, 998w, 987w, 941m, 908w, 864w, 835m, 816(sh), 805m, 769w, 747m, 718m, 700s, 694s, 630w.
(39 a)	2289vw, 2206w, 2159s, 2095s, 2018(sh).	1612m, 1585(sh), 1572m.	1298(sh), 1270s, 1220(sh), 1200s, 1197(sh).	1481m, 1436m(br), 1358m, 1157w, 1146w, 1109m, 1097m, 1071w, 1059w, 1037w, 1008(sh), 999w, 987w, 920w, 887w, 850(sh), 835m, 816m, 769w, 747s, 719m, 702(sh).

Table 10. Infrared data (continued)

Cmpd	IR (cm <sup>-1</sup> , nujol)			
	v(CN)	v(CC)	v(CF)	Other bands
(39 b)	2283vw, 2209w, 2158s, 2093s.	1610m, 1587(sh), 1572m.	1290(sh), 1270s, 1219(sh), 1200s, 1186(sh).	1481m, 1437m, 1359w, 1158w, 1147w, 1108m, 1097m, 1070w, 1068w, 1028w, 1008(sh), 999w, 987w, 942m, 881w, 831w, 812m, 769w, 746m, 719m, 702(sh), 693m, 631w.
(39 c)	2280vw, 2220vw, 2116vs.	1612w, 1572w.	1290(sh), 1270s, 1218(sh), 1201s, 1187(sh).	1482w, 1436m, 1358w, 1109m, 1097w, 1082w, 1058w, 942w, 886w, 832w, 815w, 769w, 745m, 719m, 703(sh), 692m, 631w.
(40 a)	2239vw, 2178(sh), 2151(sh), 2112s, 2018m.	1613w, 1576w.	1308(sh), 1291(sh), 1270s, 1238s, 1219m, 1198s, 1187(sh).	1532m, 1481w, 1437m, 1411w, 1346s, 1167m, 1158m, 1144w, 1109m, 1097m, 1092(sh), 1071w, 999w, 971w, 945m, 878w, 854w, 837m, 816m, 770w, 755m, 749(sh), 744m, 719m, 705m, 697(sh), 631w.
(40 b)	2241vw, 2175(sh), 2150(sh), 2117s, 2020s.	1622w, 1574w.	1272s, 1244s, 1205s.	1511w, 1482(sh), 1438m, 1357m, 1157m, 1110m, 1099m, 944w, 836w, 816w, 771w, 749m, 721m, 707s, 696s, 633w.
(42 b)	2161m, 2008s(br)	1608m, 1588vw, 1570m.	1262s, 1250s, 1200s.	1435m, 1355m, 1316m, 1185(sh), 1157w, 1128w, 1107m, 1098m, 1070w, 1059w, 1028w, 1000w, 986w, 945w, 922w, 831w, 817w, 769w, 749m, 710m, 700m, 692m, 630w.

Table 11.  $^1\text{H}$  and  $^{19}\text{F}$  NMR data for the nitrile complexes

Cmpd	$^1\text{H}$ NMR ( $\delta$ )	$^{19}\text{F}$ NMR ( $\delta$ )
d c f e		-61.8 (s, $\text{CF}_3$ ).
(29)	( $\text{CDCl}_3$ ): 7.4 - 6.5 (m, 20H, Ph); 5.27 (s, 1.5H, $\text{CH}_2\text{Cl}_2$ ); 4.41 (s, 5H, $\text{C}_5\text{H}_5$ ); 1.95 (d, $J_{\text{P-H}} = 1.2$ Hz, 3H, MeCN).	( $\text{CDCl}_3$ ): -66.2 (q, $J_{\text{F-F}} = 10$ Hz, $\text{CF}_3$ ); -66.4 (q, $J_{\text{F-F}} = 10$ Hz, $\text{CF}_3$ ).
(31)	( $\text{CDCl}_3$ ): 7.4 - 6.5 (m, 20H, Ph); 5.74 (m, 1H, CH); 5.55 (m, 2H, $\text{CH}_2$ ); 4.50 (s, 5H, $\text{C}_5\text{H}_5$ ).	Not recorded.
(32)	( $\text{C}_6\text{D}_6$ ): 7.2 - 6.5 (m, 22H, Ph + $\text{C}_6\text{H}_2$ ); 4.82 (s, 5H, $\text{C}_5\text{H}_5$ ); 4.30 (s, 1H, $\text{CH}_2\text{Cl}_2$ )	( $\text{CDCl}_3$ ): -66.1 (q, $J_{\text{F-F}} = 10$ Hz, $\text{CF}_3$ ); -66.5 (q, $J_{\text{F-F}} = 10$ Hz, $\text{CF}_3$ ).
(33)	( $\text{CDCl}_3$ ): 7.6 - 6.5 (m, 24H, Ph + $\text{C}_6\text{H}_4$ ); 4.67 (s, 5H, $\text{C}_5\text{H}_5$ ).	( $\text{CDCl}_3$ ): -66.1 (m, unresolved, $\text{CF}_3$ ); -66.4 (m, unresolved, $\text{CF}_3$ ).
(34) *	( $\text{C}_6\text{D}_6$ ): 7.1 - 6.5 (m, 20H, Ph); 4.82 (s, 5H, $\text{C}_5\text{H}_5$ ).	( $\text{CDCl}_3$ ): -66.1 (q, $J_{\text{F-F}} = 9$ Hz, 3F, $\text{CF}_3$ ); -66.4 (q, $J_{\text{F-F}} = 11$ Hz, 3F, $\text{CF}_3$ ); -127.3 (m, 1F, $\text{F}_{3,6}$ ); -128.3 (m, 1F, $\text{F}_{3,6}$ ); -142.0 (m, 1F, $\text{F}_{4,5}$ ); -144.5 (m, 1F, $\text{F}_{4,5}$ ).
(35) *	( $\text{CDCl}_3$ ): 7.4 - 6.4 (m, 20H, Ph); 4.70 (s, 5H, $\text{C}_5\text{H}_5$ ).	( $\text{CDCl}_3$ ): -66.1 (q, $J_{\text{F-F}} = 10$ Hz, 3F, $\text{CF}_3$ ); -66.4 (q, $J_{\text{F-F}} = 9$ Hz, 3F, $\text{CF}_3$ ); -128.7 (d, $J_{\text{F-F}} = 14$ Hz, 2F, $\text{F}_{3,5}$ ); -130.5 (dd, $J_{\text{F-F}} = 23, 8$ , 1F, $\text{F}_{2,6}$ ); -131.4 (dd, $J_{\text{F-F}} = 23, 11$ Hz, 1F, $\text{F}_{2,6}$ ).
(36) *	( $\text{CDCl}_3$ ): 7.4 - 6.5 (m, 20H, Ph); 6.03 (d, $J_{\text{H-H}} = 17$ Hz, 1H, CH); 5.49 (d, $J_{\text{H-H}} = 17$ Hz, 1H, CH); 4.56 (s, 5H, $\text{C}_5\text{H}_5$ ).	( $\text{CDCl}_3$ ): -66.2 (q, $J_{\text{F-F}} = 10$ Hz, $\text{CF}_3$ ); -66.4 (q, $J_{\text{F-F}} = 11$ Hz, $\text{CF}_3$ ).

\* For numbering of fluoroaromatic rings ( $\text{F}_1$ - $\text{F}_6$ ) see Section 1.2.5.

Table 11.  $^1\text{H}$  and  $^{19}\text{F}$  NMR data (continued)

Cmpd	$^1\text{H}$ NMR ( $\delta$ )	$^{19}\text{F}$ NMR ( $\delta$ )
(37)	( $\text{C}_6\text{D}_6$ ): 7.1 - 6.5 (m, 40H, Ph); 5.01 (s, 10H, $\text{C}_5\text{H}_5$ ).	( $\text{CDCl}_3$ ): -66.1 (q, $J_{\text{F-F}} = 11$ Hz, 6F, $\text{CF}_3$ ); -66.4 (q, $J_{\text{F-F}} = 10$ Hz, 6F, $\text{CF}_3$ ); -128.7 (d, $J_{\text{F-F}} = 14$ Hz, 2F, $\text{F}_{3,6}$ ); -145.5 (d, $J_{\text{F-F}} = 11$ Hz, 2F, $\text{F}_{4,5}$ ).
(38 a)	( $\text{CDCl}_3$ ): 7.4 - 6.4 (m, 40H, Ph); 5.30 (s, 2H, $\text{CH}_2\text{Cl}_2$ ); 5.14 (s, 2H, CH); 4.56 (s, 10H, $\text{C}_5\text{H}_5$ ).	( $\text{CDCl}_3$ ): -66.1 (q, $J_{\text{F-F}} = 10$ Hz, $\text{CF}_3$ ); -66.4 (q, $J_{\text{F-F}} = 10$ Hz, $\text{CF}_3$ ).
(38 b)	( $\text{CDCl}_3$ ): 7.3 - 6.5 (m, 40H, Ph); 5.30 (s, 3H, $\text{CH}_2\text{Cl}_2$ ); 5.29 (s, 2H, CH); 4.57 (s, 10H, $\text{C}_5\text{H}_5$ )	( $\text{CDCl}_3$ ): -66.1 (q, $J_{\text{F-F}} = 10$ Hz, $\text{CF}_3$ ); -66.4 (q, $J_{\text{F-F}} = 10$ Hz, $\text{CF}_3$ ).
(39 a)	( $\text{C}_6\text{D}_6$ ): 7.4 - 6.4 (m, 40H, Ph); 4.94 (s, 10H, $\text{C}_5\text{H}_5$ ).	( $\text{CDCl}_3$ ): -65.8 (q, $J_{\text{F-F}} = 10$ Hz, $\text{CF}_3$ ); -66.4 (q, $J_{\text{F-F}} = 10$ Hz, $\text{CF}_3$ ).
(39 b)	( $\text{C}_6\text{D}_6$ ): 7.2 - 6.5 (m, 40H, Ph); 4.99 (s, 10H, $\text{C}_5\text{H}_5$ ); 4.50 (s, 1H, $\text{CH}_2\text{Cl}_2$ ).	( $\text{CDCl}_3$ ): -65.7 (m, unresolved, $\text{CF}_3$ ); -66.4 (m, unresolved, $\text{CF}_3$ ).
(39 c)	( $\text{C}_6\text{D}_6$ ): 7.1 - 6.4 (m, 40H, Ph); 4.78 (d, $J_{\text{P-H}} = 1$ Hz, 10H, $\text{C}_5\text{H}_5$ ).	( $\text{CDCl}_3$ ): -66.0 (q, $J_{\text{F-F}} = 12$ Hz, $\text{CF}_3$ ); -66.4 (q, $J_{\text{F-F}} = 11$ Hz, $\text{CF}_3$ ).
(40 a)	( $\text{C}_6\text{D}_6$ ): 7.2 - 6.4 (m, 40H, Ph); 5.03 (s, 10H, $\text{C}_5\text{H}_5$ ).	( $\text{CDCl}_3$ ): -61.5 (s, 6F, dcfe); -66.0 (q, $J_{\text{F-F}} = 10$ Hz, 6F, $\text{CF}_3$ ); -66.4 (q, $J_{\text{F-F}} = 10$ Hz, 6F, $\text{CF}_3$ ).
(40 b)	( $\text{C}_6\text{D}_6$ ): 7.4 - 6.4 (m, 40H, Ph); 4.81 (s, 10H, $\text{C}_5\text{H}_5$ ).	( $\text{CDCl}_3$ ): -59.8 (s, 6F, dcfe); -65.8 (q, $J_{\text{F-F}} = 10$ Hz, 6F, $\text{CF}_3$ ); -66.3 (q, $J_{\text{F-F}} = 10$ Hz, 6F, $\text{CF}_3$ ).
(42 b)	( $\text{CDCl}_3$ ): No Signals.	Not recorded.

Table 12. UV/Visible data for the nitrile complexes†

	Compounds					
	(29)	(30)	(31)	(32)	(33)	(34)
<b>UV bands</b>	234 (4.3) 286 (0.7) 336 (0.3)	234 (4.3) 312 (2.1)	234 (4.0) 334 (1.1)	232 (4.7) 266 (2.6) 306 (1.3)	234 (5.1) 266 (1.9)	234 (4.4) 258 (2.8) 282 (2.1) 344 (0.5)
<b>CT bands</b>	-	-	-	546 (0.9) 644 (1.0)	400 (0.8) 448 (0.7)	470 (1.0) 510 (1.2)

	Compounds					
	(35)	(36)	(37)	(38a)	(38b)	(39a)
<b>UV bands</b>	238 (4.4) 256 (3.4) 290 (1.4)	234 (3.9) 256 (2.3) 292 (1.0)	234 (7.7) 276 (4.1) 342 (1.1)	234 (6.9) 256 (2.3)	234 (8.0) 256 (4.5) 290 (2.6)	232 (7.0) 288 (3.4) 328 (1.5)
<b>CT bands</b>	484 (1.2) 534 (1.3)	444 (1.1) 498 (0.8)	506 (2.1) 552 (1.9)	502 (2.1) 564 (2.4)	492 (2.4) 548 (2.7)	646 (1.9) > 900

	Compounds					
	(39b)	(39c)	(40a)	(40b)	(41)	(42b)
<b>UV bands</b>	232 (7.0)* 292 (3.0)	234 (8.0) 308 (2.4)	232 (7.4) 294 (2.9) 326 (1.0)	232 (7.4)* 240 (5.5) 324 (1.4)	234 (3.5) 284 (0.6)	234 (8.1) 274 (4.4) 350 (0.2)
<b>CT bands</b>	640 (1.6) > 900	634 (2.0) > 900	560 (1.2) 770 (1.7)	572 (0.9) 814 (1.6)	-	594 (0.5)

†  $\lambda_{\max}$ , nm ( $10^4 \epsilon$ ,  $M^{-1}cm^{-1}$ );  $CH_2Cl_2$  solutions; the mark \* indicates  $\epsilon$  are relative values.

Table 13. Electrochemical data for the nitrile complexes

		Compounds							
		(29)	(31)	(32)	(33)	(34)	(35)	(36)	(37)
<i>Square Wave Voltammetry</i>									
1st Oxid.	$E_p$	0.81	0.84	1.06	0.95	1.00	1.03	0.96	1.04
2nd Oxid.	$E_p$	-	-	-	-	-	-	-	1.10
1st Red.	$E_p$	-	-	-0.58	-1.59	-1.34	-0.97	-1.20	-1.24
2nd Red.	$E_p$	-	-	-1.61	-	-	-	-	-
<i>Cyclic Voltammetry</i>									
First Oxidation Process									
	$E_{1/2}$	0.89	0.87	1.07	0.95	1.07	1.05	0.97	1.08
	$E_{pa}$	1.26	0.96	1.13	1.02	1.31	1.16	1.07	1.18
	$E_{pc}$	0.51	0.78	1.01	0.89	0.83	0.93	0.88	0.97
	$n_{rel}$	-	-	1	1	1	1	1	2
	Reversibility	Rev.	Q-Rev.	N-Rev.	Q-Rev.	Rev.	Q-Rev.	Q-Rev.	Q-Rev.
	Diffusion control	No	No	Yes	Yes	Yes	No	No	No
First Reduction Process									
	$E_{1/2}$	-	-	-0.55	-	-	-0.97	-	-
	$E_{pa}$	-	-	-0.49	-	-	-0.85	-	-
	$E_{pc}$	-	-	-0.60	-1.66	-1.56	-1.09	-1.28	-1.50
$n_{meas}$	$n_{rel}$	-	-	1*	$\approx 1$	2	1	1	2
	Reversibility	-	-	Rev.	Irrev.	Irrev.	Rev.	Irrev.	Irrev.
	Diffusion control	-	-	Yes	Yes	No	No	No	No
Second Reduction Process									
	$E_{1/2}$	-	-	-	-	-	-	-	-
	$E_{pa}$	-	-	-	-	-	-	-	-
	$E_{pc}$	-	-	-1.64	-	-	-	-	-
	$n_{rel}$	-	-	$\approx 2$	-	-	-	-	-
	Reversibility	-	-	Irrev.	-	-	-	-	-
	Diffusion control	-	-	-	-	-	-	-	-
Rest E		-	-	-0.56	-0.93	-	-	-1.08	-1.03

Table 13. Electrochemical data (continued)

		Compounds							
		(38a)	(38b)	(39a)	(39b)	(39c)	(40a)	(40b)	(42b)
<i>Square Wave Voltammetry</i>									
1st Oxid.	$E_p$	0.92	0.94	-0.10	-0.11	-0.03	0.14	0.10	0.07
2nd Oxid.	$E_p$	1.06	1.07	1.11	1.12	1.00	0.66	0.64	0.63
1st Red.	$E_p$	-1.20	-1.20	-1.03	-1.05	-1.06	-0.46	-0.47	-
2nd Red.	$E_p$	-	-	-	-	-	-	-	-
<i>Cyclic Voltammetry</i>									
<b>First Oxidation Process</b>									
	$E_{1/2}$	0.95	0.93	-0.08	-0.09	-0.06	0.13	0.10	0.10
	$E_{pa}$	1.04	0.99	-0.02	-0.01	0.03	0.17	0.17	0.19
	$E_{pc}$	0.86	0.88	-0.14	-0.17	-0.09	0.10	0.02	-0.01
	$n_{rel}$	1	1	1	1	1	1	1	1
	Reversibility	Q-Rev.	Q-Rev.	Q-Rev.	Q-Rev.	N-Rev.	Rev.	Rev.	Rev.
	Diffusion control	Yes	Yes	No	No	No	No	No	No
<b>Second Oxidation Process</b>									
	$E_{1/2}$	1.09	1.07	1.12	1.16	1.02	0.67	0.67	0.66
	$E_{pa}$	1.12	1.09	1.17	1.24	1.07	0.72	0.74	0.76
	$E_{pc}$	1.05	1.05	1.07	1.09	0.97	0.61	0.59	0.56
	$n_{rel}$	1	1	1	1	1	1	1	1
	Reversibility	Q-Rev.	Q-Rev.	Rev.	Rev.	Q-Rev.	Rev.	Rev.	Rev.
	Diffusion control	Yes	Yes	No	No	No	No	No	No
<b>First Reduction Process</b>									
	$E_{1/2}$	-1.19	-	-0.85	-1.00	-0.88	-0.45	-0.46	-
	$E_{pa}$	-1.08	-	-0.60	-0.80	-0.58	-0.40	-0.37	-
	$E_{pc}$	-1.30	-1.27	-1.10	-1.19	-1.17	-0.50	-0.55	-
	$n_{rel}$	1	1	1	1	1	1	1	-
	Reversibility	Q-Rev.	Irrev.	Q-Rev.	Q-Rev.	Q-Rev.	Q-Rev.	Q-Rev.	-
	Diffusion control	No	No	No	No	No	No	No	-
<b>Rest E</b>		-1.08	-	-	-	-0.04	-0.18	-	0.03

Table 14. Electrochemical and UV/Visible data for the nitrile ligands†

Nitrile Ligand	Differential Pulse Voltammetry	Reversibility (CV)	UV/Visible† Absorptions
CH <sub>3</sub> CN	No processes observed	-	-
CH <sub>2</sub> =CHCN	No processes observed	-	-
C <sub>6</sub> H <sub>2</sub> (CN) <sub>4-1,2,4,5</sub>	E <sub>p</sub> <sup>red1</sup> -0.52	Quasi-Rev.	230, 250,
	E <sub>p</sub> <sup>red2</sup> -1.71	Irrev.	258, 266,
			304, 316.
C <sub>6</sub> H <sub>4</sub> (CN) <sub>2-o</sub>	E <sub>p</sub> <sup>red1</sup> -1.68	Irrev.	238, 242,
			282, 292.
C <sub>6</sub> F <sub>4</sub> (CN) <sub>2-o</sub>	E <sub>p</sub> <sup>red1</sup> -1.13	Quasi-Rev.	240, 246,
			290, 298.
C <sub>6</sub> F <sub>4</sub> (CN) <sub>2-p</sub>	E <sub>p</sub> <sup>red1</sup> -1.04	Quasi-Rev.	240, 250,
			302, 312.
<i>trans</i> -(NC)HC=CH(CN)	E <sub>p</sub> <sup>red1</sup> -1.28	Irrev.	234.
(NC) <sub>2</sub> C=C(CN) <sub>2</sub>	E <sub>p</sub> <sup>ox1</sup> 0.37	Quasi-Rev.	234, 266.
	E <sub>p</sub> <sup>red1</sup> -0.71	Quasi-Rev.	276.
(CF <sub>3</sub> ) <sub>2</sub> C=C(CN) <sub>2</sub>	E <sub>p</sub> <sup>red1</sup> -0.23	Quasi-Rev.	232.

† λ<sub>max</sub> nm ; CH<sub>2</sub>Cl<sub>2</sub> solutions.

## 1.5. References

- 1 Kostic, N.M.; Fenske, R.F. *Organometallics* **1** (1982) 974.
- 2 Bruce, M.I.; Swincer, A.G. *Adv. Organomet. Chem.* **22** (1983) 59.
- 3 Chisholm, M.H.; Rankel, L.A. *Inorg. Chem.* **16** (1977) 2177.
- 4 Tohda, Y.; Sonogashira, K.; Hagihara, N. *J. Chem. Soc., Chem. Commun.* (1975) 54.
- 5 (a) Masai, H.; Sonogashira, K.; Hagihara, N. *J. Organomet. Chem.* **34** (1972) 397; Onuma, K.; Kai, Y.; Yasuoka, N.; Kasai, N. *Bull. Chem. Soc. Jap.* **48** (1975) 1696.
- 6 Bruce, M.I.; Hambley, T.W.; Snow, M.R.; Swincer, A.G. *Organometallics* **4** (1985) 494.
- 7 Bruce, M.I.; Hambley, T.W.; Snow, M.R.; Swincer, A.G. *Organometallics* **4** (1985) 501.
- 8 Bruce, M.I.; Rodgers, J.R.; Snow, M.R.; Swincer, A.G. *J. Chem. Soc., Chem. Commun.* (1981) 271.
- 9 Bruce, M.I.; Cifuentes, M.P.; Snow, M.R.; Tiekink, E.R.T. *J. Organomet. Chem.* **359** (1989) 379.
- 10 Bruce, M.I.; Duffy, D.N.; Liddell, M.J.; Snow, M.R.; Tiekink, E.R.T. *J. Organomet. Chem.* **335** (1987) 365.
- 11 Williams, J.K.; Wiley, D.W.; McKusick, B.C. *J. Am. Chem. Soc.* **84** (1962) 2210.
- 12 (a) Huisgen, R. *Acc. Chem. Res.* **10** (1977) 177; 199.  
(b) Gotoh, T.; Padias, A.B.; Hall, H.K. *J. Am. Chem. Soc.* **108** (1986) 4920.
- 13 Bartlett, P.D. *Q. Rev. Chem. Soc.* **24** (1979) 473.
- 14 Su, S.R.; Wojcicki, A. *Acc. Chem. Res.* **7** (1974) 122.
- 15 Bruce, M.I.; Hambley, T.W.; Rodgers, J.R.; Snow, M.R.; Swincer, A.G. *J. Organomet. Chem.* **226** (1982) C1.
- 16 (a) Green, M.; Norman, N.C.; Orpen, A.G. *J. Am. Chem. Soc.* **103** (1981) 1267;  
(b) Allen, S.R.; Beevor, R.G.; Green, M.; Norman, N.C.; Orpen, A.G.; Williams, I.D. *J. Chem. Soc., Dalton Trans.* (1985) 435.
- 17 (a) Davidson, J.L.; Wilson, W.F.; Manojlovic-Muir, L.; Muir, K.W. *J. Organomet. Chem.* **254** (1983) C6; (b) Carlton, L.; Davidson, J.L.; Miller, J.C.; Muir, K.W. *J. Chem. Soc., Chem. Commun.* (1984) 11; (c) Davidson, J.L. *J. Chem. Soc., Dalton Trans.* (1987) 5715.
- 18 Brower, D.C.; Birdwhistell, K.R.; Templeton, J.R. *Organometallics* **5** (1986) 94.
- 19 Herrmann, W.A.; Fischer, R.A.; Herdtweck, E. *Angew. Chem.* **99** (1987) 1286; *Angew. Chem., Int. Ed. Engl.* **26** (1987) 1263.
- 20 Conole, G.C.; Green, M.; McPartlin, M.; Reeve, C.; Woolhouse, C.M. *J. Chem. Soc., Chem. Commun.* (1988) 1310.
- 21 Albers, M.O.; de Waal, D.J.A.; Liles, D.C.; Robinson, D.J.; Singleton, E.; Wiege, M.B. *J. Chem. Soc., Chem. Commun.* (1986) 1680.
- 22 Hirpo, W.; Curtis, M.D. *J. Am. Chem. Soc.* **108** (1986) 5218.
- 23 Thorn, D.L.; Hoffmann, R. *Nouv. J. Chim.* **3** (1979) 39; Curtis, M.D., unpublished results cited in ref. 13.
- 24 Curtis, M.D.; Real, J. *J. Am. Chem. Soc.* **108** (1986) 4668.
- 25 Ukhin, L.Y.; Sladkov, A.M.; Orlova, Zh.I. *Izv. A.N. SSSR, Ser. Khim* (1969) 705.
- 26 Brown, C.K.; Georgiou, D.; Wilkinson, G. *J. Chem. Soc.(A)*, (1971) 3120.
- 27 Bruce, M.I.; Hambley, T.W.; Snow, M.R.; Swincer, A.G. *J. Organomet. Chem.* **235** (1982) 105.
- 28 Davison, A.; Solar, J.P. *J. Organomet. Chem.* **166** (1979) C13.
- 29 Hong, P.; Sonogashira, K.; Hagihara, N. *J. Organomet. Chem.* **219** (1981) 363.
- 30 Hong, P.; Sonogashira, K.; Hagihara, N. *Tetrahedron Letters* **19** (1970) 1633.
- 31 Bell, P.B.; Wojcicki, A. *Inorg. Chem.* **20** (1981) 1585.
- 32 Bucheister, A.; Klemarczyk, P.; Rosenblum, M. *Organometallics* **1** (1982) 1679.
- 33 Kolobova, N.E.; Rozantseva, T.V.; Struchkov, Yu.T.; Batsanov, A.S.; Bakhmutov, V.I. *J. Organomet. Chem.* **292** (1985) 247.

- 34 Brekau, U.; Dziallas, M.; Werner, H. Royal Society of Chemistry, Dalton Division, 3rd International Conference on the Chemistry of Platinum Metals; University of Sheffield (1987) abstract C12.
- 35 Werner, H.; Hohn, A.; Weinand, R. *J. Organomet. Chem.* **299** (1986) C15.
- 36 Bruce, M.I.; Swincer, A.G.; Wallis, R.C. *J. Organomet. Chem.* **171** (1979) C5.
- 37 Bruce, M.I.; Humphrey, P.A.; Snow, M.R.; Tiekink, E.R.T. *J. Organomet. Chem.* **303** (1986) 417.
- 38 Schore, N.E. *Chem. Rev.* **88** (1988) 1081.
- 39 Green, M.; Heathcock, S.M.; Turney, T.W.; Mingos, D.M.P. *J. Chem. Soc., Dalton Trans.* (1977) 204.
- 40 Abel, E.W.; Crow, J.P.; Wingfield, J.N. *J. Chem. Soc., Dalton Trans.* (1972) 787.
- 41 Bruce, M.I.; Hambley, T.W.; Liddell, M.J.; Snow, M.R.; Swincer, A.G.; Tiekink, E.R.T. *Organometallics* in press.
- 42 Swincer, A.G.; Ph.D. Thesis University of Adelaide (1982).
- 43 Bruce, M.I.; Liddell, M.J. *Appl. Organomet. Chem.* **1** (1987) 191.
- 44 Valin, M.L.; Morieras, D.; Solans, X.; Miguel, D.; Riera, V. *Acta Cryst., Sect. C: Cryst. Struct. Commun.* **C42** (1986) 977.
- 45 Bruce, M.I.; Duffy, D.N.; Humphrey, M.G.; Swincer, A.G. *J. Organomet. Chem.* **282** (1985) 383.
- 46 Middleton, W.J. *J. Org. Chem.* **30** (1965) 1402.
- 47 Nakatsu, K.; Inai, Y.; Mitsudo, T.; Watanabe, Y.; Nakanishi, H.; Takegami, Y. *J. Organomet. Chem.* **159** (1978) 111.
- 48 Brisdon, B.J.; Hodson, A.G.W.; Mahon, M.F.; Molloy, K.C. *J. Organomet. Chem.* **344** (1988) C8.
- 49 King, R.B.; Saran, M.S. *Inorg. Chem.* **14** (1975) 1018.
- 50 Carty, A.J. *Am. Chem. Soc., Adv. Chem. Ser.* **196** (1982) 163.
- 51 Robinson, V.; Taylor, G.E.; Woodward, P.; Bruce, M.I.; Wallis, R.C. *J. Chem. Soc., Dalton Trans.* (1981) 1169.
- 52 Braterman, P.S.; Metal Carbonyl Spectra, *Academic Press* (1975) 145.
- 53 Ashby, G.S.; Bruce, M.I.; Tomkins, I.B.; Wallis, R.C. *Aust. J. Chem.* **32** (1979) 1003.
- 54 Bruce, M.I. *J. Chem. Soc. A* (1968) 1459.
- 55 Bruce, M.I.; Humphrey, M.G.; Liddell, M.J. *J. Organomet. Chem.* **321**(1987) 91.
- 56 Murphy, W.R.; Brewer, K.J.; Gettliffe, G.; Peterson, J.D. *Inorg. Chem.* **28** (1989) 81.
- 57 Johnson, T.J.; Bond, M.R.; Willet, R.D. *Acta Cryst.* **C44** (1988) 1890.
- 58 Bruce, M.I.; Wallis, R.C.; Skelton, B.W.; White, A.H. *J. Chem. Soc., Dalton Trans.* (1981) 2205.
- 59 (a) Gross, R.; Kaim, W. *J. Organomet. Chem.* **333** (1987) 347;  
(b) Gross, R.; Kaim, W. *Angew. Chem.* **99** (1987) 257; *Angew. Chem., Int. Ed. Engl.* **26** (1987) 251.
- 60 Bruce, M.I.; Hambley, T.W.; Rodgers, J.R.; Snow, M.R.; Wong, F.S. *Aust. J. Chem.* **35** (1982) 1323.
- 61 Bruce, M.I.; Cifuentes, M.P.; Snow, M.R.; Tiekink, E.R.T. *J. Organomet. Chem.* **359** (1989) 379.
- 62 Linn, W.J.; Webster, O.W.; Benson, R.E. *J. Am. Chem. Soc.* **85** (1963) 2032.
- 63 Bitcon, C.; Whiteley, M.W. *J. Organomet. Chem.* **336** (1987) 385.
- 64 Joseph, M.F.; Page, J.A.; Baird, M.C. *Inorg. Chim. Acta* **64** (1982) L121.
- 65 Joseph, M.F.; Page, J.A.; Baird, M.C. *Organometallics* **3** (1984) 1749.
- 66 Treichel, P.M.; Molzahn, D.C.; Wagner, K.P. *J. Organomet. Chem.* **174** (1979) 191.
- 67 Rodgers, W.N.; Page, J.A.; Baird, M.C. *J. Organomet. Chem.* **156** (1978) C37.
- 68 Armarego, W.L.F.; Perrin, D.D.; Perrin, D.R. Purification of Laboratory Chemicals, 2nd Ed., Pergamon, Oxford, (1980).
- 69 Bruce, M.I.; Humphrey, M.G.; Matisons, J.G.; Roy, S.K.; Swincer, A.G. *Aust. J. Chem.* **37** (1984) 1955.
- 70 Miguel, D.; Riera, V. *J. Organomet. Chem.* **293** (1985) 379.

- 
- 71 Bruce, M.I.; Wallis, R.C. *Aust. J. Chem.* **32** (1979) 1471; Bruce, M.I.; Swincer, A.G. *Aust. J. Chem.* **33** (1980) 1471.
- 72 E.R.T. Tiekink personal communication.

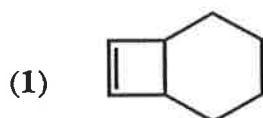
## CHAPTER TWO

### Cycloaddition reactions of *trans*-1,2-bis(carbomethoxy)-1-cyanoethene and related chemistry

	Page
2.1. Introduction	92
2.2. Results and Discussion	97
2.3. Conclusions	129
2.4. Experimental	130
2.5. References	143

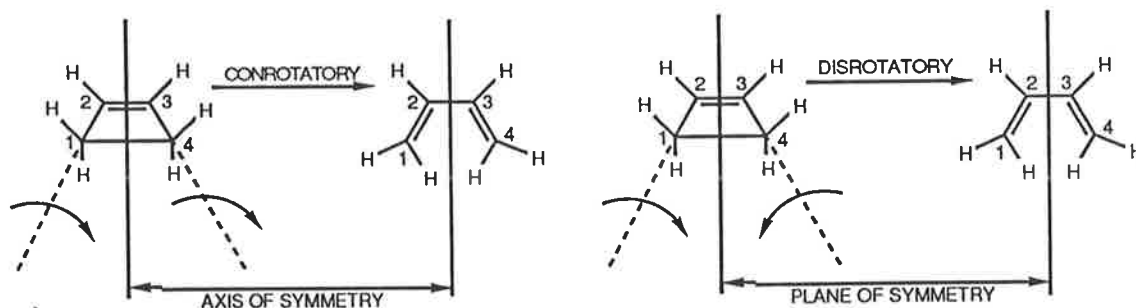
## 2.1. Introduction

The stereochemical studies by Criegee *et al.*<sup>1</sup> on the thermal ring-opening of *cis*- and *trans*-1,2,3,4-tetramethylcyclobutenes were the first to show unambiguously the conrotatory nature of the cyclobutene-butadiene electrocyclic interconversion. The 185-nm photolysis of (1) yields *cis,cis*-1,3-cyclooctadiene consistent with a disrotatory ring-opening mechanism.<sup>2</sup> In 1965, Woodward and Hoffmann<sup>3</sup> proposed a theory to rationalize such electrocyclic reactions. Since then, Brauman and Golden<sup>4</sup> have estimated that the thermally-allowed conrotatory process for cyclobutenes is more favoured (by 15.0 kcal/mol) than the disrotatory process. This experimental estimate accords with values obtained recently by Breulet and Schaefer<sup>5</sup> from *ab initio* calculations.



The concerted ring-opening reaction of cyclobutene is seen as a classic example of the use of the Woodward-Hoffmann rules and the correlation procedures introduced by Longuet-Higgins.<sup>6,7</sup> The Woodward-Hoffmann theory<sup>8</sup> has as its basis the proposition that the symmetry of the highest energy occupied molecular orbital (HOMO) in a compound determines which mode of rotation (conrotatory or disrotatory) will be preferred in cyclization and ring-opening reactions. During the course of the concerted ring-opening of cyclobutene, a twofold axis of symmetry is maintained in the conrotatory reaction, while a plane of symmetry is maintained in the disrotatory mode.

Figure 1. Conrotatory and disrotatory opening of cyclobutene



Four orbitals of the cyclobutene are involved in these transformations:  $\sigma$ ,  $\sigma^*$  between C(1) and C(4), and  $\pi$ ,  $\pi^*$  between C(2) and C(3). The symmetry of each orbital is classified as either symmetric (S) or antisymmetric (A) in relation to the symmetry elements mentioned above.

Figure 2. Correlation of orbitals

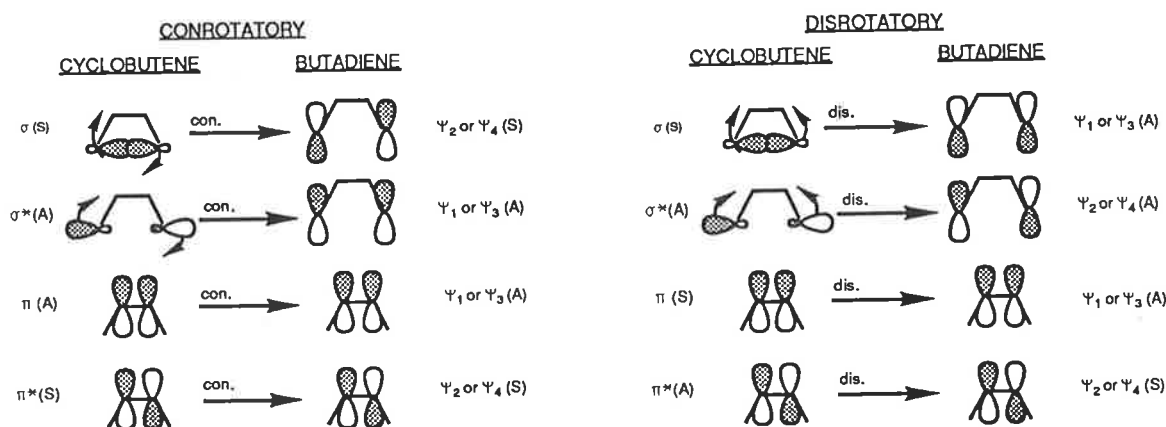
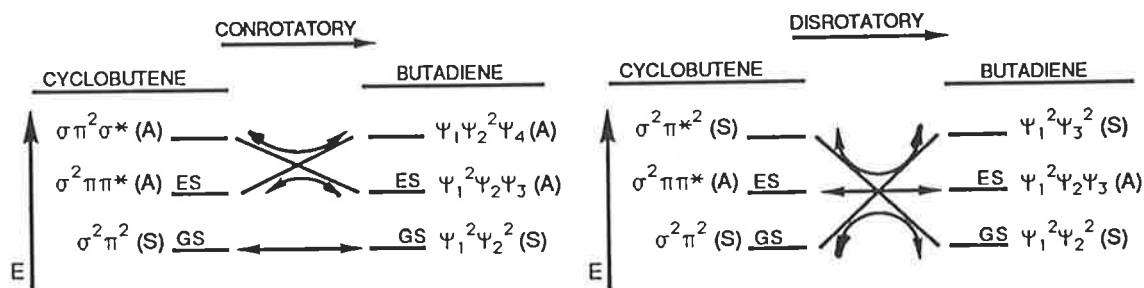


Figure 3. State correlation diagrams

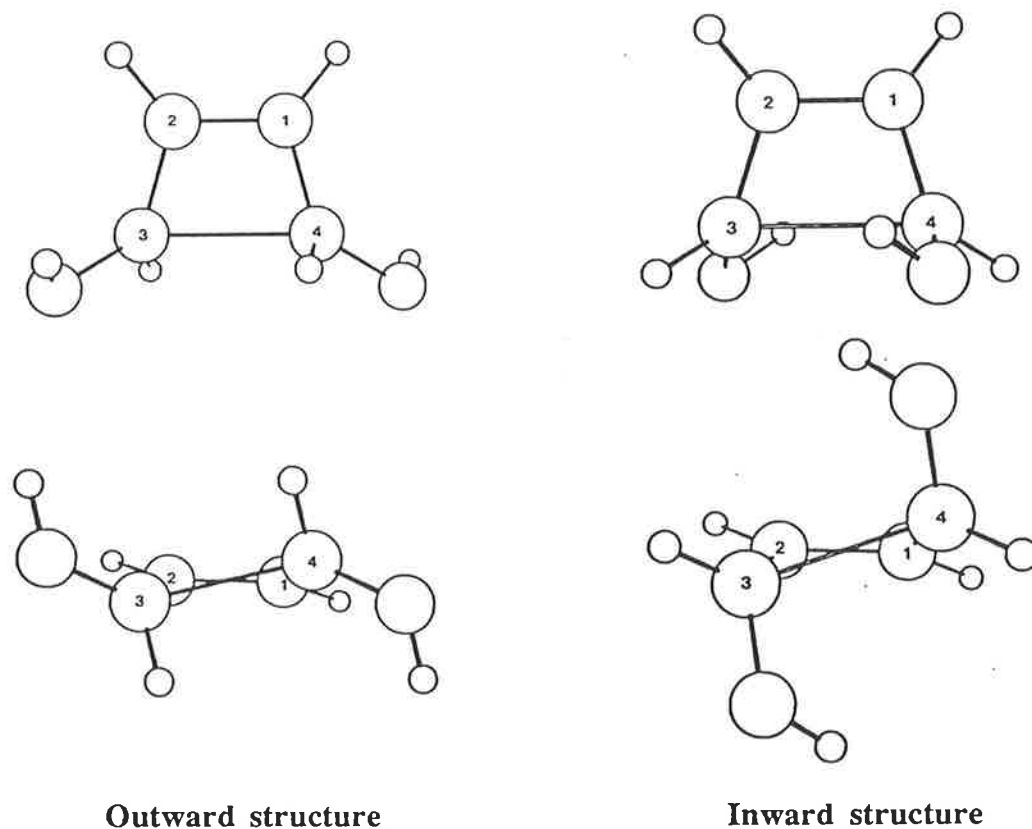


In the course of the reaction, these symmetry properties are maintained to give a correlation between the cyclobutene and the butadiene orbitals ( $\psi_1 - \psi_4$ ), as is shown in the correlation diagrams above. This avoids a change in sign of the electronic wave functions during the course of the reaction, a procedure which is disallowed. Thus, in the conrotatory reaction, the  $\sigma$ -electrons of cyclobutene are correlated with the  $\psi_2$  and  $\psi_4$  orbitals in the butadiene product. The lower energy of  $\psi_2$  means that the  $\pi$ -electrons in this orbital are formally derived from the  $\sigma$ -electrons of the cyclobutene. For any given state of the molecule, a symmetry classification

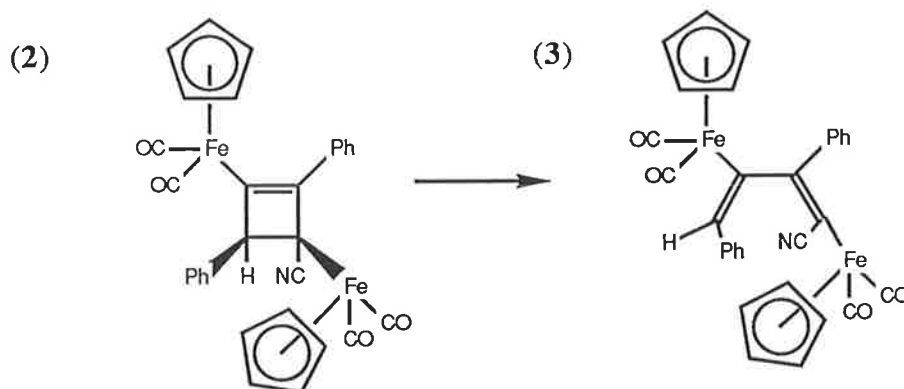
may be derived, which is the product of the symmetries of the orbitals occupied by each electron (e.g.  $\sigma^2\pi\pi^* = S.S.A.S = A$ ). By building up a state diagram for all of the states in cyclobutene and then relating these to the corresponding orbitals in butadiene, it is possible to predict which mode of reaction will be preferred. From these state diagrams it can be seen that conrotatory ring-opening from the ground-state of cyclobutene leads to the ground state of butadiene, a thermally-favoured process, while the disrotatory mode leads to an excited state of butadiene. The latter mode of ring-opening is thus favoured under photochemical conditions. Given the principle of microscopic reversibility, the reverse reactions are expected to proceed along pathways similar to those of the forward reactions (i.e. cyclization vs. ring-opening). In instances where steric limitations do not allow the electrocyclic process to follow the favoured pathway, then the disfavoured pathway may be accessed via diradical or dipolar intermediates (i.e. non-concerted mechanisms). Examples of these latter reactions are to be found in the literature.<sup>1(b),9</sup> Seemingly disrotatory thermal ring-opening reactions have also been shown to arise from *E/Z* isomerization of initially-formed conrotatory products.<sup>10</sup>

The torsional motion that is required to attain the transition state in electrocyclic reactions also plays a part in determining the direction of these reactions. Such motion has been found to be particularly crucial in cyclobutene complexes, where the products obtained from the ring-opening reactions are frequently contrary to those expected from steric considerations. Rondan and Houk<sup>11</sup> have explained the results obtained in the electrocyclic reactions of perfluorocyclobutenes<sup>12</sup> and *cis*- and *trans*-3,4 dichloro-, dimethoxy-, diethoxy- and diacetoxy-substituted cyclobutenes<sup>13</sup> as arising from the electronic effects of the cyclobutene substituents. Using *ab initio* calculations to determine transition-state structures, they established a preference for outward rotation in ring-substituents with strong electron-donor capabilities, while  $\pi$ -acceptors such as ester and keto groups were shown to have little stereochemical preference.

**Figure 4.** 'Outward' and 'inward' transition structures for conrotatory ring-opening of *trans*-3,4-dihydroxycyclobutene<sup>13</sup>



Only one organometallic electrocyclic reaction has been described that allows the stereochemistry of the reaction to be discussed. This was the thermal conversion of the cyclobutenyl diiron complex  $\text{Fe}\{\overline{\text{C}=\text{CPhC}(\text{CN})[\text{Fe}(\text{CO})_2(\eta\text{-C}_5\text{H}_5)]\text{CHPh}}\}(\text{CO})_2(\eta\text{-C}_5\text{H}_5)$  (2) to the butadienyl complex  $\text{Fe}\{\text{C}=\text{CHPh}\}\text{CPh}=\text{C}(\text{CN})[\text{Fe}(\text{CO})_2(\eta\text{-C}_5\text{H}_5)]\}(\text{CO})_2(\eta\text{-C}_5\text{H}_5)$  (3) by Kolobova *et al.*<sup>14</sup> Although not mentioned in their report, their structural studies showed that the reaction had proceeded via the expected conrotatory process. As the frontier orbitals of transition-metal vinyl complexes (of which these cyclobutenyl and butadienyl complexes are examples) are likely to be involved in ring bonding,<sup>15</sup> the dimetal-substituted complexes might have electronic properties different to those of monometal-substituted complexes. We have therefore carried out further studies on the type of electrocyclic reactions discussed in Chapter One, using substrates that have permitted the stereochemistry of the reactions to be determined.



Because the structurally-characterized cyclobutenyl and butadienyl complexes derived from *dcfe* and *tcne* are symmetrical in nature, we were unable to determine the direction of the ring-opening process. However, the availability of the olefin *trans*-bis(carbomethoxy)-1-cyanoethene [*trans*-C(CO<sub>2</sub>Me)(CN)=CH(CO<sub>2</sub>Me), *rjo*]<sup>16</sup> has allowed us to perform similar reactions with Ru(C<sub>2</sub>Ph)(CO)(PPh<sub>3</sub>)( $\eta$ -C<sub>5</sub>H<sub>5</sub>) (4). These reactions have meant that the direction of the ring-opening process could be determined and have also made possible direct structural comparisons with the cycloadducts obtained using *dcfe* (see Sections 1.2.1, 1.2.2, 1.2.3).

Although cycloaddition reactions of fluoroolefins are well documented,<sup>17</sup> there are few fluorinated cyclobutenyl complexes described in the literature. One that is readily available is Fe( $\overline{\text{C}=\text{CFCF}_2\text{CF}_2}$ )(CO)<sub>2</sub>( $\eta$ -C<sub>5</sub>H<sub>5</sub>), obtained from the salt-elimination reaction between [Fe(CO)<sub>2</sub>( $\eta$ -C<sub>5</sub>H<sub>5</sub>)]<sup>-</sup> and perfluorocyclobutene.<sup>18</sup> We have, therefore, examined the ring-opening tendencies of this complex in order to gain more information concerning the substituent effect on the course of the expected electrocyclic reaction. We have also carried out some further studies on the reaction of *tcne* with Fe(C<sub>2</sub>Ph)(CO)<sub>2</sub>( $\eta$ -C<sub>5</sub>H<sub>5</sub>),<sup>19</sup> in light of the recent work;<sup>20,21</sup> related reactions were carried out using alkynylmanganese precursors.

## 2.2. Results and Discussion

### 2.2.1. Three isomers of $\text{Ru}\{\overline{\text{C}=\text{CPhCH}(\text{CO}_2\text{Me})\text{C}(\text{CO}_2\text{Me})(\text{CN})}\}-$ $(\text{CO})(\text{PPh}_3)(\eta\text{-C}_5\text{H}_5)$

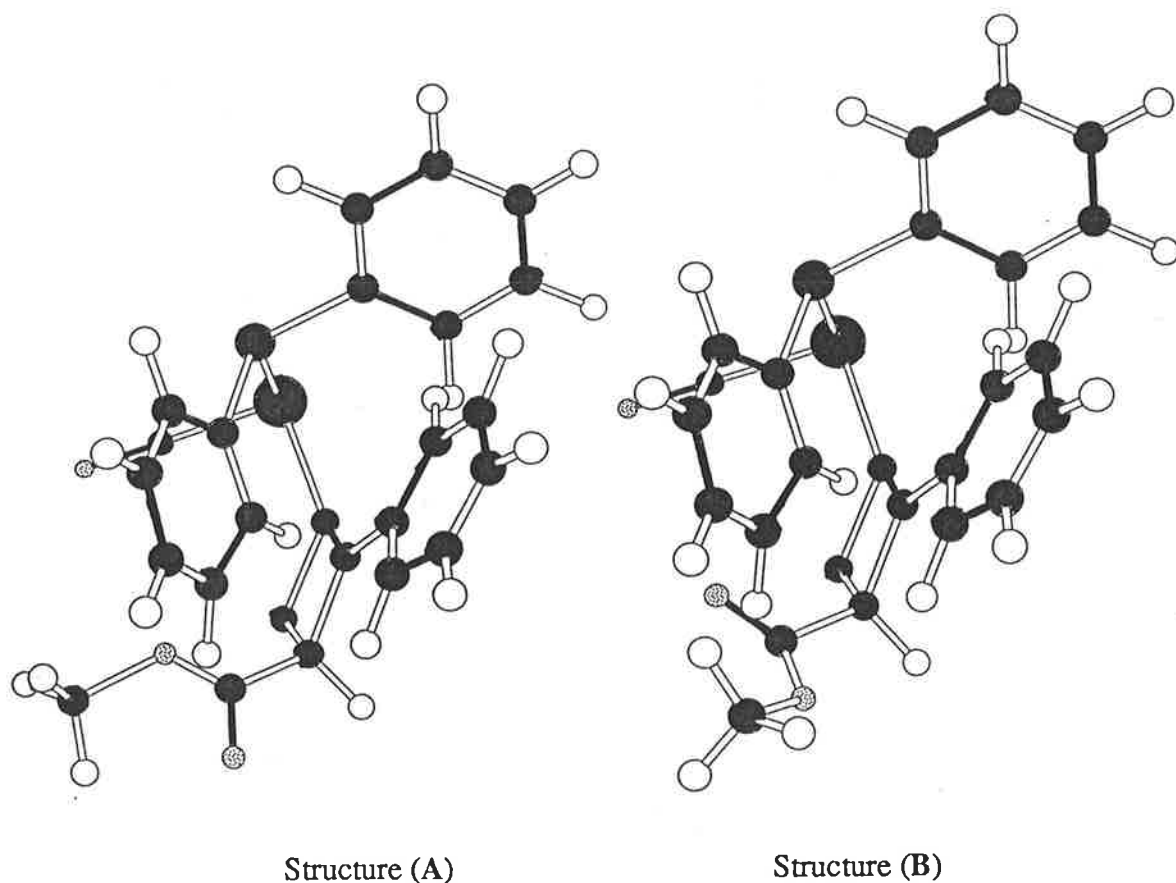
The treatment of  $\text{Ru}(\text{C}_2\text{Ph})(\text{CO})(\text{PPh}_3)(\eta\text{-C}_5\text{H}_5)$  with *trans*- $\text{C}(\text{CO}_2\text{Me})(\text{CN})=\text{C}-$   
 $\text{H}(\text{CO}_2\text{Me})$ ] in benzene resulted in the formation of two isomers of  $\text{Ru}\{\overline{\text{C}=\text{CPhCH}(\text{CO}_2\text{Me})-}$   
 $\text{C}(\text{CO}_2\text{Me})(\text{CN})\}\text{CO}(\text{PPh}_3)(\eta\text{-C}_5\text{H}_5)$  (**5a**) and (**5b**). The major isomer (59%) formed was  
(**5a**), which was separated readily from the minor isomer (27%) (**5b**) by thin-layer  
chromatography. Proton NMR investigations of similar reactions performed in  $\text{CDCl}_3$  and  
 $\text{C}_6\text{D}_6$  showed that the reaction in  $\text{CDCl}_3$  was complete within ten minutes, whereas that  
performed in benzene took 1 hour 25 minutes. The ratio of isomers (**5a**):(**5b**) [2:1  $\text{CDCl}_3$ ;  
1.5:1  $\text{C}_6\text{D}_6$ ] was only slightly altered by the differences in solvent polarity. No coloured  
intermediates were detected in these reactions and the ratio of isomers did not change after  
seven days in solution ( $\text{CDCl}_3$ ).

It was noted that both isomers slowly changed colour, from the pale yellow observed for  
(**5b**) and white for (**5a**), to a bright yellow when supported on the silica TLC medium. A  
 $^1\text{H}$  NMR study of these reactions, performed on  $d^6$ -acetone extracts of the supported samples,  
showed that when either of these complexes was adsorbed on silica, conversion to a third  
cyclobutenyl isomer (**5c**) occurred. The NMR results indicated that the conversion occurred  
only with adsorbed complexes in the solid state (dry), and control experiments with the NMR  
solvent and silica present did not reveal any formation of (**5c**). Maximum conversion of (**5a**)  
to (**5c**) was 58% after fifty hours, while (**5b**) was 25% converted after fourteen days. Several  
side reactions were also noted, but of these only the conversions (**5a**)  $\rightarrow$  (**5b**) and (**5b**)  $\rightarrow$   
(**5a**) could be correlated with the various  $\text{C}_5\text{H}_5$  and OMe resonances observed. A preparative  
scale isomerization of (**5a**) supported on silica allowed the isolation of (**5c**) in 34% yield after  
three days. Suitable crystals of this complex could not be obtained for X-ray analysis, and it  
was characterized by microanalysis and spectroscopy alone.

The infrared data for all three cyclobutenyl complexes are similar. Very weak bands were observed between 2207 and 2236  $\text{cm}^{-1}$  for the CN groups, and between 1566 and 1616  $\text{cm}^{-1}$  for the  $\nu(\text{C}=\text{C})$  absorptions. Single strong  $\nu(\text{CO})$  bands were found at  $\approx 1950 \text{ cm}^{-1}$  for the ruthenium-bound carbonyl and at  $\approx 1738 \text{ cm}^{-1}$  for the  $\text{CO}_2\text{Me}$  groups. The fingerprint region of (**5c**) was more similar to (**5a**) than to (**5b**).

In their proton NMR spectra,  $\text{C}_5\text{H}_5$ ,  $\text{CH}$ , and two OMe resonances were observed for each complex at  $\delta$  5.14, 4.52, 3.74, 3.66 (**5a**);  $\delta$  4.91, 4.52, 3.85, 3.73 (**5b**) and  $\delta$  4.88, 4.18, 3.85, 3.51 (**5c**), respectively. Phenyl resonances were observed between  $\delta$  7.4 and 6.5 for the triphenylphosphine ligand and the phenyl ring substituent. The only unusual feature of these spectra was the apparent doublet at  $\delta$  4.52 ( $J = 1.6 \text{ Hz}$ ) for the  $\text{CH}$  proton in the spectrum of (**5b**). At this stage, it is not clear how this arises, since the phosphorus is considerably removed from the proton ( $> 3 \text{ \AA}$ ) and there is no reason why  $^5J$  coupling should be observed. One proposition, however, is for the existence of two  $\text{CO}_2\text{Me}$  environments at the carbon to which the  $\text{CH}$  group is attached. This is possible if slightly different orientations of the  $\text{CO}_2\text{Me}$  groups are ascribed to the compound when it is in solution (as shown below). The second conformation [structure (B)] which differs from the solid state structure [structure (A)] is not unreasonable, as the  $\text{CO}_2\text{Me}$  group and the phenyl groups on the phosphine and the ring interact quite strongly. This interaction provides an effective barrier to rotation and two environments for the  $\text{CH}$  proton. In addition, a low-temperature (240K) spectrum of (**5b**) showed different intensities for the two peaks in the doublet (4:3), in contrast to the 1:1 intensities observed in the room-temperature spectrum.

The FAB mass spectra of all three cyclobutenyl complexes were identical. A strong molecular ion which fragmented by loss of Me, CO,  $\text{CO}_2\text{Me}$  and  $\text{C}(\text{CO}_2\text{Me})(\text{CN})=\text{CH}-$  ( $\text{CO}_2\text{Me}$ ) groups, was observed. The latter is the major ion  $[\text{M} - r\text{j}]^+$  which is characteristic of the cyclobutenyl complexes and is absent from the spectrum of the related butadienyl complex  $\text{Ru}\{\text{C}=\text{C}(\text{CO}_2\text{Me})(\text{CN})\}\text{CPh}=\text{CH}(\text{CO}_2\text{Me})\}(\text{CO})(\text{PPh}_3)(\eta\text{-C}_5\text{H}_5)$  (**6**). The other fragment ions present were associated with the loss of OMe,  $\text{O}_2\text{Me}$  and CO groups



from the ions already mentioned or with the usual breakdown patterns observed for the  $\text{Ru}(\text{PPh}_3)(\eta\text{-C}_5\text{H}_5)$  group (see Section 1.2.5).

Plots of the two structurally-characterized cyclobutenyl complexes (**5a**) and (**5b**) are shown in Figures 5 and 6, while Table 1 collects significant bond distances and angles. Both structures are chiral at the ruthenium. Compound (**5a**) crystallized in a centrosymmetric space group, whereas (**5b**) crystallized in the non-centrosymmetric space group  $Pna2_1$ , implying spontaneous resolution upon crystallization. About each ruthenium, the coordination is distorted octahedral with one face occupied by the  $\eta\text{-C}_5\text{H}_5$  group and the other face defined by the carbonyl, triphenylphosphine and  $\sigma$ -cyclobutenyl ligands. The ligand-ruthenium bond distances in complexes (**5a**) and (**5b**) Ru-C(21) [1.831(5), 1.81(1) Å, resp.], Ru-P(1) [2.299(1), 2.300(2) Å, resp.] and Ru-C(cp) [2.255(4) - 2.267(4), 2.233(9) - 2.246(8) Å, resp.] are similar to those found for other  $\text{Ru}(\text{CO})(\text{PPh}_3)(\eta\text{-C}_5\text{H}_5)$  compounds (see Section 1.2.1), the differences between the two structures being within the range of experimental error. The Ru-C( $sp^2$ ) distances [2.062(5) (**5a**) and 2.09(1) Å (**5b**)] are similar to that observed for  $\text{Ru}\{\overline{\text{C}=\text{CPhC}(\text{CF}_3)_2\text{C}(\text{CN})_2}\}(\text{CO})(\text{PPh}_3)(\eta\text{-C}_5\text{H}_5)$  [2.054(8) Å, see Section 1.2.1].

Figure 5. PLUTO plot of  $\text{Ru}\{\text{C}=\text{CPhCH}(\text{CO}_2\text{Me})\text{C}(\text{CO}_2\text{Me})(\text{CN})\}\{\text{CO}\}(\text{PPh}_3)-$   
 $(\eta\text{-C}_5\text{H}_5)$  (5a) (by D N. Duffy and E.R.T. Tiekink)

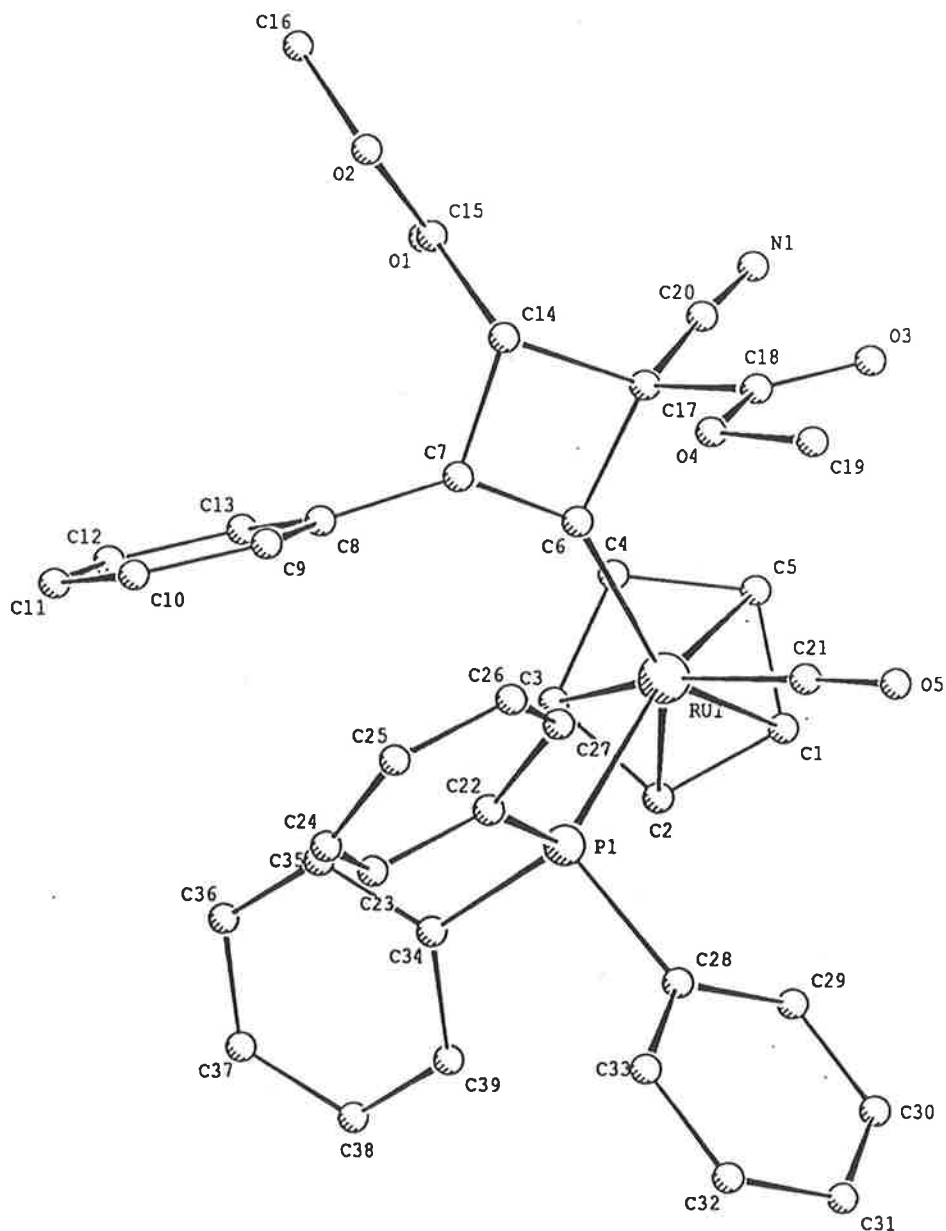
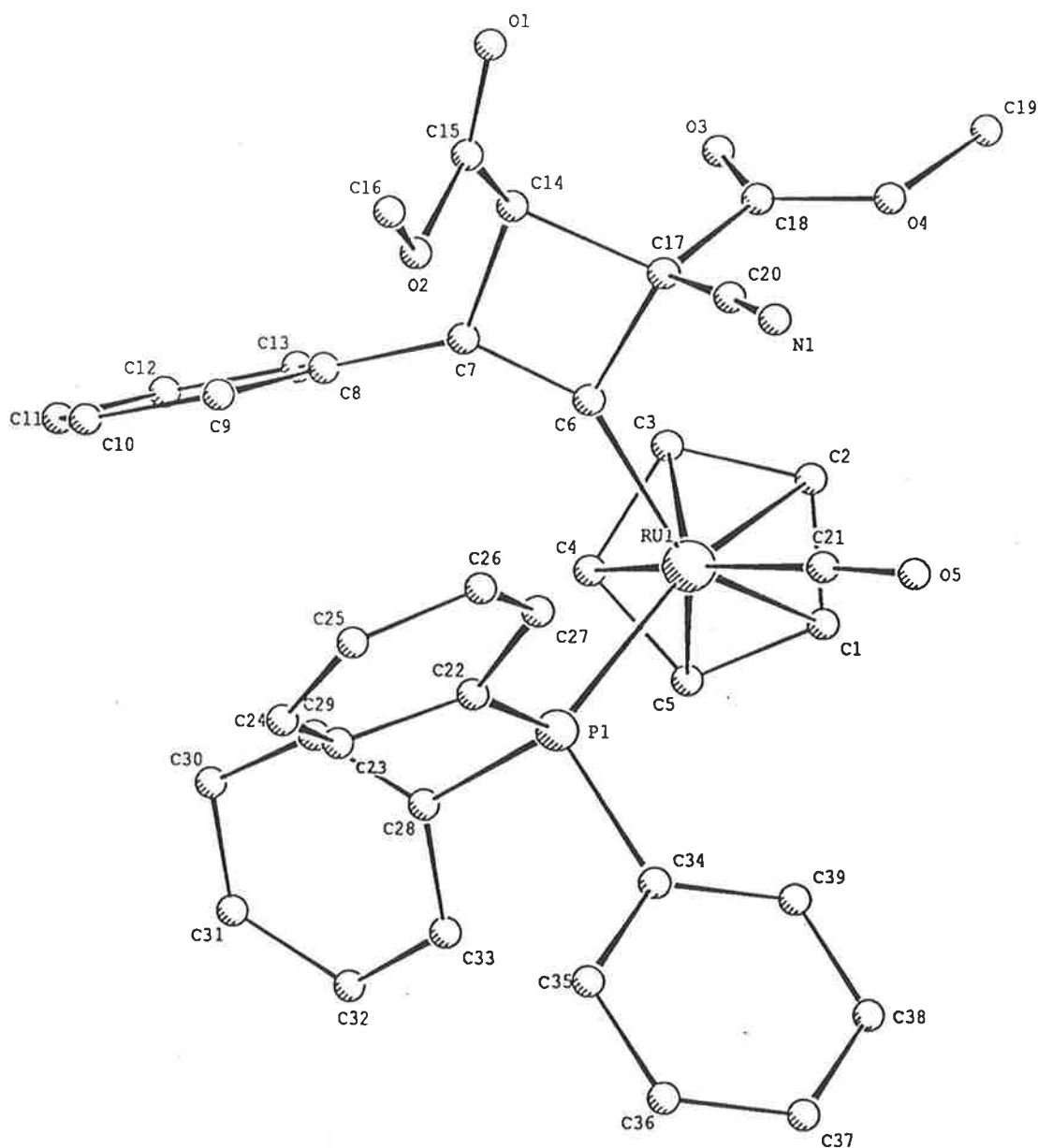


Figure 6. PLUTO plot of Ru{C=CPhCH(CO<sub>2</sub>Me)C(CO<sub>2</sub>Me)(CN)}(CO)(PPh<sub>3</sub>)-(η-C<sub>5</sub>H<sub>5</sub>) (**5b**) (by D.N. Duffy and E.R.T. Tiekink)



**Table 1.** Selected bond distances (Å) and angles (°) for complexes (5a), (5b), (6) and (7)

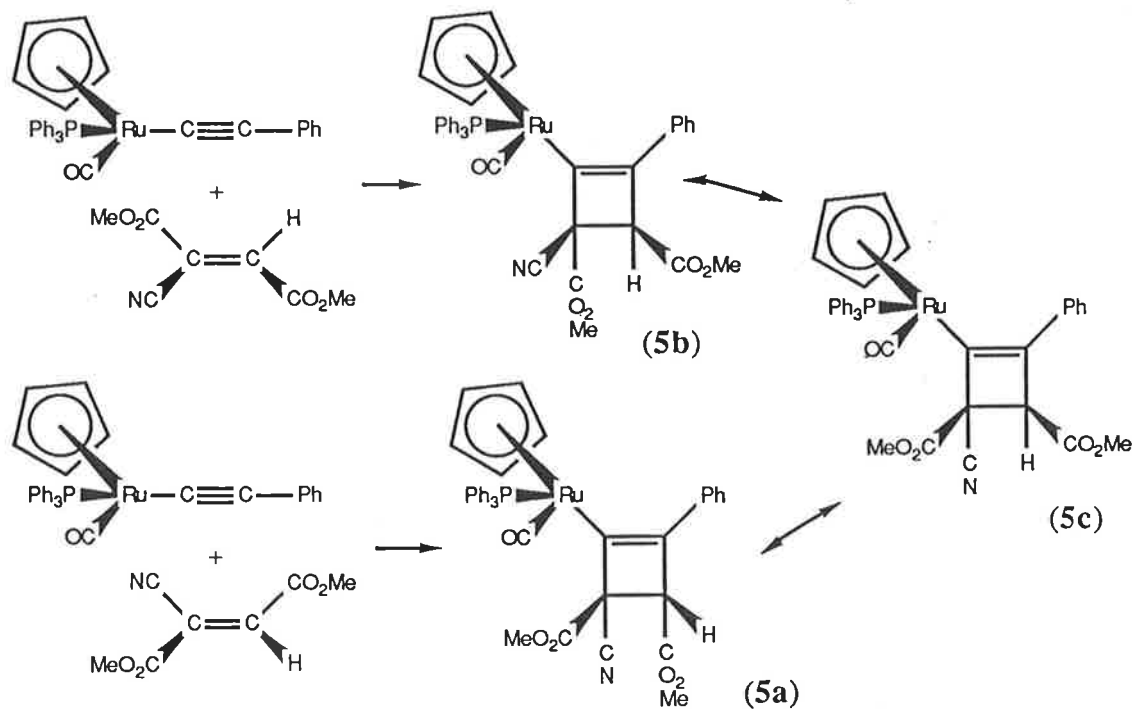
Parameter	Compound			
	(5a)	(5b)	(6)	(7) <sup>†</sup>
Ru-P(1)	2.299(1)	2.300(2)	2.318(2)	-
Ru-C(6)	2.062(5)	2.09(1)	2.109(6)	2.047(4)
Ru-C(21)	1.831(5)	1.81(1)	1.833(7)	1.875(4)
Ru-cp	2.255-	2.233(9)-	2.241-	2.227-
	2.267(4)	2.246(8)	2.273(5)	2.245(3)
C(6)-C(7)	1.357(7)	1.34(2)	1.469(8)	1.422(5)
C(6)-C(17)	1.565(7)	1.55(1)	1.363(8)	1.344(5)
C(7)-C(8)	1.471(6)	1.49(1)	1.490(7)	1.493(4)
C(7)-C(14)	1.529(7)	1.51(1)	1.346(9)	1.431(5)
C(14)-C(15)	1.511(7)	1.49(2)	1.43(1)	1.467(5)
C(14)-C(17)	1.566(4)	1.57(2)	-	-
C(17)-C(18)	1.529(7)	1.51(2)	1.479(9)	1.483(5)
C(17)-C(20)	1.477(8)	1.48(2)	1.44(1)	1.443(5)
C(20)-N(1)	1.137(7)	1.12(1)	1.140(8)	1.137(5)
C(21)-O(5)	1.160(6)	1.19(1)	1.168(7)	1.145(5)
Ru-C(6)-C(7)	142.1(4)	140.5(8)	113.9(4)	74.6(2)
Ru-C(6)-C(17)	126.5(3)	126.6(7)	126.4(7)	147.5(3)
C(7)-C(6)-C(17)	90.9(4)	91.1(8)	118.8(6)	136.5(4)
C(6)-C(7)-C(14)	96.9(4)	97.3(9)	127.5(6)	114.2(3)
C(7)-C(14)-C(15)	111.8(4)	124.3(9)	127.8(7)	121.4(3)
C(7)-C(14)-C(17)	84.8(4)	84.7(8)	-	-

<sup>†</sup> Ru-C(7) 2.160(4); Ru-C(14) 2.218(4) Å; Ru-C(7)-C(6) 66.0(2); Ru-C(14)-C(7) 68.7(2)°.

Table 1. (continued.)

Parameter	Compound			
	(5a)	(5b)	(6)	(7)
C(15)-C(14)-C(17)	117.7(4)	116.2(9)	-	-
C(6)-C(17)-C(14)	87.4(3)	86.9(7)	-	-
C(6)-C(17)-C(18)	115.0(4)	112.6(9)	122.3(6)	125.5(4)
C(6)-C(17)-C(20)	115.3(4)	115.1(8)	124.5(2)	121.7(4)
C(14)-C(17)-C(18)	115.6(4)	112(1)	-	-
C(14)-C(17)-C(20)	117.2(4)	114.9(9)	-	-
C(18)-C(17)-C(20)	106.1(4)	113.2(9)	113.1(6)	112.5(3)

Scheme 1. Interconversion of isomers (5a), (5b) and (5c)



Within the C<sub>4</sub> ring the pattern of bond lengths for (5a) and (5b) C(6)-C(7) [1.357(7), 1.34(2) Å, resp.]; C(7)-C(14) [1.529(7), 1.51(1) Å, resp.]; C(14)-C(17) [1.566(4), 1.57(2) Å, resp.]; C(17)-C(6) [1.565(7), 1.55(1) Å, resp.] is as found for the dcfе complex, the only significant difference being the slight contraction of the single bond closest to the ruthenium C(17)-C(6) [dcfе complex, 1.57(1) Å]. The angles subtended at the sp<sup>2</sup> carbon atoms range from 90.9(4) to 97.3(9)° and at the sp<sup>3</sup> carbon atoms, from 84.7(8) to 87.4(3)°. All of these fall within the normal range for the cyclobutenyl structures examined so far. The cyclobutenyl rings in the two structures are essentially planar, the ruthenium atom lying 0.222 Å below the least-squares plane through the ring in (5a) and 0.364 Å below the same plane in (5b).

The difference between the isomers is most clearly seen when one examines the disposition of the CN group. In (5a), the CN group attached to C(17) is on the same side of the ring as the ruthenium. In structure (5b), the CN group is on the other side of the ring. This suggests that the preferred direction of addition of the =C(CN)(CO<sub>2</sub>Me) group of the olefin is towards the α-carbon of the acetylide, with the CO<sub>2</sub>Me in the least sterically demanding position. Clearly, the CN group is directing the initial attack of the olefin on the acetylide, as neither of the other isomers formed by the reverse addition of the olefin was observed. The previous work with dcfе and the *ortho*-styrenes (see Section 1.1) had already led us to expect this. The similarity to the results obtained with tcne<sup>20, 21</sup> points again to the involvement of a dipolar intermediate, which converts quickly to the cyclobutenyl complexes on account of the high degree of polarizability inherent in the rjo olefin.

The structure of the third cyclobutenyl isomer was investigated by means of molecular modelling (CHEM 3D). It appears that no minor orientational forms due to restricted rotation are available, as the only appreciable interactions are intra-phenyl and these are most likely to affect crystal packing. On the basis of similarities in the phenyl region of the <sup>1</sup>H NMR and the fingerprint region of the IR spectra, we suggest a structure related to isomer (5a), but different in that the CO<sub>2</sub>Me on C(14) has rotated onto the opposite side of the ring to the ruthenium. This places both CO<sub>2</sub>Me groups on the same side of the ring, as is shown in Scheme 1.

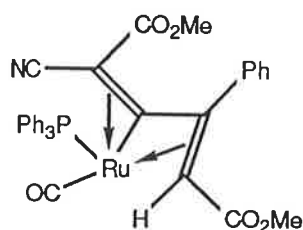
Maximum interaction of the oxygen atoms (CO<sub>2</sub>Me groups and the carbonyl group) with the surface siloxy groups of the silica, and minimum contact between the phenyl and cyclopentadienyl groups and the surface, is achieved for (5c) when the base of the ring is in contact with the surface region. As (5c) is recovered from the surface by extraction with methanol/CH<sub>2</sub>Cl<sub>2</sub> mixtures, only adsorption seems to be involved. The transformation from (5a) to (5b) and vice-versa on silica indicates that significant rearrangements of the substituents on the ring are possible. The intermediate involved in these transformations would be (5c), as illustrated in Scheme 1. The formation of (5c) shows that bond-breaking processes have occurred. At present we are inclined to favour the breaking of C(6)-C(17), followed by rotation about C(14)-C(17) and then ring-closure rather than formation of a butadiene followed by recyclization.

### 2.2.2. Conrotatory ring-opening

Pyrolysis of both of the isomers (5a) and (5b) resulted in the formation of the same complex, the butadienyl compound (6). A preparative route to (6) that did not involve the unnecessary separation of the cyclobutenyl isomers was therefore developed. This involved reacting (4) with rjo and then heating the crude reaction product [a mixture of (5a) and (5b)] for sixteen hours in benzene (80 °C), which gave yellow crystalline (6) in 60% yield.

In the IR spectrum of (6), a weak  $\nu(\text{CN})$  band was observed at 2207 cm<sup>-1</sup> and strong  $\nu(\text{CO})$  absorptions were found at 1951 and 1725 cm<sup>-1</sup> for the ruthenium-bound carbonyl and the ester carbonyls, respectively. The  $\nu(\text{C}=\text{C})$  absorptions at 1597 - 1501 cm<sup>-1</sup> had intensities varying from very weak to strong. The proton NMR spectrum contained resonances for the CH, C<sub>5</sub>H<sub>5</sub> and two CO<sub>2</sub>Me groups at  $\delta$  5.41, 4.74, 3.58 and 3.14, respectively. A collection of multiplets between  $\delta$  7.6 and 7.1 was observed for the phenyl groups. In the FAB mass spectrum of (6), a strong molecular ion, which fragmented by loss of Me, CO and C<sub>5</sub>H<sub>5</sub> groups, was observed. An interesting difference between (6) and the isomers of (5) was the loss of C<sub>5</sub>H<sub>5</sub>. This process may indicate the formation of a  $\eta^4(5e)$ -butadienyl ion such as Structure (A), which has a precedent in solution chemistry.<sup>22</sup> No loss of the olefin from the

molecular ion occurred; this confirmed the butadienyl structure.

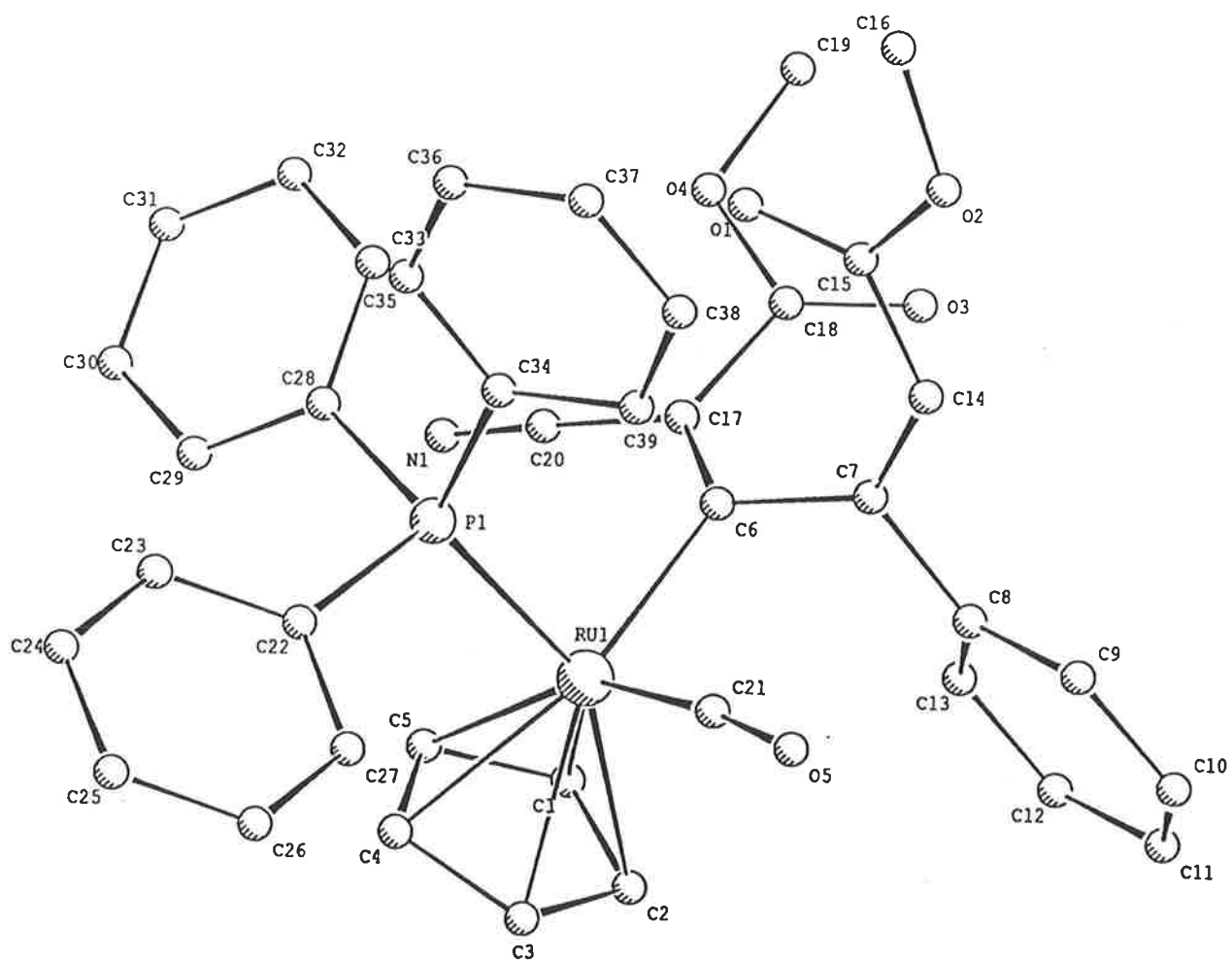


Structure (A)

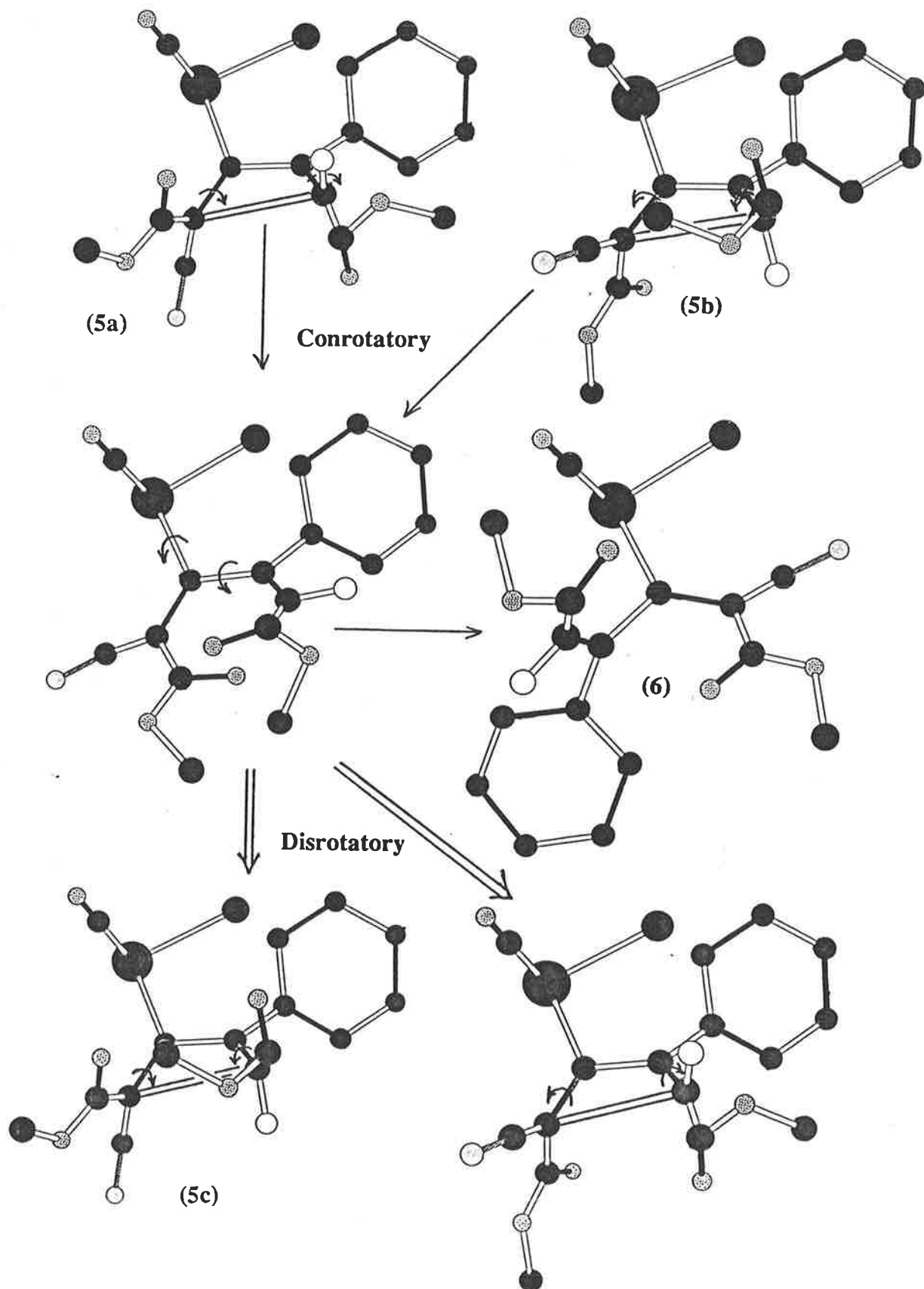
A plot of one molecule of (6) is shown in Figure 7 and significant bond distances and angles were collected in Table 1. The ruthenium is coordinated to the carbonyl, triphenylphosphine and  $\eta$ -C<sub>5</sub>H<sub>5</sub> ligands in a fashion similar to that found in (5a) and (5b). The distances Ru-C(21) [1.833(7) Å], Ru-P [2.318(2) Å], Ru-C(cp) [2.241 - 2.273(5) Å], are also comparable. The orientation of the butadienyl ligand is very similar to that observed in Ru{C[=C(CN)<sub>2</sub>]CPh=C(CF<sub>3</sub>)<sub>2</sub>}(CO)(PPh<sub>3</sub>)( $\eta$ -C<sub>5</sub>H<sub>5</sub>) (see Section 1.2.2) as are the Ru-C(sp<sup>2</sup>) [2.109(6) Å], C=C [1.346(9), 1.363(8) Å] and C-C [1.469(8) Å] bond distances [cf. dcf complex 2.100(5); 1.356(7), 1.367(7); 1.480(7) Å, resp.].

The use of modelling has shown that the cyclobutenyl rings in both isomers open in a conrotatory fashion, which is as predicted by the principles of conservation of orbital symmetry developed by Woodward and Hoffmann.<sup>3</sup> Scheme 2 depicts the two transformations and, for completeness sake, the disrotatory processes which would result in the observed butadienyl complex [complex (6) could not be obtained in a disrotatory fashion from either (5a) or (5b)]. Isomer (5c) is one of the cyclobutenyl complexes which should form (6) by a disrotatory mechanism. This isomer does not appear to be involved in the formation of (6) from (5a) and (5b), since no interconversion was found between (5a), (5b) and (5c) in solution. It is interesting to note that in these electrocyclic reactions the CO<sub>2</sub>Me substituents on C(14) and C(17) both rotate inwards in the course of the ring-opening. This result accords with recent transition-state calculations for organic cyclobutenes; these indicated that ester groups show little preference for rotation while cyano groups show a preference for outward rotation.<sup>11</sup>

**Figure 7.** PLUTO plot of  $\text{Ru}\{\text{C}=\text{C}(\text{CO}_2\text{Me})(\text{CN})\}\text{CPh}=\text{CH}(\text{CO}_2\text{Me})\}(\text{CO})(\text{PPh}_3)-(\eta\text{-C}_5\text{H}_5)$  (**6**) (by D.N. Duffy and E.R.T. Tiekink)



Scheme 2. Ring-opening transformations involving (5a) and (5b)



In the course of the ring-opening, the butadiene rotates about the Ru-C(6) bond and internally about the C(6)-C(7) bond to achieve the structure that is observed in the solid state. The coplanar diene structure is not favoured because of the overlap between the CO<sub>2</sub>Me groups, rotation about C(6)-C(7) being necessary to relieve these interactions. This in turn creates phenyl-phenyl interactions that are minimized by rotation about the Ru-C(6) bond. The torsion angle C(14)C(6)C(7)C(17) is 82.81°, reflecting these effects.

### 2.2.3. Allyl complex Ru{ $\eta^3$ -CH(CO<sub>2</sub>Me)CPhC=C(CO<sub>2</sub>Me)(CN)}(CO)-( $\eta$ -C<sub>5</sub>H<sub>5</sub>)

A minor product from the pyrolyses of (5a) and (5b) was the allyl complex Ru{ $\eta^3$ -CH(CO<sub>2</sub>Me)CPhC=C(CO<sub>2</sub>Me)(CN)}(CO)( $\eta$ -C<sub>5</sub>H<sub>5</sub>) (7). Higher yields of this complex were obtained by increasing the duration or temperature of the pyrolyses. A 57% yield of (7) was obtained after heating (5a) in refluxing xylene for 24 hours 30 minutes, and a 38% yield from (5b) after heating in refluxing toluene for 29 hours.

The IR spectrum of (7) has a weak  $\nu$ (CN) absorption at 2220 cm<sup>-1</sup>. This is the first instance where the intensity of this band has fallen below medium - strong, and shows the difficulties inherent in assigning allyl structures on the basis of the strength of this absorption. The  $\nu$ (C=C) band at 1647 cm<sup>-1</sup> was of medium intensity. An increase in the energy of the  $\nu$ (CO) band for the ruthenium-bound carbonyl to 2014 cm<sup>-1</sup> was found and suggests that the metal has a lower electron density than in (5a), (5b) and (6). The ester carbonyl absorptions were found at 1736, 1715 and 1665 cm<sup>-1</sup>.

Comparison of the relative intensities of the phenyl ( $\delta$  7.3 - 7.2) and cyclopentadienyl ( $\delta$  5.04) resonances in the proton NMR spectrum pointed to the loss of triphenylphosphine. Three other resonances were found at  $\delta$  5.09, 3.66 and 3.55 for the CH and the two CO<sub>2</sub>Me groups, respectively. In the FAB mass spectrum, a strong molecular ion was found but higher mass aggregates were also observed at  $m/z$  930, 902, 630 and 602; these correspond to [M<sub>2</sub>]<sup>+</sup>, [M<sub>2</sub> - CO]<sup>+</sup>, [M + Ru(C<sub>5</sub>H<sub>5</sub>)]<sup>+</sup> and [M - CO + Ru(C<sub>5</sub>H<sub>5</sub>)]<sup>+</sup>. The relative intensities of these aggregate ions were less than 5%, and closer examination of the spectra of the dcfe-derived

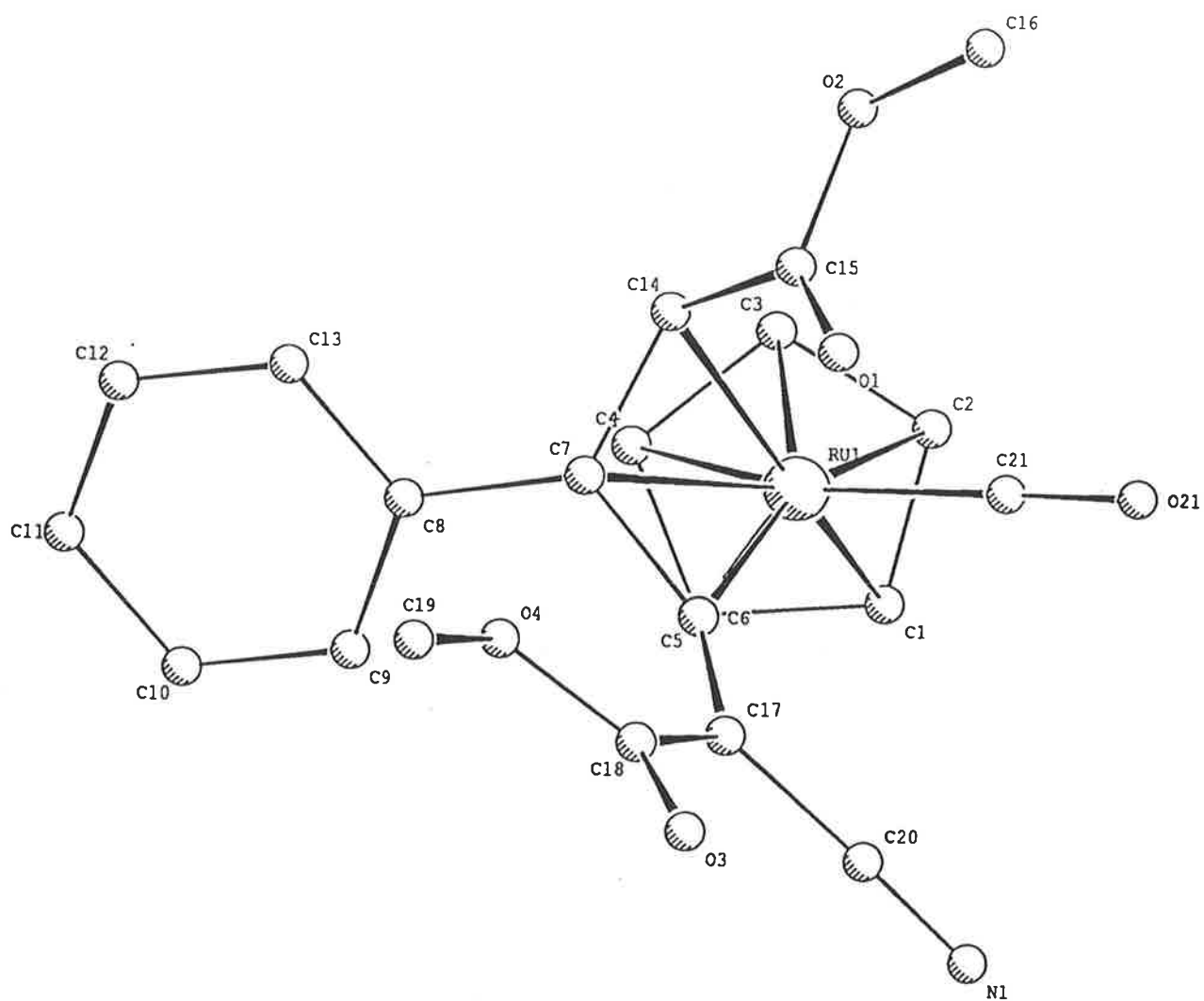
allyl complexes (see Section 1.2.3) revealed similar weak dimeric ions. The other fragment ions correspond to loss of CO and Me groups, followed by the loss of both CO<sub>2</sub>Me groups.

A plot of the structure of (7) determined by X-ray crystallography is shown in Figure 8 and significant bond distances and angles were collected in Table 1. The  $\eta$ -C<sub>5</sub>H<sub>5</sub> and CO ligands are arranged about the ruthenium in a fashion similar to that observed for the dcfe-derived allyl complex Ru{ $\eta^3$ -C(CF<sub>3</sub>)<sub>2</sub>CPhC=C(CN)<sub>2</sub>}(PPh<sub>3</sub>)( $\eta$ -C<sub>5</sub>H<sub>5</sub>) (see Section 1.2.3), except that the CO group occupies the PPh<sub>3</sub> site. The bond distances for Ru-C(21) [1.875(4) Å], Ru-C(cp) [2.227 - 2.245(3), av. 2.236 Å] are within their normal ranges (see Section 2.2.2). The Ru-C(21) distance is slightly greater ( $\approx$  0.04 Å) than those observed for (5a), (5b) and (6) [1.831(5), 1.81(1), 1.833(7) Å resp.].

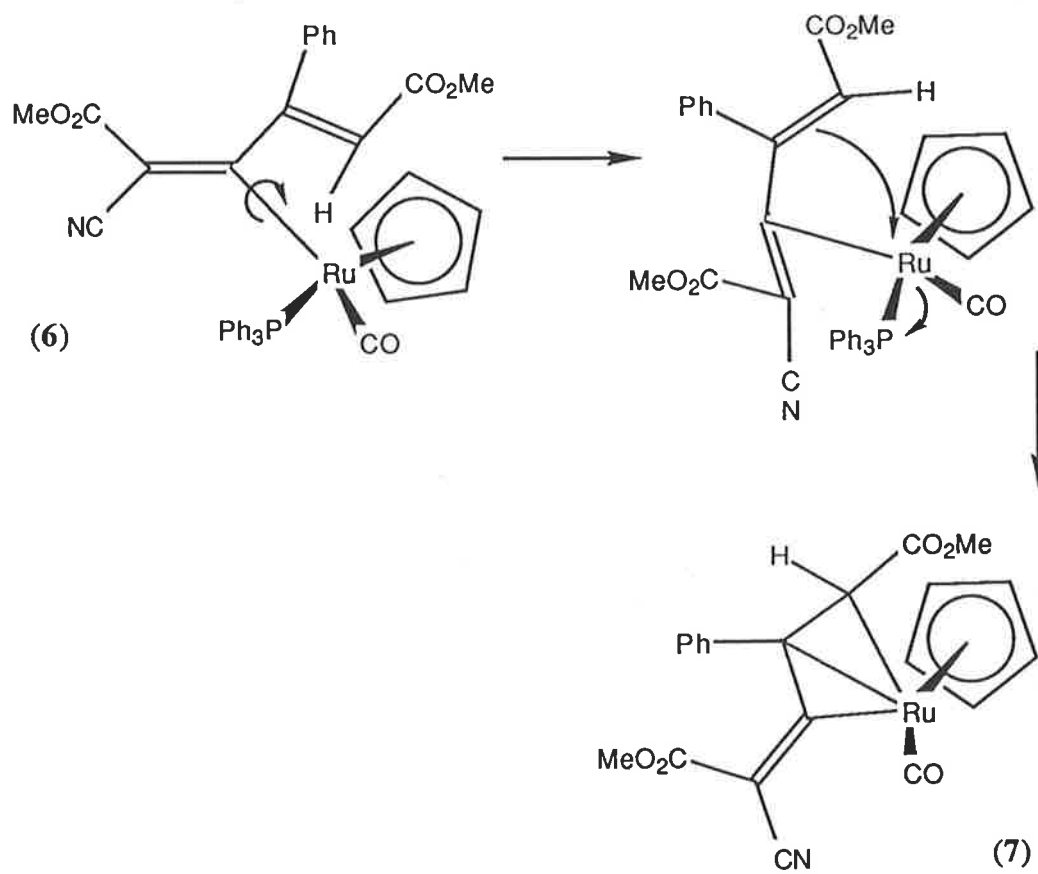
The allyl group is attached to the ruthenium in the same manner as observed for the dcfe complex mentioned above. The shortest bond is Ru-C(6) [2.047(4) Å; cf. dcfe complex 1.977(7) Å]; Ru-C(7) and Ru-C(14) are longer [2.160(4), 2.218(4) Å, resp.; cf. dcfe complex 2.138(7), 2.202(7) Å, resp.]. The distances within the allyl ligand C(6)-C(7), C(7)-C(14) [1.422(5), 1.431(5) Å, resp.; cf. dcfe complex 1.42(1), 1.46(1) Å, resp.] are normal allyl C-C separations indicative of multiple-bond order, while C(6)-C(17) [1.344(5) Å; cf. dcfe complex 1.37(1) Å] is a typical C=C double bond length. The reduction in Ru-C multiple bonding in the rjo-derived allyl compared with the other structurally-characterized allyl complexes, may arise from the absence of the PPh<sub>3</sub> (a good  $\sigma$ -donor) from the ruthenium.

It is clear from the reaction conditions that the allyl complex (7) is formed from the butadienyl compound (6). Modelling the interconversion has shown that the phenyl and =C(CN)(CO<sub>2</sub>Me) groups interact strongly with the triphenylphosphine when the butadienyl is rotated about the Ru-C(6) bond. It is probably this interaction that is responsible for the loss of the larger triphenylphosphine ligand rather than the CO group. The orientation of the allyl group is related to that of the butadienyl precursor by a rotation about Ru-C(6) (see Scheme 3). Torsion angles about RuC(6)C(7)C(14) and RuC(7)C(6)C(17) in (6) and (7) are -107.22, -169.97° and -56.91, 168.77°, respectively.

**Figure 8.** PLUTO plot of  $\text{Ru}\{\eta^3\text{-CH}(\text{CO}_2\text{Me})\text{CPhC}=\text{C}(\text{CO}_2\text{Me})(\text{CN})\}(\text{CO})(\eta\text{-C}_5\text{H}_5)$  (7)  
(by B.K. Nicholson)



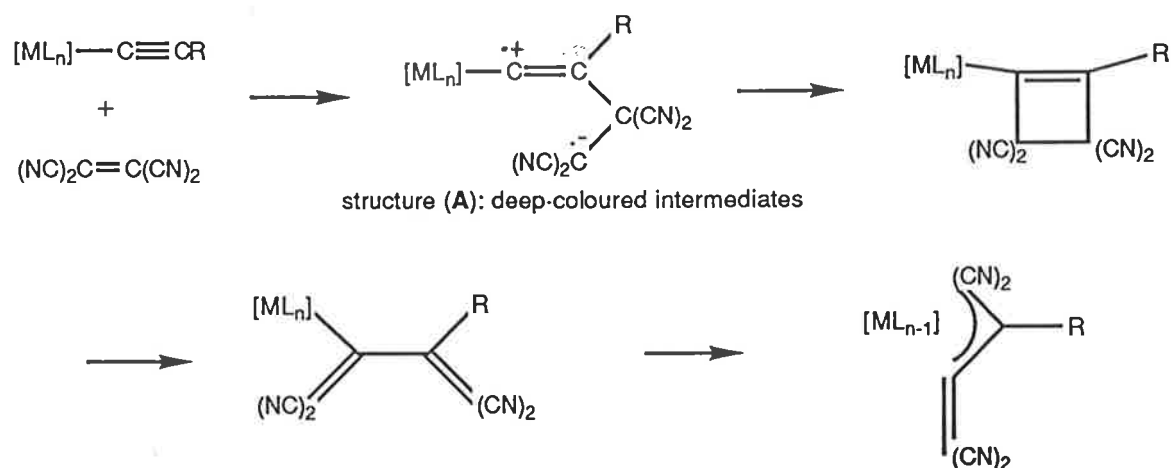
Scheme 3. Conversion of (6) to (7)



#### 2.2.4. Cycloaddition of tetracyanoethene to manganese and iron $\sigma$ -acetylide complexes

The first report of the cycloaddition of tetracyanoethene to  $\sigma$ -acetylide complexes of iron appeared in 1979,<sup>19</sup> and was followed by the initial communication by Bruce *et al.* concerning a ruthenium system.<sup>23</sup> All these reactions proceed via deep-coloured intermediates which lighten to give  $\sigma$ -cyclobutenyl complexes (see Scheme 4). These were not isolable in all cases, as the cycloadduct rapidly undergoes a ring-opening reaction to give the isomeric  $\sigma$ -butadienyl complexes. The studies reported here on the manganese and iron complexes were carried out to complement the extended accounts reported for the tungsten and ruthenium reactions.<sup>20,21</sup>

**Scheme 4.** Summary of cycloaddition reactions involving tcne



The reaction between  $\text{Mn}(\text{C}_2\text{Ph})(\text{CO})_3(\text{dppe})$  and tcne in benzene afforded a short-lived (minutes) pale green intermediate, which on standing converted to the white cyclobutenyl complex  $\text{Mn}\{\text{C}=\text{CPhC}(\text{CN})_2\text{C}(\text{CN})_2\}(\text{CO})_3(\text{dppe})$  (8). This material is characterized by very weak, single  $\nu(\text{CN})$  and  $\nu(\text{C}=\text{C})$  bands at 2234 and 1573  $\text{cm}^{-1}$ , respectively. The  $\nu(\text{CO})$  absorptions at 2017 and 1942  $\text{cm}^{-1}$  are characteristic of the *fac*- $(\text{CO})_3$  group. A similar reaction, between  $\text{Fe}(\text{C}_2\text{Ph})(\text{CO})_2(\eta\text{-C}_5\text{H}_5)$  and tcne in diethyl ether, initially gave a dark green intermediate, which then changed to pale yellow over 15 minutes, and deposited a yellow

precipitate of the cyclobutenyl derivative  $\text{Fe}\{\overline{\text{C}=\text{CPhC}(\text{CN})_2\text{C}(\text{CN})_2}\}(\text{CO})_2(\eta\text{-C}_5\text{H}_5)$  (**9**). The IR spectrum of (**9**) had a very weak  $\nu(\text{CN})$  band at  $2239\text{ cm}^{-1}$  and weak  $\nu(\text{C}=\text{C})$  bands at  $1599$ ,  $1582$  and  $1555\text{ cm}^{-1}$ . The strong  $\nu(\text{CO})$  bands at  $2045$  and  $2001\text{ cm}^{-1}$  confirmed the dicarbonyl formulation. In the proton NMR spectra, resonances at  $\delta 3.30$  for (**8**) and  $\delta 5.18$  for (**9**) confirmed the presence of dppe and  $\eta\text{-C}_5\text{H}_5$  groups, respectively. The phenyl groups had resonances between  $\delta 7.7$  and  $\delta 7.4$ . A  $^{13}\text{C}$  NMR spectrum of (**9**) had signals for the CO, Ph,  $2 \times \text{CN}$  and  $\eta\text{-C}_5\text{H}_5$  groups at  $\delta 212.5$ ,  $130.0$ ,  $112.3$ ,  $111.4$  and  $87.0$ , respectively. The FAB mass spectra of (**8**) and (**9**) show stepwise loss of CO groups from the molecular ion followed by loss of CN or phenyl groups. The base peak for (**8**) is  $[\text{Mn}(\text{CN})(\text{dppe})]^+$ , formed by CN transfer to the metal, and is similar to F-atom transfer reactions found for fluorocarbon complexes (see Section 2.2.5). Loss of the olefin from  $[\text{M}]^+$  or  $[\text{M} - 3\text{CO}]^+$  confirmed the cyclobutenyl structures. With the iron complex, the ion  $[\text{M} - \text{tcne}]^+$  forms the base peak in the spectrum. For complex (**8**) the ion  $[\text{Mn}(\text{CO})_3(\text{dppe})]^+$  is found at  $m/z 537$ , which apparently loses three CO groups simultaneously to give  $[\text{Mn}(\text{dppe})]^+$ .

When the reaction of  $\text{Mn}(\text{C}_2\text{Ph})(\text{CO})_3(\text{dppe})$  with tcne was performed in dichloromethane, a yellow crystalline material resulted. This was shown by spectroscopy to be the butadienyl complex  $\text{Mn}\{\text{C}[\text{C}(\text{CN})_2]\text{CPh}=\text{C}(\text{CN})_2\}(\text{CO})_3(\text{dppe})$  (**10**). The IR spectrum contained two weak  $\nu(\text{CN})$  bands at  $2222$  and  $2208\text{ cm}^{-1}$ . In the previous chapter, it was shown that the  $\nu(\text{CN})$  bands of the butadienyl isomer are commonly stronger than those for the cyclobutenyl isomer. The intensities of the two  $\nu(\text{C}=\text{C})$  bands found at  $1573$  and  $1533\text{ cm}^{-1}$  are also consistent with the butadienyl formulation. The spectrum contained three strong  $\nu(\text{CO})$  bands between  $1944$  and  $2018\text{ cm}^{-1}$ . Solutions of (**8**) in more polar media rapidly deepen in colour to yellow, and afford complex (**10**) upon evaporation. This example of isomerization provides additional evidence for the identities of (**8**) and (**10**), and supports the IR  $\nu(\text{CN})$  and  $\nu(\text{C}=\text{C})$  correlations with structures that were mentioned previously (see Section 1.2).

Similarly, the reaction of  $\text{Fe}(\text{C}_2\text{Ph})(\text{CO})_2(\eta\text{-C}_5\text{H}_5)$  with tcne in dichloromethane gave a yellow-green solution, from which yellow crystals of the butadienyl  $\text{Fe}\{\text{C}[\text{C}(\text{CN})_2]\text{CPh}=\text{C}(\text{CN})_2\}(\text{CO})_2(\eta\text{-C}_5\text{H}_5)$  (**11**) were isolated. In the IR spectrum of (**11**), the weak  $\nu(\text{CN})$

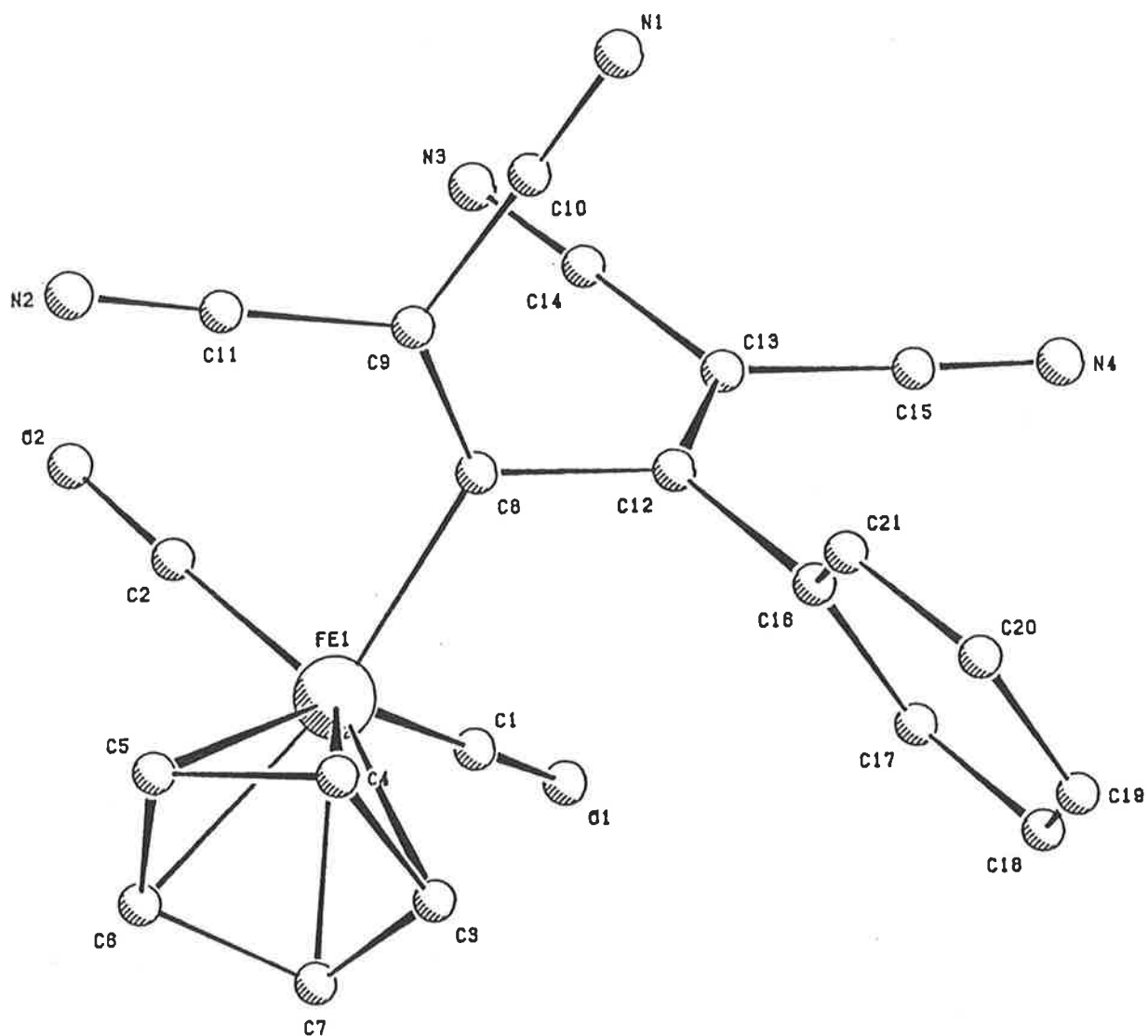
and  $\nu(\text{C}=\text{C})$  bands (2226, 1540  $\text{cm}^{-1}$ , resp.) were found at slightly lower frequencies than those of complex (9), while the  $\nu(\text{CO})$  absorptions were found at higher wavenumbers (2050, 2005  $\text{cm}^{-1}$ ). The major changes found in the  $^1\text{H}$  NMR spectra of the butadienyls were the resonances for the dppe ligand ( $\delta$  3.16) for (10) and the  $\eta\text{-C}_5\text{H}_5$  ligand ( $\delta$  4.95) in (11), both of which are at higher field than their cyclobutenyl analogues. A close comparison between the  $^{13}\text{C}$  NMR spectra of (9) and (11) was not possible, since different solvent combinations and temperatures were employed for the measurements. Two carbonyl resonances were observed for (11) at  $\delta$  211.0 and 209, and signals for the other groups were found at  $\delta$  130.7 (Ph), 115.6, 112.3, 110.5 (CN) and 86.9 ( $\text{C}_5\text{H}_5$ ). The FAB mass spectra of the butadienyls were similar to the cyclobutenyl analogues, except that loss of tcne was not observed for (10). For (11), an ion at  $m/z$  279 corresponding to the loss of tcne was observed. At this stage, it is not clear whether this is an incorrect assignment or an indication that the dicyanomethylene fragments in (11) are less stable under FAB beam conditions than the other compounds examined so far.

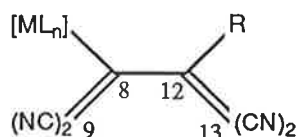
In the original report of the reaction of  $\text{Fe}(\text{C}_2\text{Ph})(\text{CO})_2(\eta\text{-C}_5\text{H}_5)$  with tcne, the same colour changes as above were noted.<sup>19</sup> The deep green intermediate was assumed to be a charge-transfer complex, the derived yellow compound a dipolar adduct formulated as Structure (A) (see Scheme 4), and the yellow-brown compound was assigned the cyclobutenyl structure of (9). The spectroscopic results discussed above, combined with a single-crystal X-ray study of (11), show that these assignments must be modified. Swincer,<sup>24</sup> in an ESR study of this reaction, found that the deep green intermediate had a signal at  $g$  1.997, which, in conjunction with the results obtained for the ruthenium and tungsten systems, suggests that the intermediate is a diradical species with a geometry similar to that of the proposed dipolar complex.

The molecular structure of the iron complex is shown in Figure 9 and confirms the butadienyl formulation, while Table 2 summarizes the pertinent bond parameters of the metal-substituted butadienyl moiety in (11) and the related ruthenium and nickel complexes  $\text{M}\{\text{C}[\text{C}(\text{CN})_2]\text{CPh}=\text{C}(\text{CN})_2\}(\text{L}_n)(\eta\text{-C}_5\text{H}_5)$  ( $\text{M} = \text{Ni}$ ,  $\text{L}_n = \text{PPh}_3$ ;  $\text{M} = \text{Ru}$ ,  $\text{L}_n = (\text{CNBu}^t)(\text{PPh}_3)$  or dppe).

Figure 9. PLUTO plot of  $\text{Fe}\{\text{C}=\text{C}(\text{CN}_2)\}\text{CPh}=\text{C}(\text{CN}_2)\}(\text{CO})_2(\eta\text{-C}_5\text{H}_5)$  (11)

(by M.R.Snow and E.R.T. Tiekink)



**Table 2.** Structural parameters for tetracyanobutadienyl ligands in four metal complexes

	[ML <sub>n</sub> ]			
	Fe(CO) <sub>2</sub> ( <b>11</b> ) (η-C <sub>5</sub> H <sub>5</sub> )	†Ru(CNBut) <sup>†</sup> (PPh <sub>3</sub> )(η-C <sub>5</sub> H <sub>5</sub> ) <sup>23</sup>	†Ru(dppe) (η-C <sub>5</sub> H <sub>5</sub> ) <sup>21</sup>	†Ni(PPh <sub>3</sub> ) (η-C <sub>5</sub> H <sub>5</sub> ) <sup>32</sup>
<i>Bond distances (Å)</i>				
M-C(8)	1.972(2)	2.074(3)	2.068(4)	1.895(6)
C(8)-C(9)	1.347(4)	1.382(5)	1.370(6)	1.338(8)
C(8)-C(12)	1.476(3)	1.478(4)	1.484(6)	1.483(6)
C(12)-C(13)	1.356(3)	1.362(4)	1.346(6)	1.356(6)
C(12)-Ph	1.485(3)	1.479(5)	1.497(6)	1.474(8)
C-CN(av.)	1.441	1.439	1.433	1.439
C-N(av.)	1.131	1.142	1.134	1.141
<i>Bond angles (°)</i>				
M-C(8)-C(9)	126.8(2)	122.5(3)	124.4(3)	125.0(6)
M-C(8)-C(12)	114.8(2)	124.7(2)	119.5(3)	114.8(6)
C(9)-C(8)-C(12)	118.4(2)	122.8(3)	114.4(4)	120.0(8)
C(8)-C(12)-C(13)	120.2(2)	117.9(3)	124.3(4)	120.1(8)
C(8)-C(9)-CN	122.8(2), 123.3(2)	123.7(4), 124.2(4)	122.3(4), 122.7(4)	122.3(8), 124.4(8)
C(12)-C(13)-CN	121.2(2), 122.5(2)	121.4(3), 126.3(4)	122.7(4), 124.3(4)	121.1(8), 125.2(8)

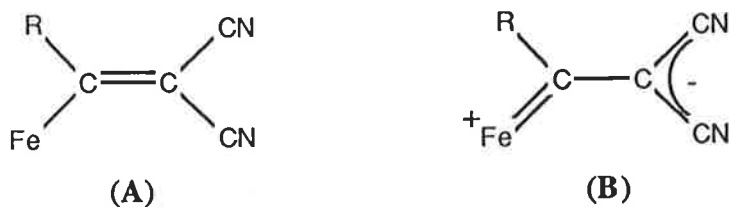
† renumbered according to (**11**)

Table 2. (continued)

	[ML <sub>n</sub> ]			
	Fe(CO) <sub>2</sub> ( <b>11</b> ) (η-C <sub>5</sub> H <sub>5</sub> )	Ru(CNBU <sup>t</sup> ) (PPh <sub>3</sub> )(η-C <sub>5</sub> H <sub>5</sub> )	Ru(dppe) (η-C <sub>5</sub> H <sub>5</sub> )	Ni(PPh <sub>3</sub> ) (η-C <sub>5</sub> H <sub>5</sub> )
<i>Bond angles</i> (°)				
NC-C(9)-CN	113.9(2)	112.0(4)	114.8(4)	113.2(8)
NC-C(13)-CN	116.5(2)	112.1(3)	112.7(4)	113.7(8)
<i>Torsion angles</i> (°)				
M-C(8)-C(12)-Ph	76.6	70.0	70.2	70.3
M-C(8)-C(12)-C(13)	99.2	111.7	112.9	108.7
C(9)-C(8)-C(12)-C(13)	81.7	81.5	80.6	67.2
C(9)-C(8)-C(12)-Ph	102.6	106.4	95.4	113.9

In (**11**), the iron atom is coordinated to the  $\eta$ -cyclopentadienyl group [Fe-C(cp) 2.075 - 2.093(3), av. 2.086 Å], two CO groups [Fe-CO 1.775(3), 1.785(3) Å] and the cyanocarbon ligand [Fe-C(8) 1.972(2) Å]. As is usually found, the angles subtended at the iron by the CO groups and C(8) [C(1)-Fe-C(2) 93.8(1), C(1)-Fe-C(8) 94.9(1), C(2)-Fe-C(8) 90.3(1)°] are all close to 90°, further substantiating the assignment of distorted octahedral stereochemistry to the iron coordination.<sup>25</sup>

The Fe-C( $sp^2$ ) distance is considerably shorter than those in Fe{CMe=C(Ph)Me}(CO)-{P(OPh)<sub>3</sub>}( $\eta$ -C<sub>5</sub>H<sub>5</sub>) [2.031(8) Å]<sup>26</sup> and Fe{C(CO<sub>2</sub>Et)=CMe<sub>2</sub>}(CO)(PPh<sub>3</sub>)( $\eta$ -C<sub>5</sub>H<sub>5</sub>) [2.030(2) Å],<sup>27</sup> although it is close to the Fe-C(O) distances in (R,S)-Fe{(Z)-C(O)CMe=C(Ph)Me}(CO){P(OPh)<sub>3</sub>}( $\eta$ -C<sub>5</sub>H<sub>5</sub>) [1.962(6) Å]<sup>28</sup> and Fe{(Z)-C(O)CMe=C(Ph)Me}(CO)-{P(OPh)<sub>3</sub>}( $\eta$ -C<sub>5</sub>H<sub>5</sub>) [1.966(3) Å]<sup>29</sup>. In this respect, it would appear that the dicyanomethylene group has a similar structural effect to oxygen. The chemical similarities have been noted earlier, both in organometallic complexes<sup>30</sup> and in organic chemistry.<sup>31</sup> The short Fe-C( $sp^2$ ) distance found here, indicating a degree of multiple bond order, probably results from a contribution from the polar form (**B**):



Within the butadienyl ligand, the mutual dispositions of the four groups in the two dicyanomethylene fragments are such as to prevent the *cisoid* diene from achieving planarity. The torsion angle C(9)C(8)C(12)C(13) for (**11**) is 81.7°. This orientation results in the presence of localized C-C single [C(8)-(12) 1.476(3) Å] and C=C double bonds [C(8)-C(9) 1.347(4); C(12)-C(13) 1.356(3) Å] in these ligands. Comparison of the four structures shows that the degree of twisting about the central C-C bond of the diene is essentially independent of the size of the ML<sub>n</sub> fragment, and is a reflection of the interaction between the overlapping CN groups. In other complexes containing non-polar *cisoid* 1,3-dienes, the torsion angles range

from  $80.6^\circ$  [in  $\text{Ru}\{\text{C}[\text{=C}(\text{CN})_2]\text{CMe}=\text{C}(\text{CF}_3)_2\}(\text{CO})(\text{PPh}_3)(\eta\text{-C}_5\text{H}_5)^{32}$ ] to  $82.4^\circ$  [in  $\text{Ru}\{\text{C}[\text{=C}(\text{CN})_2]\text{CPh}=\text{CH}(\text{C}_6\text{H}_4\text{NO}_2\text{-4})\}(\text{PPh}_3)_2(\eta\text{-C}_5\text{H}_5)^{33}$ ]. It is also of interest that no examples of reactions affording *transoid* dienes have yet been found in these systems. Modelling suggests that where the ring substituent is a phenyl group, as is the case with (11), interaction between the CN and phenyl groups would prevent the *transoid* configuration being assumed.

The transformation by UV irradiation from the butadienyl complex  $\text{W}\{\text{C}[\text{=C}(\text{CN})_2]\text{CPh}=\text{C}(\text{CN})_2\}(\text{CO})_3(\eta\text{-C}_5\text{H}_5)$  to the allylic complex  $\text{W}\{\eta^3\text{-C}(\text{CN})_2\text{CPh}=\text{C}(\text{CN})_2\}(\text{CO})_2(\eta\text{-C}_5\text{H}_5)$  was demonstrated previously.<sup>20</sup> We have attempted to achieve ring-opening and the allyl transformation by removing the CO using trimethylamine oxide. A rapid change in colour to orange was observed when  $\text{W}\{\text{C}=\text{CPhC}(\text{CN})_2\text{C}(\text{CN})_2\}(\text{CO})_3(\eta\text{-C}_5\text{H}_5)$  was treated with  $\text{Me}_3\text{NO}\cdot 2\text{H}_2\text{O}$ , and a 70% yield of a new dicarbonyl complex  $\text{W}\{\text{NH}=\text{C}(\text{OH})\text{C}(\text{CN})=\text{CPh}=\text{C}(\text{CN})_2\}(\text{CO})_2(\eta\text{-C}_5\text{H}_5)$  (12) was obtained. Microanalytical and spectroscopic data were consistent with the loss of one CO ligand and addition of one  $\text{H}_2\text{O}$  to the cyanocarbon. The IR  $\nu(\text{CO})$  spectrum contained only two equal-intensity strong bands, and absorptions assigned to  $\nu(\text{OH})$  and  $\nu(\text{NH})$  were found between 2800 and  $3350\text{ cm}^{-1}$ . A similar chelate complex derived from  $\text{W}\{\text{C}=\text{CPhC}(\text{CF}_3)_2\text{C}(\text{CN})_2\}(\text{CO})_3(\eta\text{-C}_5\text{H}_5)$  and  $\text{Me}_3\text{NO}\cdot 2\text{H}_2\text{O}$  (see Section 1.2.4), contains a  $\text{W-N}=\text{C}-\text{C}=\text{C}$  ring. In the present case, we suggest that addition of water to one of the CN groups has again occurred to give the chelating 1,1,4-tricyano-2-phenyl-5-hydroxy-5-imidopenta-1,3-dien-3-yl ligand.

### 2.2.5. Reactions of $\text{Fe}(\overline{\text{C}=\text{CFCF}_2\text{CF}_2})(\text{CO})_2(\eta\text{-C}_5\text{H}_5)$

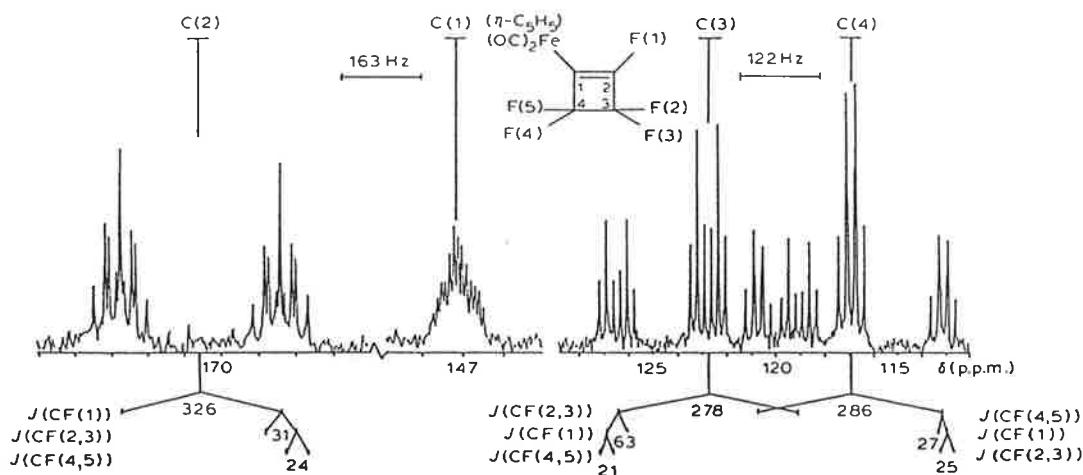
The similarity between  $\text{Fe}(\overline{\text{C}=\text{CFCF}_2\text{CF}_2})(\text{CO})_2(\eta\text{-C}_5\text{H}_5)$  (**13**)<sup>18</sup> and the cyclobutenyl compounds obtained from the reactions of transition-metal  $\sigma$ -acetylide complexes with electron-deficient olefins (see Sections 1.2.1, 2.2.1, 2.2.4) prompted us to examine the tendency of the fluorinated compounds to participate in similar ring-opening reactions.

The perfluorocyclobutenyl complex (**13**) does not undergo ring-opening under thermal or photochemical conditions. The only reactions that we have been able to carry out successfully are simple CO-substitution reactions by ligands such as acetonitrile or tertiary phosphines. Irradiation of a solution of (**13**) in acetonitrile gave the monocarbonyl  $\text{Fe}(\overline{\text{C}=\text{CFCF}_2\text{CF}_2})(\text{CO})(\text{NCMe})(\eta\text{-C}_5\text{H}_5)$  (**14**) as an orange oil in a yield greater than 95%. This complex is quite sensitive to oxidation, both in the pure state and in solution. Ready replacement of the acetonitrile by CO or tertiary phosphines, such as  $\text{PPh}_3$ , afforded complexes (**13**) or  $\text{Fe}(\overline{\text{C}=\text{CFCF}_2\text{CF}_2})(\text{CO})(\text{PPh}_3)(\eta\text{-C}_5\text{H}_5)$  (**15**) in 60 to 65% yields.

The new orange complexes (**14**) and (**15**) are soluble in hydrocarbon solvents. They were characterized by elemental analysis and from their spectra. Whereas complex (**13**) has two  $\nu(\text{CO})$  bands at 2052 and 2007  $\text{cm}^{-1}$ , the substituted complexes have only one, at 1966 (**14**) or 1964  $\text{cm}^{-1}$  (**15**). These bands show the expected lowering in frequency which results from the replacement of a CO ligand by a poorer  $\pi$ -acceptor ligand. In addition, the acetonitrile complex has a  $\nu(\text{CN})$  absorption at 2290  $\text{cm}^{-1}$ .

The  $^1\text{H}$  NMR spectra contained resonances for the  $\text{C}_5\text{H}_5$  protons at  $\delta$  5.09 (**13**), 4.68 (**14**) and 4.58 (**15**), the latter as a doublet ( $J_{\text{P-H}} = 1$  Hz); the Me resonance of the coordinated MeCN ligand (**14**) was found at  $\delta$  2.13. In the  $^{13}\text{C}$  NMR spectra, the  $\text{C}_5\text{H}_5$  signals were at  $\delta$  85.2 and  $\delta$  83.9 for (**13**) and (**15**), respectively, while the CO carbons appeared at  $\delta$  212.1 and  $\delta$  219.9. For complex (**13**), the four cyclobutenyl ring carbons gave the complex series of resonances shown in Figure 10. The fluorine-carbon couplings have permitted, for the first time, an assignment of these resonances.

**Figure 10.**  $^{13}\text{C}$  NMR spectrum of (13), cyclobutenyl ring carbon resonances, showing various  $J_{\text{F-C}}$  couplings (Hz)



The doublet of multiplets centred on  $\delta$  170.8 is assigned to C(2), each multiplet being overlapping triplets of triplets. The complex multiplet at  $\delta$  147.2 (13 peaks resolved) is assigned to C(1). Two further overlapping multiplets centred at  $\delta$  122.8 and  $\delta$  116.9 are assigned to C(3) and C(4), respectively. The  $^{31}\text{P}$  NMR spectrum of (15) contains a singlet at  $\delta$  75.3, no coupling to  $^{19}\text{F}$  being observed.

The  $^{19}\text{F}$  NMR spectra were obtained under conditions of higher resolution than was possible in 1965,<sup>18</sup> and slight changes in chemical shift values probably reflect the increased accuracy and variations in temperature. For (13) in  $\text{CS}_2$ , three signals at  $\delta$  -114.9, -114.1 and -111.0 are assigned to F(4) and F(5), F(1), and F(2) and F(3), respectively, on the basis of their mutual coupling and relative intensities (see Section 2.4.10). A marked solvent effect is observed in  $\text{CH}_2\text{Cl}_2$ , with the two high-field multiplets collapsing to a pseudo-triplet at  $\delta$  -116.0 and the low field signal shifting to  $\delta$  -111.9. The  $\text{PPh}_3$  complex (15) also exhibits a three-resonance pattern, but in this case two weakly interacting systems are present. In  $\text{CH}_2\text{Cl}_2$ , F(4) and F(5) form an AB system centred on  $\delta$  -116.7, while F(1) ( $\delta$  -116.5) and F(2), F(3) ( $\delta$  -109.9) form an  $\text{A}_2\text{X}$  system. Pronounced solvent effects on these spectra were again observed. In  $\text{CS}_2$ , the AB signals overlap with the  $\text{A}_2\text{X}$  triplet at  $\delta$  -114.5, while in benzene, the AB and X multiplets coalesce to a broad triplet ( $\delta$  -115.8). The instability of (14)

meant that a detailed  $^{19}\text{F}$  NMR spectrum could not be obtained. The three broad resonances, at  $\delta$  -110.8, -115.1, -119.7, are assigned to F(2,3), F(4,5), and F(1) respectively.

The EI mass spectrum of (13) has been described previously.<sup>34</sup> We have obtained FAB mass spectra of (14) and (15), both of which contained molecular ions and strong  $[\text{M} - \text{CO}]^+$  ions as base peaks. Common fragmentation patterns include loss of F or  $\text{C}_5\text{H}_5$  and transfer of F or  $\text{CF}_2$  to the iron atom (by elimination of neutral  $\text{C}_4\text{F}_4$  or  $\text{C}_3\text{F}_3$  fragments, respectively). Thus in (14), major ions are  $[\text{Fe}(\text{CF}_2)(\text{C}_5\text{H}_5)]^+$ ,  $[\text{FeF}(\text{C}_5\text{H}_5)]^+$  and  $[\text{Fe}(\text{C}_5\text{H}_5)]^+$ , while for (15), the  $\text{PPh}_3$  ligand is retained, giving  $[\text{Fe}(\text{CF}_2)(\text{PPh}_3)]^+$ ,  $[\text{FeF}(\text{PPh}_3)]^+$  and  $[\text{Fe}(\text{PPh}_3)]^+$ .

We have determined the molecular structures of (13) and (15) by single-crystal X-ray diffraction methods in order to establish which of the structural factors give these molecules their stability. A plot of a molecule of (13) is shown in Figure 11, and Figure 12 shows the two independent molecules, labelled A and B, comprising the asymmetric unit in (15). Selected bond parameters for these complexes are given in Table 3. In (15), the iron atoms are chiral centres, and the two molecules A and B have enantiomers generated by a centre of inversion in the centrosymmetric space group  $P\bar{1}$ , so that, in all, there are four molecules of (15) in the unit cell. Close examination of Figure 12 shows that there are major differences between A and the enantiomer of B, although to a first approximation, B has the opposite chirality to A. The relative orientations of the fluorocarbon ring and the phosphorus-bound phenyl rings differ in A and B, as is clearly shown by the torsion angles C(10)-Fe-C(1)-C(2) ( $136.5^\circ$  for A,  $7.7^\circ$  for B). In A, the cyclobutenyl ring is oriented away from the  $\text{PPh}_3$  group about the Fe-P bond. Alternatively, the C(4)=C(1)-Fe-CO(10) moieties may be regarded as *transoid* in molecule A, and *cisoid* in molecule B.

Figure 11. PLUTO plot of  $\text{Fe}(\text{C}=\text{CFCF}_2\text{CF}_2)(\text{CO})_2(\eta\text{-C}_5\text{H}_5)$  (13)

(by M.R. Snow and E.R.T. Tiekink)

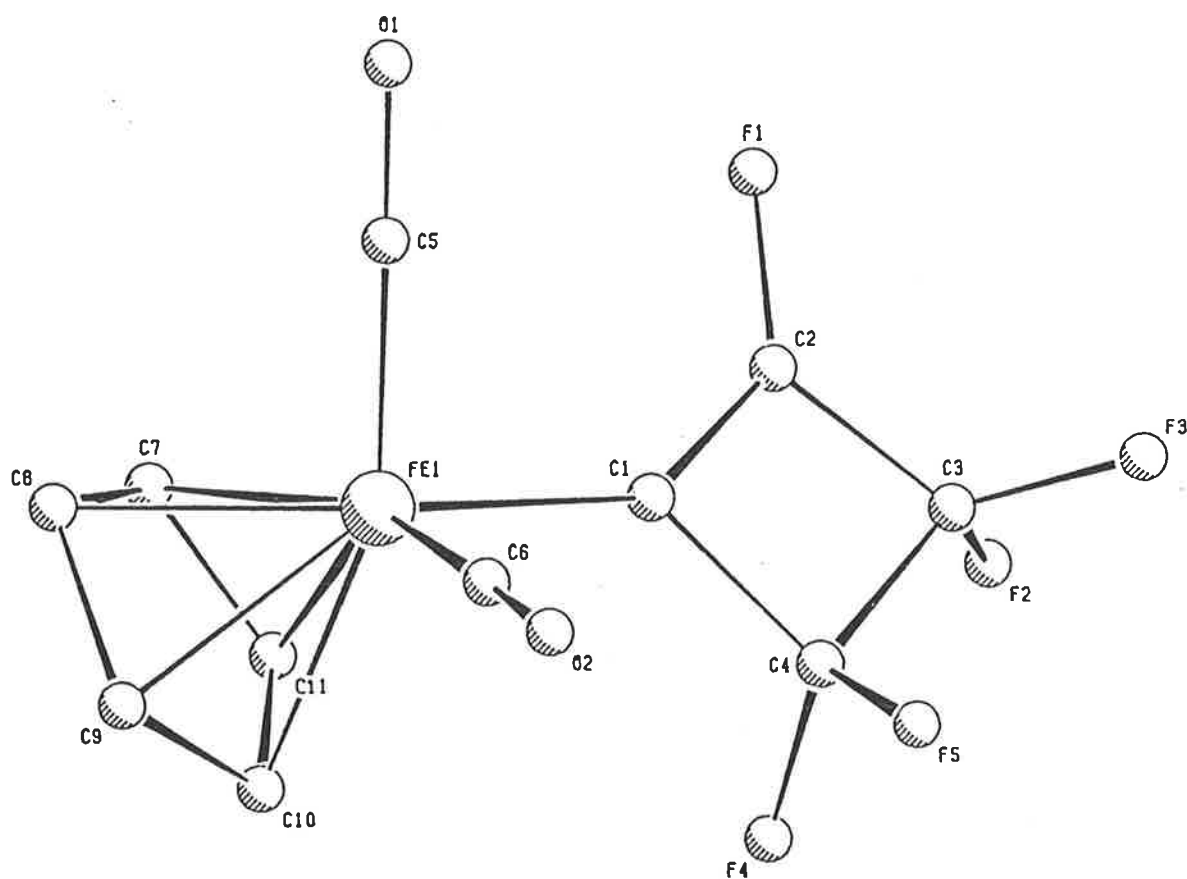
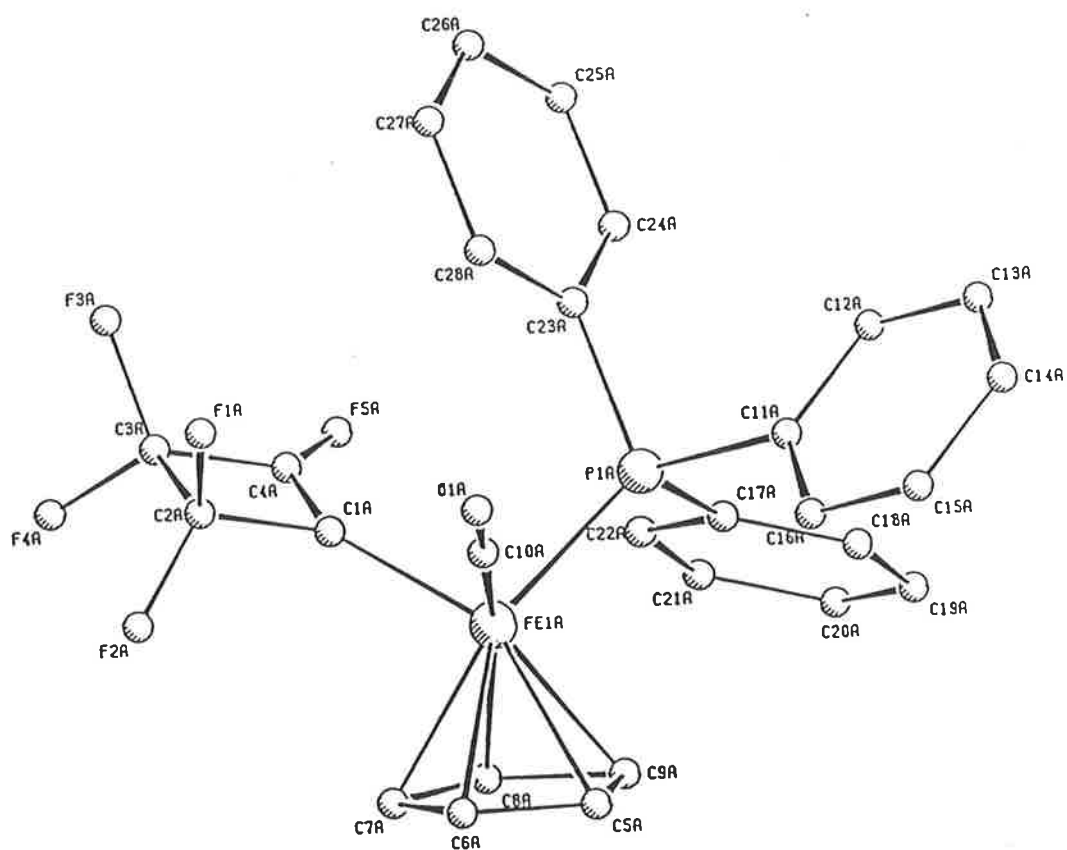
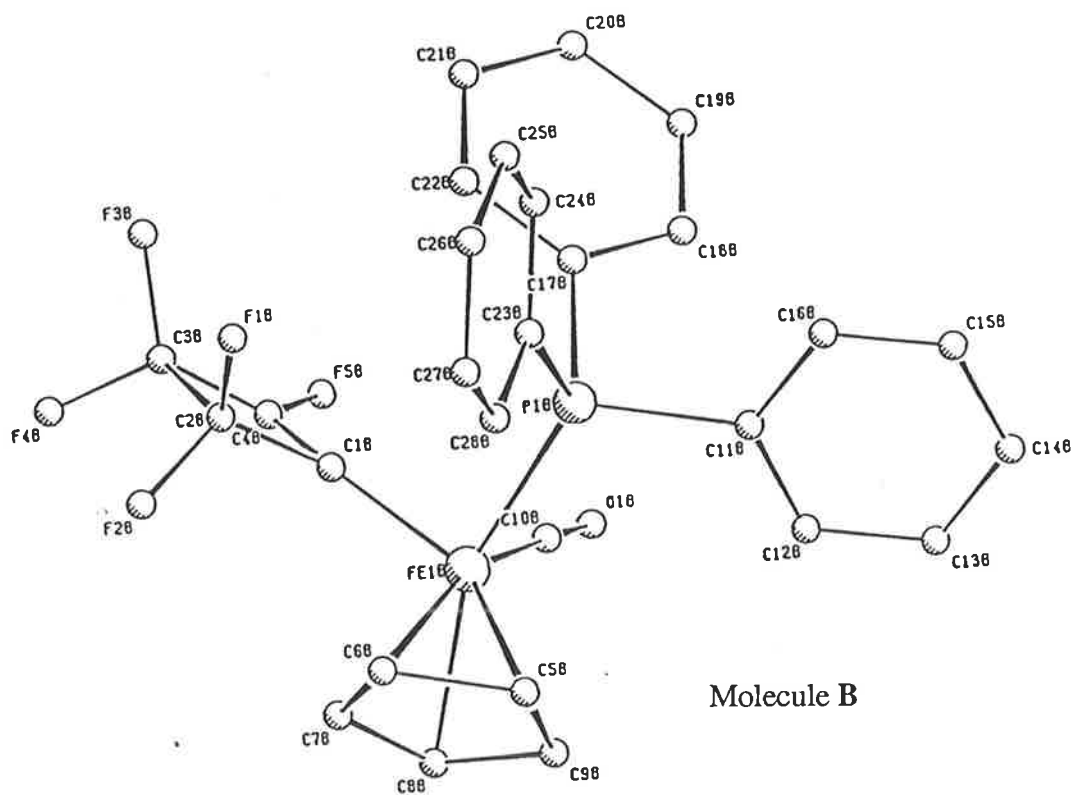


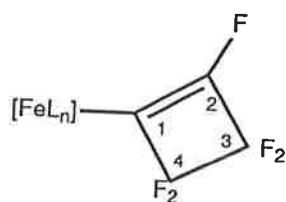
Figure 12. PLUTO plot of the two independent molecules of  $\text{Fe}(\text{C}=\text{CFCF}_2\text{CF}_2)(\text{CO})\text{-}(\text{PPh}_3)(\eta\text{-C}_5\text{H}_5)$  (15) (by M.R. Snow and E.R.T. Tiekink)



Molecule A



Molecule B

**Table 3.** Selected bond distances (Å) and angles (°) for complexes **(13)** and **(15)**

Parameter	Structure		
	(13)	(15A) <sup>†</sup>	(15B) <sup>†</sup>
Fe-cp	2.06(1)-2.09(1)	2.06(2)-2.13(2)	2.10(1)-2.12(2)
Fe-CO	1.774(9)	1.72(2)	1.73(2)
Fe-P	-	2.210(4)	2.225(4)
Fe-C(1)	1.936(9)	1.96(1)	1.89(1)
C(1)-C(4)	1.51(1)	1.46(2)	1.49(2)
C(1)-C(2)	1.32(1)	1.35(2)	1.41(2)
C(2)-C(3)	1.48(1)	1.45(2)	1.42(2)
C(3)-C(4)	1.53(1)	1.54(2)	1.50(2)
C(4)-C(1)-C(2)	88.8(8)	89(1)	84(1)
C(1)-C(2)-C(3)	99.4(8)	99(1)	100(1)
C(2)-C(3)-C(4)	82.6(7)	82(1)	83(1)
C(3)-C(4)-C(1)	89.1(7)	90(1)	93(1)

<sup>†</sup> common numbering scheme used which differs from the crystallographic numbering scheme discussed in the text.

The iron atom in (13) has distorted octahedral geometry, with one octahedral face being occupied by the C<sub>5</sub>H<sub>5</sub> group [Fe-C(cp) av. 2.07 Å] and the other by the two CO groups [Fe-C(5) 1.74(1), Fe-C(6) 1.774(9) Å] and the cyclobutenyl carbon [Fe-C(1) 1.936(9) Å]. The angles subtended at the iron by the three latter atoms [C(1)-Fe-C(5) 90.7(4), C(1)-Fe-C(6) 91.4(4), C(5)-Fe-C(6) 94.8(4)°] are all close to the expected octahedral angle. In the two molecules (A and B) of (15), the iron atoms have similar geometries. The cyclopentadienyl groups are slightly further away from the metal [Fe-C(cp) av. 2.09 Å for molecule A, 2.11 Å for molecule B]. The other three sites are occupied by the CO [Fe-C(10) 1.72(2), 1.73(2) Å], PPh<sub>3</sub> [Fe-P 2.210(4), 2.225(4) Å] and cyclobutenyl groups [Fe-C(1) 1.96(1), 1.89(1) Å]. The angles subtended at the iron by the donor atoms of these ligands [C(1)-Fe-C(10) 92.4(6), 92.0(7); C(1)-Fe-P 96.4(5), 92.2(4); C(10)-Fe-P 94.2(5), 89.2(5)°] are also close to octahedral. The Fe-C(sp<sup>2</sup>) bond lengths [1.936(9) Å in (13), 1.93(1) Å (av.) in (15)] are similar to that found in Fe{ $\overline{\text{C}=\text{CPhC}(\text{CF}_3)_2\text{C}(\text{CN})_2}$ }(CO)<sub>2</sub>(η-C<sub>5</sub>H<sub>5</sub>) [1.949(4) Å (see Section 1.2.1)], but all are shorter than that found in the butadienyl complex Fe{C[=C(CN)<sub>2</sub>]CPh=C(CN)<sub>2</sub>}(CO)<sub>2</sub>(η-C<sub>5</sub>H<sub>5</sub>) (11) [1.972(2) Å].

Of note in the context of the present investigation are the dimensions of the cyclobutenyl ring. Table 3 contains pertinent data for complexes (13) and (15). The tendency toward ring-opening in cyclobutenyl complexes so far studied is  $\overline{\text{C}=\text{CPhC}(\text{CN})_2\text{C}(\text{CN})_2} > \overline{\text{C}=\text{CPhCH}(\text{CO}_2\text{Me})\text{C}(\text{CO}_2\text{Me})(\text{CN})} > \overline{\text{C}=\text{CPhC}(\text{CF}_3)_2\text{C}(\text{CN})_2} \gg \overline{\text{C}=\text{CF}(\text{CF}_2)\text{CF}_2}$ . This tendency can be related to the interatomic parameters, particularly the length, and thus the strength, of the bond opposite the C=C double bond in the cyclobutene ring, i.e. the bond that is broken during the isomerization process.

Irradiation of (13) in non-coordinating solvents (CH<sub>2</sub>Cl<sub>2</sub>, petroleum spirit) using different UV sources (medium pressure 400W, low pressure 16W) caused gradual decomposition. Similarly, both (13) and (14) decomposed under pyrolysis when forcing conditions (120 - 140 °C) were used. This is not entirely surprising, recent results having indicated that the activation energies for the thermal electrocyclic interconversion between perfluoro-substituted cyclobutenes and butadienes are around 37 - 40 kcal/mol.<sup>12,35</sup> Dolbier *et al.*<sup>12</sup> noted a marked

increase in activation if fluorine substituents were not able to rotate outwards in the course of the ring-opening reaction. In the case of (13), the presence of fluorine substituents on both of the carbons involved in the rotation means that neither conrotatory (thermal) or disrotatory (photochemical) processes are favoured. The related cyanocyclobutenyl complexes transform to the corresponding butadienes at room temperature. These results suggest that a paramount role is played by ring substituents in the cyclobutene-butadiene isomerization reaction.

### 2.3. Conclusions

The (2 + 2) cycloaddition of the unsymmetrical olefin  $\text{rjo}$  to  $\text{Ru}(\text{C}_2\text{Ph})(\text{CO})(\text{PPh}_3)(\eta\text{-C}_5\text{H}_5)$  gave two isomers of a cyclobutenyl complex (**5a**) and (**5b**), which differ in the position of the *trans*- $\text{CO}_2\text{Me}$  groups with respect to the metal core. When they were supported on silica, complexes (**5a**) and (**5b**) isomerized to a third cyclobutenyl complex (**5c**). The thermal ring-opening reactions of both (**5a**) and (**5b**) proceeded in the conrotatory direction predicted by Woodward-Hoffmann rules to give the same butadienyl complex (**6**). Further pyrolysis gave an allyl complex (**7**), which was formed from (**6**) by the rather unexpected loss of a  $\text{PPh}_3$  ligand.

The reactions of *tcne* with iron and manganese alkynyl complexes have been investigated. The present results complement those reported earlier for the tungsten- and ruthenium-containing systems, and confirm that the *tcne* reactions proceed via an initial paramagnetic adduct. These adducts were formed by nucleophilic attack of the acetylide ligands on the olefin, and converted quickly to the cyclobutenyl complexes. The cyclobutenyls could be isolated from the reactions of the manganese and iron compounds because of their limited solubilities. In more polar solvents, the final (and often only) product isolated was one of the butadienyl complexes, of which examples containing tungsten, iron, ruthenium and nickel have now been fully characterized by X-ray studies.

Finally, we investigated the electrocyclic reactivity of  $\text{Fe}(\overline{\text{C}=\text{CFCF}_2\text{CF}_2})(\text{CO})_2(\eta\text{-C}_5\text{H}_5)$  and found that under the thermal and photolytic conditions employed, no ring-opening reactions took place. This was related structurally to the length and hence strength of the C-C bond opposite the double bond in the cyclobutenyl ring. In the photochemical reactions, simple ligand-substituted derivatives were formed by the displacement of a CO ligand.

## 2.4. Experimental

**General conditions.** General conditions and instrumentation were as outlined in Section 1.4.

**Starting Materials.** Literature methods were used to prepare  $\text{Ru}(\text{C}_2\text{Ph})(\text{CO})(\text{PPh}_3)(\eta\text{-C}_5\text{H}_5)$ ,<sup>36</sup>  $\text{Fe}(\text{C}_2\text{Ph})(\text{CO})_2(\eta\text{-C}_5\text{H}_5)$ ,<sup>37</sup>  $\text{Mn}(\text{C}_2\text{Ph})(\text{CO})_3(\text{dppe})$ ,<sup>38</sup>  $\text{W}\{\text{C}=\text{CPhC}(\text{CN})_2\text{-C}(\text{CN})_2\}(\text{CO})_3(\eta\text{-C}_5\text{H}_5)$ ,<sup>20</sup> *trans*- $\text{CH}(\text{CO}_2\text{Me})=\text{C}(\text{CN})(\text{CO}_2\text{Me})$  was provided by Professor W.R. Jackson (Monash University). Perfluorocyclobutene (Pfalz and Bauer),  $\{(\eta\text{-C}_5\text{H}_5)\text{Fe}(\text{CO})_2\}_2$  (Strem Chemicals),  $\text{C}_2(\text{CN})_4$  (Fluka) and  $\text{Me}_3\text{NO}\cdot 2\text{H}_2\text{O}$  were used as received.

## Syntheses

### 2.4.1. Synthesis of two isomers of $\text{Ru}\{\overline{\text{C}=\text{CPhCH}(\text{CO}_2\text{Me})\text{C}(\text{CO}_2\text{Me})}(\text{CN})\}(\text{CO})(\text{PPh}_3)(\eta\text{-C}_5\text{H}_5)$ (5a), (5b)

(a) The olefin  $\text{C}(\text{CO}_2\text{Me})(\text{CN})=\text{CH}(\text{CO}_2\text{Me})$  (69 mg, 0.41 mmol) was added to a solution of  $\text{Ru}(\text{C}_2\text{Ph})(\text{CO})(\text{PPh}_3)(\eta\text{-C}_5\text{H}_5)$  (200 mg, 0.36 mmol) in  $\text{CH}_2\text{Cl}_2$  (10 mL). After 17 h the solvent was removed under reduced pressure. Preparative TLC of the residue (petroleum spirit/acetone/ $\text{CH}_2\text{Cl}_2$  7:3:1) isolated two major bands. The first off-white band ( $R_f$  0.69) was collected and crystallized ( $\text{CH}_2\text{Cl}_2/\text{MeOH}$ ) to give white crystals of  $\text{Ru}\{\overline{\text{C}=\text{CPhCH}(\text{CO}_2\text{Me})\text{C}(\text{CO}_2\text{Me})}(\text{CN})\}(\text{CO})(\text{PPh}_3)(\eta\text{-C}_5\text{H}_5)\cdot 0.25\text{CH}_2\text{Cl}_2$  (5a) (160 mg, 0.21 mmol, 59%), m.p. 181-182 °C. Anal. Calcd for  $\text{C}_{39}\text{H}_{32}\text{NO}_5\text{PRu}\cdot 0.25\text{CH}_2\text{Cl}_2$ : C, 63.04; H, 4.35; N, 1.87;  $M_r$  727 (unsolvated). Found: C, 63.08; H, 4.31; N, 1.87;  $M_r$  727 (mass spectrometry). IR ( $\text{CH}_2\text{Cl}_2$ ):  $\nu(\text{CN})$  2236 vw;  $\nu(\text{CO})$  1950vs, 1738s  $\text{cm}^{-1}$ . IR (Nujol):  $\nu(\text{CC})$  1616w, 1585vw, 1572vw; other bands at 1481w, 1439m, 1437(sh), 1330m, 1260m, 1200m, 1179w, 1160m, 1097w, 1090w, 1074w, 1008w, 1011w, 998(sh), 947(sh), 936w, 912(sh), 839w, 808m, 759m, 747w, 740m, 700s, 691s  $\text{cm}^{-1}$ .  $^1\text{H NMR}$  ( $\text{CDCl}_3$ ):  $\delta$  7.4 - 6.5 (m, 20H, Ph); 5.30 (s, 0.5H,  $\text{CH}_2\text{Cl}_2$ ); 5.14 (s, 5H,  $\text{C}_5\text{H}_5$ ); 4.52 (s, 1H, CH); 3.74 (s, 3H,  $\text{CO}_2\text{Me}$ ); 3.66 (s, 3H,

CO<sub>2</sub>Me). FAB MS: 727\*, [M]<sup>+</sup>, 24; 712\*, [M - Me]<sup>+</sup>, 1; 698\*, [M - CO]<sup>+</sup>, 5; 668\*, [M - CO<sub>2</sub>Me]<sup>+</sup>, 3; 637\*, [668 - OMe]<sup>+</sup>, 2; 621\*, [668 - O<sub>2</sub>Me]<sup>+</sup>, 4; 558, [M - C(CO<sub>2</sub>Me)(CN)=CH(CO<sub>2</sub>Me)]<sup>+</sup>, 85; 529\*, [558 - CO]<sup>+</sup>, 9; 457\*, [Ru(CO)(PPh<sub>3</sub>)(C<sub>5</sub>H<sub>5</sub>)]<sup>+</sup>, 30; 429\*, [Ru(PPh<sub>3</sub>)(C<sub>5</sub>H<sub>5</sub>)]<sup>+</sup>, 100; 378\*, [Ru(CO)(PPh<sub>2</sub>)(C<sub>5</sub>H<sub>5</sub>)]<sup>+</sup>, 9; 362\*, [Ru(PPh<sub>3</sub>)]<sup>+</sup>, 13; 352\*, [Ru(PPh<sub>2</sub>)(C<sub>5</sub>H<sub>5</sub>)]<sup>+</sup>, 20; 285\*, [Ru(PPh<sub>2</sub>)]<sup>+</sup>, 9; 244, [RuPh(C<sub>5</sub>H<sub>5</sub>)]<sup>+</sup>, 13; 167, [Ru(C<sub>5</sub>H<sub>5</sub>)]<sup>+</sup>, 13.

The second pale yellow band (R<sub>f</sub> 0.61) crystallized (CH<sub>2</sub>Cl<sub>2</sub>/MeOH) as yellow crystals of Ru{ $\overline{\text{C}=\text{CPhCH}(\text{CO}_2\text{Me})\text{C}(\text{CO}_2\text{Me})(\text{CN})}$ }(CO)(PPh<sub>3</sub>)(η-C<sub>5</sub>H<sub>5</sub>) (**5b**) (83 mg, 0.11 mmol, 27%), m.p. 181-182 °C. Anal. Calcd for C<sub>39</sub>H<sub>32</sub>NO<sub>5</sub>PRu: C, 64.46; H, 4.44; N, 1.91; M<sub>r</sub> 727. Found: C, 63.96; H, 4.59; N, 1.93; M<sub>r</sub> 727 (mass spectrometry). IR (CH<sub>2</sub>Cl<sub>2</sub>): ν(CN) 2236vw; ν(CO) 1958vs, 1738s cm<sup>-1</sup>. IR (Nujol): ν(CC) 1607vw, 1572vw; other bands at 1483m, 1437m, 1277(sh), 1242s(br), 1176w, 1157(sh), 1098m, 1089w, 1075w, 1026(sh), 1012m, 997(sh), 941m, 837w, 810m, 771(sh), 760(sh), 748m, 698s cm<sup>-1</sup>. <sup>1</sup>H NMR (CDCl<sub>3</sub>): δ 7.4 - 6.8 (m, 20H, Ph); 4.91 (s, 5H, C<sub>5</sub>H<sub>5</sub>); 4.52 (d, J<sub>P-H</sub> = 1.6 Hz, 1H, CH); 3.85 (s, 3H, CO<sub>2</sub>Me); 3.73 (s, 3H, CO<sub>2</sub>Me). FAB MS: identical in observed peaks and intensities to (**5a**). A number of trace white bands (**6**) and a trace red band were observed but not identified.

(b) <sup>1</sup>H NMR Study of the formation of (**5a**) and (**5b**): Ru(C<sub>2</sub>Ph)(CO)(PPh<sub>3</sub>)(η-C<sub>5</sub>H<sub>5</sub>) (15mg, 0.027 mmol) dissolved in CDCl<sub>3</sub> (0.5 mL) was added to C(CO<sub>2</sub>Me)(CN)=CH-(CO<sub>2</sub>Me) (5 mg, 0.03 mmol) and then placed in an NMR tube. After 4 min only a trace of acetylide was found to be present and within 10 min the formation of (**5a**) and (**5b**) was complete. The equilibrium ratio of isomers (**5a**):(**5b**), (2.0:1) was the same after 7 d in solution. When a similar experiment was performed using C<sub>6</sub>D<sub>6</sub>, the total reaction time was 1h 25 min and the equilibrium ratio was (1.5:1).

#### 2.4.2. Solid state conversion of (5a) and (5b) to a third isomer of



##### (a) Conversion of (5a) to (5c)

Isomer (5a) (65 mg, 0.09 mmol) was dissolved in  $\text{CH}_2\text{Cl}_2$  (10 mL), silica (TLC grade; 800 mg) was added and the solvent removed. After 3 d in the dark, exposed to air, the silica had become yellow. Following solvent extraction ( $\text{CH}_2\text{Cl}_2/\text{MeOH}$ ) the residue was separated by TLC (petroleum spirit/ $\text{CH}_2\text{Cl}_2$ /acetone 4:2:1). Two bands were collected: the first white band ( $R_f$  0.53) was identified ( $^1\text{H}$  NMR, spot TLC) as unreacted (5a) (16 mg, 24%); the next yellow band ( $R_f$  0.44) crystallized ( $\text{CH}_2\text{Cl}_2$ /petroleum spirit) as pale yellow crystals of  $\text{Ru}\{\overline{\text{C}=\text{CPhCH}(\text{CO}_2\text{Me})\text{C}(\text{CO}_2\text{Me})(\text{CN})}\}(\text{CO})(\text{PPh}_3)(\eta\text{-C}_5\text{H}_5)$  (5c) (22 mg, 0.03 mmol, 34%), m.p. 177-179 °C. Anal. Calcd for  $\text{C}_{39}\text{H}_{32}\text{NO}_5\text{PRu}\cdot 0.1\text{CH}_2\text{Cl}_2$ : C, 63.88; H, 4.41; N, 1.91;  $M_r$  727 (unsolvated). Found: C, 63.83; H, 4.40; N, 1.92;  $M_r$  727 (mass spectrometry). IR ( $\text{CH}_2\text{Cl}_2$ ):  $\nu(\text{CN})$  2235vw, 2207vw;  $\nu(\text{CO})$  1953vs, 1737s  $\text{cm}^{-1}$ . IR (Nujol):  $\nu(\text{CC})$  1607w, 1577vw, 1566vw; other bands at 1483m, 1439s, 1428w, 1378m, 1356w, 1323w, 1311w, 1275m, 1253s, 1198m, 1179m, 1165s, 1157(sh), 1106w, 1098m, 1078m, 1027w, 1010(sh), 1004(sh), 998m, 960m, 931m, 907w, 871w, 837w, 831(sh), 816m, 807(sh), 780m, 777(sh), 750m, 748(sh), 740(sh), 696s  $\text{cm}^{-1}$ .  $^1\text{H}$  NMR ( $\text{CDCl}_3$ ):  $\delta$  7.4 - 6.6 (m, 20H, Ph); 5.30 (s, 0.2H,  $\text{CH}_2\text{Cl}_2$ ); 4.88 (s, 5H,  $\text{C}_5\text{H}_5$ ); 4.18 (s, 1H, CH); 3.85 (s, 3H,  $\text{CO}_2\text{Me}$ ); 3.51 (s, 3H,  $\text{CO}_2\text{Me}$ ).  $^1\text{H}$  NMR ( $d^6$ -acetone):  $\delta$  7.4 - 6.6 (m, 20H, Ph); 5.60 (s, 0.2H,  $\text{CH}_2\text{Cl}_2$ ); 5.00 (s, 5H,  $\text{C}_5\text{H}_5$ ); 4.19 (s, 1H, CH); 3.83 (s, 3H,  $\text{CO}_2\text{Me}$ ); 3.45 (s, 3H,  $\text{CO}_2\text{Me}$ ). FAB MS: identical in observed peaks and intensities to (5a). Instability of (5c) in solution prevented the isolation of crystals suitable for an X-ray study.

##### (b) $^1\text{H}$ NMR study of the conversion of (5a) to (5c)

(i) Isomer (5a) in  $d^6$ -acetone showed no appreciable change after 20 h in solution.

(ii) Isomer (5a) (30 mg, 0.041 mmol) in  $d^6$ -acetone (3 mL), in the presence of silica (28-280 mesh; 225mg), showed no appreciable change after 26 h in solution.

(iii) Isomer (5a) (10 mg, 0.014 mmol) was dissolved in  $\text{CH}_2\text{Cl}_2$  (10 mL), silica (TLC grade; 150 mg) was added and the solvent removed under reduced pressure. The sample was

left in contact with air under fluorescent light. NMR samples were prepared by removing 15 mg of the silica sample and extracting with  $d^6$ -acetone (0.5 mL). After 7 h approximately 50% conversion to (5c) was apparent; 30 h - 56%; 50 h - 58%. Side reactions became prominent from 50 h onwards. The only side reaction which could be correlated with the observed peaks was the conversion of (5a) to (5b).

**(c)  $^1\text{H}$  NMR Study of the conversion of (5b) to (5c)**

(i) Isomer (5b) in  $d^6$ -acetone showed no appreciable change after 20 h in solution

(ii) Isomer (5b) (10 mg, 0.014 mmol) was supported on silica (TLC grade; 125 mg) and sampled as above. After 48 h approximately 20% conversion to (5c) was indicated; at 14 d this had increased to 25% but with much side reaction (38%) and only 37% of (5b) remaining. Of the side reactions only the conversion of (5b) to (5a) could be correlated with some of the observed peaks.

**2.4.3. Thermal isomerisation of cyclobutenes (5a) and (5b) to the butadienyl complex  $\text{Ru}\{\text{C}=\text{C}(\text{CO}_2\text{Me})(\text{CN})\}\text{CPh}=\text{CH}(\text{CO}_2\text{Me})\}\{\text{CO}\}(\text{PPh}_3)-(\eta\text{-C}_5\text{H}_5)$  (6)**

**(a) Conversion of (5a) to (6)**

Isomer (5a) (62mg, 0.085 mmol) was dissolved in benzene (15 mL) and heated (oil bath, 94 °C) for 33 h. After cooling the solvent was removed under reduced pressure and the residue purified by TLC (petroleum spirit/acetone/ $\text{CH}_2\text{Cl}_2$  7:3:1). The major yellow band ( $R_f$  0.42) crystallized ( $\text{CH}_2\text{Cl}_2/\text{EtOH}$ ) as yellow crystals of  $\text{Ru}\{\text{C}=\text{C}(\text{CO}_2\text{Me})(\text{CN})\}\text{CPh}=\text{CH}(\text{CO}_2\text{Me})\}\{\text{CO}\}(\text{PPh}_3)(\eta\text{-C}_5\text{H}_5)$  (6) (45 mg, 0.062 mmol, 73%), m.p. 158-160 °C. Anal. Calcd for  $\text{C}_{39}\text{H}_{32}\text{NO}_5\text{PRu}$ : C, 64.46; H, 4.44; N, 1.91;  $M_r$  727. Found: C, 63.86; H, 4.51; N, 2.29;  $M_r$  727 (mass spectrometry). IR ( $\text{CH}_2\text{Cl}_2$ ):  $\nu(\text{CN})$  2207w;  $\nu(\text{CO})$  1951s, 1725s, 1697(sh)  $\text{cm}^{-1}$ . IR (Nujol):  $\nu(\text{CC})$  1597s, 1585vw, 1575m, 1501m; other bands at 1477(sh), 1448m, 1440m, 1437m, 1417w, 1349m, 1317w, 1269m, 1227s, 1190m, 1163s, 1118m, 1104w, 1091w, 1082w, 1057m, 1029w, 1015w, 1001m, 989m, 892w, 848s, 837s,

826m, 777m, 767m, 748m, 737w, 724m, 697s, 684(sh), 659w  $\text{cm}^{-1}$ .  $^1\text{H NMR}$  ( $\text{CDCl}_3$ ):  $\delta$  7.6 - 7.1 (m, 20H, Ph); 5.41 (s, 1H, CH); 4.74 (s, 5H,  $\text{C}_5\text{H}_5$ ); 3.58 (s, 3H,  $\text{CO}_2\text{Me}$ ); 3.14 (s, 3H,  $\text{CO}_2\text{Me}$ ). FAB MS: 727\*,  $[\text{M}]^+$ , 25; 712\*,  $[\text{M} - \text{Me}]^+$ , 2; 698\*,  $[\text{M} - \text{CO}]^+$ , 9; 662\*,  $[\text{M} - (\text{C}_5\text{H}_5)]^+$ , 15; 634\*,  $[\text{M} - \text{CO} - (\text{C}_5\text{H}_5)]^+$ , 7; 457\*,  $[\text{Ru}(\text{CO})(\text{PPh}_3)(\text{C}_5\text{H}_5)]^+$ , 47; 429\*,  $[\text{Ru}(\text{PPh}_3)(\text{C}_5\text{H}_5)]^+$ , 100; 378\*,  $[\text{Ru}(\text{CO})(\text{PPh}_2)(\text{C}_5\text{H}_5)]^+$ , 11; 362\*,  $[\text{Ru}(\text{PPh}_3)]^+$ , 16; 350\*,  $[\text{Ru}(\text{PPh}_2)(\text{C}_5\text{H}_5)]^+$ , 21; 244,  $[\text{RuPh}(\text{C}_5\text{H}_5)]^+$ , 15; 167,  $[\text{Ru}(\text{C}_5\text{H}_5)]^+$ , 25. Of five minor/trace bands, two were identified: the first white band ( $R_f$  0.89) as  $\text{PPh}_3$  (by FAB MS and comparative spot TLC), and a second white band as unreacted (5a) (4 mg, 6%) (by  $^1\text{H NMR}$  and comparative spot TLC).

#### (b) Conversion of (5b) to (6)

Isomer (5b) (45 mg, 0.062 mmol) was dissolved in benzene (20 mL) and refluxed for 17 h. After cooling and removal of solvent under reduced pressure, the residue was purified by TLC (petroleum spirit/ $\text{CH}_2\text{Cl}_2$ /acetone 4:2:1). A major yellow band ( $R_f$  0.53) was collected and crystallized ( $\text{CH}_2\text{Cl}_2$ /petroleum spirit); this was identified by (FAB MS and  $^1\text{H NMR}$ ) as (6) (13 mg, 0.018 mmol, 29%). Four white minor/trace bands were not characterized.

#### (c) Direct synthesis of (6)

A direct preparation of the butadienyl isomer that avoids unnecessary separation of the cyclobutenyl isomers is as follows: The crude reaction mixture obtained from the reaction between  $\text{Ru}(\text{C}_2\text{Ph})(\text{CO})(\text{PPh}_3)(\eta\text{-C}_5\text{H}_5)$  (220 mg, 0.39 mmol) and rjo (92 mg, 0.54 mmol) was evaporated to dryness. This residue was then precipitated from  $\text{CH}_2\text{Cl}_2/\text{MeOH}$  to give an off-white powder (200 mg, 0.28 mmol, 70%) consisting of a mixture of (5a) and (5b) (200 mg, 0.28 mmol). The powder was dissolved in benzene (30 mL) and refluxed for 16 h. After cooling the solvent was removed under reduced pressure and the residue purified by TLC (petroleum spirit/ $\text{CH}_2\text{Cl}_2$ /acetone 4:2:1). A major yellow band ( $R_f$  0.53) was crystallized ( $\text{CH}_2\text{Cl}_2/\text{EtOH}$ ) to give yellow crystalline (6) (122 mg, 0.17 mmol, 60%). Two other bands were collected: a white band ( $R_f$  0.63) identified as (5a) (by  $^1\text{H NMR}$  and FAB MS), and a yellow band ( $R_f$  0.42) identified as (7) (by FAB MS and  $^1\text{H NMR}$ , see Section 2.4.4).

**2.4.4. Thermal conversion of the cyclobutenes (5a) and (5b) to the allyl complex  $\text{Ru}\{\eta^3\text{-CH}(\text{CO}_2\text{Me})\text{CPhC}=\text{C}(\text{CO}_2\text{Me})(\text{CN})\}(\text{CO})(\eta\text{-C}_5\text{H}_5)$  (7)**

**(a) Conversion of (5a) to (7)**

Isomer (5a) (83 mg, 0.11 mmol) was heated in refluxing xylene (40 mL) for 24 h 30 min. After cooling and removal of solvent (HV, 30 °C) the residue was purified by TLC (petroleum spirit/ $\text{CH}_2\text{Cl}_2$ /acetone 8:5:2). A major yellow band ( $R_f$  0.35) crystallized ( $\text{CH}_2\text{Cl}_2$ /petroleum spirit) as large yellow crystals of  $\text{Ru}\{\eta^3\text{-CH}(\text{CO}_2\text{Me})\text{CPhC}=\text{C}(\text{CO}_2\text{Me})(\text{CN})\}(\text{CO})(\eta\text{-C}_5\text{H}_5)\cdot\text{CH}_2\text{Cl}_2$  (7) (29 mg, 0.06 mmol, 57%), m.p. 111-112 °C. Anal. Calcd for  $\text{C}_{21}\text{H}_{17}\text{NO}_5\text{Ru}\cdot\text{CH}_2\text{Cl}_2$ : C, 48.09; H, 3.48; N, 2.55;  $M_r$  465 (unsolvated). Found: C, 48.18; H, 3.46; N, 2.64;  $M_r$  465 (mass spectrometry). IR ( $\text{CH}_2\text{Cl}_2$ ):  $\nu$  (CN) 2220w;  $\nu$ (CO) 2014vs 1736(sh), 1715s, 1665w  $\text{cm}^{-1}$ . IR (Nujol):  $\nu$ (CC) 1647m; other bands at 1450m, 1444(sh), 1408w, 1295(sh), 1286m, 1275m, 1260m, 1248m, 1200w, 1190w, 1175m, 1124w, 1107w, 1067w, 1021w, 1009w, 830m, 772w, 757w, 722w, 691w, 608w  $\text{cm}^{-1}$ .  $^1\text{H}$  NMR ( $\text{CDCl}_3$ ):  $\delta$  7.3 - 7.2 (m, 5H, Ph); 5.30 (s, 2H,  $\text{CH}_2\text{Cl}_2$ ); 5.09 (s, 1H, CH); 5.04 (s, 5H,  $\text{C}_5\text{H}_5$ ); 3.66 (s, 3H,  $\text{CO}_2\text{Me}$ ); 3.55 (s, 3H,  $\text{CO}_2\text{Me}$ ). FAB MS: 465,  $[\text{M}]^+$ , 25; 437\*,  $[\text{M} - \text{CO}]^+$ , 100; 422,  $[\text{M} - \text{CO} - \text{Me}]^+$ , 38; 378\*,  $[\text{M} - \text{CO} - \text{CO}_2\text{Me}]^+$ , 52; 320,  $[\text{M} - \text{CO} - 2\text{CO}_2\text{Me}]^+$ , 13; 167\*,  $[\text{Ru}(\text{C}_5\text{H}_5)]^+$ , 27; higher mass ions are also formed with relative abundance <5%: 930\*,  $[\text{M}_2]^+$ ; 902\*,  $[\text{M}_2 - \text{CO}]^+$ ; 630\*,  $[\text{M} + \text{Ru}(\text{C}_5\text{H}_5)]^+$ ; 602\*,  $[\text{M} - \text{CO}]^+$ . Of the remaining four minor/trace bands only two were identified: a white band ( $R_f$  0.73) as  $\text{PPh}_3$  (FAB MS, spot TLC) and a yellow band ( $R_f$  0.46) as (6) ( $^1\text{H}$  NMR, FAB MS).

**(b) Conversion of (5b) to (7)**

Isomer (5b) (58 mg, 0.08 mmol) was dissolved in toluene (10 mL) and heated at reflux point for 29 h. After cooling the solvent was removed under reduced pressure and the residue purified by TLC (petroleum spirit/acetone/ $\text{CH}_2\text{Cl}_2$  7:3:1). A major yellow band ( $R_f$  0.44) was identified (by IR,  $^1\text{H}$  NMR and FAB MS) as (7) (14 mg, 0.03 mmol, 38%). Of the five minor/trace bands only one was identified, a white band ( $R_f$  0.86) as  $\text{PPh}_3$  (by FAB MS and comparative spot TLC).

## Cycloaddition reactions using tetracyanoethene

### 2.4.5. Synthesis of $\text{Mn}\{\overline{\text{C}=\text{CPhC}(\text{CN})_2\text{C}(\text{CN})_2}\}(\text{CO})_3(\text{dppe})$ (8)

$\text{Mn}(\text{C}_2\text{Ph})(\text{CO})_3(\text{dppe})$  (200 mg, 0.31 mmol) was dissolved in benzene (5 mL) and a solution of tcne (48 mg, 0.37 mmol) in benzene (15 mL) was added. After an initial green colour formed the solution became progressively paler and a white precipitate was deposited. After 4 h this was filtered off, washed with petroleum spirit (10 mL), dried, and then recrystallized quickly ( $\text{CH}_2\text{Cl}_2/\text{Et}_2\text{O}$ ) at  $-30^\circ\text{C}$  to give  $\text{Mn}\{\overline{\text{C}=\text{CPhC}(\text{CN})_2\text{C}(\text{CN})_2}\}(\text{CO})_3(\text{dppe})\cdot 0.5\text{CH}_2\text{Cl}_2$  (8) (160 mg, 0.21 mmol, 67%), m.p.  $120\text{--}125^\circ\text{C}$ . Anal. Calcd for  $\text{C}_{43}\text{H}_{29}\text{MnN}_4\text{O}_3\text{P}_2\cdot 0.5\text{CH}_2\text{Cl}_2$ : C, 64.58; H, 3.73; N, 6.92;  $M_r$  766 (unsolvated). Found: C, 64.26; H, 3.73; N, 6.92;  $M_r$  766 (mass spectrometry). IR ( $\text{CH}_2\text{Cl}_2$ ):  $\nu(\text{CN})$  2234vw;  $\nu(\text{CO})$  2017s, 1942s(br)  $\text{cm}^{-1}$ . IR (Nujol):  $\nu(\text{CC})$  1573vw; other bands at 1481w, 1440m, 1098w, 1000w, 795w, 710m, 698(sh), 690m, 688w, 667w, 650w, 628w  $\text{cm}^{-1}$ .  $^1\text{H NMR}$  ( $\text{CD}_2\text{Cl}_2$ ):  $\delta$  7.7 - 7.4 (m, 25H, Ph); 3.30 (m, 4H,  $\text{CH}_2$ ). FAB MS: 767\*,  $[\text{M}]^+$ , 8; 737\*,  $[\text{M} - \text{CO}]^+$ , 1; 711\*,  $[\text{M} - 2\text{CO}]^+$ , 2; 682\*,  $[\text{M} - 3\text{CO}]^+$ , 30; 656,  $[\text{M} - 3\text{CO} - \text{CN}]^+$ , 5; 630,  $[\text{M} - 3\text{CO} - 2\text{CN}]^+$ , 1; 605\*,  $[\text{M} - 3\text{CO} - \text{Ph}]^+$ , 3; 581,  $[\text{M} - 3\text{CO} - \text{C}_2\text{Ph}]^+$ , 9; 554,  $[\text{Mn}(\text{C}_2\text{Ph})(\text{dppe})]^+$ , 19; 537,  $[\text{Mn}(\text{CO})_3(\text{dppe})]^+$ , 14; 479,  $[\text{Mn}(\text{CN})(\text{dppe})]^+$ , 100; 453\*,  $[\text{Mn}(\text{dppe})]^+$ , 28; 425,  $[\text{Mn}(\text{PPh}_2)_2]^+$ , 9.

### 2.4.6. Synthesis of $\text{Fe}\{\overline{\text{C}=\text{CPhC}(\text{CN})_2\text{C}(\text{CN})_2}\}(\text{CO})_2(\eta\text{-C}_5\text{H}_5)$ (9)

$\text{Fe}(\text{C}_2\text{Ph})(\text{CO})_2(\eta\text{-C}_5\text{H}_5)$  (150 mg, 0.54 mmol) was dissolved in diethyl ether (10 mL) and tcne (77 mg, 0.60 mmol) was added. The solution immediately went dark green then lightened to pale yellow over 15 min with a yellow precipitate forming. This was filtered off, washed with  $\text{Et}_2\text{O}$  (10 mL), dried, and shown (by IR and FAB MS) to be  $\text{Fe}\{\overline{\text{C}=\text{CPhC}(\text{CN})_2\text{C}(\text{CN})_2}\}(\text{CO})_2(\eta\text{-C}_5\text{H}_5)$  (9) (110 mg, 0.27 mmol, 50%), m.p.  $78\text{--}79^\circ\text{C}$ . Anal. Calcd for  $\text{C}_{21}\text{H}_{10}\text{FeN}_4\text{O}_2$ : C, 62.10; H, 2.48; N, 13.79;  $M_r$  406. Found: C, 61.22; H, 2.65; N, 13.68;  $M_r$  406 (mass spectrometry). The complex is unstable in the solid state, even under nitrogen. IR ( $\text{CH}_2\text{Cl}_2$ ):  $\nu(\text{CN})$  2239vw;  $\nu(\text{CO})$  2045s, 2001s  $\text{cm}^{-1}$ . IR (Nujol):  $\nu(\text{CC})$  1599w, 1582w, 1555w; other bands at 1447w, 1435w, 1422w, 1340w, 1257m, 1187w, 1160w, 1075w,

1018m, 1005w, 915m, 885m, 861m, 840w, 781w, 772s, 721w, 692s  $\text{cm}^{-1}$  (Lit.<sup>19</sup>  $\nu(\text{CO})$  2040, 1990  $\text{cm}^{-1}$ ).  $^1\text{H}$  NMR ( $\text{CDCl}_3$ ):  $\delta$  7.55 (m, 5H, Ph); 5.18 (s, 5H,  $\text{C}_5\text{H}_5$ ).  $^{13}\text{C}\{^1\text{H}\}$  NMR ( $d^6$ -acetone/acetone 1:3, 230K):  $\delta$  212.5 (s, CO); 130.0 (m, Ph); 112.3, 111.4 (s, CN); 87.0 (s,  $\text{C}_5\text{H}_5$ ). FAB MS: 407,  $[\text{M} + \text{H}]^+$ , 18; 406,  $[\text{M}]^+$ , 20; 380,  $[\text{M} - \text{CN}]^+$ , 9; 350\*,  $[\text{M} - 2\text{CO}]^+$ , 66; 324,  $[\text{M} - 2\text{CO} - \text{CN}]^+$ , 46; 279,  $[\text{M} - \text{C}_2(\text{CN})_4]^+$ , 100; 274\*,  $[\text{M} - 2\text{CO} - \text{Ph}]^+$ , 26; 268,  $[\text{?}]^+$ , 17; 259,  $[\text{FeC}_2\text{PhC}_2(\text{CN})_3]^+$ , 11.

#### 2.4.7. Synthesis of $\text{Mn}\{\text{C}[\text{C}(\text{CN})_2]\text{CPh}=\text{C}(\text{CN})_2\}(\text{CO})_3(\text{dppe})$ (10)

$\text{Mn}(\text{C}_2\text{Ph})(\text{CO})_3(\text{dppe})$  (140 mg, 0.22 mmol) was dissolved in dichloromethane (30 mL) and tcne (31 mg, 0.24 mmol) was added. After 24 h stirring, with monitoring by IR, the mixture had become deeper yellow in colour. The solvent was then removed and the residue column chromatographed (florisil). A yellow band was eluted (petroleum spirit/acetone 3:2), and after solvent removal and recrystallization ( $\text{CH}_2\text{Cl}_2/\text{EtOH}$ ) gave yellow plates of  $\text{Mn}\{\text{C}[\text{C}(\text{CN})_2]\text{CPh}=\text{C}(\text{CN})_2\}(\text{CO})_3(\text{dppe}) \cdot 0.25\text{CH}_2\text{Cl}_2$  (10) (121 mg, 0.16 mmol, 72%), m.p. 140-145  $^\circ\text{C}$  (dec.). Anal. Calcd for  $\text{C}_{43}\text{H}_{29}\text{MnN}_4\text{O}_3\text{P}_2 \cdot 0.25\text{CH}_2\text{Cl}_2$ : C, 65.94; H, 3.77; N, 7.11;  $M_r$  766 (unsolvated). Found: C, 66.05; H, 3.85; N, 7.14;  $M_r$  766 (mass spectrometry). IR ( $\text{CH}_2\text{Cl}_2$ ):  $\nu(\text{CN})$  2222w, 2208w;  $\nu(\text{CO})$  2018s, 1957s, 1944s  $\text{cm}^{-1}$ . IR (Nujol):  $\nu(\text{CC})$  1573w, 1533m; other peaks at 1487w, 1438m, 1158w, 1103w, 1097w, 880w, 842w, 818m, 761w, 749m, 742m, 720w, 705(sh), 698s, 662m, 620w, 607w  $\text{cm}^{-1}$ .  $^1\text{H}$  NMR ( $\text{CD}_2\text{Cl}_2$ ):  $\delta$  7.6 - 7.4 (m, 25H, Ph); 3.16 (m, 4H,  $\text{CH}_2$ ). FAB MS: 767\*,  $[\text{M}]^+$ , 3; 737\*,  $[\text{M} - \text{CO}]^+$ , 1; 711\*,  $[\text{M} - 2\text{CO}]^+$ , 0.5; 682\*,  $[\text{M} - 3\text{CO}]^+$ , 27; 656\*,  $[\text{M} - 3\text{CO} - \text{CN}]^+$ , 2; 605\*,  $[\text{M} - 3\text{CO} - \text{Ph}]^+$ , 2; 537,  $[\text{Mn}(\text{CO})_3(\text{dppe})]^+$ , 18; 479,  $[\text{Mn}(\text{CN})(\text{dppe})]^+$ , 100; 453\*,  $[\text{Mn}(\text{dppe})]^+$ , 52; 425,  $[\text{Mn}(\text{PPh}_2)_2]^+$ , 9.

#### 2.4.8. Synthesis of $\text{Fe}\{\text{C}[\text{C}(\text{CN})_2]\text{CPh}=\text{C}(\text{CN})_2\}(\text{CO})_2(\eta\text{-C}_5\text{H}_5)$ (11)

$\text{Fe}(\text{C}_2\text{Ph})(\text{CO})_2(\eta\text{-C}_5\text{H}_5)$  (165 mg, 0.59 mmol) and tcne (150 mg, 1.18 mmol) were dissolved in dichloromethane (10 mL). After 1 h 30 min stirring the yellow-brown solution was filtered, EtOH (10 mL) added and the volume reduced to 5 mL. Cooling to  $-50^\circ\text{C}$  resulted in the formation of a yellow precipitate, which was collected by filtration and washed

with cold EtOH (-20 °C, 2 x 5 mL) and petroleum spirit (10 mL). Recrystallization (CH<sub>2</sub>Cl<sub>2</sub>/pentane) gave yellow crystalline Fe{C[=C(CN)<sub>2</sub>]CPh=C(CN)<sub>2</sub>}(CO)<sub>2</sub>(η-C<sub>5</sub>H<sub>5</sub>).0.125CH<sub>2</sub>Cl<sub>2</sub> (**11**) (185 mg, 0.46 mmol, 77%), m.p. 202 °C (dec.). Anal. Calcd for C<sub>21</sub>H<sub>10</sub>FeN<sub>4</sub>O<sub>2</sub>.0.125CH<sub>2</sub>Cl<sub>2</sub>: C, 60.80; H, 2.45; N, 13.43; *M<sub>r</sub>* 406 (unsolvated). Found: C, 60.79; H, 2.57; N, 13.46; *M<sub>r</sub>* 406 (mass spectrometry). IR (CH<sub>2</sub>Cl<sub>2</sub>): ν(CN) 2226w; ν(CO) 2050s, 2005s cm<sup>-1</sup>. IR (Nujol): ν(CC) 1540w; other bands at 1494w, 865w, 772w, 741w, 695w, 662w cm<sup>-1</sup> [Lit.<sup>19</sup> ν(CO) 2050, 2005 cm<sup>-1</sup>]. <sup>1</sup>H NMR (CDCl<sub>3</sub>): δ 7.60 (m, 5H, Ph); 5.30 (s, 0.25H, CH<sub>2</sub>Cl<sub>2</sub>); 4.95 (s, 5H, C<sub>5</sub>H<sub>5</sub>). <sup>13</sup>C{<sup>1</sup>H} NMR (CD<sub>2</sub>Cl<sub>2</sub>/CH<sub>2</sub>Cl<sub>2</sub> 1:4): δ 211.0, 209.0 (2 x s, CO); 130.7 (m, Ph); 15.6, 112.3, 110.5 (s, CN); 86.9 (s, C<sub>5</sub>H<sub>5</sub>). FAB MS: 407, [M + H]<sup>+</sup>, 45; 406, [M]<sup>+</sup>, 38; 379\*, [M - CO]<sup>+</sup>, 9; 363\*, [?]<sup>+</sup>, 9; 350, [M - 2CO]<sup>+</sup>, 100; 324, [M - 2CO - CN]<sup>+</sup>, 48; 279\*, [M - C<sub>2</sub>(CN)<sub>4</sub>]<sup>+</sup>, 90; 274\*, [M - 2CO - Ph]<sup>+</sup>, 48; 268, [?]<sup>+</sup>, 26; 259, [FeC<sub>2</sub>PhC<sub>2</sub>(CN)<sub>3</sub>]<sup>+</sup>, 24.

#### 2.4.9. Synthesis of $\overline{W\{NH=C(OH)C(CN)=CCPh=C(CN)_2\}(CO)_2(\eta-C_5H_5)}$ (**12**)

$\overline{W\{C=CPhC(CN)_2C(CN)_2\}(CO)_3(\eta-C_5H_5)}$  (100 mg, 0.18 mmol) was stirred with Me<sub>3</sub>NO.2H<sub>2</sub>O (65 mg, 0.58 mmol) in acetone (15 mL). After 15 min the solution had become orange and spot TLC indicated completion of reaction. The mixture was filtered and the solvent removed under vacuum. Preparative TLC of the residue (petroleum spirit/acetone/CH<sub>2</sub>Cl<sub>2</sub> 2:1:1) separated seven bands; the major orange band (R<sub>f</sub> 0.69) was collected and recrystallized (vapour diffusion of C<sub>6</sub>H<sub>6</sub>/petroleum spirit into a CH<sub>2</sub>Cl<sub>2</sub>/MeOH solution) to yield  $\overline{W\{NH=C(OH)C(CN)=CCPh=C(CN)_2\}(CO)_2(\eta-C_5H_5).0.125CH_2Cl_2}$  (**12**) (70 mg, 0.13 mmol, 70%), m.p. 110 °C (dec.). Anal. Calcd for C<sub>21</sub>H<sub>12</sub>N<sub>4</sub>O<sub>3</sub>W.0.125CH<sub>2</sub>Cl<sub>2</sub>: C, 45.08; H, 2.17; N, 9.95; *M<sub>r</sub>* 552 (unsolvated). Found: C, 45.05; H, 2.16; N, 9.97; *M<sub>r</sub>* 552 (mass spectrometry). IR (Fluorolube A): ν(OH, NH, CH) 3342s, 3240s, 3200s, 3118(sh), 2960w, 2934w, 2865w cm<sup>-1</sup>. IR (CH<sub>2</sub>Cl<sub>2</sub>): ν(CN) 2230vw, 2208w; ν(CO) 1976s, 1903s cm<sup>-1</sup>. IR (Nujol): ν(CC, CN) 1716w, 1675s, 1550s, 1540s; other peaks at 1262w, 1090(sh), 1072m, 1062(sh), 1009w, 1002w, 853m, 840w, 828m, 781w, 762m, 724w, 697m, 657w cm<sup>-1</sup>. <sup>1</sup>H NMR (d<sup>6</sup>-acetone): δ 7.67 (m, 5H, Ph); 5.80 (s, 0.25H, CH<sub>2</sub>Cl<sub>2</sub>); 5.30 (s, 5H, C<sub>5</sub>H<sub>5</sub>). FAB MS: 552, [M]<sup>+</sup>, 69; 512, [?]<sup>+</sup>, 23; 496, [M - 2CO]<sup>+</sup>, 100; 470, [M - 2CO - CN]<sup>+</sup>, 15.

Reactions of the complex  $\text{Fe}(\overline{\text{C}=\text{CFCF}_2\text{CF}_2})(\text{CO})_2(\eta\text{-C}_5\text{H}_5)$

2.4.10. Preparation of  $\text{Fe}(\overline{\text{C}=\text{CFCF}_2\text{CF}_2})(\text{CO})_2(\eta\text{-C}_5\text{H}_5)$  (13)

The method of Bruce *et al.*<sup>18</sup> was modified as follows: A solution of  $\text{Na}\{\text{Fe}(\text{CO})_2(\eta\text{-C}_5\text{H}_5)\}$  (11.3 mmol), prepared from  $\{\text{Fe}(\text{CO})_2(\eta\text{-C}_5\text{H}_5)\}_2$  (2.0 g, 5.65 mmol) and 1% Na/Hg amalgam (4 mL), in thf (50 mL), was syringed into a Carius tube. Perfluorocyclobutene (2.97 g, 18.33 mmol) was condensed in and the contents stirred at r.t. for 20 h. After removal of excess  $\text{C}_4\text{F}_6$  the orange solution was filtered through a Celite pad and the solvent removed from the filtrate at 5 °C under reduced pressure. The residue was chromatographed (column: florisil; petroleum spirit eluent) and a major orange band collected and crystallized to yield pale yellow  $\text{Fe}(\overline{\text{C}=\text{CFCF}_2\text{CF}_2})(\text{CO})_2(\eta\text{-C}_5\text{H}_5)$  (13) (2.4 g, 7.5 mmol, 66%), m.p. 50-52 °C. IR (cyclohexane):  $\nu(\text{CO})$  2052s, 2007s  $\text{cm}^{-1}$ .  $^1\text{H}$  NMR ( $\text{CDCl}_3$ ):  $\delta$  5.09 (s,  $\text{C}_5\text{H}_5$ ).  $^{13}\text{C}\{^1\text{H}\}$  NMR ( $\text{CH}_2\text{Cl}_2$ ):  $\delta$  212.1 (s, CO); 170.8 [dt;  $^1J_{\text{F}(1)\text{-C}} = 326$  Hz,  $^2J_{\text{F}(2,3)\text{-C}} = 31$  Hz,  $^3J_{\text{F}(4,5)\text{-C}} = 24$  Hz; C(2)]; 147.2 (13 peaks,  $J_{\text{av.}} = 7.6$  Hz, C(1)); 122.8 [td;  $^1J_{\text{F}(2,3)\text{-C}} = 278$  Hz,  $^2J_{\text{F}(1)\text{-C}} = 63$  Hz,  $^2J_{\text{F}(4,5)\text{-C}} = 21$  Hz; C(3)]; 116.9 [td;  $^1J_{\text{F}(4,5)\text{-C}} = 286$  Hz;  $^3J_{\text{F}(1)\text{-C}} = 27$  Hz,  $^2J_{\text{F}(2,3)\text{-C}} = 25$  Hz; C(4)]; 85.2 (s,  $\text{C}_5\text{H}_5$ ).  $^{19}\text{F}$  NMR ( $\text{CS}_2$ ):  $\delta$  -111.0 [dt;  $^3J_{\text{F}(1)\text{-F}} = 24.5$  Hz,  $^3J_{\text{F}(4,5)\text{-F}} = 22.8$  Hz; 2F; F(2,3)]; -114.1 [tt;  $^3J_{\text{F}(2,3)\text{-F}} = 24.9$  Hz,  $^4J_{\text{F}(4,5)\text{-F}} = 5.1$  Hz; 1F; F(1)]; -114.9 [td;  $^3J_{\text{F}(2,3)\text{-F}} = 22.8$  Hz,  $^4J_{\text{F}(1)\text{-F}} = 4.8$  Hz; 2F; F(4,5)].  $^{19}\text{F}$  NMR ( $\text{CH}_2\text{Cl}_2$ ):  $\delta$  -111.9 [m, 2F, F(2,3)]; -116.0 (m, 3F, F(1,4,5)]. For atom numbering scheme see Figure 10, Section 2.2.5. [Lit.<sup>18</sup> m.p. 50-51°C; IR (cyclohexane):  $\nu(\text{CO})$  2055s, 2012s  $\text{cm}^{-1}$ ;  $^{19}\text{F}$  NMR ( $\text{CS}_2$ ):  $\delta$  -119.1; -123.4; -124.1].

2.4.11. Attempted ring opening reactions of (13)

(a) Pyrolysis of  $\text{Fe}(\overline{\text{C}=\text{CFCF}_2\text{CF}_2})(\text{CO})_2(\eta\text{-C}_5\text{H}_5)$

A solution of (13) (130 mg, 0.40 mmol) in xylene (30 mL) was refluxed for 4 h, producing a cloudy solution. After cooling much decomposition was evident. Following filtration and removal of solvent the product remaining was identified (by IR and spot TLC) as unreacted starting material.

(b) Photolysis of  $\text{Fe}(\overline{\text{C}=\text{CFCF}_2\text{CF}_2})(\text{CO})_2(\eta\text{-C}_5\text{H}_5)$

(i) *In dichloromethane:* Use of a low-power lamp (16W) to irradiate a  $\text{CH}_2\text{Cl}_2$  solution of (13) (200 mg, 0.63 mmol) produced gradual decomposition over 20 h (gradual decrease in  $\nu(\text{CO})$  bands at 2034, 1996  $\text{cm}^{-1}$ ). The only product that could be identified after TLC was starting material.

(ii) *In petroleum spirit:* A medium-pressure lamp (400W, pyrex filtered) was used to irradiate a solution of (13) (150 mg, 0.47 mmol) in petroleum spirit (50 mL); after 90 min little reaction was observed. Use of an unfiltered source resulted in a 50% reduction in intensity of the  $\nu(\text{CO})$  bands over 1 h. This was accompanied by formation of an intractable brown solid.

2.4.12. Synthesis of  $\text{Fe}(\overline{\text{C}=\text{CFCF}_2\text{CF}_2})(\text{CO})(\text{NCMe})(\eta\text{-C}_5\text{H}_5)$  (14)

Irradiation (400W, pyrex filtered) of a solution of (13) (320 mg, 1.0 mmol) in MeCN (50 mL) with a  $\text{N}_2$  purge produced an orange solution after 1 h. At this stage the IR monitoring indicated completion of the photolysis (decrease in  $\nu(\text{CO})$  bands at 2047, 1999, increase in the band at 1966  $\text{cm}^{-1}$ ). After decanting into a Schlenk tube the solvent was removed (0 °C, HV), leaving an viscous orange liquid (327 mg, 98%) which was used for subsequent reactions. For analytical purposes the sample was purified by TLC (petroleum spirit/ $\text{CH}_2\text{Cl}_2$  3:2); a major orange band ( $R_f$  0.37) was separated from 3 trace bands. Removal of  $\text{CH}_2\text{Cl}_2$  from the extract (0 °C, HV) left an unstable oil characterised as  $\text{Fe}(\overline{\text{C}=\text{CFCF}_2\text{CF}_2})(\text{CO})(\text{NCMe})(\eta\text{-C}_5\text{H}_5)$  (14) (234 mg, 0.70 mmol, 70%), b.p. 65 °C/10<sup>-1</sup> mm. Anal. Calcd for  $\text{C}_{12}\text{H}_8\text{F}_5\text{FeON}$ : C, 43.28; H, 2.42; N, 4.21;  $M_r$  333. Found: C, 42.94; H, 2.48; N, 3.56;  $M_r$  333 (mass spectrometry). IR (MeCN):  $\nu(\text{CO})$  1966s  $\text{cm}^{-1}$ . IR (Neat oil):  $\nu(\text{CH})$  3420m(br), 3130w, 2832w;  $\nu(\text{CN})$  2290w;  $\nu(\text{CO})$  1970vs;  $\nu(\text{CC})$  1761w, 1692vw, 1671vw, 1609m;  $\nu(\text{CF})$  1368s, 1258s, 1157m, 1114m, 1070s; other peaks at 2047(sh), 1012w, 1003w, 929s, 839m, 827m, 787s, 771m, 670w, 839w  $\text{cm}^{-1}$ .  $^1\text{H}$  NMR ( $\text{CD}_2\text{Cl}_2$ ):  $\delta$  4.68 (s,  $\text{C}_5\text{H}_5$ ); 2.13 (s, MeCN).  $^{19}\text{F}$  NMR ( $\text{CH}_2\text{Cl}_2$ ):  $\delta$  -110.8 [m, 2F, F(2,3)]; -115.1 [m, 2F, F(4,5)]; -119.7 [m, 1F, F(1)] - broad resonances. FAB MS: 333,  $[\text{M}]^+$ , 31; 314,  $[\text{M} - \text{F}]^+$ , 51; 305,  $[\text{M} - \text{CO}]^+$ , 100; 286,  $[\text{M} - \text{F} - \text{CO}]^+$ , 42; 245\*,  $[\text{M} - \text{F} - \text{MeCN}]^+$ , 19; 240\*,

$[\text{M} - \text{CO} - (\text{C}_5\text{H}_5)]^+$ , 6; 199,  $[\text{Fe}(\text{CF}_2)(\text{CO})(\text{C}_5\text{H}_5)]^+$ , 15; 171,  $[\text{Fe}(\text{CF}_2)(\text{C}_5\text{H}_5)]^+$ , 42; 152,  $[\text{FeF}(\text{C}_5\text{H}_5)]^+$ , 27; 121,  $[\text{FeC}_5\text{H}_5]^+$ , 19. Workup of (14) was performed strictly under  $\text{N}_2$  to avoid oxidation.

### Ligand substitution reactions of (14)

#### 2.4.13. Synthesis of $\text{Fe}(\overline{\text{C}=\text{CFCF}_2\text{CF}_2})(\text{CO})(\text{PPh}_3)(\eta\text{-C}_5\text{H}_5)$ (15)

To a solution of (14) (327 mg, 0.98 mmol) dissolved in  $\text{CH}_2\text{Cl}_2$  (40 mL) was added  $\text{PPh}_3$  (262 mg, 1.00 mmol). After stirring for 3 h (25 °C) the reaction was judged to be complete (IR, spot TLC) and the solvent was removed under reduced pressure. Preparative TLC of the residue (petroleum spirit/  $\text{CH}_2\text{Cl}_2$ /Et<sub>2</sub>O 4:1:1) eluted a major orange band ( $R_f$  0.6) which crystallized by slow evaporation ( $\text{CH}_2\text{Cl}_2$ /petroleum spirit/MeOH) to give orange crystalline  $\text{Fe}(\overline{\text{C}=\text{CFCF}_2\text{CF}_2})(\text{CO})(\text{PPh}_3)(\eta\text{-C}_5\text{H}_5)$  (15) (366 mg, 0.66 mmol, 62%), m.p. 169-170 °C. Anal. Calcd for  $\text{C}_{28}\text{H}_{20}\text{F}_5\text{FeOP}$ : C, 60.67; H, 3.64;  $M_r$  554. Found: C, 60.39; H, 3.63;  $M_r$  554 (mass spectrometry). IR (cyclohexane):  $\nu(\text{CO})$  1964 vs  $\text{cm}^{-1}$ . IR (Nujol):  $\nu(\text{CC})$  1609 m;  $\nu(\text{CF})$  1358 s, 1254 s, 1183 w, 1150 m, 1106 m, 1091 s, 1071 s, 1053 s; other peaks at 1480 m, 1435 s, 1012 w, 997 w, 928 s, 850 w, 840 w, 831 m, 787 s, 748 s, 702 (sh), 697 s, 687 (sh), 640 w  $\text{cm}^{-1}$ .  $^1\text{H}$  NMR ( $\text{CDCl}_3$ ):  $\delta$  7.4 - 7.2 (m, 15H,  $\text{C}_6\text{H}_5$ ); 4.58 (d, 5H,  $^3J_{\text{P-H}} = 1\text{ Hz}$ ,  $\text{C}_5\text{H}_5$ ).  $^{13}\text{C}\{^1\text{H}\}$  NMR ( $\text{CH}_2\text{Cl}_2$ ):  $\delta$  219.9 (d,  $^2J_{\text{P-C}} = 29\text{ Hz}$ , CO); 170.4 [dm,  $^1J_{\text{F(1)-C}} = 322\text{ Hz}$ , C(2)]; 161.2 [m, C(1)]; 135.6-128.6 (m, Ph); 123.9 [tm,  $^1J_{\text{F(2,3)-C}} = 248\text{ Hz}$ , C(3)]; 117.0 [tm,  $^1J_{\text{F(4,5)-C}} = 287\text{ Hz}$ , C(4)]; 83.9 (s,  $\text{C}_5\text{H}_5$ ).  $^{19}\text{F}$  NMR ( $\text{CH}_2\text{Cl}_2$ ):  $\delta$  -109.9 [d,  $^3J_{\text{F(1)-F}} = 25.4\text{ Hz}$ , 2F, F(2,3)]; -116.0 [d,  $^1J_{\text{F-F}} = 187.8\text{ Hz}$ , 1F, F(4) or F(5)]; -116.5 [t,  $^3J_{\text{F(2,3)-F}} = 25.4\text{ Hz}$ , 1F, F(1)]; -117.2 (d,  $^1J_{\text{F-F}} = 187.5\text{ Hz}$ , 1F, F(4) or F(5)).  $^{19}\text{F}$  NMR ( $\text{CS}_2$ ):  $\delta$  -108.3 [dm,  $^3J_{\text{F(1)-F}} = 26\text{ Hz}$ , F(2,3)]; -114.5 [tm,  $^3J_{\text{F(2,3)-F}} = 27\text{ Hz}$ , F<sub>1</sub> overlap with AB system), -114.9 [d,  $^2J_{\text{F-F}} = 185\text{ Hz}$ , F(4) or F(5)]; -116.12 [d,  $^2J_{\text{F-F}} = 185\text{ Hz}$ , F(4) or F(5)].  $^{19}\text{F}$  NMR ( $\text{C}_6\text{H}_6$ ):  $\delta$  -108.6 [m, F(2,3)]; -115.8 [m, F(1,4,5)].  $^{31}\text{P}\{^1\text{H}\}$  NMR ( $\text{CH}_2\text{Cl}_2$ ):  $\delta$  75.3 (s,  $\text{PPh}_3$ ). FAB MS: 554,  $[\text{M}]^+$ , 16; 535,  $[\text{M} - \text{F}]^+$ , 10; 526,  $[\text{M} - \text{CO}]^+$ , 100; 507,  $[\text{M} - \text{CO} - \text{F}]^+$ , 3; 461,  $[\text{M} - \text{CO} - (\text{C}_5\text{H}_5)]^+$ , 3; 449,  $[\text{M} - \text{CO} - \text{Ph}]^+$ , 6; 383\*,  $[\text{Fe}(\text{PPh}_3)(\text{C}_5\text{H}_5)]^+$ , 24; 368,  $[\text{Fe}(\text{CF}_2)(\text{PPh}_3)]^+$ , 27; 337,  $[\text{FeF}(\text{PPh}_3)]^+$ , 19; 318,

[Fe(PPh<sub>3</sub>)]<sup>+</sup>, 50; 280\*, [263 + O]<sup>+</sup>, 12; 263\*, [M - CO - PPh<sub>3</sub>]<sup>+</sup>, 73; 184, [FeF(PPh)]<sup>+</sup>, 48.

#### 2.4.14. Reaction of (14) with CO

CO was bubbled through a solution of (14) (146 mg, 0.44 mmol) in CH<sub>2</sub>Cl<sub>2</sub> (50 mL) for 8 h. Solvent was removed using a nitrogen stream leaving an orange residue which was purified by TLC (petroleum spirit/CH<sub>2</sub>Cl<sub>2</sub> 4:1). A major yellow band (R<sub>f</sub> 0.45) was collected and crystallized (petroleum spirit/CH<sub>2</sub>Cl<sub>2</sub>) to yield (13) (92 mg, 0.29 mmol, 65%) identified by comparison (IR, spot TLC, FAB MS) with an authentic sample.

## 2.5. References

- 1 (a) Criegee, R.; Noll, K. *Liebigs Ann. Chem.* **672** (1959) 1; (b) *Chem. Ber.* **98** (1965) 2339.
- 2 Clark, K.B.; Leigh, W.J. *J. Am. Chem. Soc.* **109** (1987) 6086.
- 3 Woodward, R.B.; Hoffmann, R. *J. Am. Chem. Soc.* **87** (1965) 395, 2046, 2511, 4388.
- 4 Brauman, J.I.; Golden, D.M. *J. Am. Chem. Soc.* **90** (1968) 1920.
- 5 Breulet, J.; Schaefer, H.F. *J. Am. Chem. Soc.* **106** (1984) 1221.
- 6 Longuet-Higgins, H.C.; Abrahamson, E.W. *J. Am. Chem. Soc.* **87** (1965) 2045.
- 7 Vollmer, J.J.; Servis, K.L. *J. Chem. Ed.* **45** (1968) 214.
- 8 Woodward, R.B.; Hoffmann, R. *Angew. Chem.* **81** (1969) 797; *Angew. Chem., Int. Ed. Engl.* **8** (1969) 781; *The Conservation of Orbital Symmetry*, Verlag Chemie: Weinheim, (1970) pp 1-100.
- 9 Tamelen, E.E.V. *Angew. Chem.* **77** (1965) 759; *Angew. Chem., Int. Ed. Engl.* **4** (1965) 738.
- 10 Eijk, P.J.S.S.V.; Overkempe, C.; Trompenaars, W.P.; Reinhourdt, D.N.; Harkema, S. *Recl. Trav. Chim. Pays-Bas* **107** (1988) 40.
- 11 Rondan, N.G.; Houk, K.N. *J. Am. Chem. Soc.* **107** (1985) 2099.
- 12 Dolbier, W.R.; Koroniak, H.; Burton, D.J.; Heinze, P.L.; Bailey, A.R.; Shaw, G.S.; Hansen, S.W. *J. Am. Chem. Soc.* **109** (1987) 219, and references cited therein.
- 13 Kirmse, W.; Rondan, N.G.; Houk, K.N. *J. Am. Chem. Soc.* **106** (1984) 7989.
- 14 Kolobova, N.E.; Rozantseva, T.V.; Struchkov, Yu.T.; Batsanov, A.S.; Bakhmutov, V.I. *J. Organomet. Chem.* **292** (1985) 247.
- 15 Kostic, N.M.; Fenske, R.F. *Organometallics* **1** (1982) 974.
- 16 Jackson, W.R.; Lovel, C.G. *Aust. J. Chem.* **36** (1983) 1975.
- 17 Sharkey, W.H. *Fluorine Chem. Rev.* **2** (1968) 1.
- 18 Jolly, P.W.; Bruce, M.I.; Stone, F.G.A. *J. Chem. Soc.* (1965) 5830.
- 19 Davison, A.; Solar, J.P. *J. Organomet. Chem.* **166** (1979) C13.
- 20 Bruce, M.I.; Hambley, T.W.; Snow, M.R.; Swincer, A.G. *Organometallics* **4**, (1985) 494.
- 21 Bruce, M.I.; Hambley, T.W.; Snow, M.R.; Swincer, A.G. *Organometallics* **4** (1985) 501.
- 22 Conole, G.C.; Green, M.; McPartlin, M.; Reeve, C.; Woolhouse, C.M. *J. Chem. Soc., Chem. Commun.* (1988) 1310.
- 23 Bruce, M.I.; Rodgers, J.R.; Snow, M.R.; Swincer, A.G. *J. Chem. Soc., Chem. Commun.* (1981) 271.
- 24 Bruce, M.I.; Hambley, T.W.; Rodgers, J.R.; Snow, M.R.; Swincer, A.G. *J. Organomet. Chem.* **226** (1982) C1.
- 25 Seeman, J.I.; Davies, S.G. *J. Am. Chem. Soc.* **107** (1985) 6522.
- 26 Reger, D.L.; Belmore, K.A.; Mintz, E.; Charles, N.G.; Griffith, E.A.H.; Amma, E.L. *Organometallics* **2** (1983) 101.
- 27 Reger, D.L.; McElligott, P.J.; Charles, N.G.; Griffith, E.A.H.; Amma, E.L. *Organometallics* **1** (1982) 443.
- 28 Davies, S.G.; Easton, R.J.C.; Sutton, K.H.; Walker, J.C.; Jones, R.H. *J. Chem. Soc., Perkin Trans. I* (1987) 489.
- 29 Reger, D.L.; Mintz, E.; Lebioda, L. *J. Am. Chem. Soc.* **108** (1986) 1940.
- 30 King, R.B.; in Ishii, Y.; Tsutsui, M. (Eds.) *Organo-transition Metal Chemistry*, Plenum, New York, (1975).
- 31 Wallenfels, K. *Chimia* **20** (1966) 303.
- 32 Bruce, M.I.; Hambley, T.W.; Liddell, M.J.; Snow, M.R.; Swincer, A.G.; Tiekink, E.R.T. *Organometallics*, in press.
- 33 Bruce, M.I.; Humphrey, P.A.; Snow, M.R.; Tiekink, E.R.T. *J. Organomet. Chem.* **303** (1986) 417.
- 34 Bruce, M.I. *Org. Mass. Spectrom.* **1** (1968) 503.
- 35 Epiotis, N.D. *Nouv. J. Chim.* **11** (1987) 310.
- 36 Bruce, M.I.; Hameister, C.; Swincer, A.G.; Wallis, R.C. *Inorg. Synth.* **21** (1982) 82.

- 
- 37 Bruce, M.I.; Humphrey, J.G.; Matison, J.G.; Roy, S.K.; Swincer, A.G. *Aust. J. Chem.* **37** (1984) 1955.
- 38 Miguel, D.; Riera, V. *J. Organomet. Chem.* **293** (1985) 379.

## CHAPTER THREE

### New reactions of $\text{Ru}_5(\mu_5\text{-}\eta^2, P\text{-C}_2\text{PPh}_2)(\mu\text{-PPh}_2)(\text{CO})_{13}$

	Page
3.1. Introduction	146
3.2. Results and Discussion	161
3.3. Conclusions	238
3.4. Experimental	241
3.5. References	270

### 3.1. Introduction

In recent years, there has been a considerable expansion in the chemistry of pentanuclear ruthenium carbonyl cluster complexes. Although binary  $Ru_5$  carbonyl clusters are unknown, a large number containing hetero-atoms have been synthesized. For the purposes of this discussion, the carbonyl clusters have been divided into classes according to their hetero-atoms. These divisions are: (i) clusters containing only hydrocarbyl and/or phosphane-based ligands; (ii) those containing C, N, P or S atoms either wholly or partially encapsulated; (iii) clusters containing other metal atoms, i.e. higher nuclearity heteronuclear clusters with  $Ru_5$  cores (see Table 1). The clusters have also been analyzed structurally in terms of the geometries of the  $Ru_5$  cores (see Scheme 1): this is not as accurate geometrically as an analysis which considers the heteroatoms bound to the metal core, but it does provide a consistent basis for comparison and gives a better account of the structures in terms of polyhedral skeletal electron-pair theory.<sup>1</sup>

**Scheme 1.** Core transformations for pentaruthenium clusters

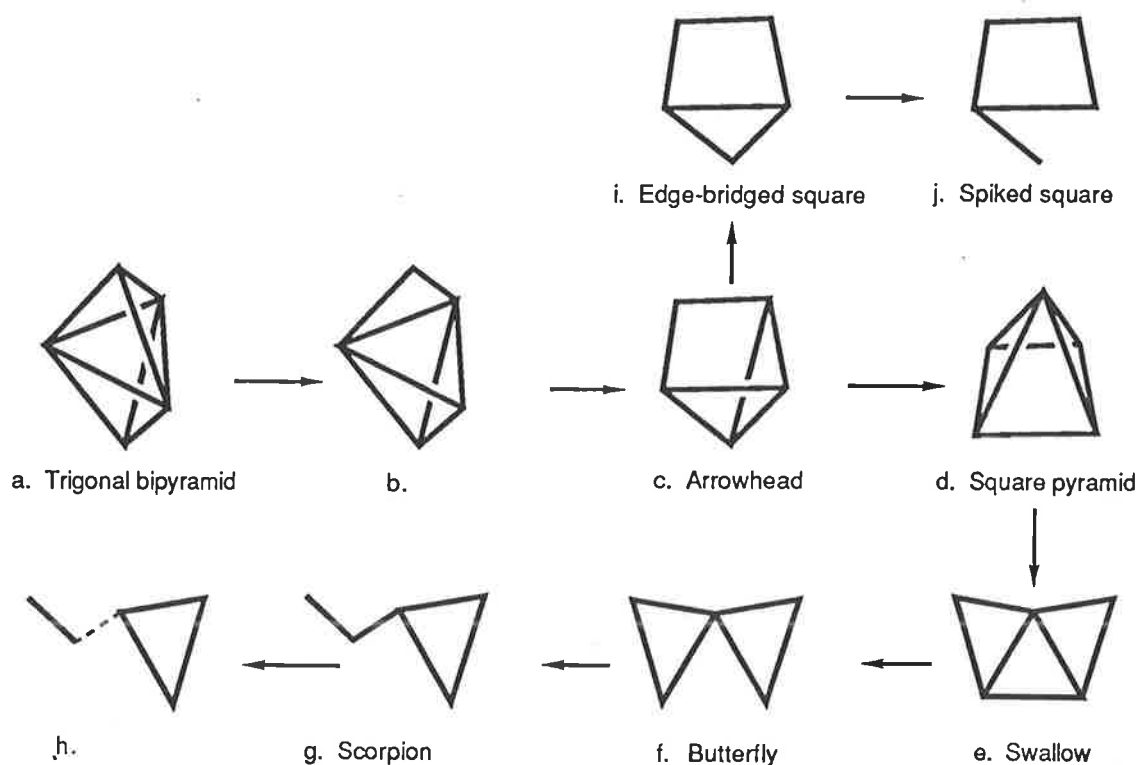


**Table 1.** Crystallographically characterized pentaruthenium clusters

Cluster	Reagents and conditions	Ru <sub>5</sub> Core Structure	Reference
<b>Class (i)</b>			
Ru <sub>5</sub> (CO) <sub>6</sub> (cp) <sub>4</sub>	Ru <sub>2</sub> (CO) <sub>2</sub> (cp) <sub>2</sub> , Δ	a	2
[Ru <sub>3</sub> (CO) <sub>3</sub> (cp) <sub>3</sub> ](μ-CCH <sub>2</sub> CHC)- {Ru <sub>2</sub> (CO) <sub>3</sub> (cp) <sub>2</sub> }	[Ru <sub>2</sub> (CO) <sub>3</sub> (CMe)(cp) <sub>2</sub> ] <sup>+</sup> + Ru <sub>2</sub> (CO) <sub>3</sub> (CCH <sub>2</sub> )(cp) <sub>2</sub>	h	3
Ru <sub>5</sub> (CO) <sub>10</sub> (PhC <sub>2</sub> Ph)(PPh)(PPh <sub>2</sub> ) <sub>2</sub>	Ru <sub>5</sub> (CO) <sub>13</sub> (C <sub>2</sub> PPh <sub>2</sub> )(PPh <sub>2</sub> ) + PPh <sub>3</sub> , Δ	d	4
HRu <sub>5</sub> (CO) <sub>10</sub> {CCPh(C <sub>6</sub> H <sub>4</sub> )}(PPh) <sub>2</sub>	Ru <sub>5</sub> (CO) <sub>13</sub> (C <sub>2</sub> PPh <sub>2</sub> )(PPh <sub>2</sub> ), Δ	c	4
HRu <sub>5</sub> (CO) <sub>10</sub> (PPh) <sub>3</sub> (PPh <sub>2</sub> )	Ru <sub>5</sub> (CO) <sub>13</sub> (C <sub>2</sub> Ph)(PPh <sub>2</sub> ) + PPhH <sub>2</sub>	c	5
Ru <sub>5</sub> (CO) <sub>11</sub> {CCPh(C <sub>6</sub> H <sub>4</sub> )}(PPh){P(OMe)Ph}	HRu <sub>5</sub> (CO) <sub>10</sub> {CCPh(C <sub>6</sub> H <sub>4</sub> )}(PPh) <sub>2</sub> + MeOH	c	4
Ru <sub>5</sub> (CO) <sub>11</sub> {C <sub>5</sub> H <sub>3</sub> Me(CHCH <sub>2</sub> )}(PPh)(PPh <sub>2</sub> )	Ru <sub>5</sub> (CO) <sub>13</sub> (C <sub>2</sub> PPh <sub>2</sub> )(PPh <sub>2</sub> ) + C <sub>2</sub> H <sub>4</sub> , Δ	d	4
Ru <sub>5</sub> (CO) <sub>11</sub> (C <sub>2</sub> PPh <sub>2</sub> )(PPh <sub>2</sub> ){P(OEt) <sub>3</sub> } <sub>2</sub>	Ru <sub>5</sub> (CO) <sub>13</sub> (C <sub>2</sub> PPh <sub>2</sub> )(PPh <sub>2</sub> ) + P(OEt) <sub>3</sub>	e	4
Ru <sub>5</sub> (CO) <sub>11</sub> {CCC(O)C <sub>3</sub> H <sub>5</sub> }Br(PPh <sub>2</sub> ) <sub>2</sub>	Ru <sub>5</sub> (CO) <sub>13</sub> (C <sub>2</sub> PPh <sub>2</sub> )(PPh <sub>2</sub> ) + C <sub>3</sub> H <sub>5</sub> Br, Δ	j	4
{Ru <sub>3</sub> (CO) <sub>6</sub> (NPh)C}O- {Ru <sub>2</sub> (CO) <sub>5</sub> [PhNC(O)C(C <sub>6</sub> H <sub>4</sub> )CPh]}	Ru <sub>3</sub> (CO) <sub>10</sub> (NPh) + Ru <sub>2</sub> (CO) <sub>5</sub> [PhNC(O)CPhCPh], Δ	h	6
Ru <sub>5</sub> (CO) <sub>12</sub> {CCPh(PPh <sub>2</sub> )}(PPh)	Ru <sub>5</sub> (CO) <sub>13</sub> (C <sub>2</sub> PPh <sub>2</sub> )(PPh <sub>2</sub> ), Δ	d	4
Ru <sub>5</sub> (CO) <sub>12</sub> (C <sub>2</sub> Ph)(N <sub>2</sub> CPh <sub>2</sub> )(PPh <sub>2</sub> )	Ru <sub>5</sub> (CO) <sub>13</sub> (C <sub>2</sub> Ph)(PPh <sub>2</sub> ) + N <sub>2</sub> CPh <sub>2</sub>	i	7
Ru <sub>5</sub> (CO) <sub>12</sub> (CCH <sub>2</sub> Pr <sup>i</sup> )(PPh)(PPh <sub>2</sub> )	Ru <sub>5</sub> (CO) <sub>13</sub> (C <sub>2</sub> Pr <sup>i</sup> )(PPh <sub>2</sub> ) + PPhH <sub>2</sub> , Δ	d	5
Ru <sub>5</sub> (CO) <sub>12</sub> (C <sub>2</sub> Ph)(PhC <sub>2</sub> C <sub>2</sub> Ph)(PPh <sub>2</sub> )	Ru <sub>5</sub> (CO) <sub>13</sub> (C <sub>2</sub> Ph)(PPh <sub>2</sub> ) + PhC <sub>2</sub> C <sub>2</sub> Ph	e	8
Ru <sub>5</sub> (CO) <sub>12</sub> (C <sub>2</sub> PPh <sub>2</sub> )(PPh <sub>2</sub> ){P(OEt) <sub>3</sub> } (2 isomers)	Ru <sub>5</sub> (CO) <sub>13</sub> (C <sub>2</sub> PPh <sub>2</sub> )(PPh <sub>2</sub> ) + P(OEt) <sub>3</sub>	e	4
Ru <sub>5</sub> (CO) <sub>12</sub> {CC(CCH <sub>2</sub> )(CHCH <sub>2</sub> )}(PPh)(PPh <sub>2</sub> )	Ru <sub>5</sub> (CO) <sub>13</sub> (C <sub>2</sub> PPh <sub>2</sub> )(PPh <sub>2</sub> ) + C <sub>2</sub> H <sub>4</sub> , Δ	c	4
HRu <sub>5</sub> (CO) <sub>12</sub> (CNMe <sub>2</sub> )(PMe <sub>2</sub> Ph) <sub>2</sub>	HRu <sub>5</sub> (CO) <sub>14</sub> (CNMe <sub>2</sub> ) + PMe <sub>2</sub> Ph	b	9
HRu <sub>5</sub> (CO) <sub>12</sub> (C <sub>2</sub> PPh <sub>2</sub> )I(PPh <sub>2</sub> )	Ru <sub>5</sub> (CO) <sub>13</sub> (C <sub>2</sub> PPh <sub>2</sub> )(PPh <sub>2</sub> ) + HI	g	4
H <sub>2</sub> Ru <sub>5</sub> (CO) <sub>12</sub> (CCH <sub>2</sub> PPh <sub>2</sub> )(PPh <sub>2</sub> )	Ru <sub>5</sub> (CO) <sub>13</sub> (C <sub>2</sub> PPh <sub>2</sub> )(PPh <sub>2</sub> ), H <sub>2</sub> , Δ	d	10
Ru <sub>5</sub> (CO) <sub>13</sub> (C <sub>2</sub> Ph)(PPh <sub>2</sub> )	Ru <sub>3</sub> (CO) <sub>11</sub> (PhC <sub>2</sub> PPh <sub>2</sub> ), Δ	d	11
Ru <sub>5</sub> (CO) <sub>13</sub> (C <sub>2</sub> PPh <sub>2</sub> )(PPh <sub>2</sub> )	{Ru <sub>3</sub> (CO) <sub>11</sub> } <sub>2</sub> dppa, Δ	e	12
Ru <sub>5</sub> (CO) <sub>13</sub> (PhC <sub>2</sub> Ph)(PPh)	Ru <sub>5</sub> (CO) <sub>13</sub> (C <sub>2</sub> Ph)(PPh <sub>2</sub> ), Δ	d	13

Table 1. (continued)

Cluster	Reagents and conditions	Ru <sub>5</sub> Core Structure	References
<b>Class (i) (continued)</b>			
Ru <sub>5</sub> (CO) <sub>13</sub> (C <sub>6</sub> H <sub>4</sub> )(PPh)	Ru <sub>3</sub> (CO) <sub>11</sub> (PPh <sub>3</sub> ), Δ	i	14
Ru <sub>5</sub> (CO) <sub>13</sub> (C <sub>2</sub> Pr <sup>i</sup> )(NC(O)NCPh <sub>2</sub> )(PPh <sub>2</sub> )	Ru <sub>5</sub> (CO) <sub>12</sub> (C <sub>2</sub> Pr <sup>i</sup> )(N <sub>2</sub> CPh <sub>2</sub> )(PPh <sub>2</sub> ), CO	j	7
Ru <sub>5</sub> (CO) <sub>13</sub> (CNMe <sub>2</sub> ) <sub>2</sub>	HRu <sub>3</sub> (CO) <sub>10</sub> (CNMe <sub>2</sub> ), Δ	b	15
HRu <sub>5</sub> (CO) <sub>13</sub> (C <sub>2</sub> Ph)(PPh <sub>2</sub> ) <sub>2</sub>	Ru <sub>5</sub> (CO) <sub>13</sub> (C <sub>2</sub> Ph)(PPh <sub>2</sub> ) + HPPH <sub>2</sub>	f	16
HRu <sub>5</sub> (CO) <sub>13</sub> (CCHPPH <sub>2</sub> )(PPh <sub>2</sub> )	Ru <sub>5</sub> (CO) <sub>13</sub> (C <sub>2</sub> PPh <sub>2</sub> )(PPh <sub>2</sub> ), H <sub>2</sub> , Δ	e	17
HRu <sub>5</sub> (CO) <sub>13</sub> (PPh)(P(OPr <sup>n</sup> )Ph)	Ru <sub>3</sub> (CO) <sub>12</sub> + PPhH <sub>2</sub> , Δ	d	18
HRu <sub>5</sub> (CO) <sub>13</sub> (C <sub>2</sub> PPh <sub>2</sub> )Br(PPh <sub>2</sub> )	Ru <sub>5</sub> (CO) <sub>13</sub> (C <sub>2</sub> PPh <sub>2</sub> )(PPh <sub>2</sub> ) + HBr	g	4
Ru <sub>5</sub> (CO) <sub>14</sub> (CNBu <sup>t</sup> ) <sub>2</sub>	Ru <sub>3</sub> (CO) <sub>11</sub> (CNBu <sup>t</sup> ), Δ	e	19
Ru <sub>5</sub> (CO) <sub>14</sub> (C <sub>2</sub> Ph)(PPh <sub>2</sub> )	Ru <sub>5</sub> (CO) <sub>13</sub> (C <sub>2</sub> Ph)(PPh <sub>2</sub> ), CO	e	20
Ru <sub>5</sub> (CO) <sub>15</sub> (C <sub>2</sub> PPh <sub>2</sub> )(PPh <sub>2</sub> ) (2 isomers)	Ru <sub>5</sub> (CO) <sub>13</sub> (C <sub>2</sub> PPh <sub>2</sub> )(PPh <sub>2</sub> ), CO, Δ	g	21
Ru <sub>5</sub> (CO) <sub>15</sub> (PR) (R = Ph, Et)	Ru <sub>3</sub> (CO) <sub>12</sub> + Mn(CO) <sub>2</sub> (PRCl <sub>2</sub> )(cp), Δ	d	22
<b>Class (ii)</b>			
Ru <sub>5</sub> C(CO) <sub>13</sub> (dppb)	Ru <sub>5</sub> C(CO) <sub>15</sub> + dppb, Δ	d	23
Ru <sub>5</sub> C(CO) <sub>13</sub> (PPh <sub>3</sub> ) <sub>2</sub>	Ru <sub>5</sub> C(CO) <sub>15</sub> + PPh <sub>3</sub>	d	24
Ru <sub>5</sub> C(CO) <sub>14</sub> (PPh <sub>3</sub> )	Ru <sub>5</sub> C(CO) <sub>15</sub> + PPh <sub>3</sub>	d	24
Ru <sub>5</sub> C(CO) <sub>15</sub>	Ru <sub>6</sub> C(CO) <sub>17</sub> , CO, Δ	d	24
Ru <sub>5</sub> C(CO) <sub>15</sub> (MeCN)	Ru <sub>5</sub> C(CO) <sub>15</sub> + MeCN	c	24
HRu <sub>5</sub> C(CO) <sub>12</sub> (SEt)(PPh <sub>3</sub> )	HRu <sub>5</sub> (CO) <sub>13</sub> (SEt)(PPh <sub>3</sub> ), Δ	d	25
HRu <sub>5</sub> C(CO) <sub>13</sub> (PPh <sub>2</sub> )	Ru <sub>5</sub> C(CO) <sub>15</sub> + HPPH <sub>2</sub> ; Δ	d	26
HRu <sub>5</sub> C(CO) <sub>13</sub> (SEt)(PPh <sub>3</sub> )	HRu <sub>5</sub> C(CO) <sub>14</sub> (SEt), Δ; + PPh <sub>3</sub>	c	25
HRu <sub>5</sub> C(CO) <sub>14</sub> (SEt)	Ru <sub>5</sub> C(CO) <sub>15</sub> + EtSH	c	25
H <sub>2</sub> Ru <sub>5</sub> C(CO) <sub>12</sub> (dppe)	Ru <sub>5</sub> C(CO) <sub>15</sub> + dppe; H <sub>2</sub> , Δ	d	24
H <sub>3</sub> Ru <sub>5</sub> C(CO) <sub>11</sub> (PPh <sub>2</sub> )(PMePh <sub>2</sub> )	Ru <sub>5</sub> (CO) <sub>13</sub> (C <sub>2</sub> PPh <sub>2</sub> )(PPh <sub>2</sub> ), H <sub>2</sub> , Δ	d	10

Table 1. (continued)

Cluster	Reagents and conditions	Ru <sub>5</sub> Core Structure	References
<b>Class (ii) (continued)</b>			
[Ru <sub>5</sub> N(CO) <sub>14</sub> ] <sup>-</sup>	Ru <sub>3</sub> (CO) <sub>12</sub> + [ppn][N <sub>3</sub> ], Δ	d	27
Ru <sub>5</sub> P(CO) <sub>16</sub> (PPh <sub>2</sub> )	HRu <sub>3</sub> (CO) <sub>9</sub> (PPh <sub>2</sub> ), Δ	g	28
Ru <sub>5</sub> S(CO) <sub>14</sub> (HC <sub>2</sub> Ph)	Ru <sub>3</sub> S(CO) <sub>9</sub> (HC <sub>2</sub> Ph) + Ru(CO) <sub>5</sub> , Δ	i	29
Ru <sub>5</sub> S(CO) <sub>15</sub>	Ru <sub>3</sub> S(CO) <sub>10</sub> + Ru(CO) <sub>5</sub> , Δ	d	30
HRu <sub>5</sub> S(CO) <sub>12</sub> (1,5-Me <sub>2</sub> C <sub>5</sub> H <sub>5</sub> )	Ru <sub>5</sub> S(CO) <sub>15</sub> + <i>trans</i> -2-heptene, Δ	d	31
Ru <sub>5</sub> S <sub>2</sub> (CO) <sub>14</sub>	Ru <sub>3</sub> S <sub>2</sub> (CO) <sub>9</sub> + Ru <sub>3</sub> (CO) <sub>12</sub> , <i>hν</i>	i	32
<b>Class (iii)</b>			
AuRu <sub>5</sub> C(CO) <sub>13</sub> (PPh <sub>3</sub> )(C <sub>5</sub> H <sub>5</sub> )	Ru <sub>5</sub> C(CO) <sub>15</sub> + [C <sub>5</sub> H <sub>5</sub> ] <sup>-</sup> ; [Au(PPh <sub>3</sub> )] <sup>+</sup>	c	33
AuRu <sub>5</sub> C(CO) <sub>13</sub> I(PPh <sub>3</sub> ) <sub>2</sub>	Ru <sub>5</sub> C(CO) <sub>15</sub> + AuI(PPh <sub>3</sub> ); Δ; + PPh <sub>3</sub>	c	24
AuRu <sub>5</sub> C(CO) <sub>13</sub> (NO)(PEt <sub>3</sub> ) (2 isomers)	[Ru <sub>5</sub> C(CO) <sub>13</sub> (NO)] <sup>-</sup> + [Au(PEt <sub>3</sub> )] <sup>+</sup>	d	34
AuRu <sub>5</sub> C(CO) <sub>14</sub> {C(Me)O}(PPh <sub>3</sub> )	Ru <sub>5</sub> C(CO) <sub>15</sub> + LiMe; AuCl(PPh <sub>3</sub> )	c	33
AuRu <sub>5</sub> C(CO) <sub>14</sub> Br(PPh <sub>3</sub> )	Ru <sub>5</sub> C(CO) <sub>15</sub> + AuBr(PPh <sub>3</sub> ); N <sub>2</sub>	c	35
AuRu <sub>5</sub> C(CO) <sub>15</sub> Cl(PPh <sub>3</sub> )	Ru <sub>5</sub> C(CO) <sub>15</sub> + AuCl(PPh <sub>3</sub> )	c	35
AuRu <sub>5</sub> RhC(CO) <sub>14</sub> (cod)(PPh <sub>3</sub> )	[Ru <sub>5</sub> C(CO) <sub>14</sub> ] <sup>2-</sup> + [Rh(COD) <sub>2</sub> ] <sup>+</sup> /AuCl(PPh <sub>3</sub> )	*	36
AuRu <sub>5</sub> RhC(CO) <sub>16</sub> (PPh <sub>3</sub> )	AuRu <sub>5</sub> RhC(CO) <sub>14</sub> (COD)(PPh <sub>3</sub> ) + CO, Δ	*	36
Au <sub>2</sub> Ru <sub>5</sub> (CO) <sub>11</sub> (C <sub>2</sub> PPh <sub>2</sub> )(PPh <sub>2</sub> ){P(OEt) <sub>3</sub> }(PPh <sub>3</sub> ) <sub>2</sub>	Ru <sub>5</sub> (CO) <sub>13</sub> (C <sub>2</sub> PPh <sub>2</sub> ) + 'Au <sub>2</sub> (PPh <sub>3</sub> ) <sub>2</sub> '; P(OEt) <sub>3</sub> , Δ	j	4
Au <sub>2</sub> Ru <sub>5</sub> C(CO) <sub>14</sub> (PEt <sub>3</sub> ) <sub>2</sub>	[Ru <sub>5</sub> C(CO) <sub>14</sub> ] <sup>2-</sup> + [Au(PEt <sub>3</sub> )] <sup>-</sup>	*	36
Au <sub>2</sub> Ru <sub>5</sub> WC(CO) <sub>17</sub> (PEt <sub>3</sub> ) <sub>2</sub>	[Ru <sub>5</sub> C(CO) <sub>14</sub> ] <sup>2-</sup> + W(CO) <sub>3</sub> (MeCN) <sub>3</sub> ; [Au(PPh <sub>3</sub> )] <sup>+</sup>	d	37
{Ru <sub>2</sub> (CO) <sub>8</sub> }Bi{HRu <sub>3</sub> (CO) <sub>10</sub> }	[HRu <sub>3</sub> (CO) <sub>11</sub> ] <sup>-</sup> + Bi(NO <sub>3</sub> ) <sub>3</sub> ·5H <sub>2</sub> O/MeOH	h	38
HCuRu <sub>5</sub> (CO) <sub>18</sub> (PPh <sub>3</sub> )	H <sub>3</sub> CuRu <sub>4</sub> (CO) <sub>12</sub> (PPh <sub>3</sub> ), CO, Δ	g	39
Mo <sub>2</sub> Ru <sub>5</sub> S(CO) <sub>16</sub> (cp) <sub>2</sub>	Mo <sub>2</sub> RuS(CO) <sub>7</sub> (cp) <sub>2</sub> + Ru(CO) <sub>5</sub> , Δ	g	40
Ru <sub>5</sub> RhC(CO) <sub>14</sub> (C <sub>5</sub> Me <sub>5</sub> )	[Ru <sub>5</sub> C(CO) <sub>14</sub> ] <sup>2-</sup> + [Rh(C <sub>5</sub> Me <sub>5</sub> )(MeCN) <sub>2</sub> ] <sup>2+</sup>	*	36

\* Structure solved but core geometry not reported in reference 36.

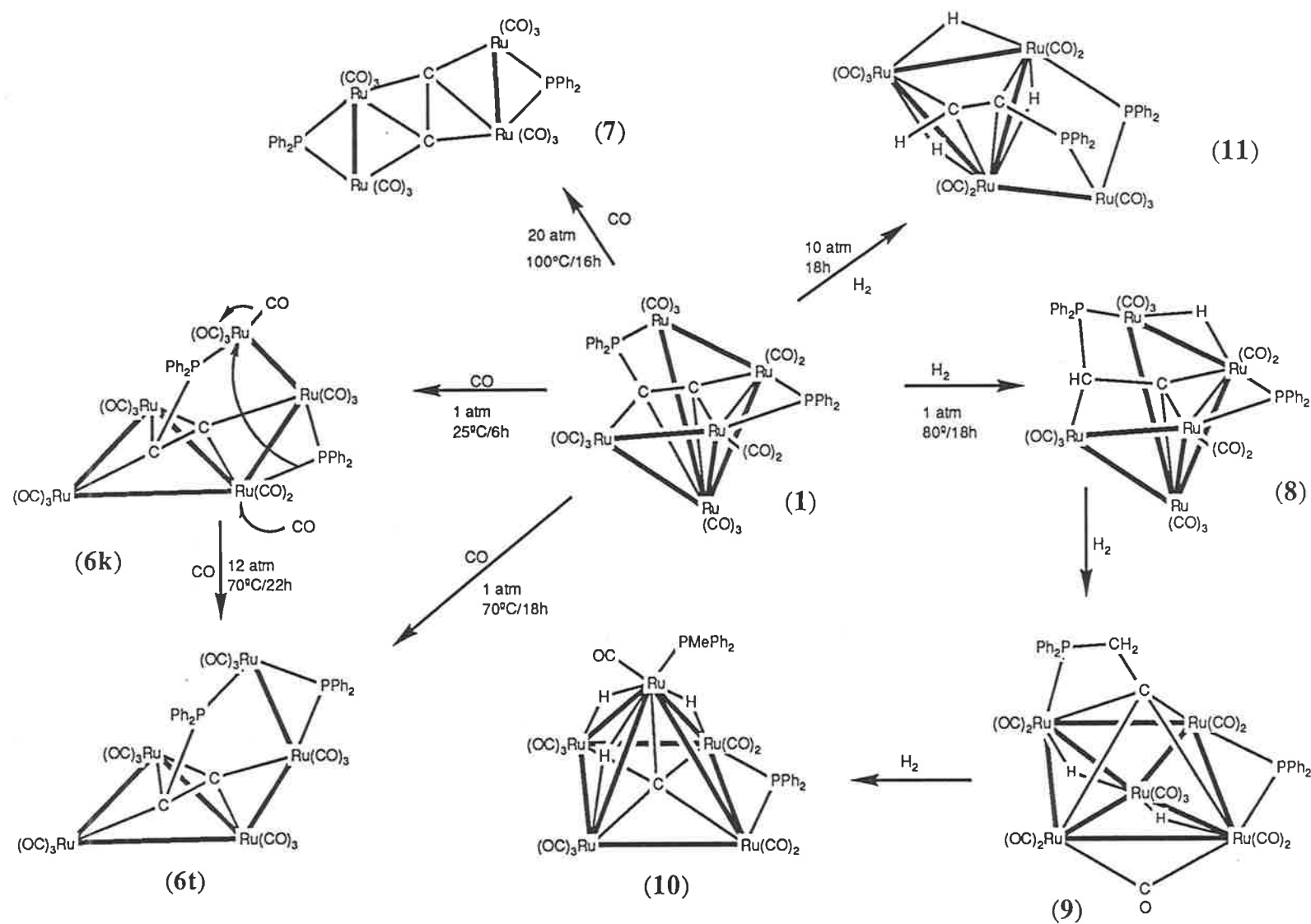
Frequently, the cluster structures are intermediate between two of the core types shown in Scheme 1. The compound  $\text{AuRu}_5\text{C}(\mu\text{-Br})(\text{CO})_{14}(\text{PPh}_3)$ ,<sup>35</sup> for instance, where the structure is that of a distorted square pyramid lacking one metal-metal vector, has been classified in Table 1 as an 'arrowhead' structure. A recent article on polyhedral rearrangements in clusters has described the use of geometric transformations in determining the alternative structures available for a molecule.<sup>41</sup> Interconversion between the core structures shown in Scheme 1 is achieved through metal-metal bond cleavage accompanied by changes in the overall electron count. At present the direct transformations (c)  $\leftrightarrow$  (d), (d)  $\leftrightarrow$  (e), (i)  $\rightarrow$  (j) have been observed.<sup>7,20,24</sup>

Pentaruthenium clusters are generally synthesized by the condensation of smaller clusters under pyrolytic or photolytic conditions, or by the addition of  $\text{Ru}(\text{CO})_5$  or ' $\text{Ru}(\text{CO})_4$ ' to  $\text{Ru}_3$  clusters. The latter route has been that most systematically used in the synthesis of  $\text{Ru}_5$  clusters.<sup>30-32</sup> However, reactions of this sort do not give particularly high yields, since the related  $\text{Ru}_4$ ,  $\text{Ru}_6$  and  $\text{Ru}_7$  clusters (not all combinations) are also obtained. The chemistry of only three  $\text{Ru}_5$  systems has been investigated in detail:  $\text{Ru}_5(\mu_5\text{-}\eta^2, P\text{-C}_2\text{PPh}_2)(\mu\text{-PPh}_2)(\text{CO})_{13}$  (**1**),  $\text{Ru}_5(\mu_4\text{-}\eta^2\text{-C}_2\text{Ph})(\mu\text{-PPh}_2)(\text{CO})_{13}$  (**2**) and  $\text{Ru}_5\text{C}(\text{CO})_{15}$  (**3**). The first two of these complexes have provided much information on the reactivity of Class (i) clusters (Table 1). The carbido compound has been the starting material used in the synthesis of nearly all the  $\text{Ru}_5$ -carbido clusters in Classes (ii) and (iii). There has been little development in the chemistry of Class (iii) clusters, since most of these compounds have been synthesized only recently. At present, most of the complexes in this class contain at least one gold atom and were produced by adding  $[\text{Au}(\text{PR}_3)]^+$  ( $\text{R} = \text{Et}, \text{Ph}$ ) to  $\text{Ru}_5$  anions, or by the oxidative addition of  $\text{AuX}(\text{PR}_3)$  ( $\text{X} = \text{Cl}, \text{Br}, \text{I}$ ) to neutral  $\text{Ru}_5$  clusters. The synthesis of the unusual bismuth complex  $\{\text{Ru}_2(\text{CO})_8\}(\mu_4\text{-Bi})\{\text{Ru}_3(\mu\text{-H})(\text{CO})_{10}\}$ ,<sup>38</sup> from  $[\text{Ru}_3\text{H}(\text{CO})_{11}]^-$  and  $\text{Bi}(\text{NO}_3)_3 \cdot 5\text{H}_2\text{O}$ , suggests that a variety of new complexes may be accessible by choosing suitable metal fragments. The cluster  $\{\text{Ru}_3(\text{CO})_6(\text{NPh})\text{C}\}\text{O}\{\text{Ru}_2(\text{CO})_5[\text{PhNC}(\text{O})\text{-C}(\text{C}_6\text{H}_4)\text{CPh}]\}$ ,<sup>6</sup> for example, was isolated in 49% yield by the combination of  $\text{Ru}_3$  and  $\text{Ru}_2$  fragments.

The complex  $\text{Ru}_5(\mu_5\text{-}\eta^2, P\text{-C}_2\text{PPh}_2)(\mu\text{-PPh}_2)(\text{CO})_{13}$  (**1**) is a brown crystalline material obtained in 88% yield from the pyrolysis of  $\{\text{Ru}_3(\text{CO})_{11}\}_2(\mu\text{-dppa})$  (**4**) (toluene, 90 °C, 1 h),<sup>12</sup> and has also been obtained from the thermal reaction of  $\text{Ru}_3(\text{CO})_{12}$  with dppa [1,2-bis-(diphenylphosphino)ethyne] in thf.<sup>42</sup> Two other compounds,  $\{\text{Ru}_2(\mu\text{-PPh}_2)(\mu\text{-C}_2\text{PPh}_2)(\text{CO})_5\}_2$  and  $\text{Ru}_4(\mu_4\text{-PPh})\{\mu_4\text{-}\eta^2, P\text{-PhC}_2\text{PPh}_2\}(\mu\text{-CO})_2(\text{CO})_8$  (**5**), were also obtained from the latter reaction. Recently, the osmium analogue of (**1**) has been synthesized and was found to be isostructural with (**1**).<sup>43</sup> The synthesis of (**2**), a blue-green crystalline complex, was achieved by the thermolysis of  $\text{Ru}_3(\text{CO})_{11}(\text{PhC}_2\text{PPh}_2)$  in heptane (70 °C, 8 h, 30%).<sup>11</sup> A similar cluster with the acetylide group  $\text{C}_2\text{Pr}^i$  has also been prepared.<sup>7</sup> In contrast to these compounds which were synthesized from smaller clusters, the dark brown complex (**3**) was obtained in almost 100% yield from the reaction between  $\text{Ru}_6\text{C}(\text{CO})_{17}$  and CO (80 atm, 70 °C, 3 h).<sup>24</sup> It has also been isolated in  $\approx 1\%$  yield by heating  $\text{Ru}_4(\mu\text{-H})_4(\text{CO})_{12}$  under ethene.<sup>44</sup>

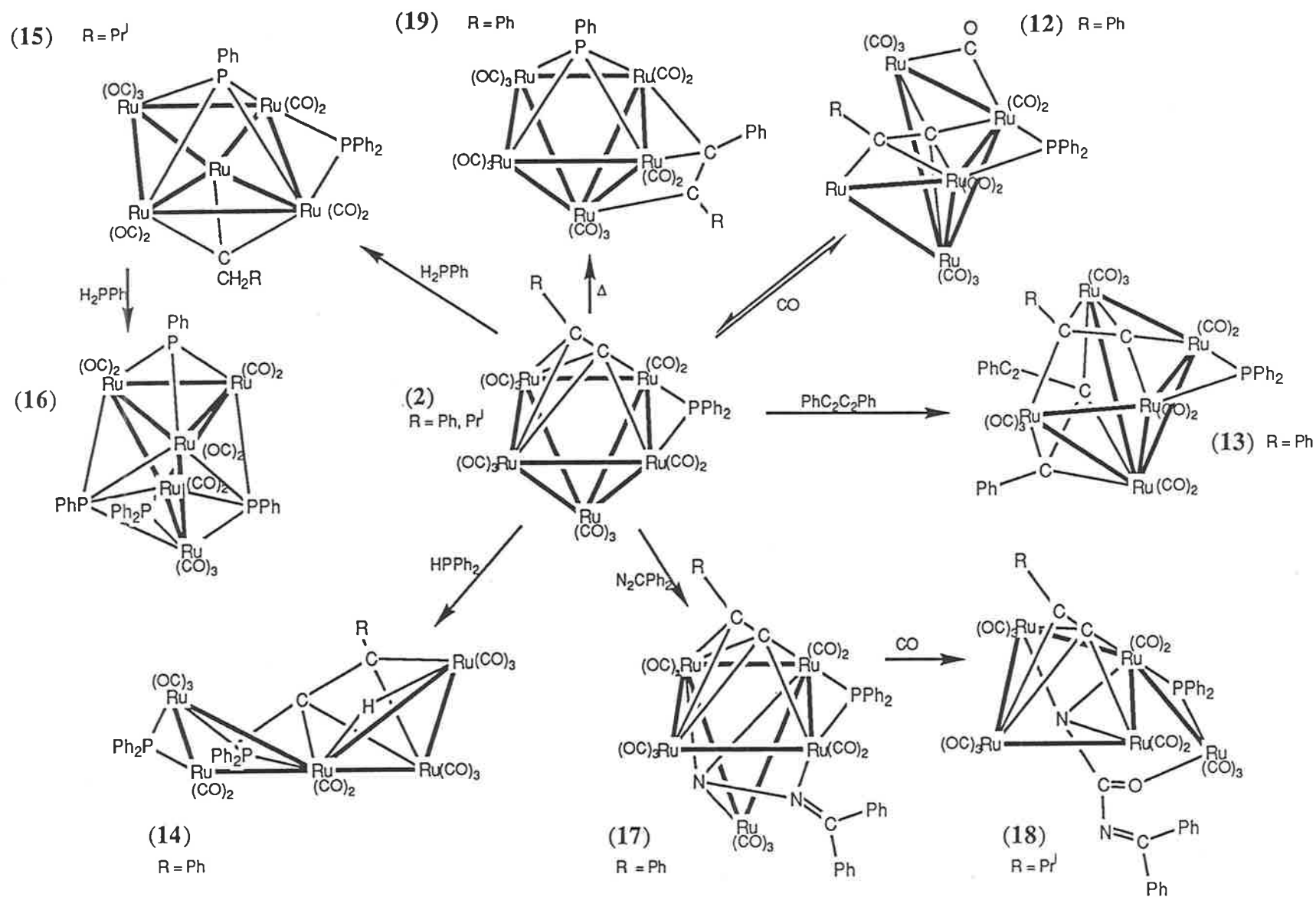
Some chemistry of (**1**) is illustrated in Scheme 2. The reactions of (**1**) with CO proceeded to give the 'kinetic' isomer of  $\text{Ru}_5(\mu_5\text{-}\eta^2, P\text{-C}_2\text{PPh}_2)(\mu\text{-PPh}_2)(\text{CO})_{15}$  (**6k**) (1 atm, 25 °C, 6 h) and the 'thermodynamic' isomer (**6t**) (1 atm, 70 °C, 18 h); (**6k**) and (**6t**) interconverted in solution under some conditions.<sup>21</sup> Under higher CO pressures (20 atm, 100 °C, 16 h), these complexes formed the tetranuclear complex  $\text{Ru}_4(\mu_4\text{-}\eta^2\text{-C}_2)(\mu\text{-PPh}_2)_2(\text{CO})_{12}$  (**7**), which contains a  $\text{C}_2$  ligand.<sup>45</sup> Under mild conditions (1 atm, 80 °C, 18 h), the hydrogenation of (**1**) proceeded by the reduction of the phosphinoacetylide ligand and the addition of hydride ligands to the metal core;<sup>10</sup> the complexes formed were  $\text{Ru}_5(\mu\text{-H})(\mu_5\text{-CCHPPh}_2)(\mu\text{-PPh}_2)(\text{CO})_{13}$  (**8**), then  $\text{Ru}_5(\mu\text{-H})_2(\mu_4\text{-CCH}_2\text{PPh}_2)(\mu\text{-PPh}_2)(\text{CO})_{12}$  (**9**), and finally  $\text{Ru}_5\text{C}(\mu\text{-H})_3(\mu\text{-PPh}_2)(\text{CO})_{11}(\text{PMePh}_2)$  (**10**). Complex (**8**) was also obtained by successive addition of  $\text{H}^-$  and then  $\text{H}^+$  to (**1**). A notable feature of these hydrogenations is the progressive tightening of the attachment of the  $\alpha$ -carbon to the cluster, it being ultimately incorporated as a carbide atom into the  $\text{Ru}_5$  core. The reaction of (**1**) with  $\text{H}_2$  under mild conditions is a striking illustration of the increased reactivity of the  $\text{C}_2$  unit when it is attached to four metals. Under higher  $\text{H}_2$  pressures (10 atm, 18 h), partial breakdown of (**1**) gave the alkyne cluster  $\text{Ru}_4(\mu\text{-H})_3(\mu_4\text{-HC}_2\text{PPh}_2)(\mu\text{-PPh}_2)(\text{CO})_{10}$  (**11**).<sup>46</sup>

Scheme 2. Reactivity patterns of (1)



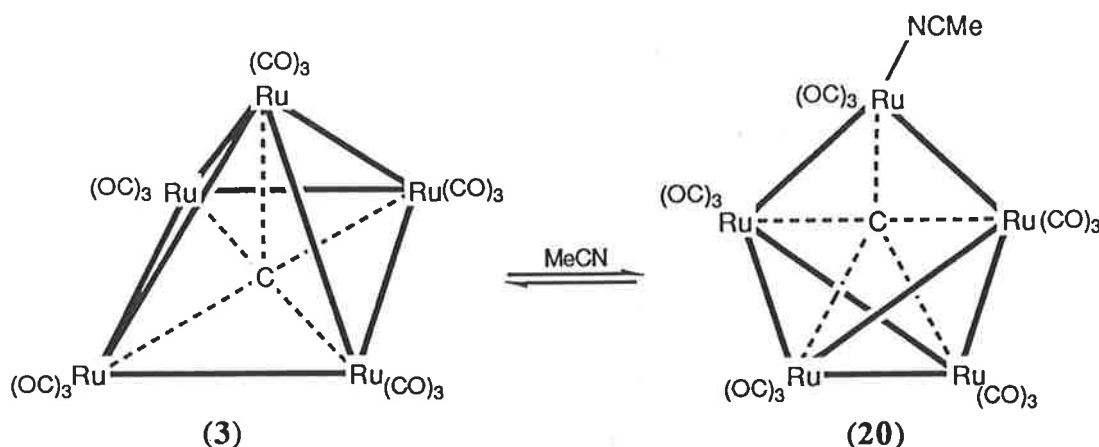
An extensive chemistry has been developed for (2): the reactions published to date are illustrated in Scheme 3. Facile Ru-Ru bond cleavage was found to occur when (2) was treated with Lewis bases (CO, MeCN, PhCN, Pr<sup>i</sup>NH<sub>2</sub>, Bu<sup>s</sup>NH<sub>2</sub> and C<sub>5</sub>H<sub>5</sub>N), converting its square pyramidal structure into a 'swallow' structure related to that of (1). The crystal structure of the CO adduct Ru<sub>5</sub>(μ<sub>5</sub>-η<sup>2</sup>-C<sub>2</sub>Ph)(μ-PPh<sub>2</sub>)(CO)<sub>14</sub> (12) has been determined.<sup>20</sup> The reaction of (2) with CO was found to be reversible and labelling experiments established that all carbonyl groups were exchanged equally. The variable temperature <sup>13</sup>C NMR spectrum of (2) showed that intermetallic CO exchange was slow. Diphenyldiacetylene was found to react with (2) to give Ru<sub>5</sub>(μ<sub>5</sub>-C<sub>2</sub>Ph)(μ<sub>3</sub>-η<sup>2</sup>-PhC<sub>2</sub>C<sub>2</sub>Ph)(μ-PPh<sub>2</sub>)(CO)<sub>12</sub> (13), the addition of the four-electron donor being accompanied by CO loss and the cleavage of a Ru-Ru bond.<sup>8</sup> An unusual reaction occurred between diphenylphosphine and (2), where four-electron oxidative addition of (H + PPh<sub>2</sub>), without loss of CO, was accompanied by the cleavage of two M-M bonds; the result was the 'bow-tie' cluster Ru<sub>5</sub>(μ-H)(μ<sub>4</sub>-η<sup>2</sup>-C<sub>2</sub>Ph)(μ-PPh<sub>2</sub>)<sub>2</sub>(CO)<sub>13</sub> (14).<sup>16</sup> The reaction of phenylphosphine with (2) (107 °C, 4.5 h) gave the alkylidyne cluster Ru<sub>5</sub>(μ<sub>4</sub>-PPh)(μ<sub>3</sub>-C-CH<sub>2</sub>Pr<sup>i</sup>)(μ-PPh<sub>2</sub>)(CO)<sub>12</sub> (15), which was shown to react further with two equivalents of phenylphosphine to give the cluster Ru<sub>5</sub>(μ-H)(μ<sub>4</sub>-PPh)<sub>2</sub>(μ<sub>3</sub>-PPh)(μ-PPh<sub>2</sub>)(CO)<sub>10</sub> (16).<sup>5</sup> The reaction of diphenyldiazomethane with (2) (75 °C, 4 h) gave Ru<sub>5</sub>(μ<sub>4</sub>-η<sup>2</sup>-C<sub>2</sub>Ph)(μ<sub>4</sub>-N<sub>2</sub>CPh<sub>2</sub>)(μ-PPh<sub>2</sub>)(CO)<sub>12</sub> (17).<sup>7</sup> A similar product was obtained with the isopropyl analogue of (2): treatment of this product with CO (3.5 h) gave Ru<sub>5</sub>(μ<sub>4</sub>-η<sup>2</sup>-C<sub>2</sub>Pr<sup>i</sup>){μ<sub>4</sub>-NC(O)NCPPh<sub>2</sub>}(μ-PPh<sub>2</sub>)(CO)<sub>13</sub> (18), formed by insertion of CO into the N=N bond. The reaction with N<sub>2</sub>CPh<sub>2</sub> was unusual in that no C-C coupled products were found: these are generally observed in the reactions of binuclear and trinuclear ruthenium complexes with diazo compounds.<sup>47</sup> Pyrolysis of (2) gave the diphenylacetylene cluster Ru<sub>5</sub>(μ<sub>4</sub>-PPh)(μ<sub>3</sub>-η<sup>2</sup>-PhC<sub>2</sub>Ph)(CO)<sub>13</sub> (19), the transformation being accomplished by P-C cleavage and phenyl migration to the acetylide.<sup>13</sup>

Scheme 3. Reactivity patterns of (2)



The most extensively studied pentaruthenium cluster to date is  $\text{Ru}_5\text{C}(\text{CO})_{15}$  (**3**), a square pyramidal cluster where the carbide atom is situated  $0.11(2)$  Å below the square base.<sup>24(a), (c)</sup> The addition of triphenylphosphine to (**3**) results in substitution at one or two basal sites. The disubstituted cluster has the phosphines in *trans*-axial positions.<sup>24(a), (c)</sup> This arrangement was also favoured by the bidentate phosphine dppb, where the bite of the ligand was sufficient to span the base of the cluster.<sup>23</sup> The series of clusters  $\text{Ru}_5\text{C}(\text{CO})_{13}\{(\text{PPh}_2)_2(\text{CH}_2)_n(\text{PPh}_2)_2\}$  ( $n = 1-4$ ) was prepared by Evans *et al.*,<sup>23</sup> who found that the clusters existed in three isomeric forms in solution. The  $^{31}\text{P}$  NMR spectra showed the presence of two isomers with different axial-equatorial substitution patterns, and the *trans*-axial isomer mentioned previously.

The first  $\text{Ru}_5$  cluster to be found with a arrowhead or 'bridged butterfly' geometry was  $\text{Ru}_5\text{C}(\text{CO})_{15}(\text{NCMe})$  (**20**), where the acetonitrile ligand had added to the bridging ruthenium atom.<sup>24</sup>



Complex (**20**) was formed from (**3**) by cleavage of a Ru-Ru bond. This cleavage came about as a result of the addition of two electrons from the acetonitrile ligand. Hydrogenation of  $\text{Ru}_5\text{C}(\text{CO})_{13}(\text{dppe})$  gave  $\text{Ru}_5(\mu\text{-H})_2\text{C}(\text{CO})_{12}(\text{dppe})$ , which has a square pyramidal core structure with dppe chelating a basal ruthenium; two carbonyls were found bridging the basal edges.<sup>24(c)</sup> Tri-substitution of (**3**) was obtained using the smaller phosphine  $\text{PMePh}_2$ .<sup>24(c)</sup> Addition of diphenylphosphine to (**3**) gave  $\text{Ru}_5\text{C}(\text{CO})_{14}(\text{PPh}_2)$ , which was then pyrolyzed ( $70^\circ\text{C}$ , 2 h) to give the square pyramidal complex  $\text{Ru}_5\text{C}(\mu\text{-H})(\mu\text{-PPh}_2)(\text{CO})_{13}$ .<sup>26</sup> A silylated version of this complex,  $\text{Ru}_5\text{C}(\mu\text{-H})\{\mu\text{-PPhCH}_2\text{CH}_2\text{Si}(\text{OEt})_3\}(\text{CO})_{13}$ , was also prepared and then tethered to both silica and alumina via the silyl group. A recent approach to obtaining

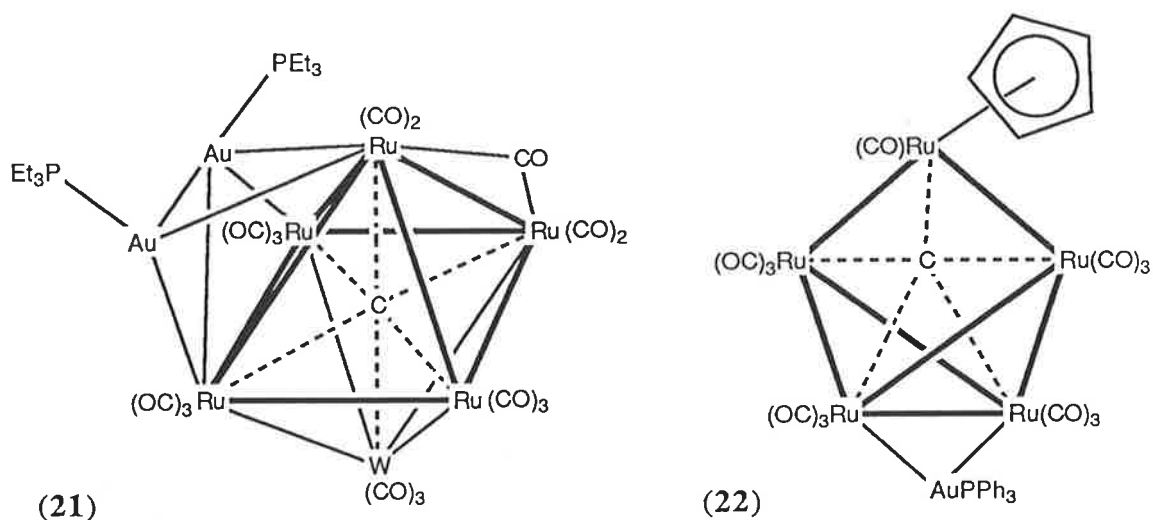
substituted derivatives of (3) has been the oxidation of the anion  $[\text{Ru}_5\text{C}(\text{CO})_{14}]^{2-}$  in the presence of the required ligand.<sup>48</sup> Using  $[\text{Ph}_3\text{C}][\text{BF}_4]$  or  $[\text{C}_7\text{H}_7][\text{BF}_4]$  in the presence of  $\text{PPh}_3$  or  $\text{C}_2\text{Ph}_2$ , the compounds  $\text{Ru}_5\text{C}(\text{CO})_{14}(\text{PPh}_3)$  and  $\text{Ru}_5\text{C}(\text{PhC}_2\text{Ph})(\text{CO})_{13}$  have been obtained in yields of 82% and 76%, respectively.

Complex (3) was found to react with  $\text{HER}$  ( $\text{E} = \text{S}, \text{Se}$ ;  $\text{R} = \text{H}, \text{Me}$  or  $\text{Et}$ ) to give  $\text{Ru}_5\text{C}(\mu\text{-H})(\text{CO})_{14}(\text{ER})$ . Of these compounds, the complex  $\text{Ru}_5\text{C}(\mu\text{-H})(\mu\text{-SEt})(\text{CO})_{14}$  has an arrowhead geometry with the sulphide ligand bridging a square face of the cluster.<sup>25</sup> When  $\text{Ru}_5\text{C}(\mu\text{-H})(\mu\text{-SEt})(\text{CO})_{14}$  was heated (81 °C, 30 min), carbonyl loss occurred and  $\text{Ru}_5\text{C}(\mu\text{-H})(\mu\text{-SEt})(\text{CO})_{13}$  was formed. A  $\text{PPh}_3$  derivative of this complex,  $\text{Ru}_5\text{C}(\mu\text{-H})(\mu\text{-SEt})(\text{CO})_{13}(\text{PPh}_3)$ , was prepared; this also had an arrowhead structure. Further carbonyl loss took place when  $\text{Ru}_5\text{C}(\mu\text{-H})(\mu\text{-SEt})(\text{CO})_{13}(\text{PPh}_3)$  was heated, resulting in the isolation of two isomers of  $\text{Ru}_5\text{C}(\mu\text{-H})(\mu\text{-SEt})(\text{CO})_{12}(\text{PPh}_3)$ , one of which has a square pyramidal structure with the sulphide bridging two basal rutheniums.

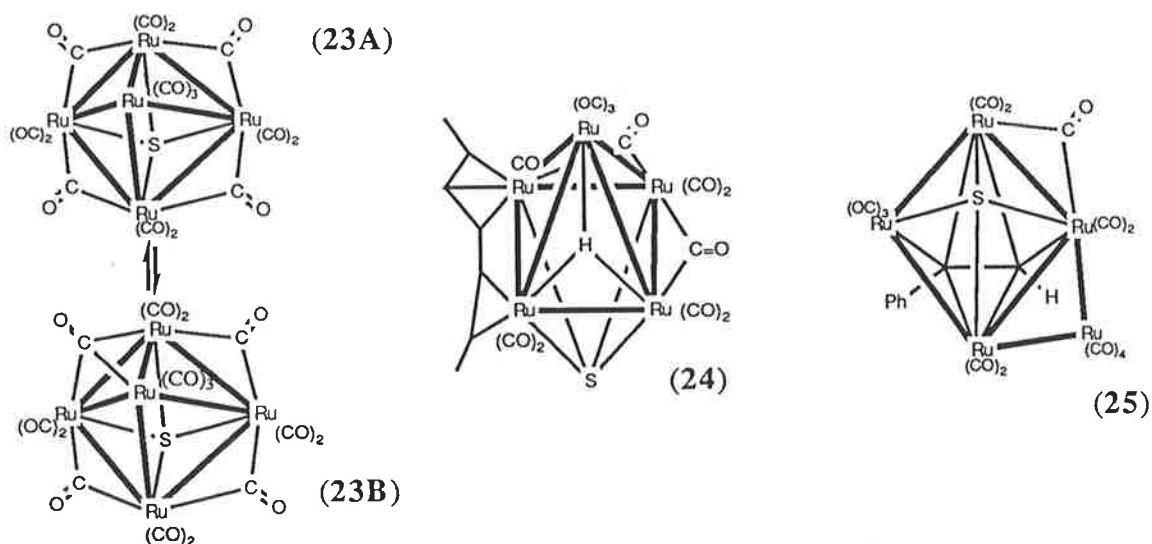
The addition of  $\text{HX}$  ( $\text{X} = \text{Cl}, \text{Br}$ ) to (3) or protonation of the products obtained by treating (3) with  $\text{X}^-$  ( $\text{X} = \text{Cl}, \text{Br}, \text{F}, \text{I}$ ), gave the compounds  $\text{Ru}_5\text{C}(\mu\text{-H})(\text{X})(\text{CO})_{15}$ .<sup>24(c)</sup> Arrowhead structures were assigned to these complexes on the basis of far-infrared and approximate normal-coordinate analysis studies.<sup>49</sup> Related  $\text{AuRu}_5\text{C}(\text{X})(\text{CO})_{15}(\text{PPh}_3)$  ( $\text{X} = \text{Cl}, \text{Br}$ ) complexes were obtained by treating (3) with  $\text{AuX}(\text{PPh}_3)$ , and exhibited the expected arrowhead structures, with the halide ligand terminally bound. In contrast, the addition of  $\text{AuI}(\text{PPh}_3)$  to (3) gave  $\text{AuRu}_5\text{C}(\mu\text{-I})(\text{CO})_{14}(\text{PPh}_3)$ .<sup>25</sup> Treatment of  $\text{AuRu}_5\text{C}(\text{X})(\text{CO})_{15}(\text{PPh}_3)$  ( $\text{X} = \text{Cl}, \text{Br}$ ) with  $\text{PPh}_3$  gave  $\text{Ru}_5\text{C}(\text{CO})_{14}(\text{PPh}_3)$  and  $\text{AuX}(\text{PPh}_3)$ , while the reaction with  $\text{AuRu}_5\text{C}(\mu\text{-I})(\text{CO})_{13}(\text{PPh}_3)$  [obtained by pyrolysis of  $\text{AuRu}_5\text{C}(\mu\text{-I})(\text{CO})_{14}(\text{PPh}_3)$ ] gave  $\text{AuRu}_5\text{C}(\mu\text{-I})(\text{CO})_{13}(\text{PPh}_3)$ ,<sup>25</sup> an arrowhead cluster with the iodide bridging a square face. Carbonyl loss occurred when  $\text{AuRu}_5\text{C}(\text{Br})(\text{CO})_{15}(\text{PPh}_3)$  was heated, giving  $\text{AuRu}_5\text{C}(\mu\text{-Br})(\text{CO})_{14}(\text{PPh}_3)$ , where the bromide ligand bridges a square face of the arrowhead structure.<sup>35</sup> Addition of  $\text{Cl}_2$  and  $\text{Br}_2$  to (3) gave  $\{\text{RuX}_2(\text{CO})_3\}_2$  ( $\text{X} = \text{Cl}, \text{Br}$ ), while the addition of  $\text{I}_2$  gave  $\text{Ru}_5\text{C}(\text{CO})_{15}\text{I}_2$ .<sup>24(c)</sup> Pyrolysis of (3) under argon (10 atm, 200 °C) gave  $\text{Ru}_6\text{C}(\text{CO})_{17}$  and ruthenium metal, but under  $\text{CO}$  (400 atm, 100 °C) no reaction was

observed.<sup>24(a)</sup> Other reactions that have been noted for (3) are hydrogenation, which gave  $\text{Ru}_5\text{C}(\mu\text{-H})_2(\text{CO})_{15}$ , and protonation, which gave  $[\text{Ru}_5\text{C}(\mu\text{-H})(\text{CO})_{15}]^+$ , the  $\text{H}^+$  ion in this case being associated with the cluster rather than with the carbide atom. In the square pyramidal structures, the partially-exposed carbide is shielded by the envelope of ligands below the basal plane, while in the arrowhead arrangement the carbide is in a slightly more open position. At this stage, no reactions of the carbide atom have been described.

A number of mixed-metal derivatives have been prepared from (3). The dianion  $[\text{Ru}_5\text{C}(\text{CO})_{14}]^{2-}$  was shown to react with  $\text{M}(\text{CO})_3\text{L}_3$  ( $\text{M} = \text{Cr}$ ,  $\text{L} = \text{pyridine}$ ;  $\text{M} = \text{Mo}$ ,  $\text{W}$ ,  $\text{L} = \text{MeCN}$ ) to give the anions  $[\text{Ru}_5\text{MC}(\text{CO})_{17}]^{2-}$ , which in turn reacted with  $\{\text{Au}(\text{PEt}_3)\}^+$  to form  $\text{Au}_2\text{Ru}_5\text{M}(\text{CO})_{17}(\text{PEt}_3)_2$ .<sup>37</sup> The structure of  $\text{Au}_2\text{Ru}_5\text{WC}(\text{CO})_{17}(\text{PEt}_3)_2$  (21) has been determined and shows that the tungsten has capped the square pyramid to form an octahedron with the carbide fully encapsulated. The  $\text{Au}_2$  unit interacts with the cluster in the familiar  $\text{Au}_2\text{Ru}_3$  trigonal bipyramid fashion, which comes about when one  $\text{Au}(\text{PR}_3)$  caps an  $\text{Ru}_3$  face and the second  $\text{Au}(\text{PR}_3)$  face-caps the  $\text{AuRu}_3$  unit.<sup>50</sup> A nitrosyl anion  $[\text{Ru}_5\text{C}(\text{CO})_{13}(\text{NO})]^-$  was prepared by treating (3) with  $[\text{ppn}][\text{NO}_2]$ . The reaction between  $[\text{Ru}_5\text{C}(\text{CO})_{13}(\text{NO})]^-$  and  $[\text{Au}(\text{PEt}_3)]^+$  gave  $\text{AuRu}_5\text{C}(\text{CO})_{13}(\text{NO})(\text{PEt}_3)$ , which was shown by an X-ray study to exist in the solid state in two isomeric square pyramidal forms, with the nitrosyl either  $\mu_3$ - or  $\mu_2$ -bound.<sup>34</sup> The cluster  $\text{AuRu}_5\text{C}(\mu\text{-}\eta^2\text{-MeCO})(\text{CO})_{14}(\text{PPh}_3)$  has been isolated by treating (3) with  $\text{LiMe}$  then with  $\text{AuCl}(\text{PPh}_3)$ , or by treating (3) with  $\text{AuMe}(\text{PPh}_3)$ .<sup>33</sup> Similarly, the cluster  $\text{AuRu}_5\text{C}(\text{CO})_{13}(\text{PPh}_3)(\eta^5\text{-C}_5\text{H}_5)$  (22) was obtained when (3) was treated with  $\text{Na}[\text{C}_5\text{H}_5]$ , and then with  $\text{AuCl}(\text{PPh}_3)$ .<sup>33</sup> Both the acyl and cyclopentadienyl complexes have arrowhead structures with the gold unit bridging the two hinge rutheniums: the acyl ligand in the former is bonded across a square face and the cyclopentadienyl ligand in the latter is attached to the bridging ruthenium. The action of  $\text{HI}$  on  $\text{AuRu}_5\text{C}(\mu\text{-}\eta^2\text{-MeCO})(\text{CO})_{14}(\text{PPh}_3)$  has been investigated spectroscopically and was found to give  $\text{Ru}_5\text{C}(\mu\text{-H})(\mu\text{-MeCO})(\text{CO})_{14}$  and  $\text{AuI}(\text{PPh}_3)$ . The addition of  $\text{H}^-$  to the acyl clusters at low temperatures probably gave formyl derivatives, which, on warming to room temperature, decomposed and liberated acetaldehyde.<sup>51</sup>



Recently, Adams and co-workers have synthesized several pentaruthenium sulphido clusters by adding mononuclear ruthenium carbonyl units to smaller clusters. In this way,  $\text{Ru}_5(\mu_4\text{-S})(\text{CO})_{15}$  (**23**) was prepared from  $\text{Ru}_3(\mu_3\text{-S})(\mu_3\text{-CO})(\text{CO})_9$  and  $\text{Ru}(\text{CO})_5$  (68 °C, CO, 10 min) (62% yield).<sup>30</sup> The structure of (**23**), which was determined by X-ray analysis, was unusual in that the two independent molecules present showed markedly different arrangements for the carbonyl ligands about the metal core. It was found that further ' $\text{Ru}(\text{CO})_3$ ' units could be added to (**23**) to form, sequentially,  $\text{Ru}_6(\mu_4\text{-S})(\text{CO})_{18}$  and then  $\text{Ru}_7(\mu_4\text{-S})(\text{CO})_{21}$ , each additional ' $\text{Ru}(\text{CO})_3$ ' unit bridging a basal edge of the square pyramid. All three complexes were degraded under CO (1 atm, 98 °C) by the stepwise removal of mononuclear carbonyl groups. Complex (**23**) was found to react with either *trans*-2-heptene or 2,4-heptadiene (80 °C, 40-75 min) to give  $\text{Ru}_5(\mu_3\text{-H})(\mu_4\text{-S})(\mu\text{-}\eta^2, \eta^3\text{-1,5-Me}_2\text{C}_5\text{H}_5)(\text{CO})_{12}$  (**24**), which has a square pyramidal metal core with the pentadienyl ligand bonded through olefinic and allylic interactions to two basal rutheniums.<sup>31</sup> Reaction of the diene cluster with  $\text{Ru}(\text{CO})_5$  gave  $\text{Ru}_6(\mu_3\text{-H})(\mu_4\text{-S})(\mu\text{-}\eta^2, \eta^3\text{-1,5-Me}_2\text{C}_5\text{H}_5)(\text{CO})_{15}$ , where the extra ruthenium bridged a basal edge opposite the diene. Formation of the 1,5-dimethylpentadienyl ligands from the precursor olefins on these clusters is a clear demonstration of CH activation by the pentaruthenium cluster. Under CO (98 °C, 45 min), the  $\text{Ru}_6$  cluster re-formed  $\text{Ru}_5(\mu_3\text{-H})(\mu_4\text{-S})(\mu\text{-}\eta^2, \eta^3\text{-1,5-Me}_2\text{C}_5\text{H}_5)(\text{CO})_{12}$  in 30% yield.



The cluster  $\text{Ru}_5(\mu_4\text{-S})_2(\text{CO})_{14}$  was synthesized in 20% yield from  $\text{Ru}_3(\mu_3\text{-S})_2(\text{CO})_9$  and  $\text{Ru}_3(\text{CO})_{12}$  under UV irradiation (5 h).<sup>32</sup> The metal skeleton of  $\text{Ru}_5(\mu_4\text{-S})_2(\text{CO})_{14}$  is that of an edge-bridged square. Addition of further  $\text{Ru}(\text{CO})_3$  units to edges of the square was observed in the syntheses of  $\text{Ru}_6(\mu_4\text{-S})_2(\text{CO})_{17}$  and  $\text{Ru}_7(\mu_4\text{-S})_2(\text{CO})_{20}$ , which were obtained by treating  $\text{Ru}_5(\mu_4\text{-S})_2(\text{CO})_{14}$  with  $\text{Ru}(\text{CO})_5$  (UV irradiation, 10h). An alkyne cluster  $\text{Ru}_5(\mu_4\text{-S})(\mu_4\text{-}\eta^2\text{-HC}_2\text{Ph})(\mu\text{-CO})(\text{CO})_{13}$  (**25**) was obtained from the reactions of either  $\text{Ru}_3(\mu_3\text{-S})(\mu_3\text{-}\eta^2\text{-HC}_2\text{Ph})(\text{CO})_9$  or  $\text{Ru}_4(\mu_4\text{-S})(\mu_4\text{-}\eta^2\text{-HC}_2\text{Ph})(\mu\text{-CO})_2(\text{CO})_9$  with  $\text{Ru}(\text{CO})_5$  (70 °C, CO, 60 min).<sup>29</sup> The structure of  $\text{Ru}_5(\mu_4\text{-S})(\mu_4\text{-}\eta^2\text{-HC}_2\text{Ph})(\mu\text{-CO})(\text{CO})_{13}$  is an edge-bridged square, the faces of which are capped by the sulphido and acetylene groups. Further reaction of  $\text{Ru}_5(\mu_4\text{-S})(\mu_4\text{-}\eta^2\text{-HC}_2\text{Ph})(\mu\text{-CO})(\text{CO})_{13}$  with  $\text{Ru}(\text{CO})_5$  gave  $\text{Ru}_6(\mu_4\text{-S})(\mu_4\text{-}\eta^2\text{-HC}_2\text{Ph})(\text{CO})_{17}$ , where the additional ruthenium bridges an edge adjacent to the other  $\text{Ru}(\text{CO})_4$  fragment.<sup>29</sup> It was found that the  $\text{Ru}(\text{CO})_4$  fragments could be cleaved sequentially from the  $\text{Ru}_6$  cluster by treatment with CO. The heptanuclear cluster  $\text{Mo}_2\text{Ru}_5(\mu_4\text{-S})(\mu_4\text{-}\eta^2\text{-CO})_2(\text{CO})_{14}(\eta\text{-C}_5\text{H}_5)_2$  has recently been synthesized by adding  $\text{Ru}(\text{CO})_5$  to  $\text{Mo}_2\text{Ru}(\mu_3\text{-S})(\text{CO})_7(\eta\text{-C}_5\text{H}_5)_2$  or to  $\text{Mo}_2\text{Ru}_4(\mu_4\text{-S})(\mu_4\text{-}\eta^2\text{-CO})(\text{CO})_{13}(\eta\text{-C}_5\text{H}_5)_2$  (80 °C, 1-3 h).<sup>40</sup> The presence of quadruply-bridging CO ligands in both the  $\text{Mo}_2\text{Ru}_4$  and  $\text{Mo}_2\text{Ru}_5$  clusters is an indication that this type of carbonyl ligand may be involved in the cluster growth process.

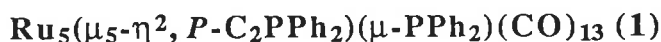
Within the chemistry developed for pentaruthenium clusters, many reactions have been found that show that the higher nuclearity clusters behave differently from the smaller Ru<sub>3</sub> and Ru<sub>4</sub> clusters. This accords with a recent statistical study by Struchkov *et al.*,<sup>52</sup> which has pointed to the intermediate nature of M<sub>5</sub> clusters, where the bonding may be considered to be in between localized and delocalized bonding modes. In the study of available structures made by Struchkov in 1987, the total number of M<sub>5</sub> carbonyl clusters of the Fe and Co subgroups was 37. The rapid expansion in Ru<sub>5</sub> chemistry in recent years becomes evident when one compares this result with the listing in Table 1.

As the chemistry of (1) had been examined only briefly prior to the work reported in this thesis, a number of important questions remained about the reactivity of the molecule. From the point of view of synthesis, the preparation of (1) gives a relatively high yield, which makes it an attractive starting material for pentaruthenium chemistry. The presence of the phosphine and phosphido ligands in (1) has already been shown to be useful in maintaining the integrity of the cluster. The open structure of complex (1) also provides a useful model for the interaction, and hence reactions, of acetylides at metal surfaces.

This chapter examines the synthesis and reactivity of Ru<sub>5</sub>(μ<sub>5</sub>-η<sup>2</sup>, P-C<sub>2</sub>PPh<sub>2</sub>)(μ-PPh<sub>2</sub>)-(CO)<sub>13</sub> (1).<sup>12</sup> As has been shown previously,<sup>10</sup> this cluster reacts with H<sub>2</sub> and CO under quite mild conditions to give a variety of Ru<sub>5</sub> and Ru<sub>4</sub> compounds. In the present study, further reactions using (1) were undertaken to yield a new range of clusters. These have been discussed, as far as possible, within the context of the earlier work.

## 3.2. Results and Discussion

### 3.2.1. Further observations on the synthesis of



When the synthesis of (1) from  $\{\text{Ru}_3(\text{CO})_{11}\}_2(\mu\text{-dppa})$  (4) was performed on a gram scale, a variety of products was obtained in addition to (1). The major complexes isolated and identified were:  $\text{Ru}_5(\mu_5\text{-}\eta^2, P\text{-C}_2\text{PPh}_2)(\mu\text{-PPh}_2)(\text{CO})_{13}$  (1),  $\text{Ru}_4(\mu_4\text{-PPh})\{\mu_4\text{-}\eta^2, P\text{-PhC}_2\text{PPh}_2\}(\mu\text{-CO})_2(\text{CO})_8$  (5),<sup>53</sup>  $\text{Ru}_5(\mu_5\text{-}\eta^2, P\text{-C}_2\text{PPh}_2)(\mu\text{-PPh}_2)(\text{CO})_{15}$  (6t),<sup>21</sup>  $\text{Ru}_4(\mu_4\text{-}\eta^2\text{-C}_2)(\mu\text{-PPh}_2)_2(\text{CO})_{12}$  (7),<sup>45</sup>  $\text{Ru}_5(\mu_4\text{-PPh})\{\mu_3\text{-}\eta^2, P\text{-CCPh}(\text{PPh}_2)\}(\text{CO})_{12}$  (26) and  $\text{Ru}_5(\mu\text{-H})(\mu_4\text{-PPh})\{\mu_4\text{-}\eta^4\text{-CCPh}(\text{C}_6\text{H}_4)\}(\mu_3\text{-PPh})(\text{CO})_{10}$  (27). Complexes (26) and (27) were also obtained by pyrolysis of (1) and are described in Section 3.2.2. The relative yields of the products could be varied by altering reaction parameters such as temperature, duration and control of the reaction atmosphere. Most critical of these parameters was the pyrolysis temperature for the conversion of  $\{\text{Ru}_3(\text{CO})_{11}\}_2(\mu\text{-dppa})$  to (1). If the temperature was increased from 90 °C to 111 °C, the major products formed were  $\text{Ru}_3(\text{CO})_{12}$ , (1), (5), (26) and (27). Two orange clusters were also observed, and were formulated as  $\text{Ru}_8(\text{CO})_{17}\text{(dppa}^*)^\dagger$  and  $\text{Ru}_5(\text{CO})_{13}\text{(dppa}^*)$ . If the duration of the reflux was increased (from 1 h 30 min to 3 h), as well as the temperature, then significant proportions of complexes (26) and (27) were formed. If the conversion was not performed with a  $\text{N}_2$  purge, the evolved CO reacted under the pyrolysis conditions with (1) to form the clusters  $\text{Ru}_5(\mu_5\text{-}\eta^2, P\text{-C}_2\text{PPh}_2)(\mu\text{-PPh}_2)(\text{CO})_{15}$  (6t) and  $\text{Ru}_4(\mu_4\text{-}\eta^2\text{-C}_2)(\mu\text{-PPh}_2)_2(\text{CO})_{12}$  (7). Both these clusters have been synthesized previously in the reaction of (1) with CO.<sup>21,45</sup> Separation of (5) and (6t) from (1) on a large scale was found to be difficult, so the reaction conditions had to be carefully controlled in order to avoid low yields of (1).

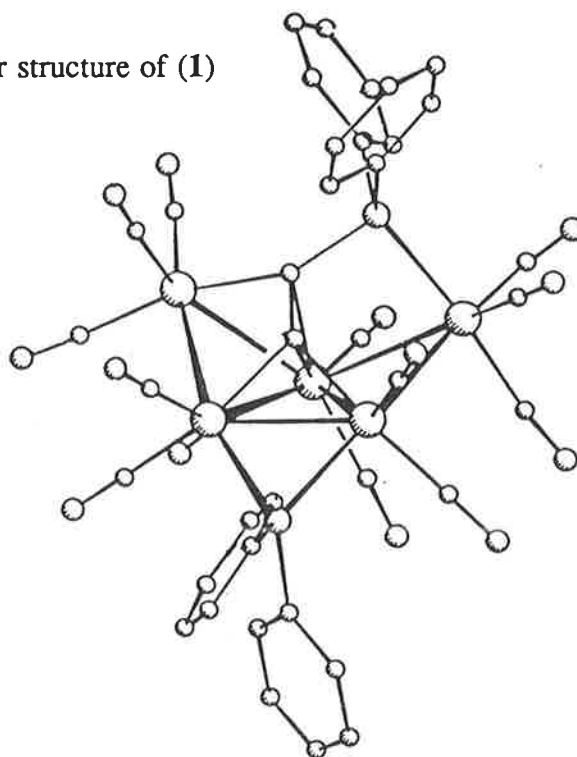
---

† (dppa\*) is used throughout this chapter to indicate the incorporation of the elements of dppa in the cluster; the ligand does not necessarily correspond to structurally intact dppa.

New spectroscopic data has been obtained for (1). The fast atom bombardment (FAB) mass spectrum showed a molecular ion and sequential loss of 13 carbonyl groups. After prolonged periods in the FAB beam, ions at  $m/z$  1321 and 1293 corresponding to  $\text{Ru}_5(\text{CO})_{15}(\text{dppa}^*)$  and  $\text{Ru}_5(\text{CO})_{14}(\text{dppa}^*)$  were observed. These have the same nominal mass as ions noted in the spectra of (6k) and (6t) (see below) and suggest that intermolecular reactions such as CO transfer are occurring in the matrix or in the selva region directly above the surface.<sup>54</sup> Generally, such reactions have not proved a problem in the examination of the clusters, except when particularly labile ligands have been present. The FAB mass spectra for (6t) and (6k) were identical and showed molecular ions at  $m/z$  1321 and loss of 15 carbonyl groups.

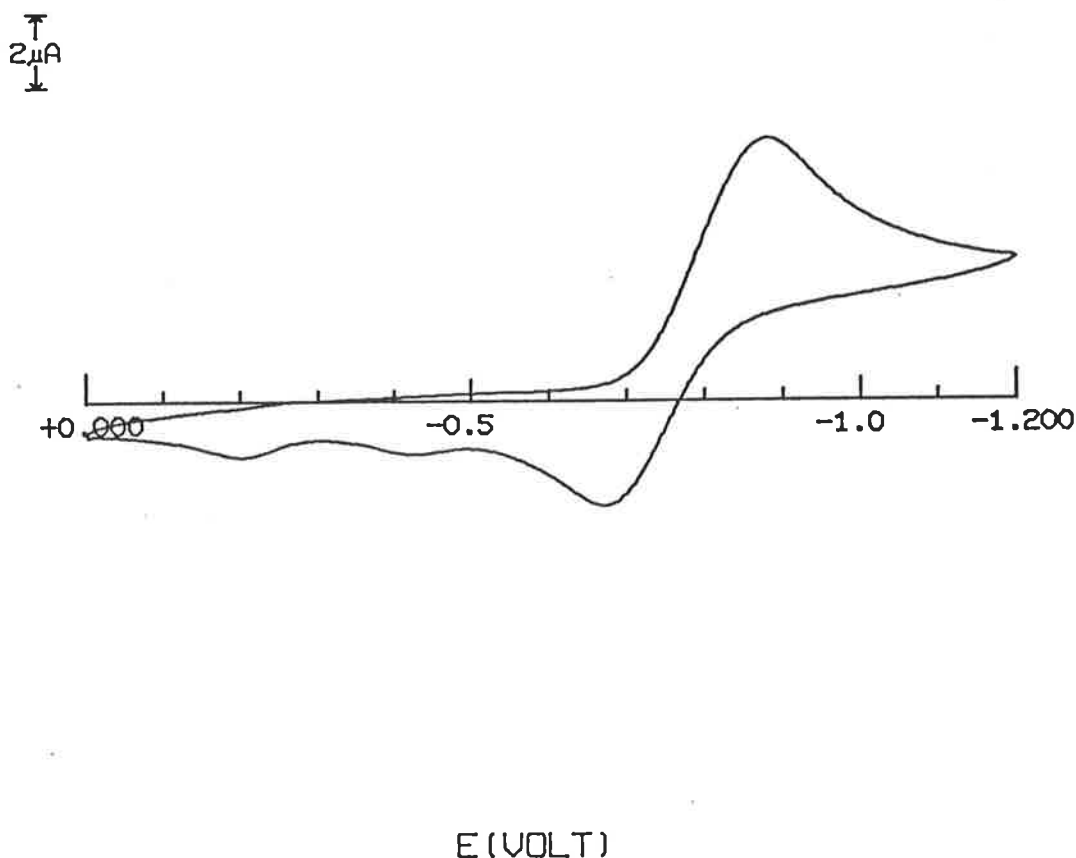
The  $^{13}\text{C}$  NMR spectrum of (1) suggested that several of the carbonyl ligands are either fluxional at room temperature<sup>55</sup> or are accidentally equivalent, as only nine signals were found between  $\delta$  202.5 and 192.5 in contrast to the 13 CO environments expected from the  $C_1$  symmetry of (1)<sup>12</sup> (see Figure 1). The chemical shifts noted for  $\text{C}_\alpha$  and  $\text{C}_\beta$  at  $\delta$  239.0 (doublet,  $J_{\text{P-C}} = 23$  Hz) and  $\delta$  108.8 (doublet,  $J_{\text{P-C}} = 22$  Hz), respectively, are similar to those found for other  $\mu_4\text{-}\eta^2$ -acetylide complexes.<sup>56</sup> The  $\alpha$ -carbon is particularly electron-deficient and should be susceptible to nucleophilic attack.

**Figure 1.** Molecular structure of (1)



An electrochemical study of (1) was carried out to determine whether a stable anion could be generated. A cyclic voltammogram at  $200 \text{ mV s}^{-1}$  is shown in Figure 2. The process was quasi-reversible with  $E_{1/2} -0.78 \text{ V}$ , suggesting that it should be possible to reduce (1) chemically with a reagent such as sodium amalgam ( $E_{1/2} -2.0 \text{ V DMF}^{57}$ ). Treatment of (1) with sodium amalgam gave a black solution, which had  $\nu(\text{CO})$  bands at  $2021(\text{sh})$ ,  $2005(\text{sh})$ ,  $1968\text{vs}$  and  $1948(\text{sh}) \text{ cm}^{-1}$ . It has not been possible to isolate a product from this reduced solution. Treatment of the reduced solution with  $[\text{ppn}]\text{Cl}$  in MeCN resulted in further reaction, and the anion so obtained gave an IR spectrum different from that of the original reduced solution. A FAB mass spectrum of the ppn salt of this anion showed a molecular negative ion  $[\text{M}]^-$  at  $m/z$  1236, which corresponds to  $[\text{Ru}_5(\text{CO})_{12}(\text{dppa}^*)]^-$  (this does not rule out the possibility of ions such as  $[\text{Ru}_5\text{H}(\text{CO})_{12}(\text{dppa}^*)]^-$  formed from  $[\text{Ru}_5(\text{CO})_{12}(\text{dppa}^*)]^{2-}$  in the spectrometer).

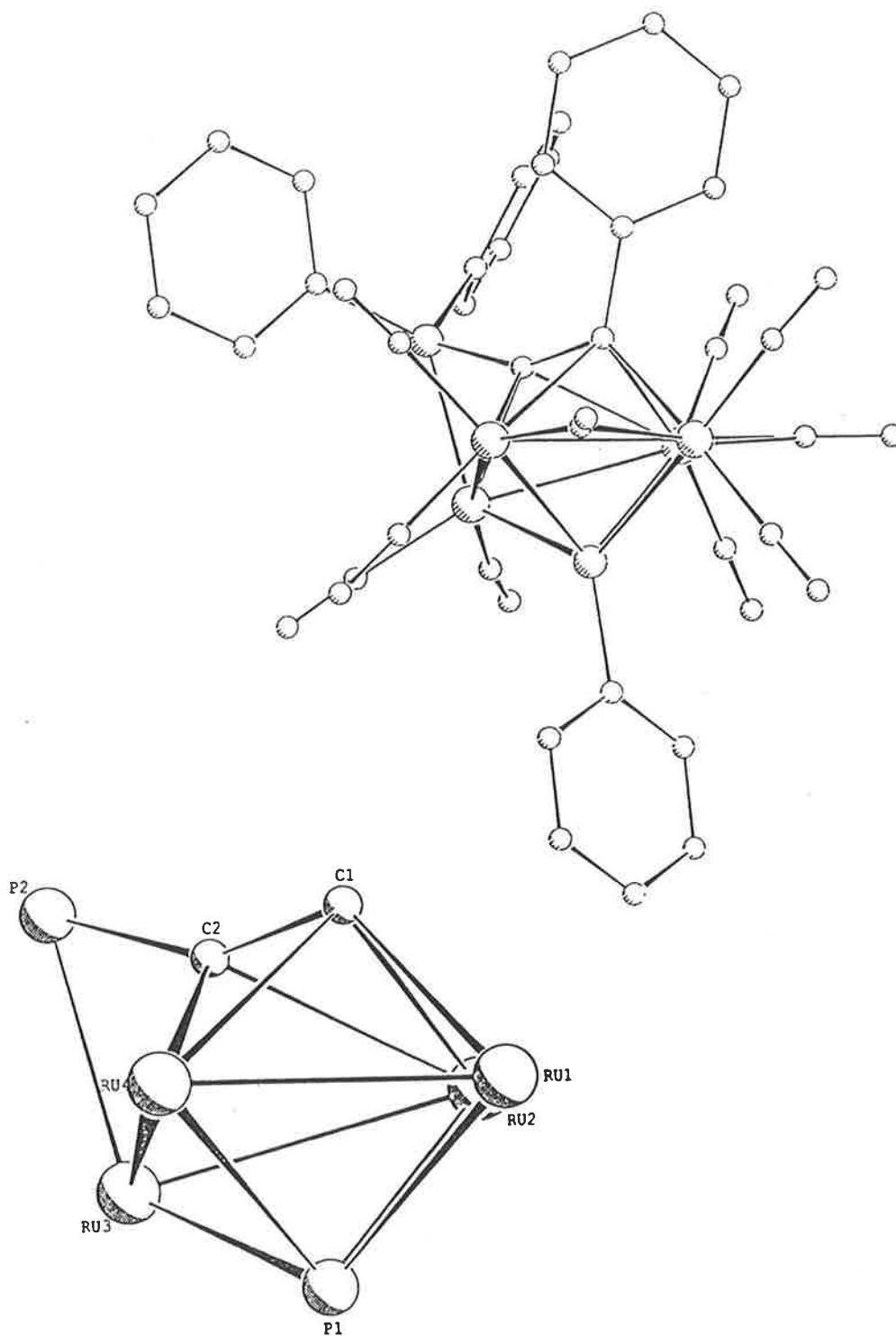
**Figure 2.** Cyclic voltammogram of (1) ( $200 \text{ mV s}^{-1}$ ) in  $\text{CH}_2\text{Cl}_2$



At this stage it is not clear whether the product formed initially is a '(CO)<sub>12</sub>' or '(CO)<sub>13</sub>' species, or whether it is a monoanion or a dianion. Some indirect evidence has been gained from the addition of two AuCl(PPh<sub>3</sub>) units to the anion, which suggests that the [Ru<sub>5</sub>(CO)<sub>12</sub>-(dppa\*)]<sup>2-</sup> formulation may be correct (see Section 3.2.6). The appearance of the small anodic waves at E -0.43 V and -0.20 V, suggest that CO loss or skeletal changes may have been occurring.<sup>58,59</sup> An attempt to initiate an ETC reaction between (1) and dppa using the catalyst Na/BPK<sup>57</sup> was unsuccessful.

Complex (5) gave a FAB mass spectrum which showed a molecular ion at *m/z* 1080 followed by loss of ten carbonyl groups. In conjunction with analytical, <sup>1</sup>H NMR and <sup>31</sup>P NMR data a formulation similar to that reported by Daran *et al.*<sup>53</sup> for the complex Ru<sub>4</sub>(μ<sub>4</sub>-PPh){μ<sub>4</sub>-η<sup>2</sup>, *P*-PhC<sub>2</sub>PPh<sub>2</sub>}(μ-CO)<sub>2</sub>(CO)<sub>8</sub> was suggested. The IR data reported for their complex (2065w, 2030vs, 1985(sh), 1980s, 1970s, 1842vs cm<sup>-1</sup>) were significantly different from that obtained for (5) (2061w, 2030vs, 2008m, 2001w, 1982w, 1964w, 1878vw, 1851w cm<sup>-1</sup>). An X-ray crystallographic study was therefore carried out on (5), to determine whether a structure different to that reported by Daran was present. However, it was found to be identical, except for the presence of a molecule of solvated MeOH in our sample (this altered the unit cell dimensions). Separation of clusters with R<sub>f</sub> values similar to (5) could not be achieved under the column chromatography conditions specified by Daran, and co-crystallization of (5) and other Ru<sub>5</sub> clusters [e.g. (1), (6t)] occurs readily, which probably accounts for the major differences in the IR spectra noted above. A PLUTO plot of a molecule of (5) is shown in Figure 3. In the redetermination of the structure of (5), the greatest variation in bond lengths was found for Ru(2)-C(2) 2.429(9) Å [Lit.<sup>53</sup> 2.310(8) Å]; most other differences are within 3 esd's. A cluster with a related geometry, Ru<sub>4</sub>{μ<sub>4</sub>-η<sup>3</sup>-P(Ph)CHCH}-(μ<sub>4</sub>-PPh)(μ-CO)(CO)<sub>10</sub>, has been synthesized recently by insertion of acetylene into the Ru-P bonds of a phosphinidene group in Ru<sub>4</sub>(μ<sub>4</sub>-PPh)<sub>2</sub>(μ-CO)(CO)<sub>10</sub>.<sup>60</sup>

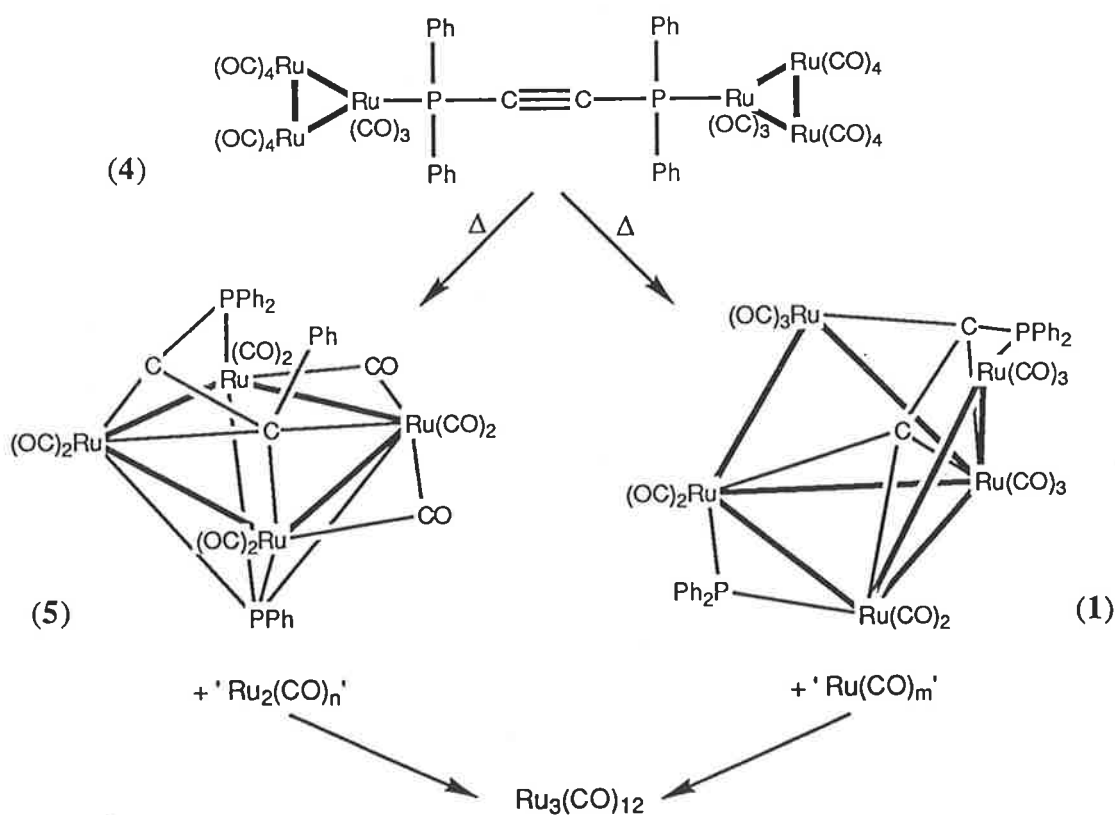
**Figure 3.** PLUTO plot of  $\text{Ru}_4(\mu_4\text{-PPh})\{\mu_4\text{-}\eta^2, P\text{-PhC}_2\text{PPh}_2\}(\mu\text{-CO})_2(\text{CO})_8\cdot\text{MeOH}$  (5)<sup>†</sup>  
(by E.R.T. Tiekink)



<sup>†</sup> Throughout this chapter, for the sake of clarity, only the core structures showing atoms of interest have been labelled. Full structures have been left unlabelled.

It appears that (5) is formed through condensation of (4) under a slight CO partial pressure, as no evidence was found for the formation of (5) during the pyrolysis of (1). Small amounts of (5) were always recovered in the synthesis of (1), even with a nitrogen purge. A bimolecular process may be involved whereby the lost ' $\text{Ru}_2(\text{CO})_n$ ' fragment formed in the synthesis of (5) combines with the lost ' $\text{Ru}(\text{CO})_m$ ' fragment formed in the synthesis of (1) to form  $\text{Ru}_3(\text{CO})_{12}$  (see Scheme 4).

**Scheme 4.** Syntheses of (1) and (5) from (4)



In terms of Polyhedral Skeletal Electron Pair (PSEP) theory,<sup>1</sup> (5) is a 64-electron, 8-SEP cluster. Further examples of this type of cluster are the compounds  $\text{Fe}_4(\mu_4\text{-PPh})_2(\text{CO})_{11}(\text{L})$  ( $\text{L} = \text{CO}, \text{PR}_3$ ):<sup>61</sup> these 64-electron clusters lose CO reversibly to form  $\text{Fe}_4(\mu_4\text{-PPh})_2(\text{CO})_{10}(\text{L})$  which are 62-electron, 7-SEP clusters. It is interesting to note that molecular orbital calculations have indicated that the 64-electron, 8-SEP configuration is favoured for the iron clusters whereas the ruthenium analogues are expected to exist only as 62-electron, 7-SEP

clusters.<sup>62</sup> This is seen for instance, in the complex  $\text{Ru}_4(\mu_4\text{-PPh})_2(\text{CO})_{11}$ , a 7-SEP cluster, which does not convert to the related 8-SEP cluster  $\text{Ru}_4(\mu_4\text{-PPh})_2(\text{CO})_{12}$ .<sup>63</sup> The 8-SEP count found for (5) appears to be due to the presence of the phosphino-alkyne and phosphido ligands. In complex (5) the acetylene, a six-electron donor, is assumed to be involved in a  $\pi$ -interaction with Ru(4), two  $\sigma$ -interactions with Ru(1) and Ru(2) and a carbenic interaction with Ru(3).

The direct synthesis of (7) from (1) was attempted in the hope of increasing the yield of this compound, which contains a novel  $\mu_4\text{-}\eta^1,\eta^2$ -ethynediyl dianion. In fact, the yield by this route (11%) was lower than that previously obtained (28%).<sup>45</sup> Further spectroscopic data has been collected for (7). The FAB mass spectrum showed a molecular ion at  $m/z$  1137 and loss of twelve CO groups. A  $^{13}\text{C}$  NMR spectrum contained three resonances for the CO groups (all multiplets). As the molecule displays  $C_2$  symmetry, six unique CO sites are expected. The signals observed, therefore, indicate either accidental equivalence of signals or that carbonyl exchange processes are occurring. The doublet at  $\delta$  141.1 ( $J_{\text{P-C}} = 37$  Hz) was assigned to the carbons of the  $C_2$  fragment and suggests that both carbons are equivalent and that each carbon is coupled to only one phosphorus. Carty *et al.*<sup>56</sup> have shown that the  $C_\alpha$  resonances have quite large  $^{31}\text{P}\text{-}^{13}\text{C}$  couplings ( $J_{\text{P-C}} = 27.4 - 27.8$  Hz) for  $\text{Ru}_2(\mu_2\text{-}\eta^2\text{-C}_2\text{R})(\mu\text{-PPh}_2)(\text{CO})_6$  ( $\text{R} = \text{Ph}, \text{Bu}^t$ ), whereas  $C_\beta$  couplings are in the range 7.7 - 8.0 Hz.

### 3.2.2. Pyrolysis reactions of (1)

In the course of studying the pyrolytic behaviour of (1), we isolated  $\text{Ru}_5(\mu_4\text{-PPh})\{\mu_3\text{-}\eta^2, P\text{-CCPh}(\text{PPh}_2)\}(\text{CO})_{12}$  (26) and  $\text{Ru}_5(\mu\text{-H})(\mu_4\text{-PPh})\{\mu_4\text{-}\eta^4\text{-CCPh}(\text{C}_6\text{H}_4)\}(\mu_3\text{-PPh})(\text{CO})_{10}$  (27). Both these complexes have been fully characterized by X-ray studies. Plots of the two molecular structures are shown in Figures 4 and 5, and significant bond distances and angles are collected in Tables 2 and 3. Complexes (26) and (27) were formed sequentially when (1) was heated in toluene. After 2 h 30 min at reflux, complex (26) was isolated in 22% yield as a brown crystalline material and complex (27) in > 65% yield as a dark green crystalline material.

Figure 4. PLUTO plot of  $\text{Ru}_5(\mu_4\text{-PPh})\{\mu_3\text{-}\eta^2, P\text{-CCPh}(\text{PPh}_2)\}(\text{CO})_{12}$  (26)

(by E.R.T. Tiekink)

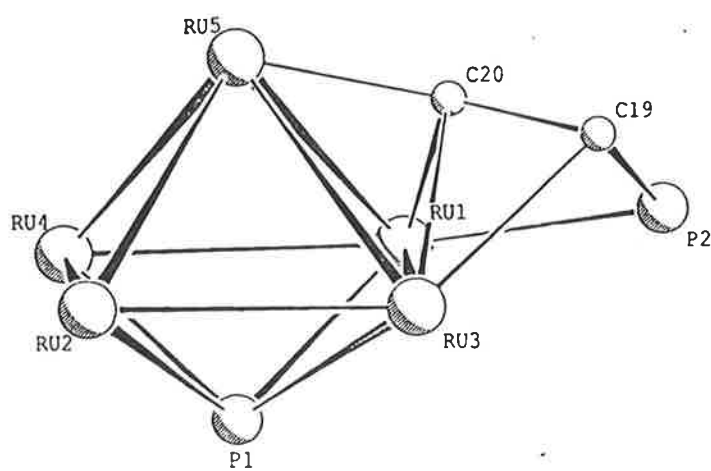
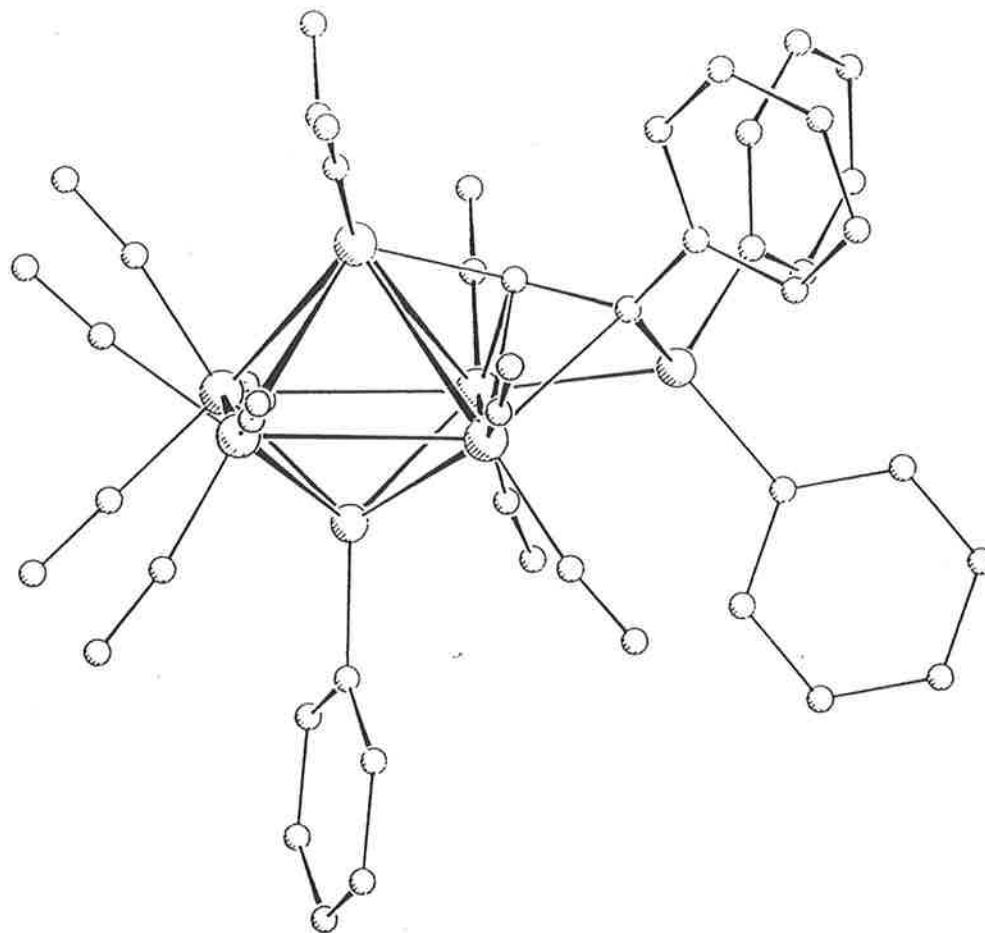


**Table 2.** Selected bond distances (Å) and angles (°) for (26)

Ru(1)-Ru(3)	2.776(4)	Ru(1)-Ru(4)	2.961(5)
Ru(1)-Ru(5)	2.826(5)	Ru(2)-Ru(3)	2.874(5)
Ru(2)-Ru(4)	2.870(5)	Ru(2)-Ru(5)	2.808(5)
Ru(3)-Ru(5)	2.832(6)	Ru(4)-Ru(5)	2.810(5)
Ru(1)-P(1)	2.44(1)	Ru(2)-P(1)	2.38(4)
Ru(3)-P(1)	2.36(1)	Ru(4)-P(1)	2.36(1)
P(2)-Ru(1)	2.33(1)	Ru(3)-C(19)	2.24(5)
Ru(1)-C(20)	2.08(4)	Ru(3)-C(20)	2.15(4)
Ru(5)-C(20)	1.88(5)	C(19)-P(2)	1.84(5)
C(19)-C(20)	1.45(6)		
Ru(3)Ru(1)Ru(4)	89.1(1)	Ru(3)Ru(2)Ru(4)	89.0(1)
Ru(1)Ru(3)Ru(2)	92.7(1)	Ru(1)Ru(4)Ru(2)	89.1(1)
Ru(1)Ru(5)Ru(2)	93.1(2)	Ru(3)Ru(5)Ru(4)	91.1(2)
Ru(3)C(19)P(2)	101(2)	Ru(1)P(2)C(19)	88(2)
Ru(3)C(19)C(20)	67(3)	Ru(1)C(20)Ru(3)	82(1)
Ru(1)C(20)Ru(5)	91(2)	Ru(3)C(20)Ru(5)	89(2)
Ru(1)C(20)C(19)	110(3)	Ru(3)C(20)C(19)	74(3)
Ru(5)C(20)C(19)	151(3)	P(2)C(19)C(20)	90(3)

**Figure 5.** PLUTO plot of  $\text{Ru}_5(\mu\text{-H})(\mu_4\text{-PPh})(\mu_4\text{-}\eta^4\text{-CCPh(C}_6\text{H}_4\text{)}) (\mu_3\text{-PPh})(\text{CO})_{10}$  (27)  
(by E.R.T. Tiekink)

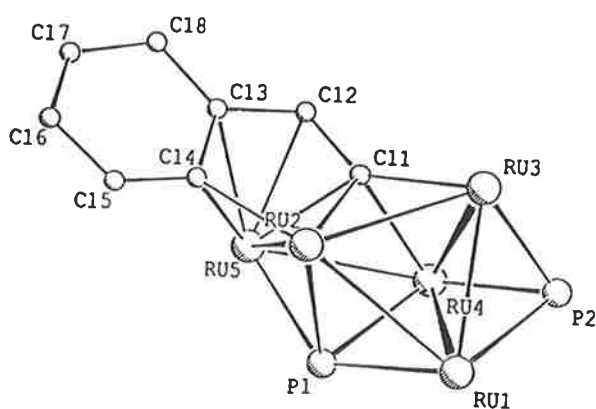
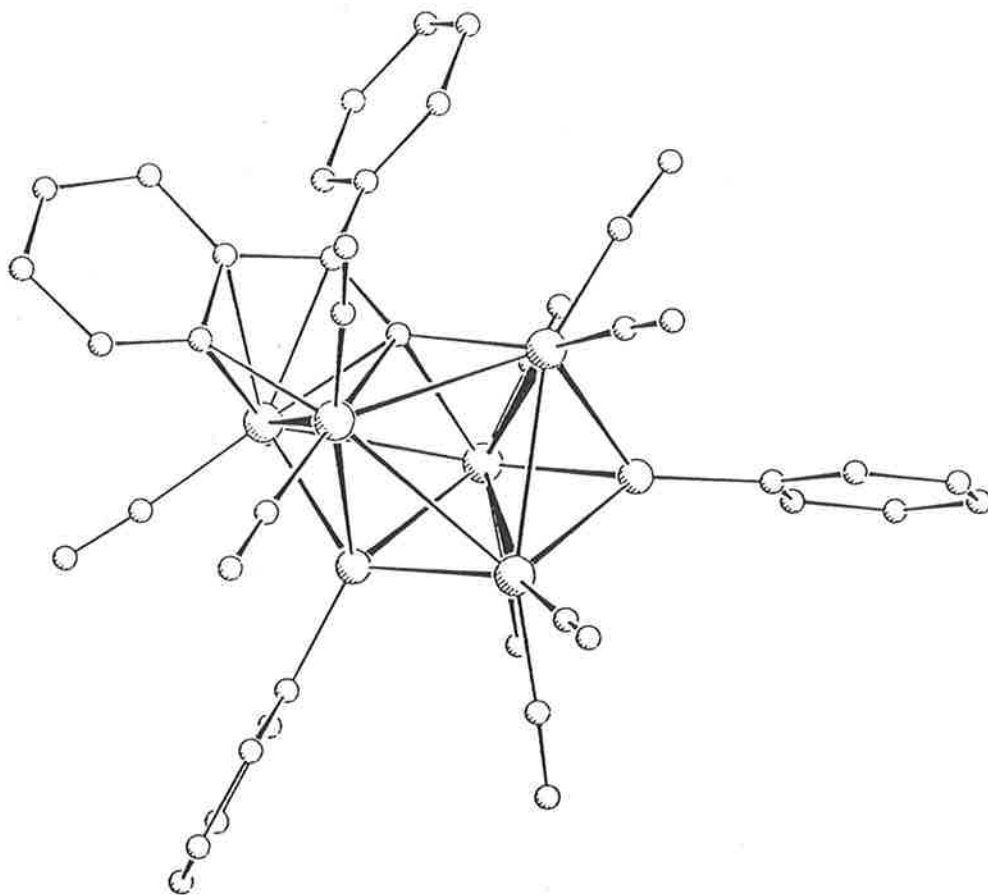


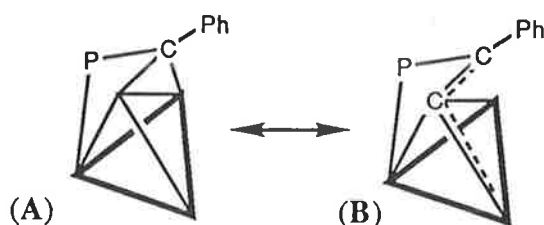
**Table 3.** Selected bond distances (Å) and angles (°) for (27)

Ru(1)-Ru(2)	3.065(1)	Ru(1)-Ru(3)	2.874(1)
Ru(1)-Ru(4)	2.840(1)	Ru(2)-Ru(4)	3.605(1)
Ru(2)-Ru(3)	2.895(1)	Ru(2)-Ru(5)	2.743(1)
Ru(3)-Ru(4)	2.855(1)	Ru(4)-Ru(5)	2.854(1)
Ru(1)-P(1)	2.300(3)	Ru(2)-P(1)	2.488(3)
Ru(4)-P(1)	2.479(3)	Ru(5)-P(1)	2.326(3)
Ru(1)-P(2)	2.280(3)	Ru(3)-P(2)	2.243(3)
Ru(4)-P(2)	2.273(3)	C(11)-Ru(2)	2.14(1)
Ru(3)-C(11)	2.09(1)	Ru(4)-C(11)	2.37(1)
Ru(5)-C(11)	2.25(1)	Ru(5)-C(12)	2.26(1)
Ru(5)-C(13)	2.33(1)	Ru(2)-C(14)	2.14(1)
Ru(5)-C(14)	2.23(1)	C(11)-C(12)	1.41(2)
C(12)-C(13)	1.47(2)	C(13)-C(14)	1.44(2)
Ru(2)Ru(1)Ru(4)	75.1(1)	Ru(1)Ru(2)Ru(5)	93.0(1)
Ru(3)Ru(2)Ru(5)	94.5(1)	Ru(2)Ru(3)Ru(4)	77.6(1)
Ru(1)Ru(4)Ru(5)	95.6(1)	Ru(3)Ru(4)Ru(5)	93.0(1)
Ru(2)Ru(5)Ru(4)	80.2(1)	Ru(1)P(1)Ru(5)	131.5(1)
Ru(2)P(1)Ru(4)	93.1(1)	Ru(1)P(2)Ru(3)	78.9(1)
Ru(1)P(2)Ru(4)	77.2(1)	Ru(3)P(2)Ru(4)	78.4(1)
Ru(2)C(11)Ru(4)	106.1(5)	Ru(3)C(11)Ru(5)	145.6(6)
C(11)C(12)C(13)	114(1)	C(12)C(13)C(14)	116(1)
C(13)C(14)Ru(2)	113.3(8)	C(13)C(14)Ru(5)	75.4(7)

The IR spectrum of (26) had an all-terminal  $\nu(\text{CO})$  seven-band pattern. No cluster-bound hydrides were found in the  $^1\text{H}$  NMR spectrum, which contained resonances for the phenyl groups between  $\delta$  7.9 and 6.8. In the  $^{13}\text{C}$  NMR spectrum of complex (26), only four CO signals were found at  $\delta$  202.6, 197.0, 192.6 and 192.3. The  $\text{C}_\alpha$  ( $\delta$  148.8, d,  $J_{\text{P-C}} = 15$  Hz) and the  $\text{C}_\beta$  ( $\delta$  109.2, multiplet) signals were in environments similar to those of  $\mu_3\text{-}\eta^2\text{-acetylide}$  cluster complexes.<sup>56</sup> The FAB mass spectrum showed a molecular ion at  $m/z$  1236 which fragmented by loss of ten CO groups.

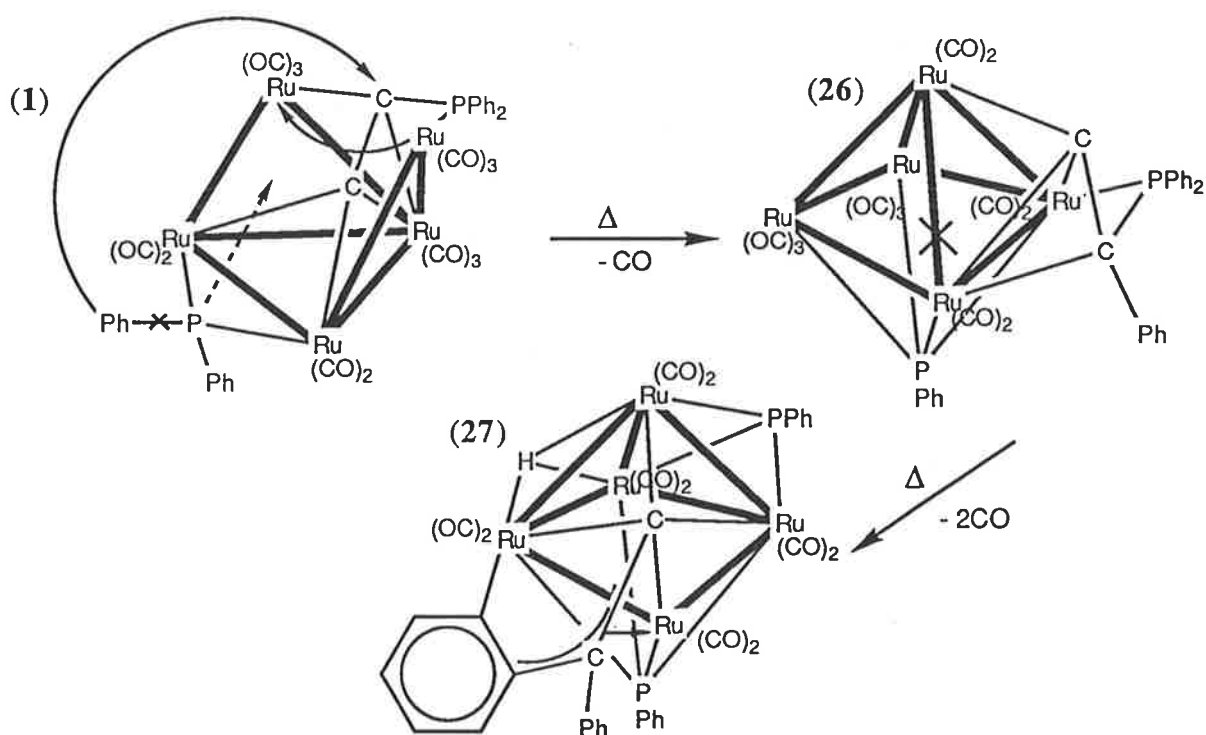
In the structure of (26), the five Ru atoms form a square pyramid, the square face of which is capped by a PPh group, equidistant from Ru(2), Ru(3) and Ru(4) [Ru-P<sub>av.</sub> 2.37 Å, RuPRu<sub>av.</sub> 74.6°] but somewhat further away from Ru(1) [2.44(1) Å]. The phosphino-vinylidene ligand is asymmetrically coordinated: C(20) is displaced towards Ru(5) [Ru(5)-C(20) 1.88(5) Å], while C(19) interacts rather weakly with Ru(3) [Ru(3)-C(19) 2.24(5) Å]. The C=C bond length [1.45(6) Å] is typical of cluster-bound vinylidenes.<sup>64</sup> Several carbonyls are bent (RuCO 162 - 169 °); these appear to reflect steric interactions within the cluster, since the Ru-C distances are clearly non-bonding (>3.0 Å). In terms of SEP electron counting, (26) is a 7-SEP, 74-electron *nido* octahedral cluster.

Cluster (26) is formed from (1) by P-C cleavage and phenyl migration to the acetylide, which generates a phosphino-vinylidene. Contraction of the open Ru<sub>5</sub> cluster found in (1) to the square-pyramidal arrangement in (26) occurs as a result of the loss of one CO ligand. A similar transformation occurs when Ru<sub>5</sub>( $\mu_4\text{-}\eta^2\text{-C}_2\text{Ph}$ )( $\mu\text{-PPh}_2$ )(CO)<sub>14</sub> (12) is warmed.<sup>20</sup> Formation of the CCPh(PPh<sub>2</sub>) ligand (A) occurs by formal cluster-assisted transfer of a phenyl group from the  $\mu\text{-PPh}_2$  group in (1) to the  $\beta$ -carbon of the phosphino-acetylide. Consideration of the Ru-C distances, particularly Ru(5)-C(20) and Ru(3)-C(19) (see above), suggests that a tautomeric methylidyne form of the ligand (B) may also be contributing to the structure. This



suggestion is supported by the close resemblance of the structure of (26) to that of  $\text{Ru}_5(\mu_4\text{-PPh})\{\mu_3\text{-CCH}_2(\text{i-Pr})\}(\mu\text{-PPh}_2)(\text{CO})_{12}$  (15),<sup>5</sup> which contains an alkylidyne capping a triangular face of a square pyramid. The formation of phosphinidene groups through phenyl loss has been noted previously,<sup>13</sup> and the migration of phenyl groups from phosphorus to carbon has been recognized as a metal-assisted process.<sup>65</sup> To our knowledge, however, this is the first occasion on which migration of a phenyl group from P to C to generate a vinylidene ligand has been demonstrated (see Scheme 5). Related compounds containing cluster-bound alkynes have already been synthesized, examples being (5)<sup>53</sup> and  $\text{Ru}_5(\mu_4\text{-PPh})(\mu_3\text{-}\eta^2\text{-PhC}_2\text{Ph})(\text{CO})_{13}$  (19).<sup>13</sup>

Scheme 5. Formation of (26) and (27) from (1)

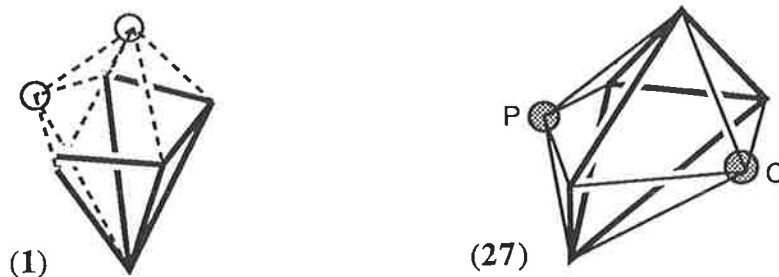


In the IR spectrum of (27), eight  $\nu(\text{CO})$  bands were found in the terminal region. A hydride resonance was found at  $\delta -15.38$  (dd,  $J_{\text{P-H}} = 10.3, 7.3$  Hz) and phenyl and  $\text{C}_6\text{H}_4$  resonances between  $\delta 7.9$  and  $6.1$  in the  $^1\text{H}$  NMR spectrum. The FAB mass spectrum of (27) had a molecular ion at  $m/z$  1181, which, in conjunction with analytical,  $^1\text{H}$  and  $^{31}\text{P}$  NMR data, allowed the formulation as  $\text{Ru}_5(\mu\text{-H})(\mu_4\text{-PPh})\{\mu_4\text{-}\eta^4\text{-CCPh}(\text{C}_6\text{H}_4)\}(\mu_3\text{-PPh})(\text{CO})_{10}$ . The

$^{31}\text{P}$  NMR data confirmed the presence of two phosphinidene groups with signals at  $\delta$  455.9 (d,  $J_{\text{P-P}} = 78$  Hz) and  $\delta$  480.4 (d,  $J_{\text{P-P}} = 80$  Hz), both of which were apparently in *trans* dispositions (on the basis of the observed couplings). In the  $^{13}\text{C}$  NMR spectrum of (27), the chemical shifts for  $\text{C}_\alpha$  ( $\delta$  243.2) and  $\text{C}_\beta$  ( $\delta$  117.1) are similar to those found in ruthenium acetylide clusters.<sup>13,56</sup> This suggests that the electronic differences between acetylide and vinylidene ligands on clusters are not large. Signals for seven different carbonyl environments were also observed (2 singlets, 4 doublets, 1 triplet) in the  $^{13}\text{C}$  NMR spectrum at room temperature. On the basis of the observed  $\text{C}_i$  symmetry for (27), 10 carbonyl environments are expected, so it appears that either some signals are accidentally degenerate or carbonyl scrambling is occurring.

In complex (27), the five ruthenium atoms define a arrowhead framework as found previously in many  $\text{Ru}_5\text{C}$  clusters (see Table 1, Section 1.1).<sup>24</sup> When the phosphorus and vinylidene  $\text{C}_\alpha$  atoms [P(1), C(11)] are included, the atom skeleton is that of a pentagonal bipyramid. A least-squares plane passes through P(1)Ru(5)C(11)Ru(3)Ru(1) (maximum deviations  $< 0.08$  Å), the atoms which define the pentagon. Distortion from the typical butterfly arrangement is evident in the metal framework of (27), with Ru(1)-Ru(2) [3.065(1) Å] longer than Ru(2)-Ru(3) [2.895(1) Å]. The  $\mu_3$ -phosphinidene displays a reasonably symmetrical disposition about the Ru(4)Ru(1)Ru(5) face in (27), while the  $\mu_4$ -phosphinidene is distorted towards Ru(1)Ru(5). The  $\mu_4$ -carbon is also asymmetrically bonded to a  $\text{Ru}_4$  face (Ru(2)-C(11) [2.14(1) Å], Ru(4)-C(11) [2.37(1) Å]). Presumably, the bonding interactions of the allyl system with the metal core affect the disposition of  $\text{C}_\alpha$ . The C=C bond length [1.41(3) Å] is comparable to those of other cluster-bound vinylidenes.<sup>64</sup> The vinylidene substituents are a phenyl ring and a metallated  $\text{C}_6\text{H}_4$  ring, the latter involved in an allylic interaction with Ru(5) [Ru(5)-C(12) 2.26(1) Å, Ru(5)-C(13) 2.33(1) Å, Ru(5)-C(14) 2.23(1) Å] and a  $\sigma$ -interaction with Ru(2) [Ru(2)-C(14) 2.14(1) Å].

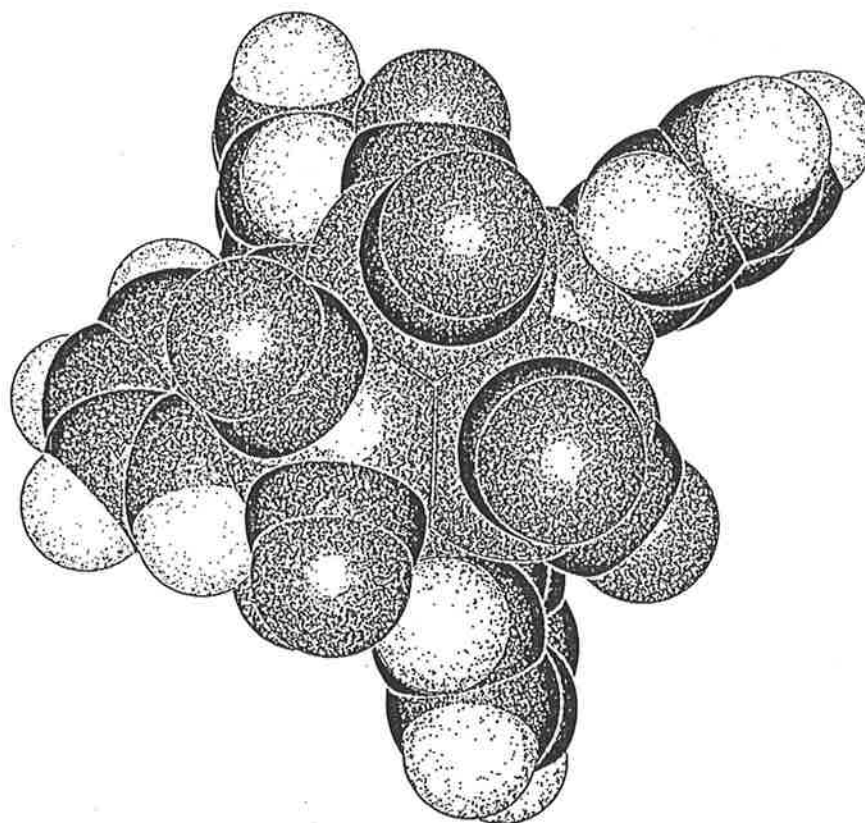
Structures (1) and (27) are both based on a pentagonal bipyramid. Complex (1) has an *arachno* structure and complex (27) a *closo* structure, although in each case it is different atoms that define the pentagon: Ru(1)Ru(2)Ru(3)Ru(4) (1) (other vertex missing), and



$P(1)Ru(5)C(11)Ru(3)Ru(1)$  (27). The formation of these clusters may therefore be thought of as demonstrating the interconversion between an open cluster (1), where the organic unit interacts with the surface, and a closed cluster (27), where the organic moiety is incorporated into the cluster.

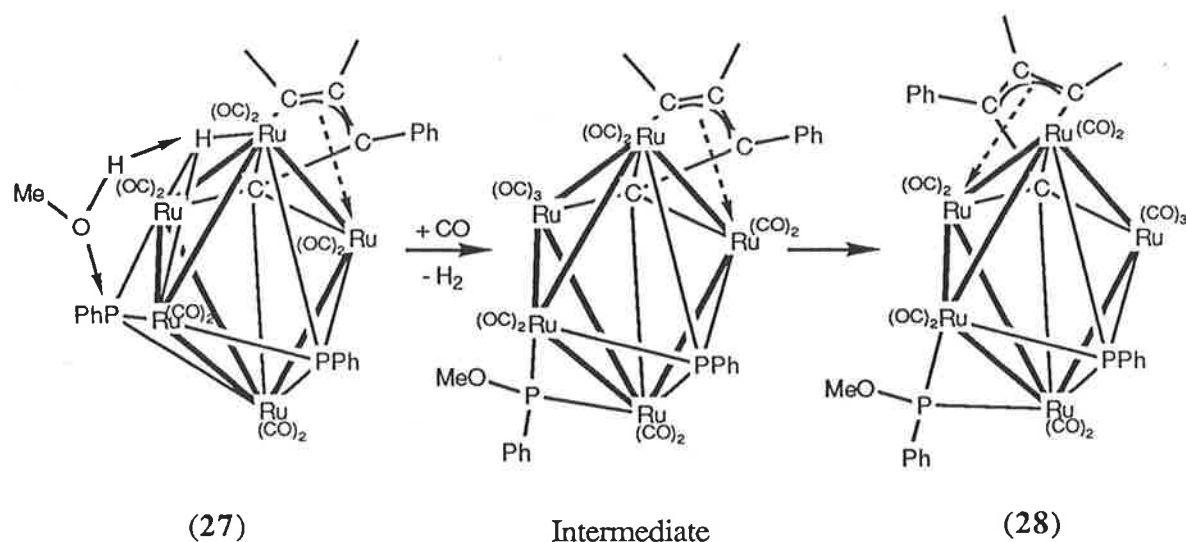
Although no other intermediates were detected, it is probable that the conversion from (1) to (27) proceeds by stepwise loss of the three carbonyl groups accompanied by skeletal rearrangements. In (27), the acetylide has been transformed, through phenyl migration (via P-C bond cleavage) into a vinylidene unit; this is coordinated via  $C_{\beta}$  and the metallated phenyl ring [C(12)C(13)C(14)] to Ru(5) and Ru(2). In the course of metallation, a hydrogen atom has been transferred to the cluster framework. Such a transfer has been noted previously in the formation of  $Os_3(\mu-H)\{\mu_3-(C_6H_4)PPh_2\}(CO)_8(PPh_3)$ .<sup>66</sup> The bond elongations Ru(1)-Ru(2) [3.065(1) Å], Ru(2)-Ru(3) [2.895(1) Å] (Ru-Ru<sub>av.</sub> 2.833 Å)<sup>67</sup> and coupling to two phosphinidene groups in the <sup>1</sup>H NMR hydride signal suggest that the hydride is  $\mu_3$ -bonding the Ru(1)Ru(2)Ru(3) face. This is also supported by structural similarities with the complex  $HRu_5(\mu_4-PPh)_2(\mu_3-PPh)(\mu-PPh_2)(CO)_{10}$  (16)<sup>5</sup> where the hydride was located on a similar face, and by the space-filling model of (27) (Figure 6) where the dispositions of the carbonyl ligands on the Ru(1)Ru(2)Ru(3) face reveal a cavity in which the  $\mu_3$ -H atom could reside.<sup>68</sup>

**Figure 6.** JACKAL space filling plot of (27) [view showing Ru(1)Ru(2)Ru(3) face].



When (27) was stirred for twenty-four hours in methanol, transformation to  $\text{Ru}_5(\mu_4\text{-PPh})\{\mu_4\text{-}\eta^4\text{-CCPh(C}_6\text{H}_4)\}\{\mu\text{-PPh(OMe)}\}(\text{CO})_{11}$  (28) occurred; the brown product was isolated in 38% yield after thin layer chromatography. In the proton NMR a doublet at  $\delta$  3.14 ( $J_{\text{P-H}} = 14.2$  Hz) indicated the presence of a Me group coupled to phosphorus; no metal-hydride ligands were present. The FAB mass spectrum confirmed that addition of 'MeO' and CO had occurred, with a molecular ion at  $m/z$  1238. Eight carbonyl resonances (5 singlets, 1 doublet, 2 multiplets) were observed in the  $^{13}\text{C}$  NMR spectrum of (28) at room temperature. On the basis of the observed  $\text{C}_i$  symmetry for (28) (see Figure 7), it appears that either some signals are accidentally degenerate or that carbonyl scrambling is occurring. The  $\alpha$ - and  $\beta$ -carbon environments ( $\delta$  258.4, 107.7, resp.) are similar to those of complex (27). A second brown band that was collected quickly converted into (28) (15 min for total conversion in  $\text{CH}_2\text{Cl}_2/\text{cyclohexane}$  solution, at 25 °C). The speed of the conversion precluded a detailed

Scheme 6. Reaction of (27) with MeOH to form (28)



characterization of this band, but data provided by the FAB mass spectrum, low temperature  $^1\text{H}$  and  $^{31}\text{P}$  NMR led us to give this complex the same formulation as (28). This isomer is probably related to (28) by a structural transformation such as is shown in Scheme 6. The origin of the extra CO ligand in (28) has not been determined, but because of the large amount of decomposition observed in the reaction, it seems likely that intermolecular CO transfer is involved. The other eight minor bands and a large amount of intractable material on the base of the TLC plates were not isolated. A X-ray crystal structure determination was carried out on (28), and it confirmed the addition of 'MeO' to a PPh ligand to form the  $\mu$ -phosphido group. The molecular structure is shown in Figure 7 and bond distances and angles are listed in Table 4.

Compounds (27) and (28) share a common metal core, the five ruthenium atoms defining, as noted above, a wingtip-bridged butterfly framework. When the phosphorus and  $\text{C}_\alpha$  vinylidene carbon atoms [P(1), C(13)] are included in the atom skeleton of complex (28), the geometry is again that of a pentagonal bipyramid with a least-squares plane passing through P(1)Ru(5)C(13)Ru(3)Ru(1) (maximum deviations  $< 0.13 \text{ \AA}$ ). An appreciable interaction was found between Ru(2) and Ru(4) in both structures [ $3.605(1) \text{ \AA}$  (27),  $3.596(1) \text{ \AA}$  (28)], as is also implied in each case by the relatively small angles subtended at the bridgehead atoms [Ru(2)Ru(5)Ru(4)  $80.2(1)^\circ$  (27),  $76.9(1)^\circ$  (28)] and the small dihedral angle at the hinge

Figure 7. PLUTO plot of  $\text{Ru}_5(\mu_4\text{-PPh})\{\mu_4\text{-}\eta^4\text{-CCPh(C}_6\text{H}_4)\}\{\mu\text{-PPh(OMe)}\}(\text{CO})_{11}$ .  
 $2\text{MeOH}\cdot\text{H}_2\text{O}$  (28)

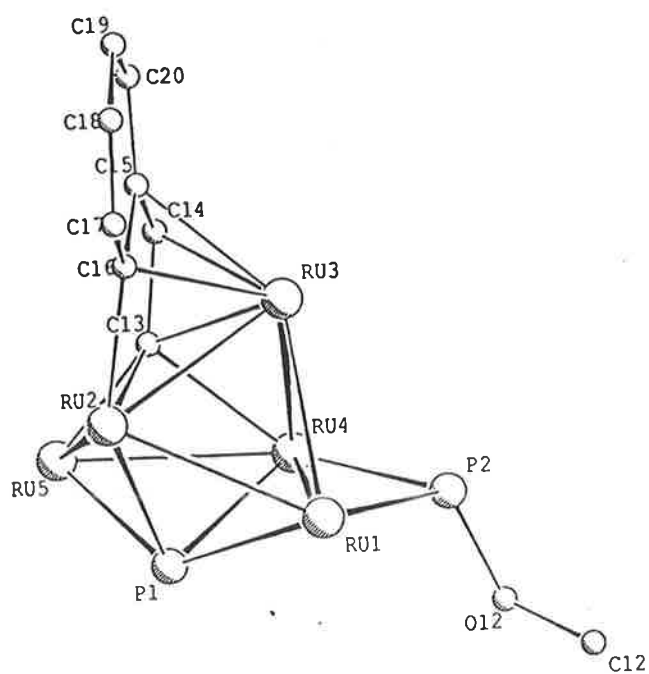
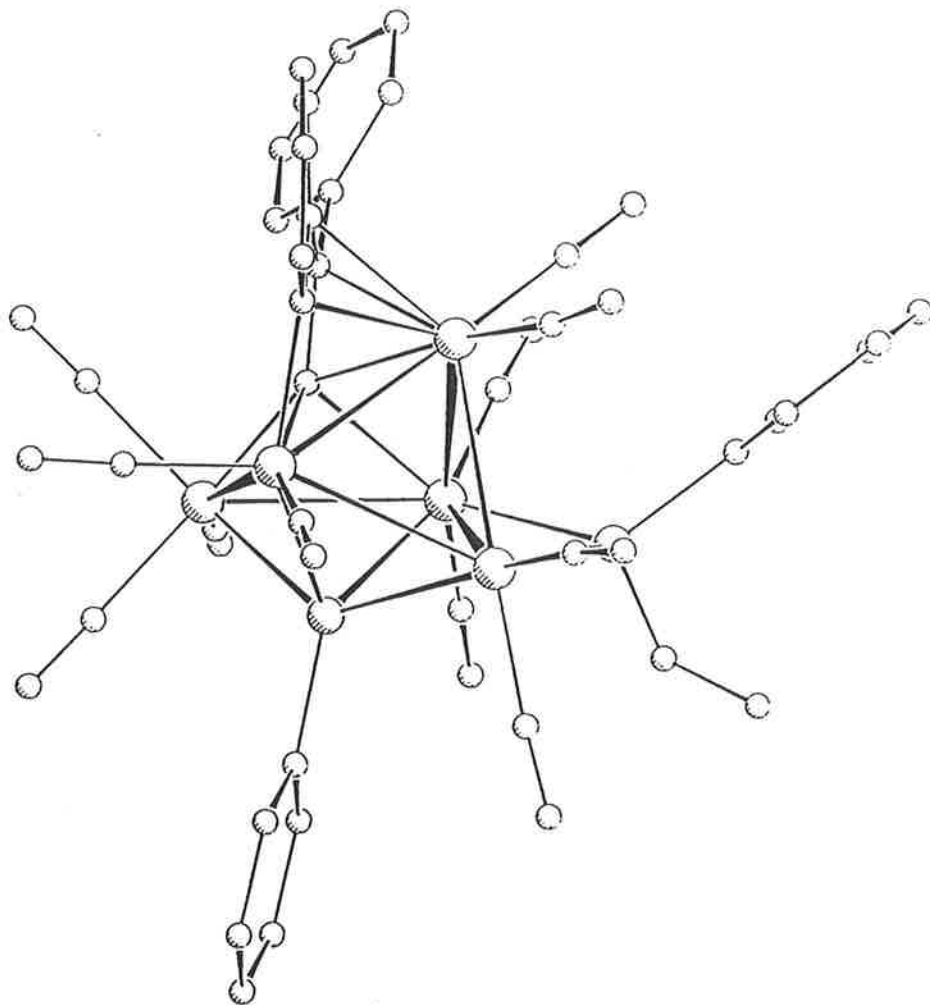


**Table 4.** Selected bond distances (Å) and angles (°) for (28)

Ru(1)-Ru(2)	2.929(2)	Ru(1)-Ru(3)	2.820(2)
Ru(1)-Ru(4)	2.811(2)	Ru(2)-Ru(3)	2.752(2)
Ru(2)-Ru(4)	3.596(2)	Ru(2)-Ru(5)	2.842(2)
Ru(3)-Ru(4)	2.902(2)	Ru(4)-Ru(5)	2.941(2)
Ru(1)-P(1)	2.394(4)	Ru(2)-P(1)	2.370(4)
Ru(4)-P(1)	2.484(4)	Ru(5)-P(1)	2.357(4)
Ru(1)-P(2)	2.225(5)	Ru(4)-P(2)	2.256(5)
Ru(2)-C(13)	2.18(2)	Ru(3)-C(13)	2.19(1)
Ru(4)-C(13)	2.41(2)	Ru(5)-C(13)	2.05(1)
Ru(3)-C(14)	2.21(1)	Ru(3)-C(15)	2.30(2)
Ru(2)-C(16)	2.07(1)	Ru(3)-C(16)	2.29(2)
P(2)-O(12)	1.65(1)	O(12)-C(12)	1.38(2)
C(13)-C(14)	1.41(2)	C(14)-C(15)	1.51(2)
C(15)-C(16)	1.45(2)		
Ru(1)Ru(2)Ru(5)	96.8(1)	Ru(2)Ru(3)Ru(4)	78.9(1)
Ru(1)Ru(4)Ru(5)	97.2(1)	Ru(3)Ru(4)Ru(5)	88.9(1)
Ru(2)Ru(5)Ru(4)	76.9(1)	Ru(1)P(1)Ru(5)	130.7(2)
Ru(2)P(1)Ru(4)	95.6(1)	Ru(1)P(2)Ru(4)	77.7(1)
Ru(2)C(13)Ru(4)	102.9(6)	Ru(3)C(13)Ru(5)	149.5(8)
Ru(2)C(16)Ru(3)	78.1(5)	Ru(2)C(16)C(15)	120(1)
Ru(3)C(16)C(15)	71.9(9)	P(2)O(12)C(12)	119(1)
C(13)C(14)C(15)	112(1)	C(14)C(15)C(16)	113(1)

[90.5°(27), 93.0°(28)]. These appear to be the first examples of  $M_5$  clusters that are held together by both  $\mu_4$ -vinylidene and  $\mu_4$ -phosphinidene groups to form *closo* structures. In (28), the effect of the phosphinidene and phosphido groups bridging Ru(1)-Ru(4) is to shorten this bond [2.840(1) Å (27), 2.811(2) Å (28), resp.]; Ru(1)-Ru(2) [2.929(2) Å] and Ru(2)-Ru(3) [2.752(2) Å] are also shorter than in (27). The difference in the latter two bond lengths in similar  $Ru_5C$  clusters is typically only 0.01 Å.<sup>24</sup> The distortion of the  $\mu_4$ -phosphinidene in complex (28) is towards Ru(2)Ru(5).

The  $\alpha$ -carbon is asymmetrically bonded to the  $Ru_4$  face with Ru(2)-C(13) much shorter than Ru(4)-C(13) [2.18(2) Å; 2.41(2), Å resp.]. The C=C bond length [1.41(2) Å] is comparable to that in (27) [1.41(3) Å]. Complexes (27) and (28) are the first examples of clusters containing a  $\mu_4$ - $\eta^3$  vinylidene without a hydrogen substituent on  $C_\beta$ . The switch of the allyl interaction from Ru(5) (27) to Ru(3) (28) occurs as a result of the new bonding requirements and the formation of the alkoxyphosphido group. The rearrangement shown in Scheme 6 is postulated because it assumes the smallest number of bonds broken/formed in the course of the reaction. The addition of methanol to the phosphinidene in (27) appears to be without precedent,<sup>69</sup> and presumably occurs through nucleophilic attack by the methoxy group in conjunction with hydrogen transfer to the cluster, followed by loss of  $H_2$ .

### 3.2.3. CO substitution by $P(OEt)_3$ in (1)

Two routes to carbonyl substitution in (1) by  $P(OEt)_3$  were investigated: (i) trimethylamine oxide-promoted, and (ii) thermally assisted. The first method involved treating an acetone solution of (1) with  $Me_3NO$  and  $P(OEt)_3$  at 0 °C. The two products isolated from this reaction were found to be isomers of  $Ru_5(\mu_5-\eta^2, P-C_2PPh_2)(\mu-PPh_2)(CO)_{12}\{P(OEt)_3\}$ , (29a) and (29b). A third isomer of this complex, (29c), was the major product isolated from the thermal reaction of (1) with  $P(OEt)_3$  in cyclohexane at 45 °C. From the latter reaction, (29a), (29b) and a disubstituted product  $Ru_5(\mu_5-\eta^2, P-C_2PPh_2)(\mu-PPh_2)(CO)_{11}\{P(OEt)_3\}_2$  (30) were also formed. When the thermal reaction was carried out in acetone, a lower yield of (29c) and a higher yield of (30) were obtained. A side product,  $Ru_5(CO)_{14}(dppa^*)\{P(OEt)_3\}$ , obtained in

this last reaction was apparently formed by ligand substitution of (6k); the appearance of the IR spectrum suggests that the product may be related structurally to isomer (6t).

The four complexes (29a) - (29c) and (30) are dark brown crystalline solids, which were characterized in the first instance by spectroscopy and microanalysis and later by X-ray studies for (29a), (29c) and (30). The FAB mass spectra for the three monosubstituted isomers showed molecular ions at  $m/z$  1402, followed by loss of twelve CO ligands. The molecular ion for (30) at  $m/z$  1542 fragmented by loss of nine CO groups. Proton NMR spectra for the complexes exhibited signals between  $\delta$  8.1 and  $\delta$  7.2 for the phenyl groups. Two multiplets were found for each P(OEt)<sub>3</sub> ligand. The low field multiplet for the phosphite ligand [ $\delta$  3.92 (29a); 4.03 (29b); 3.41 (29c); 3.92(P3)<sup>†</sup>, 3.77(P4) (30)] was assigned to the CH<sub>2</sub> groups and in some cases was coupled to the phosphorus as well as to the CH<sub>3</sub> groups. A quintet was found for this signal in complexes (29a) and (29b). Complex (29a) does not have a phosphido-group attached to the phosphite-bound ruthenium. The quintet, therefore, appears as a result of two overlapping quartets, and accords with each proton on the CH<sub>2</sub> group being slightly inequivalent. Of the two CH<sub>2</sub> signals found for (30), the pseudo-quartet at  $\delta$  3.92 was assigned to P(3), as it showed coupling to P(1), and the quintet at  $\delta$  3.77 was assigned to P(4). The fourteen-line pattern at  $\delta$  3.41 in (29c) is a result of long range coupling. A detailed theoretical account of X<sub>n</sub>AA'X'<sub>n</sub> coupling patterns has been given by Harris<sup>70</sup> for complexes containing two P-donor ligands at a metal centre. From this it is apparent that an Y<sub>9</sub>X<sub>6</sub>AA'X'<sub>6</sub>Y'<sub>9</sub> spin system would be very complex. For small  $J_{AA'}$  the spectrum will tend towards the first-order spectrum, which for the CH<sub>2</sub> signal is a quartet ( $J_{H-H}$ ) of doublets ( $J_{P-H}$ ) of doublets ( $J_{P'-H}$ ), as observed for complexes (29c) and (30).

The location of the phosphite in (29b) was established on the basis of the spectroscopic data. The sites available include Ru(1), Ru(2), Ru(5) [see below for results for (29a) and (29c)] and the acetylide. It has been established that nucleophilic attack of

---

<sup>†</sup> For common numbering scheme see Figures 8-10.

phosphine ligands can occur at the  $\alpha$ -carbon of  $\mu_3$ - $\eta^2$ -acetylide and vinylidene ligands; this may be followed by transfer of the phosphorus ligand to the metal core.<sup>71,72</sup> A substantial study of mono- and bis-substituted triruthenium clusters<sup>73</sup> found no evidence for the presence of isomers formed through substitution at the different equatorial positions on the same metal site. The <sup>31</sup>P NMR spectrum for complex (29b) showed that there were other isomers of this complex (with near-identical signals) present in solution (see Table 13, Section 3.2.11). The environment for P(1) ( $\delta$  43.5) was very similar to that of (29c) ( $\delta$  43.9), although the P(2) and P(3) environments had changed substantially [ $\delta$  300.0, 134.1, resp. (29b); 292.5, 137.6, resp. (29c)], and phosphorus-phosphorus coupling was apparent ( $J_{av.} = 34.5$  Hz). In the IR spectrum the  $\nu(\text{CO})$  pattern was similar to that of (29a), and a bridging carbonyl absorption was found at 1801  $\text{cm}^{-1}$ . A bridging carbonyl absorption at 1791  $\text{cm}^{-1}$  was also found for (30), where the CO bridges the Ru(1)-Ru(5) bond. Complex (30), which has been shown to be substituted at Ru(1) and Ru(4), was the major product obtained from the reaction of (29b) with further  $\text{P}(\text{OEt})_3$ . These observations lead us to believe that in the formation of (29b), phosphite substitution took place at Ru(1), with the phosphite *trans* to the phosphino-acetylide.

X-ray crystallographic studies were carried out for complexes (29a), (29c) and (30) to determine their molecular structures. Figures 8 - 10 illustrate the three molecules, and Table 5 collects significant bond distances and angles.

All three structures share the same open metal framework with (1), which comprises three edge-fused  $\text{Ru}_3$  triangles. Thermal reaction was seen to favour mono-substitution at Ru(3), a basal ruthenium, whereas  $\text{Me}_3\text{NO}$ -promoted reaction resulted in wingtip-substitution at Ru(4). The identity of the third monosubstituted isomer (29b) can only be inferred from spectroscopic data, as this complex was not stable in solution for prolonged periods. The bis-triethylphosphite complex (30) was substituted at the wingtip rutheniums Ru(1) and Ru(4). Conversion between these products is illustrated in Scheme 7. The Ru-Ru bonds are in the ranges 2.754(1) - 2.901(1) Å (29a), 2.747(1) - 2.958(1) Å (29c) and 2.828(3) - 3.009(2) Å (30). The monosubstituted clusters have a shortest bond in common with (1), *viz.* Ru(2)-Ru(3), the bond bridged by the phosphido group.

**Figure 8.** PLUTO plot of  $\text{Ru}_5(\mu_5\text{-}\eta^2\text{-}P\text{-C}_2\text{PPh}_2)(\mu\text{-PPh}_2)(\text{CO})_{12}\{\text{P}(\text{OEt})_3\}$  (**29a**)  
(by B.W. Skelton and A.H. White)

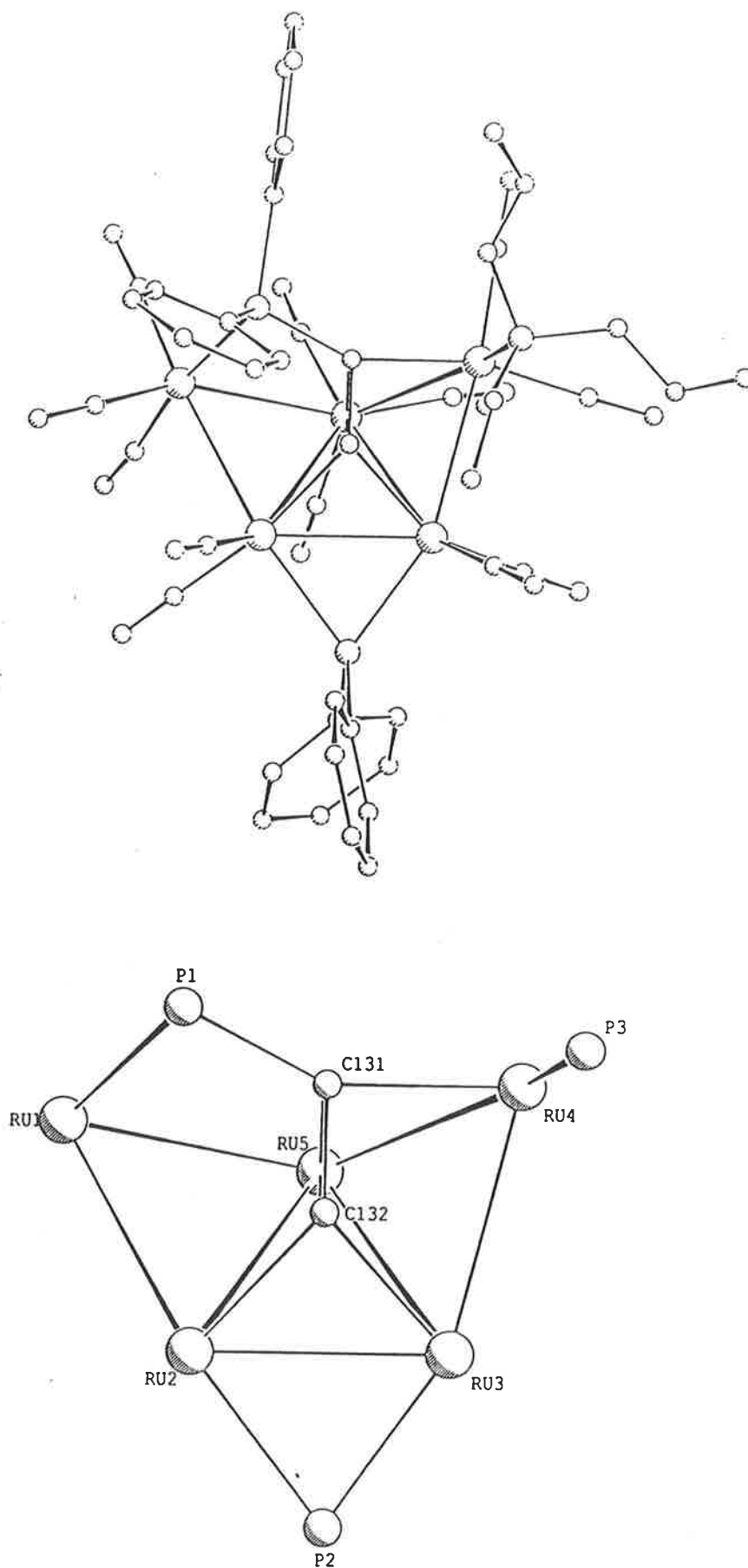


Figure 9. PLUTO plot of  $\text{Ru}_5(\mu_5\text{-}\eta^2\text{-}P\text{-C}_2\text{PPh}_2)(\mu\text{-PPh}_2)(\text{CO})_{12}\{\text{P}(\text{OEt})_3\}$  (29c)

(by E.R.T. Tiekink)

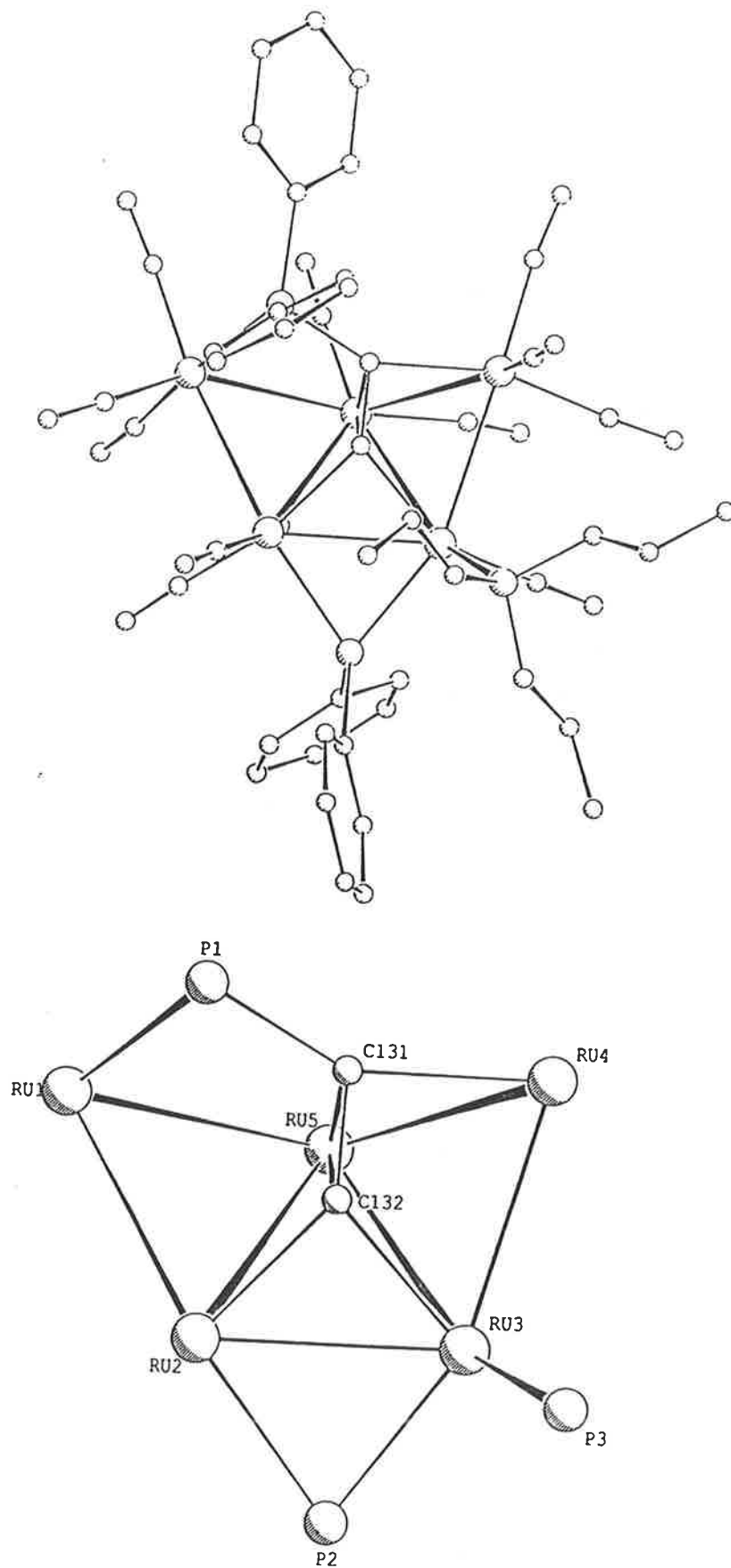
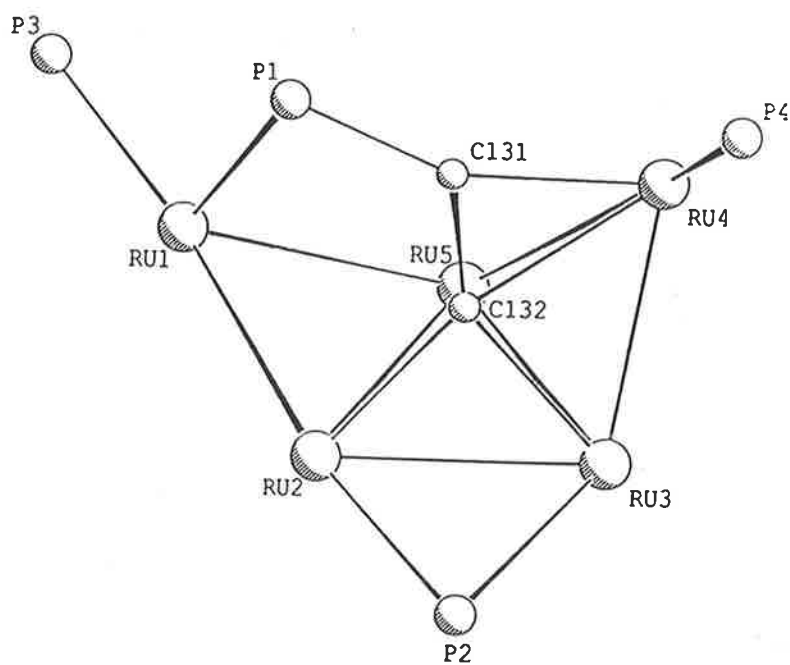
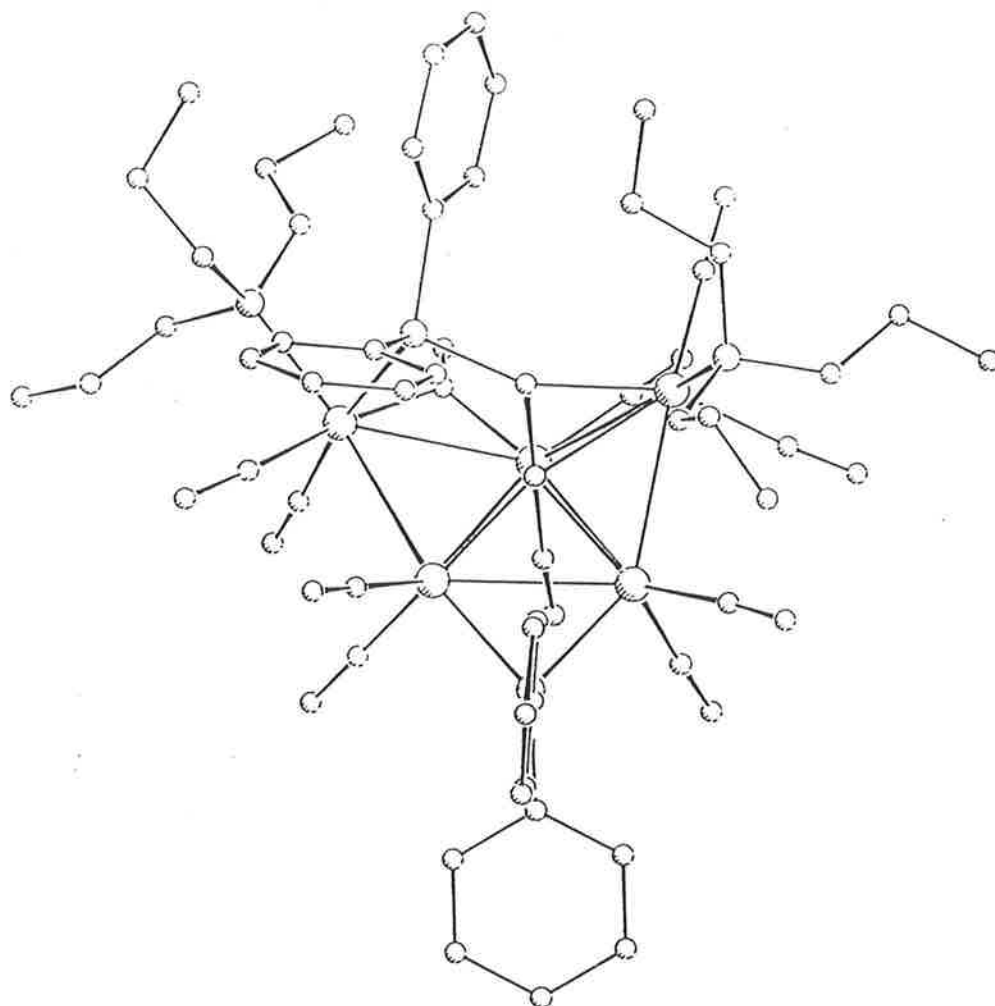


Figure 10. PLUTO plot of  $\text{Ru}_5(\mu_5\text{-}\eta^2\text{-}P\text{-C}_2\text{PPh}_2)(\mu\text{-PPh}_2)(\text{CO})_{11}\{\text{P}(\text{OEt})_3\}_2$  (**30**)

(by B.K. Nicholson)



**Table 5.** Selected bond distances (Å) and angles (°) for complexes (29a), (29c) and (30)

Parameter	Structure		
	(29a)(a)	(29c)(b)	(30)(c)
Ru(1)-Ru(2)	2.898(1)	2.894(1)	3.009(2)
Ru(1)-Ru(5)	2.882(1)	2.932(1)	2.891(1)
Ru(2)-Ru(3)	2.754(1)	2.747(1)	2.849(1)
Ru(2)-Ru(5)	2.878(1)	2.882(1)	2.854(2)
Ru(3)-Ru(4)	2.901(1)	2.872(1)	2.855(1)
Ru(3)-Ru(5)	2.901(1)	2.958(1)	2.870(2)
Ru(4)-Ru(5)	2.841(1)	2.857(1)	2.828(3)
Ru(1)-P(1)	2.369(2)	2.368(2)	2.391(6)
Ru(2)-P(2)	2.346(3)	2.351(3)	2.283(5)
Ru(3)-P(2)	2.266(3)	2.271(2)	2.251(4)
Ru(1)-P(3)	-	-	2.273(5)
Ru(3)-P(3)	-	2.220(2)	-
Ru(4)-P(3)	2.242(2)	-	-
Ru(4)-P(4)	-	-	2.246(7)
Ru(4)-C(131)	2.088(9)	2.089(8)	2.07(1)
Ru(5)-C(131)	2.323(6)	2.240(9)	2.30(2)
Ru(2)-C(132)	2.092(8)	2.081(8)	2.14(1)

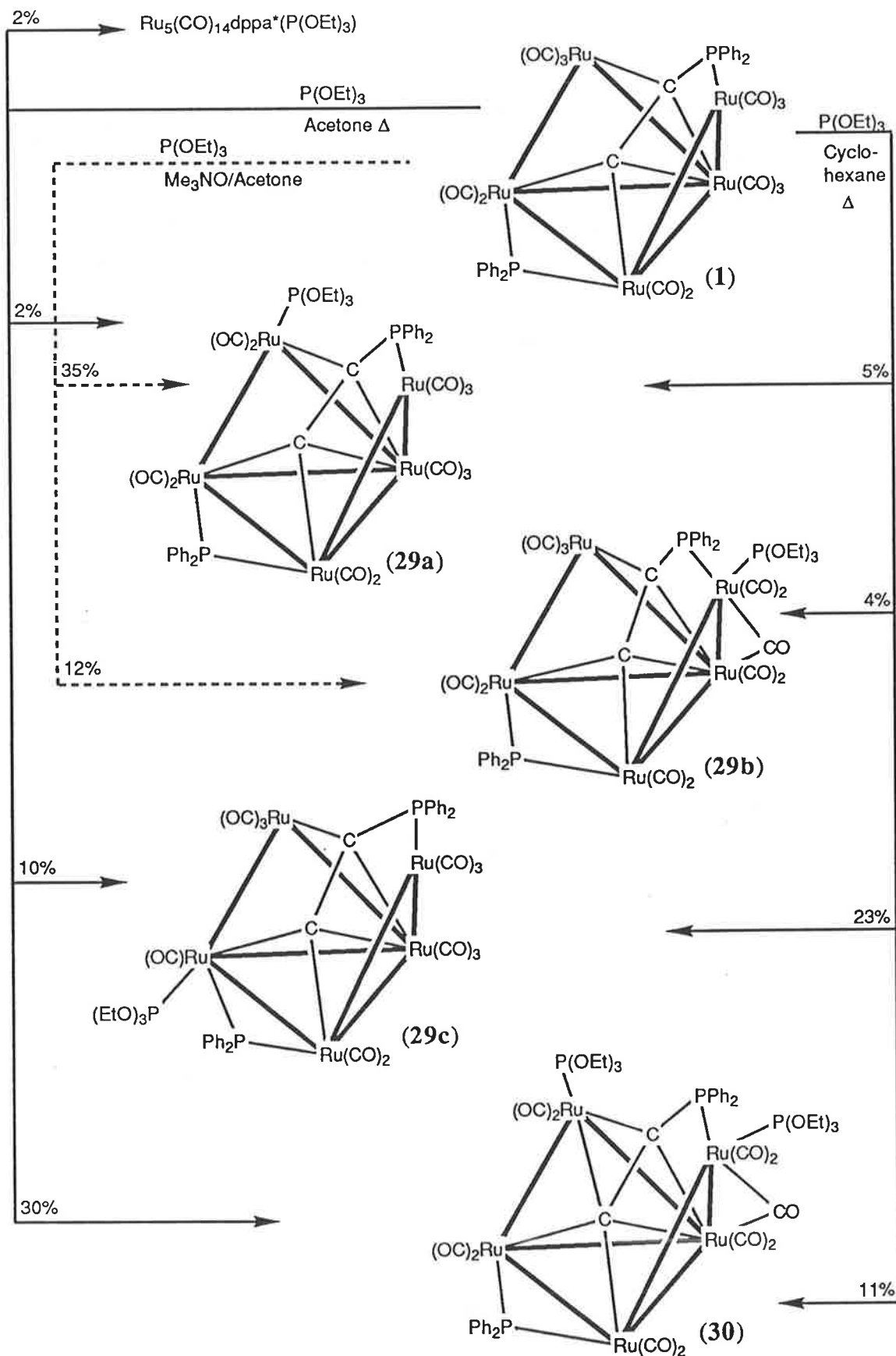
a) Ru(4)-C(51) 2.549(8); Ru(5)-C(51) 1.89(1); Ru(4)C(51)O(51) 123.0(7);  
Ru(5)C(51)O(51) 159.0(7).

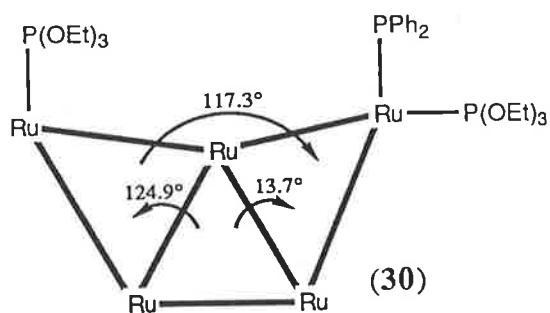
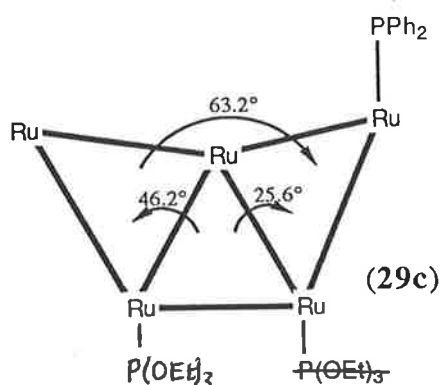
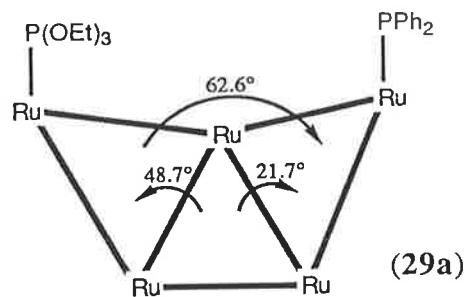
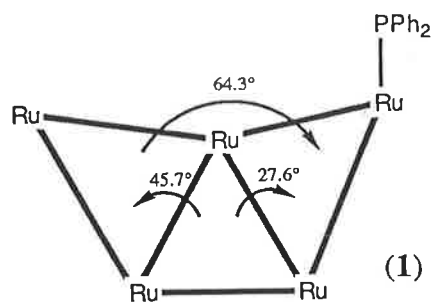
(b) Ru(4)-C(51) 2.64(1) Å; Ru(5)-C(51) 1.94(1) Å; Ru(4)C(51)O(51) 123.2(8);  
Ru(5)C(51)O(51) 161.2(9).

(c) Ru(1)-C(52) 2.15(2); Ru(5)-C(52) 2.02(2);  
Ru(1)C(52)O(52) 135(1); Ru(5)C(52)O(52) 136(1).

Table 5. (continued)

<u>Parameter</u>	<u>Structure</u>		
	(29a)	(29c)	(30)
Ru(3)-C(132)	2.048(8)	2.051(9)	2.13(1)
Ru(4)-C(132)	2.487(9)	2.507(8)	2.33(1)
Ru(5)-C(132)	2.183(7)	2.165(8)	2.22(3)
C(131)-C(132)	1.35(1)	1.33(1)	1.35(2)
P(1)-C(131)	1.759(9)	1.773(9)	1.78(1)
Ru(2)Ru(1)Ru(5)	59.72(3)	59.3(1)	57.8(1)
Ru(1)Ru(2)Ru(3)	118.24(4)	119.2(1)	118.1(1)
Ru(2)Ru(3)Ru(4)	103.97(4)	105.0(1)	99.7(1)
Ru(3)Ru(4)Ru(5)	60.69(3)	62.2(1)	60.7(1)
Ru(1)Ru(5)Ru(4)	118.67(3)	117.6(1)	121.3(1)
Ru(1)P(1)C(131)	97.0(2)	94.4(3)	99.6(6)
Ru(2)P(2)Ru(3)	73.29(7)	72.9(1)	77.9(2)
Ru(2)C(132)Ru(3)	83.4(3)	83.3(3)	83.5(4)
Ru(2)C(132)Ru(5)	84.6(2)	85.5(3)	81.8(8)
Ru(3)C(132)Ru(5)	86.5(3)	89.1(4)	82.6(8)
Ru(5)C(131)P(1)	107.3(3)	111.4(3)	105.9(9)
Ru(4)C(131)Ru(5)	80.0(3)	82.5(3)	80.4(5)
Ru(4)C(131)P(1)	153.0(5)	152.2(5)	157.9(7)
C(131)Ru(5)C(132)	34.6(3)	35.0(3)	34.8(5)
P(1)C(131)C(132)	116.8(7)	115.6(6)	119.3(9)

Scheme 7. Reaction of (1) with  $P(OEt)_3$ 



The introduction of two phosphite ligands flattens out the swallow structure; this may be seen by comparing the dihedral angles between the  $\text{Ru}_3$  planes. The addition of the phosphite ligands is seen to lengthen the metal-metal bonds slightly in complexes (29c) and (30) [ $\text{Ru-Ru}_{\text{av}}$ , 2.869 Å (1), 2.865 Å (29a), 2.877 Å (29c), 2.879 Å (30)]. This effect is not as pronounced as it is in triruthenium clusters,<sup>73</sup> and suggests that the pentaruthenium clusters are able to redistribute electron density more effectively. The redistribution is also accomplished in part by the presence of semibridging and bridging carbonyl ligands. Semibridging carbonyls were found between Ru(4) and Ru(5) [Ru(5)C(51)O(51)  $159.0(7)^\circ$ ,  $161.2(9)^\circ$  (29a) and (29c), resp.; Ru(4)-C(51) 2.549(8) Å, 2.64(1) Å, (29a) and (29c), resp.]. In complex (30), an asymmetric bridging carbonyl was found between Ru(1) and Ru(5) [Ru(1)-C(52) 2.15(2) Å, Ru(5)-C(52) 2.02(2) Å]. The phosphido, phosphite and phosphino-acetylde Ru-P distances are in the ranges 2.242(2) - 2.369(2) Å (29a), 2.220(2) - 2.368(2) Å (29c), 2.246(7) - 2.391(6) Å (30), with the longest values being obtained for the phosphines and the shortest values for the phosphite ligands. Coordination of the phosphino-acetylde to the metal core is essentially the same as in (1); Ru-C distances are 2.048(8) - 2.323(6) Å (29a), 2.051(9) - 2.240(9) Å (29c) and 2.07(1) - 2.33(2) Å (30), the shorter bonds being Ru(2)-C(132), Ru(3)-C(132) and Ru(4)-C(131). For (29a) and (29c), the interaction between

C(132) and Ru(4) is non-bonding [2.487(9) Å, 2.507(8) Å, resp.], whereas in (30) the distance of 2.33(2) Å indicates a rather long Ru-C bond. The acetylide C≡C distances are 1.35(1) Å (29a), 1.33(1) Å (29c) and 1.35(2) Å (30), all slightly shorter than the 1.383(6) Å found for (1).

It seems likely that all five ruthenium sites were available for substitution, as several other minor products were also noted in the reactions with P(OEt)<sub>3</sub>. The thermal substitution at Ru(3) suggests that the carbonyl ligands on Ru(3) are the most labile, presumably as a result of electronic and steric effects.<sup>74</sup> This does, however, suppose the phosphite is attached to the ruthenium from which CO dissociation has occurred. Previous studies on phosphite substitution reactions of Fe<sub>2</sub>O<sub>s</sub>(CO)<sub>12</sub><sup>75</sup> have indicated that this is not always the case.

Changing the solvent polarity for the thermal reactions resulted in different yields of the same products (see Scheme 7). Thus, in cyclohexane, the ratio of (29c) to (30) was 23%:11%, whereas in acetone the ratio was 10%:30%. Separate experiments have demonstrated that the formation of (30) does not proceed through (29c), and that the isomers of (29) do not interconvert in solution. The disubstituted cluster (30) may be formed through substitution of either (29a) or (29b). The addition of *P*-donor ligands to metal carbonyl clusters has been shown to accelerate the CO-substitution process in some cases.<sup>74-79</sup> Such acceleration may be involved in the formation of (30), which occurred even with a 1:1 ratio of reactants. Under conditions similar to those used in the formation of (30) from (1), complete reaction of isomers (29a), (29b) and (29c) with P(OEt)<sub>3</sub> required an excess of the ligand and longer times. The rates of these reactions need to be investigated to determine whether phosphite substitution does result in acceleration of CO dissociation from (1), or if multiple CO loss is involved to form an intermediate such as 'Ru<sub>5</sub>(CO)<sub>11</sub>(dppa\*)'.

These results suggest that the Me<sub>3</sub>NO-promoted reaction proceeded via the generation of unstable 'Ru<sub>5</sub>(CO)<sub>12</sub>(dppa\*)' intermediates.<sup>80</sup> The attack of Me<sub>3</sub>NO on cluster carbonyl ligands has been shown to occur by nucleophilic attack on the C atom of the carbonyl ligand.<sup>80</sup> Formation of (29a), (29b) and (30) suggests that the most electrophilic carbonyls are those on Ru(1) and Ru(4). Further reaction with Me<sub>3</sub>NO/P(OEt)<sub>3</sub> was not observed. The thermal

reactions proceeded through dissociative CO loss<sup>77,81,82</sup> at Ru(1), Ru(3) or Ru(4) to generate 'Ru<sub>5</sub>(CO)<sub>12</sub>(dppa\*)' intermediates, which then underwent phosphite addition to form (29a), (29b) and (29c). The most favoured pathway was that resulting in the formation of (29c). A competing process involved in the thermal reactions was the substitution of two CO ligands in (1) resulting in the formation of the disubstituted complex (30).

#### 3.2.4. CO substitution by PMe<sub>2</sub>Ph in (1)

A complex formulated as Ru<sub>5</sub>(μ<sub>5</sub>-η<sup>2</sup>, *P*-C<sub>2</sub>PPh<sub>2</sub>)(μ-PPh<sub>2</sub>)(CO)<sub>11</sub>(PMe<sub>2</sub>Ph)<sub>2</sub> (31) was isolated from the reaction of a two-fold excess of PMe<sub>2</sub>Ph with (1). A reliable analysis could not be obtained for this rather unstable compound, which was characterized spectroscopically. The IR ν(CO) pattern was similar to that of (30), in that the terminal bands were approximately 40 cm<sup>-1</sup> lower than those of (1), and a bridging carbonyl absorption was present at 1775 cm<sup>-1</sup>. It is likely that (31) is substituted at Ru(1), since a bridging carbonyl absorption was also found for (29b) and (30), and at Ru(3), because of spectroscopic similarities with a partially characterized bis-phosphite derivative obtained from (29c). In the FAB mass spectrum, a molecular ion was found at *m/z* 1485, which fragmented by loss of eleven CO groups. The <sup>1</sup>H NMR spectrum contained two signals for the Me groups at δ 1.19 and 0.93, while the phenyl resonances were between δ 7.8 and 6.5. The <sup>31</sup>P NMR spectrum showed two PMe<sub>2</sub>Ph resonances at δ 1.5 and 23.7; the C<sub>2</sub>PPh<sub>2</sub> resonance was found at δ 39.2 and the μ-PPh<sub>2</sub> resonance at δ 269.6. The latter two resonances were similar to those of the phosphite-substituted products (see Table 13, Section 3.2.11). No P-P coupling between the PMe<sub>2</sub>Ph ligands and C<sub>2</sub>PPh<sub>2</sub> was observed. However, this does not conflict with substitution having occurred at Ru(3), as coupling was not observed in (29c), where the phosphite is in a *cis*-configuration with respect to the phosphido group.

### 3.2.5. CO substitution by PPh<sub>3</sub> in (1)

Two methods of substituting CO ligands in (1) by PPh<sub>3</sub> were examined. The first method, using Me<sub>3</sub>NO to remove a CO ligand, permitted the isolation of dark brown crystalline Ru<sub>5</sub>(μ<sub>5</sub>-η<sup>2</sup>, *P*-C<sub>2</sub>PPh<sub>2</sub>)(μ-PPh<sub>2</sub>)(CO)<sub>12</sub>(PPh<sub>3</sub>) (32) in 46% yield. In the FAB mass spectrum, a molecular ion was found at *m/z* 1499, which fragmented by loss of twelve CO groups. The IR ν(CO) region was similar to that of (29a) in both the appearance and position of the bands. The <sup>31</sup>P NMR spectrum (see Table 13, Section 3.2.11) confirmed that the cluster was monosubstituted, and from the IR data it seems likely that the substitution occurred at Ru(4).

The second method involved a twenty-hour reflux in CH<sub>2</sub>Cl<sub>2</sub>. From this reaction mixture, complex (32) and dark green crystalline Ru<sub>5</sub>(μ<sub>4</sub>-PPh)(μ<sub>3</sub>-η<sup>2</sup>-PhC<sub>2</sub>Ph)(μ-PPh<sub>2</sub>)<sub>2</sub>(CO)<sub>10</sub> (33) were isolated. Studies on Ru<sub>3</sub>(CO)<sub>12</sub> clusters have shown that P(OEt)<sub>3</sub> substitution occurs at slightly slower rates than PPh<sub>3</sub> under Me<sub>3</sub>NO activation,<sup>80</sup> but at considerably faster rates under thermal activation.<sup>83</sup> Our results accord with this observation. Molecular modelling showed that significant interaction exists between a PPh<sub>3</sub> ligand on Ru(3) and the μ-phosphido ligand. The P(OEt)<sub>3</sub> [at Ru(3)] and the phosphido ligands in (29c) show considerably less interaction. This probably accounts for the differences between phosphine and phosphite substitution of (1) under thermal activation.

Complex (33) crystallized as a hexane solvate in 22% yield. A similar complex Ru<sub>5</sub>(μ<sub>4</sub>-PPh){μ<sub>3</sub>-η<sup>2</sup>-PhC<sub>2</sub>(*p*-tolyl)}(μ-PPh<sub>2</sub>){μ-P(*p*-tolyl)<sub>2</sub>}(CO)<sub>10</sub> (34) was isolated from the reaction of P(*p*-tolyl)<sub>3</sub> with (1). Complex (32) was converted into (33) by heating in CH<sub>2</sub>Cl<sub>2</sub>, demonstrating the intermediacy of (32) in the synthesis of (33). The FAB mass spectra of (33) and (34) showed molecular ions at *m/z* 1444 and *m/z* 1485 respectively, each of which fragmented by loss of ten carbonyl groups. These data indicated that the complexes were related to (1) by addition of PR<sub>3</sub> and loss of three carbonyl groups. The proton NMR spectrum of (34) indicated that there were two equivalent Me groups and one inequivalent Me group; these were assigned to the tolyl groups on the μ-P(*p*-tolyl)<sub>2</sub> and PhC<sub>2</sub>(*p*-tolyl) ligands, respectively. The <sup>31</sup>P NMR spectrum of (33) showed that the two μ-PPh<sub>2</sub> groups were nearly equivalent, a broad signal being found at δ 203.7.

In contrast, there were two phosphido environments in complex (34): these appeared as separate broad signals at  $\delta$  208.7 and 203.7 in acetone, but in  $\text{CH}_2\text{Cl}_2$  as an apparent triplet formed by two overlapping doublets ( $\delta$  205.2, 202.4;  $J_{\text{P-P}} = 340$  Hz). By comparison with (33), it seems likely that the high field signal was due to the  $\mu$ -PPh<sub>2</sub> group and the low field signal to  $\mu$ -P(*p*-tolyl)<sub>2</sub>. The  $\mu_4$ -PPh groups in (33) and (34) had signals at  $\delta$  451.5 and  $\delta$  451.4 respectively.

The molecular structure of (33) was determined by an X-ray study and a plot of a molecule is shown in Figure 11. Significant bond distances and angles are collected in Table 6. Rather large esd's result from twinning in the crystal used for the determination. As found for complex (26), the geometry is a square-pyramidal Ru<sub>5</sub> metal skeleton, which becomes an octahedron when the phosphinidene P-atom is included in the core. The phosphinidene P-atom is 1.280 Å below the square base and Ru(1) is 1.952 Å above. Two edges are bridged by phosphido groups, one of which is derived from the triphenylphosphine. A  $\mu_3$ - $\eta^2$ -PhC<sub>2</sub>Ph ligand bridges the Ru(1)Ru(2)Ru(3) face.

The Ru-Ru bond distances [2.726(2) - 2.958(3) Å] are within the usual values, the shortest distance being Ru(1)-Ru(3). Two carbonyls are found on each of the rutheniums. The Ru-P distances of the phosphido and phosphinidene ligands are in the range 2.232(4) - 2.499(4) Å. The phosphinidene is coordinated in a similar fashion to (26), with three normal Ru-P bonds [Ru-P<sub>av.</sub> 2.36 Å] and one long bond Ru(5)-P(2) [2.499(4) Å]. Two long Ru-C bonds [Ru(2)-C(1) 2.33(2), Ru(3)-C(2) 2.24(1) Å] and two short bonds [Ru(1)-C(2) 2.01(1), Ru(3)-C(1) 2.09(2) Å] were found to the acetylene, a pattern suggesting a bonding mode in between  $\eta^2$ -|| and  $\eta^2$ -⊥. This is possibly due to a solid state freezing out of oscillatory motion that has been noted for other  $\eta^2$ -|| complexes in solution.<sup>84</sup> The C=C bond length of 1.34(3) Å is similar to that found in other  $\mu_3$ - $\eta^2$  acetylene complexes.<sup>85</sup>

From the above results, it is evident that the reaction of (1) with triphenylphosphine under mild conditions resulted in initial ligand substitution, followed by P-C cleavage of the phosphido, phosphino-acetylide and the phosphine ligands. Migration of the aryl groups to the C<sub>2</sub> unit generated a disubstituted alkyne, and the phosphorus groups formed phosphido and

**Figure 11.** PLUTO plot of  $\text{Ru}_5(\mu_4\text{-PPh})(\mu_3\text{-}\eta^2\text{-PhC}_2\text{Ph})(\mu\text{-PPh}_2)_2(\text{CO})_{10}\cdot\text{CH}_2\text{Cl}_2$  (**33**)

(by B.W. Skelton and A.H. White)

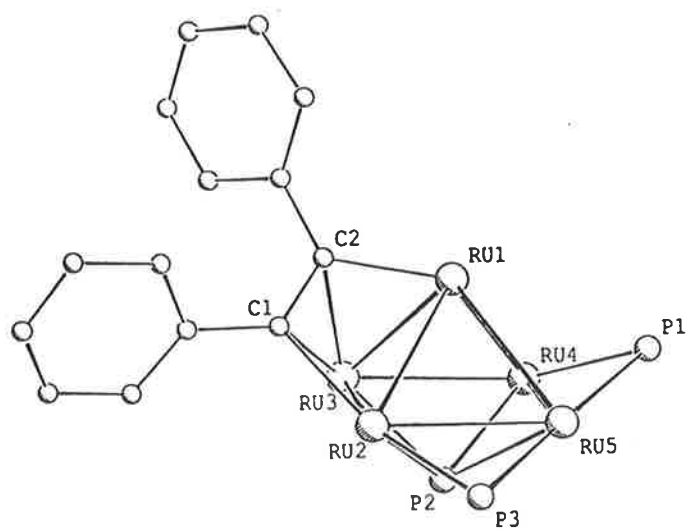
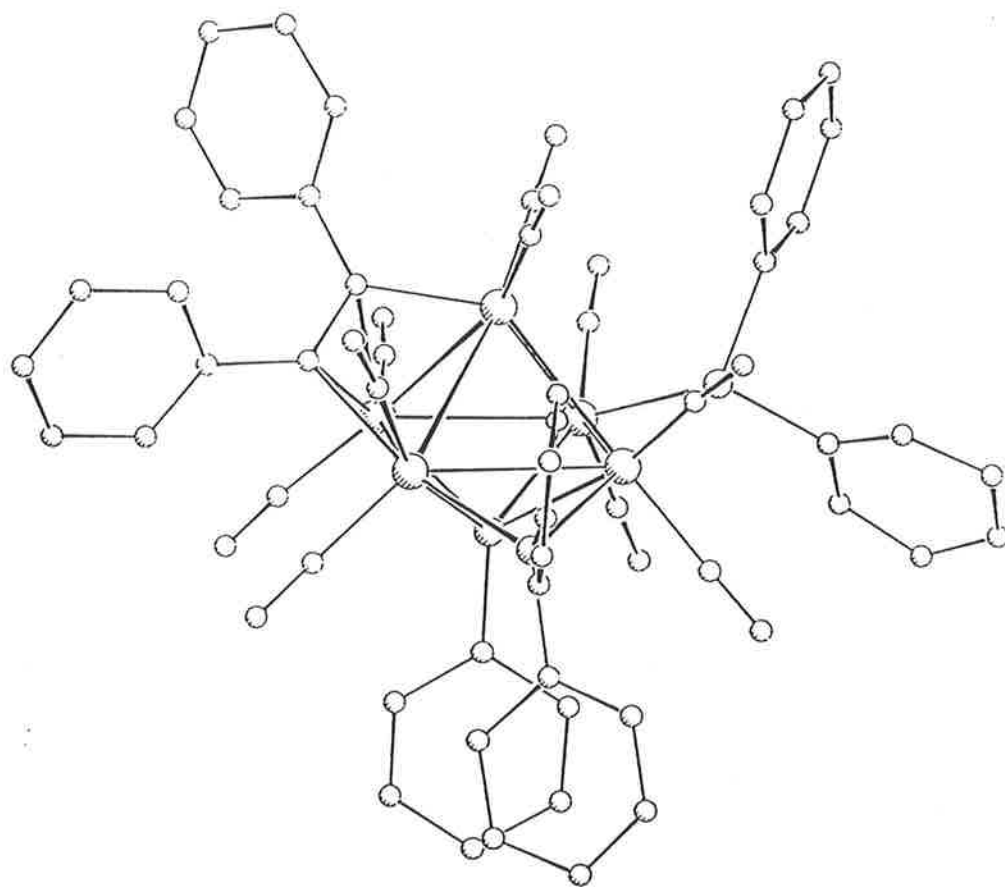


**Table 6.** Selected bond distances (Å) and angles (°) for complex **(33)**

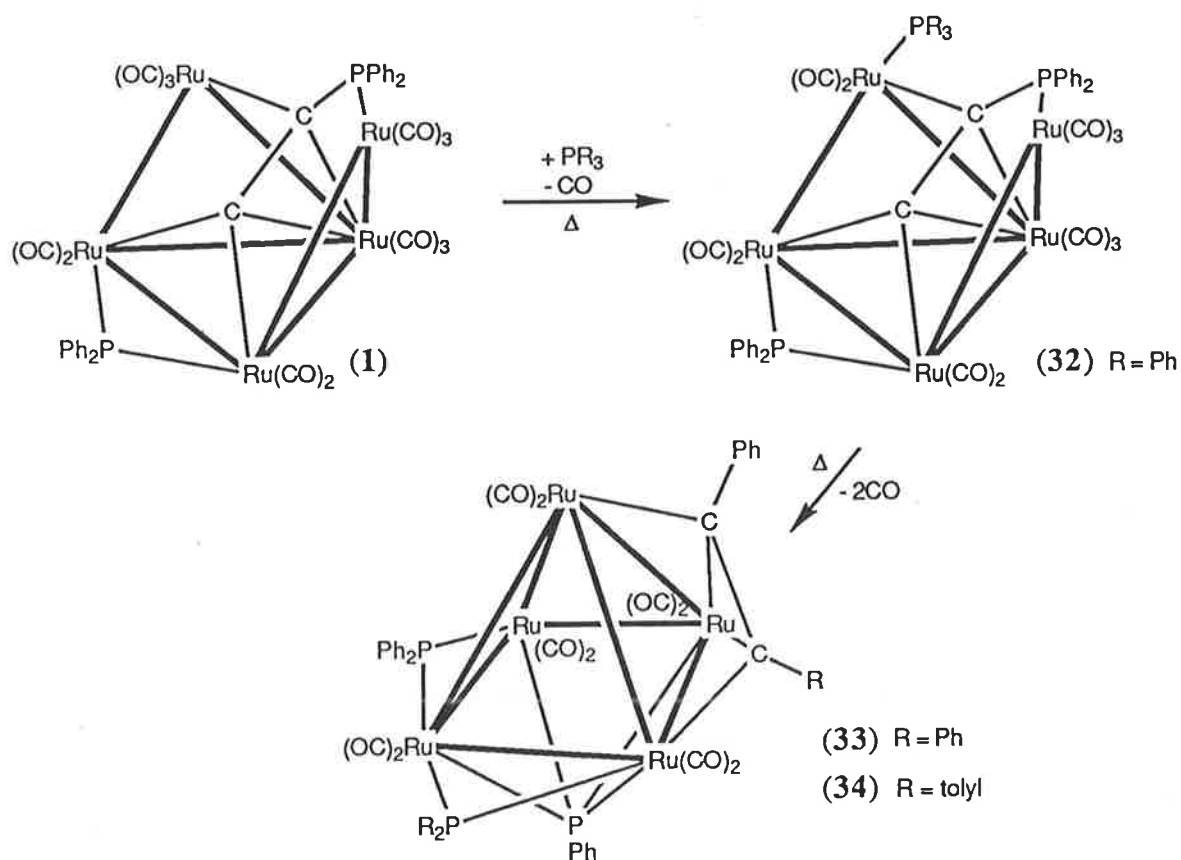
Ru(1)-Ru(2)	2.826(3)	Ru(1)-Ru(3)	2.726(2)
Ru(1)-Ru(4)	2.822(3)	Ru(1)-Ru(5)	2.874(3)
Ru(2)-Ru(3)	2.798(4)	Ru(2)-Ru(5)	2.958(3)
Ru(3)-Ru(4)	2.825(3)	Ru(4)-Ru(5)	2.842(4)
Ru(4)-P(1)	2.232(4)	Ru(5)-P(1)	2.389(6)
Ru(2)-P(2)	2.380(5)	Ru(3)-P(2)	2.324(5)
Ru(4)-P(2)	2.369(6)	Ru(5)-P(2)	2.499(4)
Ru(2)-P(3)	2.297(5)	Ru(5)-P(3)	2.390(6)
Ru(1)-C(1)	2.75	Ru(2)-C(1)	2.33(2)
Ru(3)-C(1)	2.09(2)	Ru(1)-C(2)	2.01(1)
Ru(2)-C(2)	3.07	Ru(3)-C(2)	2.24(1)
C(1)-C(2)	1.34(3)		
Ru(2)Ru(1)Ru(3)	60.50(8)	Ru(2)Ru(1)Ru(4)	90.93(7)
Ru(2)Ru(1)Ru(5)	62.52(9)	Ru(3)Ru(1)Ru(4)	61.20(8)
Ru(3)Ru(1)Ru(5)	92.6(1)	Ru(4)Ru(1)Ru(5)	59.86(6)
Ru(3)Ru(2)Ru(5)	98.4(1)	Ru(2)Ru(3)Ru(4)	91.4(1)
Ru(3)Ru(4)Ru(5)	92.1(1)	Ru(2)Ru(5)Ru(4)	87.8(1)
Ru(4)P(1)Ru(5)	75.9(2)	P(1)Ru(5)P(2)	100.5(2)
P(1)Ru(4)P(2)	109.5(2)	P(1)Ru(5)P(3)	178.5(1)
Ru(2)P(2)Ru(3)	73.0(1)	Ru(2)P(2)Ru(4)	115.9(2)

**Table 6.** (continued)

Ru(2)P(2)Ru(5)	74.6(2)	Ru(3)P(2)Ru(4)	74.0(2)
Ru(3)P(2)Ru(5)	114.2(2)	Ru(4)P(2)Ru(5)	71.4(1)
P(2)Ru(2)P(3)	85.2(2)	P(2)Ru(5)P(3)	80.70(2)
Ru(2)P(3)Ru(5)	78.2(2)	Ru(2)C(1)Ru(3)	78.3(5)
Ru(2)Ru(3)C(1)	54.8(5)	Ru(3)Ru(2)C(1)	46.9(5)
Ru(1)Ru(3)C(2)	46.6(3)	Ru(3)Ru(1)C(2)	54.0(4)
Ru(1)C(2)Ru(3)	79.5(5)	Ru(2)C(1)C(2)	110.8(9)
Ru(3)C(1)C(2)	78(1)	Ru(1)C(2)C(1)	109(1)
Ru(3)C(2)C(1)	66(1)		

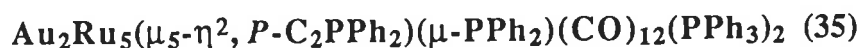
phosphinidene ligands (see Scheme 8). Carty *et al.*<sup>13</sup> have reported the formation of a diphenylacetylene cluster  $\text{Ru}_5(\mu_4\text{-PPh})(\mu_3\text{-}\eta^2\text{-PhC}_2\text{Ph})(\text{CO})_{13}$  (**19**) by pyrolysis of the phenylacetylide cluster  $\text{Ru}_5(\mu_4\text{-}\eta^2\text{-C}_2\text{Ph})(\mu\text{-PPh}_2)(\text{CO})_{13}$  (**2**). The formation of (**33**) is somewhat different in that two aryl groups have migrated to the  $\text{C}_2$  unit, one of these originating from the phosphine rather than from a phosphido group. Although P-C cleavage reactions of  $\text{PPh}_3$  generating phosphido groups are well known,<sup>66,86</sup> the reaction conditions have generally been quite severe (refluxing toluene, xylene, decalin). The reaction of  $\text{Ru}_3(\mu\text{-dppm})(\text{CO})_{10}$  with K-Selectride resulted in the formation of  $[\text{Ru}_3\{\mu_3\text{-PPhCH}_2\text{PPh}_2\}(\text{CO})_9]^-$ , this dephenylation occurring at room temperature.<sup>87</sup> In the present case, loss of the aryl group from the phosphine has occurred under thermal conditions which were less forcing than were used by Knox *et al.*<sup>14</sup> in their synthesis of the benzyne complex  $\text{Ru}_5(\mu_5\text{-}\eta^6\text{-C}_6\text{H}_4)(\mu_4\text{-PPh})(\text{CO})_{13}$  from  $\text{Ru}_3(\text{CO})_{11}(\text{PPh}_3)$ , and indicates considerable activation of  $\text{PPh}_3$  by (**1**).

Scheme 8. Reactions of (**1**) with  $\text{PPh}_3$  and  $\text{P}(p\text{-tolyl})_3$



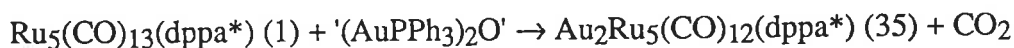
The syntheses of (33) and (34) illustrate a new pattern of reactivity for (1), where the ready transformation between different structural types has allowed P-C bond cleavage and C-C coupling reactions to occur at 40 °C. These reactions have previously been shown to occur under high temperature pyrolysis conditions (see Section 3.2.2). The reactions of  $\text{Ru}_3(\text{CO})_{12}$  and  $\text{Os}_3(\text{CO})_{12}$  with  $\text{PPh}_3$ <sup>66,86</sup> produced complexes that contained orthometallated phenyl and benzyne groups, the formation of these ligands being accompanied by hydride transfer to the clusters. A different mechanism is likely in the formation of (33) and (34), as no hydride-containing intermediates were detected. We suggest that a possible mechanism for the formation of the disubstituted acetylene involves phosphido P-C cleavage with migration of the phenyl group to the  $\beta$ -carbon to generate a phosphino-vinylidene [cf (26)]. This is followed by cleavage of the P-C bond of the phosphino-vinylidene to generate a phenylacetylide. Further cleavage of an aryl group from the phosphine and migration to the  $\text{C}_2$  unit forms the acetylene  $\text{PhC}_2\text{R}$  ( $\text{R} = \text{Ph}, p\text{-tolyl}$ ).<sup>88</sup> Complex (1) is stable in refluxing  $\text{CH}_2\text{Cl}_2$ . The formation of (33) from (32) by multiple CO loss under the same conditions indicates that the triarylphosphine-substitution of (1) has rendered the cluster more susceptible to CO dissociation. Kinetic studies on the  $\text{Ir}_4(\text{CO})_{12}$  system have indicated that arylphosphines induce greater labilization of CO than the smaller ligands such as alkylphosphines or CO.<sup>74</sup>

### 3.2.6. Synthesis of and ligand substitution in



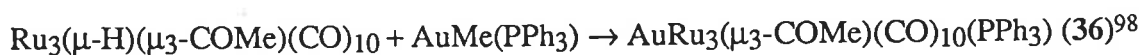
Formal addition of the digold unit  $\text{Au}_2(\text{PPh}_3)_2$ <sup>89</sup> to (1) resulted in the formation of the hexanuclear cluster (35). This cluster was characterized by microanalysis and spectroscopic data. The FAB mass spectrum had a molecular ion at  $m/z$  2155 which fragmented by loss of twelve CO groups. In the  $^1\text{H}$  NMR spectrum, resonances were found between  $\delta$  7.5 and 6.6 for the phenyl groups. In the  $^{13}\text{C}$  NMR spectrum, resonances were found for the carbonyl ligands ( $\delta$  215.3, 214.7, 212.8, 206.2, 202.1, 198.0, 194.6) and the phenyl groups ( $\delta$  141.2 - 126.0); a signal at  $\delta$  144.1 showing coupling to two phosphorus ligands was assigned to the  $\alpha$ -carbon of the acetylide. Various routes to (35) have been investigated. For preparative purposes, it was found that the addition of  $[\text{ppn}][\text{Co}(\text{CO})_4]$  and  $[(\text{AuPPh}_3)_3\text{O}][\text{BF}_4]$  to (1) in

thf at room temperature gave (35) in 83% yield. The binuclear compound  $\text{AuCo}(\text{CO})_4\text{PPh}_3$  was also isolated in 83% yield. Treatment of (1) with  $[\text{ppn}][\text{Mn}(\text{CO})_5]/[(\text{AuPPh}_3)_3\text{O}][\text{BF}_4]$  or  $\text{Na}[\text{Co}(\text{CO})_4]/[(\text{AuPPh}_3)_3\text{O}][\text{BF}_4]$  gave (35) in 73% and 35% yields respectively. The addition of  $[\text{ppn}][\text{Co}(\text{CO})_4]$  to the oxonium salt in thf gave an orange solution, which did not react with (1) to form (35). This suggests that the cluster may have been reacting with an unstable intermediate ' $(\text{AuPPh}_3)_2\text{O}$ ', formed by removal of a ' $[\text{Au}(\text{PPh}_3)]^+$ ' unit from  $[(\text{AuPPh}_3)_3\text{O}]^+$ :



It appears that this reagent may be useful in introducing ' $\text{Au}_2(\text{PR}_3)_2$ ' units into clusters under mild conditions,<sup>72</sup> without the requirement that the cluster be a dianion or multihydride complex. At this stage, it seems that the cluster must be capable of facile CO loss for the above reaction to work successfully. Various sources of ' $\text{Au}(\text{PR}_3)$ ' and ' $\{\text{Au}(\text{PR}_3)\}_3$ ' have been developed, but no systematic route to digold substitution of neutral clusters has appeared.<sup>50,90-99</sup> The three principal routes to introducing  $\text{Au}(\text{PR}_3)$  units involve:

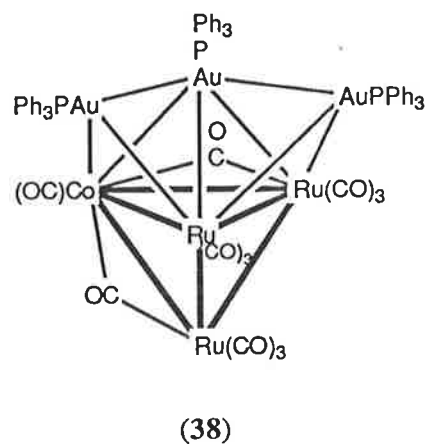
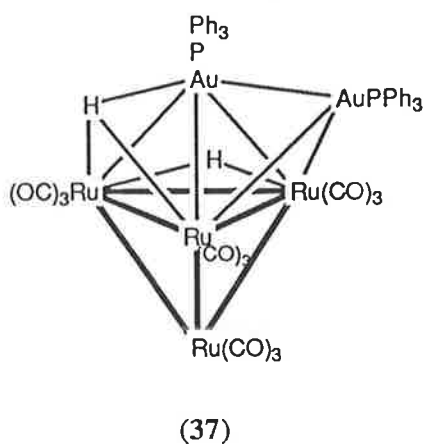
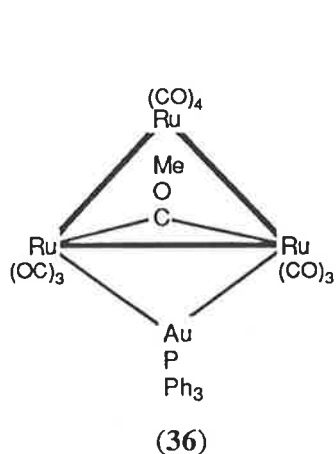
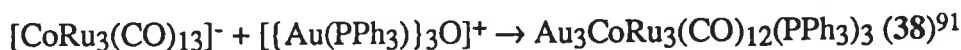
(i) replacement of hydrido ligands by  $\text{AuMe}(\text{PPh}_3)$



(ii) substitution of a cluster anion by a source of  $[\text{Au}(\text{PR}_3)]^+$



(iii) addition of  $\{[\text{Au}(\text{PPh}_3)]_3\text{O}\}^+$  to anionic clusters

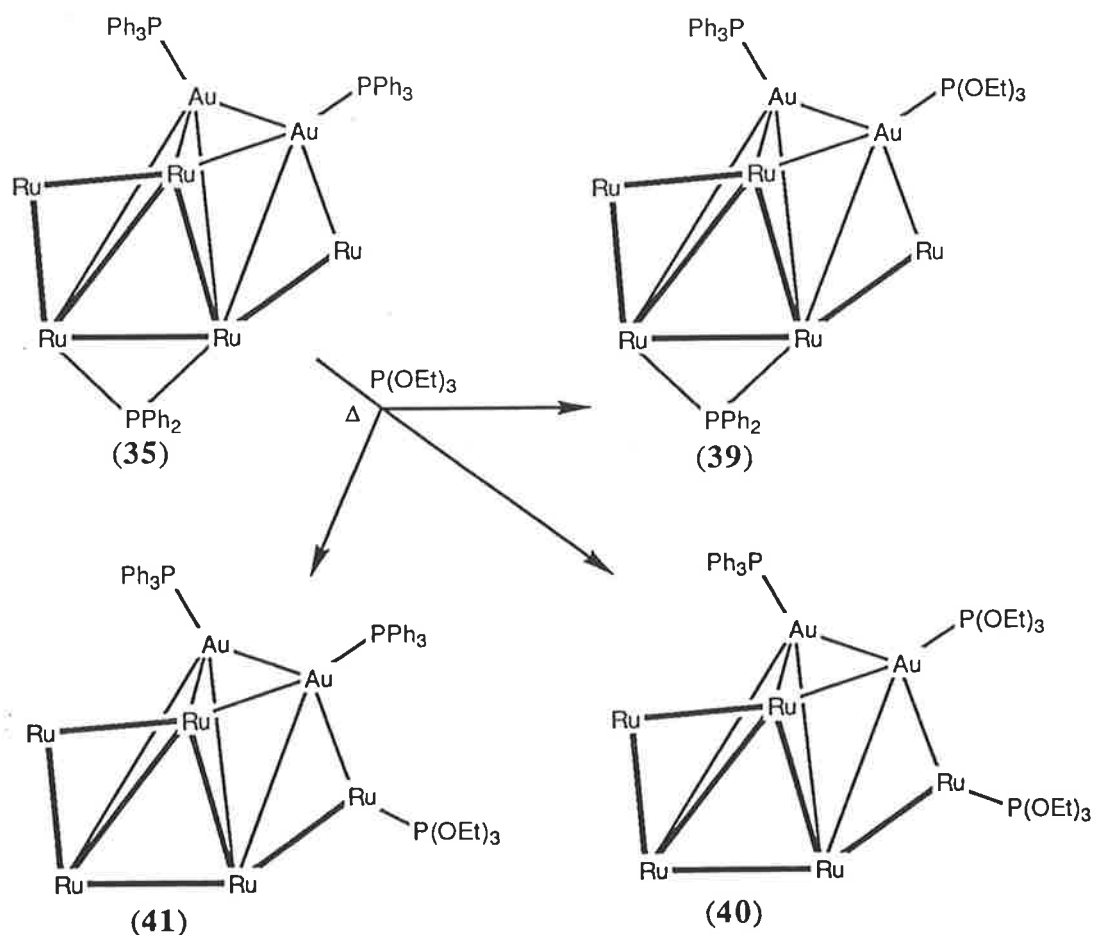


The reaction of (1) with [(AuPPh<sub>3</sub>)<sub>3</sub>O][BF<sub>4</sub>] alone also gave (35), but the yield was considerably lower (22%) and the reaction did not go to completion. A side product from this reaction, Au<sub>3</sub>Ru<sub>5</sub>(CO)<sub>10</sub>(dppa\*)(PPh<sub>3</sub>)<sub>3</sub> (identified by FAB MS), was apparently formed by addition of a third 'Au(PPh<sub>3</sub>)' fragment to (35). Another route to the synthesis of (35) was the reaction between AuCl(PPh<sub>3</sub>) and the reduced solution formed by reacting (1) with sodium amalgam (see Section 3.2.1); complex (35) was obtained in 85% yield. From this result, it seems likely that the reduced species is [Ru<sub>5</sub>(CO)<sub>12</sub>(dppa\*)]<sup>2-</sup>, since dianions generally react with two '[Au(PR<sub>3</sub>)]<sup>+</sup>' units to give neutral species, whereas monoanions react with only one Au(PR<sub>3</sub>) moiety.

The reaction of [ppn][Co(CO)<sub>4</sub>] / [(AuPPh<sub>3</sub>)<sub>3</sub>O][BF<sub>4</sub>] with (1) demonstrates formally the substitution of a CO group by neutral 'Au<sub>2</sub>(PPh<sub>3</sub>)<sub>2</sub>'. In contrast, the reaction between '[Ru<sub>5</sub>(CO)<sub>12</sub>(dppa\*)]<sup>2-</sup>' and AuCl(PPh<sub>3</sub>) involves salt elimination to generate a neutral species. No reaction of complex (1) occurred when it was treated with a solution of Na[Co(CO)<sub>4</sub>] in thf.

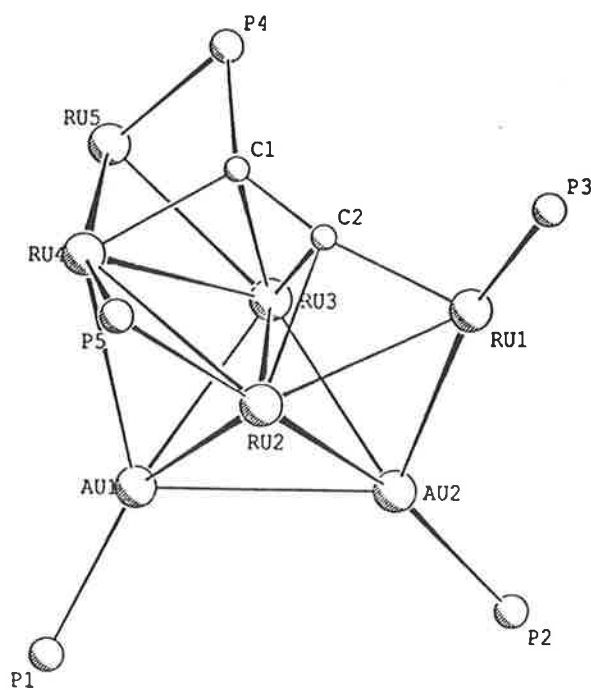
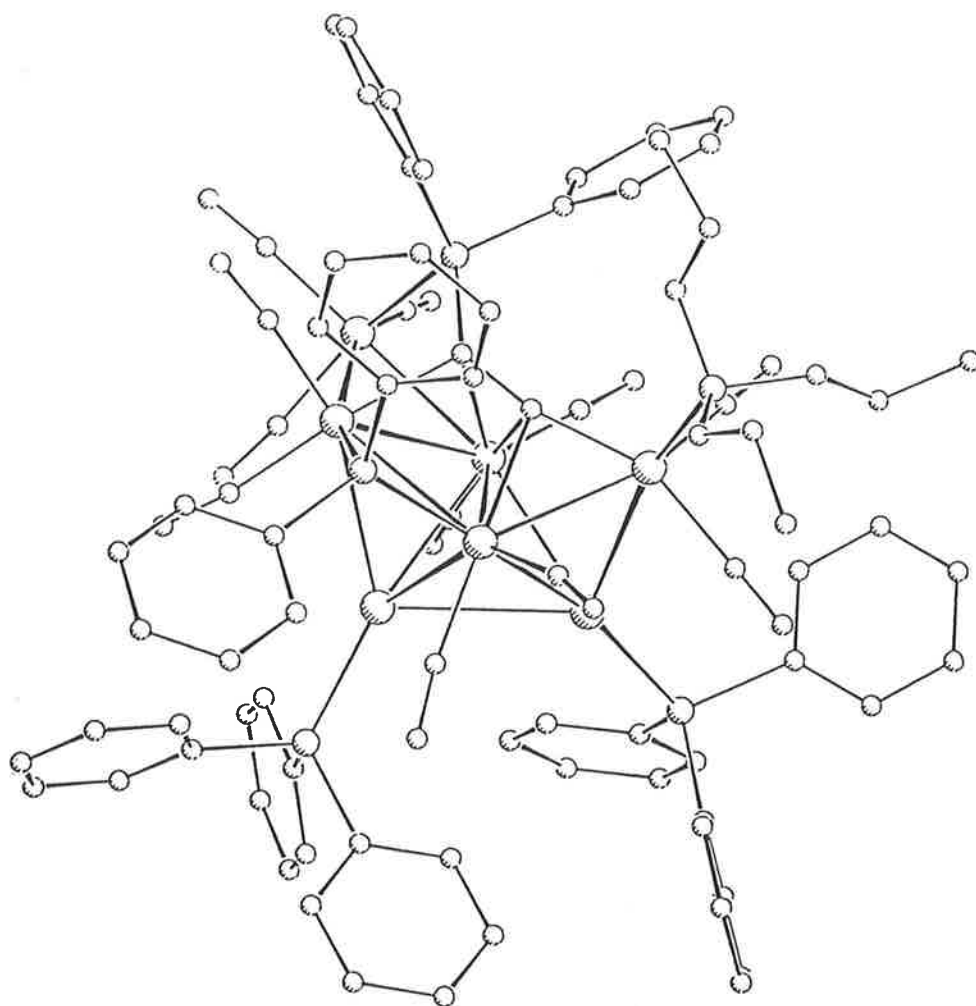
X-ray quality crystals of (35) could not be obtained, so a triethylphosphite-substituted derivative was synthesized. The reaction of (35) with P(OEt)<sub>3</sub> was not entirely straightforward: three products were obtained when a 2:1 ratio of phosphite to (35) was used, while at a lower phosphite/cluster ratio the reaction did not go to completion. The three green phosphite-substituted compounds Au<sub>2</sub>Ru<sub>5</sub>(μ<sub>5</sub>-η<sup>2</sup>, *P*-C<sub>2</sub>PPh<sub>2</sub>)(μ-PPh<sub>2</sub>)(CO)<sub>12</sub>(PPh<sub>3</sub>)-{P(OEt)<sub>3</sub>} (39), Au<sub>2</sub>Ru<sub>5</sub>(μ<sub>5</sub>-η<sup>2</sup>, *P*-C<sub>2</sub>PPh<sub>2</sub>)(μ-PPh<sub>2</sub>)(CO)<sub>11</sub>(PPh<sub>3</sub>){P(OEt)<sub>3</sub>}<sub>2</sub> (40) and Au<sub>2</sub>Ru<sub>5</sub>(μ<sub>5</sub>-η<sup>2</sup>, *P*-C<sub>2</sub>PPh<sub>2</sub>)(μ-PPh<sub>2</sub>)(CO)<sub>11</sub>(PPh<sub>3</sub>)<sub>2</sub>{P(OEt)<sub>3</sub>} (41) were characterized by analytical and spectroscopic data. The IR spectrum of (39) was very similar to that of (35), while (40) and (41) showed shifts to lower wavenumber and band patterns different to (35). Molecular ions were observed in the FAB mass spectra of these complexes at *m/z* 2059 (39), 2197 (40) and 2292 (41). The number of phosphite ligands was easily ascertained by <sup>1</sup>H NMR. The CH<sub>2</sub> environments in all the complexes demonstrated the long range coupling patterns mentioned in Section 3.2.3.

Figure 12. Possible core structures for complexes (35), (39) and (40)



Possible core structures for the products (39) and (40) are shown in Figure 12, while the molecular structure of (41) is shown in Figure 13. Table 7 collects significant bond distances and angles for (41). The structure of (41) is quite closely related to that of (1). The cleavage of the Ru(1)-Ru(3) bond resulted in a spiked-square structure: deviations from the least-squares plane through the square defined by Ru(2)Ru(3)Ru(4)Ru(5) are less than 0.06 Å; Ru(1) is 1.909 Å below this plane. This is the second example of a Ru<sub>5</sub> core with this geometry, Carty *et al.*<sup>7</sup> having found a rather distorted form of the arrangement in the cluster  $\text{Ru}_5(\mu_4\text{-}\eta^2\text{-C}_2\text{Pr}^i)\{\mu_4\text{-NC(O)NCPh}_2\}(\mu\text{-PPh}_2)(\text{CO})_{13}$ .<sup>18</sup>

**Figure 13.** PLUTO plot of  $\text{Au}_2\text{Ru}_5(\mu_5\text{-}\eta^2\text{-}P\text{-C}_2\text{PPh}_2)(\mu\text{-PPh}_2)(\text{CO})_{11}(\text{PPh}_3)_2\{\text{P}(\text{OEt})_3\}$   
(41) (by B.K. Nicholson)

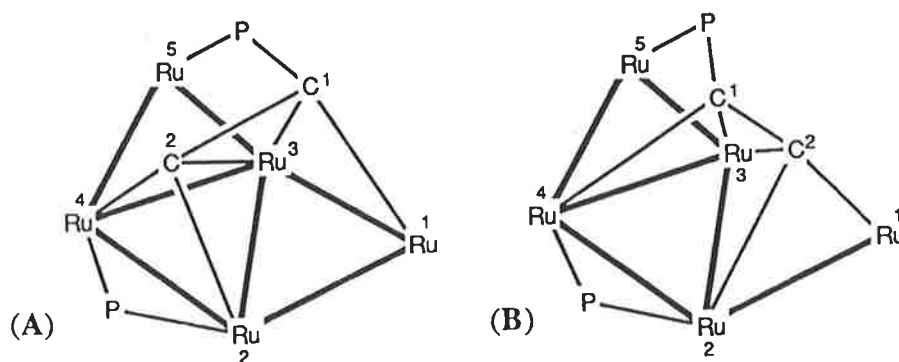


**Table 7.** Selected bond distances (Å) and angles (°) for complex (41)

Au(1)-Au(2)	3.085(1)	Au(1)-Ru(2)	2.792(2)
Au(1)-Ru(3)	2.794(2)	Au(1)-Ru(4)	3.020(1)
Au(2)-Ru(1)	2.855(2)	Au(2)-Ru(2)	2.854(1)
Au(2)-Ru(3)	2.758(2)	Ru(1)-Ru(2)	2.751(2)
Ru(1)-Ru(3)	3.238(3)	Ru(2)-Ru(3)	2.965(2)
Ru(2)-Ru(4)	2.990(2)	Ru(3)-Ru(4)	2.809(2)
Ru(3)-Ru(5)	2.825(2)	Ru(4)-Ru(5)	2.825(2)
Au(1)-P(1)	2.321(5)	Au(2)-P(2)	2.323(4)
Ru(1)-P(3)	2.235(6)	Ru(5)-P(4)	2.360(6)
Ru(2)-P(5)	2.296(4)	Ru(4)-P(5)	2.299(6)
Ru(3)-C(1)	2.30(2)	Ru(4)-C(1)	2.11(2)
Ru(1)-C(2)	1.94(2)	Ru(2)-C(2)	2.21(2)
Ru(3)-C(2)	2.29(2)	C(1)-C(2)	1.39(3)
P(4)-C(1)	1.79(2)		
Ru(1)Ru(2)Ru(4)	109.6(1)	Ru(1)Ru(2)Ru(3)	68.9(1)
Ru(2)Ru(4)Ru(5)	121.4(1)	Ru(3)Ru(5)Ru(4)	59.6(1)
Ru(2)Ru(3)Ru(4)	62.3(1)	Ru(4)Au(1)Au(2)	103.0(1)
Ru(2)Ru(1)Au(2)	61.2(1)	Ru(2)Au(1)Ru(3)	64.1(1)
Ru(2)Au(2)Ru(3)	63.8(1)	Au(1)Ru(2)Au(2)	66.2(1)
Au(1)Ru(3)Au(2)	67.5(1)	Ru(1)Au(2)Au(1)	107.3(1)
Ru(4)C(1)Ru(3)	79.2(6)	C(1)Ru(3)C(2)	35.3(7)
Ru(2)C(2)Ru(3)	82.6(7)	Ru(1)C(2)C(1)	161(1)
Ru(5)P(4)C(1)	89.9(7)	P(4)C(1)C(2)	135(2)
P(1)Au(1)Au(2)	135.9(2)	P(2)Au(2)Au(1)	127.3(2)

The structure of (41) is best thought of as a trigonal bipyramid [formed by Ru(4), Au(1), Ru(2), Ru(3), Au(2)], edge-bridged by Ru(1), Ru(5) and P(5). The trigonal-bipyramidal structure results from the addition of one gold to a triangular face [Ru(2)Ru(3)Ru(4)], the Au(1)Ru(2)Ru(3) face being then capped by the second gold fragment. This polyhedron has been noted previously in clusters such as Au<sub>2</sub>Ru<sub>3</sub>(μ<sub>3</sub>-S)(CO)<sub>9</sub>(PPh<sub>3</sub>)<sub>2</sub><sup>93</sup> and Au<sub>2</sub>Ru<sub>4</sub>(μ-H)<sub>2</sub>(CO)<sub>12</sub>(PPh<sub>3</sub>)<sub>2</sub>.<sup>95(b)</sup> The most reasonable approach for electron counting of clusters containing multi-gold units is to include the valence *d*-electrons of the gold atoms in the total electron count.<sup>101</sup> For (41), this gives a 100-electron, 8-SEP count for the cluster.

In (41), the eleven CO ligands are distributed two to each ruthenium except Ru(5), which has three. Semibridging carbonyl interactions are found for C(21) and C(22) on Ru(2), the angles and non-bonded distances for Ru(2)C(21)O(21), Au(1)-C(21) and Ru(2)C(22)O(22), Ru(1)-C(22) being 166(2)°, 2.64 Å and 168(2)°, 2.79 Å, respectively. Gold-carbonyl interactions have been noted previously in the complex [AuOs<sub>10</sub>C(CO)<sub>24</sub>(PPh<sub>3</sub>)]<sup>-</sup> where Au-C contacts of 2.661 Å and 2.668 Å were found.<sup>102</sup> The phosphino-acetylide is bonded in a μ<sub>5</sub>-η<sup>2</sup>, *P* mode, as found for (1) [Structure (A)], but C(1) bridges Ru(3)-Ru(4) and C(2) bridges Ru(1)-Ru(2), Ru(2)-Ru(3) [Structure (B)]. The C(1)-C(2) separation [1.39(3) Å] is similar to that in (1) [1.383(6) Å], and the Ru-C separations are all normal, except for Ru(1)-C(2) which is rather short at 1.94(2) Å.



The metal-metal separations are of three types: six Ru-Ru [2.751(2) - 2.990(2) Å], six Au-Ru [2.758(2) - 3.020(1) Å], and one Au-Au [3.085(1) Å]. All values fall within the ranges already reported for complexes containing ruthenium-gold cores.<sup>90</sup> The major change from the structure of (1) are the breaking of Ru(1)-Ru(3) and the elongation of Ru(2)-Ru(3): this was

the shortest Ru-Ru bond [2.731(2) Å] in (1), whereas here it is the longest [2.990(2) Å]. The difference in length appears to be due to the presence of the Au<sub>2</sub>(PPh<sub>3</sub>)<sub>2</sub> fragment bridging this bond.

The reaction of 'Au<sub>2</sub>(PPh<sub>3</sub>)<sub>2</sub>' with (1) is somewhat different to that between H<sub>2</sub> and (1) (although the digold fragment is isolobal with H<sub>2</sub>). In the hydrogenation, the complex Ru<sub>5</sub>(μ<sub>5</sub>-CCHPPh<sub>2</sub>)(μ-H)(μ-PPh<sub>2</sub>)(CO)<sub>13</sub> (8) was the first product formed.<sup>17</sup> This complex has been shown to possess a vinylidene ligand [C=CH(PPh<sub>2</sub>)] and a μ-hydrido ligand which is bridging the Ru(4)-Ru(5) edge (in terms of the Au<sub>2</sub>Ru<sub>5</sub> structure). It has been pointed out by Bruce<sup>91</sup> and Mingos<sup>99</sup> that the isolobal relationship between Au(PR<sub>3</sub>) and H is of limited use in predicting structures when more than one gold atom is present. This is due to the strong propensity of gold to form Au-Au bonds. Examination of the structure of (1) using molecular modelling suggests that there is insufficient room to introduce a Au(PPh<sub>3</sub>) unit at the β-carbon, because of interactions with the phosphido group.

The formal addition of H<sub>2</sub> to (1) has also been demonstrated previously using H<sup>-</sup>/H<sup>+</sup>.<sup>17</sup> When the reduced solution from (1) (see Section 3.2.1) was treated with H<sup>+</sup>, no evidence for formation of the vinylidene cluster (8) was found. Neither was any reaction found when (1) was treated with HBF<sub>4</sub>.Et<sub>2</sub>O. These results confirm that the H<sup>-</sup>/H<sup>+</sup> reaction actually proceeds by addition of H<sup>-</sup> to the β-carbon of the acetylide, followed by addition of H<sup>+</sup> to the cluster. Such a mechanism cannot operate for the gold system as the approach to the acetylide is hindered. The reaction of hydrogen with (1) is not likely to give a stable analogue of (35), as there does not exist the potential for multicentre bonds that the Au<sub>2</sub>(PPh<sub>3</sub>)<sub>2</sub> fragment possesses.

The substitution of the phosphite on Ru(1) is similar to that observed for (29a) (different crystallographic numbering schemes have been used), and presumably arises from the formal electron-deficiency at this ruthenium (17e) and the steric constraints that are present. The other products formed in the substitution, (39) and (40), demonstrate the lability of the phosphines on the gold atoms. It seems likely that interphenyl interactions are responsible for replacement of a bulky phosphine for a phosphite group (cone angles 145°, 109° respectively). This is

seen in the torsion angle P(1)Au(1)Au(2)P(2), which is 25.18 °. Previous work<sup>37</sup> has demonstrated phosphine exchange between the clusters  $\text{Au}_2\text{Ru}_6\text{C}(\text{CO})_{16}(\text{PET}_3)_2$  and  $\text{Au}_2\text{Ru}_6\text{C}(\text{CO})_{16}(\text{PPh}_3)_2$ , where equilibrium was attained in eight hours. Another equilibrium situation was found for the complex  $\text{Au}_2\text{Fe}_4\text{BH}(\text{CO})_{12}(\text{PET}_3)_2$ ,<sup>97</sup> which underwent phosphine exchange with  $[\text{ppn}]\text{Cl}$  to form complexes containing  $\text{Au}_2(\text{PPh}_3)_2$  and  $\text{Au}_2(\text{PET}_3)(\text{PPh}_3)$ .

### 3.2.7. Oxidative addition of haloacids and $\text{AuCl}(\text{PPh}_3)$ to (1)

Four oxidative adducts have been synthesized from the reaction of HX (X = Cl, Br, I) or  $\text{AuCl}(\text{PPh}_3)$  (an aurated equivalent of HCl) with (1). The reactions of the aqueous acids with (1) proceeded at r.t. quickly (5 - 20 minutes) to give the orange complexes  $\text{Ru}_5(\mu\text{-H})(\mu_5\text{-}\eta^2, P\text{-C}_2\text{PPh}_2)(\mu\text{-PPh}_2)(\mu\text{-X})(\text{CO})_{13}$  [X = Cl, (42); Br, (43)] and the purple complex  $\text{Ru}_5(\mu\text{-H})(\mu_5\text{-}\eta^2, P\text{-C}_2\text{PPh}_2)(\mu_3\text{-I})(\mu\text{-PPh}_2)(\text{CO})_{12}$  (44). The reaction with  $\text{AuCl}(\text{PPh}_3)$  proceeded more slowly (24 hours) to give orange  $\text{AuRu}_5(\mu_5\text{-}\eta^2, P\text{-C}_2\text{PPh}_2)(\mu\text{-PPh}_2)(\mu\text{-Cl})(\text{CO})_{13}(\text{PPh}_3)$  (45) in 41% yield.

The infrared spectra of (42), (43) and (45) all show similar  $\nu(\text{CO})$  band patterns, the gold derivative having intensities different from the other two. A simpler pattern was found for the HI complex. In the  $^1\text{H}$  NMR, high field signals were found for the hydride ligands in (42), (43) and (44) at  $\delta$  -21.25, -20.71 and -25.33 respectively. These values are within the normal range for  $\mu$ -hydride ligands. The FAB mass spectra of the four compounds showed molecular ions at  $m/z$  1300 (42), 1345 (43), 1365 (44) and 1759 (45), which fragmented by loss of the appropriate number of carbonyl ligands.

To determine the molecular structures of the complexes, X-ray studies were carried out on (43) and (44). Plots of the two structures are shown in Figures 14 and 15, while significant bond distances and angles are collected in Table 8.

Figure 14. PLUTO plot of  $\text{Ru}_5(\mu\text{-H})(\mu_5\text{-}\eta^2, P\text{-C}_2\text{PPh}_2)(\mu\text{-PPh}_2)(\mu\text{-Br})(\text{CO})_{13}$  (43)

(by B.K. Nicholson)

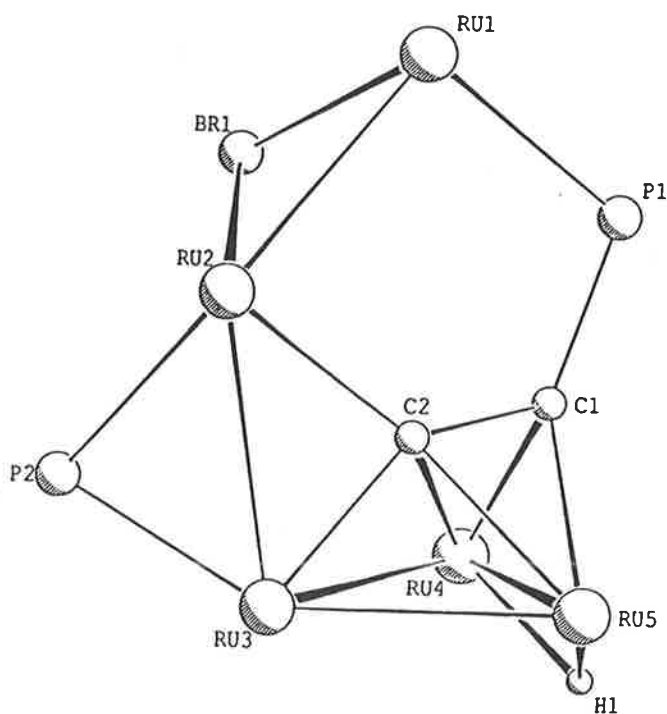
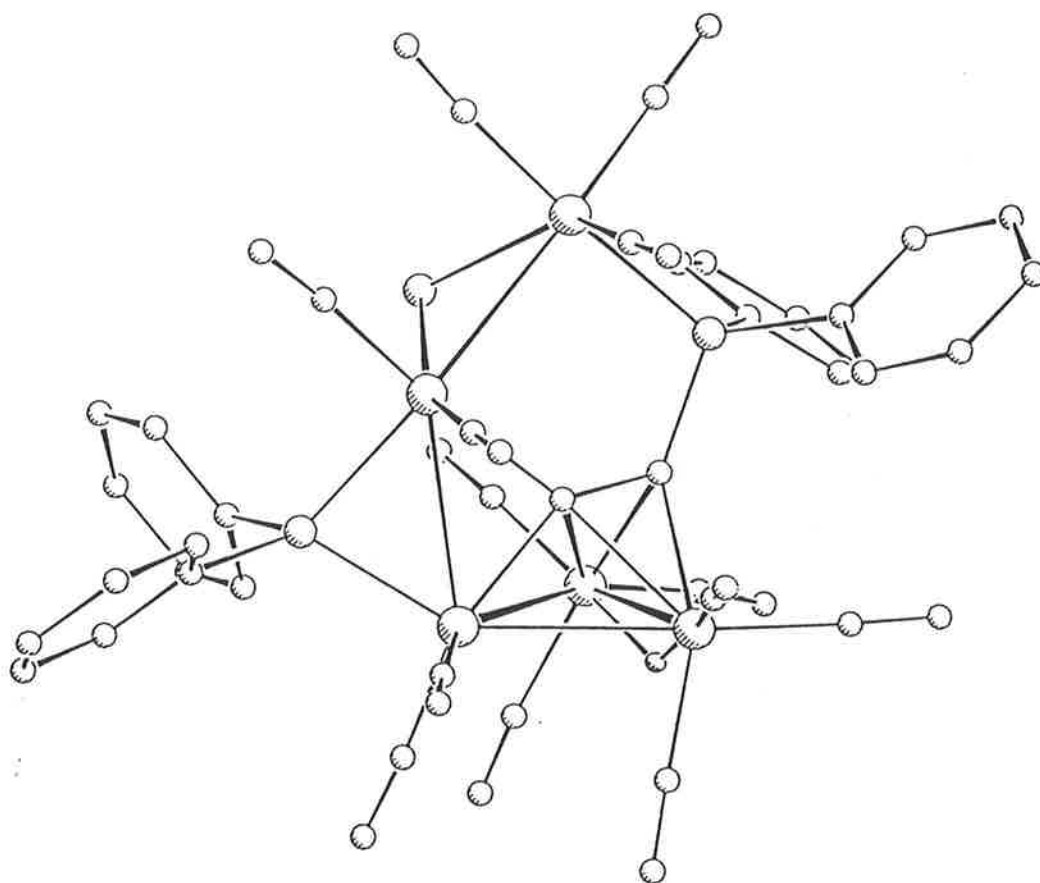
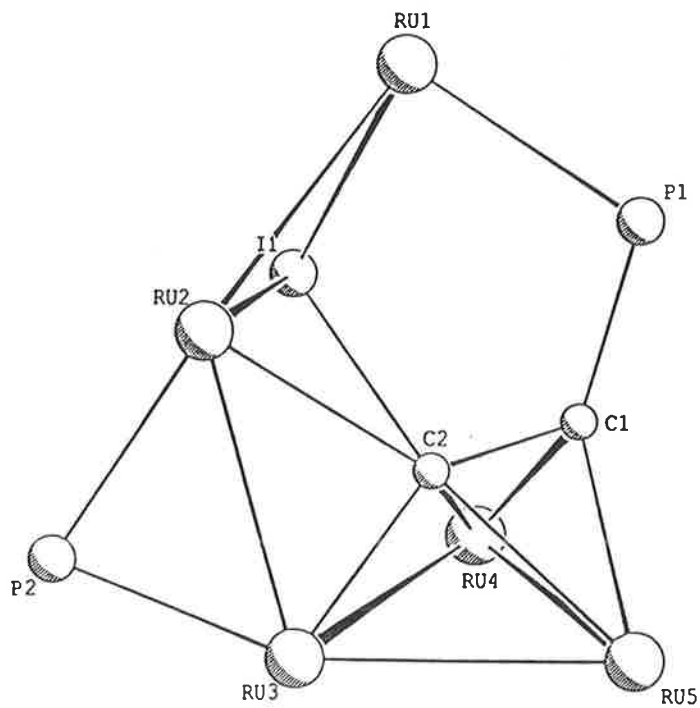
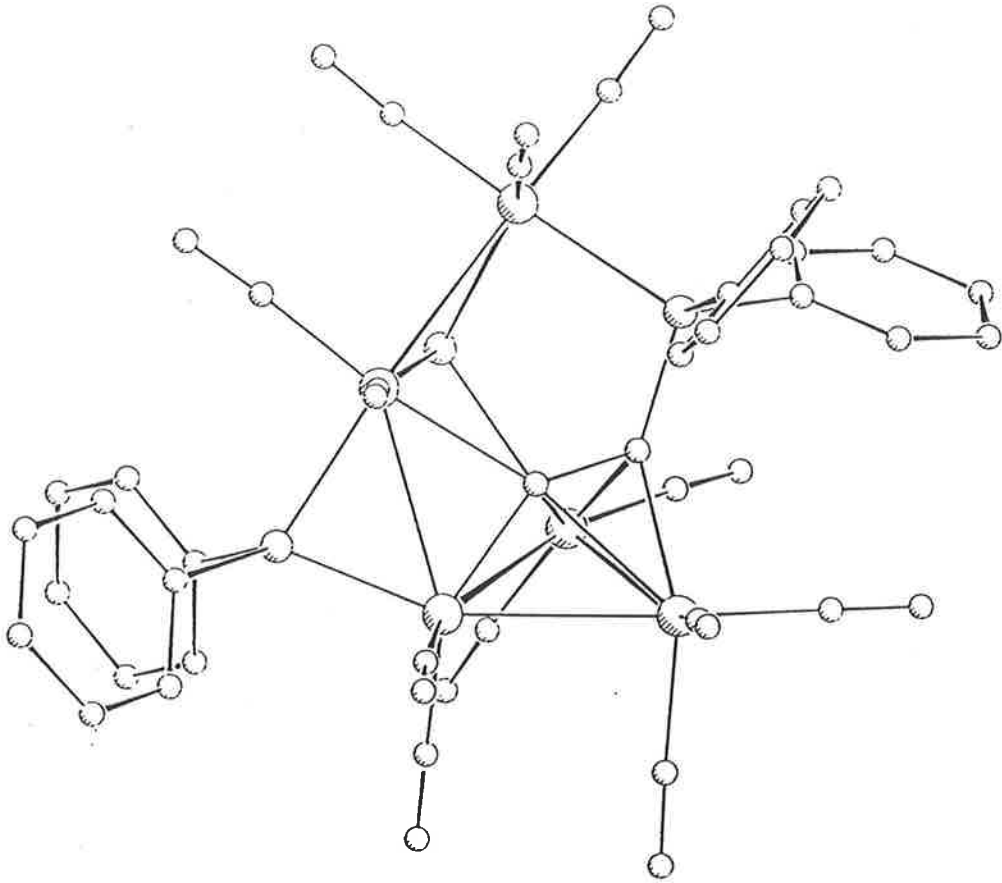


Figure 15. PLUTO plot of  $\text{Ru}_5(\mu\text{-H})(\mu_5\text{-}\eta^2\text{-}P\text{-C}_2\text{PPh}_2)(\mu_3\text{-I})(\mu\text{-PPh}_2)(\text{CO})_{12}$  (44)

(by B.K. Nicholson )



**Table 8.** Selected bond distances (Å) and angles (°) for complexes (43) and (44)

<u>Parameter</u>	<u>Structure</u>	
	(43)(a)	(44)(b)
Ru(1)-Ru(2)	2.862(1)	2.936(1)
Ru(2)-Ru(3)	2.917(1)	2.881(1)
Ru(3)-Ru(4)	2.909(1)	2.858(1)
Ru(3)-Ru(5)	2.821(1)	2.848(1)
Ru(4)-Ru(5)	2.808(1)	2.775(1)
Ru(1)-P(1)	2.397(1)	2.400(2)
Ru(2)-P(2)	2.359(1)	2.332(3)
Ru(3)-P(2)	2.268(1)	2.264(2)
Ru(4)-C(1)	2.203(5)	2.176(9)
Ru(5)-C(1)	2.195(6)	2.129(8)
Ru(2)-C(2)	2.276(5)	2.277(8)
Ru(3)-C(2)	2.042(6)	1.962(9)
Ru(5)-C(2)	2.291(5)	2.355(8)
Ru(1)-X	2.565(1)	2.751(1)
Ru(2)-X	2.560(1)	2.740(1)
P(1)-C(1)	1.796(5)	1.774(9)
C(1)-C(2)	1.316(8)	1.33(1)
Ru(1)Ru(2)Ru(3)	129.0(1)	125.2(1)
Ru(2)Ru(3)Ru(5)	98.3(1)	106.8(1)
Ru(2)Ru(3)Ru(4)	92.7(1)	78.2(1)
Ru(3)Ru(4)Ru(5)	59.1(1)	60.7(1)

(a) Ru(4)-H(1) 1.79(8); Ru(5)-H(1) 1.72; X = Br.

(b) Ru(4)-I 2.727(1); Ru(1)IRu(4) 103.1(1); Ru(2)IRu(4) 83.0(1); X = I.

Table 8. (continued)

<u>Parameter</u>	<u>Structure</u>	
	(43)	(44)
Ru(3)Ru(5)Ru(4)	62.2(1)	61.1(1)
Ru(4)Ru(3)Ru(5)	58.7(1)	58.2(1)
Ru(1)P(1)C(1)	108.8(2)	106.8(3)
Ru(2)P(2)Ru(3)	78.1(1)	77.6(1)
Ru(1)XRu(2)	67.9(1)	64.7(1)
Ru(4)C(1)Ru(5)	79.4(2)	80.2(3)
Ru(2)C(2)Ru(3)	84.8(2)	85.3(3)
Ru(3)C(2)Ru(4)	84.5(2)	87.0(3)
Ru(3)C(2)Ru(5)	81.0(2)	82.0(3)
C(1)C(2)Ru(2)	131.0(4)	129.7(6)
C(2)C(1)Ru(5)	77.0(4)	83.0(1)

Both structures are closely related to that of the kinetic isomer  $\text{Ru}_5(\mu_5\text{-}\eta^2, P\text{-C}_2\text{PPh}_2)(\mu\text{-PPh}_2)(\text{CO})_{15}$  (**6k**), obtained by carbonylation of (**1**).<sup>21</sup> The metal core consists of a  $\text{Ru}_3$  triangle spiked by a  $\text{Ru}_2$  chain in a so-called 'scorpion' geometry. Such a geometry is formed from (**1**) by the breaking of two Ru-Ru bonds, and is consistent with the addition of the four-electron donor (H+Br) (**43**), and the six-electron donor (H+I) (**44**). The addition of HI is accompanied by loss of a carbonyl ligand from Ru(4). In both (**43**) and (**44**), the phosphino-acetylide ligand is attached to Ru(1) by a normal two-electron donor interaction with P(1), and to the Ru(3)Ru(4)Ru(5) triangle by a  $\mu_3\text{-}\eta^2$  ( $\perp$ ) attachment of the acetylide unit. The interactions between C(2) and Ru(5) are not particularly strong, as may be seen from the bond lengths [2.291(5) Å (**43**) and 2.355(8) Å (**44**)]. There is also a weak interaction between Ru(2) and C(2) [2.276(5) Å (**43**); 2.277(8) Å (**44**)]. A phosphido group bridges the Ru(2)-Ru(3) vector in each complex, and the carbonyl groups are arranged thus: three to each of Ru(1), Ru(4), Ru(5) in (**43**), or Ru(1), Ru(5) in (**44**), and two each to the other ruthenium centres. In (**43**), the bromide ligand bridges the Ru(2)-Ru(3) bond, and the hydride is located on the Ru(4)-Ru(5) edge of the  $\text{Ru}_3$  triangle. The iodide ligand in (**44**) is  $\mu_3$ -bonded to Ru(1), Ru(2) and Ru(4). The hydride was not located in (**44**), but from the disposition of carbonyl ligands, and by comparison with (**43**), it may be assumed that it lies across the Ru(4)-Ru(5) bond.

The five Ru-Ru bonds are in the ranges 2.808(1) - 2.917(1) Å (av. 2.863 Å) (**43**) and 2.775(1) - 2.936(1) Å (av. 2.860 Å) (**44**), and have similar variations, the shortest bond in the structures being Ru(4)-Ru(5) and the longest Ru(2)-Ru(3) (**43**) and Ru(1)-Ru(2) (**44**). These variations are also in accordance with the structure of (**6k**). The environment around Ru(1) is approximately octahedral with coordination by three CO ligands, P(1), Ru(2) and either Br or I. Since the P(1)→Ru(1) bond [2.397(1) Å (**43**); 2.400(2) Å (**44**)] is a normal two-electron donor link, the metal atom achieves an 18-electron count from this tertiary phosphine and the halide and CO ligands. The Ru(1)-Ru(2) bond [2.862(1) Å (**43**); 2.936(1) Å (**44**)] is therefore another example of a supported donor bond. Both structures have 80-electron electron-precise structures.

The major structural difference between the two complexes is in the orientation of the metal cores. A least-squares plane passes through C(1), C(2), Ru(1), Ru(2), Ru(3), P(1) (maximum deviation  $< 0.02 \text{ \AA}$ ) in complex (43). In (44), there are substantial deviations from this plane: C(1)  $0.06 \text{ \AA}$ , C(2)  $-0.10 \text{ \AA}$ , Ru(1)  $-0.09 \text{ \AA}$ , Ru(2)  $-0.48 \text{ \AA}$ , Ru(3)  $0.10 \text{ \AA}$ , P(1)  $-0.17 \text{ \AA}$ ; implying that the Ru(2)-Ru(3) bond is twisted towards the iodide atom. The different geometries probably reflect the effect of the  $\mu_3$ -I spanning the open side Ru(1)Ru(2)Ru(4) in (44). This non-face-capping  $\mu_3$ -coordination mode has not been observed previously. The only other structurally characterized clusters containing  $\mu_3$ -I groups,  $\text{Ru}_3(\mu\text{-H})(\mu_3\text{-I})(\text{CO})_9$ <sup>103</sup> and  $[\text{Na}(18\text{-crown-6})][\text{Ru}_3(\mu_3\text{-I})(\text{CO})_9]$ ,<sup>104</sup> show the ligand in a triangular face-capping position. As both these clusters were derived from a  $\text{Ru}_3(\mu\text{-I})(\text{CO})_{10}$  precursor by CO loss, it seems likely that (44) is also formed through CO loss from an intermediate related to (43), probably  $\text{Ru}_5(\mu\text{-H})(\mu_5\text{-}\eta^2, P\text{-C}_2\text{PPh}_2)(\mu\text{-PPh}_2)(\mu\text{-I})(\text{CO})_{13}$ . The FAB mass spectrum of (44) supports this idea, as an ion  $[\text{M} + \text{CO}]^+$  is formed after short periods in the FAB beam. However, no intermediates were detected in the formation of (44).

The addition of HX or AuCl(PPh<sub>3</sub>) to (1) appears to proceed by oxidative addition at Ru(2), with the H ligand migrating to the Ru<sub>3</sub> triangle that results. The halide ligand may exist as a two-, three- ( $\mu$ ) or five-electron ( $\mu_3$ ) donor. Previous studies<sup>25,35,49</sup> have demonstrated both terminal and  $\mu$ -bonding modes for iodide and bromide ligands attached to Ru<sub>5</sub> carbido clusters. Isolobal principles,<sup>99,105</sup> suggest that the Au(PPh<sub>3</sub>) group in (45) is likely to occupy the same position as the hydride in (43). The similarity of the IR spectra for (42) and (43) suggests that the chloride occupies a position similar to that of the bromide ligand; it is presumably in the same position in (45).

### 3.2.8. Addition of allyl halides to (1)

As an extension of the experiments with the halo-acids, it was decided to investigate the reaction of allyl halides with (1). These reactions proceed quite slowly (20 - 24 hours, refluxing CH<sub>2</sub>Cl<sub>2</sub>), to give moderate yields of a number of isomers of Ru<sub>5</sub>X(CO)<sub>12</sub>(dppa\*)-(allyl) (X = Cl, Br). Two isomers were isolated from the reaction of allyl chloride with (1)

[(46b), (46o)] and, similarly, two isomers [(47b), (47o)] were obtained from the allyl bromide reaction. Of these complexes, orange crystalline (47o) was identified by an X-ray study as  $\text{Ru}_5\{\mu_4\text{-}\eta^4, O\text{-C}_2\text{C(O)C}_3\text{H}_5\}\{\mu\text{-PPh}_2\}_2(\mu\text{-Br})(\text{CO})_{11}$ . The brown complex  $\text{Ru}_5\text{Br}(\text{CO})_{12}(\text{dppa}^*)(\text{allyl})$  (47b) exists in solution as two isomers which were not separable by thin layer chromatography. The related products from the allyl chloride reaction, orange  $\text{Ru}_5\{\mu_4\text{-}\eta^4, O\text{-C}_2\text{C(O)C}_3\text{H}_5\}\{\mu\text{-PPh}_2\}_2(\mu\text{-Cl})(\text{CO})_{11}$  (46o) and brown  $\text{Ru}_5\text{Cl}(\text{CO})_{12}(\text{dppa}^*)(\text{allyl})$  (46b), were isolated in 19% and 42% yields, respectively.

The infrared spectra for (46o) and (47o) were very similar, and suggest that the two complexes have related structures, but with a  $\mu\text{-Cl}$  in (46o) replacing the  $\mu\text{-Br}$  in (47o). Very weak bands at  $1535\text{ cm}^{-1}$  (46o) and  $1534\text{ cm}^{-1}$  (47o) were assigned to the coordinated ketonic carbonyls; a band was found at  $1588\text{ cm}^{-1}$  for a similar group in  $\text{Ru}_4\{\mu_4\text{-}\eta^2, P, O\text{-C}_5\text{H}_4\text{O}(\text{PPh}_2)\}\{\mu\text{-PPh}_2\}(\text{CO})_{11}$  (see Section 3.2.10). The spectra for (46b) and (47b) are also closely related, but are quite different from those of the orange isomers. As no evidence was found for ketonic or bridging CO groups in the spectra of (46b) or (47b), these complexes appear to possess twelve terminal carbonyl groups. The most closely related band pattern for the  $\text{Ru}_5(\text{CO})_{12}$  structures examined so far is that of complex (44).

Molecular ions corresponding to  $\text{Ru}_5\text{X}(\text{CO})_{12}(\text{dppa}^*)(\text{allyl})$  were found in the FAB mass spectra at  $m/z$  1313 for (46o) and (46b), and at  $m/z$  1357 for (47o) and (47b). The orange isomers showed loss of twelve carbonyl groups, while the brown isomers fragmented by loss of seven carbonyl groups. An ion  $[\text{M} - \text{CO} - \text{allyl}]^+$  was also found for the brown isomers, suggesting that the allyl ligand may be intact.

The proton NMR spectra of the orange complexes were similar, the coordinated allyl group displaying a five-resonance pattern, which demonstrates the inequivalence of the five protons. The low field multiplet was assigned to the proton on C(5), the three doublets (in order of increasing field) to the *syn* proton on C(4), the *anti* proton on C(4) and the *syn* proton on C(6), while the doublet of doublets was assigned to the *anti* proton on C(6) on the basis of coupling constant and chemical shift data (for atom numbering see Figure 16). A complex pattern of ten resonances was observed for the allyl protons in each of (46b) and (47b). Two multiplets

were found at approximately  $\delta$  4.4. Of the other eight signals, two doublets showed H-H coupling, two doublets showed P-H coupling, two doublets of doublets showed both H-H and P-H coupling, and two multiplets were unresolved. The intensity of these resonances suggested the presence of two isomers of each complex in solution, in a ratio of 2:1 for (46b) and 1:1 for (47b) in  $C_6D_6$ . The environments of the protons were quite different from those in the orange complexes and suggest a different bonding mode for the allyl group. What is apparent from these results is that the allyl group in (46b) [or (47b)] is attached to the cluster in an unsymmetrical manner, probably involving a unsymmetrical  $\eta^3$ -CH<sub>2</sub>CHCH<sub>2</sub> interaction with a phosphorus-bound ruthenium.

The <sup>31</sup>P NMR chemical shifts for the  $\mu$ -PPh<sub>2</sub> group bridging the non-bonded Ru(2)-Ru(5) vector appeared at  $\delta$  54.9 and 57.3 in (46o) and (47o), respectively. The signals observed for (46b) and (47b) were at  $\delta$  65.5, 60.8 [two isomers of (46b)] and  $\delta$  67.2, 60.9 [two isomers of (47b)], a region similar to that found for the C<sub>2</sub>PPh<sub>2</sub> group in (44) ( $\delta$  64.1). A signal for the  $\mu$ -PPh<sub>2</sub> group bridging a Ru-Ru bond was found in the range  $\delta$  249.8 - 271.3 for each of the complexes.

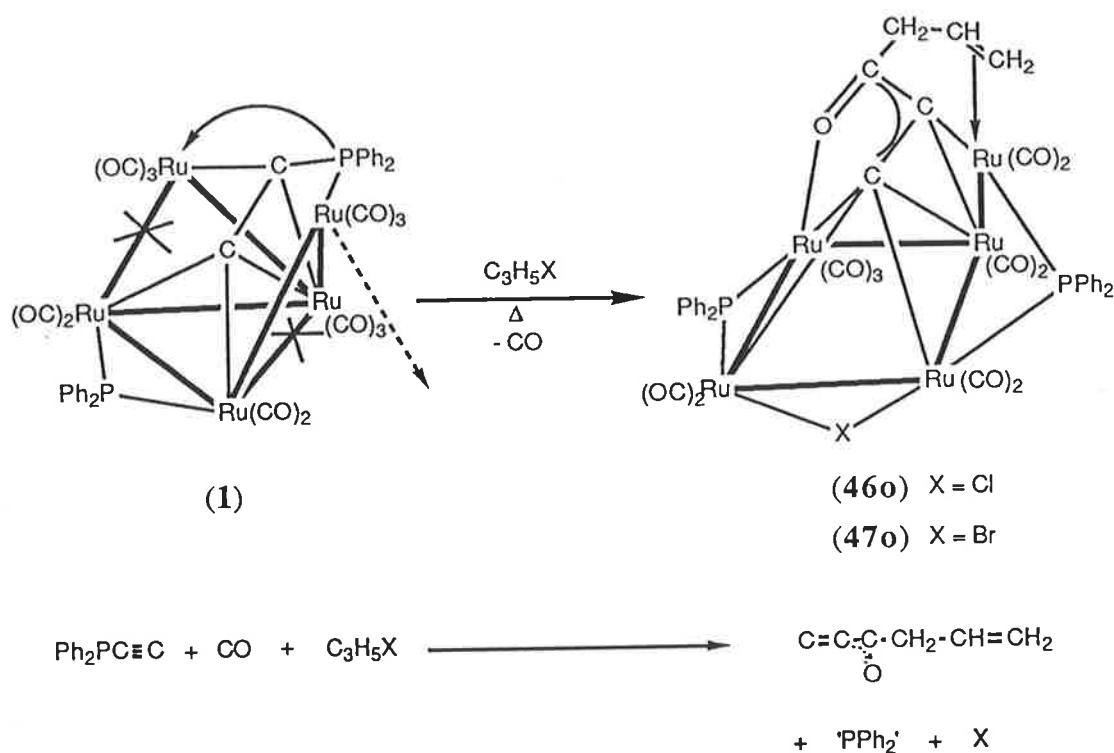
The formation of (47o) is demonstrated in Scheme 9. No interconversion between (47o) and (47b) was noted after heating in refluxing in CH<sub>2</sub>Cl<sub>2</sub> for 20 hours. On the basis of the spectroscopic data mentioned above it appears (46b) and (47b) have significantly different metal skeletons to those of the orange isomers (46o) and (47o). The spectroscopic results suggest that the structures may be based on the scorpion geometry.

An X-ray structure determination for (47o) revealed the molecular structure shown in Figure 16. A listing of significant bond distances and angles is presented in Table 9. The metal framework of (47o) consists of a distorted square [diagonals Ru(2)-Ru(4) 3.99 Å, Ru(1)-Ru(3) 4.06 Å], spiked by Ru(5). Carbon-carbon coupling between the acetylide, a carbonyl ligand and the allyl group has formed a metallated hex-1-en-4-one ligand<sup>†</sup>

---

<sup>†</sup> Because of the delocalized bonding and the multisite nature of the ligand-cluster interaction, the nomenclature of the C-C coupled ligands is not precise.

Scheme 9. Reactions of (1) with allyl halides



coordinated to all five Ru atoms of the cluster via a  $\eta^2$ -linkage through C(1), C(2), a  $\eta^2$ -interaction through C(5), C(6) and a Ru-O bond from the ketonic oxygen. The interaction between C(1), C(2) and the square base of the cluster is reminiscent of the  $\mu_4$ ,  $\eta^2$  interactions between acetylides and  $\text{Ru}_4$  butterfly clusters.<sup>13</sup> The distance between the C(1) carbon and the least-squares plane through Ru(1)Ru(2)Ru(3)Ru(4) (deviations 0.200, -0.194, 0.191, 0.197 Å, resp.) is 0.74 Å. A phosphido group has been formed by P-C cleavage of the phosphino-acetylide. As a result, there are two phosphido groups present, one bridging the Ru(1)-Ru(4) bond and the other bridging the non-bonded Ru(2)-Ru(5) vector.

Within the organic ligand, the C-C distances suggest significant double bond character for C(1)-C(2), C(2)-C(3) and C(5)-C(6) [1.47(5), 1.42(4), 1.34(4) Å, resp.], while C(3)-C(4) and C(4)-C(5) are normal single bonds [1.55(5), 1.58(4) Å, resp.]. The ketonic interaction with Ru(4) [Ru(4)-O(1) 2.11(2) Å] is a normal Ru→O distance.<sup>106</sup> The  $\alpha$ -carbon, C(1), is symmetrically bound to Ru(1), Ru(2), Ru(3) (2.09 Å av.), with a longer bond to Ru(4) [2.32(4) Å]. The Ru-Ru bond distances [2.828(4) - 2.937(4) Å] are all within normal values, the longest bond Ru(2)-Ru(3) probably reflecting the strain present in the Ru(5)-P(1) bridge

**Figure 16.** PLUTO plot of  $\text{Ru}_5\{\mu_4\text{-}\eta^4\text{-}O\text{-C}_2\text{C}(\text{O})\text{C}_3\text{H}_5\}(\mu\text{-PPh}_2)_2(\mu\text{-Br})(\text{CO})_{11}$  (**47o**)  
(by B.K. Nicholson)

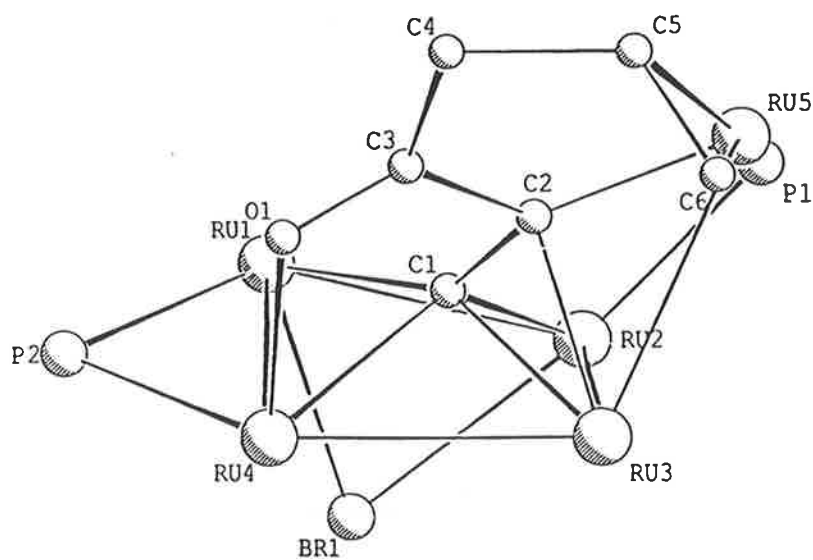
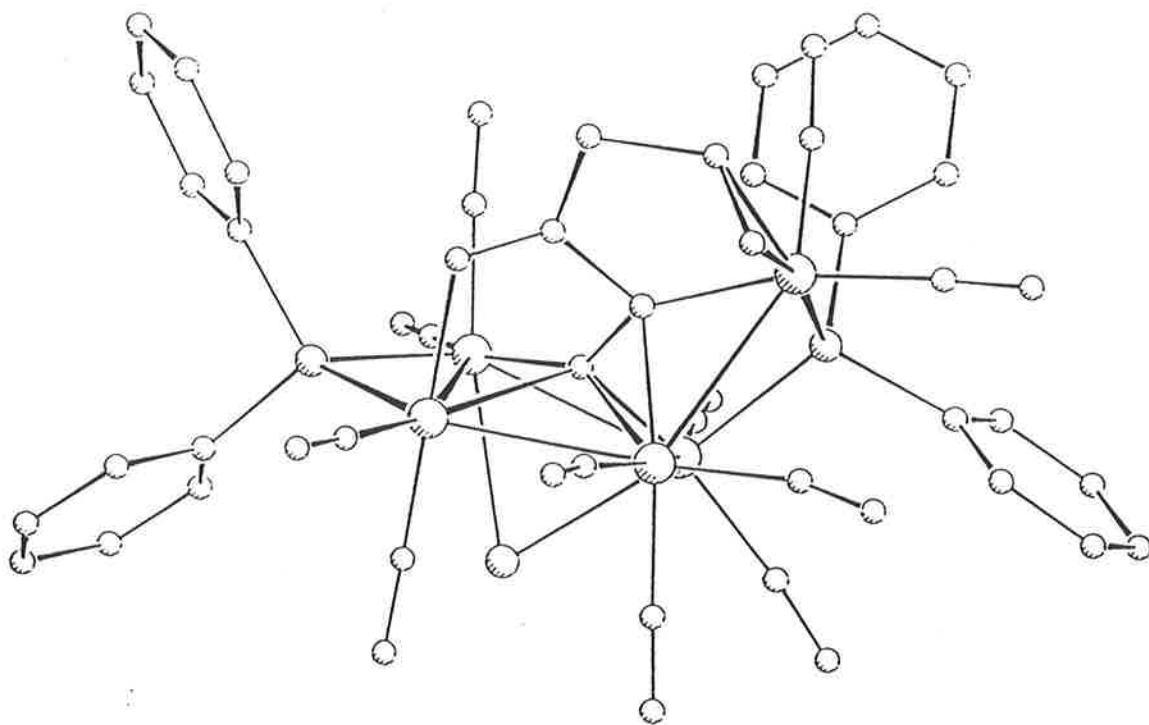


**Table 9.** Selected bond distances (Å) and angles (°) for complex (47o)

Ru(1)-Ru(2)	2.828(4)	Ru(1)-Ru(4)	2.849(4)
Ru(2)-Ru(3)	2.937(4)	Ru(3)-Ru(5)	2.889(4)
Ru(3)-Ru(4)	2.870(4)	Ru(2)-P(1)	2.312(9)
Ru(5)-P(1)	2.362(9)	Ru(1)-P(2)	2.296(9)
Ru(4)-P(2)	2.290(9)	Ru(1)-Br	2.581(4)
Ru(2)-Br	2.260(4)	Ru(1)-C(1)	2.08(4)
Ru(2)-C(1)	2.06(4)	Ru(3)-C(1)	2.12(4)
Ru(4)-C(1)	2.32(4)	Ru(3)-C(2)	2.13(3)
Ru(5)-C(2)	2.07(3)	Ru(5)-C(5)	2.38(3)
Ru(5)-C(6)	2.42(3)	Ru(4)-O(1)	2.11(2)
C(1)-C(2)	1.47(5)	C(2)-C(3)	1.42(4)
C(3)-C(4)	1.55(5)	C(4)-C(5)	1.58(4)
C(5)-C(6)	1.34(4)	C(3)-O(1)	1.26(3)
Ru(2)Ru(1)Ru(4)	89.2(1)	Ru(1)Ru(2)Ru(3)	89.5(1)
Ru(2)Ru(3)Ru(4)	86.7(1)	Ru(4)Ru(3)Ru(5)	114.7(1)
Ru(2)Ru(3)Ru(5)	82.1(1)	Ru(1)Ru(4)Ru(3)	90.4(1)
Ru(2)P(1)Ru(5)	109.8(3)	Ru(1)P(2)Ru(4)	76.8(3)
Ru(1)C(1)Ru(3)	150(2)	Ru(2)C(1)Ru(4)	131(2)
Ru(3)C(2)Ru(5)	87(1)	C(1)Ru(3)C(2)	40(1)
Ru(5)C(5)C(4)	107(2)	C(5)Ru(5)C(6)	32(1)
Ru(4)O(1)C(3)	112(2)	Ru(1)BrRu(2)	65.9(1)
C(1)C(2)C(3)	117(3)	C(2)C(3)C(4)	122(3)
C(3)C(4)C(5)	107(3)	C(4)C(5)C(6)	125(3)

[Ru(2)-Ru(5) 3.83 Å]. The carbonyl ligands are distributed three to Ru(3) and two to the remaining four rutheniums. A semibridging interaction is found for CO(32) situated between Ru(3) and Ru(5) [Ru(3)C(32)O(32) 163(3)°, Ru(3)-C(32) 1.91(3) Å, Ru(5)-C(32) 2.70 Å]. The bromine ligand is involved in a bridging three-electron interaction with Ru(1)-Ru(2) and the addition of the allyl group formally adds three electrons to the cluster. As a carbonyl ligand has also been lost, the net electronic change amounts to the addition of four electrons, resulting in the cleavage of two M-M bonds. The cluster (47o) is an 80-electron, 10-SEP compound, this assessment being obtained within PSEP theory<sup>1</sup> by condensing the electron counts for a four-membered ring and a binuclear unit (i.e. 64 + 34 - 18 = 80).

Other cluster complexes containing C<sub>3</sub>H<sub>5</sub> groups include Ru<sub>3</sub>(μ-η<sup>3</sup>-C<sub>3</sub>H<sub>5</sub>)(μ<sub>3</sub>-PPhCH<sub>2</sub>-PPh<sub>2</sub>)(CO)<sub>8</sub>,<sup>107</sup> [Os<sub>3</sub>(η<sup>3</sup>-C<sub>3</sub>H<sub>5</sub>)(CO)<sub>11</sub>][BF<sub>4</sub>],<sup>108</sup> and [PPh<sub>4</sub>][Rh<sub>6</sub>(η<sup>3</sup>-C<sub>3</sub>H<sub>5</sub>)(CO)<sub>14</sub>].<sup>109</sup> In these clusters, the allyl group is bonded to either one or two metals, with no interaction with the other ligands on the cluster. Carbon-carbon coupling reactions are well known between cluster acetylides and various substrates, including alkynes, isocyanates, isocyanides, diazoalkanes and carbon monoxide.<sup>13,47,110-112</sup>

There is no precedent for coupling involving an allyl group and carbon monoxide with a cluster-bound acetylide. This reaction, therefore, is a useful model for the interaction of an allyl group with carbon and carbon monoxide at a ruthenium surface.

### 3.2.9. Reaction of (1) with mercuric chloride

Addition of mercuric chloride to a solution of (1) in dichloromethane gave two orange-yellow isomers of Ru<sub>6</sub>(CO)<sub>11</sub>(dppa\*), (48o) and (48y). These products were obtained as crystalline solids in 13% and 19% yields respectively. Neither complex gave crystals suitable for X-ray analysis. A PPh<sub>3</sub> derivative was made by treating (32) with mercuric chloride, but this did not have a crystalline habit and was not characterized further.

The IR ν(CO) bands for (48o) and (48y) suggest all-terminal carbonyl structures in both cases, with quite different symmetries in each of the clusters. Conversion from (48y) to

(48o) was noted after 24 hours in solution, but not from (48o) to (48y). The proton NMR spectra for both compounds confirmed the presence of phenyl groups and the absence of hydride ligands. The FAB mass spectra for (48o) and (48y) showed molecular ions at  $m/z$  1308 which fragmented by successive loss of twelve 28 mass unit groups. An ion present at  $m/z$  1218 in both spectra suggested the loss of a CPh group from the molecular ion. Analytical results indicated that the compounds are best formulated as isomers of  $\text{Ru}_6(\text{CO})_{11}(\text{dppa}^*)$  (no mercury or halide elements were found by electron microprobe analyses). The  $^{31}\text{P}$  NMR spectra showed two signals for each complex at  $\delta$  258.6, 4.4 (48o) and  $\delta$  242.8, 1.3 (48y). The low field signals were assigned to a phosphido group bridging a Ru-Ru bond and the high field signals to a phosphino-acetylide (see Section 3.2.11).

The clusters appear to be electron-deficient as no evidence was found in the  $^1\text{H}$  NMR for bridging benzyne groups.<sup>14</sup> According to the spectral data, the difference between the isomers is not great and may be related to the kinetic and thermodynamic structural isomerism noted for complexes (6k) and (6t).<sup>21</sup> The treatment of a neutral cluster with  $\text{HgCl}_2$  to create new, non-mercury containing clusters such as (48o) and (48y) is an unusual reaction which deserves further investigation. Generally, the reaction of  $\text{Hg}(\text{II})$  compounds with clusters proceeds to give Hg-containing clusters such as  $\{\text{Ru}_3(\text{CO})_{11}\text{Hg}\}_3$ <sup>113</sup> and  $\text{Os}_3(\mu_3\text{-C}_2\text{Ph}_2)(\mu\text{-Cl})(\text{CO})_9\text{-(HgCl)}_2$ ,<sup>114</sup> where the mercury atoms link several cluster units (see also references 115-117), and  $\text{RuCo}_3(\text{CO})_{12}\{\mu_3\text{-HgCo}(\text{CO})_4\}$ ,<sup>118</sup> which contains a face-bridging mercury atom.

### 3.2.10. Reaction of (1) with ethene or 1-butene

Reactions involving the addition of the olefins ethene or 1-butene to (1) have been investigated under a variety of conditions. Pressurized reactions were performed in Carius tubes or in an autoclave (20 atmospheres). A red tetraruthenium cluster  $\text{Ru}_4\{\mu_4\text{-}\eta^2, P, O\text{-C}_5\text{H}_4\text{O}(\text{PPh}_2)\}(\mu\text{-PPh}_2)(\text{CO})_{11}$  (49) and two isomers of  $\text{Ru}_5(\mu_4\text{-PPh})\{\mu_3\text{-}\eta^3\text{-CC}(\text{C}_2\text{H}_2)\text{-}(\text{C}_2\text{H}_3)\}(\mu\text{-PPh}_2)(\text{CO})_{12}$  [(50b) brown, (50o) orange] were obtained from the thermal reaction of (1) and ethene under pressure. A reaction performed in the autoclave was checked at five hours, by which time the reaction was still incomplete and no other complexes were

detected. Higher yields of (49) (27%) were obtained from the Carius tube reactions, a small amount of  $\text{Ru}_3(\text{CO})_{12}$  also being isolated. Two isomers of  $\text{Ru}_5(\mu_4\text{-PPh})\{\mu_3\text{-}\eta^3\text{-CC}(\text{C}_4\text{H}_6)(\text{C}_4\text{H}_7)\}(\mu\text{-PPh}_2)(\text{CO})_{12}$  [(51b), (51o)] were obtained from the thermal reaction of 1-butene and (1) after fourteen days in a Carius tube. When ethene was passed through a heated solution of (1) in cyclohexane,  $\text{Ru}_5(\mu_4\text{-PPh})(\mu\text{-PPh}_2)(\mu\text{-CO})(\text{CO})_{10}\{\eta^5\text{-C}_5\text{H}_3(\text{C}_2\text{H}_3)\text{Me}\}$  (52) was obtained as a minor product, along with (50b) and (50o). A product with a related formulation,  $\text{Ru}_5(\text{CO})_{12}(\text{PPh})(\text{PPh}_2)\text{C}_2(\text{C}_4\text{H}_8)_3$ , was obtained from the 1-butene reaction but could not be fully characterized. Complex (50b) was converted into (52) under conditions similar to those used in the synthesis of (52) from (1). A number of minor products from these reactions were partially characterized by FAB MS and IR spectra, but as the number of olefin molecules incorporated was not always clear, these complexes are not discussed further.

An investigation of the isomer pair (50b), (50o) has shown that equilibrium concentrations of each compound are set up when the solids are dissolved in cyclohexane. The position of this equilibrium is affected by the presence of  $\text{O}_2$  in the solution and by the overall concentration, but not significantly by the presence of ethene. No exchange was found to take place between 1-butene and isomer (50o) after 15 days in solution: only (50o) and (50b) were isolated. Isomers (51b) and (51o) were found to interconvert in solution. These results suggest that intramolecular rearrangements occur in solution to give structurally-related isomers.

The infrared spectrum of (49) has nine terminal  $\nu(\text{CO})$  bands between 2082 and 1958  $\text{cm}^{-1}$ , a bridging carbonyl absorption at 1820  $\text{cm}^{-1}$ , and a weak band assigned to the ketonic carbonyl absorption at 1588  $\text{cm}^{-1}$ . A similar ketonic absorption was found for (50o) at 1532  $\text{cm}^{-1}$ , which otherwise had an all-terminal  $\nu(\text{CO})$  pattern. The 1-butene derivatives (51b) and (51o) had band patterns similar to the ethene isomers (50b) and (50o), respectively. A bridging carbonyl absorption was found for (52) at 1779  $\text{cm}^{-1}$ .

The FAB mass spectra for all the  $\text{Ru}_5$  complexes showed molecular ions which fragmented

by loss of carbonyl groups. Because of similar nominal masses for CO and ethene, and two carbonyls and butene, the exact nature of these fragmentation patterns cannot be determined from low resolution spectra. No molecular ion was found in the positive ion spectrum of (49); the negative ion spectrum, however, gave a  $[M]^-$  ion at  $m/z$  1163.

The proton NMR spectra of these compounds are complicated by the number of olefin groups attached to the clusters and also by the interconversion in solution which has been referred to previously. Phenyl resonances were found between  $\delta$  8.1 and 6.2 for all of the complexes. Four signals at  $\delta$  2.83, 2.73, 2.20 and 1.47 were assigned to the protons on the pentenone ligand in (49). The low temperature (240K) spectrum of (50b) had resonances at  $\delta$  5.58, 2.37, 1.72, 1.63 and 0.86 for the alkene and allyl protons. In the low temperature spectrum of (50o), three major resonances appeared at  $\delta$  5.04, 1.27 and 0.51; these suggested that some of the CH and CH<sub>2</sub> protons were in environments similar to those of (50b). Room temperature spectra of complexes (51b) and (51o) contained peaks that were not readily assignable, except for triplets at  $\delta$  0.96, 0.73 (51b) and at  $\delta$  0.87, 0.70 (51o), which correspond to the CH<sub>3</sub> substituents on the butene groups. The signals for the CH protons on the C<sub>5</sub> ring in complex (52) were found at  $\delta$  5.86, 5.49 and 4.61, and resonances for the CH, CH<sub>2</sub> and CH<sub>3</sub> groups at  $\delta$  2.44, 2.17 and 1.96, respectively.

The <sup>31</sup>P NMR spectra were useful in relating (50b) to (50o), as similar phosphido and phosphinidene environments were found at  $\delta$  236.7, 353.4 (50b) and  $\delta$  232.6, 374.3 (50o). Phosphido signals were found at  $\delta$  236.0, 233.2 and phosphinidene signals at  $\delta$  350.6 and 375.9 for (51b) and (51o), respectively. Phosphorus-phosphorus coupling was observed in each case, implying that the structures of these isomers are not markedly different and that the phosphido groups are *trans* to the phosphinidene ligands.

X-ray structural studies have been performed on (49), (50b) and (52). The structures determined demonstrate that incorporation of ethene and C-C coupling reactions have occurred in each instance. Plots of the three molecules are shown in Figures 17-19 and selected bond distances and angles are given in Tables 10-12.

Figure 17. PLUTO plot of  $\text{Ru}_4\{\mu_4\text{-}\eta^2\text{-}P,O\text{-C}_5\text{H}_4\text{O(PPh}_2)\}\{\mu\text{-PPh}_2\}(\text{CO})_{11}$  (49)

(by B.W. Skelton and A.H. White)

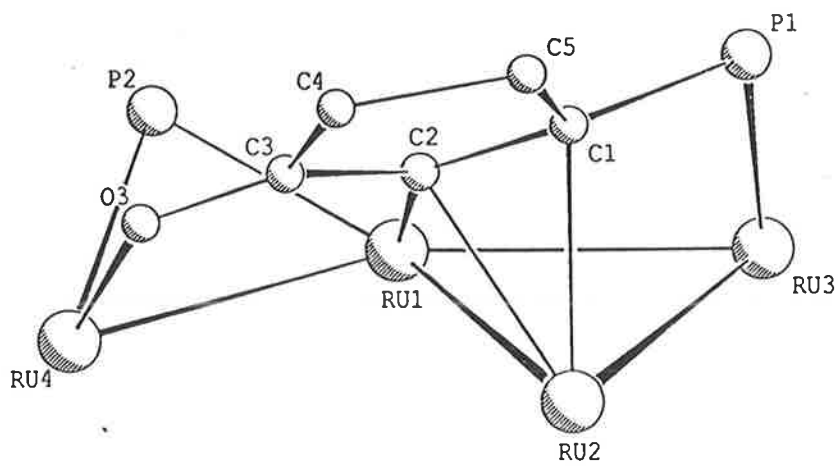
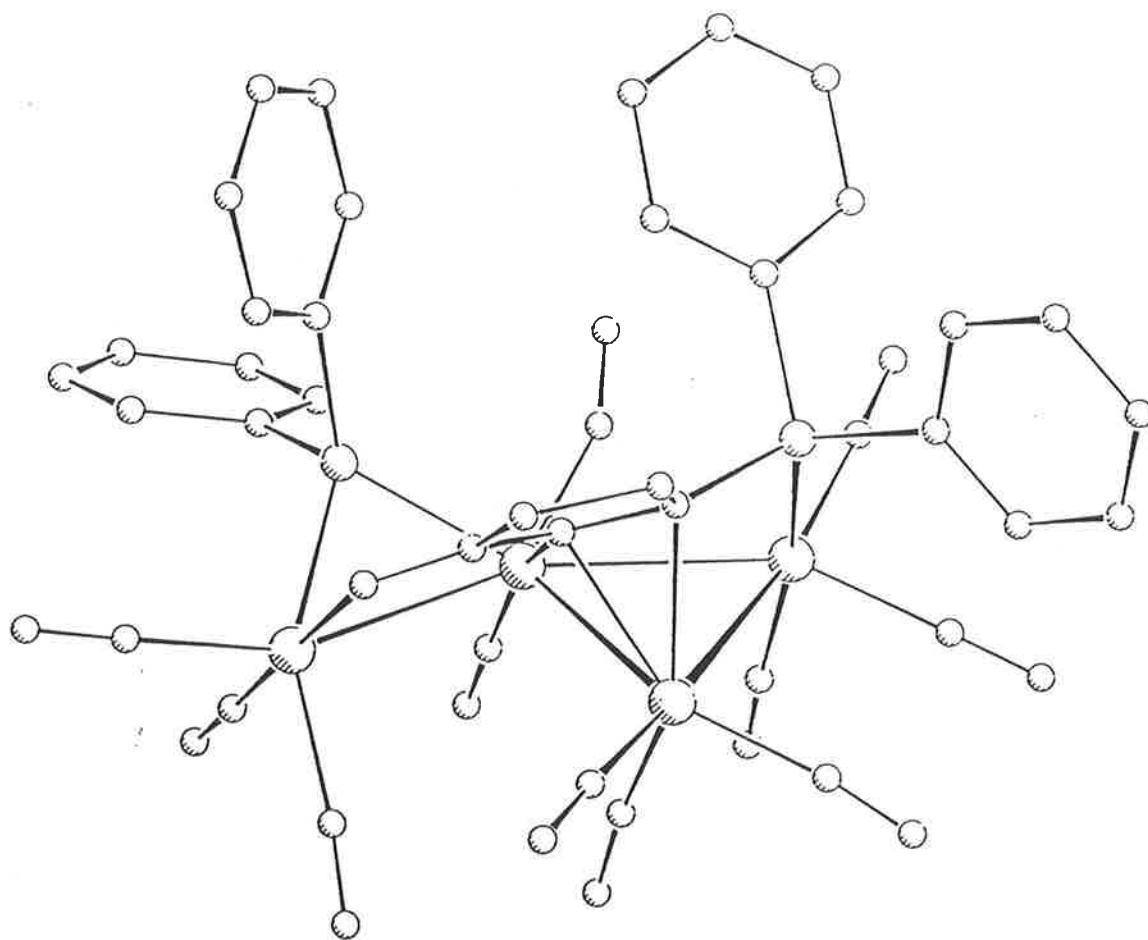


**Table 10.** Selected bond distances (Å) and angles (°) for complex (49)

Ru(1)-Ru(2)	2.787(1)	Ru(1)-Ru(3)	2.899(2)
Ru(1)-Ru(4)	2.868(2)	Ru(2)-Ru(3)	2.865(2)
Ru(3)-P(1)	2.360(2)	Ru(1)-P(2)	2.282(2)
Ru(4)-P(2)	2.306(2)	Ru(1)C(2)	2.072(7)
Ru(2)-C(1)	2.301(7)	Ru(2)-C(2)	2.202(7)
Ru(4)-O(3)	2.142(5)	C(1)-C(2)	1.43(1)
C(1)-C(5)	1.54(1)	C(2)-C(3)	1.43(1)
C(3)-C(4)	1.51(1)	C(4)-C(5)	1.53(1)
P(1)-C(1)	1.773(7)	C(3)-O(3)	1.243(9)
Ru(1)Ru(2)Ru(3)	61.69(3)	Ru(1)Ru(3)Ru(2)	57.84(4)
Ru(2)Ru(1)Ru(3)	60.47(2)	Ru(2)Ru(1)Ru(4)	96.31(2)
Ru(3)Ru(1)Ru(4)	156.48(3)	Ru(3)P(1)C(1)	103.3(2)
Ru(1)P(2)Ru(4)	77.36(8)	C(1)Ru(2)C(2)	36.9(2)
Ru(1)C(2)C(1)	129.6(5)	Ru(1)C(2)Ru(2)	81.3(2)
Ru(4)O(3)C(3)	121.8(4)	O(3)C(3)C(4)	120.6(8)
P(1)C(1)C(2)	117.9(5)	P(1)C(1)C(5)	125.3(5)
C(2)C(1)C(5)	11.9(6)	C(1)C(2)C(3)	106.7(6)
C(2)C(3)C(4)	112.1(6)	C(3)C(4)C(5)	105.2(6)
C(1)C(5)C(4)	103.7(6)		

**Figure 18.** PLUTO plot of  $\text{Ru}_5(\mu_4\text{-PPh})\{\mu_3\text{-}\eta^3\text{-CC}(\text{C}_2\text{H}_2)(\text{C}_2\text{H}_3)\}(\mu\text{-PPh}_2)(\text{CO})_{12}$ .  
 $\text{CH}_2\text{Cl}_2\cdot\text{MeOH}$  (50b) (by E.R.T. Tiekink)

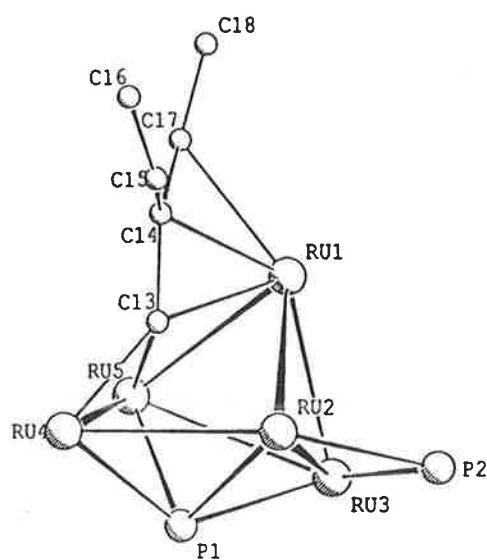
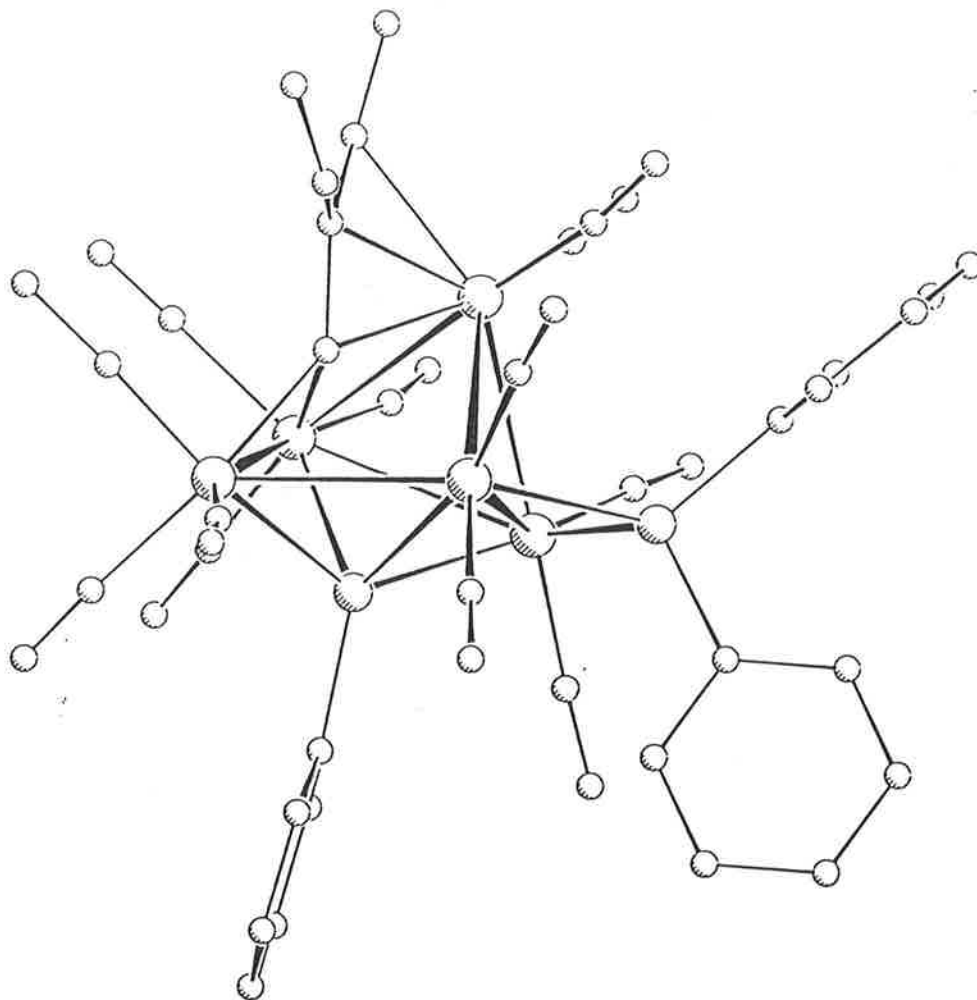


**Table 11.** Selected bond distances (Å) and angles (°) for complex (**50b**)

Ru(1)-Ru(2)	2.899(2)	Ru(1)-Ru(3)	2.829(3)
Ru(1)-Ru(5)	2.898(2)	Ru(2)-Ru(3)	2.812(3)
Ru(2)-Ru(4)	2.986(2)	Ru(3)-Ru(5)	2.985(2)
Ru(4)-Ru(5)	2.835(2)	Ru(2)-P(1)	2.472(6)
Ru(3)-P(1)	2.360(5)	Ru(4)-P(1)	2.354(7)
Ru(5)-P(1)	2.410(5)	Ru(2)-P(2)	2.311(6)
Ru(3)-P(2)	2.254(5)	Ru(1)-C(13)	2.04(2)
Ru(2)-C(13)	2.52(2)	Ru(4)-C(13)	2.07(2)
Ru(5)-C(13)	2.21(2)	Ru(1)-C(14)	2.20(3)
Ru(1)-C(17)	2.33(3)	C(13)-C(14)	1.47(4)
C(14)-C(15)	1.50(5)	C(14)-C(17)	1.55(3)
C(15)-C(16)	1.36(7)	C(17)-C(18)	1.35(4)
Ru(2)Ru(1)Ru(5)	81.3(1)	Ru(1)Ru(2)Ru(3)	59.4(1)
Ru(1)Ru(2)Ru(4)	85.3(1)	Ru(3)Ru(2)Ru(4)	95.0(1)
Ru(2)Ru(3)Ru(5)	81.3(1)	Ru(2)Ru(4)Ru(5)	80.9(1)
Ru(1)Ru(5)Ru(3)	57.5(1)	Ru(1)Ru(5)Ru(4)	88.1(1)
Ru(3)Ru(5)Ru(4)	94.5(1)	Ru(3)P(1)Ru(4)	130.2(2)
Ru(2)P(1)Ru(5)	101.3(2)	Ru(2)P(2)Ru(3)	76.0(2)
Ru(1)C(13)Ru(4)	152.2(1)	Ru(4)C(13)Ru(5)	82.9(7)
Ru(1)C(13)Ru(5)	85.8(8)	C(13)Ru(1)C(14)	40.3(9)
Ru(1)C(13)C(14)	76(1)	Ru(4)C(13)C(14)	131(2)
Ru(5)C(13)C(14)	127(1)	C(13)Ru(1)C(17)	72.9(8)
C(14)Ru(1)C(17)	39.8(8)	C(13)C(14)C(15)	118(2)
C(13)C(14)C(17)	120(2)	C(14)C(15)C(16)	137(3)
C(14)C(17)C(18)	125(3)		

**Figure 19.** PLUTO plot of  $\text{Ru}_5(\mu_4\text{-PPh})(\mu\text{-PPh}_2)(\mu\text{-CO})(\text{CO})_{10}\{\eta^5\text{-C}_5\text{H}_3(\text{C}_2\text{H}_3)\text{Me}\}$ .  
 $\text{C}_6\text{H}_{14}$  (52) (by B.W. Skelton and A.H. White)

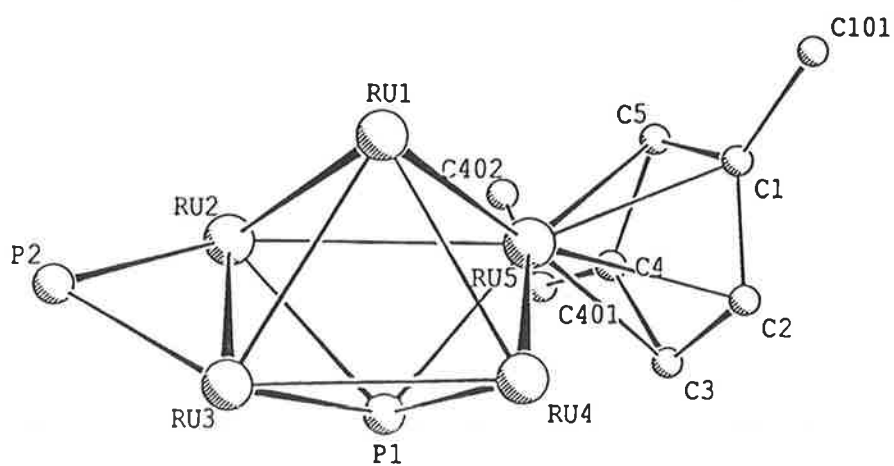
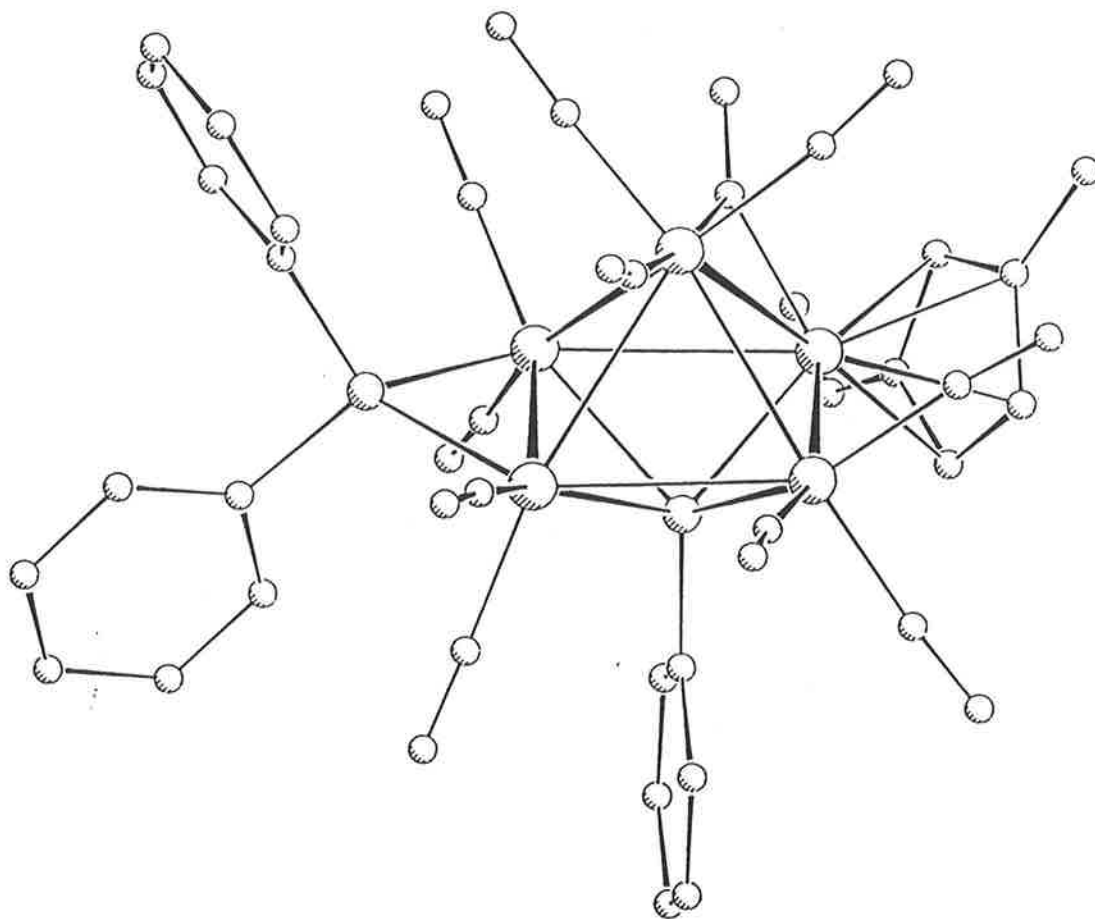


**Table 12.** Selected bond distances (Å) and angles (°) for complex (52)

Ru(1)-Ru(2)	2.874(2)	Ru(1)-Ru(3)	2.920(1)
Ru(1)-Ru(4)	2.807(2)	Ru(1)-Ru(5)	2.857(1)
Ru(2)-Ru(3)	2.794(1)	Ru(2)-Ru(5)	2.951(1)
Ru(3)-Ru(4)	2.911(1)	Ru(4)-Ru(5)	2.845(1)
Ru(2)-P(1)	2.393(2)	Ru(3)-P(1)	2.377(2)
Ru(4)-P(1)	2.355(2)	Ru(5)-P(1)	2.296(2)
Ru(2)-P(2)	2.285(2)	Ru(3)-P(2)	2.265(2)
Ru(5)C(1)	2.258(6)	Ru(5)-C(2)	2.221(6)
Ru(5)-C(3)	2.172(7)	Ru(5)-C(4)	2.232(7)
Ru(5)-C(5)	2.228(6)	Ru(1)-C(51)	2.353(7)
Ru(2)-C(51)	2.600(6)	Ru(5)-C(51)	1.925(6)
C(1)-C(2)	1.40(1)	C(1)-C(5)	1.423(9)
C(2)-C(3)	1.40(1)	C(3)-C(4)	1.42(1)
C(4)-C(5)	1.43(1)	C(1)-C(101)	1.51(1)
C(4)-C(401)	1.48(1)	C(401)-C(402)	1.21(2)
Ru(2)Ru(1)Ru(3)	57.65(3)	Ru(2)Ru(1)Ru(4)	91.40(5)
Ru(2)Ru(1)Ru(5)	61.97(4)	Ru(3)Ru(1)Ru(4)	61.07(4)
Ru(3)Ru(1)Ru(5)	89.41(5)	Ru(4)Ru(1)Ru(5)	60.29(3)
Ru(3)Ru(2)Ru(5)	90.03(5)	Ru(2)Ru(3)Ru(4)	90.91(5)
Ru(3)Ru(4)Ru(5)	89.83(5)	Ru(2)Ru(5)Ru(4)	89.10(5)
Ru(2)P(1)Ru(3)	71.72(5)	Ru(2)P(1)Ru(4)	117.87(8)
Ru(2)P(1)Ru(5)	77.99(6)	Ru(3)P(1)Ru(4)	75.93(6)
Ru(3)P(1)Ru(5)	120.86(8)	Ru(4)P(1)Ru(5)	75.41(6)
Ru(2)P(2)Ru(3)	75.73(5)	Ru(1)C(51)O(51)	125.3(5)
Ru(2)C(51)O(51)	123.5(4)	Ru(5)C(51)O(51)	146.3(5)
Ru(5)C(51)Ru(1)	83.2(2)	C(4)C(401)C(402)	122(1)

The metal-core structure of (49) is that of a spiked triangle, which is held together by a phosphino-cyclopentenone ligand and a bridging phosphido group. Electronically, (49) is a 64-electron, 8-SEP cluster. The metal core is related to (1) by cleavage of a 'Ru(CO)' fragment [which appears as Ru<sub>3</sub>(CO)<sub>12</sub>]. The 'spike' atom Ru(4) lies 0.199 Å above the least-squares plane through Ru(1)Ru(2)Ru(3) and at a distance of 2.868(2) Å from Ru(1). Within the Ru<sub>3</sub> triangle, the two Ru-Ru separations Ru(1)-Ru(3) [2.899(2) Å], Ru(2)-Ru(3) [2.865(2) Å] are normal,<sup>73</sup> while Ru(1)-Ru(2) [2.787(1) Å] is rather short and appears to reflect the clamping effect of the pentenone ligand. The P-Ru distances [2.282(2) - 2.306(2) Å] are unexceptional. Three carbonyl ligands are attached to each of Ru(2), Ru(3) and Ru(4), while two are attached to Ru(1). A semibridging carbonyl interaction is found between Ru(1) and Ru(3), with a Ru(1)C(12)O(12) angle of 157.7(6)° and Ru(3)-C(12) contact of 2.56(8) Å. As there is no obvious electronic imbalance at Ru(1) or Ru(3) the reason for this mode of bonding appears to lie with the steric interactions of the phosphido group attached to Ru(1). The ketonic carbonyl group is attached to Ru(4) [Ru(4)-O(1) 2.11(2) Å] in a manner similar to that found for (47o). Within the organic ligand, delocalized double bonds were found for C(1)-C(2), C(2)-C(3) [1.43(1) Å for both] and localized C-C single bonds for C(1)-C(5), C(3)-C(4), C(4)-C(5) [1.54(1), 1.51(1), 1.53(1) Å, resp.], confirming the σ-vinyl interaction of the cyclopentenone ligand with the cluster.

Carty *et al.*<sup>119</sup> have recently reported the synthesis of a tetranuclear cyclopentadienyl complex [Ru<sub>2</sub>{μ-σ(C,O), η<sup>7</sup>-C<sub>5</sub>MePh<sub>2</sub>(C<sub>6</sub>H<sub>4</sub>)(O)}(μ-PPh<sub>2</sub>)]<sub>2</sub>, obtained by diphenylacetylene-allenyl coupling. The mechanism proposed for the formation of the cyclopentadienyl ligand involves the addition of alkyne and CO to the η<sup>2</sup>-coordinated double bond of the allenyl ligand. In the formation of (49), we see the addition of CO and ethene to a η<sup>2</sup>-coordinated acetylide moiety. In Section 3.2.8, the generation of a hexenone ligand from the original C<sub>2</sub> unit, a carbonyl ligand and an allyl group was mentioned. Here we have found the formation of a C<sub>5</sub> ring from the C<sub>2</sub> unit, an ethene molecule and a carbonyl ligand. Organometallic compounds containing the related pentadienone ligand include Os<sub>3</sub>{ $\overline{\text{C(Me)C(Me)C(O)C(Me)-C(Me)}}$ }(CO)<sub>9</sub>,<sup>120</sup> Os<sub>3</sub>(μ-H){ $\overline{\text{CHC(CHMe)C(O)CEtCH}}$ }(CO)<sub>8</sub><sup>121</sup> and

$\text{Rh}_2\{\overline{\text{C}(\text{CF}_3)\text{C}(\text{CF}_3)\text{CHC}(\text{Bu}^t)\text{C}(\text{O})}\}(\text{CO})(\eta\text{-C}_5\text{H}_5)_2$ ;<sup>122</sup> these complexes were formed from alkyne-carbonyl-alkyne coupling reactions.

The structure of (50b) is related to those of (27) and (28), in that the  $\text{Ru}_5$  core is a wingtip-bridged butterfly (the dihedral angle of the butterfly core is  $96.5^\circ$ ). All three clusters have 76-electron, 8-SEP electron counts. A substituted vinyl-allyl ligand has been formed by the addition of two ethene units to the  $\beta$ -carbon of the acetylide. The  $\alpha$ -carbon is  $\mu_4$ -bonded to one face of the cluster and a  $\mu_4$ -phosphinidene ligand caps the other  $\text{Ru}_4$  face. Inclusion of these main group elements in the cluster core defines a *closo* pentagonal bipyramid [a least-squares plane through  $\text{Ru}(4)\text{P}(1)\text{Ru}(3)\text{Ru}(1)\text{C}(13)$  has maximum deviations of  $0.11(2) \text{ \AA}$ , with  $\text{Ru}(2)$  and  $\text{Ru}(5)$  symmetrically displaced about this plane [ $-1.894(2)$  and  $1.877(2) \text{ \AA}$ , resp.]. A phosphido group bridges  $\text{Ru}(2)$ - $\text{Ru}(3)$ . Three carbonyls are bonded to each of  $\text{Ru}(4)$  and  $\text{Ru}(5)$ , and two to each of  $\text{Ru}(1)$ ,  $\text{Ru}(2)$  and  $\text{Ru}(3)$ . A carbonyl on  $\text{Ru}(5)$  is in a bent arrangement [ $\text{Ru}(5)\text{C}(10)\text{O}(10) 165.9(2)^\circ$ ]: this is probably due to steric effects, since the non-bonding distances  $\text{Ru}(1)\cdots\text{C}(10)$  and  $\text{Ru}(3)\cdots\text{C}(10)$  are both quite large [ $3.06$ ,  $2.98 \text{ \AA}$ , resp.]. The  $\text{Ru}$ - $\text{Ru}$  bonds are within the range  $2.812(2) - 2.986(2) \text{ \AA}$  and  $\text{Ru}$ - $\text{P}$  separations are in the range  $2.311(6) - 2.472(6) \text{ \AA}$ . The  $\mu_4$ -phosphinidene has two shorter  $\text{Ru}$ - $\text{P}$  bonds, involving  $\text{Ru}(3)$  and  $\text{Ru}(4)$  [ $2.360(5)$ ,  $2.354(7) \text{ \AA}$ , resp.] and two longer bonds to the wingtip rutheniums  $\text{Ru}(2)$  and  $\text{Ru}(5)$  [ $2.472(6)$ ,  $2.410(5) \text{ \AA}$ , resp.]. The  $\alpha$ -carbon of the vinyl-allyl ligand,  $\text{C}(13)$ , is bonded to  $\text{Ru}(1)$ ,  $\text{Ru}(2)$ ,  $\text{Ru}(4)$  and  $\text{Ru}(5)$  [ $2.04(2)$ ,  $2.52(2)$ ,  $2.07(2)$ ,  $2.21(2) \text{ \AA}$ , resp.]. The interaction with  $\text{Ru}(2)$  is rather long but is apparently bonding, as there is a formal electronic deficiency at this ruthenium 17(e). An allylic interaction between  $\text{C}(13)$ ,  $\text{C}(14)$ ,  $\text{C}(17)$  and  $\text{Ru}(1)$  [ $\text{C}(14)$ - $\text{Ru}(1) 2.20(3)$ ,  $\text{C}(17)$ - $\text{Ru}(1) 2.33(3) \text{ \AA}$ , resp.] is necessary to fulfil the electronic requirements at this atom. Within the organic group, there are both delocalized and localized  $\text{C}=\text{C}$  double bonds  $\text{C}(13)$ - $\text{C}(14)$ ,  $\text{C}(15)$ - $\text{C}(16)$ ,  $\text{C}(17)$ - $\text{C}(18)$  [ $1.47(3)$ ,  $1.36(7)$ ,  $1.35(4) \text{ \AA}$ , resp.] and  $\text{C}$ - $\text{C}$  single bonds  $\text{C}(14)$ - $\text{C}(15)$ ,  $\text{C}(14)$ - $\text{C}(17)$  [ $1.50(5)$ ,  $1.55(3) \text{ \AA}$ , resp.].

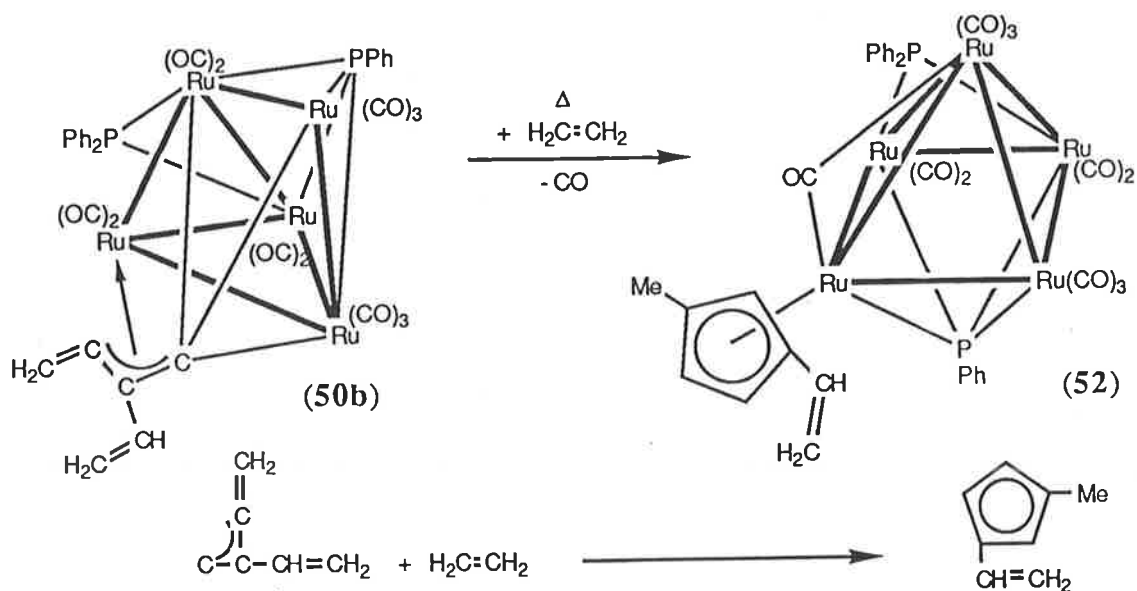
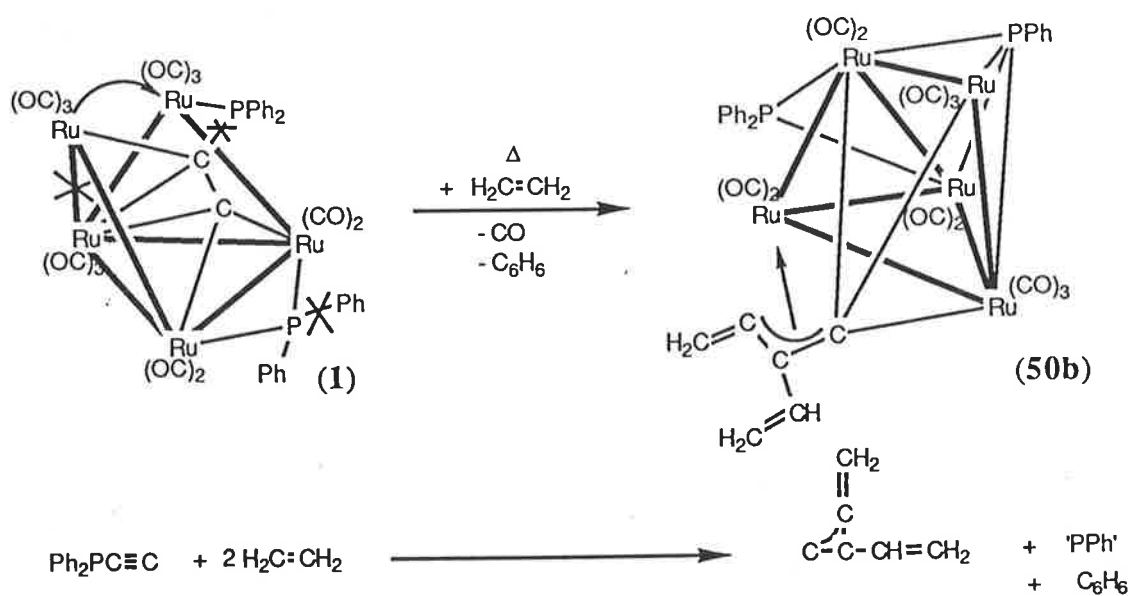
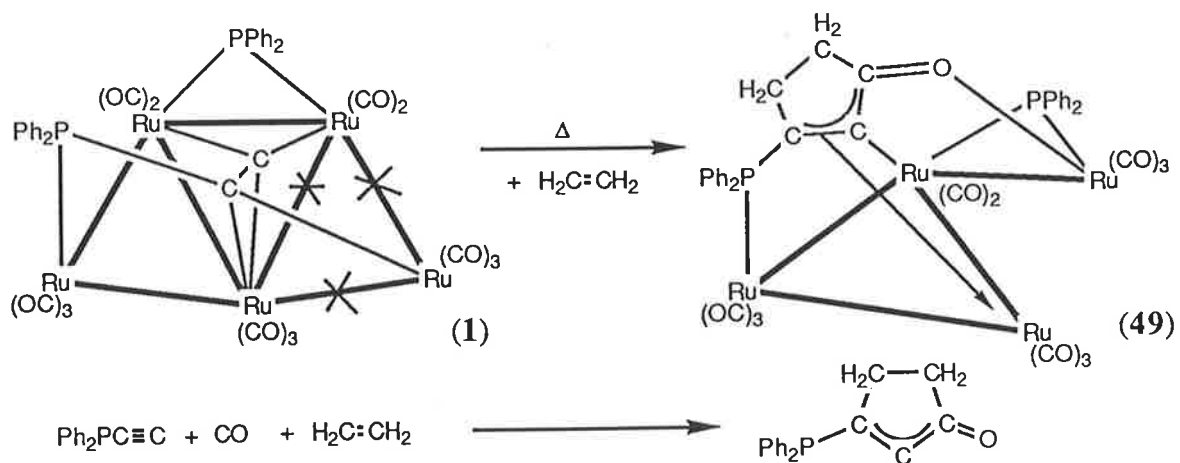
The last structure to be examined in this study is that of (52), which has a metal core based on a square pyramidal geometry. The phosphinidene  $\text{P}$  atom is situated  $2.017 \text{ \AA}$  below the

square base with Ru(1) 1.187 Å above it. The 1-methyl-3-vinylcyclopentadienyl ligand attached to Ru(5) is formed by the addition of a further ethene molecule to the vinyl-allyl ligand in (50b). There are eleven carbonyl groups in the molecule, two being attached to each of Ru(2) and Ru(3), and three to each of Ru(1) and Ru(4). A bridging carbonyl is asymmetrically situated over the Ru(1)-Ru(5) bond [Ru(1)-C(51) 2.353(7), Ru(5)-C(51) 1.925(6) Å] with a rather short non-bonding distance to Ru(2) [Ru(2)··C(51) 2.600(6) Å]. A semibridging carbonyl interaction is present between Ru(1) and Ru(3) [Ru(1)C(12)O(12) 168.8(6)°, Ru(3)··C(12) 2.95 Å]. The eight Ru-Ru bonds are in the range 2.794(1) - 2.920(1) Å. The phosphinidene and phosphido ligands are attached to the cluster in a manner similar to (33), the Ru-P distances being between 2.265(2) and 2.396(2) Å. The cyclopentadienyl ligand is almost symmetrically bonded to Ru(1) [Ru-C distances 2.172(7) - 2.258(6) Å], and within the cyclopentadienyl ligand the C-C separations are between 1.40(1) and 1.43(1) Å. The C(401)-C(402) bond distance [1.21(2) Å] confirms that the ring substituent at this position is indeed a vinyl group. Like (26) and (33), the square pyramidal structure of (52) has a 74-electron, 7-SEP electron count. Clusters containing cyclopentadienyl ligands are relatively rare, the only pentaruthenium clusters noted to date being Ru<sub>5</sub>(CO)<sub>6</sub>(η-C<sub>5</sub>H<sub>5</sub>)<sub>4</sub><sup>2</sup> and AuRu<sub>5</sub>C(CO)<sub>13</sub>(PPh<sub>3</sub>)(η-C<sub>5</sub>H<sub>5</sub>) (22),<sup>33</sup> while some smaller clusters are mentioned in a recent review on ruthenium and osmium complexes containing η<sup>5</sup>-dienyl ligands.<sup>123</sup>

The addition of two ethene molecules to the phosphino-acetylide in (1) to form (50b) involves two P-C cleavage reactions and loss of a CO ligand and a phenyl group. As several protons have been cleaved from the ethene molecules on coupling it is likely that the phenyl group is lost as benzene.<sup>124</sup> The core transformations are similar to those involved in the formation of (27). No reaction between (27) and ethene was seen to occur in refluxing cyclohexane, conditions under which (1) reacted to form (50b) and (52). The conversion of (50b) to (52) by reaction with further ethene is illustrated in Scheme 10. The addition of the incoming ethene molecule to the vinyl-allyl group is accompanied by loss of a carbonyl ligand and a major structural rearrangement. There is a possibility that the other isomer (50o) is involved in this transformation, as this product was also isolated from the reaction mixture.

The alkene-acetylide coupling reactions examined here are without precedent in cluster chemistry and are therefore of considerable interest. Reactions of ethene with clusters have generally given  $\eta^2$ -bonded complexes.<sup>125-127</sup> The reactions of  $\text{Ru}_3(\text{CO})_{12}$  with ethene have been shown to give C-C coupled products such as  $\text{Ru}_4(\mu_4-\eta^2\text{-MeCCMe})(\text{CO})_{12}$  and  $\text{Ru}_6\text{C}(\mu-\eta^2, \eta^2\text{-MeCH=CHCH=CHMe})(\text{CO})_{15}$  through oligomerization of the olefin.<sup>128</sup> Clusters (49) - (52) may be seen as model compounds for C-C bond-forming reactions which occur at metal surfaces.<sup>129</sup> The chemisorption and decomposition of ethyne and ethene on oxygen-covered  $\text{Ru}(001)$  surfaces has been studied.<sup>130,131</sup> Ethyne chemisorbs initially and then decomposes between 200 and 350K to produce a number of stable intermediates including an acetylide species (CCH); under similar conditions ethene initially chemisorbs irreversibly and then dehydrogenates to form the stable intermediates ethylidyne (CCH<sub>3</sub>) and vinylidene (CCH<sub>2</sub>). These intermediates have been implicated in the carbon-carbon chain growth process of Fischer-Tropsch catalysis. Although clusters can act as catalysts it has not yet been established whether they are the actual species involved in the catalytic process.<sup>132</sup> For example, the cluster  $\text{Ru}_3(\mu\text{-H})_2(\mu_3\text{-O})(\text{CO})_5(\text{dppm})_2$  has been shown to be an active catalyst precursor for ethene hydrogenation reactions, the reaction proceeding through olefin coordination and activation by the dihydride cluster.<sup>133</sup> Recent work has established that alkyne-alkene,<sup>134</sup> alkyne-alkyne,<sup>120,135</sup> alkyne-alkylidyne,<sup>136</sup> alkyne-carbide,<sup>137</sup> alkyne-carbyne,<sup>138</sup> alkyne-methylene,<sup>139</sup> carbyne-ethylidene,<sup>140</sup> and ethene-methylene<sup>141</sup> coupling reactions all occur readily for multinuclear organometallic complexes. The structural characterization of complexes (49), (50b) and (52) shows that acetylide-alkene coupling is also a facile process for transition-metal cluster complexes. C-C coupling involving three different components is a new development in the chemistry of large clusters.

Scheme 10. Reaction of (1) with ethene



### 3.2.11. $^{31}\text{P}$ NMR studies on some $\text{Ru}_4$ , $\text{Ru}_5$ and $\text{Au}_2\text{Ru}_5$ clusters

The  $^{31}\text{P}$  NMR data gathered in the course of this work is presented in Table 13. Wherever the complexes containing phosphine, phosphite, phosphido and phosphinidene ligands have been crystallographically characterized, correlations between the  $^{31}\text{P}$  NMR spectra and these structures have been made. A number of related compounds, which were not crystallographically characterized, are also listed in the table.

A recent review<sup>142</sup> has shown the usefulness of  $^{31}\text{P}$  NMR chemical shift and coupling constant information in defining the stereochemistry of transition metal complexes which contain phosphido and phosphinidene ligands. Huttner *et al.*<sup>22</sup> have recorded a series of chemical shifts for various  $\text{Ru}_5(\mu_4\text{-PR}_3)(\text{CO})_{15}$  ( $\text{R} = \text{Ph, Et, Me, CH}_2\text{Ph}$ ) clusters, and a small number of other  $\text{Ru}_5$  clusters were also mentioned in the review article.<sup>142</sup> The work presented here extends considerably the amount of information pertaining to pentanuclear ruthenium clusters.

*Phosphinidene Ligands* : Phosphinidene ligands, in both the  $\mu_4$  and  $\mu_3$  modes of coordination, were found in several of these complexes. Two structural types containing  $\mu_4$ -PPh groups have been found for the  $\text{Ru}_5$  clusters: the first was the arrowhead core, which has an open  $\text{Ru}_4$  face capped by a phosphinidene ligand. Complexes (27), (28) and (50b) have this geometry and the chemical shifts for the phosphinidenes were found at  $\delta$  480.4, 326.1 and 353.4, respectively. [The assignment of the signal for (27) is somewhat arbitrary as there is also a  $\mu_3$ -phosphinidene present at  $\delta$  455.9.] Both phosphinidenes in complex (27) are coupled ( $J_{\text{av.}} = 79$  Hz). Similar coupling was found between the phosphido and phosphinidene ligands in (28) and (50b), these groups being attached to the Ru(1)-Ru(4) bond [but numbered Ru(2)-Ru(3) in (50b)] as is the  $\mu_3$ -PPh in (27). The second structural type is that based on a square pyramid, examples being (26), (33) and (52). The chemical shifts for the phosphinidene ligands in these clusters were at  $\delta$  475.7, 451.5 and 422.2, respectively. No coupling was observed between the phosphino-vinylidene and phosphinidene ligands in (26). The phosphinidene ligand in (5) had a signal at  $\delta$  191.6 showing P-P

coupling (100 Hz) to the phosphino-alkyne ligand. This high field shift has a precedent in the signal found at  $\delta$  -34 for one of the phosphinidene ligands in  $\text{Ru}_4(\mu_4\text{-PPh})_2(\mu\text{-PPhH})_2(\text{CO})_8$ .<sup>18</sup>

*Bridging phosphido ligands:* The chemical shift for the phosphido bridge in (1) is at particularly low field ( $\delta$  310.6). Similar shifts ( $\delta$  277.3 - 292.9) were found for the swallow-geometry, phosphite-substituted clusters (29a), (29c) and (30). No phosphorus coupling was observed between the  $\text{P}(\text{OEt})_3$  ligand in (29c) and the phosphido ligand; this is not surprising as the phosphite is attached in a *cis* fashion to the phosphido-bound ruthenium [P(2)Ru(3)P(3) 102.3(1)]. In the arrowhead arrangement of (50b), the  $\mu\text{-PPh}_2$  ligand had a higher field signal at  $\delta$  236.7, whereas the  $\mu\text{-PPh}(\text{OMe})$  ligand in (28) showed had a signal at  $\delta$  297.2. The lower field shift of the latter is consistent with differences observed between phosphite and phosphine ligands. For the square pyramidal clusters (33) and (52), the phosphido signals appeared at  $\delta$  203.7 and  $\delta$  263.6, respectively. In the cluster with the spiked square geometry (47o), the phosphido bridging the Ru(1)-Ru(4) bond had a chemical shift of  $\delta$  269.4, while the phosphido ligand bridging the open distance between Ru(5) and Ru(2) (see Figure 16) had a high field signal at  $\delta$  57.3. The latter signal is comparable to the shift observed for the phosphido ligand in  $\text{Ru}_5(\mu_4\text{-}\eta^2\text{-C}_2\text{Pr}^i)\{\mu_4\text{-NC(O)NCPh}_2\}(\mu\text{-PPh}_2)(\text{CO})_{13}$ <sup>7</sup> ( $\delta$  79.7), which bridges a similar open vector. The third pentanuclear framework to have been examined was that of the scorpion geometry, of which (6k), (6t), (43) and (44) are examples. The chemical shifts for the phosphido groups in these complexes are  $\delta$  192.1, 187.0, 194.3 and 236.6, respectively. There was a large P-P coupling constant ( $J_{\text{av.}} = 124$  Hz) between the phosphido and phosphino-acetylide ligands in (6t), as these ligands are in a *trans* arrangement [RuPRu 141.0(1)<sup>o</sup>]. A normal shift of  $\delta$  185.4 was found for the phosphido ligand in the  $\text{Ru}_4$  cluster (49) and a signal was found at  $\delta$  131.9 for the two equivalent phosphido groups bridging the  $\text{Ru}_3$  triangles in (7). The heptanuclear cluster (41) showed a higher field shift for the phosphido group ( $\delta$  203.4) than did (29a) (which is the most closely related  $\text{Ru}_5$  complex).

*Phosphine and phosphite ligands:* The phosphino-acetylide ligands in the pentaruthenium clusters showed chemical shifts in the range  $\delta$  38.1 - 44.8 for the swallow clusters and  $\delta$  7.7 - 64.1 for the scorpion clusters. Coordination and rearrangement of the dppa ligand has moved the chemical shift of the phosphorus to a lower field than that of the free ligand ( $\delta$  -31.0). The  $\text{Au}_2\text{Ru}_5$  clusters had signals for the  $\text{C}_2\text{PPh}_2$  ligand between  $\delta$  -6.3 and 1.3, the effect of adding the digold unit to (1) being to shield the phosphorus nuclei. Complex (30) showed P-P coupling (40 Hz) between the phosphino-acetylide and the  $\text{P}(\text{OEt})_3$  ligand on Ru(1). As mentioned above, a large P-P coupling constant (100 Hz) was found between the phosphino-alkyne and phosphinidene ligands in the tetranuclear cluster (5); the chemical shift of the phosphino-alkyne was  $\delta$  0.1. The novel phosphino-vinylidene ligand present in (26) has a chemical shift of  $\delta$  -34.7. The substituted derivatives (29a), (29c), (30) and (41) had chemical shifts for the triethylphosphite ligands in the normal region for such ligands  $\delta$  129.2 - 140.8, while the triphenylphosphine ligands in complex (41) had signals at  $\delta$  62.3 and 74.7.

The utility of  $^{31}\text{P}$  NMR studies in characterizing multinuclear clusters relies on a sufficiently large body of data having been correlated with the known structural types. When such information becomes available, the combination of analytical results, FAB MS,  $^1\text{H}$  NMR,  $^{13}\text{C}$  NMR and  $^{31}\text{P}$  NMR data may provide quite detailed information on the stereochemistry of new complexes without recourse to X-ray studies. In favourable circumstances, the time required to obtain an X-ray crystal structure is likely to be shorter than that required for an analytical and spectroscopic characterization, and the result more certain. In particular, for complexes that are likely to have new structural geometries, the  $^{31}\text{P}$  NMR results must be treated cautiously, as the chemical shift regions of the various phosphorus ligands examined have been shown to overlap and X-ray studies become essential.

Table 13.  $^{31}\text{P}\{^1\text{H}\}$  NMR data for some  $\text{Ru}_4$ ,  $\text{Ru}_5$  and  $\text{Au}_2\text{Ru}_5$  clusters<sup>§</sup>

Compd	$\text{C}_2\text{PPh}_2$ or <sup>a</sup> $\text{C}_2\text{PhPPh}_2$	$\mu\text{-PPh}_2$ <sup>b</sup> $\mu\text{-PPh(OMe)}$	$\mu_3\text{-PPh}$	$\mu_4\text{-PPh}$	$\text{P(OEt)}_3^1$	$\text{PPh}_3^1$ or <sup>c</sup> $\text{PMe}_2\text{Ph}^1$	$\text{PPh}_3^2$ or <sup>d</sup> $\text{P(OEt)}_3^2$
d p p a	-31.0	-	-	-	-	-	-
(1)	38.1	310.6	-	-	-	-	-
(5)	-	0.1	-	191.6	-	-	-
(6k)	7.7	(d, $J = 100$ ) 192.1	-	(d, $J = 100$ ) -	-	-	-
(6t)	10.5	187.0	-	-	-	-	-
(7)	(d, $J = 123$ ) -	(d, $J = 125$ ) 131.9	-	-	-	-	-
(26)	-34.7 <sup>a</sup>	-	-	475.7	-	-	-
(27)	-	-	455.9	480.4	-	-	-
(28)	-	297.2 <sup>b</sup>	(d, $J = 78$ ) -	(d, $J = 80$ ) 326.1	-	-	-
(29a)	44.2	(d, $J = 30$ ) 292.9	-	(d, $J = 30$ ) -	140.8	-	-
(29b)	43.5	300.0	-	-	134.1	-	-
(29c)	(m) 43.9	(m) 292.5	-	-	(2xd, $J=35,34$ ) 137.6	-	-
(30)	44.8	277.3	-	-	142.8	-	137.1 <sup>d</sup>
(31)	(d, $J = 40$ ) 39.2	269.6	-	-	-	23.7 <sup>c</sup>	(d, $J = 40$ ) 1.5 <sup>c</sup>
(32)	41.0	281.3	-	-	-	-	-
(33)	-	203.7	-	451.5	-	-	-
(35)	-6.0	(m) 213.8	-	-	-	74.9	62.6
(39)	-6.3	214.3	-	-	186.3	71.3	-
(40)	0.4	202.5	-	-	185.7	71.0	130.2 <sup>d</sup>
(41)	1.3	203.4	-	-	129.2	74.7	62.3
(42)	44.5	194.8	-	-	-	-	-
(43)	40.3	194.3	-	-	-	-	-

<sup>§</sup>All spectra were recorded in  $\text{CH}_2\text{Cl}_2$ ; peak positions are relative to ext. 85%  $\text{H}_3\text{PO}_4$ .

Table 13. (continued)<sup>§</sup>

Compd	C <sub>2</sub> PPh <sub>2</sub> or e <sub>μ</sub> -PPh <sub>2</sub> <sup>2</sup>	μ-PPh <sub>2</sub>	μ <sub>3</sub> -PPh	μ <sub>4</sub> -PPh	P(OEt) <sub>3</sub> <sup>1</sup>	PPh <sub>3</sub> <sup>1</sup>	PPh <sub>3</sub> <sup>2</sup> or P(OEt) <sub>3</sub> <sup>2</sup>
(44)	64.1	236.6	-	-	-	-	-
(45)	49.5	189.1	-	-	-	60.4	-
(46o)	54.9 <sup>e</sup>	271.3	-	-	-	-	-
(46b) <i>i</i>	65.5	252.4	-	-	-	-	-
<i>ii</i>	60.8	249.8	-	-	-	-	-
(47o)	57.3 <sup>e</sup>	269.4	-	-	-	-	-
(47b) <i>i</i>	67.2	252.8	-	-	-	-	-
<i>ii</i>	60.9	251.0	-	-	-	-	-
(48o)	4.4	258.6	-	-	-	-	-
(48y)	1.3	242.8	-	-	-	-	-
(49)	40.4	185.4	-	-	-	-	-
(50o)	-	232.6 (d, <i>J</i> = 38)	-	374.3 (d, <i>J</i> = 38)	-	-	-
(50b)	-	236.7 (d, <i>J</i> = 34)	-	353.4 (d, <i>J</i> = 32)	-	-	-
(51o)	-	233.2 (d, <i>J</i> = 38)	-	375.9 (d, <i>J</i> = 41)	-	-	-
(51b)	-	236.0 (d, <i>J</i> = 38)	-	350.6 (d, <i>J</i> = 35)	-	-	-
(52)	-	263.6 (m)	-	422.2 (m)	-	-	-

<sup>§</sup>All spectra were recorded in CH<sub>2</sub>Cl<sub>2</sub>; peak positions are relative to ext. 85% H<sub>3</sub>PO<sub>4</sub>.

### 3.3. Conclusions

Many reactions have now been investigated for complex (1) and some reactivity patterns have been established:

(i) Thermal activation of the cluster results in carbonyl loss, P-C bond cleavage and, under forcing conditions, orthometallation. Upon pyrolysis, the acetylide ligand is transformed into a vinylidene ligand [in (26), (27)] by phenyl migration from a phosphido ligand, the formation of bridging phosphinidene and phosphido ligands helping to maintain cluster integrity. The generation of smaller clusters ( $Ru_3$ ,  $Ru_4$ ) occurs only when excess reagents are present.

(ii) The oxidative addition of substrates such as HX ( $X = Cl, Br$ ),  $AuCl(PPh_3)$  (four-electron donors) or HI (six-electron donor) proceeds to give complexes with scorpion structures. The addition of two CO groups (four electrons) gives complexes with the same metal core geometry.<sup>21</sup>

(iii) Substitution of carbonyl ligands by two-electron donors such as phosphites or phosphines results principally in substitution at wingtip positions when  $Me_3NO$  is used, and at the phosphido-bridged rutheniums under thermal conditions. As further *P*-donor ligands are introduced into the cluster, the electronic balance in the molecule is maintained by bridging and semibridging carbonyl interactions.

(iv) The reduction of the acetylide ligand by hydrogen proceeds through successive addition of H to  $C_\beta$  to give a vinylidene ligand [ $CCH(PPh_2)$ ], followed by an alkylidyne ligand [ $CCH_2(PPh_2)$ ] and finally, cleavage of the  $C\equiv C$  bond to give a carbide ligand and a Me group (in  $PMePh_2$ ). Three H atoms are added stepwise to the cluster framework.<sup>10</sup> The addition of the first  $H_2$  molecule results in an electronic rearrangement within the cluster, but the overall electron count remains at 76 electrons. The next addition of  $H_2$  is accompanied by the loss of a CO molecule, and the electron count on the cluster drops to 74 electrons. This change in the electron count is consistent with the structural change from swallow to square pyramidal geometry. The final addition of  $H_2$  results in the loss of a further CO, which is offset electronically by the incorporation of the carbide (4e) into the cluster.

(v) Reduction of (1), followed by the addition of AuCl(PPh<sub>3</sub>), results in the synthesis of the heptanuclear digold cluster (35). The phosphite derivative (41) has an open Ru<sub>5</sub> core with six Ru-Ru bonds, which is one less than (1). The breaking of one metal-metal bond accords with the addition of two one-electron Au(PPh<sub>3</sub>) units. In (41), the acetylide still contributes five electrons to the overall electron count, but the mode of distribution within the cluster has changed.

(vi) The reactions of allyl halides and alkenes with (1) gave C-C coupled products. The reaction with allyl bromide gave the spiked square cluster (47o), which was found to have a hexenone ligand formed from the allyl group, a carbonyl ligand and the C<sub>2</sub> unit. The reaction between ethene and (1) gave three crystallographically-characterized complexes (49), (50b) and (52). The Ru<sub>4</sub> cluster (49) contained a cyclopentenone ligand formed by the combination of ethene, CO and C<sub>2</sub> groups. Complex (50b) is a 74-electron cluster with an allylic linkage involving a CC(CCH<sub>2</sub>)(CHCH<sub>2</sub>) ligand, which has been formed by linking two ethene units with the acetylide. Upon treatment with further ethene, complex (50b) converts into (52), which contains a substituted cyclopentadienyl ligand formed by the addition of an ethene molecule to the allyl ligand in (50b). In complexes (50b) and (52), a phenyl ligand was lost from (1), presumably as benzene. This is the first time that the incorporation of carbonyl ligands into organic units on these Ru<sub>5</sub> clusters has been observed. The structural and electronic flexibility of complex (1) has permitted a variety of new C-C coupling reactions to be undertaken. In all cases, cleavage of P-C bonds from the C<sub>2</sub> unit has occurred.

A survey of the reactions which have been examined for complex (1) is presented in Scheme 11, with an emphasis on the transformations of the organic and phosphane ligands during these reactions.



### 3.4. Experimental

**General conditions.** General conditions and instrumentation were as outlined in Section 1.4. The matrix for the FAB mass spectrometry was usually 3-nitrobenzyl alcohol, but for low solubility complexes (such as the Au<sub>2</sub>Ru<sub>5</sub> complexes), a mixture of 18-crown-6 ether and 3-nitrobenzyl alcohol 1:2 (v/v) was found successful. In the case of the Ru<sub>4</sub>, Ru<sub>5</sub>, Au<sub>2</sub>Ru<sub>5</sub> and Ru<sub>6</sub> clusters studied here the ions observed were all related to their assigned formulations by addition or loss of one or two H atoms; this procedure was in part occasioned by the relatively weak ion intensities which tended to obscure the true isotope patterns. The carbonyl loss patterns almost invariably had some ions of very low intensity relative to the base peak. Many of the clusters were found to be unstable under FAB beam conditions, apparently undergoing intermolecular reactions such as CO transfer. As a result, most of the spectra were recorded within 2 min of sample introduction.

**Starting materials.** Literature methods were used to prepare [ppn][Co(CO)<sub>4</sub>],<sup>143</sup> [ppn]-[Mn(CO)<sub>5</sub>],<sup>144</sup> AuClPPh<sub>3</sub>,<sup>145</sup> [(AuPPh<sub>3</sub>)<sub>3</sub>O][BF<sub>4</sub>]<sup>146</sup> and Ru<sub>5</sub>(μ<sub>5</sub>-η<sup>2</sup>, P-C<sub>2</sub>PPh<sub>2</sub>)(μ-PPh<sub>2</sub>)(CO)<sub>15</sub> [thermodynamic (6t) and kinetic (6k) isomers].<sup>21</sup> Ru<sub>3</sub>(CO)<sub>12</sub> was made by carbonylation (60 atm) of RuCl<sub>3</sub>.xH<sub>2</sub>O (3 x 7g lots, Johnson Matthey) in MeOH (600 mL, AR) at 125 °C for 16 h.<sup>147</sup> P(OEt)<sub>3</sub>, PMe<sub>2</sub>Ph, PPh<sub>3</sub>, P(tolyl-*p*)<sub>3</sub> and dppa were purchased from Strem Chemicals and were used as received, except for P(OEt)<sub>3</sub>, which was distilled from 4 Å molecular sieves. Me<sub>3</sub>NO.2H<sub>2</sub>O (Aldrich) was dehydrated by sublimation at 100 °C/10<sup>-1</sup> mm in a glass tube. HCl(aq.), HBr(aq.), HI(aq.), allyl chloride and allyl bromide (free from halide impurities) were commercial products (BDH), as were HgCl<sub>2</sub> (May and Baker), ethene (Commonwealth Industrial Gases), carbon monoxide (Matheson Gas Products) and 1-butene (Fluka). Na/BPK solutions were prepared according to literature procedures.<sup>148</sup>

## Syntheses

### 3.4.1. A large scale preparation of $\text{Ru}_5(\mu_5\text{-}\eta^2, P\text{-C}_2\text{PPh}_2)(\mu\text{-PPh}_2)(\text{CO})_{13}$ (**1**)

Ten drops of Na/BPK solution (approx. 0.1 M)<sup>148</sup> were added to a degassed solution of  $\text{Ru}_3(\text{CO})_{12}$  (1.0 g, 1.56 mmol, finely ground) and dppa (310 mg, 0.79 mmol) in thf (90 mL). A  $\text{N}_2$  stream was used to remove evolved CO. After 15 min another six drops of Na/BPK solution were added. Spot TLC analysis (petroleum spirit/ $\text{CH}_2\text{Cl}_2$  4:1) of the deep orange solution indicated the presence of a trace amount of unreacted  $\text{Ru}_3(\text{CO})_{12}$  ( $R_f$  0.77), two minor orange-red bands and the major orange product ( $R_f$  0.57)  $\{\text{Ru}_3(\text{CO})_{11}\}_2(\mu\text{-dppa})$ . The solvent was then removed under vacuum, the residue extracted with toluene (50 mL) and filtered through Celite into a two-neck flask (100 mL). Nitrogen was passed through the solution using a glass sinter, and the reaction heated to between 88 and 92 °C for 1 h 30 min. The dark brown solution was monitored by TLC and IR for the disappearance of  $\{\text{Ru}_3(\text{CO})_{11}\}_2(\mu\text{-dppa})$ . After cooling to -15 °C for 15 h, the yellow precipitate of  $\text{Ru}_3(\text{CO})_{12}$  (150 mg, 0.23 mmol, 15%) was filtered off, washed with cold toluene (-15 °C, 2 x 5 mL) and the filtrates evaporated to dryness. The residue was extracted with  $\text{CH}_2\text{Cl}_2$  (20 mL), and MeOH (5 mL) was then added. Following volume reduction (to 7 mL) the solution was layered with MeOH (20 mL) and cooled to -15 °C (3 h). This gave a first crop of dark brown crystalline  $\text{Ru}_5(\mu_5\text{-}\eta^2, P\text{-C}_2\text{PPh}_2)(\mu\text{-PPh}_2)(\text{CO})_{13}$  (**1**) (600 mg). The process of crystallization was repeated to give a further crop of (**1**) (210 mg) for a total yield of (**1**) (810 mg, 0.64 mmol, 82%). These crystallizations had to be performed carefully and reasonably quickly to avoid co-crystallization of  $\text{Ru}_4(\mu_4\text{-PPh})\{\mu_4\text{-}\eta^2, P\text{-PhC}_2\text{PPh}_2\}(\mu\text{-CO})_2(\text{CO})_8$  (**5**) (orange crystals). Although these complexes could be separated by TLC it was not possible on this scale to achieve reasonable separations by column chromatography on florisil or silica.

*New spectroscopic data for  $\text{Ru}_5(\mu_5\text{-}\eta^2, P\text{-C}_2\text{PPh}_2)(\mu\text{-PPh}_2)(\text{CO})_{13}$  (**1**):* FAB MS: 1265,  $[\text{M}]^+$ ; loss of 13 CO groups. [After prolonged periods in the FAB beam peaks corresponding to the carbonylation isomers  $\text{Ru}_5(\mu_5\text{-}\eta^2, P\text{-C}_2\text{PPh}_2)(\mu\text{-PPh}_2)(\text{CO})_{15}$  (**6k**), (**6t**) were observed, viz. 1321,  $[\text{M} + 2\text{CO}]^+$ ; 1293,  $[\text{M} + \text{CO}]^+$ .]  $^{13}\text{C}\{^1\text{H}\}$  NMR ( $\text{CDCl}_3$ ):  $\delta$  239.0 (d,  $J_{\text{P-C}} = 23$  Hz,  $\text{C}_\alpha$ ); 202.5 (s), 201.5(s), 199.2(s), 198.9(d,  $J_{\text{P-C}} = 4$  Hz), 197.7 (s), 194.5 (s),

194.1 (d,  $J_{P-C} = 3$  Hz), 193.9 (d,  $J_{P-C} = 3$  Hz), 192.5 (s) - CO; 143.5 - 128.4 (m, Ph); 108.8 (d,  $J_{P-C} = 22$  Hz,  $C_{\beta}$ ). Electrochemistry ( $CH_2Cl_2$ ): Differential pulse  $E_p^{red} -0.76$  V; CV  $E_{1/2}^{red} -0.78$  V,  $E_{pc}^{red} -0.88$  V,  $E_{pa}^{red} -0.67$  V; this reduction process is quasi-reversible and is not diffusion controlled.

The supernatant from the above synthesis was evaporated to dryness to give a brown residue. This residue was converted to  $Ru_5(\mu-H)(\mu_4-PPh)\{\mu_4-\eta^4-CCPh(C_6H_4)\}(\mu_3-PPh)(CO)_{10}$  (**27**) by the following procedure: the residue was first dissolved in  $CH_2Cl_2$  and then supported on florisil; the florisil was then extracted with petroleum spirit/ $CH_2Cl_2$  (1:1) and the solvent removed under vacuum (to remove all traces of MeOH). The resulting product was then pyrolyzed in toluene and worked up as for the synthesis of (**27**) from (**1**) (see Section 3.4.5 below).

The two minor products observed in the ETC reaction of  $Ru_3(CO)_{12}$  with dppa were purified by preparative TLC (petroleum spirit/ $CH_2Cl_2$  4:1). An orange compound ( $R_f$  0.28) was formulated as  $Ru_5(CO)_{13}(dppa^*)^\dagger$  IR (cyclohexane):  $\nu(CO)$  2095m, 2074w, 2056(sh), 2044s, 2025(sh), 2013s  $cm^{-1}$ . FAB MS: 1265,  $[M]^+$ ; loss of 2 CO groups. The second, red, compound ( $R_f$  0.45) was formulated as  $Ru_6(CO)_{16}(dppa^*)(Ph)$  IR (cyclohexane):  $\nu(CO)$  2092(sh), 2085m, 2057s, 2048(sh), 2024(sh), 2017s, 1989(sh), 1967(sh)  $cm^{-1}$ . FAB MS 1526,  $[M]^+$ ; loss of two CO groups.

### 3.4.2. Pyrolysis of $\{Ru_3(CO)_{11}\}_2(\mu-dppa)$ under different conditions

(a) The reaction product from  $Ru_3(CO)_{12}$  (1 g, 1.56 mmol) and dppa (308 mg, 0.78 mmol) (see Section 3.4.1) was heated (under a  $N_2$  blanket) in toluene (50 mL) for 4 h at 90 °C. After removing  $Ru_3(CO)_{12}$  (142 mg, 0.22 mmol, 14%) by cooling (-15 °C), further crystallization ( $CH_2Cl_2/MeOH$ ) gave a crop of (**1**) (510 mg, 0.40 mmol, 52%).

---

† (dppa\*) is used throughout this chapter to indicate the incorporation of the elements of dppa in the cluster; the ligand does not necessarily correspond to structurally intact dppa.

The residue was purified by TLC (petroleum spirit/CH<sub>2</sub>Cl<sub>2</sub> 4:1); five bands were collected, the first four being identified (IR, FAB MS) as: (1) R<sub>f</sub> 0.77 yellow, Ru<sub>3</sub>(CO)<sub>12</sub>; (2) R<sub>f</sub> 0.57, orange, {Ru<sub>3</sub>(CO)<sub>11</sub>}<sub>2</sub>(μ-dppa); (3) R<sub>f</sub> 0.50, brown, (1); (4) R<sub>f</sub> 0.52, yellow, Ru<sub>4</sub>(μ<sub>4</sub>-η<sup>2</sup>-C<sub>2</sub>)(μ-PPh<sub>2</sub>)<sub>2</sub>(CO)<sub>12</sub> (7) (see Section 3.4.3). The fifth band (R<sub>f</sub> 0.48, orange) was fractionally crystallized (CH<sub>2</sub>Cl<sub>2</sub>/petroleum spirit) and the first crop of fine orange crystals identified as Ru<sub>4</sub>(μ<sub>4</sub>-PPh){μ<sub>4</sub>-η<sup>2</sup>, *P*-PhC<sub>2</sub>PPh<sub>2</sub>}(μ-CO)<sub>2</sub>(CO)<sub>8</sub>.0.5CH<sub>2</sub>Cl<sub>2</sub> (5) (15 mg, 0.013 mmol, 2%), m.p. (160-163 colour change), 175-176 °C. Anal. Calcd for C<sub>36</sub>H<sub>20</sub>O<sub>10</sub>P<sub>2</sub>Ru<sub>4</sub>.0.5CH<sub>2</sub>Cl<sub>2</sub>: C, 39.10; H, 1.89; M<sub>r</sub> 1079 (unsolvated). Found: C, 39.24; H, 1.96; M<sub>r</sub> 1079 (mass spectrometry, [M + H]<sup>+</sup> = 1080). IR (cyclohexane): ν(CO) 2061w, 2030vs, 2008m, 2001w, 1982w, 1964w, 1878vw, 1851w cm<sup>-1</sup>. <sup>1</sup>H NMR (CDCl<sub>3</sub>): δ 7.7 - 7.2 (m, 20H, Ph); 5.30 (s, 1H, CH<sub>2</sub>Cl<sub>2</sub>). FAB MS: 1080, [M]<sup>+</sup>; loss of 10 CO groups. Slow evaporation of the supernatant gave a further batch of orange crystals which were found to be Ru<sub>5</sub>(μ<sub>5</sub>-η<sup>2</sup>, *P*-C<sub>2</sub>PPh<sub>2</sub>)(μ-PPh<sub>2</sub>)(CO)<sub>15</sub> [(6t), thermodynamic isomer]<sup>21</sup> (22 mg, 0.016 mmol, 2%), identified by IR and spot TLC comparison with an authentic sample. *New spectroscopic data for Ru<sub>5</sub>(μ<sub>5</sub>-η<sup>2</sup>, *P*-C<sub>2</sub>PPh<sub>2</sub>)(μ-PPh<sub>2</sub>)(CO)<sub>15</sub>*: FAB MS (6t): 1321, [M]<sup>+</sup>; loss of 15 CO groups. FAB MS (6k): 1321, [M]<sup>+</sup>; fragmentation pattern identical to (6t).

(b) A solution of {Ru<sub>3</sub>(CO)<sub>11</sub>}<sub>2</sub>(μ-dppa) (450 mg, 0.28 mmol) in toluene (50 mL) was refluxed for 1h 30 mins (under a N<sub>2</sub> blanket), and cooled, the Ru<sub>3</sub>(CO)<sub>12</sub> side product was removed by crystallization (-15 °C). Of the large number of products (12) isolated by preparative TLC (petroleum spirit/CH<sub>2</sub>Cl<sub>2</sub> 4:1), the major product was (1) (R<sub>f</sub> 0.45). A green band (R<sub>f</sub> 0.53) was identified (IR, FAB MS) as Ru<sub>5</sub>(μ-H)(μ<sub>4</sub>-PPh){μ<sub>4</sub>-η<sup>4</sup>-CCPh(C<sub>6</sub>H<sub>4</sub>)}(μ<sub>3</sub>-PPh)(CO)<sub>10</sub> (27). Fractional crystallization of a brown band (R<sub>f</sub> 0.42) gave a first batch of orange crystals (CH<sub>2</sub>Cl<sub>2</sub>/petroleum spirit, -15 °C) which were identified (IR, FAB MS) as (5). Following volume reduction and cooling of the supernatant, brown crystals of Ru<sub>5</sub>(μ<sub>4</sub>-PPh){μ<sub>3</sub>-η<sup>2</sup>, *P*-CCPh(PPh<sub>2</sub>)}(CO)<sub>12</sub> (26), (identified by IR, FAB MS) were separated from an orange powder. The orange powder was given the formulation Ru<sub>8</sub>(CO)<sub>17</sub>(dppa\*) from FAB MS data (*m/z* 1681, [M]<sup>+</sup>). The last product may also be obtained by pyrolysis of (27) and Ru<sub>3</sub>(CO)<sub>12</sub> in *n*-octane. Unfortunately, because of the low yields of this complex it was

not possible to grow single crystals suitable for an X-ray study. Another complex of the formulation  $\text{Ru}_5(\text{CO})_{13}(\text{dppa}^*)$  was also isolated in the initial TLC separation (orange,  $R_f$  0.38, 4 mg); this had the following properties: IR (cyclohexane):  $\nu(\text{CO})$  2088m, 2081w, 2068s, 2044vs, 2038(sh), 2020vs, 2011(sh), 2002s(sh), 1990m, 1978(sh), 1963m. FAB MS: 1265,  $[\text{M}]^+$ ; loss of 13 CO groups.

### 3.4.3. Synthesis of $\text{Ru}_4(\mu_4\text{-}\eta^2\text{-C}_2)(\mu\text{-PPh}_2)_2(\text{CO})_{12}$ (7)

Compound (1) (100 mg, 0.079 mmol) was dissolved in benzene (30 mL) and then placed under 22 atm of CO. The solution was then heated at 105 °C for 21 h. After cooling, the solvent was removed from the yellow solution under reduced pressure and the residue chromatographed (TLC: petroleum spirit/ $\text{CH}_2\text{Cl}_2$  4:1). Most of the reaction product was absorbed on the base-line. A yellow band ( $R_f$  0.8) was identified (IR, spot TLC) as  $\text{Ru}_3(\text{CO})_{12}$  (11 mg, 0.017 mmol, 22%) and a minor yellow band ( $R_f$  0.52) crystallized ( $\text{CH}_2\text{Cl}_2$ /petroleum spirit) as yellow cubes of  $\text{Ru}_4(\mu_4\text{-}\eta^2\text{-C}_2)(\mu\text{-PPh}_2)_2(\text{CO})_{12}$  (7) (10 mg, 0.0088 mmol, 11%),<sup>45</sup> identified by comparison with an authentic sample (IR, unit cell dimensions).

*New spectroscopic data for  $\text{Ru}_4(\mu_4\text{-}\eta^2\text{-C}_2)(\mu\text{-PPh}_2)_2(\text{CO})_{12}$  (7):* m.p. 158-160 °C (dec.).

<sup>1</sup>H NMR ( $\text{C}_6\text{D}_6$ ):  $\delta$  7.2 - 6.2 (m, Ph). <sup>13</sup>C{<sup>1</sup>H} NMR ( $\text{CDCl}_3$ ):  $\delta$  198.0 (m), 196.6(m), 194.3(m) - CO; 141.1 (d,  $J_{\text{P-C}} = 37$  Hz,  $\text{C}_2$ ); 133.2 - 128.4 (m, Ph). FAB MS: 1137,  $[\text{M}]^+$ ; loss of 12 CO groups.

### Thermolysis reactions of $\text{Ru}_5(\mu_5-\eta^2, P\text{-C}_2\text{PPh}_2)(\mu\text{-PPh}_2)(\text{CO})_{13}$

#### 3.4.4. Synthesis of $\text{Ru}_5(\mu_4\text{-PPh})\{\mu_3-\eta^2, P\text{-CCPh}(\text{PPh}_2)\}(\text{CO})_{12}$ (26)

A solution of (1) (250 mg, 0.20 mmol) in toluene (60 mL) was heated (oil bath, 170 °C) for 2 h 30 min, with  $\text{N}_2$  passing through the solution. The solvent was removed under reduced pressure and the residue separated by chromatography (column: florisil). A major green band was removed (petroleum spirit) and identified (IR, FAB MS) as (27) (110mg, 0.093 mmol, 47%). The next brown band (eluent petroleum spirit/ $\text{CH}_2\text{Cl}_2$  2:1) was collected, and further purified by TLC (petroleum spirit/ $\text{CH}_2\text{Cl}_2$  4:1). A small amount of (27) was recovered ( $R_f$  0.68, green band), followed by a major brown band ( $R_f$  0.58) which was crystallized ( $\text{CH}_2\text{Cl}_2/\text{MeOH}$ ) to give dark brown crystals of  $\text{Ru}_5(\mu_4\text{-PPh})\{\mu_3-\eta^2, P\text{-CCPh}(\text{PPh}_2)\}(\text{CO})_{12}$  (26) (54 mg, 0.044 mmol, 22%), m.p. 205-207 °C. Anal. Calcd for  $\text{C}_{38}\text{H}_{20}\text{O}_{12}\text{P}_2\text{Ru}_5$ : C, 36.93; H, 1.63;  $M_r$  1236. Found: C, 36.81; H, < 2%;  $M_r$  1236 (mass spectrometry). IR (cyclohexane):  $\nu(\text{CO})$  2072m, 2041s, 2025s, 2008s, 1985w, 1968w, 1953w  $\text{cm}^{-1}$ .  $^1\text{H}$  NMR ( $\text{C}_6\text{D}_6$ ):  $\delta$  7.9 - 6.8 (m, Ph).  $^{13}\text{C}\{^1\text{H}\}$  NMR [ $\text{CDCl}_3$ ,  $\text{Cr}(\text{acac})_3$ ]:  $\delta$  202.6 (m), 197.0(m), 192.6(s), 192.3(s) - CO; 148.8(d,  $J_{\text{P-C}} = 15$  Hz,  $\text{C}_\alpha$ ); 133.6 - 127.8 (m, Ph); 109.2 (m,  $\text{C}_\beta$ ). FAB MS: 1236,  $[\text{M}]^+$ ; loss of 10 CO groups.

#### 3.4.5. Synthesis of $\text{Ru}_5(\mu\text{-H})(\mu_4\text{-PPh})\{\mu_4-\eta^4\text{-CCPh}(\text{C}_6\text{H}_4)\}(\mu_3\text{-PPh})(\text{CO})_{10}$ (27)

##### (a) Conversion of (1) to (27)

A solution of (1) (200 mg, 0.16 mmol) in toluene (50 mL) was refluxed for 2 h (oil bath, 155 °C), with  $\text{N}_2$  flowing through the solution. During this time the reaction mixture became green and monitoring by spot TLC confirmed the disappearance of the starting material. The solvent was removed under vacuum and the residue purified by TLC (petroleum spirit/ $\text{CH}_2\text{Cl}_2$  4:1). A major green band ( $R_f$  0.53) crystallized (hexane /cyclohexane) by slow evaporation as dark green-black crystals of  $\text{Ru}_5(\mu\text{-H})(\mu_4\text{-PPh})\{\mu_4-\eta^4\text{-CCPh}(\text{C}_6\text{H}_4)\}(\mu_3\text{-PPh})(\text{CO})_{10}\cdot 0.5\text{C}_6\text{H}_{14}$  (27) (122 mg, 0.10 mmol, 65 %), m.p. 170-172 °C. Anal. Calcd for

$C_{36}H_{20}O_{10}P_2Ru_5 \cdot 0.5C_6H_{14}$ : C, 38.30; H, 2.33;  $M_r$  1180 (unsolvated). Found: C, 38.20; H, 2.22;  $M_r$  1180 (mass spectrometry, 1181 =  $[M + H]^+$ ). IR (cyclohexane):  $\nu(\text{CO})$  2056vw, 2030vs, 2024(sh), 2016s, 2012(sh), 1982m, 1977(sh), 1966m  $\text{cm}^{-1}$ .  $^1\text{H}$  NMR ( $C_6D_6$ ):  $\delta$  7.9 - 6.1 (m, 19 H, Ph +  $C_6H_4$ ); 0.99 (m, 4H,  $\text{CH}_2$ , hexane); 0.58 (m, 3H,  $\text{CH}_3$ , hexane); -15.38 (dd,  $J_{\text{P-H}} = 10.3, 7.3$  Hz, 1H, RuH).  $^{13}\text{C}\{^1\text{H}\}$  NMR ( $\text{CH}_2\text{Cl}_2$ ):  $\delta$  243.2 (d,  $J_{\text{P-C}} = 11$  Hz,  $C_\alpha$ ); 199.0 (s), 198.1 (s), 197.5 (d,  $J_{\text{P-C}} = 13$  Hz), 193.7 (t,  $J_{\text{P-C}} = 31$  Hz), 192.6 (d,  $J_{\text{P-C}} = 29$  Hz), 191.4 (d,  $J_{\text{P-C}} = 27$  Hz), 190.1 (d,  $J_{\text{P-C}} = 31$  Hz) - CO; 149.3 - 124.6 (m, Ph); 117.1 (s,  $C_\beta$ ). FAB MS: 1181,  $[M]^+$ ; loss of 10 CO groups. Two minor bands were also observed; of these the brown band ( $R_f$  0.42) contained (26) (IR, FAB MS). For preparative purposes it was found that a slightly longer reaction duration (2 h 30 min), and column chromatography (florisil, eluent petroleum spirit) allowed the isolation of (27) in higher yields. Due to the high solubility of this compound in hydrocarbon solvents the product was generally evaporated to dryness under vacuum to obtain a sample suitable for further reactions.

#### (b) Conversion of (26) to (27)

Complex (26) (9 mg, 0.007 mmol) was refluxed in toluene (15 mL) for 4 h 15 min, with  $\text{N}_2$  flowing through the solution. After cooling, the solvent was removed and the residue chromatographed (TLC: petroleum spirit/ $\text{CH}_2\text{Cl}_2$  4:1). A major green band ( $R_f$  0.50) was identified (IR, spot TLC) as  $\text{Ru}_5(\mu\text{-H})(\mu_4\text{-PPh})\{\mu_4\text{-}\eta^4\text{-CCPh}(C_6H_4)\}(\mu_3\text{-PPh})(\text{CO})_{10}$  (27) (6 mg, 0.005 mmol, 73%) and a minor brown band ( $R_f$  0.38) was collected and identified (IR, spot TLC) as unreacted (26) (1 mg, 0.008 mmol, 11%); two trace bands and a brown baseline were also observed.

**3.4.6. Synthesis of  $\text{Ru}_5(\mu_4\text{-PPh})\{\mu_4\text{-}\eta^4\text{-CCPh}(\text{C}_6\text{H}_4)\}\{\mu\text{-PPh}(\text{OMe})\}(\text{CO})_{11}$  (28)**

Methanol (15 mL) was added to complex (27) (100 mg, 0.085 mmol), and the reaction mixture was stirred vigorously for 24 h. The solvent was removed from the brown solution under reduced pressure and the residue purified by TLC (petroleum spirit/ $\text{CH}_2\text{Cl}_2$  8:3). A major brown band ( $R_f$  0.50) was collected and crystallized ( $\text{CH}_2\text{Cl}_2/\text{MeOH}$ ) as dark brown rhomboids of  $\text{Ru}_5(\mu_4\text{-PPh})\{\mu_4\text{-}\eta^4\text{-CCPh}(\text{C}_6\text{H}_4)\}\{\mu\text{-PPh}(\text{OMe})\}(\text{CO})_{11}$  (28) (40 mg, 0.032 mmol, 38%), m.p. 115-117 °C. Anal. Calcd for  $\text{C}_{38}\text{H}_{22}\text{O}_{12}\text{P}_2\text{Ru}_5$ : C, 36.87; H, 1.79;  $M_r$  1238. Found: C, 36.32; H, 2.04;  $M_r$  1238 (mass spectrometry). IR (cyclohexane):  $\nu(\text{CO})$  2081m, 2038s, 2033(sh), 2021s, 2001s, 1995(sh), 1990m, 1982vw, 1973w, 1969(sh), 1952w  $\text{cm}^{-1}$ .  $^1\text{H}$  NMR ( $\text{CD}_2\text{Cl}_2$ ):  $\delta$  8.4 - 6.9 (m, 19H, Ph +  $\text{C}_6\text{H}_4$ ); 3.14 (d,  $J_{\text{P-H}} = 14.2$  Hz, 3H, OMe).  $^{13}\text{C}\{^1\text{H}\}$  NMR ( $\text{CH}_2\text{Cl}_2$ ):  $\delta$  258.4 (d,  $J_{\text{P-C}} = 14$  Hz,  $\text{C}_\alpha$ ); 210.3 (d,  $J_{\text{P-C}} = 36$  Hz), 206.9 (s), 202.0 (s), 200.4 (s), 198.0 (s), 193.7 (m), 192.8 (m), 189.2 (s) - CO; 146.3 - 123.1 (m, Ph); 107.7 (s,  $\text{C}_\beta$ ); - OMe resonance probably under  $\text{CH}_2\text{Cl}_2$  peak.<sup>149</sup> FAB MS: 1238,  $[\text{M}]^+$ ; loss of 10 CO groups. Of the ten other minor/trace bands only a brown band ( $R_f$  0.15) was collected. This was precipitated quickly ( $\text{CH}_2\text{Cl}_2/\text{petroleum spirit}$ ) as a brown powder which was unstable in solution. In cyclohexane conversion of this product to (28) was complete (IR, spot TLC) within 15 min. The brown powder also has the formulation  $\text{Ru}_5(\mu_4\text{-PPh})\{\text{CCPh}(\text{C}_6\text{H}_4)\}\{\mu\text{-PPh}(\text{OMe})\}(\text{CO})_{11}$  (15 mg, 0.012 mmol, 14%). IR (cyclohexane):  $\nu(\text{CO})$  2050w, 2025s, 2017s, 1980w, 1962w  $\text{cm}^{-1}$ .  $^1\text{H}$  NMR ( $d^6$ -acetone, 240K):  $\delta$  8.2 - 6.9 (m, Ph); 3.17 (d,  $J_{\text{P-H}} = 14.4$  Hz, OMe).  $^{31}\text{P}\{^1\text{H}\}$  NMR ( $d^6$ -acetone, 240K):  $\delta$  305.5 (d,  $J_{\text{P-P}} = 26$  Hz,  $\mu_4$  - PPh); 299.2 (d,  $J_{\text{P-P}} = 26$  Hz,  $\mu$  - P(OMe)Ph). FAB MS: 1239,  $[\text{M}]^+$ ; loss of 10 CO groups. A major base-line was also observed in the original TLC separation of the reaction product.

*Crystallography.* General techniques and details given below apply to the structure of complex (28), determined by the author.

Crystal data:  $\text{Ru}_5(\mu_4\text{-PPh})\{\mu_4\text{-}\eta^4\text{-CCPh}(\text{C}_6\text{H}_4)\}\{\mu\text{-PPh}(\text{OMe})\}(\text{CO})_{11}\cdot 2\text{MeOH}\cdot \text{H}_2\text{O}$  (28)  $\equiv \text{C}_{40}\text{H}_{32}\text{O}_{15}\text{P}_2\text{Ru}_5$ ,  $M$  1317.9,  $D_m$  1.89,  $Z$  4,  $D_c$  1.87  $\text{g cm}^{-3}$ , monoclinic,

space group  $P2_1/c$  ( $C_{2h}^5$ , No. 14),  $a$  20.556(5),  $b$  10.698(2),  $c$  21.536(3) Å,  $\beta$  98.62(2)°,  $U$  4682.4 Å<sup>3</sup>,  $F(000)$  2568.

A suitable crystal (0.12 x 0.34 x 0.22 mm) of (28) was grown from CH<sub>2</sub>Cl<sub>2</sub>/MeOH at -15 °C and was mounted on a glass fibre using cyanoacrylate 'super' glue. The density of the crystal was measured by flotation in aqueous zinc bromide solution. Lattice parameters were determined from a least-squares fit to the setting angles of 25 high angle reflections on an Enraf-Nonius CAD-4F four-circle diffractometer using graphite monochromated Mo- $K_\alpha$  radiation ( $\lambda = 0.7107$  Å). The crystal was found to be monoclinic with systematic absences  $h0l: l = 2n + 1$  and  $0k0: k = 2n + 1$  defining the space group  $P 2_1/c$  ( $C_{2h}^5$ , No. 14).

Intensity data were measured at room temperature using a  $\omega:2\theta$  scan mode ( $\theta$  range 1.5 - 22.5°). The intensities of three standard reflections were monitored every 60 min to check for crystal and machine stability. Data reduction and application of Lorentz and polarization corrections were undertaken with the programs PREABS and PROCES.<sup>150</sup> Absorption corrections ( $\mu$  16.45 mm<sup>-1</sup>, maximum and minimum transmission factors 0.8056 and 0.6866) were applied using the SHELX-76<sup>151</sup> system of programs which were also used for all the solution and refinement work. Reflections with intensities  $I < 2.5 \sigma(I)$  and systemically absent reflections were rejected, while equivalent reflections were averaged ( $R_{\text{amal}} = 0.030$ ); of the 8012 measured reflections 6126 were found to be unique.

The structure was solved by direct methods to give the metal atom positions; all other non-hydrogen atoms were located by means of Fourier difference maps of successive blocked-matrix least-squares refinements in which the function  $\sum w\Delta^2$  was minimized, and where  $w$  was the weight applied to each reflection and  $\Delta = |F_o| - |F_c|$ . Phenyl rings were included as hexagonal rigid groups (C-C 1.395 Å) with individual isotropic thermal parameters. Hydrogen atoms were placed in calculated positions (0.97 Å) with common group thermal parameters.

At this stage of the refinement several residual electron density peaks were located in a difference map; these were consistent with the presence of solvent molecules of crystallization.

They were assigned to one H<sub>2</sub>O molecule and one MeOH molecule. A third solvent molecule was refined as a disordered [about (0.5, 0, 0)] MeOH molecule. In the final refinement cycles (with all non-hydrogen atoms and non-phenyl carbons anisotropic), the following weighting was employed:  $w = [\sigma^2(F) + |g| F^2]^{-1}$ ; at convergence  $g = 0.004$ ,  $R = 0.039$  and  $R_w = 0.042$ . Bond lengths, valence angles, non-bonded distances and their standard deviations were all calculated using SHELX-76. Least-squares planes and dihedral angles were calculated using the program LSPLAN<sup>152</sup> and diagrams plotted by PLUTO.<sup>153</sup> All programs were implemented on the VAX 11/785 computing system at the University of Adelaide. Neutral atom scattering factors for C, H, O and P were those listed in SHELX-76 and those for Ru were obtained from the International Tables,<sup>154</sup> the values being corrected for anomalous dispersion.

The listings of observed ( $F_o$ ) and calculated ( $F_c$ ) structure factors, bond distances and angles, and positional and thermal parameters for the structure are given in Appendix 1.

### Ligand Substitution Reactions of $\text{Ru}_5(\mu_5\text{-}\eta^2, P\text{-C}_2\text{PPh}_2)(\mu\text{-PPh}_2)(\text{CO})_{13}$

#### 3.4.7. Syntheses of three isomers of $\text{Ru}_5(\mu_5\text{-}\eta^2, P\text{-C}_2\text{PPh}_2)(\mu\text{-PPh}_2)(\text{CO})_{12}\text{-}\{\text{P}(\text{OEt})_3\}$ (29a), (29b), (29c) and $\text{Ru}_5(\mu_5\text{-}\eta^2, P\text{-C}_2\text{PPh}_2)(\mu\text{-PPh}_2)(\text{CO})_{11}\{\text{P}(\text{OEt})_3\}_2$ (30)

##### (a) $\text{Me}_3\text{NO}$ -assisted reaction

A solution of (1) (100 mg, 0.079 mmol) in acetone (50 mL) was cooled to 0 °C and then  $\text{Me}_3\text{NO}$  (6 mg, 0.08 mmol) and  $\text{P}(\text{OEt})_3$  (16 mg, 0.096 mmol) were added in quick succession. The solution was allowed to warm to r.t. over 30 min and further portions of  $\text{P}(\text{OEt})_3$  (8 mg, 0.048 mmol) and  $\text{Me}_3\text{NO}$  (3 mg, 0.04 mmol) were added. After a further 15 min all the starting cluster had been consumed (spot TLC) and the solvent was removed under vacuum. Preparative TLC of the residue (petroleum spirit/acetone/ $\text{CH}_2\text{Cl}_2$  14:2:1) separated nine bands of which only the major two were collected. The first brown band ( $R_f$  0.35) crystallized ( $\text{CH}_2\text{Cl}_2$ /petroleum spirit) as dark brown crystals of  $\text{Ru}_5(\mu_5\text{-}\eta^2, P\text{-C}_2\text{PPh}_2)(\mu\text{-PPh}_2)(\text{CO})_{12}\{\text{P}(\text{OEt})_3\}.0.5\text{CH}_2\text{Cl}_2$  (29a) (39 mg, 0.028 mmol, 35%), m.p. 270 °C (dec.). Anal. Calcd for  $\text{C}_{44}\text{H}_{35}\text{O}_{15}\text{P}_3\text{Ru}_5.0.5\text{CH}_2\text{Cl}_2$ : C, 37.00; H, 2.51;  $M_r$  1402 (unsolvated). Found: C, 36.96; H, 2.51;  $M_r$  1402 (mass spectrometry). IR (cyclohexane):  $\nu(\text{CO})$  2061m, 2029s, 2007(sh), 2001s, 1990(sh), 1971m, 1953w, 1933w  $\text{cm}^{-1}$ .  $^1\text{H}$  NMR ( $\text{CDCl}_3$ ):  $\delta$  7.9 - 7.3 (m, 20H, Ph); 5.30 (s, 1H,  $\text{CH}_2\text{Cl}_2$ ); 3.92 (p,  $J = 7.0$  Hz, 6H,  $\text{CH}_2$ ); 1.17 (t,  $J_{\text{H-H}} = 7.0$  Hz, 9H,  $\text{CH}_3$ ). FAB MS: 1402,  $[\text{M}]^+$ ; loss of 12 CO groups. A second brown band ( $R_f$  0.38) was rechromatographed (TLC: petroleum spirit/ $\text{Et}_2\text{O}$ /acetone 17:3:1). The major brown band ( $R_f$  0.25) that developed was quickly removed from the TLC medium, precipitated ( $\text{CH}_2\text{Cl}_2$ /MeOH) by volume reduction (at -70 °C), and washed with EtOH and pentane (-70 °C). This product, an isomer of  $\text{Ru}_5(\mu_5\text{-}\eta^2, P\text{-C}_2\text{PPh}_2)(\mu\text{-PPh}_2)(\text{CO})_{12}\{\text{P}(\text{OEt})_3\}$  (29b) (13 mg, 0.0093 mmol, 12%), was unstable in solution and a crystalline sample suitable for X-ray or elemental analysis could not be prepared. IR (cyclohexane):  $\nu(\text{CO})$  2070m, 2034s, 2012s, 2002s, 1980(sh), 1953w, 1948w, 1934w, 1801w  $\text{cm}^{-1}$ .  $^1\text{H}$  NMR ( $\text{CDCl}_3$ ):  $\delta$  7.6 - 7.2 (m, 20H, Ph); 4.03 (p,  $J = 6.7$  Hz, 6H,  $\text{CH}_2$ ); 1.20 (t,  $J_{\text{H-H}} = 6.9$  Hz, 9H,  $\text{CH}_3$ ).

FAB MS: 1402,  $[M]^+$ ; loss of 12 CO groups.

### (b) Thermal Reactions

(i) *In cyclohexane*: A solution of (1) (100 mg, 0.079 mmol) dissolved in cyclohexane (30 mL) was heated (45 °C), and  $P(OEt)_3$  (24 mg, 0.145 mmol) was then added portion-wise over 45 min. Following this the solvent was removed under reduced pressure and the residue purified by TLC (petroleum spirit/acetone/ $CH_2Cl_2$  14:2:1). Five bands were collected, the first ( $R_f$  0.50, brown) being identified (IR, FAB MS) as unreacted (1) (34 mg, 0.027 mmol, 34%). The second band ( $R_f$  0.40, ochre) crystallized ( $CH_2Cl_2/MeOH$ ) as dark red-brown crystalline  $Ru_5(\mu_5-\eta^2, P-C_2PPh_2)(\mu-PPh_2)(CO)_{12}\{P(OEt)_3\}$  (29c) (25 mg, 0.017 mmol, 23%), m.p. 219-220 °C. Anal. Calcd for  $C_{44}H_{35}O_{15}P_3Ru_5$ : C, 37.70; H, 2.40;  $M_r$  1402. Found: C, 37.33; H, 2.48;  $M_r$  1402 (mass spectrometry). IR (cyclohexane):  $\nu(CO)$  2071w, 2052s, 2005s, 1984(sh), 1971(sh), 1945w  $cm^{-1}$ .  $^1H$  NMR ( $CDCl_3$ ):  $\delta$  8.0 - 7.3 (m, 20H, Ph); 3.41 (m, 6H,  $CH_2$ ); 0.96 (t,  $J_{H-H} = 7.0$  Hz, 9H,  $CH_3$ ). FAB MS: 1402,  $[M]^+$ ; loss of 12 CO groups. The two middle brown bands ( $R_f$  0.35 and 0.33) were identified (IR, FAB MS) as (29b) (4 mg, 0.003 mmol, 4%), and (29a) (6 mg, 0.004 mmol, 5%). The last band ( $R_f$  0.28, brown) was crystallized ( $CH_2Cl_2$ /petroleum spirit) by slow evaporation and cooling to give dark brown crystals of  $Ru_5(\mu_5-\eta^2, P-C_2PPh_2)(\mu-PPh_2)(CO)_{11}\{P(OEt)_3\}_2$  (30) (14 mg, 0.0091 mmol, 11%), m.p. 213-214 °C. Anal. Calcd for  $C_{49}H_{50}O_{17}P_4Ru_5$ : C, 38.21; H, 3.27;  $M_r$  1540. Found: C, 38.01; H, 3.19;  $M_r$  1540 (mass spectrometry,  $[M + 2H]^+ = 1542$ ). IR (cyclohexane):  $\nu(CO)$  2038m, 2018s, 1992s, 1983(sh), 1965m, 1943m, 1926(sh), 1791w  $cm^{-1}$ .  $^1H$  NMR ( $CDCl_3$ ):  $\delta$  8.1 - 7.3 (m, 20H, Ph); 3.92 (m, 6H,  $CH_2$ ); 3.77 (p,  $J = 7.0$  Hz, 6H,  $CH_2$ ); 1.18 (t,  $J_{H-H} = 7.0$  Hz, 9H,  $CH_3$ ); 1.11 (t,  $J_{H-H} = 7.0$  Hz, 9H,  $CH_3$ ). FAB MS: 1542,  $[M]^+$ ; loss of 9 CO groups. Three other minor/trace bands were not characterized further. No conversion between the three isomers of (29) was detected by  $^1H$  or  $^{31}P$  NMR ( $CDCl_3$  or  $CH_2Cl_2$ , 2h, r.t.).

(ii) *In acetone*: To (1) (200 mg, 0.16 mmol) in acetone (40 mL) was added  $P(OEt)_3$  (46 mg, 0.28 mmol) over 1 h at r.t. After a further 20 min the solvent was removed under vacuum. Preparative TLC of the residue (petroleum spirit/acetone/ $CH_2Cl_2$  14:2:1) eluted

eleven bands, of which five were collected and identified spectroscopically (IR, FAB MS) as: (1)  $R_f$  0.85, brown, (1) (23 mg, 0.018 mmol, 11%); (2)  $R_f$  0.78, ochre, (29c) (22 mg, 0.016 mmol, 10%); (3)  $R_f$  0.68, brown, (29a) (5 mg, 0.004 mol, 2%); (4)  $R_f$  0.60, brown, (30) (75 mg, 0.049 mmol, 30%); and (5)  $R_f$  0.50, orange,  $\text{Ru}_5(\text{CO})_{14}(\text{dppa}^*)\{\text{P}(\text{OEt})_3\}$  (4 mg, 0.003 mmol, 2%) [IR (cyclohexane):  $\nu(\text{CO})$  2048m, 2042(sh), 2031s, 2011w, 1996s, 1977w, 1956w, 1945w  $\text{cm}^{-1}$ . FAB MS: 1457,  $[\text{M}]^+$ ; loss of 14 CO groups.].

**(c) Attempted formation of (30) from (29a), (29b) or (29c)**

(i) *From (29a)*: A solution of (29a) (7 mg, 0.005 mmol) in acetone (40 mL) was treated with  $\text{P}(\text{OEt})_3$  (12 mg, 0.072 mmol) at 33 °C. After 16 h the solvent was removed under reduced pressure and the residue purified by TLC (petroleum spirit/ $\text{CH}_2\text{Cl}_2$ /acetone 7:2:1) to give a major brown band ( $R_f$  0.32) that was identified as (30) (IR, FAB MS).

(ii) *From (29b)*: A solution of (29b) (9 mg, 0.006 mmol) in acetone (40 mL) was treated with  $\text{P}(\text{OEt})_3$  (12 mg, 0.072 mmol) at 33 °C. After 16 h the solvent was removed under reduced pressure and the residue purified by TLC (petroleum spirit/ $\text{CH}_2\text{Cl}_2$ /acetone 7:2:1) to give a major brown band ( $R_f$  0.32) that was identified as (30) (IR, FAB MS).

(iii) *From (29c)*: A solution of (29c) (15 mg, 0.0011 mmol) in acetone (15 mL) was treated portionwise with  $\text{P}(\text{OEt})_3$  (11 mg, 0.066 mmol) at 45 °C. After 1 h 15 min the solvent was removed under reduced pressure and the residue purified by TLC (petroleum spirit/ $\text{CH}_2\text{Cl}_2$ /acetone 14:2:1) to give four brown bands. Two bands ( $R_f$  0.26, 0.20) were identified (FAB MS, IR) as isomers of  $\text{Ru}_5(\text{CO})_{11}(\text{dppa}^*)\{\text{P}(\text{OEt})_3\}_2$   $\{[\text{M}]^+ 1542, \text{IR significantly different from (30)}\}$  and the fourth ( $R_f$  0.37) as unreacted (29c).

**3.4.8. Synthesis of  $\text{Ru}_5(\mu_5\text{-}\eta^2, P\text{-C}_2\text{PPh}_2)(\mu\text{-PPh}_2)(\text{CO})_{11}(\text{PMe}_2\text{Ph})_2$  (31)**

An immediate reaction occurred when  $\text{PMe}_2\text{Ph}$  (11 mg, 0.080 mmol) was added to a solution of (1) (50 mg, 0.040 mmol) in acetone (20 mL). After 30 min the solvent was removed under vacuum and the products separated by TLC (petroleum spirit/ $\text{CH}_2\text{Cl}_2$  4:3). A major brown band ( $R_f$  0.30) was separated from the four other minor bands and crystallized

(CH<sub>2</sub>Cl<sub>2</sub>/MeOH) as brown plates of Ru<sub>5</sub>(μ<sub>5</sub>-η<sup>2</sup>, *P*-C<sub>2</sub>PPh<sub>2</sub>)(μ-PPh<sub>2</sub>)(CO)<sub>11</sub>-(PMe<sub>2</sub>Ph)<sub>2</sub> (**31**) (43 mg, 0.029 mmol, 72%), m.p. 241-243 °C. Reliable analyses could not be obtained for this complex. IR (cyclohexane): ν(CO) 2038(sh), 2034m, 2014s, 1988vs, 1962w, 1953w, 1933m, 1775w cm<sup>-1</sup>. <sup>1</sup>H NMR (C<sub>6</sub>D<sub>6</sub>): 7.8 - 6.5 (m, 30H, Ph); 1.19 (d, *J*<sub>P-H</sub> = 10.0 Hz, 6H, Me); 0.93 (d, *J*<sub>P-H</sub> = 10.5 Hz, 6H, Me). FAB MS: 1485, [M]<sup>+</sup>; loss of 11 CO groups.

### 3.4.9. Syntheses of Ru<sub>5</sub>(μ<sub>5</sub>-η<sup>2</sup>, *P*-C<sub>2</sub>PPh<sub>2</sub>)(μ-PPh<sub>2</sub>)(CO)<sub>12</sub>(PPh<sub>3</sub>) (**32**) and Ru<sub>5</sub>(μ<sub>4</sub>-PPh)(μ<sub>3</sub>-η<sup>2</sup>-PhC<sub>2</sub>Ph)(μ-PPh<sub>2</sub>)<sub>2</sub>(CO)<sub>10</sub> (**33**)

#### (a) Me<sub>3</sub>NO-assisted reaction

To a solution of (**1**) (100 mg, 0.079 mmol) and PPh<sub>3</sub> (21 mg, 0.080 mmol) in acetone (45 mL) was added Me<sub>3</sub>NO (6 mg, 0.080 mmol). After 1 h a further portion of Me<sub>3</sub>NO (6 mg, 0.080 mmol) was added and 5 minutes later complete reaction was indicated by spot TLC. The solvent was removed under vacuum and the residue chromatographed (column: silica). Elution with petroleum spirit/CH<sub>2</sub>Cl<sub>2</sub> (7:3) gave a trace orange band followed by a major brown band which was crystallized (CH<sub>2</sub>Cl<sub>2</sub>/petroleum spirit) as black crystalline Ru<sub>5</sub>(μ<sub>5</sub>-η<sup>2</sup>, *P*-C<sub>2</sub>PPh<sub>2</sub>)(μ-PPh<sub>2</sub>)(CO)<sub>12</sub>(PPh<sub>3</sub>) (**32**) (55 mg, 0.037 mmol, 46%), m.p. 184-186 °C. Anal. Calcd for C<sub>56</sub>H<sub>35</sub>O<sub>12</sub>P<sub>3</sub>Ru<sub>5</sub>: C, 44.89; H, 2.35; *M*<sub>r</sub> 1498. Found: C, 44.45; H, 2.57; *M*<sub>r</sub> 1498 (mass spectrometry, 1499 = [M + H]<sup>+</sup>). IR (cyclohexane): ν(CO) 2062s, 2028s, 2008m, 2001(sh), 1993m, 1974w, 1968(sh), 1952m cm<sup>-1</sup>. <sup>1</sup>H NMR (C<sub>6</sub>H<sub>6</sub>): δ 7.9 - 6.6 (m, Ph). FAB MS: 1499, [M]<sup>+</sup>; loss of 12 CO groups. Two other minor bands were eluted but not characterized and a large amount of material was also left on the column.

#### (b) Thermal reactions

(i) In CH<sub>2</sub>Cl<sub>2</sub>: A solution of (**1**) (100 mg, 0.079 mmol) and PPh<sub>3</sub> (21 mg, 0.080 mmol) was refluxed in CH<sub>2</sub>Cl<sub>2</sub> (20 mL) for 20 h. After cooling and removal of solvent under reduced pressure the residue was purified by TLC (petroleum spirit/CH<sub>2</sub>Cl<sub>2</sub> 3:2); a major brown band (R<sub>f</sub> 0.44) was separated from seven other bands and further TLC (petroleum spirit/CH<sub>2</sub>Cl<sub>2</sub>/acetone 16:2:1) resolved this product into two bands. A brown band (R<sub>f</sub> 0.36) was found to be (**32**) (54 mg, 0.036 mmol, 45%) (identified by IR, FAB MS) and the remaining green band

( $R_f$  0.43) crystallized ( $\text{CH}_2\text{Cl}_2$ /hexane) to give dark green-black crystals of  $\text{Ru}_5(\mu_4\text{-PPh})(\mu_3\text{-}\eta^2\text{-PhC}_2\text{Ph})(\mu\text{-PPh}_2)_2(\text{CO})_{10}\cdot 0.5\text{C}_6\text{H}_{14}$  (**33**) (25 mg, 0.017 mmol, 22%), m.p. 238-40 °C. Anal. Calcd for  $\text{C}_{54}\text{H}_{35}\text{O}_{10}\text{P}_3\text{Ru}_5\cdot 0.5\text{C}_6\text{H}_{14}$ : C, 46.09; H, 2.85;  $M_r$  1442 (unsolvated). Found: C, 46.15; H, 2.94;  $M_r$  1442 (mass spectrometry, 1444 =  $[\text{M} + 2\text{H}]^+$ ). IR (cyclohexane):  $\nu(\text{CO})$  2044vw, 2025s, 2013(sh), 1996vs, 1976vw, 1970vw, 1947vw  $\text{cm}^{-1}$ .  $^1\text{H}$  NMR ( $\text{CDCl}_3$ ): 7.7 - 6.9 (m, 35H, Ph); 1.42 (m, 4H, hexane); 0.88 (m, 3H, hexane). FAB MS: 1444,  $[\text{M}]^+$ ; loss of 10 CO groups.

(ii) *Conversion of (32) to (33) in  $\text{CH}_2\text{Cl}_2$* : Complex (**32**) (15 mg, 0.010 mmol) was heated in  $\text{CH}_2\text{Cl}_2$  (25 mL) at reflux for 20 h. The solvent was then removed and the residue purified by TLC (petroleum spirit/ $\text{CH}_2\text{Cl}_2$ /acetone 16:2:1) to give four bands, of which a green band ( $R_f$  0.32) was identified (FAB MS, IR) as (**33**) (2 mg, 0.007 mmol, 14%) and a brown band ( $R_f$  0.29) as unreacted (**32**) (12 mg, 80%).

(iii) *1,2-dichloroethane*: Heating a solution of (**1**) (50 mg, 0.040 mmol) and  $\text{PPh}_3$  (11 mg, 0.042 mmol) in 1,2-dichloroethane (20 mL) for 20 h (oil bath, 106 °C) gave an orange-brown solution. The solvent was removed and the residue separated by TLC (petroleum spirit/ $\text{CH}_2\text{Cl}_2$ /acetone 16:2:1) giving a complicated array of products (11 bands), of which only a green band ( $R_f$  0.30) (**33**) (7 mg, 0.005 mmol, 12 %) was characterized (IR, FAB MS).

#### 3.4.10. Synthesis of $\text{Ru}_5(\mu_4\text{-PPh})(\mu_3\text{-}\eta^2\text{-PhC}_2(p\text{-tolyl}))(\mu\text{-PPh}_2)\text{-}\{\mu\text{-P}(p\text{-tolyl})_2\}(\text{CO})_{10}$ (**34**)

A reaction between (**1**) (90 mg, 0.071 mmol) and  $\text{P}(p\text{-tolyl})_3$  (22 mg, 0.071 mmol) in refluxing  $\text{CH}_2\text{Cl}_2$  (20 mL) gave a brown-green solution. The solvent was removed and the residue purified by TLC (petroleum spirit/ $\text{CH}_2\text{Cl}_2$ /acetone 16:2:1); a major green band was collected and precipitated from  $\text{CH}_2\text{Cl}_2$ /petroleum spirit to give a green solid  $\text{Ru}_5(\mu_4\text{-PPh})(\mu_3\text{-}\eta^2\text{-PhC}_2(p\text{-tolyl}))(\mu\text{-PPh}_2)\{\mu\text{-P}(p\text{-tolyl})_2\}(\text{CO})_{10}\cdot 0.5\text{C}_6\text{H}_{14}$  (**34**) (39 mg, 0.026 mmol, 37%), m.p. 250 °C (dec.) Anal. Calcd for  $\text{C}_{57}\text{H}_{41}\text{O}_{10}\text{P}_3\text{Ru}_5\cdot 0.5\text{C}_6\text{H}_{14}$ : C, 47.19; H, 3.17;  $M_r$  (unsolvated) 1484. Found: C, 47.11; H, 3.11;  $M_r$  1484 (mass spectrometry, 1485 =  $[\text{M} + \text{H}]^+$ ). IR (cyclohexane):  $\nu(\text{CO})$  2045vw, 2025s, 2013(sh), 1997vs, 1980vw, 1972vw, 1949vw  $\text{cm}^{-1}$ .  $^1\text{H}$  NMR ( $\text{C}_6\text{D}_6$ ):  $\delta$  7.8 - 6.6 (m, 32H, Ph +  $\text{C}_6\text{H}_4$ ); 1.87 (s, 6H, Me); 1.85

(m, 3H, Me); 1.30 (m, 4H, C<sub>6</sub>H<sub>14</sub>), 0.88 (m, 3H, C<sub>6</sub>H<sub>14</sub>). <sup>31</sup>P{<sup>1</sup>H} (CH<sub>2</sub>Cl<sub>2</sub>): δ 451.4 (s, PPh); 203.8 [m, PPh<sub>2</sub> + P(tolyl)<sub>2</sub>]. <sup>31</sup>P{<sup>1</sup>H} (acetone): δ 452.3 (s, PPh); 203.7 (m, PPh<sub>2</sub>); 208.7 [m, P(tolyl)<sub>2</sub>]. FAB MS: 1485, [M]<sup>+</sup>; loss of 10 CO groups.

### 3.4.11. Syntheses of Au<sub>2</sub>Ru<sub>5</sub>(μ<sub>5</sub>-η<sup>2</sup>, *P*-C<sub>2</sub>PPh<sub>2</sub>)(μ-PPh<sub>2</sub>)(CO)<sub>12</sub>(PPh<sub>3</sub>)<sub>2</sub> (35)

#### (a) Using [(AuPPh<sub>3</sub>)<sub>3</sub>O][BF<sub>4</sub>]/[ppn][Co(CO)<sub>4</sub>]

A mixture of (1) (51 mg, 0.040 mmol), [(AuPPh<sub>3</sub>)<sub>3</sub>O][BF<sub>4</sub>] (62 mg, 0.041 mmol) and [ppn][Co(CO)<sub>4</sub>] (30 mg, 0.042 mmol) in thf (20 mL) was stirred at r.t. for 24 h giving a green solution. The solvent was removed under vacuum and the residue extracted with CH<sub>2</sub>Cl<sub>2</sub> (minimum volume). Diethyl ether (20 mL) was then added and the volume reduced; after cooling (-15 °C), the resulting white precipitate was filtered off and identified (IR, FAB MS) as [ppn][BF<sub>4</sub>] (7 mg, 0.01 mmol, 26%). The filtrate was evaporated to dryness under reduced pressure and purified by TLC (petroleum spirit/CH<sub>2</sub>Cl<sub>2</sub> 2:1). A minor white band (R<sub>f</sub> 0.60) was identified as AuCo(CO)<sub>4</sub>(PPh<sub>3</sub>) IR (cyclohexane): ν(CO) 2055s, 1988m, 1958vs cm<sup>-1</sup>; FAB MS: 630, [M]<sup>+</sup>; loss of 4 CO groups [Lit.<sup>155</sup> IR (CS<sub>2</sub>) 2054s, 1988s, 1957s cm<sup>-1</sup>]. The major band (R<sub>f</sub> 0.24) was crystallized (CH<sub>2</sub>Cl<sub>2</sub>/petroleum spirit) as dark green-black crystals of Au<sub>2</sub>Ru<sub>5</sub>(μ<sub>5</sub>-η<sup>2</sup>, *P*-C<sub>2</sub>PPh<sub>2</sub>)(μ-PPh<sub>2</sub>)(CO)<sub>12</sub>(PPh<sub>3</sub>)<sub>2</sub> (35) (66 mg, 0.031 mmol, 77%), m.p. > 330 °C (dec.). Anal. Calcd for C<sub>74</sub>H<sub>50</sub>Au<sub>2</sub>O<sub>12</sub>P<sub>4</sub>Ru<sub>5</sub>: C, 41.26; H, 2.34; M<sub>r</sub> 2154. Found: C, 41.61; H, 2.62; M<sub>r</sub> 2154 (mass spectrometry, 2155 = [M + H]<sup>+</sup>). IR (CH<sub>2</sub>Cl<sub>2</sub>): ν(CO) 2057w, 2036s, 1984vs, 1957(sh), 1917m cm<sup>-1</sup>. <sup>1</sup>H NMR (CDCl<sub>3</sub>): δ 7.5 - 6.6 (m, Ph). <sup>13</sup>C{<sup>1</sup>H} NMR (CH<sub>2</sub>Cl<sub>2</sub>): δ 215.3, 214.7, 212.8, (3 x s, CO); 206.2, 202.1, 198.0, 194.6 (4 x m, CO); 144.1 (dd, J<sub>P-C</sub> = 27, 11 Hz, C<sub>α</sub>); 141.2 - 126.0 (m, Ph). FAB MS: 2155, [M]<sup>+</sup>; loss of 12 CO groups.

A larger scale reaction { (1) (100 mg), [(AuPPh<sub>3</sub>)<sub>3</sub>O][BF<sub>4</sub>] (124 mg), [ppn][Co(CO)<sub>4</sub>] (60 mg), thf (35 mL) } was worked up after 24 h by removing the solvent under vacuum and purifying the residue by column chromatography (florisil). AuCo(CO)<sub>4</sub>(PPh<sub>3</sub>) (41 mg, 0.065 mmol, 83%) was removed first (petroleum spirit/CH<sub>2</sub>Cl<sub>2</sub> 8:1, colourless band), followed by (35) (140 mg, 0.065 mmol, 83%) (petroleum spirit/CH<sub>2</sub>Cl<sub>2</sub> 3:1, green band).

$\text{Au}_2\text{Ru}_5(\mu_5\text{-}\eta^2, P\text{-C}_2\text{PPh}_2)(\mu\text{-PPh}_2)(\text{CO})_{12}(\text{PPh}_3)_2$  (**35**), unlike most of the other  $\text{Ru}_5$  clusters, is virtually insoluble in hydrocarbon solvents and although it crystallizes readily the crystals are not suitable for an X-ray study.

**(b) Using  $[(\text{AuPPh}_3)_3\text{O}][\text{BF}_4]/[\text{ppn}][\text{Mn}(\text{CO})_5]$**

Similarly (**1**) (50 mg, 0.040 mmol),  $[(\text{AuPPh}_3)_3\text{O}][\text{BF}_4]$  (60 mg, 0.041 mmol) and  $[\text{ppn}][\text{Mn}(\text{CO})_5]$  (29 mg, 0.041 mmol) in thf (25 mL) were stirred at r.t. for 20 h. Following removal of the solvent under vacuum, TLC (petroleum spirit/ $\text{CH}_2\text{Cl}_2$  2:1) of the residue gave two bands: white ( $R_f$  0.65)  $\text{AuMn}(\text{CO})_5(\text{PPh}_3)$  (7 mg, 0.01 mmol, 27%) identified spectroscopically IR (cyclohexane):  $\nu(\text{CO})$  2067m, 1962vs  $\text{cm}^{-1}$ , FAB MS: 654,  $[\text{M}]^+$  - loss of 2 CO groups [Lit.<sup>155</sup> IR ( $\text{CCl}_4$ ) 2062m, 1961vs  $\text{cm}^{-1}$ ]; and green ( $R_f$  0.24) (**35**) (63 mg, 0.029 mmol, 73%), identified by IR.

**(c) Using  $[(\text{AuPPh}_3)_3\text{O}][\text{BF}_4]/\text{Na}[\text{Co}(\text{CO})_4]$**

$\text{Ru}_5(\mu_5\text{-}\eta^2, P\text{-C}_2\text{PPh}_2)(\mu\text{-PPh}_2)(\text{CO})_{13}$  (**1**) (100 mg, 0.079 mmol) was added to a filtered (Celite) solution of  $\text{NaCo}(\text{CO})_4$  (0.12 mmol), prepared from  $\text{Co}_2(\text{CO})_8$  (20 mg, 0.058 mmol) and 1% Na amalgam in thf (15 mL). No reaction was apparent after 20 h, and spot TLC indicated that both starting materials were still present. Addition of  $[(\text{AuPPh}_3)_3\text{O}][\text{BF}_4]$  (118 mg, 0.080 mmol) gave a green solution after 4 h. The solvent was removed under vacuum and the residue purified by TLC (petroleum spirit/acetone 8:5). A major green band ( $R_f$  0.35) was collected and identified (IR, FAB MS) as (**35**) (59 mg, 0.027 mmol, 35%).

**(d) Using only  $[(\text{AuPPh}_3)_3\text{O}][\text{BF}_4]$**

A solution of (**1**) (50 mg, 0.040 mmol) and  $[(\text{AuPPh}_3)_3\text{O}][\text{BF}_4]$  (59 mg, 0.041 mmol) in thf (20 mL) were stirred at r.t. for 20 h. The solvent was then removed under vacuum. Preparative TLC (petroleum spirit/acetone 8:5) of the residue eluted six bands of which three were collected and identified (IR, spot TLC) as: (1) a brown band ( $R_f$  0.53) of unreacted (**1**) (5 mg, 0.004 mmol, 10%); (2) a green band ( $R_f$  0.35) of (**35**) (19 mg, 0.009 mmol, 22%);

(3) a major brown base-line (extracted  $\text{CH}_2\text{Cl}_2/\text{MeOH}$ ) contained  $\text{Au}_3\text{Ru}_5(\text{CO})_{10}(\text{dppa}^*)(\text{PPh}_3)_3$  IR (cyclohexane):  $\nu(\text{CO})$  2047w, 2024w, 2014(sh), 2006(sh), 1978vs, 1916(sh)  $\text{cm}^{-1}$ ; FAB MS: 2556,  $[\text{M}]^+$ .

#### (e) Using sodium amalgam and $\text{AuClPPh}_3$

Reduction of a solution of (1) (50 mg, 0.040 mmol) in thf (24 mL) with sodium amalgam (4 mL, 1% amalgam) for 40 mins gave a black solution [IR (thf):  $\nu(\text{CO})$  2021(sh), 2005(sh), 1968vs (overlap with thf), 1948(sh)  $\text{cm}^{-1}$ ]. This was then syringed into a flask containing  $\text{AuClPPh}_3$  (40 mg, 0.081 mmol). The solution immediately turned green and after stirring for 15 min the reaction mixture was filtered (Celite) and evaporated to dryness under reduced pressure. The residue was purified by TLC (petroleum spirit/ $\text{CH}_2\text{Cl}_2$  2:1) and a major green band ( $R_f$  0.27) was collected and precipitated ( $\text{CH}_2\text{Cl}_2/\text{petroleum spirit}$ ) as (35) (73 mg, 0.034 mmol, 85%) (identified by IR and FAB MS).

*N.B.* The reduced solution produced from (1) (50 mg, 0.040 mmol) and sodium amalgam in thf (24 mL) (as above) was added to  $[\text{ppn}]\text{Cl}$  (50 mg, 0.087 mmol) in MeCN (10 mL) and stirred for 20 min. A colour change to brown was observed. The solution was filtered (Celite) and evaporated to dryness under reduced pressure. The residue was extracted with  $\text{CH}_2\text{Cl}_2$  and EtOH was added; volume reduction of this solution gave a red-brown precipitate. This product is thought to be  $[\text{ppn}]_2[\text{Ru}_5(\text{CO})_{12}\text{dppa}]$  (65 mg, 0.028 mmol, 70%). IR ( $\text{CH}_2\text{Cl}_2$ ):  $\nu(\text{CO})$  2025m, 1987vs, 1970(sh)  $\text{cm}^{-1}$ . IR (thf):  $\nu(\text{CO})$  2020m, 1983vs  $\text{cm}^{-1}$ . FAB MS: 1236,  $[\text{M}]^-$ ; loss of 8 CO groups; 538,  $[\text{ppn}]^+$ ; no Ru-containing peaks in the positive ion spectrum.  $^1\text{H NMR}$  ( $\text{C}_6\text{D}_6/d^6\text{-acetone}$  3:1):  $\delta$  7.4 - 7.2 (m, Ph). No reaction occurred when this product was treated with  $\text{AuCl}(\text{PPh}_3)$ .

#### 3.4.12. Synthesis of $\text{Au}_2\text{Ru}_5(\mu_5\text{-}\eta^2, P\text{-C}_2\text{PPh}_2)(\mu\text{-PPh}_2)(\text{CO})_{12}(\text{PPh}_3)\text{-}\{\text{P}(\text{OEt})_3\}$ (39), $\text{Au}_2\text{Ru}_5(\mu_5\text{-}\eta^2, P\text{-C}_2\text{PPh}_2)(\mu\text{-PPh}_2)(\text{CO})_{11}(\text{PPh}_3)\text{-}\{\text{P}(\text{OEt})_3\}_2$ (40) and $\text{Au}_2\text{Ru}_5(\mu_5\text{-}\eta^2, P\text{-C}_2\text{PPh}_2)(\mu\text{-PPh}_2)(\text{CO})_{11}\text{-}\{\text{PPh}_3\}_2\{\text{P}(\text{OEt})_3\}$ (41)

Complex (35) (70 mg, 0.033 mmol) and  $\text{P}(\text{OEt})_3$  (9 mg, 0.054 mmol) were heated in

refluxing  $\text{CH}_2\text{Cl}_2$  (15 mL) for 1 h. A further portion of  $\text{P}(\text{OEt})_3$  (6 mg, 0.037 mmol) was added and heating was continued for 15 min. At this stage reaction appeared to be complete (by spot TLC). The volume was then reduced to 1 mL and petroleum spirit (10 mL) was added to precipitate a green solid, which was washed with further petroleum spirit. Preparative TLC (petroleum spirit/ $\text{CH}_2\text{Cl}_2$ /acetone 8:2:1) of this product gave three green bands. The first band ( $R_f$  0.53) was crystallized ( $\text{CH}_2\text{Cl}_2$ /cyclohexane) as microcrystalline  $\text{Au}_2\text{Ru}_5(\mu_5\text{-}\eta^2, P\text{-C}_2\text{PPh}_2)(\mu\text{-PPh}_2)(\text{CO})_{12}(\text{PPh}_3)\{\text{P}(\text{OEt})_3\}$  (**39**) (8 mg, 0.004 mmol, 12%), m.p. 230 °C(dec.). Anal. Calcd for  $\text{C}_{62}\text{H}_{50}\text{Au}_2\text{O}_{15}\text{P}_4\text{Ru}_5$ : C, 36.18; H, 2.45;  $M_r$  2058. Found: C, 35.82; H, 2.44;  $M_r$  2058 (mass spectrometry, 2059 =  $[\text{M} + \text{H}]^+$ ). IR ( $\text{CH}_2\text{Cl}_2$ ):  $\nu(\text{CO})$  2058w, 2036s, 1998(sh), 1988vs, 1962(sh), 1921m  $\text{cm}^{-1}$ .  $^1\text{H}$  NMR ( $\text{CDCl}_3$ ):  $\delta$  7.9 - 6.9 (m, 35H, Ph); 3.62 (m, 6H,  $\text{CH}_2$ ); 0.85 (t,  $J_{\text{H-H}} = 7.0$  Hz, 9H,  $\text{CH}_3$ ). FAB MS: 2059,  $[\text{M}]^+$ ; loss of 2 CO groups. The second band ( $R_f$  0.40) crystallized ( $\text{CH}_2\text{Cl}_2$ /petroleum spirit) as green microcrystalline  $\text{Au}_2\text{Ru}_5(\mu_5\text{-}\eta^2, P\text{-C}_2\text{PPh}_2)(\mu\text{-PPh}_2)(\text{CO})_{11}(\text{PPh}_3)\{\text{P}(\text{OEt})_3\}_2$  (**40**) (26 mg, 0.012 mmol, 36%), m.p. 174-178 °C. Anal. Calcd for  $\text{C}_{67}\text{H}_{65}\text{Au}_2\text{O}_{17}\text{P}_5\text{Ru}_5$ : C, 36.63; H, 2.98;  $M_r$  2196. Found: C, 37.15; H, 2.82;  $M_r$  2196 (mass spectrometry, 2197 =  $[\text{M} + \text{H}]^+$ ). IR ( $\text{CH}_2\text{Cl}_2$ ):  $\nu(\text{CO})$  2035m, 2002m, 1976vs, 1965(sh), 1912m  $\text{cm}^{-1}$ .  $^1\text{H}$  NMR ( $\text{CDCl}_3$ ):  $\delta$  8.2 - 6.9 (m, 35H, Ph); 4.18 (m, 6H,  $\text{CH}_2$ ); 3.58 (m, 6H,  $\text{CH}_2$ ); 1.30 (t,  $J_{\text{H-H}} = 7.0$  Hz, 9H,  $\text{CH}_3$ ); 0.83 (t,  $J_{\text{H-H}} = 7.0$  Hz, 9H,  $\text{CH}_3$ ). FAB MS: 2197,  $[\text{M}]^+$ ; loss of 10 CO groups. The last band ( $R_f$  0.33) crystallized ( $\text{CH}_2\text{Cl}_2$ /petroleum spirit) as large green-black crystals of  $\text{Au}_2\text{Ru}_5(\mu_5\text{-}\eta^2, P\text{-C}_2\text{PPh}_2)(\mu\text{-PPh}_2)(\text{CO})_{11}(\text{PPh}_3)_2\{\text{P}(\text{OEt})_3\}$  (**41**) (11 mg, 0.0048 mmol, 15%), m.p. 275 °C (dec.). Anal. Calcd for  $\text{C}_{79}\text{H}_{65}\text{Au}_2\text{O}_{14}\text{P}_5\text{Ru}_5$ : C, 41.39; H, 2.86;  $M_r$  2292. Found: C, 41.46; H, 2.95;  $M_r$  2292 (mass spectrometry). IR ( $\text{CH}_2\text{Cl}_2$ ):  $\nu(\text{CO})$  2036m, 2005m, 1977vs, 1964(sh), 1911m  $\text{cm}^{-1}$ .  $^1\text{H}$  NMR ( $\text{CDCl}_3$ ):  $\delta$  8.2 - 6.6 (m, 50H, Ph); 4.18 (m, 6H,  $\text{CH}_2$ ); 1.29(t,  $J_{\text{H-H}} = 7.0$  Hz, 9H,  $\text{CH}_3$ ). FAB MS: 2292,  $[\text{M}]^+$ ; loss of 10 CO groups.

#### 3.4.13. Synthesis of $\text{Ru}_5(\mu\text{-H})(\mu_5\text{-}\eta^2, P\text{-C}_2\text{PPh}_2)(\mu\text{-PPh}_2)(\mu\text{-Cl})(\text{CO})_{13}$ (**42**)

Two drops of HCl (aq. 33%; 58 mg, approx. 1.61 mmol) were added to a solution of (**1**) (100 mg, 0.079 mmol) dissolved in acetone/ $\text{CH}_2\text{Cl}_2$  (1:1, 20 mL). After stirring for 20 min

no starting material remained (spot TLC). At this stage  $\text{CH}_2\text{Cl}_2$  (20 mL) and water (10 mL) were added to the orange solution. The organic layer was then extracted with a further two aliquots of water, dried over  $\text{MgSO}_4$  and evaporated to dryness. Crystallization ( $\text{CH}_2\text{Cl}_2$ /petroleum spirit) gave  $\text{Ru}_5(\mu\text{-H})(\mu_5\text{-}\eta^2, P\text{-C}_2\text{PPh}_2)(\mu\text{-PPh}_2)(\mu\text{-Cl})(\text{CO})_{13}$  (87 mg, 0.067 mmol, 85%). The analytical sample was prepared by preparative TLC (petroleum spirit/ $\text{CH}_2\text{Cl}_2$  2:1) of this product. A major orange band ( $R_f$  0.52) was separated from three trace bands and crystallized ( $\text{CH}_2\text{Cl}_2$ /petroleum spirit) to give orange crystalline  $\text{Ru}_5(\mu\text{-H})(\mu_5\text{-}\eta^2, P\text{-C}_2\text{PPh}_2)(\mu\text{-PPh}_2)(\mu\text{-Cl})(\text{CO})_{13}$  (**42**) (30 mg, 0.023 mmol, 29%), m.p. 193-194 °C. Anal. Calcd for  $\text{C}_{39}\text{H}_{21}\text{ClO}_{13}\text{P}_2\text{Ru}_5$ : C, 36.03; H, 1.63;  $M_r$  1300. Found: C, 36.55; H, 1.84;  $M_r$  1300 (mass spectrometry). IR (cyclohexane):  $\nu(\text{CO})$  2087w, 2070s, 2061s, 2050(sh), 2023vs, 2014(sh), 2009(sh), 1998(sh), 1976m, 1958(sh), 1948(sh), 1944m  $\text{cm}^{-1}$ .  $^1\text{H}$  NMR ( $\text{C}_6\text{D}_6$ ):  $\delta$  7.5 - 6.7 (m, 20H, Ph); -21.25 (s, 1H, RuH).  $^{13}\text{C}\{^1\text{H}\}$  NMR ( $\text{CH}_2\text{Cl}_2$ ):  $\delta$  292.9 (s,  $\text{C}_\alpha$ ); 205.4 (s), 203.3 (s), 199.2 (m), 197.6 (m), 196.1 (s), 194.6 (m), 191.8 (s), 189.2 (m), 185.1 (s), 183.9 (s), 176.0 (s) -CO; 154.3 (d,  $J_{\text{P-C}} = 15$  Hz,  $\text{C}_\beta$ ); 141.2 - 128.6 (m, Ph). FAB MS: 1300,  $[\text{M}]^+$ ; loss of 13 CO groups.

*N.B.* An attempted protonation of (**1**) with  $\text{HBF}_4\cdot\text{Et}_2\text{O}$  was unsuccessful. After 5 h at r.t. with an excess of acid no reaction was observed and unreacted starting material was recovered.

#### 3.4.14. Synthesis of $\text{Ru}_5(\mu\text{-H})(\mu_5\text{-}\eta^2, P\text{-C}_2\text{PPh}_2)(\mu\text{-PPh}_2)(\mu\text{-Br})(\text{CO})_{13}$ (**43**)

Three drops of HBr (aq. 48%, approx. 4.5 mmol) were added to (**1**) (100 mg, 0.079 mmol) dissolved in acetone/ $\text{CH}_2\text{Cl}_2$  (1:1, 20 mL). After stirring for 20 min the orange solution was poured into water (30 mL), and the organic layer then separated, dried over  $\text{MgSO}_4$  and evaporated to dryness. Preparative TLC (petroleum spirit/ $\text{CH}_2\text{Cl}_2$  2:1) of this product gave a major orange band ( $R_f$  0.67) which was collected and crystallized ( $\text{CH}_2\text{Cl}_2$ /EtOH), giving light orange crystals of  $\text{Ru}_5(\mu\text{-H})(\mu_5\text{-}\eta^2, P\text{-C}_2\text{PPh}_2)(\mu\text{-PPh}_2)(\mu\text{-Br})(\text{CO})_{13}$  (**43**) (60 mg, 0.045 mmol, 56%), m.p. 195-197 °C (crystals darkened at 175 °C). Anal. Calcd for  $\text{C}_{39}\text{H}_{21}\text{BrO}_{13}\text{P}_2\text{Ru}_5$ : C, 34.83; H, 1.57;  $M_r$  1345. Found: C, 34.58; H, 1.57;  $M_r$  1345 (mass spectrometry). IR (cyclohexane):  $\nu(\text{CO})$  2088w, 2071s, 2063s, 2051(sh), 2037(sh), 2031(sh), 2025vs, 2020(sh), 2014(sh), 2000(sh), 1989(sh), 1981m, 1962sh,

1954w cm<sup>-1</sup>. <sup>1</sup>H NMR (C<sub>6</sub>D<sub>6</sub>): δ 7.9 - 6.9 (m, 20H, Ph); -20.71 (s, 1H, RuH). FAB MS: 1345, [M]<sup>+</sup>; loss of 13 CO groups.

#### 3.4.15. Synthesis of Ru<sub>5</sub>(μ-H)(μ<sub>5</sub>-η<sup>2</sup>, *P*-C<sub>2</sub>PPh<sub>2</sub>)(μ<sub>3</sub>-I)(μ-PPh<sub>2</sub>)(CO)<sub>12</sub> (44)

Two drops of HI (aq. 57%, approx. 2.8 mmol) were added to a solution of (1) (100 mg, 0.079 mmol) dissolved in CH<sub>2</sub>Cl<sub>2</sub>/acetone (1:1, 20 mL). An instant colour change to a dark orange-brown was observed and 5 min later the solution was added to water (30 mL). The organic layer was extracted with water and then dried over MgSO<sub>4</sub>. After removing the solvent under reduced pressure the residue was purified by TLC (petroleum spirit/CH<sub>2</sub>Cl<sub>2</sub> 2:1). A major burgundy-coloured band (R<sub>f</sub> 0.71) was separated from two other trace bands and an orange base-line. This product was then crystallized (CH<sub>2</sub>Cl<sub>2</sub>/heptane) to give Ru<sub>5</sub>(μ-H)(μ<sub>5</sub>-η<sup>2</sup>, *P*-C<sub>2</sub>PPh<sub>2</sub>)(μ<sub>3</sub>-I)(μ-PPh<sub>2</sub>)(CO)<sub>12</sub>·0.33C<sub>7</sub>H<sub>16</sub> (44) (75 mg, 0.055 mmol, 70%), m.p. 187-189 °C (darkened at 112 °C). Anal. Calcd for C<sub>38</sub>H<sub>21</sub>IO<sub>12</sub>P<sub>2</sub>Ru<sub>5</sub>·0.33C<sub>7</sub>H<sub>16</sub>: C, 34.67; H, 1.90; M<sub>r</sub> 1364 (unsolvated). Found: C, 34.86; H, 1.81; M<sub>r</sub> 1364 (mass spectrometry, 1365 = [M + H]<sup>+</sup>). IR (cyclohexane): ν(CO) 2081w, 2061s, 2021vs, 2006vw, 1996w, 1982w, 1953vw cm<sup>-1</sup>. <sup>1</sup>H NMR (*d*<sup>6</sup>-acetone): δ 8.2 - 7.4 (m, 20H, Ph); 1.28(m 3H, CH<sub>2</sub>, C<sub>7</sub>H<sub>16</sub>); 0.88 (m, 2H, CH<sub>3</sub>, C<sub>7</sub>H<sub>16</sub>); -25.33 (s, 1H, RuH). FAB MS: 1365, [M]<sup>+</sup>; loss of 12 CO groups. This complex also forms an ion at *m/z* 1391, [M + CO]<sup>+</sup> after short periods in the FAB beam.

#### 3.4.16. Synthesis of AuRu<sub>5</sub>(μ<sub>5</sub>-η<sup>2</sup>, *P*-C<sub>2</sub>PPh<sub>2</sub>)(μ-PPh<sub>2</sub>)(μ-Cl)(CO)<sub>13</sub>(PPh<sub>3</sub>) (45)

A mixture of (1) (60 mg, 0.047 mmol) and AuCl(PPh<sub>3</sub>) (50 mg, 0.10 mmol) was stirred at r.t. for 24 h. The solvent was then removed under vacuum and the residue purified by TLC (petroleum spirit/CH<sub>2</sub>Cl<sub>2</sub> 4:1) giving a minor brown band (R<sub>f</sub> 0.62) identified (IR, FAB MS) as (1) (5 mg, 0.004 mmol, 8%). A major orange band (R<sub>f</sub> 0.37) was also collected and crystallized (CH<sub>2</sub>Cl<sub>2</sub>/petroleum spirit) as AuRu<sub>5</sub>(μ<sub>5</sub>-η<sup>2</sup>, *P*-C<sub>2</sub>PPh<sub>2</sub>)(μ-PPh<sub>2</sub>)(μ-Cl)(CO)<sub>13</sub>(PPh<sub>3</sub>) (45) (34 mg, 0.019 mmol, 41%), m.p. 162 °C (dec.). Anal. Calcd for C<sub>57</sub>H<sub>35</sub>AuClO<sub>13</sub>P<sub>3</sub>Ru<sub>5</sub>: C, 38.93; 2.01; M<sub>r</sub> 1759. Found: C, 38.71; H, 2.06; M<sub>r</sub> 1759 (mass spectro-

metry). IR (cyclohexane):  $\nu(\text{CO})$  2066m, 2050m, 2038vs, 2013m, 2001(sh), 1992m, 1980(sh), 1970m, 1953(sh), 1932w  $\text{cm}^{-1}$ .  $^1\text{H NMR}$  ( $\text{C}_6\text{D}_6$ ):  $\delta$  7.9 - 6.5 (m, Ph). FAB MS: 1759,  $[\text{M}]^+$ ; loss of 13 CO groups.

**3.4.17. Synthesis of  $\text{Ru}_5\{\mu_4\text{-}\eta^4, O\text{-C}_2\text{C}(\text{O})\text{C}_3\text{H}_5\}(\mu\text{-PPh}_2)_2(\mu\text{-Cl})(\text{CO})_{11}$  (46o) and an isomer  $\text{Ru}_5\text{Cl}(\text{CO})_{12}(\text{allyl})(\text{dppa}^*)$  (46b)**

Allyl chloride (250 mg, 3.29 mmol) and (1) (50 mg, 0.040 mmol) were refluxed in  $\text{CH}_2\text{Cl}_2$  (30 mL) for 20 h. After cooling the solvent was removed under reduced pressure and the residue was purified by TLC (petroleum spirit/ $\text{CH}_2\text{Cl}_2$  3:2). Two bands were collected: the first brown band ( $R_f$  0.50) was crystallized ( $\text{CH}_2\text{Cl}_2/\text{MeOH}$ ) by slow evaporation to give light brown crystals of  $\text{Ru}_5\text{Cl}(\text{CO})_{12}(\text{allyl})(\text{dppa}^*)$  (46b) (22 mg, 0.017 mmol, 42%), m.p. 225-226 °C. Anal. Calcd for  $\text{C}_{41}\text{H}_{25}\text{ClO}_{12}\text{P}_2\text{Ru}_5$ : C, 37.52; H, 1.92;  $M_r$  1312. Found: C, 37.14; H, 1.94;  $M_r$  1312 (mass spectrometry, 1313 =  $[\text{M} + \text{H}]^+$ ). IR (cyclohexane):  $\nu(\text{CO})$  2069w, 2058(sh), 2049vs, 2032(sh), 2020(sh), 2015s, 2005m, 1991s, 1980m, 1956vw, 1942vw  $\text{cm}^{-1}$ .  $^1\text{H NMR}$  ( $\text{C}_6\text{D}_6$ ):  $\delta$  8.1 - 6.6<sup>++</sup> (m, 20H, Ph); 4.52<sup>++</sup> (m, CH); 3.87<sup>+</sup> (d,  $J_{\text{H-H}} = 7.6$  Hz,  $\text{CH}_2$ ); 3.55<sup>+</sup> (m,  $\text{CH}_2$ ); 3.28<sup>\*</sup> (m, 1H,  $\text{CH}_2$ ); 3.15<sup>\*</sup> (dd,  $J_{\text{P-H}} = 13.0$ ,  $J_{\text{H-H}} = 5.0$  Hz,  $\text{CH}_2$ ); 3.02<sup>+</sup> (dd,  $J_{\text{P-H}} = 13.0$ ,  $J_{\text{H-H}} = 5.0$  Hz,  $\text{CH}_2$ ); 2.21<sup>+</sup> (d,  $J_{\text{P-H}} = 12.9$  Hz,  $\text{CH}_2$ ); 2.12<sup>\*</sup> (d,  $J_{\text{H-H}} = 8.0$  Hz,  $\text{CH}_2$ ); 1.87<sup>\*</sup> (d,  $J_{\text{P-H}} = 13.0$  Hz,  $\text{CH}_2$ ); ratio of isomer 1 (marked \*) to isomer 2 (marked +) is 2:1. FAB MS: 1313,  $[\text{M}]^+$ ; loss of 7 CO groups; 1244,  $[\text{M} - \text{CO} - \text{allyl}]^+$ .

A second band ( $R_f$  0.37, orange) was collected and crystallized ( $\text{CH}_2\text{Cl}_2/\text{petroleum spirit}$ ) giving orange crystals of  $\text{Ru}_5\{\mu_4\text{-}\eta^4, O\text{-C}_2\text{C}(\text{O})\text{C}_3\text{H}_5\}(\mu\text{-PPh}_2)_2(\mu\text{-Cl})(\text{CO})_{11}$  (46o) (10 mg, 0.0076 mmol, 19%), m.p. 200 °C (dec.). Anal. Found: C, 37.39; H, 2.09;  $M_r$  1312 (mass spectrometry, 1313 =  $[\text{M} + \text{H}]^+$ ). IR (cyclohexane):  $\nu(\text{CO})$  2060m, 2043(sh), 2038s, 2032s, 2026(sh), 1992s, 1987(sh), 1975w, 1951vw, 1928vw, 1535vw  $\text{cm}^{-1}$ .  $^1\text{H NMR}$  ( $\text{C}_6\text{D}_6$ ):  $\delta$  8.2 - 6.7 (m, 20H, Ph); 3.57 (m, 1H, CH); 3.36 (d,  $J_{\text{H-H}} = 8.7$  Hz, 1H,  $\text{CH}_2$ ); 2.92 (d,  $J_{\text{P-H}} = 14.9$  Hz, 1H,  $\text{CH}_2$ ); 2.23 (d,  $J_{\text{P-H}} = 19.3$  Hz, 1H,  $\text{CH}_2$ ); 1.96 (dd,  $J_{\text{P-H}} = 19.3$ ,  $J_{\text{H-H}} = 8.0$  Hz, 1H,  $\text{CH}_2$ ). FAB MS: 1313,  $[\text{M}]^+$ ; loss of 12 CO groups.

**3.4.18. Synthesis of  $\text{Ru}_5\{\mu_4\text{-}\eta^4\text{-}O\text{-C}_2\text{C(O)C}_3\text{H}_5\}(\mu\text{-PPh}_2)_2(\mu\text{-Br})(\text{CO})_{11}$  (47o) and an isomer  $\text{Ru}_5\text{Br}(\text{CO})_{12}(\text{allyl})(\text{dppa}^*)$  (47b)**

Allyl bromide (500 mg, 4.13 mmol) and (1) (130 mg, 0.10 mmol) were heated in refluxing  $\text{CH}_2\text{Cl}_2$  (20 mL) for 24 h. After cooling the solvent was removed under reduced pressure and the residue was purified by TLC (petroleum spirit/ $\text{CH}_2\text{Cl}_2$  3:2). Two bands were collected: the major brown band ( $R_f$  0.60) was rechromatographed (TLC: petroleum spirit/ $\text{Et}_2\text{O}/\text{CH}_2\text{Cl}_2$  16:2:1) to give a band ( $R_f$  0.47) which was precipitated from  $\text{CH}_2\text{Cl}_2/\text{cyclohexane}$  as a brown powder of  $\text{Ru}_5\text{Br}(\text{CO})_{12}(\text{allyl})(\text{dppa}^*)\cdot 0.5\text{C}_6\text{H}_{12}$  (47b) (24 mg, 0.018 mmol, 18%), m.p. 145-147 °C. Anal. Calcd for  $\text{C}_{41}\text{H}_{25}\text{BrO}_{12}\text{P}_2\text{Ru}_5\cdot 0.5\text{C}_6\text{H}_{12}$ : C, 37.78; H, 2.23;  $M_r$  (unsolvated) 1357. Found: C, 37.58; H, 2.30;  $M_r$  1357 (mass spectrometry). IR (cyclohexane):  $\nu(\text{CO})$  2068w, 2056(sh), 2049vs, 2016(sh), 2014s, 2004w, 1992m, 1980w, 1956vw  $\text{cm}^{-1}$ .  $^1\text{H NMR}$  ( $\text{C}_6\text{D}_6$ ):  $\delta$  7.9 - 6.8 (m, 20H, Ph); 4.45\* (m, CH); 4.31+ (m, CH); 3.83+ (d,  $J_{\text{H-H}} = 7.5$  Hz,  $\text{CH}_2$ ); 3.44+ (m,  $\text{CH}_2$ ); 3.29\* (dd,  $J_{\text{P-H}} = 13.1$ ,  $J_{\text{H-H}} = 5.2$  Hz,  $\text{CH}_2$ ); 3.11\*\* (dd + m,  $J_{\text{P-H}} = 12.2$ ,  $J_{\text{H-H}} = 5.4$  Hz,  $\text{CH}_2$ ); 2.32+ (d,  $J_{\text{P-H}} = 13.1$  Hz,  $\text{CH}_2$ ); 2.15\* (d,  $J_{\text{H-H}} = 6.3$  Hz,  $\text{CH}_2$ ); 1.97\* (d,  $J_{\text{P-H}} = 13.1$  Hz,  $\text{CH}_2$ ); ratio of isomer 1 (marked \*) to isomer 2 (marked +) is 1:1. FAB MS: 1357,  $[\text{M}]^+$ ; loss of 7 CO groups; 1288,  $[\text{M} - \text{CO} - \text{allyl}]^+$ , loss of 9 CO groups.

The other minor band ( $R_f$  0.40, orange) was collected and crystallized ( $\text{CH}_2\text{Cl}_2/\text{petroleum spirit}$ ) giving orange cube-like crystals of  $\text{Ru}_5\{\mu_4\text{-}\eta^4\text{-}O\text{-C}_2\text{C(O)C}_3\text{H}_5\}(\mu\text{-PPh}_2)_2(\mu\text{-Br})(\text{CO})_{11}$  (47o) (7 mg, 0.005 mmol, 5%), m.p. 230-232 °C. Anal. Calcd for  $\text{C}_{41}\text{H}_{25}\text{BrO}_{12}\text{P}_2\text{Ru}_5\cdot 0.5\text{CH}_2\text{Cl}_2$ : C, 35.62; H, 1.87;  $M_r$  (unsolvated) 1357. Found: C, 35.53; H, 1.96;  $M_r$  1357 (mass spectrometry). IR (cyclohexane):  $\nu(\text{CO})$  2059w, 2038s, 2031s, 2026(sh), 1995(sh), 1989m, 1975w, 1955vw, 1925vw. IR ( $\text{CH}_2\text{Cl}_2$ ):  $\nu(\text{CO})$  1534vw  $\text{cm}^{-1}$ .  $^1\text{H NMR}$  ( $\text{C}_6\text{D}_6$ ):  $\delta$  8.3 - 6.9 (m, 20H, Ph); 4.26 (s, 1H,  $\text{CH}_2\text{Cl}_2$ ); 3.56 (m, 1H, CH); 3.35 (d,  $J_{\text{H-H}} = 8.9$  Hz, 1H,  $\text{CH}_2$ ); 2.94 (d,  $J_{\text{P-H}} = 13.9$  Hz, 1H,  $\text{CH}_2$ ); 2.24 (d,  $J_{\text{P-H}} = 19.4$  Hz, 1H,  $\text{CH}_2$ ); 1.96 (dd,  $J_{\text{P-H}} = 19.2$ ,  $J_{\text{H-H}} = 7.8$  Hz, 1H,  $\text{CH}_2$ ). FAB MS: 1357,  $[\text{M}]^+$ ; loss of 12 CO groups. A large base-line was also observed in the TLC separation.

*N.B.* No reaction was observed when either (47b) or (47o) was refluxed in  $\text{CH}_2\text{Cl}_2$  for 48 h.

### 3.4.19. Synthesis of two isomers of $\text{Ru}_6(\text{CO})_{11}(\text{dppa}^*)$ (48o), (48y)

Addition of  $\text{HgCl}_2$  (22 mg, 0.081 mmol) to a solution of (1) (100 mg, 0.079 mmol) in  $\text{CH}_2\text{Cl}_2$  (20 mL) resulted in the solution turning orange. After 30 min a further portion of  $\text{HgCl}_2$  (16 mg, 0.059 mmol) was added and the reaction stirred for 15 min. A grey precipitate was then filtered off (Celite) and the solvent removed under reduced pressure. Preparative TLC (petroleum spirit/acetone 2:1) of the residue separated two main bands and left a large base-line (brown). A yellow band ( $R_f$  0.36) was quickly removed from the silica and crystallized ( $\text{CH}_2\text{Cl}_2/\text{MeOH}$ ) as yellow microcrystalline  $\text{Ru}_6(\text{CO})_{11}(\text{dppa}^*)$  (48y) (20 mg, 0.015 mmol, 19%), m.p. 170-172 °C (colour darkened at 110 °C). Anal. Calcd for  $\text{C}_{37}\text{H}_{20}\text{O}_{11}\text{P}_2\text{Ru}_6$ : C, 33.95; H, 1.54;  $M_r$  1307. Found: C, 33.72; H < 2%; (Cl, Hg < 0.1%)  $M_r$  1308 (mass spectrometry). IR (cyclohexane):  $\nu(\text{CO})$  2112vw, 2077s, 2045s, 2035(sh), 2027s, 2014s, 1996(sh), 1986m, 1976(sh), 1963m  $\text{cm}^{-1}$ .  $^1\text{H}$  NMR ( $\text{CS}_2$ ):  $\delta$  7.9 - 7.2 (m, Ph). FAB MS: 1308,  $[\text{M}]^+$ ; loss of 12 CO groups; 1218  $[\text{M} - \text{CPh}]^+$ .

The second band ( $R_f$  0.50, orange) crystallized ( $\text{CH}_2\text{Cl}_2/\text{petroleum spirit}$ ) as pale orange crystals of  $\text{Ru}_6(\text{CO})_{11}(\text{dppa}^*)$  (48o) (13 mg, 0.01 mmol, 13%), m.p. 150 °C (dec.). Anal. Found: C, 34.02; H, 1.64; (Cl, Hg < 0.1%)  $M_r$  1308 (mass spectrometry). IR (cyclohexane):  $\nu(\text{CO})$  2090m, 2073w, 2055m, 2045(sh), 2038s, 2033s, 2025(sh), 2014w, 2006w, 1995m, 1985(sh), 1975(sh), 1947vw  $\text{cm}^{-1}$ .  $^1\text{H}$  NMR ( $\text{CS}_2$ ):  $\delta$  7.8 - 7.2 (m, Ph). FAB MS: 1308,  $[\text{M}]^+$ ; fragmentation pattern identical to (48y).

### 3.4.20. Synthesis of $\text{Ru}_4\{\mu_4\text{-}\eta^2, P, O\text{-C}_5\text{H}_4\text{O}(\text{PPh}_2)\}\mu\text{-PPh}_2(\text{CO})_{11}$ (49) and two isomers of $\text{Ru}_5(\mu_4\text{-PPh})\{\mu_3\text{-}\eta^3\text{-CC}(\text{C}_2\text{H}_2)(\text{C}_2\text{H}_3)\}\mu\text{-PPh}_2(\text{CO})_{12}$ (50b), (50o)

#### (a) Under 20 atmospheres of ethene

A solution of (1) (200 mg, 0.158 mmol) in benzene (15 mL) was placed in a small autoclave (100 mL) and pressurized to 20 atm with ethene. After heating at 80 °C for 8.5 h the reaction was cooled (pressure had dropped to 10 atm) and the orange solution was then

evaporated to dryness under reduced pressure. Preparative TLC (petroleum spirit/acetone 9:1) of the residue gave ten bands of which the major three were collected. A red band ( $R_f$  0.33) was removed from the silica quickly and crystallized ( $\text{CH}_2\text{Cl}_2/\text{MeOH}$ ) by slow evaporation to give small red needles of  $\text{Ru}_4\{\mu_4\text{-}\eta^2, P, O\text{-C}_5\text{H}_4\text{O}(\text{PPh}_2)\}(\mu\text{-PPh}_2)(\text{CO})_{11}\cdot 0.5\text{CH}_2\text{Cl}_2$  (**49**) (31 mg, 0.027 mmol, 17%), m.p. > 280 °C. Anal. Calcd for  $\text{C}_{40}\text{H}_{24}\text{O}_{12}\text{P}_2\text{Ru}_4\cdot 0.5\text{CH}_2\text{Cl}_2$ : C, 40.36; H, 2.09;  $M_r$  1163. Found: C, 40.76; H, 2.06;  $M_r$  1163 (mass spectrometry). IR (cyclohexane):  $\nu(\text{CO})$  2082m, 2064m, 2025s, 2019(sh), 2002(sh), 1998m, 1976w, 1968m, 1958(sh), 1820w  $\text{cm}^{-1}$ . IR ( $\text{CH}_2\text{Cl}_2$ ):  $\nu(\text{CO})$  1588w  $\text{cm}^{-1}$ .  $^1\text{H}$  NMR ( $\text{CD}_2\text{Cl}_2$ , 240K):  $\delta$  7.8 - 6.7 (m, 20H, Ph); 2.83 (m, 1H,  $\text{CH}_2$ ); 2.73 (dd,  $J = 14.8, 4.7$  Hz, 1H,  $\text{CH}_2$ ); 2.20 (dd,  $J = 20.2, 6.7$  Hz, 1H,  $\text{CH}_2$ ); 1.47 (ddd,  $J = 14.6, 9.8, 3.5$  Hz 1H,  $\text{CH}_2$ ). FAB MS Negative ion: 1163,  $[\text{M}]^-$ ; loss of 7 CO groups; 942  $[\text{?}]^+$ , loss of 6 CO groups. FAB MS Positive ion: 1135,  $[\text{M} - \text{CO}]^+$ ; loss of 10 CO groups. This compound was unstable in solution and apparently reacted with MeOH to form larger clusters (FAB MS analysis of the products).

The brown band ( $R_f$  0.59) crystallized ( $\text{CH}_2\text{Cl}_2/\text{petroleum spirit}$ ) as  $\text{Ru}_5(\mu_4\text{-PPh})\{\mu_3\text{-}\eta^3\text{-CC}(\text{C}_2\text{H}_2)(\text{C}_2\text{H}_3)\}(\mu\text{-PPh}_2)(\text{CO})_{12}\cdot\text{CH}_2\text{Cl}_2$  (**50b**) (27 mg, 0.022 mmol, 14%), m.p. 209-210 °C. Anal. Calcd for  $\text{C}_{36}\text{H}_{20}\text{O}_{12}\text{P}_2\text{Ru}_5\cdot\text{CH}_2\text{Cl}_2$ : C, 34.24; H, 1.78;  $M_r$  1213. Found: C, 33.97; H, 1.84;  $M_r$  1213 (mass spectrometry, 1214 =  $[\text{M} + \text{H}]^+$ ). IR (cyclohexane):  $\nu(\text{CO})$  2079m, 2048m, 2030(sh), 2024s, 2013s, 1997m, 1978(sh), 1971m, 1958w, 1952w  $\text{cm}^{-1}$ .  $^1\text{H}$  NMR ( $\text{CD}_2\text{Cl}_2$ , 240K):  $\delta$  8.1 - 6.2 (m, 15H, Ph); 5.58 (d,  $J = 36.2$  Hz, 1H, CH); 5.53 (d,  $J = 29.3$  Hz, 0.5H, ?); 2.37 (d,  $J = 6.3$  Hz, 1H,  $\text{CH}_2$ ); 1.72 (m, 1H,  $\text{CH}_2$ ); 1.63 (d,  $J = 5.9$  Hz, 1H,  $\text{CH}_2$ ); 0.86 (dt,  $J = 9.4, 6.2$  Hz, 1H,  $\text{CH}_2$ ). FAB MS: 1214,  $[\text{M}]^+$ ; loss of 12 CO groups.

The last band collected ( $R_f$  0.47, orange) was removed from the silica with  $\text{CH}_2\text{Cl}_2$  (-15 °C) and crystallized ( $\text{CH}_2\text{Cl}_2/\text{petroleum spirit}$ ) quickly to give orange plate-like crystals of  $\text{Ru}_5(\mu_4\text{-PPh})\{\mu_3\text{-}\eta^3\text{-CC}(\text{C}_2\text{H}_2)(\text{C}_2\text{H}_3)\}(\mu\text{-PPh}_2)(\text{CO})_{12}$  (**50o**) (43 mg, 0.035 mmol, 22%), m.p. 173-174 °C. Anal. Calcd for  $\text{C}_{36}\text{H}_{20}\text{O}_{12}\text{P}_2\text{Ru}_5$ : C, 35.65; H, 1.74;  $M_r$  1213. Found: C, 35.17; H, 1.83;  $M_r$  1213 (mass spectrometry, 1214 =  $[\text{M} + \text{H}]^+$ ). IR (cyclohexane):  $\nu(\text{CO})$  2070m, 2042(sh), 2037s, 2023s, 2016s, 1984(sh), 1975w, 1958w  $\text{cm}^{-1}$ . IR ( $\text{CH}_2\text{Cl}_2$ ):  $\nu(\text{CO})$  1532  $\text{cm}^{-1}$ .  $^1\text{H}$  NMR ( $\text{CD}_2\text{Cl}_2$ , 240K):  $\delta$  7.9 - 6.9 (m, 15H, Ph); 5.23 (t,  $J = 5.8$  Hz,

0.5H, ?); 5.04 (d,  $J = 6.7$  Hz, 1H, CH); 1.27 (d,  $J = 6.3$  Hz, 3H, CH<sub>2</sub>); 0.51 (dt,  $J = 6.1$ , 6.1 Hz, 1H, CH<sub>2</sub>). FAB MS: 1214, [M]<sup>+</sup>; loss of 12 CO groups, intensities similar to (50b). This complex decomposes on standing at r.t. in solution and in the solid state (1-2 d). After 2 d in solution (Et<sub>2</sub>O/pentane) at -15 °C, (50b) was detected in both the crystalline solid deposited (approx. 2%) and in the supernatant (approx. 10%). Infrared and TLC monitoring of the reaction at 5 h indicated the presence of (49), (50o), (50b) and a trace of unreacted (1).

### (b) Reaction performed in a Carius tube

A solution of (1) (150 mg, 0.12 mmol) in benzene (20 mL) was placed in a Carius tube (40 mL internal volume) and ethene (1.0 g, 35.7 mmol) was added. After heating at 85 °C for 24 h the solution was cooled and the excess ethene vented. The solvent was removed under reduced pressure and the residue purified by TLC (petroleum spirit/acetone 9:1). Four bands were collected: a yellow band ( $R_f$  0.85) near the solvent front was identified (IR, spot TLC) as Ru<sub>3</sub>(CO)<sub>12</sub> (4 mg, 0.006 mmol, 5%); the next three bands were identified (IR) as: (2)  $R_f$  0.55, brown, (50b) (15 mg, 0.012 mmol, 10%); (3)  $R_f$  0.45, orange, (50o) (22 mg, 0.018 mmol, 15%); (4)  $R_f$  0.33, red, (49) (37 mg, 0.032 mmol, 27%). Five other minor bands and the brown base-line were not investigated.

### (c) Interconversion of (50o) and (50b)

(i) *In a Carius tube under nitrogen*: Isomer (50o) (6 mg, 0.005 mmol) was dissolved in cyclohexane (5 mL), degassed with N<sub>2</sub> and placed in a Carius tube (10 mL) in the dark at r.t.. Infrared and TLC monitoring of the solution indicated the attainment of equilibrium 3:1 (50o):(50b) after 5d. A small amount of air was then admitted to the solution and the vessel covered with foil. After 5 d the equilibrium of the mixture had changed to 1:1 (50o):(50b).

(ii) *Under N<sub>2</sub> blanket*: Isomers (50o) (10 mg, 0.008 mmol) and (50b) (5 mg, 0.004 mmol) were placed in separate foil-covered flasks (under N<sub>2</sub> blanket). Cyclohexane (5 mL) was added to each and the reactions were left at r.t.. Infrared and TLC monitoring of the solutions showed that both isomers reached an equilibrium mixture [(50b):(50o) 9:7] after 5 d in solution. Immediately after dissolving (50o) an appreciable amount of (50b) was found to

be present in solution (IR, spot TLC), and *vice versa*. The joints on the Schlenk flasks were not greased and so presumably after 5 d a small amount of air would have entered the solutions.

(iii) *In a Carius tube under ethene*: Isomer (**50o**) (6 mg, 0.005 mmol) was dissolved in cyclohexane (5 mL), degassed with C<sub>2</sub>H<sub>4</sub> and placed in a Carius tube (10 mL) in the dark at r.t. Infrared and TLC monitoring of the solution indicated a smaller degree of interconversion than (i). Preparative TLC after 17 d indicated the equilibrium ratio was 3.8:1 (**50o**):(**50b**).

(iv) *In a Carius tube under 1-butene*: Isomer (**50o**) (20 mg, 0.016 mmol) was dissolved in cyclohexane (10 mL), degassed with C<sub>4</sub>H<sub>8</sub> and placed in a Carius tube (10 mL) in the dark at r.t. Preparative TLC after 15 d indicated the equilibrium ratio was 3.3:1 (**50o**):(**50b**). The products were identified by IR, spot TLC and FAB MS. No incorporation of butene was observed.

#### 3.4.21. Synthesis of two isomers of Ru<sub>5</sub>(μ<sub>4</sub>-PPh){μ<sub>3</sub>-η<sup>3</sup>-CC(C<sub>4</sub>H<sub>6</sub>)(C<sub>4</sub>H<sub>7</sub>)}-(μ-PPh<sub>2</sub>)(CO)<sub>12</sub> (**51b**), (**51o**)

A solution of (**1**) (150 mg, 0.12 mmol) in benzene (15 mL) was added to a Carius tube (40 mL) and 1-butene (1.84 g, 32.9 mmol) was condensed into it. After heating at 87 °C for 14 d the excess gas was vented and the solvent removed under reduced pressure. Preparative TLC (petroleum spirit/acetone 9:1) of the residue separated seventeen bands, of which four were collected. A brown band (R<sub>f</sub> 0.55) was crystallized (CH<sub>2</sub>Cl<sub>2</sub>/petroleum spirit) as brown microcrystalline Ru<sub>5</sub>(μ<sub>4</sub>-PPh){μ<sub>3</sub>-η<sup>3</sup>-CC(C<sub>4</sub>H<sub>6</sub>)(C<sub>4</sub>H<sub>7</sub>)}(μ-PPh<sub>2</sub>)(CO)<sub>12</sub>.CH<sub>2</sub>Cl<sub>2</sub> (**51b**) (16 mg, 0.013 mmol, 10%), m.p. 139-141 °C. Anal. Calcd for C<sub>40</sub>H<sub>28</sub>O<sub>12</sub>P<sub>2</sub>Ru<sub>5</sub>.0.5-CH<sub>2</sub>Cl<sub>2</sub>: C, 36.66; H, 2.15; M<sub>r</sub> 1268 (unsolvated). Found: C, 36.73; H, 2.09; M<sub>r</sub> 1268 (mass spectrometry, 1270 = [M + 2H]<sup>+</sup>). IR (cyclohexane): ν(CO) 2078m, 2047s, 2029s, 2023(sh), 2013s, 1997m, 1989(sh), 1979m, 1972w, 1951vw cm<sup>-1</sup>. <sup>1</sup>H NMR (C<sub>6</sub>D<sub>6</sub>): 8.1 - 6.4 (m, 15H, Ph); 6.21 (dt, J = 15.6, 6.2 Hz, 1H, CH); 6.00 (m, 1H, CH); 5.40 (d, J = 15.7 Hz, 1H, CH); 4.27 (s, 2H, CH<sub>2</sub>Cl<sub>2</sub>); 1.90 (m, 2H, CH<sub>2</sub>); 1.75 (m, 2H, CH<sub>2</sub>); 1.37 (m, 2H, CH<sub>2</sub>); 1.00 (m, 2H, CH<sub>2</sub>); 0.96 (t, J = 7.6 Hz, 3H, CH<sub>3</sub>); 0.73 (t, J = 7.2 Hz, 3H, CH<sub>3</sub>). FAB MS: 1270, [M]<sup>+</sup>; loss of 10 CO groups. This compound decomposed readily in solution.

The following major orange band ( $R_f$  0.45) was crystallized quickly ( $\text{CH}_2\text{Cl}_2/\text{pentane}$ ) to give orange plates of  $\text{Ru}_5(\mu_4\text{-PPh})\{\mu_3\text{-}\eta^3\text{-CC}(\text{C}_4\text{H}_6)(\text{C}_4\text{H}_7)\}(\mu\text{-PPh}_2)(\text{CO})_{12}$  (**51o**) (31 mg, 0.024 mmol, 20%), m.p. 170 °C (dec.). Anal. Calcd for  $\text{C}_{40}\text{H}_{28}\text{O}_{12}\text{P}_2\text{Ru}_5$ : C, 37.89; H, 2.23;  $M_r$  1271. Found: C, 37.58; H, 2.36;  $M_r$  1268 (mass spectrometry, 1270,  $[\text{M} + 2\text{H}]^+$ ). IR (cyclohexane):  $\nu(\text{CO})$  2069m, 2037s, 2022(sh), 2016s, 2008(sh), 1994(sh), 1982vw, 1958w  $\text{cm}^{-1}$ .  $^1\text{H NMR}$  ( $\text{C}_6\text{D}_6$ ): 7.9 - 6.7 (m, 15H, Ph); 5.44 (dt,  $J = 15.9, 6.1$  Hz, 2H, CH); 4.99 (d,  $J = 16.0$  Hz, 1H, CH); 1.81 (m, 2H,  $\text{CH}_2$ ); 1.51 (m, 2H,  $\text{CH}_2$ ); 1.38 (m, 1H,  $\text{CH}_2$ ); 1.23 (m, 1H,  $\text{CH}_2$ ); 0.87 (t,  $J = 7.4$  Hz, 3H,  $\text{CH}_3$ ); 0.70 (t,  $J = 7.0$  Hz, 3H,  $\text{CH}_3$ ). FAB MS: 1270,  $[\text{M}]^+$ ; loss of 9 CO groups, intensities similar to (**51b**). Within 30 min of being placed in solution, isomer-pure (**51o**) was partially converted to (**51b**) and, conversely, pure (**51b**) to (**51o**).

The next minor band removed ( $R_f$  0.38, brown) was fractionally crystallized ( $\text{CH}_2\text{Cl}_2/\text{cyclohexane}$ ) to give an orange powder which was formulated as  $\text{Ru}_5(\text{CO})_{12}(\text{PPh})(\text{PPh}_2)\text{C}_2\text{-(C}_4\text{H}_8)_3$ . IR (cyclohexane):  $\nu(\text{CO})$  2070w, 2037s, 2023(sh), 2010vs, 1978w, 1972w  $\text{cm}^{-1}$ ; FAB MS: 1382,  $[\text{M}]^+$ , loss of 11 CO groups. The last band removed ( $R_f$  0.25, red) was given the formulation  $\text{Ru}_5(\text{CO})_{11}(\text{dppa}^*)(\text{C}_4\text{H}_8)$  on the basis of spectroscopic data: IR (cyclohexane): 2081w, 2053m, 2037(sh), 2025vs, 2013s, 200(sh), 1992m, 1982(sh), 1967w, 1950w, 1768vw  $\text{cm}^{-1}$ ; FAB MS: 1265,  $[\text{M}]^+$ , loss of 8 CO groups. Insufficient amounts of these last two products were obtained to allow full characterization.

### 3.4.22. Synthesis of $\text{Ru}_5(\mu_4\text{-PPh})(\mu\text{-PPh}_2)(\mu\text{-CO})(\text{CO})_{10}\{\eta^5\text{-C}_5\text{H}_3(\text{C}_2\text{H}_3)\text{Me}\}$ (**52**)

#### (a) Reaction of (1) with ethene

Ethene was bubbled through a solution of (1) (100 mg, 0.079 mmol) in cyclohexane (50 mL) at slow reflux (oil bath 105 °C). After 48 h the reaction mixture was cooled and the solvent removed under reduced pressure. Preparative TLC (petroleum spirit/ $\text{CH}_2\text{Cl}_2$  7:1) of the reaction product separated nine bands from a large base-line; five were collected. A trace green band ( $R_f$  0.51) was identified (IR, FAB MS) as (**27**). The next orange band was further

chromatographed (TLC: petroleum spirit/acetone 9:1) to give two bands, a brown band ( $R_f$  0.44) identified (IR, FAB MS) as **(50b)** and an orange band ( $R_f$  0.33) which contained **(50o)**. Two other products obtained from the original separation (brown bands at  $R_f$  0.43, 0.40 respectively) have the same nominal formulation, viz.  $Ru_5(CO)_{12-n}(dppa^*)(C_2H_4)_n$  (FAB MS: 1237,  $[M]^+$ ). The last brown band collected ( $R_f$  0.29) was repurified (TLC: petroleum spirit/ $CH_2Cl_2$ /acetone 8:2:1) to give a major brown band ( $R_f$  0.55), this in turn was fractionally crystallized ( $CH_2Cl_2$ /petroleum spirit) to give brown crystals of  $Ru_5(\mu_4-PPh)(\mu-PPh_2)(\mu-CO)(CO)_{10}\{\eta^5-C_5H_3(C_2H_3)Me\}.C_6H_{14}$  (**(52)**) (9 mg, 0.007 mmol, 9%), m.p. 110-115 °C. Anal. Calcd for  $C_{37}H_{24}O_{11}P_2Ru_5.C_6H_{14}$ : C, 39.78; H, 2.95;  $M_r$  1212 (unsolvated). Found: C, 39.78; H, 3.08;  $M_r$  1212 (mass spectrometry, 1214 =  $[M + 2H]^+$ ). IR (cyclohexane):  $\nu(CO)$  2060m, 2029vs, 2021(sh), 2012m, 1997(sh), 1987m, 1972w, 1967(sh), 1779vw  $cm^{-1}$ .  $^1H$  NMR ( $CDCl_3$ ):  $\delta$  7.9 - 6.9 (m, 15H, Ph); 5.86 (s, 1H, CH); 5.49 (s, 1H, CH); 4.61 (s, 1H, CH); 2.44 (m, 2H, CH +  $CH_2$ ); 2.17 (s, 1H,  $CH_2$ ); 1.96 (s, 3H,  $CH_3$ ). FAB MS: 1214,  $[M]^+$ ; loss of 11 CO groups.

#### (b) Conversion of **(50b)** to **(52)**

A solution of **(50b)** (12 mg, 0.01 mmol) was dissolved in cyclohexane (30 mL) and heated (oil bath, 98 °C, 24 h) with ethene bubbling through the solution. After cooling the solvent was removed under reduced pressure and the residue purified by TLC (petroleum spirit/ $CH_2Cl_2$ /acetone 8:2:1). Of the seven bands which separated from the base-line only three were collected and identified (IR, spot TLC) as: (1)  $R_f$  0.69, brown, **(50b)** (0.5 mg, 0.0004 mmol, 4%); (2)  $R_f$  0.63, orange, **(50o)** (2.0 mg, 0.0016 mmol, 16%); (3)  $R_f$  0.50, brown, **(52)** (2.4 mg, 0.02 mmol, 19%), also identified by FAB MS.

### 3.5. References

- 1 (a) Wade, K. *Inorg. Nucl. Chem. Letters* **8** (1972) 559.  
(b) Mingos, D.M.P. *Acc. Chem. Res.* **17** (1984) 311.
- 2 Knox, S.A.R.; Morris, M.J. *J. Chem. Soc., Dalton Trans.* (1987) 2087.
- 3 Davies, D.L.; Howard, J.A.K.; Knox, S.A.R.; Mardsen, K.; Mead, K.A.; Morris, M.J.; Rendle, M.C. *J. Organomet. Chem.* **279** (1985) C37.
- 4 This work.
- 5 Kwek, K.; Taylor, N.J.; Carty, A.J. *J. Am. Chem. Soc.* **106** (1984) 4636.
- 6 Han, S.H.; Geoffroy, G.L.; Rheingold, A.L. *Organometallics* **5** (1986) 2561.
- 7 Nucciarone, D.; Taylor, N.J.; Carty, A.J. *Organometallics* **5** (1986) 2565.
- 8 MacLaughlin, S.A.; Taylor, N.J.; Carty, A.J. *Organometallics* **3** (1984) 392.
- 9 Adams, R.D.; Babin, J.E.; Tanner, J.T. *Organometallics* **7** (1988) 2027.
- 10 Bruce, M.I.; Williams, M.L.; Skelton, B.W.; White, A.H. *J. Organomet. Chem.* in press.
- 11 MacLaughlin, S.A.; Taylor, N.J.; Carty, A.J. *J. Am. Chem. Soc.* **103** (1981) 2456.
- 12 Bruce, M.I.; Williams, M.L.; Patrick, J.M.; White, A.H. *J. Chem. Soc., Dalton Trans.* (1985) 1229.
- 13 Carty, A.J. *Pure Appl. Chem.* **54** (1982) 113.
- 14 Knox, S.A.R.; Lloyd, B.R.; Orpen, A.G.; Vinas, J.M.; Weber, M. *J. Chem. Soc., Chem. Commun.* (1987) 1498.
- 15 Adams, R.D.; Babin, J.E.; Tanner, J. *Organometallics* **7** (1988) 765.
- 16 Kwek, K.; Taylor, N.J.; Carty, A.J. *J. Chem. Soc., Chem. Commun.* (1986) 230.
- 17 Bruce, M.I.; Skelton, B.W.; White, A.H.; Williams, M.L. *J. Chem. Soc., Chem. Commun.* (1985) 744.
- 18 Field, J.S.; Haines, R.J.; Smit, D.N. *J. Chem. Soc., Dalton Trans.* (1988) 1315.
- 19 Bruce, M.I.; Matisons, J.G.; Rodgers, J.R.; Wallis, R.C. *J. Chem. Soc., Chem. Commun.* (1981) 1070.
- 20 MacLaughlin, S.A.; Taylor, N.J.; Carty, A.J. *Organometallics* **2** (1983) 1194.
- 21 Bruce, M.I.; Williams, M.L. *J. Organomet. Chem.* **282** (1985) C11.
- 22 Natarajan, K.; Zsolnai, L.; Huttner, G. *J. Organomet. Chem.* **209** (1981) 85.
- 23 Evans, J.; Gracey, B.P.; Gray, L.R.; Webster, M. *J. Organomet. Chem.* **240** (1982) C61.
- 24 (a) Farrar, D.H.; Jackson, P.F.; Johnson, B.F.G.; Lewis, J.; Nicholls, J.N. *J. Chem. Soc., Chem. Commun.* (1981) 415; (b) Johnson, B.F.G.; Lewis, J.; Nicholls, J.N.; Oxtan, I.A.; Raithby, P.R. *J. Chem. Soc., Chem. Commun.* (1982) 289; (c) Johnson, B.F.G.; Lewis, J.; Nicholls, J.N.; Puga, J.; Raithby, P.R.; Rosales, M.J.; McPartlin, M.; Clegg, W. *J. Chem. Soc., Dalton Trans.* (1983) 277.
- 25 Cowie, A.G.; Johnson, B.F.G.; Lewis, J.; Nicholls, J.N.; Raithby, P.R.; Rosales, M.J. *J. Chem. Soc., Dalton Trans.* (1983) 2311.
- 26 Cook, S.L.; Evans, J.; Gray, L.R.; Webster, M. *J. Chem. Soc., Dalton Trans.* (1986) 2149.
- 27 Blohm, M.L.; Gladfelter, W.L. *Organometallics* **4** (1985) 45.
- 28 MacLaughlin, S.A.; Taylor, N.J.; Carty, A.J. *Inorg. Chem.* **22** (1983) 1409.
- 29 Adams, R.D.; Babin, J.E.; Tasi, M.; Wolfe, T.A. *Organometallics* **6** (1987) 2228; *Polyhedron* **7** (1988) 1071.
- 30 Adams, R.D.; Babin, J.E.; Tasi, M. *Organometallics* **7** (1988) 503.
- 31 Adams, R.D.; Babin, J.E.; Tasi, M.; Wolfe, T.A. *J. Am. Chem. Soc.* **110** (1988) 7093.
- 32 Adams, R.D.; Babin, J.E.; Tasi, M. *Inorg. Chem.* **26** (1987) 2807.
- 33 Cowie, A.G.; Johnson, B.F.G.; Lewis, J.; Nicholls, J.N.; Raithby, P.R.; Swanson, A.G. *J. Chem. Soc., Chem. Commun.* (1984) 637.
- 34 Henrick, K.; Johnson, B.F.G.; Lewis, J.; Mace, J.; McPartlin, M.; Morris, J. *J. Chem. Soc., Chem. Commun.* (1985) 1617.

- 35 Johnson, B.F.G.; Lewis, J.; Nicholls, J.N.; Puga, J.; Whitmire, K.H. *J. Chem. Soc., Dalton Trans.* (1983) 787.
- 36 Vargas, M.D.; Nicholls, J.N. *Adv. Inorg. Chem. Radiochem.* **30** (1986) 123, unpublished results cited in reference 70.
- 37 Bunkall, S.R.; Holden, H.D.; Johnson, B.F.G.; Lewis, J.; Pain, G.N.; Raithby, P.R.; Taylor, M.J. *J. Chem. Soc., Chem. Commun.* (1984) 25.
- 38 Johnson, B.F.G.; Lewis, J.; Raithby, P.R.; Whitton, A.J. *J. Chem. Soc., Chem. Commun.* (1988) 401.
- 39 Evans, J.; Street, A.C.; Webster, M. *J. Chem. Soc., Chem. Commun.* (1987) 637.
- 40 Adams, R.D.; Babin, J.E.; Tasi, M. *Inorg. Chem.* **27** (1988) 2618; *Polyhedron* **7** (1988) 2263; *Angew. Chem.* **99** (1987) 691; *Angew. Chem., Int. Ed. Engl.* **26** (1987) 685.
- 41 Rodger, A.; Johnson, B.F.G. *Polyhedron* **7** (1988) 1107.
- 42 Daran, J-C.; Kristiansson, O.; Jeannin, Y. *C. R. Acad. Sc. Paris., Section C* **300** (1985) 943.
- 43 Daran, J-C.; Cabrera, E.; Bruce, M.I.; Williams, M.L. *J. Organomet. Chem.* **319** (1987) 239.
- 44 Eady, C.R.; Johnson, B.F.G.; Lewis, J.; Matheson, T. *J. Organomet. Chem.* **57** (1973) C82.
- 45 Bruce, M.I.; Snow, M.R.; Tiekink, E.R.T.; Williams, M.L. *J. Chem. Soc., Chem. Commun.* (1986) 701.
- 46 Bruce, M.I.; Williams, M.L.; Skelton, B.W.; White, A.H. *J. Organomet. Chem.* **282** (1985) C53.
- 47 (a) Nucciarone, D.; Taylor, N.J.; Carty, A.J. *Organometallics* **5** (1986) 1179;  
(b) Nucciarone, D.; MacLaughlin, S.A.; Taylor, N.J.; Carty, A.J. *Organometallics* **7** (1988) 106; (c) Nucciarone, D.; Taylor, N.J.; Carty, A.J.; Tiripicchio, A.; Tiripicchio-Camellini, M. *Organometallics* **7** (1988) 118.
- 48 Drake, S.R.; Johnson, B.F.G.; Lewis, J. *J. Chem. Soc., Chem. Commun.* (1988) 1033.
- 49 Oxtton, I.A.; Powell, D.B.; Farrar, D.H.; Johnson, B.F.G.; Lewis, J.; Nicholls, J.N. *Inorg. Chem.* **20** (1981) 4302.
- 50 Bruce, M.I.; Horn, E.; Shawkataly, O. bin; Snow, M.R. *J. Organomet. Chem.* **280** (1985) 289.
- 51 Cowie, A.G.; Johnson, B.F.G.; Lewis, J. *J. Chem. Soc., Dalton Trans.* (1987) 2839.
- 52 Slovokhotov, Yu.L.; Struchkov, Yu.T. *J. Organomet. Chem.* **333** (1987) 217.
- 53 Daran, J-C.; Jeannin, Y.; Kristiansson, O. *Organometallics* **4** (1985) 1882.
- 54 Detter, L.D.; Hand, O.W.; Cooks, R.G.; Walton, R.A. *Mass Spectrom. Rev.* **7** (1988) 465.
- 55 Ewing, P.; Farrugia, L.J.; Rycroft, D.S. *Organometallics* **7** (1988) 859.
- 56 Carty, A.J.; Cherkas, A.A.; Randall, L.H. *Polyhedron* **7** (1988) 1045.
- 57 Astruc, D. *Angew. Chem.* **100** (1988) 662; *Angew. Chem., Int. Ed. Engl.* **27** (1988) 643.
- 58 Cyr, J.C.; DeGray, J.A.; Gosser, D.K.; Lee, E.S.; Rieger, P.H. *Organometallics* **4** (1985) 950.
- 59 Lemoine, P. *Coord. Chem. Rev.* **83** (1988) 169.
- 60 Field, J.S.; Haines, R.J.; Minshall, E.; Smit, D.N. *J. Organomet. Chem.* **310** (1986) C69.
- 61 (a) Jaeger, T.; Aime, S.; Vahrenkamp, H. *Organometallics* **5** (1986) 245;  
(b) Ohst, H.H.; Kochi, J.K. *Organometallics* **5** (1986) 1359.
- 62 Halet, J-F.; Saillard, J-Y. *New J. Chem.* **11** (1987) 315 and references therein.
- 63 Field, J.S.; Haines, R.J.; Smit, D.N.; Natarajan, K.; Scheidsteger, O.; Huttner, G. *J. Organomet. Chem.* **240** (1982) C23.
- 64 Bruce, M.I.; Swincer, A.G. *Adv. Organomet. Chem.* **22** (1983) 59.
- 65 Vierling, P.; Reiss, J.G.; Grand, A. *J. Am. Chem. Soc.* **103** (1981) 2466.
- 66 (a) Gainsford, G.J.; Guss, J.M.; Ireland, P.R.; Mason, R.; Bradford, C.W.; Nyholm, R.S. *J. Organomet. Chem.* **40** (1972) C70; (b) Bradford, C.W.; Nyholm, R.S.; Gainsford, G.J.; Guss, J.M.; Ireland, P.R.; Mason, R. *J. Chem. Soc., Chem.*

- Commun.* (1972) 87; (c) Bradford, C.W.; Nyholm, R.S. *J. Chem. Soc., Dalton Trans.* (1973) 529.
- 67 Mitchell, G.F.; Welch, A.J. *J. Chem. Soc., Dalton Trans.* (1987) 1017.
- 68 Churchill, M.R.; Hollander, F.J. *Inorg. Chem.* **18** (1979) 161.
- 69 Huttner, G.; Knoll, K. *Angew. Chem.* **99** (1987) 765; *Angew. Chem., Int. Ed. Engl.* **26** (1987) 743.
- 70 Harris, R.K. *Canad. J. Chem.* **42** (1964) 2275.
- 71 Albiez, T.; Vahrenkamp, H. *Angew. Chem.* **99** (1987) 561; *Angew. Chem., Int. Ed. Engl.* **26** (1987) 572.
- 72 Bruce, M.I.; Koutsantonis, G.A. unpublished results.
- 73 Bruce, M.I.; Hughes, C.A.; Liddell, M.J.; Skelton, B.W.; White, A.H. *J. Organomet. Chem.* **347** (1988) 157, 181.
- 74 (a) Darensbourg, D.J.; Baldwin-Zuschke, B.J. *J. Am. Chem. Soc.* **104** (1982) 3906; (b) Sonnenberger, D.C.; Atwood, J.D. *J. Am. Chem. Soc.* **104** (1982) 2113.
- 75 Shojaie, R.; Atwood, J.D. *Inorg. Chem.* **27** (1988) 2558.
- 76 Ros, R.; Scrivanti, A.; Albano, V.G.; Braga, D.; Garlaschelli, L. *J. Chem. Soc., Dalton Trans.* (1986) 2411.
- 77 Johnson, B.F.G. *Inorg. Chim. Acta* **115** (1986) L39 and references therein.
- 78 Karel, K.J.; Norton, J.R. *J. Am. Chem. Soc.* **96** (1974) 6812.
- 79 Malik, S.K.; Poe, A.J. *Inorg. Chem.* **17** (1978) 1484.
- 80 (a) Shen, J.K.; Shi, Q.Z.; Basolo, F. *Inorg. Chem.* **27** (1988) 4236; (b) Shen, J.K.; Shi, Y.L.; Gao, Y.C.; Shi, Q.Z.; Basolo, F. *J. Am. Chem. Soc.* **110** (1988) 2414.
- 81 Shojaie, R.; Atwood, J.D. *Inorg. Chem.* **26** (1987) 2199 and references therein.
- 82 Candlin, J.P.; Shortland, A.C. *J. Organomet. Chem.* **16** (1969) 289.
- 83 Poe, A.; Twigg, M.V. *J. Chem. Soc., Dalton Trans.* (1974) 1860.
- 84 Aime, S.; Bertocello, R.; Busetti, V.; Gobetto, R.; Granozzi, G.; Osella, D. *Inorg. Chem.* **25** (1986) 4004.
- 85 Gastel, F.V.; MacLaughlin, S.A.; Lynch, M.; Carty, A.J.; Sappa, E.; Tiripicchio, A.; Tiripicchio-Camellini, M. *J. Organomet. Chem.* **326** (1987) C65.
- 86 (a) Bruce, M.I.; Shaw, G.; Stone, F.G.A. *J. Chem. Soc., Dalton Trans.* (1972) 2727; (b) Blickensderfer, J.R.; Kaesz, H.D. *J. Am. Chem. Soc.* **97** (1975) 2681.
- 87 Bruce, M.I.; Horn, E.; Snow, M.R.; Williams, M.L. *J. Organomet. Chem.* **276** (1984) C53.
- 88 Bernhardt, W.; Schering, C.; Vahrenkamp, H. *Angew. Chem.* **98** (1986) 285; *Angew. Chem., Int. Ed. Engl.* **25** (1986) 279.
- 89 Mingos, D.M.P. *Pure Appl. Chem.* **52** (1980) 705.
- 90 Braunstein, P.; Rose, J. *Gold Bull.* **18** (1985) 17 and references cited therein.
- 91 Bruce, M.I.; Nicholson, B.K. *Organometallics* **3** (1984) 101 and references cited therein.
- 92 Bruce, M.I.; Nicholson, B.K. *J. Organomet. Chem.* **252** (1983) 243 and references cited therein.
- 93 Bruce, M.I.; Shawkataly, O. bin; Nicholson, B.K. *J. Organomet. Chem.* **286** (1985) 427.
- 94 Alexander, B.D.; Gomez-Sal, M.P.; Gannon, P.R.; Blaine, C.A.; Boyle, P.D.; Mueting, A.M.; Pignolet, L.H. *Inorg. Chem.* **27** (1988) 3301.
- 95 (a) Brown, S.S.D.; Salter, I.D.; Dyson, D.B.; Parish, R.V.; Bates, P.A.; Hursthouse, M.B. *J. Chem. Soc., Dalton Trans.* (1988) 1795 and references therein. (b) Freeman, M.J.; Green, M.; Orpen, A.G.; Salter, I.D.; Stone, F.G.A. *J. Chem. Soc., Chem. Commun.* (1983) 1332.
- 96 Sutherland, B.R.; Ho, D.M.; Huffman, J.C.; Caulton, K.G. *Angew. Chem.* **99** (1987) 147; *Angew. Chem., Int. Ed. Engl.* **26** (1987) 135.
- 97 Harpp, K.S.; Housecroft, C.E. *J. Organomet. Chem.* **340** (1988) 389.
- 98 Bateman, L.W.; Green, M.; Mead, K.A.; Mills, R.M.; Salter, I.D.; Stone, F.G.A.; Woodward, P. *J. Chem. Soc., Dalton Trans.* (1983) 2599.
- 99 Hall, K.P.; Mingos, D.M.P. *Prog. Inorg. Chem.* **32** (1984) 237 and references cited therein.
- 100 Freeman, M.J.; Orpen, A.G.; Salter, I.D. *J. Chem. Soc., Dalton Trans.* (1987) 397.

- 101 Owen, S.M. *Polyhedron* **7** (1988) 253.
- 102 Johnson, B.F.G.; Lewis, J.; Nelson, W.J.H.; Vargas, M.D.; Braga, D.; McPartlin, M. *J. Organomet. Chem.* **246** (1983) C69.
- 103 Kampe, C.E.; Boag, N.M.; Knobler, C.B.; Kaesz, H.D. *Inorg. Chem.* **23** (1984) 1390.
- 104 Han, S.H.; Geoffroy, G.L.; Dombek, B.D.; Rheingold, A.L. *Inorg. Chem.* **27** (1988) 4355.
- 105 (a) Hoffmann, R. *Angew. Chem.* **94** (1982) 725; *Angew. Chem., Int. Ed. Engl.* **21** (1982) 711; (b) Stone, F.G.A. *Angew. Chem.* **96** (1984) 85; *Angew. Chem., Int. Ed. Engl.* **23** (1984) 89.
- 106 Basu, A.; Bhaduri, S.; Khwaja, H.; Jones, P.G.; Schroeder, T.; Sheldrick, G.M. *J. Organomet. Chem.* **290** (1985) C19.
- 107 Bruce, M.I.; Williams, M.L. *J. Organomet. Chem.* **288** (1985) C55.
- 108 Krivykh, V.V.; Asunta, T.; Gusev, O.V.; Rybinskaya, M.I. *J. Organomet. Chem.* **338** (1988) 55.
- 109 Ciani, G.; Sironi, A.; Chini, P.; Ceriotti, A.; Martinengo, S. *J. Organomet. Chem.* **192** (1980) C39.
- 110 Sappa, E.; Tiripicchio, A.; Braunstein, P. *Chem. Rev.* **83** (1983) 203.
- 111 Adams, R.D.; Horvath, I.T. *Prog. Inorg. Chem.* **33** (1985) 127.
- 112 Raithby, P.R.; Rosales, M.J. *Adv. Inorg. Chem. Radiochem.* **29** (1986) 169.
- 113 Fajardo, M.; Holden, H.D.; Johnson, B.F.G.; Lewis, J.; Raithby, P.R. *J. Chem. Soc., Chem. Commun.* (1984) 24.
- 114 Fernandez-G, J.M.; Rosales, M.J.; Toscano, R.A. *Polyhedron* **21** (1988) 2159.
- 115 Ermer, S.; King, K.; Hardcastle, K.I.; Rosenberg, E.; Lanfredi, A.M.M.; Tiripicchio, A.; Tiripicchio-Camellini, M. *Inorg. Chem.* **22** (1983) 1339.
- 116 Yamamoto, Y.; Yamazaki, H.; Sakurai, T. *J. Am. Chem. Soc.* **104** (1982) 2329.
- 117 Iggo, J.A.; Mays, M.J. *J. Chem. Soc., Dalton Trans.* (1984) 643.
- 118 Braunstein, P.; Rose, J.; Tiripicchio, A.; Tiripicchio-Camellini, M. *J. Chem. Soc., Chem. Commun.* (1984) 39.
- 119 Randall, S.M.; Taylor, N.J.; Carty, A.J.; Haddah, T.B.; Dixneuf, P.H. *J. Chem. Soc., Chem. Commun.* (1988) 870.
- 120 (a) Deeming, A.J.; Hasso, S.; Underhill, M. *J. Chem. Soc., Dalton Trans.* (1975) 1614; (b) Johnson, B.F.G.; Khattar, R.; Lewis, J.; Raithby, P.R.; Smit, D.N. *J. Chem. Soc., Dalton Trans.* (1988) 1421.
- 121 Churchill, M.R.; Lashewycz, R.A. *Inorg. Chem.* **17** (1978) 1291.
- 122 Dickson, R.S.; Fallon, G.D.; McLure, F.I.; Nesbit, R.J. *Organometallics* **6** (1987) 215.
- 123 Albers, M.O.; Robinson, D.J.; Singleton, E. *Coord. Chem. Rev.* **79** (1987) 1.
- 124 Foley, H.C.; Finch, W.C.; Pierpoint, C.G.; Geoffroy, G.L. *Organometallics* **1** (1982) 1379.
- 125 Ros, R.; Scrivanti, A.; Roulet, R. *J. Organomet. Chem.* **303** (1986) 273.
- 126 Tachikawa, M.; Shapley, J.R. *J. Organomet. Chem.* **124** (1977) C19.
- 127 Chen, Y.J.; Knobler, C.B.; Kaesz, H.D. *Polyhedron* **7** (1988) 1891.
- 128 Jackson, P.F.; Johnson, B.F.G.; Lewis, J.; McPartlin, M.; Nelson, W.J.H. *J. Chem. Soc., Chem. Commun.* (1980) 1190.
- 129 Maire, G.; Garin, F. *J. Mol. Catal.* **48** (1988) 99.
- 130 Hills, M.M.; Parmeter, J.E.; Weinberg, W.H. *J. Am. Chem. Soc.* **109** (1987) 597, 4224; *J. Am. Chem. Soc.* **110** (1988) 7952.
- 131 Henderson, M.A.; Mitchell, G.E.; White, J.M. *Surface Sci.* **203** (1988) 378.
- 132 Braunstein, P.; Rose, J. *Stereochem. Organomet. Inorg. Comp.* **3** (1989) 000.
- 133 Bergounhou, C.; Fompeyrine, P.; Commenges, G.; Bonnet, J.J. *J. Mol. Catal.* **48** (1988) 285.
- 134 Dickson, R.S.; Fallon, G.D.; Jenkins, S.M.; Skelton, B.W.; White, A.H. *J. Organomet. Chem.* **314** (1986) 333.
- 135 Green, M.; Jetha, N.K.; Mercer, R.J.; Norman, N.C.; Orpen, A.G. *J. Chem. Soc., Dalton Trans.* (1988) 1843.
- 136 (a) Churchill, M.R.; Ziller, J.W.; Shapley, J.R.; Yeh, W.Y. *J. Organomet. Chem.* **353** (1988) 103; (b) Lentz, D.; Michael, H. *Chem. Ber.* **121** (1988) 1413; (c) Hart, S.J.; Stone, F.G.A. *J. Chem. Soc., Dalton Trans.* (1988) 1899.

- 137 Dutton, T.; Johnson, B.F.G.; Lewis, J.; Owen, S.M.; Raithby, P.R. *J. Chem. Soc., Chem. Commun.* (1988) 1423.
- 138 (a) Ros, J.; Commenges, G.; Mathieu, R.; Solans, X.; Font-Altaba, M. *J. Chem. Soc., Dalton Trans.* (1985) 1087; (b) Garcia, M.E.; Jeffrey, J.C.; Sherwood, P.; Stone, F.G.A. *J. Chem. Soc., Dalton Trans.* (1988) 2431.
- 139 Navarre, D.; Parlier, A.; Rudler, H.; Daran, J-C. *J. Organomet. Chem.* **103** (1987) 103.
- 140 Fong, R.H.; Hersh, W.H. *Organometallics* **7** (1988) 794.
- 141 Howard, J.A.K.; Knox, S.A.R.; Terrill, N.J.; Yates, M.I. Royal Society of Chemistry, Dalton Division, 3rd International Conference on the Chemistry of Platinum Metals; University of Sheffield (1987), abstract E6.
- 142 Carty, A.J.; MacLaughlin, S.A.; Nucciarone, D. in Phosphorus-31 NMR Spectroscopy in Stereochemical Analysis: Organic Compounds and Metal Complexes; Verkade, J.G., Quin, L.D., Eds.; VCH Publishers: New York, 1986; Chapter 16.
- 143 Steinhardt, P.C.; Gladfelter, W.L.; Harley, A.D.; Fox, J.R.; Geoffroy, G.L. *Inorg. Chem.* **19** (1980) 332.
- 144 Faltynek, R.A.; Wrighton, M.S. *J. Am. Chem. Soc.* **100** (1978) 2701.
- 145 Kowala, C.; Swan, J.M. *Aust. J. Chem.* **19** (1966) 547.
- 146 Nesmeyanov, A.N.; Perevalova, E.G.; Struchkov, Yu.T.; Antipin, M.Yu.; Grandberg, I.K.; Dyadchenko, V.P. *J. Organomet. Chem.* **201** (1980) 343.
- 147 Bruce, M.I.; Matisons, J.G.; Patrick, J.M.; Skelton, B.W.; Wallis, R.C.; White, A.H. *J. Chem. Soc., Dalton Trans.* (1983) 2365.
- 148 Bruce, M.I.; Matisons, J.G.; Nicholson, B.K. *J. Organomet. Chem.* **243** (1983) 321.
- 149 Bruce, M.I.; Cifuentes, M.P.; Snow, M.R.; Tiekink, E.R.T. *J. Organomet. Chem.* **359** (1989) 379.
- 150 PREABS and PROCES, Data reduction programs for CAD4 diffractometer, University of Melbourne, 1981.
- 151 SHELX-76, Program for crystal structure determination, Sheldrick, G.M., University of Cambridge, 1976.
- 152 LSPLAN, Program for calculation of least-squares planes in molecular structures, Pippy, M.E.; Ahmed, F.R., National Research Council, Ottawa, 1967.
- 153 PLUTO, Plotting program for molecular structures, W.D.S. Motherwell, University of Cambridge, 1978.
- 154 Ibers, J.A.; Hamilton, W.C. (Eds.), *International Tables for X-ray Crystallography*, Kynoch Press, Birmingham, 1974, Vol IV, p. 99, 149.
- 155 Coffey, C.E.; Lewis, J.; Nyholm, R.S. *J. Chem. Soc.* (1964) 1741.

## APPENDIX 1. Supplementary data for

 $\text{Ru}_5(\mu_4\text{-PPh})\{\mu_4\text{-}\eta^4\text{-CCPh}(\text{C}_6\text{H}_4)\}\{\mu\text{-PPh}(\text{OMe})\}(\text{CO})_{11}$  (28)

(crystallographic numbering differs slightly from that discussed in the text: Ru(2) and Ru(4) are interchanged)

Table 14. Bond distances (Å)

Ru (2)	----	Ru (1)	2.811 (2)	Ru (3)	----	Ru (1)	2.820 (2)
Ru (4)	----	Ru (1)	2.929 (2)	P (1)	----	Ru (1)	2.394 (4)
P (2)	----	Ru (1)	2.225 (5)	C (1)	----	Ru (1)	1.899 (19)
C (2)	----	Ru (1)	1.921 (21)	Ru (3)	----	Ru (2)	2.902 (2)
Ru (4)	----	Ru (2)	3.596 (2)	Ru (5)	----	Ru (2)	2.941 (2)
P (1)	----	Ru (2)	2.484 (4)	P (2)	----	Ru (2)	2.256 (5)
C (3)	----	Ru (2)	1.911 (17)	C (4)	----	Ru (2)	1.879 (18)
C (13)	----	Ru (2)	2.412 (15)	Ru (4)	----	Ru (3)	2.752 (2)
C (5)	----	Ru (3)	1.882 (18)	C (6)	----	Ru (3)	1.875 (19)
C (13)	----	Ru (3)	2.194 (14)	C (14)	----	Ru (3)	2.212 (14)
C (15)	----	Ru (3)	2.301 (16)	C (16)	----	Ru (3)	2.292 (16)
Ru (5)	----	Ru (4)	2.842 (2)	P (1)	----	Ru (4)	2.370 (4)
C (7)	----	Ru (4)	1.901 (20)	C (8)	----	Ru (4)	1.868 (19)
C (13)	----	Ru (4)	2.182 (15)	C (16)	----	Ru (4)	2.068 (14)
P (1)	----	Ru (5)	2.357 (4)	C (9)	----	Ru (5)	2.012 (21)
C (10)	----	Ru (5)	1.852 (20)	C (11)	----	Ru (5)	1.925 (18)
C (13)	----	Ru (5)	2.046 (14)	C (27)	----	P (1)	1.813 (12)
O (12)	----	P (2)	1.645 (12)	C (33)	----	P (2)	1.822 (12)
O (1)	----	C (1)	1.133 (20)	O (2)	----	C (2)	1.118 (21)
O (3)	----	C (3)	1.131 (17)	O (4)	----	C (4)	1.132 (18)
O (5)	----	C (5)	1.156 (18)	O (6)	----	C (6)	1.145 (19)
O (7)	----	C (7)	1.132 (20)	O (8)	----	C (8)	1.139 (20)
O (9)	----	C (9)	1.089 (20)	O (10)	----	C (10)	1.157 (20)
O (11)	----	C (11)	1.129 (19)	O (12)	----	C (12)	1.383 (22)
C (14)	----	C (13)	1.408 (20)	C (15)	----	C (14)	1.507 (21)
C (21)	----	C (14)	1.487 (17)	C (16)	----	C (15)	1.451 (20)
C (20)	----	C (15)	1.398 (21)	C (17)	----	C (16)	1.434 (22)
C (18)	----	C (17)	1.340 (22)	C (19)	----	C (18)	1.408 (24)
O (15)	----	C (40)	1.412 (-)	O (14)	----	C (39)	1.411 (-)

Table 15. Valence angles (°)

Ru (3) - Ru (1) - Ru (2)	62.1 (1)	Ru (4) - Ru (1) - Ru (2)	77.6 (1)
Ru (4) - Ru (1) - Ru (3)	57.2 (1)	P (1) - Ru (1) - Ru (2)	56.3 (1)
P (1) - Ru (1) - Ru (3)	90.4 (1)	P (1) - Ru (1) - Ru (4)	51.7 (1)
P (2) - Ru (1) - Ru (2)	51.6 (1)	P (2) - Ru (1) - Ru (3)	81.8 (1)
P (2) - Ru (1) - Ru (4)	126.4 (1)	P (2) - Ru (1) - P (1)	101.5 (2)
C (1) - Ru (1) - Ru (2)	151.4 (6)	C (1) - Ru (1) - Ru (3)	97.2 (6)
C (1) - Ru (1) - Ru (4)	108.8 (6)	C (1) - Ru (1) - P (1)	149.0 (6)
C (1) - Ru (1) - P (2)	109.2 (6)	C (2) - Ru (1) - Ru (2)	114.5 (6)
C (2) - Ru (1) - Ru (3)	176.0 (6)	C (2) - Ru (1) - Ru (4)	124.9 (5)
C (2) - Ru (1) - P (1)	89.0 (5)	C (2) - Ru (1) - P (2)	94.5 (6)
C (2) - Ru (1) - C (1)	85.3 (8)	Ru (3) - Ru (2) - Ru (1)	59.1 (1)
Ru (4) - Ru (2) - Ru (1)	52.7 (1)	Ru (4) - Ru (2) - Ru (3)	48.7 (1)
Ru (5) - Ru (2) - Ru (1)	97.2 (1)	Ru (5) - Ru (2) - Ru (3)	88.9 (1)
Ru (5) - Ru (2) - Ru (4)	50.3 (1)	P (1) - Ru (2) - Ru (1)	53.3 (1)
P (1) - Ru (2) - Ru (3)	86.7 (1)	P (1) - Ru (2) - Ru (4)	41.0 (1)
P (1) - Ru (2) - Ru (5)	50.6 (1)	P (2) - Ru (2) - Ru (1)	50.7 (1)
P (2) - Ru (2) - Ru (3)	79.5 (1)	P (2) - Ru (2) - Ru (4)	101.5 (1)
P (2) - Ru (2) - Ru (5)	147.3 (1)	P (2) - Ru (2) - P (1)	97.9 (2)
C (3) - Ru (2) - Ru (1)	137.7 (5)	C (3) - Ru (2) - Ru (3)	91.2 (5)
C (3) - Ru (2) - Ru (4)	129.6 (5)	C (3) - Ru (2) - Ru (5)	112.6 (5)
C (3) - Ru (2) - P (1)	163.1 (5)	C (3) - Ru (2) - P (2)	98.1 (5)
C (4) - Ru (2) - Ru (1)	116.1 (5)	C (4) - Ru (2) - Ru (3)	171.5 (5)
C (4) - Ru (2) - Ru (4)	135.5 (5)	C (4) - Ru (2) - Ru (5)	99.0 (5)
C (4) - Ru (2) - P (1)	95.6 (5)	C (4) - Ru (2) - P (2)	92.1 (5)
C (4) - Ru (2) - C (3)	89.0 (7)	C (13) - Ru (2) - Ru (1)	85.5 (4)
C (13) - Ru (2) - Ru (3)	47.7 (3)	C (13) - Ru (2) - Ru (4)	36.3 (4)
C (13) - Ru (2) - Ru (5)	43.6 (3)	C (13) - Ru (2) - P (1)	70.5 (3)
C (13) - Ru (2) - P (2)	125.4 (4)	C (13) - Ru (2) - C (3)	95.9 (6)
C (13) - Ru (2) - C (4)	140.8 (6)	Ru (2) - Ru (3) - Ru (1)	58.8 (1)
Ru (4) - Ru (3) - Ru (1)	63.4 (1)	Ru (4) - Ru (3) - Ru (2)	78.9 (1)
C (5) - Ru (3) - Ru (1)	118.1 (6)	C (5) - Ru (3) - Ru (2)	90.4 (5)
C (5) - Ru (3) - Ru (4)	166.3 (5)	C (6) - Ru (3) - Ru (1)	81.9 (5)
C (6) - Ru (3) - Ru (2)	132.4 (6)	C (6) - Ru (3) - Ru (4)	108.2 (5)
C (6) - Ru (3) - C (5)	85.4 (7)	C (13) - Ru (3) - Ru (1)	89.5 (4)
C (13) - Ru (3) - Ru (2)	54.4 (4)	C (13) - Ru (3) - Ru (4)	50.8 (4)
C (13) - Ru (3) - C (5)	115.8 (6)	C (13) - Ru (3) - C (6)	158.7 (6)

Table 15. (continued)

C (13) - Ru (5) - Ru (2)	54.3 (4)	C (13) - Ru (5) - Ru (4)	49.8 (4)
C (13) - Ru (5) - P (1)	79.5 (4)	C (13) - Ru (5) - C (9)	87.6 (6)
C (13) - Ru (5) - C (10)	116.0 (6)	C (13) - Ru (5) - C (11)	153.1 (8)
Ru (2) - P (1) - Ru (1)	70.4 (1)	Ru (4) - P (1) - Ru (1)	75.9 (1)
Ru (4) - P (1) - Ru (2)	95.6 (1)	Ru (5) - P (1) - Ru (1)	130.7 (2)
Ru (5) - P (1) - Ru (2)	74.8 (1)	Ru (5) - P (1) - Ru (4)	73.9 (1)
C (27) - P (1) - Ru (1)	114.6 (4)	C (27) - P (1) - Ru (2)	129.3 (4)
C (27) - P (1) - Ru (4)	135.1 (4)	C (27) - P (1) - Ru (5)	114.4 (4)
Ru (2) - P (2) - Ru (1)	77.7 (1)	O (12) - P (2) - Ru (1)	116.3 (5)
O (12) - P (2) - Ru (2)	110.5 (5)	C (33) - P (2) - Ru (1)	126.9 (4)
C (33) - P (2) - Ru (2)	124.1 (4)	C (33) - P (2) - O (12)	100.9 (6)
O (1) - C (1) - Ru (1)	175.7 (20)	O (2) - C (2) - Ru (1)	175.6 (18)
O (3) - C (3) - Ru (2)	175.5 (15)	O (4) - C (4) - Ru (2)	179.6 (9)
O (5) - C (5) - Ru (3)	178.6 (16)	O (6) - C (6) - Ru (3)	171.5 (16)
O (7) - C (7) - Ru (4)	178.0 (18)	O (8) - C (8) - Ru (4)	177.1 (17)
O (9) - C (9) - Ru (5)	176.0 (19)	O (10) - C (10) - Ru (5)	178.0 (16)
O (11) - C (11) - Ru (5)	174.9 (20)	C (12) - O (12) - P (2)	118.8 (12)
Ru (3) - C (13) - Ru (2)	78.0 (5)	Ru (4) - C (13) - Ru (2)	102.9 (6)
Ru (4) - C (13) - Ru (3)	77.9 (5)	Ru (5) - C (13) - Ru (2)	82.1 (5)
Ru (5) - C (13) - Ru (3)	149.5 (8)	Ru (5) - C (13) - Ru (4)	84.4 (5)
C (14) - C (13) - Ru (2)	121.0 (10)	C (14) - C (13) - Ru (3)	72.1 (8)
C (14) - C (13) - Ru (4)	118.2 (11)	C (14) - C (13) - Ru (5)	138.4 (11)
C (13) - C (14) - Ru (3)	70.6 (9)	C (15) - C (14) - Ru (3)	73.7 (8)
C (15) - C (14) - C (13)	112.2 (13)	C (21) - C (14) - Ru (3)	124.9 (8)
C (21) - C (14) - C (13)	126.7 (13)	C (21) - C (14) - C (15)	121.0 (12)
C (14) - C (15) - Ru (3)	67.3 (8)	C (16) - C (15) - Ru (3)	71.3 (9)
C (16) - C (15) - C (14)	113.3 (13)	C (20) - C (15) - Ru (3)	131.8 (11)
C (20) - C (15) - C (14)	125.2 (14)	C (20) - C (15) - C (16)	121.4 (15)
Ru (4) - C (16) - Ru (3)	78.1 (5)	C (15) - C (16) - Ru (3)	71.9 (9)
C (15) - C (16) - Ru (4)	119.5 (11)	C (17) - C (16) - Ru (3)	126.3 (11)
C (17) - C (16) - Ru (4)	125.9 (12)	C (17) - C (16) - C (15)	114.3 (14)
C (18) - C (17) - C (16)	124.9 (16)	C (19) - C (18) - C (17)	118.7 (17)
C (20) - C (19) - C (18)	121.1 (15)	C (19) - C (20) - C (15)	119.2 (15)
C (21) - C (26) - C (25)	120.0 (1)	C (22) - C (21) - C (14)	121.1 (6)
C (26) - C (21) - C (14)	118.8 (6)	C (26) - C (21) - C (22)	120.0 (1)
C (27) - C (32) - C (31)	120.0 (1)	C (28) - C (27) - P (1)	120.2 (3)
C (32) - C (27) - P (1)	119.8 (3)	C (32) - C (27) - C (28)	120.0 (1)
C (33) - C (38) - C (37)	120.0 (1)	C (34) - C (33) - P (2)	122.0 (3)
C (38) - C (33) - P (2)	118.0 (3)	C (38) - C (33) - C (34)	120.0 (1)

Table 15. (continued)

C (14) - Ru (3) - Ru (1)	126.7 (4)	C (14) - Ru (3) - Ru (2)	81.0 (4)
C (14) - Ru (3) - Ru (4)	76.6 (3)	C (14) - Ru (3) - C (5)	93.4 (6)
C (14) - Ru (3) - C (6)	146.5 (7)	C (14) - Ru (3) - C (13)	37.3 (5)
C (15) - Ru (3) - Ru (1)	137.1 (4)	C (15) - Ru (3) - Ru (2)	117.8 (4)
C (15) - Ru (3) - Ru (4)	73.8 (4)	C (15) - Ru (3) - C (5)	104.3 (7)
C (15) - Ru (3) - C (6)	109.1 (7)	C (15) - Ru (3) - C (13)	65.1 (5)
C (15) - Ru (3) - C (14)	38.9 (5)	C (16) - Ru (3) - Ru (1)	104.0 (4)
C (16) - Ru (3) - Ru (2)	121.1 (3)	C (16) - Ru (3) - Ru (4)	47.3 (4)
C (16) - Ru (3) - C (5)	136.9 (7)	C (16) - Ru (3) - C (6)	91.9 (7)
C (16) - Ru (3) - C (13)	71.3 (5)	C (16) - Ru (3) - C (14)	66.5 (5)
C (16) - Ru (3) - C (15)	36.8 (5)	Ru (2) - Ru (4) - Ru (1)	49.8 (1)
Ru (3) - Ru (4) - Ru (1)	59.4 (1)	Ru (3) - Ru (4) - Ru (2)	52.4 (1)
Ru (5) - Ru (4) - Ru (1)	96.8 (1)	Ru (5) - Ru (4) - Ru (2)	52.8 (1)
Ru (5) - Ru (4) - Ru (3)	94.0 (1)	P (1) - Ru (4) - Ru (1)	52.4 (1)
P (1) - Ru (4) - Ru (2)	43.4 (1)	P (1) - Ru (4) - Ru (3)	92.5 (1)
P (1) - Ru (4) - Ru (5)	52.8 (1)	C (7) - Ru (4) - Ru (1)	78.6 (5)
C (7) - Ru (4) - Ru (2)	128.2 (5)	C (7) - Ru (4) - Ru (3)	108.3 (6)
C (7) - Ru (4) - Ru (5)	150.0 (6)	C (7) - Ru (4) - P (1)	105.0 (6)
C (8) - Ru (4) - Ru (1)	155.9 (5)	C (8) - Ru (4) - Ru (2)	135.3 (5)
C (8) - Ru (4) - Ru (3)	144.7 (5)	C (8) - Ru (4) - Ru (5)	82.6 (5)
C (8) - Ru (4) - P (1)	112.1 (6)	C (8) - Ru (4) - C (7)	89.9 (8)
C (13) - Ru (4) - Ru (1)	86.9 (4)	C (13) - Ru (4) - Ru (2)	40.8 (4)
C (13) - Ru (4) - Ru (3)	51.2 (4)	C (13) - Ru (4) - Ru (5)	45.8 (4)
C (13) - Ru (4) - P (1)	76.6 (4)	C (13) - Ru (4) - C (7)	159.4 (7)
C (13) - Ru (4) - C (8)	108.7 (7)	C (16) - Ru (4) - Ru (1)	106.7 (4)
C (16) - Ru (4) - Ru (2)	103.0 (4)	C (16) - Ru (4) - Ru (3)	54.6 (4)
C (16) - Ru (4) - Ru (5)	115.3 (4)	C (16) - Ru (4) - P (1)	146.2 (4)
C (16) - Ru (4) - C (7)	94.2 (7)	C (16) - Ru (4) - C (8)	95.2 (7)
C (16) - Ru (4) - C (13)	75.9 (6)	Ru (4) - Ru (5) - Ru (2)	76.9 (1)
P (1) - Ru (5) - Ru (2)	54.6 (1)	P (1) - Ru (5) - Ru (4)	53.3 (1)
C (9) - Ru (5) - Ru (2)	132.5 (5)	C (9) - Ru (5) - Ru (4)	101.1 (5)
C (9) - Ru (5) - P (1)	153.6 (5)	C (10) - Ru (5) - Ru (2)	80.5 (5)
C (10) - Ru (5) - Ru (4)	157.3 (5)	C (10) - Ru (5) - P (1)	111.1 (6)
C (10) - Ru (5) - C (9)	95.2 (7)	C (11) - Ru (5) - Ru (2)	134.0 (6)
C (11) - Ru (5) - Ru (4)	103.9 (6)	C (11) - Ru (5) - P (1)	88.4 (5)
C (11) - Ru (5) - C (9)	93.1 (7)	C (11) - Ru (5) - C (10)	90.8 (8)

Table 16. Fractional atomic coordinates ( $\times 10^5$  for Ru;  $\times 10^4$  for remaining non-hydrogen atoms) and thermal parameters ( $\times 10^4$  for Ru;  $\times 10^3$  for remaining non-hydrogen atoms)

Atom	x	y	z	U(11)	U(22)	U(33)	U(23)	U(13)	U(12)
Ru(1)	2579(1)	913(1)	3435(1)	35(1)	35(1)	41(1)	-6(1)	8(1)	-2(1)
Ru(2)	2651(1)	-1706(1)	3363(1)	29(1)	35(1)	34(1)	4(1)	12(1)	2(1)
Ru(3)	2662(1)	-165(1)	2255(1)	31(1)	29(1)	35(1)	3(1)	13(1)	1(1)
Ru(4)	1417(1)	301(1)	2524(1)	31(1)	33(1)	34(1)	-3(1)	9(1)	4(1)
Ru(5)	1241(1)	-2167(1)	2958(1)	33(1)	37(1)	32(1)	-3(1)	13(1)	-6(1)
P(1)	1688(2)	-454(4)	3566(2)	34(2)	40(3)	34(2)	-3(2)	13(2)	-2(2)
P(2)	3444(2)	-317(4)	3725(2)	32(2)	49(3)	39(2)	1(2)	12(2)	-3(2)
C(1)	2877(9)	2536(17)	3256(9)	60(12)	38(12)	73(13)	-3(10)	-6(10)	-1(9)
O(1)	3047(9)	3526(14)	3185(9)	183(18)	41(10)	155(17)	-3(10)	14(14)	-51(11)
C(2)	2557(8)	1551(16)	4266(10)	48(11)	48(12)	80(15)	-19(11)	26(11)	-2(9)
O(2)	2582(7)	1886(14)	4760(6)	97(11)	108(12)	59(9)	-56(9)	34(8)	-26(9)
C(3)	3197(8)	-2928(15)	3048(8)	51(10)	34(10)	44(10)	6(8)	9(8)	5(8)
O(3)	3534(6)	-3671(12)	2902(6)	76(9)	57(8)	76(9)	-8(7)	26(8)	28(7)
C(4)	2755(8)	-2566(16)	4132(8)	40(9)	68(12)	30(9)	9(9)	3(8)	-1(9)
O(4)	2821(6)	-3086(12)	4595(6)	88(10)	92(10)	43(8)	30(8)	28(7)	11(8)
C(5)	3468(9)	-876(15)	2127(8)	57(12)	35(10)	58(12)	7(9)	19(10)	5(9)
O(5)	3957(5)	-1337(12)	2046(6)	31(6)	81(9)	86(10)	-10(7)	24(7)	22(6)
C(6)	3060(8)	1372(18)	2128(8)	39(10)	61(13)	57(12)	-2(10)	18(9)	-9(9)
O(6)	3325(6)	2243(12)	1985(7)	78(9)	55(8)	127(13)	10(8)	42(9)	-32(8)
C(7)	1319(9)	2057(19)	2608(8)	62(12)	61(14)	44(11)	-14(10)	-7(9)	25(10)
O(7)	1242(7)	3097(14)	2662(8)	93(11)	65(10)	113(13)	-21(9)	-20(10)	29(9)
C(8)	519(9)	162(16)	2227(9)	42(11)	51(11)	68(12)	-8(10)	12(10)	3(9)
O(8)	-23(7)	45(12)	2026(7)	46(8)	76(10)	109(12)	8(8)	-20(8)	2(7)
C(9)	741(9)	-2959(16)	2183(9)	51(11)	50(11)	56(12)	10(10)	28(10)	-16(9)
O(9)	447(7)	-3333(16)	1761(6)	87(11)	139(14)	45(8)	-26(9)	-16(8)	-26(10)
C(10)	1471(9)	-3664(17)	3364(8)	58(11)	47(11)	39(10)	-3(9)	20(9)	-21(9)
O(10)	1603(7)	-4618(14)	3603(6)	93(11)	76(10)	67(9)	24(9)	5(8)	-10(8)
C(11)	472(9)	-2043(17)	3366(9)	54(11)	67(13)	70(13)	-23(11)	26(11)	-15(10)
O(11)	10(6)	-1891(14)	3581(7)	55(8)	121(13)	125(13)	-54(10)	61(9)	-31(8)
C(12)	4095(9)	370(23)	4806(9)	43(11)	156(22)	56(12)	18(15)	-10(10)	-16(14)
O(12)	3671(5)	-496(11)	4486(5)	40(6)	84(9)	37(6)	-8(6)	8(5)	-16(6)
C(13)	1887(7)	-1494(14)	2403(7)	32(8)	38(10)	35(9)	2(7)	12(8)	0(7)
C(14)	2079(6)	-1759(14)	1816(7)	14(7)	37(9)	43(9)	-7(8)	9(7)	-8(6)
C(15)	1947(7)	-681(15)	1365(7)	24(8)	49(11)	49(10)	1(9)	9(7)	2(7)
C(16)	1700(7)	423(14)	1644(7)	37(9)	36(10)	44(9)	11(9)	15(7)	-8(8)
C(17)	1610(8)	1486(15)	1234(9)	44(10)	36(10)	64(13)	0(9)	1(9)	5(8)

Table 16. (continued)

Atom	x	y	z	U(11)	U(22)	U(33)	U(23)	U(13)	U(12)
C(18)	1714(8)	1491(18)	635(8)	59(12)	69(14)	42(11)	18(9)	16(9)	17(10)
C(19)	1899(9)	367(18)	368(8)	68(13)	77(13)	47(11)	14(11)	22(10)	20(11)
C(20)	2024(7)	-712(14)	731(7)	38(10)	49(10)	29(9)	5(8)	5(7)	15(8)
C(21)	2361(5)	-2952(8)	1623(5)	34(4)					
C(22)	2808(5)	-2964(8)	1195(5)	44(4)					
C(23)	3034(5)	-4099(8)	990(5)	59(5)					
C(24)	2814(5)	-5222(8)	1215(5)	68(5)					
C(25)	2368(5)	-5210(8)	1643(5)	56(5)					
C(26)	2142(5)	-4075(8)	1847(5)	42(4)					
C(27)	1356(5)	-237(9)	4293(6)	47(4)					
C(28)	1440(5)	-1162(9)	4754(6)	60(5)					
C(29)	1168(5)	-1007(9)	5305(6)	82(6)					
C(30)	813(5)	73(9)	5395(6)	74(6)					
C(31)	729(5)	997(9)	4933(6)	66(5)					
C(32)	1001(5)	843(9)	4382(6)	56(5)					
C(33)	4242(5)	-232(9)	3455(6)	48(4)					
C(34)	4452(5)	843(9)	3176(6)	57(5)					
C(35)	5065(5)	862(9)	2973(6)	76(6)					
C(36)	5468(5)	-193(9)	3049(6)	73(6)					
C(37)	5258(5)	-1267(9)	3327(6)	72(6)					
C(38)	4645(5)	-1287(9)	3530(6)	60(5)					
O(13)	5423(16)	11764(33)	9489(16)	267(15)					
O(14)	16(11)	5752(22)	5482(11)	176(9)					
C(39)	199(18)	5843(34)	4877(12)	176(14)					
O(15)	6050(24)	9333(41)	9434(22)	393(24)					
C(40)	5456(28)	9688(59)	9057(28)	333(36)					

Where the anisotropic thermal parameter is given by the following expression:

$$T_{aniso} = \exp[-2\pi^2(h^2a^*U_{11} + k^2b^*U_{22} + l^2c^*U_{33} + 2hka^*b^*U_{12} + 2hla^*c^*U_{13} + 2klb^*c^*U_{23})]$$

Table 17. Positional ( $\times 10^4$ ) and thermal parameters ( $\times 10^3$ ) for hydrogen atoms

Atom	x	y	z	U(11)
H(12A)	4185(9)	147(23)	5247(9)	88(38)
H(12B)	3893(9)	1192(23)	4763(9)	88(38)
H(12C)	4503(9)	382(23)	4632(9)	88(38)
H(17)	1462(8)	2258(15)	1404(9)	59(24)
H(18)	1664(8)	2253(18)	389(8)	59(24)
H(19)	1940(9)	344(18)	-74(8)	59(24)
H(20)	2163(7)	-1474(14)	545(7)	59(24)
H(22)	2960(5)	-2183(8)	1039(5)	94(15)
H(23)	3344(5)	-4107(8)	692(5)	94(15)
H(24)	2972(5)	-6011(8)	1073(5)	94(15)
H(25)	2215(5)	-5991(8)	1799(5)	94(15)
H(26)	1831(5)	-4066(8)	2145(5)	94(15)
H(28)	1687(5)	-1912(9)	4692(6)	94(15)
H(29)	1227(5)	-1650(9)	5626(6)	94(15)
H(30)	624(5)	180(9)	5778(6)	94(15)
H(31)	482(5)	1748(9)	4995(6)	94(15)
H(32)	943(5)	1486(9)	4061(6)	94(15)
H(34)	4172(5)	1576(9)	3124(6)	94(15)
H(35)	5211(5)	1610(9)	2780(6)	94(15)
H(36)	5895(5)	-179(9)	2908(6)	94(15)
H(37)	5538(5)	-2001(9)	3380(6)	94(15)
H(38)	4499(5)	-2034(9)	3724(6)	94(15)

Table 18. Observed and calculated structure factors

OBSERVED AND CALCULATED STRUCTURE FACTORS FOR RU5(CO)11(C2PH(C6H4)) (PPH) (PPH(OME))												PAGE 1												
H	K	L	10FO	10FC	H	K	L	10FO	10FC	H	K	L	10FO	10FC	H	K	L	10FO	10FC					
2	0	0	5725	-6604	5	2	0	1783	1740	5	5	0	808	-765	10	9	0	797	-789	-21	2	1	595	-612
3	0	0	1593	-1572	6	2	0	701	607	8	5	0	611	-650	11	9	0	667	-658	-20	2	1	566	-531
4	0	0	1497	1310	7	2	0	523	516	9	5	0	609	-563	12	9	0	991	1004	-18	2	1	651	690
5	0	0	2817	-2862	9	2	0	1412	-1323	12	5	0	425	413	13	9	0	727	745	-16	2	1	477	-387
6	0	0	1049	-1118	10	2	0	1627	-1600	16	5	0	964	-917	4	10	0	590	592	-15	2	1	711	752
7	0	0	5263	5254	11	2	0	867	818	19	5	0	647	631	6	10	0	903	-948	-13	2	1	1243	-1223
8	0	0	4421	4454	12	2	0	1504	1503	0	6	0	1495	1480	8	10	0	640	686	-12	2	1	650	-620
9	0	0	1760	-1861	14	2	0	598	644	2	6	0	833	-822	-19	1	1	555	-519	-11	2	1	1029	979
10	0	0	3325	-3310	16	2	0	699	-668	3	6	0	419	298	-18	1	1	837	-883	-10	2	1	918	988
11	0	0	1341	1344	17	2	0	957	-995	4	6	0	700	686	-16	1	1	1715	1702	-8	2	1	404	509
12	0	0	596	605	20	2	0	710	728	7	6	0	1050	1069	-14	1	1	1714	-1740	-7	2	1	816	840
13	0	0	2408	-2359	1	3	0	1560	-1436	8	6	0	501	453	-13	1	1	515	616	-6	2	1	566	-543
15	0	0	3170	3203	2	3	0	1505	-1612	9	6	0	985	-987	-12	1	1	613	599	-5	2	1	1320	-1315
16	0	0	679	812	5	3	0	1610	-1557	10	6	0	501	-600	-11	1	1	2115	-2058	-3	2	1	784	736
17	0	0	1331	-1319	6	3	0	2133	2103	11	6	0	468	-446	-9	1	1	2680	2832	-2	2	1	471	516
19	0	0	817	852	7	3	0	1994	1971	13	6	0	745	764	-8	1	1	1531	1513	1	2	1	614	-501
21	0	0	1082	-1053	8	3	0	810	-885	15	6	0	593	-619	-7	1	1	2050	-1993	2	2	1	245	-202
1	1	0	2492	2536	9	3	0	1326	-1344	17	6	0	1477	1469	-5	1	1	2025	1963	3	2	1	449	-306
2	1	0	1103	1008	14	3	0	570	607	1	7	0	1286	-1272	-3	1	1	1717	-1707	4	2	1	340	231
3	1	0	353	406	15	3	0	767	764	2	7	0	1477	1469	-2	1	1	2603	2056	5	2	1	1653	1622
4	1	0	563	454	16	3	0	604	-614	3	7	0	2116	-2148	-1	1	1	5845	6164	7	2	1	422	-412
6	1	0	470	-523	17	3	0	870	-854	4	7	0	995	1021	1	1	1	5382	-5342	10	2	1	805	817
7	1	0	650	-705	0	4	0	1610	1602	5	7	0	2175	2193	3	1	1	1182	1025	11	2	1	485	614
8	1	0	368	314	1	4	0	1470	1411	7	7	0	970	-1031	4	1	1	686	640	12	2	1	521	-528
9	1	0	785	797	2	4	0	367	-149	10	7	0	1570	-1543	5	1	1	1538	1257	13	2	1	547	-579
11	1	0	1052	1037	3	4	0	699	-678	11	7	0	864	-855	6	1	1	3677	3601	17	2	1	511	524
12	1	0	878	847	4	4	0	1542	-1602	12	7	0	1745	1750	7	1	1	1862	1803	18	2	1	565	421
13	1	0	851	-830	5	4	0	869	-822	13	7	0	1078	1098	8	1	1	3536	-3458	-16	3	1	597	721
14	1	0	1379	-1399	6	4	0	631	578	14	7	0	862	-831	9	1	1	2464	-2450	-15	3	1	1733	1697
16	1	0	516	295	7	4	0	1592	1637	15	7	0	484	-508	10	1	1	2052	2093	-13	3	1	1087	-1088
19	1	0	728	720	8	4	0	863	774	16	7	0	391	363	11	1	1	1544	1564	-12	3	1	456	-531
21	1	0	629	-537	10	4	0	499	-589	9	8	0	485	-90	12	1	1	1590	-1590	-10	3	1	350	-415
0	2	0	3423	3012	11	4	0	659	-659	2	9	0	835	-871	14	1	1	1969	2030	-8	3	1	1914	1824
1	2	0	357	-354	12	4	0	601	-616	3	9	0	806	-816	16	1	1	1778	-1817	-7	3	1	1304	1442
2	2	0	511	-623	14	4	0	970	981	5	9	0	940	991	18	1	1	1149	1141	-6	3	1	1261	-1308
3	2	0	952	-890	15	4	0	726	672	7	9	0	596	-645	20	1	1	571	-489	-5	3	1	1378	-1383

OBSERVED AND CALCULATED STRUCTURE FACTORS FOR RU5(CO)11(C2PH(C6H4)) (PPH) (PPH(OME))												PAGE 2												
H	K	L	10FO	10FC	H	K	L	10FO	10FC	H	K	L	10FO	10FC	H	K	L	10FO	10FC					
-4	3	1	2140	2085	10	4	1	441	436	-8	6	1	771	734	-1	8	1	613	-676	-13	0	2	704	729
-3	3	1	462	435	12	4	1	858	893	-6	6	1	774	-784	0	8	1	769	779	-12	0	2	1199	-1160
-1	3	1	1596	1589	13	4	1	820	756	-5	6	1	895	-898	1	8	1	1814	-1874	-11	0	2	2193	2252
0	3	1	668	684	14	4	1	626	-639	-4	6	1	603	551	2	8	1	1476	-1396	-10	0	2	2527	2706
2	3	1	853	-850	15	4	1	1456	-1400	-3	6	1	712	681	3	8	1	1931	1923	-9	0	2	2295	-2253
3	3	1	347	-412	17	4	1	777	777	-2	6	1	637	-644	4	8	1	2494	2518	-8	0	2	4348	-4403
4	3	1	1322	1349	-19	5	1	670	659	-1	6	1	600	595	6	8	1	1566	-1559	-7	0	2	482	-493
5	3	1	709	678	-16	5	1	713	731	0	6	1	1087	1100	7	8	1	438	-328	-6	0	2	2596	2593
6	3	1	849	-845	-14	5	1	1647	-1625	1	6	1	411	-413	9	8	1	1107	-1089	-5	0	2	2385	2374
8	3	1	421	357	-13	5	1	577	-754	2	6	1	971	-911	11	8	1	2165	2189	-4	0	2	1218	-1247
9	3	1	940	-970	-12	5	1	548	494	6	6	1	1154	-1078	12	8	1	854	842	-3	0	2	2276	2283
11	3	1	1372	1342	-11	5	1	391	443	8	6	1	902	970	13	8	1	1144	-1190	-2	0	2	3518	2950
12	3	1	622	616	-9	5	1	981	978	11	6	1	1004	1032	14	8	1	518	-589	-1	0	2	4626	-4235
14	3	1	516	-507	-8	5	1	831	817	13	6	1	1443	-1428	-7	9	1	423	-433	0	0	2	6142	-7028
19	3	1	802	786	-7	5	1	737	-719	16	6	1	689	602	-6	9	1	628	-597	1	0	2	1695	1814
-18	4	1	753	714	-6	5	1	1749	-1752	-16	7	1	649	702	-4	9	1	647	583	2	0	2	3513	3276
-16	4	1	1367	-1353	-5	5	1	1341	-1302	-10	7	1	1018	-1054	-3	9	1	599	771	3	0	2	577	413
-15	4	1	801	-788	-4	5	1	604	574	-8	7	1	973	1017	7	9	1	637	630	4	0	2	1348	1405
-14	4	1	661	625	-2	5	1	977	973	-7	7	1	477	307	10	9	1	784	-733	5	0	2	2828	2462
-11	4	1	719	733	-1	5	1	1339	1366	-5	7	1	728	678	-6	10	1	553	-564	6	0	2	2345	-2198
-10	4	1	781	829	1	5	1	2016	-2002	-3	7	1	1040	-1085	-4	10	1	326	230	7	0	2	4886	-5110
-9	4	1	456	-490	2	5	1	1636	-1688	-2	7	1	859	-896	4	10	1	459	469	8	0	2	1413	-1506
-8	4	1	2508	-2569	3	5	1	483	-452	0	7	1	599	534	6	10	1	603	-638	9	0	2	2964	2970
-7	4	1	850	-921	5	5	1	743	700	3	7	1	794	775	-6	11	1	405	449	10	0	2	1673	1691
-6	4	1	1226	1238	6	5	1	1166	1221	5	7	1	942	-975	-5	11	1	1341	1328	11	0	2	921	-923
-3	4	1	2338	2246	7	5	1	569	570	6	7	1	384	-332	-3	11	1	1067	-1119	12	0	2	1643	1711
-1	4	1	2090	-2079	8	5	1	917	-940	10	7	1	731	711	2	11	1	1023	1020	13	0	2	1768	1825
0	4	1	2434	-2409	9	5	1	1418	-1448	-14	8	1	900	-919	3	11	1	873	884	14	0	2	1479	-1495
1	4	1	466	-408	13	5	1	1037	1041	-12	8	1	1661	1703	4	11	1	829	-843	15	0	2	2788	-2674

Table 18. (continued)

OBSERVED AND CALCULATED STRUCTURE FACTORS FOR RUS(CO)11(C2PH(C6H4)) (PPH) (PPH(OME))												PAGE 3												
H	K	L	10FO	10FC	H	K	L	10FO	10FC	H	K	L	10FO	10FC	H	K	L	10FO	10FC					
-13	1	2	514	561	-4	2	2	1485	-1433	3	3	2	948	1023	18	4	2	710	710	8	6	2	671	-659
-12	1	2	607	643	-3	2	2	529	-445	4	3	2	1099	1072	-19	5	2	1166	1128	10	6	2	381	388
-10	1	2	460	516	-2	2	2	2260	2096	5	3	2	1425	-1521	-17	5	2	838	-835	-13	7	2	1464	1499
-9	1	2	454	496	-1	2	2	1609	1553	6	3	2	2824	-2847	-16	5	2	515	-450	-12	7	2	553	464
-8	1	2	931	-878	1	2	2	326	-353	8	3	2	1779	1721	-12	5	2	669	654	-11	7	2	1034	-1042
-7	1	2	2531	-2474	2	2	2	1110	1104	9	3	2	1611	1679	-11	5	2	1257	1256	-10	7	2	522	-309
-6	1	2	607	-612	3	2	2	1411	1211	10	3	2	963	965	-9	5	2	1270	-1305	-7	7	2	1074	-1121
-5	1	2	928	1005	4	2	2	2955	-2958	12	3	2	562	-556	-7	5	2	433	278	-5	7	2	2036	1988
-4	1	2	1238	1207	5	2	2	1284	-1398	13	3	2	1599	-1545	-6	5	2	1272	-1320	-3	7	2	1928	-1916
-3	1	2	820	869	6	2	2	1538	1439	14	3	2	776	-717	-4	5	2	2172	2141	-1	7	2	613	625
-2	1	2	1044	947	8	2	2	1061	-1088	16	3	2	1158	1154	-2	5	2	1054	-1037	0	7	2	1809	-1771
-1	1	2	699	743	9	2	2	1505	1522	-20	4	2	832	771	-1	5	2	992	-949	2	7	2	2254	2181
0	1	2	1322	-1464	10	2	2	1763	1693	-18	4	2	796	-773	1	5	2	388	407	3	7	2	1414	1414
1	1	2	1988	-1862	11	2	2	1601	-1606	-15	4	2	1247	-1256	3	5	2	405	401	4	7	2	1323	-1279
2	1	2	991	-1213	12	2	2	1221	-1278	-14	4	2	789	-812	4	5	2	1193	1363	5	7	2	1756	-1694
4	1	2	1160	1079	17	2	2	933	905	-13	4	2	910	852	5	5	2	963	-917	8	7	2	760	-747
5	1	2	387	350	18	2	2	535	293	-12	4	2	1063	1080	6	5	2	1005	-950	9	7	2	763	791
6	1	2	1465	-1465	19	2	2	791	-782	-9	4	2	655	673	7	5	2	668	641	10	7	2	1724	1732
8	1	2	542	-574	20	2	2	720	-673	-8	4	2	951	-953	8	5	2	1043	1119	12	7	2	2009	-2005
10	1	2	442	412	-18	3	2	337	-468	-7	4	2	3062	-3103	13	5	2	669	-654	14	7	2	825	832
11	1	2	508	-487	-17	3	2	1351	-1376	-6	4	2	474	-502	15	5	2	908	925	-11	8	2	601	-566
14	1	2	842	813	-16	3	2	677	641	-5	4	2	3352	3338	16	5	2	549	525	-7	8	2	623	-640
18	1	2	554	-586	-15	3	2	1471	1496	-4	4	2	1420	1396	17	5	2	664	-656	-3	8	2	750	-754
19	1	2	560	-586	-13	3	2	357	-272	-3	4	2	961	-921	-17	6	2	805	800	-1	8	2	890	847
-21	2	2	782	-775	-12	3	2	577	594	-1	4	2	1079	-1071	-15	6	2	1020	-1010	4	8	2	636	-616
-17	2	2	1411	1430	-10	3	2	1198	-1181	0	4	2	2233	-2126	-13	6	2	535	494	8	8	2	466	-502
-16	2	2	1094	1142	-9	3	2	1128	-1151	1	4	2	2557	-2558	-11	6	2	641	-670	-13	9	2	592	611
-15	2	2	961	-934	-8	3	2	897	971	2	4	2	988	1074	-9	6	2	1035	1031	-10	9	2	557	-312
-14	2	2	1457	-1453	-7	3	2	1282	1279	3	4	2	2777	2827	-7	6	2	1242	-1221	-5	9	2	866	844
-13	2	2	826	-841	-6	3	2	390	-291	5	4	2	1051	-1066	-5	6	2	716	682	-3	9	2	678	-660
-12	2	2	521	-548	-4	3	2	1631	1593	7	4	2	618	-681	-4	6	2	548	-649	-2	9	2	328	-310
-10	2	2	1563	1607	-2	3	2	3030	-2986	8	4	2	1626	-1707	-2	6	2	1082	1020	0	9	2	883	-888
-9	2	2	1858	1936	-1	3	2	344	-342	9	4	2	644	-719	0	6	2	1387	-1389	2	9	2	1298	1209
-7	2	2	2727	-2672	0	3	2	1731	1583	10	4	2	1776	1830	1	6	2	695	-675	3	9	2	1015	1032
-6	2	2	1114	-1093	1	3	2	1195	1381	11	4	2	1315	1301	6	6	2	463	451	5	9	2	1126	-1082
-5	2	2	1171	1206	2	3	2	921	771	16	4	2	968	-933	7	6	2	354	-384	6	9	2	393	-362

OBSERVED AND CALCULATED STRUCTURE FACTORS FOR RUS(CO)11(C2PH(C6H4)) (PPH) (PPH(OME))												PAGE 4												
H	K	L	10FO	10FC	H	K	L	10FO	10FC	H	K	L	10FO	10FC	H	K	L	10FO	10FC					
10	9	2	1186	1160	-14	2	3	1059	1069	1	3	3	680	582	5	4	3	1957	-2034	-18	6	3	846	-884
12	9	2	1194	-1209	-13	2	3	937	922	2	3	3	1368	1449	6	4	3	2723	2777	-14	6	3	1096	1135
13	9	2	557	-513	-12	2	3	256	-285	3	3	3	1014	-1147	7	4	3	2665	2817	-13	6	3	725	726
-4	11	2	815	850	-11	2	3	778	-730	4	3	3	1825	-1863	9	4	3	1642	-1621	-10	6	3	998	-975
5	11	2	465	-524	-9	2	3	663	657	5	3	3	1926	1837	12	4	3	1745	-1795	-9	6	3	890	-907
-18	1	3	510	498	-8	2	3	896	-847	6	3	3	740	762	14	4	3	1903	1913	-7	6	3	464	446
-17	1	3	407	-352	-7	2	3	968	-920	7	3	3	1935	-1916	15	4	3	1025	978	-6	6	3	1618	1565
-16	1	3	930	-885	-6	2	3	2036	1978	8	3	3	400	-364	16	4	3	803	-795	-5	6	3	1122	1145
-12	1	3	988	1078	-4	2	3	1411	-1409	9	3	3	2185	2194	18	4	3	347	336	-4	6	3	946	-957
-11	1	3	689	735	-2	2	3	689	561	11	3	3	2034	-2088	-19	5	3	626	-640	-3	6	3	1070	-996
-10	1	3	1229	-1163	-1	2	3	791	-630	12	3	3	427	-230	-16	5	3	836	-842	-2	6	3	441	-406
-9	1	3	1161	-1080	0	2	3	368	-488	13	3	3	1071	1016	-14	5	3	1502	1444	-1	6	3	811	-770
-8	1	3	1283	-1273	1	2	3	389	377	15	3	3	713	-683	-12	5	3	1191	-1149	1	6	3	1360	1420
-7	1	3	1494	1515	2	2	3	1821	1612	17	3	3	543	580	-11	5	3	465	-503	2	6	3	816	906
-6	1	3	1224	1287	4	2	3	978	963	18	3	3	1018	-989	-10	5	3	462	435	4	6	3	979	-934
-4	1	3	1460	1455	5	2	3	1028	937	19	3	3	1047	-977	-9	5	3	800	-798	6	6	3	629	685
-3	1	3	558	480	6	2	3	657	648	-18	4	3	826	-775	-8	5	3	975	-962	7	6	3	473	-500
-2	1	3	2289	-2360	10	2	3	325	-381	-17	4	3	627	708	-7	5	3	1537	1536	11	6	3	731	-766
-1	1	3	2345	-2183	14	2	3	446	433	-16	4	3	1212	1151	-6	5	3	1775	1748	12	6	3	433	481
0	1	3	2351	2093	17	2	3	526	-558	-15	4	3	749	-699	-5	5	3	542	-529	13	6	3	963	957
1	1	3	620	558	19	2	3	490	474	-14	4	3	886	-860	-4	5	3	1794	-1877	15	6	3	491	-304
2	1	3	581	566	-21	3	3	860	854	-12	4	3	375	374	-2	5	3	659	-675	-16	6	3	605	-527
3	1	3	844	-1102	-18	3	3	890	876	-11	4	3	1469	-1424	-1	5	3	1220	-1196	-16	7	3	1013	-1051
4	1	3	3274	3402	-16	3	3	1616	-1646	-10	4	3	854	-860	0	5	3	426	322	-15	7	3	457	-417
6	1	3	3018	-2954	-15	3	3	1676	-1712	-9	4	3	2263	2283	1	5	3	2552	2543	-10	7	3	1055	1002
7	1	3	520	-595	-14	3	3	569	614	-8	4	3	1801	1780	2	5	3	1944	1848	-8	7	3	1339	-1346
8	1	3	2682	2731	-13	3	3	1369	1339	-7	4	3	1566	-1545	3	5	3	858	-868	-5	7	3	508	-466
9	1	3	1123	1126	-10	3	3	1503	1511	-6	4	3	647	-687	4	5	3	1486	-1564	-3	7	3	1100	1069
10	1	3	1082	-1079	-8	3	3	3339	-3352	-5	4	3	2131	2104	6	5	3	931	-886	-2	7	3	685	

Table 18. (continued)

OBSERVED AND CALCULATED STRUCTURE FACTORS FOR												RUS(CO)11(C2PH(C6H4)) (PPH) (PPH(OME))												PAGE 5
H	K	L	10FO	10FC	H	K	L	10FO	10FC	H	K	L	10FO	10FC	H	K	L	10FO	10FC	H	K	L	10FO	10FC
-13	8	3	634	-644	6	10	3	705	694	-9	1	4	1117	1078	17	2	4	956	-963	-6	4	4	896	-867
-12	8	3	1056	-1099	8	10	3	464	-523	-8	1	4	1789	1835	19	2	4	856	869	-5	4	4	2912	-2781
-7	8	3	763	750	-6	11	3	889	-859	-7	1	4	1447	1460	-21	3	4	462	416	-3	4	4	1310	1328
-5	8	3	1415	-1355	2	11	3	1104	-1066	-5	1	4	1208	-1131	-18	3	4	809	779	-1	4	4	387	-438
-4	8	3	1687	-1679	4	11	3	930	959	-4	1	4	629	-679	-16	3	4	1132	-1143	0	4	4	2161	2155
-2	8	3	975	954	-16	0	4	673	666	-3	1	4	1035	-911	-14	3	4	773	747	1	4	4	1892	1878
0	8	3	889	890	-12	0	4	684	-716	-1	1	4	1207	1234	-12	3	4	900	-896	2	4	4	2346	-2470
1	8	3	1251	1321	-11	0	4	2036	-1998	0	1	4	1691	1577	-11	3	4	657	641	3	4	4	2720	-2819
2	8	3	622	-622	-10	0	4	692	678	4	1	4	1033	-1115	-10	3	4	1627	1644	4	4	4	1238	1212
3	8	3	1730	-1743	-9	0	4	1514	1626	5	1	4	1606	-1759	-9	3	4	821	-771	6	4	4	1184	-1253
4	8	3	1164	-1196	-8	0	4	2098	2081	7	1	4	802	721	-8	3	4	1820	-1801	7	4	4	1133	1096
6	8	3	665	603	-6	0	4	2450	-2275	8	1	4	671	699	-7	3	4	663	681	8	4	4	2191	2190
8	8	3	1178	1142	-5	0	4	1628	-1649	9	1	4	944	869	-6	3	4	614	625	10	4	4	2154	-2244
9	8	3	723	753	-4	0	4	3852	-3546	20	1	4	419	-444	-5	3	4	1735	-1574	11	4	4	1024	-1048
10	8	3	1245	-1222	-3	0	4	975	-996	-17	2	4	1522	-1506	-4	3	4	793	-759	15	4	4	1132	1088
11	8	3	1805	-1845	-2	0	4	3024	3023	-15	2	4	1646	1627	-3	3	4	2178	2111	16	4	4	935	944
13	8	3	948	952	-1	0	4	4039	3962	-14	2	4	2132	2115	-2	3	4	2422	2332	17	4	4	1078	-1037
-12	9	3	865	-925	0	0	4	969	973	-13	2	4	759	717	0	3	4	1851	-1936	18	4	4	1144	-1129
-11	9	3	815	-767	3	0	4	1119	-1353	-12	2	4	745	-712	3	3	4	1616	-1683	-19	5	4	1062	-1043
-4	9	3	795	-811	4	0	4	3165	-2992	-11	2	4	482	-465	4	3	4	850	929	-18	5	4	589	602
-3	9	3	428	-428	5	0	4	276	-416	-10	2	4	1003	-953	5	3	4	2797	2818	-14	5	4	488	493
1	9	3	958	922	6	0	4	2589	2715	-9	2	4	2691	-2622	6	3	4	902	1006	-12	5	4	1458	-1398
2	9	3	614	598	7	0	4	2040	2004	-8	2	4	601	636	7	3	4	1612	-1706	-11	5	4	1454	-1437
4	9	3	561	-434	11	0	4	1332	-1335	-7	2	4	2937	2972	8	3	4	1360	-1425	-10	5	4	1400	1362
7	9	3	487	-565	12	0	4	2178	-2092	-6	2	4	1030	1029	12	3	4	955	990	-9	5	4	703	718
9	9	3	925	929	14	0	4	1965	1985	-4	2	4	670	767	13	3	4	1611	1641	-8	5	4	871	-872
11	9	3	480	-534	15	0	4	1682	1649	-2	2	4	1147	-1013	15	3	4	1277	-1288	-7	5	4	1163	1148
-10	10	3	952	-969	17	0	4	979	-975	-1	2	4	782	-858	16	3	4	640	-610	-6	5	4	1600	1522
-6	10	3	557	571	18	0	4	512	-583	0	2	4	1063	1143	-17	4	4	939	-938	-5	5	4	1674	-1682
-5	10	3	642	645	19	0	4	693	-657	1	2	4	2298	2160	-15	4	4	1473	1418	-4	5	4	2800	-2786
-4	10	3	487	-493	20	0	4	568	-578	3	2	4	822	668	-13	4	4	1100	-1083	-3	5	4	628	655
-3	10	3	797	-805	-16	1	4	812	847	4	2	4	1611	1703	-12	4	4	1010	-990	-2	5	4	1996	2066
2	10	3	562	483	-15	1	4	1237	1208	6	2	4	2259	-2360	-11	4	4	1435	1344	-1	5	4	1018	1038
3	10	3	431	442	-14	1	4	307	-231	8	2	4	1442	1459	-9	4	4	1609	-1557	1	5	4	478	538
4	10	3	727	-794	-13	1	4	998	-991	12	2	4	444	437	-8	4	4	1139	1156	3	5	4	2060	-2112
5	10	3	482	-460	-10	1	4	700	-656	15	2	4	495	465	-7	4	4	2337	2328	4	5	4	539	-410

OBSERVED AND CALCULATED STRUCTURE FACTORS FOR												RUS(CO)11(C2PH(C6H4)) (PPH) (PPH(OME))												PAGE 6
H	K	L	10FO	10FC	H	K	L	10FO	10FC	H	K	L	10FO	10FC	H	K	L	10FO	10FC	H	K	L	10FO	10FC
5	5	4	2603	2616	10	7	4	710	-741	1	1	5	862	-949	-7	3	5	886	-874	2	4	5	1436	-1475
6	5	4	537	632	11	7	4	1111	1144	2	1	5	2757	-2652	-6	3	5	2854	-2730	3	4	5	2039	1987
7	5	4	1440	-1520	12	7	4	731	812	3	1	5	1223	1104	-4	3	5	1439	1475	4	4	5	3619	3789
8	5	4	816	-818	-15	8	4	812	722	4	1	5	978	1028	-3	3	5	1790	-1769	6	4	5	3089	-3174
9	5	4	934	923	-11	8	4	712	672	5	1	5	1417	1358	-2	3	5	399	-349	7	4	5	656	-638
11	5	4	723	-758	-7	8	4	832	797	6	1	5	1298	1355	-1	3	5	3916	3870	8	4	5	1317	1355
13	5	4	725	776	-5	8	4	625	-613	8	1	5	630	-646	0	3	5	1912	2003	11	4	5	1243	1263
15	5	4	1042	-1034	-4	8	4	438	435	9	1	5	986	-948	1	3	5	962	-1043	13	4	5	923	-949
17	5	4	686	693	-3	8	4	721	703	10	1	5	647	-631	2	3	5	1342	-1342	14	4	5	1409	-1412
-18	6	4	504	-475	-2	8	4	694	-689	12	1	5	1545	1549	3	3	5	1367	1336	19	4	5	994	1075
-15	6	4	897	857	0	8	4	883	857	13	1	5	1049	1066	5	3	5	1780	-1873	-9	5	5	906	865
-10	6	4	630	-595	1	8	4	682	706	20	1	5	619	607	6	3	5	841	853	-7	5	5	1324	-1355
-9	6	4	961	-994	2	8	4	751	-801	-16	2	5	446	399	7	3	5	2532	2651	-6	5	5	1014	-1004
-7	6	4	1088	1045	6	8	4	666	-730	-15	2	5	611	-597	9	3	5	1152	1215	-5	5	5	1041	956
-5	6	4	772	-760	-9	9	4	675	700	-14	2	5	811	-839	11	3	5	685	-672	-4	5	5	1330	1289
-4	6	4	612	636	-5	9	4	560	-467	-11	2	5	406	412	13	3	5	912	914	-1	5	5	966	982
-2	6	4	1187	-1193	5	9	4	1056	1091	-7	2	5	916	-828	14	3	5	1164	-1156	1	5	5	2003	-1990
0	6	4	1048	1000	-5	11	4	781	-703	-6	2	5	1266	-1234	16	3	5	1254	1281	2	5	5	1027	-1113
1	6	4	658	675	-4	11	4	969	-911	-5	2	5	575	596	18	3	5	825	865	3	5	5	1483	1568
2	6	4	601	-697	-3	11	4	480	443	-4	2	5	740	693	-19	4	5	1048	-1077	4	5	5	1561	1596
3	6	4	622	-596	-2	11	4	831	784	-2	2	5	1359	1324	-17	4	5	1351	1309	6	5	5	842	892
6	6	4	709	-757	1	11	4	367	235	0	2	5	729	-842	-15	4	5	1056	-1061	8	5	5	1102	-1109
8	6	4	623	674	3	11	4	732	-754	2	2	5	1494	-1564	-13	4	5	2131	2161	9	5	5	1780	-1899
-14	7	4	669	-742	-20	1	5	555	-585	5	2	5	693	617	-11	4	5	900	-834	11	5	5	1202	1246
-13	7	4	503	-489	-15	1	5	1127	1078	11	2	5	653	-644	-10	4	5	2310	-2252	17	5	5	1011	-978
-8	7	4	1045	1035	-13	1	5	2041	-1954	16	2	5	472	521	-9	4	5	973	981	-18	6	5	876	927
-6	7	4	1333	-1310	-12	1	5	1067	-1013	-21	3	5	978	-907	-7	4	5	1454	1466	-14	6	5	936	-881
-5	7	4	803	-777	-11	1	5	1482	1507	-18	3	5	953	-907	-6	4	5	876	-849	-12	6	5	459	-447
-4	7	4	569	573	-10	1	5	707	756	-16	3	5												

Table 18. (continued)

OBSERVED AND CALCULATED STRUCTURE FACTORS FOR										RUS (CO)11 (C2PH (C6H4)) (PPH) (PPH(OME))										PAGE 7				
H	K	L	10FO	10FC	H	K	L	10FO	10FC	H	K	L	10FO	10FC	H	K	L	10FO	10FC	H	K	L	10FO	10FC
-1	6	5	436	-431	-10	10	5	869	898	14	0	6	1079	-1014	-3	2	6	737	-698	18	3	6	624	585
0	6	5	988	-1066	-9	10	5	502	-496	17	0	6	616	657	-2	2	6	2136	2150	-17	4	6	806	807
1	6	5	924	-893	-6	10	5	835	-781	18	0	6	1100	1138	-1	2	6	2172	2099	-15	4	6	972	-984
2	6	5	725	-649	-5	10	5	685	-722	19	0	6	902	838	0	2	6	2191	-2060	-13	4	6	984	979
4	6	5	740	819	-4	10	5	712	670	-21	1	6	626	514	1	2	6	3576	-3625	-11	4	6	1465	-1465
-16	7	5	958	945	-3	10	5	1084	1064	-18	1	6	530	510	5	2	6	1236	1268	-10	4	6	411	485
-15	7	5	356	363	2	10	5	818	-860	-16	1	6	1046	-1127	6	2	6	1622	1671	-9	4	6	961	947
-11	7	5	578	-583	4	10	5	913	856	-14	1	6	613	623	8	2	6	1737	-1764	-8	4	6	1799	-1690
-10	7	5	460	-460	-1	11	5	395	-339	-13	1	6	1015	991	9	2	6	500	-581	-7	4	6	769	-816
-9	7	5	628	645	1	11	5	849	857	-12	1	6	1021	987	10	2	6	892	875	-6	4	6	1677	1673
-8	7	5	1625	1666	3	11	5	586	-600	-11	1	6	797	776	11	2	6	725	665	-5	4	6	1891	1757
-6	7	5	748	-827	-21	0	6	679	-700	-9	1	6	1708	-1657	17	2	6	904	870	-4	4	6	511	-483
-3	7	5	1076	-1047	-19	0	6	675	664	-8	1	6	1401	-1426	19	2	6	572	-630	0	4	6	2276	-2422
-1	7	5	1465	1400	-18	0	6	452	-470	-5	1	6	1645	1631	-17	3	6	846	854	2	4	6	2138	2139
0	7	5	1453	1330	-17	0	6	697	-682	-4	1	6	1673	1583	-15	3	6	539	-591	3	4	6	837	876
2	7	5	477	-572	-16	0	6	1208	1190	-3	1	6	308	-282	-11	3	6	873	-888	4	4	6	1275	-1357
5	7	5	869	-910	-14	0	6	1868	-1854	-2	1	6	456	-494	-9	3	6	1016	1068	5	4	6	533	507
7	7	5	696	683	-13	0	6	789	703	-1	1	6	1439	-1361	-6	3	6	658	697	6	4	6	517	470
13	7	5	696	-761	-12	0	6	2163	2238	1	1	6	503	447	-5	3	6	1065	1022	7	4	6	1730	-1783
-8	8	5	838	-794	-11	0	6	534	-560	2	1	6	2113	2198	-4	3	6	699	-659	8	4	6	1528	-1661
-6	8	5	589	657	-10	0	6	2626	-2609	3	1	6	509	476	-3	3	6	2209	-2184	9	4	6	1115	1118
-5	8	5	944	945	-9	0	6	669	-672	4	1	6	1014	1100	-2	3	6	900	-843	10	4	6	2174	2253
-1	8	5	829	-826	-5	0	6	2712	2725	5	1	6	1019	856	-1	3	6	1306	1324	11	4	6	631	650
0	8	5	1746	-1722	-4	0	6	3119	3298	6	1	6	517	-487	0	3	6	1708	1758	15	4	6	1517	-1551
2	8	5	1786	1785	-2	0	6	2973	-2711	7	1	6	884	-963	1	3	6	535	-515	17	4	6	1489	1471
3	8	5	803	885	0	0	6	2432	2542	12	1	6	816	759	2	3	6	651	717	18	4	6	806	791
7	8	5	1140	-1202	1	0	6	1719	-1717	-17	2	6	1129	1089	3	3	6	659	629	-17	5	6	390	-274
8	8	5	966	-964	3	0	6	2515	2660	-15	2	6	1827	-1830	4	3	6	1738	-1710	-15	5	6	777	-752
10	8	5	1336	1389	4	0	6	3391	3421	-14	2	6	2316	-2285	5	3	6	2388	-2556	-14	5	6	494	-519
14	8	5	540	-555	5	0	6	1531	-1576	-12	2	6	1627	1690	6	3	6	435	411	-12	5	6	2003	1999
-12	9	5	1052	1011	6	0	6	3065	-3238	-10	2	6	987	1018	7	3	6	1658	1715	-10	5	6	1569	-1501
-10	9	5	566	-594	7	0	6	992	-999	-9	2	6	1934	1873	8	3	6	662	643	-7	5	6	1126	-1116
-4	9	5	975	972	10	0	6	1291	1249	-8	2	6	851	-767	10	3	6	524	471	-5	5	6	2058	2083
1	9	5	1132	-1107	11	0	6	2678	2718	-7	2	6	2745	-2713	12	3	6	1066	-1054	-4	5	6	1187	1181
3	9	5	1196	1205	12	0	6	428	476	-6	2	6	1752	-1639	13	3	6	1146	-1123	-3	5	6	1341	-1322
9	9	5	696	-751	13	0	6	1990	-2029	-5	2	6	1280	1267	15	3	6	952	1048	-2	5	6	1414	-1467

OBSERVED AND CALCULATED STRUCTURE FACTORS FOR										RUS (CO)11 (C2PH (C6H4)) (PPH) (PPH(OME))										PAGE 8				
H	K	L	10FO	10FC	H	K	L	10FO	10FC	H	K	L	10FO	10FC	H	K	L	10FO	10FC	H	K	L	10FO	10FC
1	5	6	1198	-1105	6	7	6	915	-911	-1	1	7	361	369	-7	3	7	1247	1254	15	4	7	635	-647
2	5	6	654	658	8	7	6	1291	1362	0	1	7	3732	-3482	-6	3	7	1956	1983	10	4	7	923	-926
3	5	6	1866	1973	9	7	6	738	712	1	1	7	1182	1174	-3	3	7	856	923	-4	5	7	1594	-1603
4	5	6	451	-450	10	7	6	740	-832	2	1	7	3471	3704	-2	3	7	836	-802	-3	5	7	829	-862
5	5	6	1873	-1818	-9	8	6	649	607	3	1	7	953	-884	-1	3	7	2950	-2943	-2	5	7	498	448
7	5	6	825	887	-7	8	6	764	-743	4	1	7	2402	-2557	1	3	7	1710	1724	1	5	7	1129	1172
12	5	6	520	-485	-3	8	6	379	-358	5	1	7	1186	-1111	2	3	7	832	849	2	5	7	382	295
13	5	6	426	-507	-2	8	6	623	668	6	1	7	897	913	4	3	7	561	535	3	5	7	1330	-1260
14	5	6	711	760	0	8	6	808	-779	8	1	7	780	-799	6	3	7	1127	-1251	4	5	7	1128	-1225
16	5	6	835	-802	2	8	6	1011	973	9	1	7	1666	1768	7	3	7	1667	-1702	8	5	7	895	850
-14	6	6	442	-370	4	8	6	889	-975	10	1	7	1597	1680	8	3	7	538	521	9	5	7	1149	1171
-10	6	6	493	432	6	8	6	754	796	11	1	7	1430	-1493	9	3	7	1424	1399	11	5	7	1270	-1332
-7	6	6	661	-637	13	0	6	414	473	12	1	7	2097	-2075	11	3	7	605	-641	16	5	7	925	936
-5	6	6	495	508	-12	9	6	692	709	14	1	7	479	457	14	3	7	1067	-1070	-18	6	7	1111	-1155
-3	6	6	797	744	-4	9	6	682	650	19	1	7	984	-950	16	3	7	1140	1130	-17	6	7	653	-622
0	6	6	695	-692	-2	9	6	1328	-1313	-17	2	7	1080	-1087	-16	4	7	778	-751	-15	6	7	642	669
1	6	6	673	-733	0	9	6	952	874	-15	2	7	981	953	-15	4	7	709	-582	-14	6	7	826	754
3	6	6	470	465	5	9	6	836	-795	-14	2	7	477	476	-13	4	7	1024	997	-11	6	7	1745	-1701
8	6	6	668	-673	8	9	6	762	751	-11	2	7	486	-501	-10	4	7	1038	971	-10	6	7	1631	-1590
12	6	6	411	-406	-10	10	6	609	-618	-10	2	7	691	-708	-8	4	7	1185	-1118	-8	6	7	1436	1421
-17	7	6	718	-661	-2	11	6	742	-700	-8	2	7	574	581	-7	4	7	523	487	-7	6	7	1263	1232
-16	7	6	828	-814	-21	1	7	871	835	-7	2	7	1520	1374	-6	4	7	876	899	-4	6	7	905	-895
-12	7	6	534	534	-20	1	7	686	648	-6	2	7	683	744	-5	4	7	1336	-1307	-3	6	7	2377	-2449
-11	7	6	1114	1100	-17	1	7	606	614	-5	2	7	546	-563	-4	4	7	1831	-1703	-2	6	7	601	-596
-10	7	6	421	-419	-15	1	7	2144	-2133	-4	2	7	750	-686	-3	4	7	1214	1179	-1	6	7	1291	1342
-9	7	6	1493	-1467	-13	1	7	2091	2223	-3	2	7	436	-450	-2	4	7	2170	2170	0	6	7	874	846
-8	7	6	539	-547	-12	1	7	493	-495	-2	2	7	789	-770	0	4	7	1049	-1044	2	6	7	697	685
-7	7	6	1122	1116	-11	1	7	1609	-1525	0	2	7	343	333	1	4	7	640	599	4	6	7	942	-1000
-6	7	6	779	813	-10	1	7	542	504	2	2	7	808	905	3	4								

Table 18. (continued)

OBSERVED AND CALCULATED STRUCTURE FACTORS FOR												RUS (CO) 11 (C2PH (C6H4)) (PPH) (PPH (OME))				PAGE 9								
H	K	L	10FO	10FC	H	K	L	10FO	10FC	H	K	L	10FO	10FC	H	K	L	10FO	10FC					
-1	7	7	1120	-1145	-12	0	8	947	-1031	-2	1	8	1361	1294	-18	3	8	733	-796	-2	5	8	811	854
0	7	7	998	-950	-11	0	8	2201	2190	-1	1	8	1372	1518	-15	3	8	849	863	0	5	8	431	481
7	7	7	797	-784	-10	0	8	2128	2125	1	1	8	760	-759	-10	3	8	556	-548	2	5	8	1077	-1084
12	7	7	639	602	-9	0	8	2320	-2244	2	1	8	1297	-1255	-6	3	8	773	-710	3	5	8	575	-566
15	7	7	671	-570	-8	0	8	2880	-2844	3	1	8	830	-827	-4	3	8	1441	1495	4	5	8	804	839
-14	8	7	895	-924	-7	0	8	2248	2329	4	1	8	884	-858	-3	3	8	831	827	7	5	8	740	745
-13	8	7	653	624	-6	0	8	1959	2018	6	1	8	539	547	-2	3	8	596	-558	8	5	8	565	536
-12	8	7	1168	1161	-5	0	8	3877	-3598	7	1	8	838	836	-1	3	8	542	-530	11	5	8	382	-293
-11	8	7	702	-721	-4	0	8	2391	-2249	11	1	8	1030	-1053	0	3	8	705	-635	17	5	8	680	-670
-10	8	7	1147	-1129	-3	0	8	2747	2888	14	1	8	521	441	3	3	8	1027	1046	-16	6	8	605	-585
-9	8	7	822	844	-2	0	8	1929	1927	-19	2	8	635	-601	4	3	8	1253	1331	-14	6	8	1176	1158
-8	8	7	1175	1122	-1	0	8	3103	-2930	-15	2	8	1577	1637	6	3	8	1457	-1533	-12	6	8	977	-969
-6	8	7	1192	-1176	0	0	8	875	-722	-14	2	8	1348	1323	11	3	8	448	541	-11	6	8	520	-446
-3	8	7	1075	-1036	1	0	8	4115	4316	-13	2	8	740	-723	12	3	8	1204	1173	-10	6	8	394	418
-1	8	7	1915	1881	2	0	8	2852	-2662	-12	2	8	887	-915	-14	4	8	376	339	-7	6	8	874	846
0	8	7	915	907	3	0	8	4571	-4398	-11	2	8	769	-723	-6	4	8	558	-534	-6	6	8	1022	1046
1	8	7	1586	-1629	5	0	8	3177	3487	-10	2	8	1492	-1476	-1	4	8	653	612	-5	6	8	929	-897
2	8	7	925	-877	8	0	8	2026	2070	-9	2	8	1621	-1526	0	4	8	1231	1161	-4	6	8	832	-798
7	8	7	1524	1508	10	0	8	3583	-3573	-7	2	8	2601	2591	1	4	8	914	-881	3	6	8	953	948
9	8	7	1194	-1192	11	0	8	2142	-2079	-6	2	8	1554	1565	2	4	8	1486	-1508	15	6	8	405	271
-12	9	7	835	-802	12	0	8	2051	2030	-5	2	8	1681	-1531	7	4	8	1004	993	-13	7	8	442	459
-5	9	7	775	-767	13	0	8	1722	1661	-4	2	8	1089	-1138	9	4	8	1135	-1102	-12	7	8	1384	-1319
-4	9	7	802	-755	18	0	8	1782	-1742	-3	2	8	904	-837	10	4	8	534	510	-11	7	8	1046	-1038
1	9	7	671	628	-17	1	8	955	974	-2	2	8	1993	-1961	12	4	8	582	-591	-10	7	8	1246	1240
3	9	7	1035	-1041	-16	1	8	1106	1104	-1	2	8	914	-824	16	4	8	900	-947	-9	7	8	1696	1639
-6	10	7	597	595	-14	1	8	1066	-1117	0	2	8	2656	2757	17	4	8	582	-591	-7	7	8	1395	-1377
-4	10	7	921	-871	-13	1	8	872	-896	1	2	8	2288	2367	-15	5	8	939	901	-5	7	8	462	391
-3	10	7	1195	-1245	-12	1	8	822	-839	2	2	8	1264	-1206	-13	5	8	1250	-1241	-4	7	8	1405	-1339
2	10	7	776	864	-11	1	8	641	-615	3	2	8	845	-730	-12	5	8	1231	-1152	-2	7	8	2459	2463
4	10	7	794	-829	-10	1	8	803	774	4	2	8	1211	-1214	-10	5	8	628	721	0	7	8	2056	-2033
-21	0	8	670	686	-9	1	8	2530	2467	5	2	8	992	-956	-9	5	8	700	658	2	7	8	1132	1117
-20	0	8	846	-845	-8	1	8	817	865	6	2	8	1303	1319	-8	5	8	1253	1167	4	7	8	1045	-1009
-18	0	8	1414	1459	-7	1	8	1355	-1351	8	2	8	577	546	-6	5	8	1664	-1577	6	7	8	1608	1676
-16	0	8	2360	-2370	-6	1	8	848	-815	9	2	8	899	-923	-5	5	8	1389	-1480	8	7	8	1471	-1517
-14	0	8	2163	2135	-5	1	8	714	-746	10	2	8	759	-790	-3	5	8	789	736	11	7	8	948	-952
-13	0	8	886	-926	-4	1	8	897	-838	11	2	8	759	-790	-3	5	8	789	736	11	7	8	948	-952

OBSERVED AND CALCULATED STRUCTURE FACTORS FOR												RUS (CO) 11 (C2PH (C6H4)) (PPH) (PPH (OME))				PAGE 10								
H	K	L	10FO	10FC	H	K	L	10FO	10FC	H	K	L	10FO	10FC	H	K	L	10FO	10FC					
13	7	8	1190	1214	6	1	9	1445	-1473	8	3	9	391	-395	-7	6	9	757	-811	-7	10	9	583	-610
-12	9	8	1009	-1015	8	1	9	499	543	14	3	9	550	573	-4	6	9	1190	1201	-4	10	9	808	866
-11	9	8	379	-421	9	1	9	2094	-2137	-19	4	9	675	-672	-3	6	9	2362	2395	-3	10	9	1022	1020
-10	9	8	782	815	10	1	9	844	-865	-17	4	9	810	805	-1	6	9	1482	-1482	1	10	9	420	-449
-9	9	8	705	656	11	1	9	2113	2152	-15	4	9	867	-842	0	6	9	928	-977	4	10	9	650	611
-5	9	8	405	-398	12	1	9	799	822	-11	4	9	615	-699	4	6	9	879	856	-19	0	10	901	-876
-4	9	8	821	-838	13	1	9	915	-940	-9	4	9	983	992	5	6	9	1208	1254	-18	0	10	659	-673
-3	9	8	760	775	17	1	9	975	-977	-7	4	9	951	-933	7	6	9	1075	-1148	-17	0	10	1513	1537
-2	9	8	1289	1324	-18	2	9	595	617	-5	4	9	1312	1279	12	6	9	970	1012	-16	0	10	1622	1629
0	9	8	995	-1003	-15	2	9	763	-766	-3	4	9	1426	-1412	-14	7	9	469	-427	-15	0	10	1059	-1057
6	9	8	857	836	-11	2	9	883	867	2	4	9	759	771	-13	7	9	1178	-1144	-14	0	10	1126	-1243
8	9	8	928	-976	-10	2	9	1145	1098	3	4	9	1126	1218	-6	7	9	1078	-1082	-11	0	10	2022	-2013
-5	10	8	729	-740	-8	2	9	1709	-1743	4	4	9	770	-816	-5	7	9	1127	-1108	-9	0	10	2417	2528
-3	10	8	903	938	-7	2	9	846	-878	5	4	9	1507	-1468	-3	7	9	636	656	-8	0	10	625	649
5	10	8	544	536	-3	2	9	703	762	8	4	9	530	-434	-1	7	9	539	562	-7	0	10	3245	-3233
-21	1	9	739	-791	-2	2	9	1074	1091	10	4	9	1029	1052	0	7	9	755	801	-6	0	10	1047	-964
-19	1	9	710	660	-1	2	9	912	-844	12	4	9	759	-748	2	7	9	764	-770	-5	0	10	1978	2168
-17	1	9	838	-815	0	2	9	538	-510	13	4	9	786	-885	-13	8	9	1210	-1240	-3	0	10	1402	-1261
-16	1	9	1130	1143	4	2	9	604	679	-17	5	9	846	-829	-12	8	9	763	-770	-2	0	10	1308	1297
-15	1	9	1436	1435	6	2	9	995	1083	-15	5	9	801	786	-11	8	9	970	999	-1	0	10	957	1065
-14	1	9	1202	-1222	7	2	9	621	-614	-9	5	9	1094	-1052	-9	8	9	897	-834	0	0	10	2681	-2436
-13	1	9	1288	-1306	-20	3	9	690	-688	-7	5	9	951	937	-7	8	9	1198	1142	1	0	10	2419	-2189
-12	1	9	706	735	-13	3	9	589	-568	-4	5	9	863	857	-6	8	9	394	394	2	0	10	2886	2923
-10	1	9	1855	-1783	-10	3	9	1134	1160	-3	5	9	783	782	-5	8	9	1225	-1170	3	0	10	3240	3413
-8	1	9	2787	2716	-9	3	9	1044	969	-2	5	9	704	-681	-3	8	9	1298	1283	4	0	10	2517	-2416
-7	1	9	1056	1002	-6	3	9	1159	-1174	4	5	9	1166	1181	-1	8	9	1641	-1614	5	0	10	2937	-2760
-6	1	9	3010	-3022	-5	3	9	1791	-1724	6	5	9	632	-616	1	8	9	1550	1574	6	0	10	1573	1628
-5	1	9	1320	-1154	-4	3	9	909	-886	9	5	9	674	-668	4	8	9	577	613	8	0	10	2244	-2280
-4	1	9	1794	1872	-3	3	9	488	500	11	5	9	837	811	5	8	9							

Table 18. (continued)

OBSERVED AND CALCULATED STRUCTURE FACTORS FOR										RUS (CO)11 (C2PH(C6H4)) (PPH) (PPH(OME))										PAGE 11									
H	K	L	10FO	10FC	H	K	L	10FO	10FC	H	K	L	10FO	10FC	H	K	L	10FO	10FC	H	K	L	10FO	10FC					
-12	1	10	763	745	-19	3	10	770	721	-8	5	10	824	-799	0	7	10	1031	1030	-16	2	11	712	711					
-10	1	10	1499-1552		-18	3	10	825	850	-7	5	10	1048	1003	3	7	10	1006	981	-14	2	11	658	-675					
-9	1	10	1775-1716		-16	3	10	545	-615	-6	5	10	1417	1372	4	7	10	612	599	-11	2	11	908	-898					
-7	1	10	1304	1311	-13	3	10	639	-630	-3	5	10	420	426	5	7	10	1490-1469		-10	2	11	837	-867					
-5	1	10	821	761	-11	3	10	796	822	-2	5	10	856	-868	6	7	10	1119-1065		-9	2	11	679	667					
-4	1	10	637	660	-10	3	10	909	844	-1	5	10	1267-1242		7	7	10	1256	1268	-8	2	11	1576	1466					
-3	1	10	885	-891	-9	3	10	650	-623	1	5	10	1188	1231	8	7	10	632	623	-4	2	11	549	-534					
-2	1	10	1622-1696		-5	3	10	1018-1079		2	5	10	1079	1059	12	7	10	595	-568	-3	2	11	1617-1622						
-1	1	10	1011	-966	-4	3	10	655	-607	3	5	10	342	-327	13	7	10	992	-995	-2	2	11	349	-335					
2	1	10	743	793	-3	3	10	1139	1065	6	5	10	1301-1365		-8	8	10	440	419	-1	2	11	1063	1150					
3	1	10	937	977	-2	3	10	995	1016	7	5	10	734	-706	1	8	10	381	-369	4	2	11	1295-1250						
5	1	10	1238-1300		0	3	10	386	-355	9	5	10	876	872	-5	9	10	404	501	5	2	11	734	-679					
6	1	10	1403-1391		3	3	10	1461-1466		-16	6	10	656	763	-4	9	10	683	688	7	2	11	805	824					
7	1	10	526	-499	5	3	10	829	876	-14	6	10	1238-1224		-3	9	10	676	-643	-18	3	11	816	-798					
10	1	10	701	771	9	3	10	594	578	-12	6	10	946	965	-1	9	10	384	284	-15	3	11	856	-815					
11	1	10	925	925	11	3	10	1037	-986	-10	6	10	774	-710	-18	1	11	763	789	-13	3	11	1287	1267					
-15	2	10	1009-1012		-16	4	10	884	909	-8	6	10	670	684	-16	1	11	1141-1177		-12	3	11	1620	1539					
-14	2	10	960	-924	-15	4	10	783	770	-7	6	10	1166-1176		-15	1	11	805	-790	-11	3	11	1025-1009						
-12	2	10	1077	1049	-14	4	10	1194-1119		-6	6	10	864	-864	-13	1	11	779	814	-10	3	11	1670-1686						
-11	2	10	1369	1384	-13	4	10	1254-1185		-5	6	10	1229	1249	-10	1	11	807	765	-7	3	11	646	-648					
-10	2	10	701	714	-11	4	10	891	819	-4	6	10	943	925	-9	1	11	422	-540	-6	3	11	1551	1520					
-8	2	10	799	-779	-10	4	10	658	-644	-3	6	10	468	-463	-8	1	11	1626-1574		-5	3	11	2397	2297					
-7	2	10	2289-2240		-8	4	10	1149	1138	0	6	10	584	-607	-6	1	11	2381	2386	-3	3	11	2269-2157						
-6	2	10	1399-1400		-6	4	10	905	-890	1	6	10	1047-1018		-4	1	11	1224-1189		-2	3	11	1312-1301						
-5	2	10	1610	1692	-4	4	10	1420	1414	3	6	10	1164	1200	-3	1	11	415	534	2	3	11	2015	1952					
-4	2	10	2798	2668	3	4	10	637	633	10	6	10	687	662	-1	1	11	2109-1926		3	3	11	1636	1670					
-3	2	10	1120	1214	4	4	10	657	634	-14	7	10	660	-662	0	1	11	925	-832	4	3	11	1702-1645						
-2	2	10	1242	1182	5	4	10	1204-1183		-12	7	10	1271	1265	1	1	11	1923	1931	5	3	11	1591-1578						
-1	2	10	762	-732	6	4	10	786	-806	-10	7	10	1320-1329		2	1	11	1584	1672	9	3	11	485	462					
0	2	10	2496-2364		8	4	10	371	330	-8	7	10	1075	1071	3	1	11	918	-966	10	3	11	993	1035					
1	2	10	1758-1704		10	4	10	578	621	-6	7	10	1017-1000		4	1	11	1750-1708		12	3	11	981	-1028					
3	2	10	1917	1938	-17	5	10	636	-663	-5	7	10	582	584	7	1	11	1109-1033		13	3	11	585	-552					
4	2	10	1753	1810	-16	5	10	853	-863	-4	7	10	1385	1342	8	1	11	844	826	14	3	11	363	352					
8	2	10	1249-1204		-14	5	10	935	928	-3	7	10	1007-989		9	1	11	1666	1644	-19	4	11	552	600					
10	2	10	791	816	-13	5	10	761	807	-2	7	10	1769-1789		11	1	11	1145-1047		-17	4	11	1246-1135						
11	2	10	631	600	-9	5	10	1183-1191		-1	7	10	694	656	17	1	11	962	821	-15	4	11	999	993					

OBSERVED AND CALCULATED STRUCTURE FACTORS FOR										RUS (CO)11 (C2PH(C6H4)) (PPH) (PPH(OME))										PAGE 12									
H	K	L	10FO	10FC	H	K	L	10FO	10FC	H	K	L	10FO	10FC	H	K	L	10FO	10FC	H	K	L	10FO	10FC					
-12	4	11	1041	950	-11	6	11	849	-826	-18	0	12	994	-981	5	1	12	1486	1494	10	3	12	913	899					
-11	4	11	1099	1081	-9	6	11	1117	1108	-17	0	12	1677-1749		6	1	12	1029	1004	-16	4	12	1095-1140						
-10	4	11	1397-1401		-8	6	11	1330	1352	-15	0	12	691	685	-20	2	12	516	-515	-14	4	12	1540	1577					
-9	4	11	1272-1229		-4	6	11	1342-1274		-14	0	12	649	630	-19	2	12	622	-670	-13	4	12	797	857					
-8	4	11	878	774	-3	6	11	1449-1451		-13	0	12	651	645	-14	2	12	1172	1140	-12	4	12	967	-979					
-6	4	11	1086-1058		-1	6	11	1031	1000	-10	0	12	1533-1550		-12	2	12	1560-1567		-11	4	12	737	-727					
-4	4	11	1368	1383	0	6	11	815	837	-9	0	12	1135-1192		-11	2	12	1627-1669		-10	4	12	729	781					
-2	4	11	1362-1310		1	6	11	488	425	-8	0	12	489	462	-10	2	12	411	401	-9	4	12	824	-776					
0	4	11	1369	1378	4	6	11	1299-1314		-7	0	12	1302	1394	-9	2	12	732	742	-8	4	12	1073-1047						
1	4	11	350	-366	5	6	11	1097-1083		-6	0	12	1231-1068		-7	2	12	1761	1693	-7	4	12	1219	1177					
2	4	11	1817-1793		6	6	11	1063	1084	-4	0	12	1416	1391	-5	2	12	1784-1783		-6	4	12	1478	1474					
3	4	11	961	968	7	6	11	1014	1020	-3	0	12	605	-564	-4	2	12	2494-2486		-5	4	12	792	-792					
4	4	11	1237	1234	12	6	11	772	-710	-2	0	12	1281-1188		-3	2	12	881	-887	-4	4	12	1658-1664						
5	4	11	673	-689	-14	7	11	695	725	0	0	12	604	685	-2	2	12	882	918	-3	4	12	662	647					
7	4	11	979	1010	-13	7	11	991	955	2	0	12	1631-1644		-1	2	12	1081	1172	-2	4	12	921	918					
9	4	11	939	-938	-12	7	11	491	-448	3	0	12	923	-902	0	2	12	526	595	-1	4	12	990-1043						
10	4	11	1142-1146		-6	7	11	1067	1039	4	0	12	2049	2037	1	2	12	832	922	0	4	12	1049-1043						
12	4	11	875	835	-5	7	11	921	862	6	0	12	1286-1230		2	2	12	399	-374	1	4	12	948	902					
-17	5	11	836	812	-3	7	11	782	-834	7	0	12	791	719	3	2	12	2294-2331		3	4	12	1438-1468						
-15	5	11	1428-1358		0	7	11	690	-670	9	0	12	1509-1522		4	2	12	1246-1179		5	4	12	1700	1672					
-13	5	11	1233	1193	2	7	11	1189	1158	10	0	12	1241-1242		8	2	12	791	876	7	4	12	980-1002						
-12	5	11	372	427	3	7	11	447	411	12	0	12	768	738	11	2	12	1239-1206		11	4	12	879	-807					
-10	5	11	1031	1005	9	7	11	802	780	17	0	12	1129-1090		16	2	12	814	758	13	4	12	970	970					
-9	5	11	1360	1342	10	7	11	778	797	-18	1	12	1273	1231	-19	3	12	1027-1026		15	4	12	729	-676					
-8	5	11	1452-1452		-13	8	11	882	877	-17	1	12	635	617	-13	3	12	1175	1132	-17	5	12	849	824					
-7	5	11	1581-1559		-7	8	11	695	-691	-15	1	12	620	-615	-11	3	12	1979-1969		-16	5	12	610	597					
-6	5	11	994	947	-5	8	11	830	818	-11	1	12	842	892	-9	3	12	1287	1283	-11									

Table 18. (continued)

OBSERVED AND CALCULATED STRUCTURE FACTORS FOR										RU5 (CO) 11 (C2PH (C6H4)) (PPH) (PPH (OME))										PAGE 13									
H	K	L	10FO	10FC	H	K	L	10FO	10FC	H	K	L	10FO	10FC	H	K	L	10FO	10FC	H	K	L	10FO	10FC					
-13	6	12	837	-859	-11	2	13	745	768	-3	4	13	1462	1452	-12	7	13	818	783	-9	1	14	533	532					
-12	6	12	741	-773	-9	2	13	1022	-1026	-2	4	13	1659	1649	-11	7	13	887	893	-8	1	14	663	681					
-7	6	12	1083	1068	-4	2	13	766	760	-1	4	13	1103	-1086	-6	7	13	758	-773	-6	1	14	847	796					
-5	6	12	1033	-1012	-3	2	13	703	684	0	4	13	1354	-1309	-5	7	13	658	-641	-3	1	14	1367	-1349					
-4	6	12	822	-792	-2	2	13	659	-682	1	4	13	1447	1435	-4	7	13	611	643	0	1	14	722	672					
1	6	12	1004	968	-1	2	13	1063	-1099	2	4	13	557	588	2	7	13	1052	-1047	4	1	14	1183	-1183					
3	6	12	1286	-1330	0	2	13	652	-617	3	4	13	1387	-1445	4	7	13	796	787	5	1	14	1039	-1046					
5	6	12	545	544	4	2	13	761	831	5	4	13	1001	1059	9	7	13	624	-623	9	1	14	868	859					
-7	7	12	603	587	7	2	13	583	-645	7	4	13	1139	-1107	10	7	13	716	-687	-19	2	14	838	818					
-5	7	12	1137	-1115	-19	3	13	589	596	9	4	13	1223	1249	-7	8	13	568	-560	-14	2	14	1106	-1096					
-4	7	12	363	-381	-17	3	13	548	-541	11	4	13	985	-949	-6	8	13	884	-894	-12	2	14	1913	1856					
-3	7	12	728	724	-15	3	13	1042	1039	-15	5	13	1094	1087	1	8	13	448	-462	-11	2	14	544	523					
2	7	12	568	-547	-13	3	13	1554	-1601	-10	5	13	981	-910	2	8	13	357	-406	-10	2	14	1375	-1358					
3	7	12	785	-814	-12	3	13	758	-794	-8	5	13	1305	1299	-7	9	13	987	1029	-9	2	14	619	-668					
5	7	12	1453	1461	-11	3	13	2069	2076	-7	5	13	856	806	0	9	13	501	579	-7	2	14	452	-512					
7	7	12	511	-579	-10	3	13	664	664	-6	5	13	893	-844	-19	0	14	831	850	-6	2	14	424	-415					
10	7	12	581	-559	-9	3	13	864	-902	-5	5	13	690	-643	-18	0	14	1523	1591	-5	2	14	1209	1142					
-12	8	12	606	-620	-6	3	13	1978	-1972	-2	5	13	761	-723	-14	0	14	867	-854	-4	2	14	2393	2407					
-8	8	12	616	-640	-5	3	13	2215	-2198	0	5	13	863	882	-13	0	14	1525	-1491	-2	2	14	1816	-1806					
-6	8	12	507	559	-4	3	13	1038	1012	2	5	13	690	-677	-12	0	14	573	573	1	2	14	1283	-1250					
-4	8	12	621	-586	-3	3	13	2729	2732	4	5	13	714	657	-11	0	14	1897	1767	3	2	14	1902	1962					
1	8	12	628	564	-1	3	13	988	-1013	5	5	13	486	-544	-10	0	14	1027	1078	4	2	14	810	835					
-5	9	12	423	-354	0	3	13	1297	1284	6	5	13	835	-863	-8	0	14	749	-744	5	2	14	460	-424					
-19	1	13	676	-626	2	3	13	2437	-2433	-15	6	13	400	-428	-5	0	14	1383	-1493	9	2	14	936	-821					
-13	1	13	905	-926	4	3	13	2071	2172	-9	6	13	592	-595	-4	0	14	551	516	10	2	14	930	965					
-12	1	13	1295	-1305	5	3	13	739	727	-8	6	13	771	-755	-3	0	14	1577	1527	11	2	14	1317	1335					
-9	1	13	759	693	9	3	13	855	-853	-5	6	13	725	731	-1	0	14	657	-642	-12	3	14	875	870					
-8	1	13	485	489	10	3	13	1586	-1522	-4	6	13	995	981	3	0	14	801	-781	-11	3	14	1355	1332					
-7	1	13	531	-589	12	3	13	1477	1424	-1	6	13	847	-809	5	0	14	1093	1081	-9	3	14	878	-940					
-6	1	13	578	-574	15	3	13	422	444	0	6	13	1422	-1465	7	0	14	658	-671	-7	3	14	776	-790					
-4	1	13	808	-790	-18	4	13	1146	1190	3	6	13	898	917	8	0	14	1115	1116	-6	3	14	901	-907					
-2	1	13	896	946	-12	4	13	1196	-1269	4	6	13	1120	1157	10	0	14	483	-541	-4	3	14	1763	1728					
6	1	13	748	785	-10	4	13	1756	1770	6	6	13	899	-908	14	0	14	695	-687	-3	3	14	773	776					
8	1	13	937	-960	-8	4	13	299	-334	7	6	13	988	-1009	-18	1	14	761	-792	-2	3	14	974	-967					
16	1	13	793	-757	-5	4	13	1486	-1447	10	6	13	568	554	-16	1	14	716	786	-1	3	14	734	-717					
-17	2	13	763	-771	-4	4	13	906	-899	-14	7	13	574	-618	-11	1	14	978	-972	2	3	14	999	-979					

OBSERVED AND CALCULATED STRUCTURE FACTORS FOR										RU5 (CO) 11 (C2PH (C6H4)) (PPH) (PPH (OME))										PAGE 14									
H	K	L	10FO	10FC	H	K	L	10FO	10FC	H	K	L	10FO	10FC	H	K	L	10FO	10FC	H	K	L	10FO	10FC					
3	3	14	635	670	3	6	14	840	863	-1	2	15	455	433	-7	5	15	591	-572	-10	1	16	478	-475					
6	3	14	406	-482	-8	7	14	746	-779	5	2	15	316	344	-5	5	15	722	719	-6	1	16	1106	-1111					
7	3	14	584	617	-6	7	14	1073	1080	-15	3	15	771	-735	0	5	15	848	-785	-4	1	16	1238	1253					
9	3	14	578	-624	-5	7	14	643	637	-14	3	15	648	573	-8	6	15	634	-676	-3	1	16	767	728					
10	3	14	811	-789	-1	7	14	747	-785	-13	3	15	1384	1383	-5	6	15	1009	-979	0	1	16	647	-629					
-16	4	14	865	865	1	7	14	592	637	-11	3	15	1308	-1321	-1	6	15	1056	1047	1	1	16	1073	-1059					
-14	4	14	1340	-1361	2	7	14	943	1024	-6	3	15	1471	1395	0	6	15	1021	998	8	1	16	611	-554					
-9	4	14	1227	1182	4	7	14	890	-834	-5	3	15	1019	1011	2	6	15	775	-830	9	1	16	804	-767					
-8	4	14	586	572	9	7	14	663	618	-4	3	15	1518	-1483	3	6	15	884	-925	11	1	16	573	567					
-7	4	14	1130	-1133	3	8	14	805	810	-3	3	15	1253	-1216	6	6	15	644	602	-14	2	16	728	744					
-6	4	14	904	-904	5	8	14	584	-613	-2	3	15	875	855	7	6	15	1097	1125	-12	2	16	1053	-1079					
-4	4	14	659	735	1	9	14	652	654	0	3	15	1118	-1087	4	7	15	844	-851	-10	2	16	907	916					
-3	4	14	824	-822	-18	1	15	883	-907	1	3	15	906	911	-9	8	15	1143	-1133	-9	2	16	638	583					
-1	4	14	1659	1628	-15	1	15	673	-699	2	3	15	1564	1590	-7	8	15	1392	1384	-5	2	16	1105	-1089					
1	4	14	1467	-1423	-14	1	15	761	-753	4	3	15	1103	-1119	-14	0	16	1567	1592	-4	2	16	1325	-1323					
3	4	14	995	984	-13	1	15	1370	1354	9	3	15	1432	1429	-13	0	16	1310	1256	-3	2	16	728	655					
-1	4	14	682	-639	-12	1	15	1138	1201	10	3	15	1087	1088	-12	0	16	1188	-1185	-2	1	16	986	926					
7	4	14	851	913	-11	1	15	671	-645	11	3	15	762	-754	-11	0	16	1741	-1749	1	2	16	703	693					
9	4	14	870	-865	-10	1	15	1110	-1108	12	3	15	952	-934	-9	0	16	920	934	3	2	16	1377	-1351					
13	4	14	661	-682	-8	1	15	653	671	-17	4	15	398	-489	-8	0	16	967	-992	5	2	16	634	562					
-16	5	14	401	-351	-7	1	15	691	-731	-13	4	15	1210	1139	-6	0	16	2796	2710	6	2	16	750	765					
-15	5	14	833	837	-5	1	15	2103	2154	-11	4	15	1391	-1426	-5	0	16	1077	1016	8	2	16	699	701					
-10	5	14	735	-702	-4	1	15	843	843	-10	4	15	955	-1013	-4	0	16	2189	-2218	10	2	16	1064	-1071					
-9	5	14	840	-812	-3	1	15	1374	-1425	-9	4	15	653	642	-3	0	16	1214	-1260	11	2	16	1090	-1053					
-7	5	14	614	586	-2	1	15	692	-694	-6	4	15	651	598	-2	0	16	580	558	13	2	16	832	769					
-2	5	14	1960	-1862	-1	1	15	907	827	-5	4	15	1372	1375	0	0	16	1057	-1029	-15	3	16	746	764					
-1	5	14	1294	-1318	1	1	15	693	-724	-3	4	15	1848	-1908	1	0	16	1115	1103	-13	3	16	778	-753					
0	5	14	1300	1315	3	1	15																						



**APPENDIX 2. Publications by the author arising from this work**

- (1) Reactions of transition metal  $\sigma$ -acetylide complexes. Part X. Cycloaddition of tetracyanoethene to manganese, iron and nickel complexes, and hydration of a related tungsten complex. X-Ray structures of  $\text{Fe}\{\overline{\text{C}=\text{C}(\text{CN})_2}\text{CPh}=\text{C}(\text{CN})_2\}(\text{CO})_2(\eta\text{-C}_5\text{H}_5)$  and  $\text{Ni}\{\text{C}[\text{C}(\text{CN})_2]\text{CPh}=\text{C}(\text{CN})_2\}(\text{PPh}_3)(\eta\text{-C}_5\text{H}_5)$  (with M.I. Bruce, D.N. Duffy, M.R. Snow and E.R.T. Tiekink) *J. Organomet. Chem.* **335** (1987) 365.
- (2) Reactions of transition metal  $\sigma$ -acetylide complexes. Part 11. Cycloaddition reactions with 1,1-dicyano-2,2-bis(trifluoromethyl)ethene. X-Ray structures of  $\text{W}\{\overline{\text{C}=\text{CPhC}(\text{CF}_3)_2\text{C}(\text{CN})_2}\}(\text{CO})_3(\eta\text{-C}_5\text{H}_5)$ ,  $\text{Mn}\{\overline{\text{C}=\text{CPhC}(\text{CF}_3)_2\text{C}(\text{CN})_2}\}(\text{CO})_3(\text{dppe})$ , and  $\text{Fe}\{\overline{\text{C}=\text{CPhC}(\text{CF}_3)_2\text{C}(\text{CN})_2}\}(\text{CO})_2(\eta\text{-C}_5\text{H}_5)$  and of a hydration product  $\overline{\text{W}\{\text{NH}=\text{C}(\text{OH})\text{C}(\text{CN})=\text{CCPh}=\text{C}(\text{CF}_3)_2\}}(\text{CO})_2(\eta\text{-C}_5\text{H}_5)$  (with M.I. Bruce, M.R. Snow and E.R.T. Tiekink) *Organometallics* **7** (1988) 343.
- (3) Stability of the cyclobutenyl group in  $\text{Fe}(\text{C}=\text{CFCF}_2\text{CF}_2)(\text{CO})_2(\eta\text{-C}_5\text{H}_5)$  towards isomerisation by ring-opening. X-Ray crystal structures of  $\text{Fe}\{\overline{\text{C}=\text{CFCF}_2\text{CF}_2}\}(\text{CO})(\text{L})(\eta\text{-C}_5\text{H}_5)$  ( $\text{L} = \text{CO}$  and  $\text{PPh}_3$ ) (with M.I. Bruce, M.R. Snow and E.R.T. Tiekink) *J. Organomet. Chem.* **352** (1988) 199.